РАЗКОПКИ И ПРОУЧВАНИЯ XLVIII(1)

1892 - 1921 - 1948

БЪЛГАРСКА АКАДЕМИЯ НА НАУКИТЕ
НАЦИОНАЛЕН АРХЕОЛОГИЧЕСКИ
ИНСТИТУТ С МУЗЕЙ

Lyudmil Vagalinski, Sven Conrad, Lyuba Traykova,
Nadezhda Kecheva, Raiko Krauß

NOVGRAD – TASH BAIR I

ARCHAEOLOGICAL INVESTIGATIONS AT THE SOUTHERNMOST POINT OF THE DANUBE



София • 2023

NOVGRAD – TASH BAIR I

ARCHAEOLOGICAL INVESTIGATIONS AT THE SOUTHERNMOST POINT OF THE DANUBE

НОВГРАД – ТАШ БАИР I

АРХЕОЛОГИЧЕСКИ ПРОУЧВАНИЯ В НАЙ-ЮЖНАТА ТОЧКА НА ДУНАВ

Разкопки и проучвания е поредица издавана от Националния археологически институт с музей при Българската академия на науките

Разкопки и проучвания (Archaeological Excavations and Research) Series is published by the National Archaeological Institute with Museum at the Bulgarian Academy of Sciences

1892 - 1921 - 1948

Funded by DFG Deutsche Forschungsgemeinschaft German Research Foundation

EBERHARD KARLS UNIVERSITÄT TÜBINGEN

Германската фондация за научни изследвания (Deutsche Forschungsgemeinschaft – DFG) финансира научен проект с № 388543935 / CO-288 / 2-1, подаден от Свен Конрад чрез Университета в Тюбинген, Германия. Проектът е изпълнен чрез договор между НАИМ – БАН и Университета в Тюбинген.

The German Research Foundation (Deutsche Forschungsgemeinschaft – DFG) funded the research project submitted by Sven Conrad under No. 388543935 / CO-288 / 2-1 via the University of Tübingen, Germany. The project was implemented by a contract between NAIM–BAS and the University of Tübingen.

©Национален археологически институт с музей при Българската академия на науките

©Издателство на БАН „Проф. Марин Дринов“

©Автори: *Людмил Вагалински, Свен Конрад, Люба Трайкова, Надежда Кечева, Райко Краус* с приноси от *Андреас Лопес дел Олмо, Буркарт Улрих, Ернст Перницка, Херт Верстраетен, Хенинг Цьолнер, Мария Гюрова, Надежда Карастоянова, Николаас Ноорда, Нилс Бротхаертс, Петър Зидаров, Силва Събкова, Виктория Русева*

©National Archaeological Institute with Museum at the Bulgarian Academy of Sciences

©Prof. Marin Drinov Publishing House of BAS

©Authors: *Lyudmil Vagalinski, Sven Conrad, Lyuba Traykova, Nadezhda Kecheva, Raiko Krauß* with contributions by *Andreas López del Olmo, Burkart Ullrich, Ernst Pernicka, Gert Verstraeten, Henning Zoellner, Maria Gurova, Nadezhda Karastoyanova, Nikolaas Noorda, Nils Brothaerts, Petar Zidarov, Silva Sabkova, Victoria Russeva*

Редактори: *Людмил Вагалински, Свен Конрад, Райко Краус*
Рецензенти: *Христо Попов, Иво Д. Чолаков, Здравко Димитров*
Технически редактор: *Надежда Кечева*
Езикова редакция на английски: *Каталина Лабра-Оде, Амбър Рой*
Езиков коректор на български: *Гергана Ангелова*
Предпечат: *Галя Герасимова, Бойко Киряков*
Снимка на корицата: *поглед към Таш баир от юг-югозапад (снимка от Б. Борисов, април 2022 г.)*
Печат: *Издателство на БАН „Проф. Марин Дринов“*
София 2023

Editors: *Lyudmil Vagalinski, Sven Conrad, Raiko Krauß*
Reviewers: *Hristo Popov, Ivo D. Cholakov, Zdravko Dimitrov*
Technical assistant: *Nadezhda Kecheva*
English language editing: *Catalina Labra-Odde, Amber Roy*
Bulgarian language proofreading: *Gergana Angelova*
Prepress: *Galya Gerasimova, Boyko Kiryakov*
Front cover photo: *view of Tash Bair locality from the south-southwest (photo by B. Borisov, April 2022)*
Printed by *Prof. Marin Drinov Publishing House of BAS*
Sofia 2023

ISSN 0205-0722 (print)
ISSN 2683-0833 (online)
ISBN 978-619-245-386-2 (print)
ISBN 978-619-254-029-6 (online)

Редакционна колегия на поредицата *Разкопки и проучвания*:
Марио Иванов (главен редактор),
Дочка Владимирова-Аладжова, Мария Гюрова,
Стефан Александров, Маргарит Дамянов,
Деян Рабовянов, Николай Шаранков

Editorial Board of *Разкопки и проучвания* (Archaeological Excavations and Research) Series:
Mario Ivanov (Editor-in-Chief),
Dochka Vladimirova-Aladzhova, Maria Gurova,
Stefan Alexandrov, Margarit Damyanov,
Deyan Rabovyanov, Nicolay Sharankov

Всички права са запазени. Нито една част от тази книга не може да бъде репродуцирана, публикувана, изцяло или отчасти, или в съкратен вариант, преразказана или преработена с фабрични или електронни средства, препечатана или записвана под каквато и да било форма без изричното писмено разрешение на издателя.

All rights reserved. No part of this book may be reproduced, or transmitted in any form or by any means, electronic or mechanical including photocopying, recording or by any information storage and retrieval system, without permission from the publisher in writing.

Цитиране на цялата книга / Citation of the whole book:
Vagalinski, L., Conrad, S., Traykova, L., Kecheva, N., Krauß, R. 2023. Novgrad – Tash Bair I. Archaeological Investigations at the Southernmost Point of the Danube. – Разкопки и проучвания, 48(1). Sofia: Prof. Marin Drinov Publishing House of BAS.

1892 - 1921 - 1948

БЪЛГАРСКА АКАДЕМИЯ НА НАУКИТЕ
НАЦИОНАЛЕН АРХЕОЛОГИЧЕСКИ ИНСТИТУТ С МУЗЕЙ
BULGARIAN ACADEMY OF SCIENCES
NATIONAL ARCHAEOLOGICAL INSTITUTE WITH MUSEUM

РАЗКОПКИ И ПРОУЧВАНИЯ – XLVIII(1)
ARCHAEOLOGICAL EXCAVATIONS AND RESEARCH – 48(1)

**Lyudmil Vagalinski, Sven Conrad, Lyuba Traykova,
Nadezhda Kecheva, Raiko Krauß**

with contributions by

Andreas López del Olmo, Burkart Ullrich, Ernst Pernicka, Gert Verstraeten,
Henning Zoellner, Maria Gurova, Nadezhda Karastoyanova, Nikolaas Noorda,
Nils Brothaerts, Petar Zidarov, Silva Sabkova, Victoria Russeva

Novgrad – Tash Bair I

Archaeological investigations at the southernmost point of the Danube

**Людмил Вагалински, Свен Конрад, Люба Трайкова,
Надежда Кечева, Райко Краус**

с приноси от

Андреас Лопес дел Олмо, Буркарт Улрих, Ернст Перницка, Херт Верстраетен,
Хеннинг Цьолнер, Мария Гюрова, Надежда Карастоянова, Николаас Ноорда,
Нилс Бротхаертс, Петър Зидаров, Силва Събкова, Виктория Русева

Новград – Таш баир I

Археологически проучвания в най-южната точка на Дунав

Издателство на БАН „Проф. Марин Дринов“

София • Sofia
2023

CONTENTS / СЪДЪРЖАНИЕ

VOLUME 48(1) / КНИГА XLVIII(1)

Affiliations of the authors in alphabetical order / Афилиации на авторите по азбучен ред ix

List of figures / Списък на фигурите xiii

List of tables / Списък на таблиците xxvi

List of plates / Списък на таблата xxviii

1. Preface 1
Sven Conrad, Raiko Krauß, Lyudmil Vagalinski
Увод 3
Свен Конрад, Райко Краус, Людмил Вагалински

2. History of research and aims of the project 5
Sven Conrad, Raiko Krauß
История на проучванията и цели на проекта (Резюме) 13
Свен Конрад, Райко Краус

3. Environmental conditions in the study area 15
Andreas López del Olmo, Raiko Krauß, Sven Conrad
Състояние на околната среда в района на изследване (Резюме) 27
Андреас Лопес дел Олмо, Райко Краус, Свен Конрад

4. Palaeo-river course reconstruction in the floodplain of the Yantra River, North-Central Bulgaria 29
Andreas López del Olmo, Gert Verstraeten, Nils Brothaerts
Реконструкция на палеоречното течение в заливната низина на р. Янтра, Централна Северна България (Резюме) 66
Андреас Лопес дел Олмо, Херт Верстраетен, Нилс Бротхаертс

5. Methodology of archaeological research / Методи при археологическите проучвания 69

5.1. The measurement system 69
Nadezhda Kecheva, Sven Conrad
Системи за измерване и документиране (Резюме) 73
Надежда Кечева, Свен Конрад

5.2. Field survey methods 73
Nadezhda Kecheva
Методи при теренните издирвания (Резюме) 89
Надежда Кечева

5.3. Archaeological excavation methods / Методи при археологическите разкопки 90

5.3.1. Archaeological excavation methods 90
Lyudmil Vagalinski, Lyuba Traykova
Методи при археологическите разкопки (Резюме) 92
Людмил Вагалински, Люба Трайкова

5.3.2. Archaeological excavation methods for the trenches 1.2, 3.1 and 5.1 93
Sven Conrad
Методи при археологическите разкопки на сондажи 1.2, 3.1 и 5.1 (Резюме) 94
Свен Конрад

5.4. Find recording / Документиране на находки 95
5.4.1. Recording of pottery finds, silex and animal bones 95
Sven Conrad
Документиране на керамични находки, кремъци и животински кости (Резюме) 95
Свен Конрад
5.4.2. Small find recording 96
Lyuba Traykova
Документиране на малки находки (Резюме) 96
Люба Трайкова
5.5. Sampling 96
Sven Conrad
Взимане на проби (Резюме) 98
Свен Конрад
6. The geophysical prospections. Methods and results / Геофизични проучвания. Методи и резултати 99
6.1. Geophysical prospections at sites 1 and 3–5 99
Burkart Ullrich, Nikolaas Noorda, Henning Zoellner
Геофизични проучвания на обекти 1 и 3 – 5 (Резюме) 108
Буркарт Улрих, Николаас Ноорда, Хенниг Цьолнер
6.2. Geomagnetic survey at site 2 109
Petar Zidarov
Геомагнитни проучвания на обект 2 (Резюме) 116
Петър Зидаров
6.3. Two ERT profiles through the ditches on site 3 116
Gert Verstraeten
Два ERT профила през рововете на обект 3 (Резюме) 118
Херт Верстраетен
7. The intensive field surveys at the Tash Bair and in its surroundings 119
Nadezhda Kecheva, Lyudmil Vagalinski, Lyuba Traykova, Silva Sabkova
Интензивни теренни издирвания в района на Таш баир (Резюме) 139
Надежда Кечева, Людмил Вагалински, Люба Трайкова, Силва Събкова
8. Archaeological excavations / Археологически разкопки 141
8.1. The Late Neolithic ditches at site 1 (trench 1.2) 141
Raiko Krauß, Sven Conrad
Късноенеолитни ровове на обект 1 (сондаж 1.2) (Резюме) 148
Райко Краус, Свен Конрад
8.2. Bronze Age / Бронзова епоха 148
8.2.1. The inner ditch of the enclosure in trench 3.6 148
Lyudmil Vagalinski, Lyuba Traykova, Nadezhda Kecheva
Вътрешен ров на оградена площ в сондаж 3.6 (Резюме) 156
Людмил Вагалински, Люба Трайкова, Надежда Кечева
8.2.2. The structure in trenches 3.2–5 159
Lyudmil Vagalinski, Lyuba Traykova
Структура в сондажи 3.2 – 5 (Резюме) 164
Людмил Вагалински, Люба Трайкова

8.2.3. The pit in trench 3.1 165
Sven Conrad, Raiko Krauß
Яма в сондаж 3.1 (Резюме) 170
Свен Конрад, Райко Краус
8.2.4. Bronze Age. Conclusion 171
Lyudmil Vagalinski, Lyuba Traykova, Nadezhda Kecheva
Бронзова епоха. Заключение (Резюме) 172
Людмил Вагалински, Люба Трайкова, Надежда Кечева
8.3. Late Iron Age / Късна желязна епоха 172
8.3.1. The Late Iron Age ditch in trench 1.1 173
Lyudmil Vagalinski, Lyuba Traykova, Nadezhda Kecheva
Ров от късната желязна епоха в сондаж 1.1 (Резюме) 183
Людмил Вагалински, Люба Трайкова, Надежда Кечева
8.3.2. The Early Roman pits 5.1.2 and 5.1.6 185
Sven Conrad
Раннримски ями 5.1.2 и 5.1.6 (Резюме) 190
Свен Конрад
8.3.3. The grave in pit 5.1.5 191
Lyudmil Vagalinski, Lyuba Traykova, Nadezhda Kecheva
Гроб в яма 5.1.5 (Резюме) 201
Людмил Вагалински, Люба Трайкова, Надежда Кечева
8.3.4. Late Iron Age. Conclusion 203
Lyudmil Vagalinski, Lyuba Traykova, Nadezhda Kecheva
Късна желязна епоха. Заключение (Резюме) 204
Людмил Вагалински, Люба Трайкова, Надежда Кечева
8.4. The Early Medieval fortifications in trenches 1.1 and 1.2 205
Lyudmil Vagalinski, Lyuba Traykova, Nadezhda Kecheva
Ранносредновековни фортификации в сондажи 1.1 и 1.2 (Резюме) 221
Людмил Вагалински, Люба Трайкова, Надежда Кечева
9. Pottery and small finds / Керамични и малки находки 225
9.1. The pottery finds (with catalogue) / Керамични находки (с каталог) 225
9.1.1. Prehistoric pottery 225
Raiko Krauß
Керамика от праисторията (Резюме) 238
Райко Краус
9.1.2. Late Iron Age to Medieval pottery 242
Sven Conrad
Керамика от късната желязна епоха до Средновековието (Резюме) 261
Свен Конрад
9.1.3. Pottery statistics from the excavations of different features 262
Sven Conrad, Raiko Krauß
Статистика на керамични находки от разкопките на различни структури (Резюме) 283
Свен Конрад, Райко Краус
9.2. Small finds (with catalogue) / Малки находки (с каталог) 382

9.2.1. Small finds from prehistory 382
Raiko Krauß
Малки находки от праисторията (Резюме) 387
Райко Краус
9.2.2. Small finds from Antiquity and Early Middle Ages 398
Lyuba Traykova
Малки находки от Античността и Ранното средновековие (Резюме) 407
Люба Трайкова

VOLUME 48(2) / КНИГА XLVIII(2)

Affiliations of the authors in alphabetical order / Афилиации на авторите по азбучен ред ... xxxix
List of figures / Списък на фигурите xliii
List of tables / Списък на таблиците xlix
10. Interdisciplinary research / Интердисциплинарни проучвания 431
10.1. A bronze knife from site 3 431
Raiko Krauß, Ernst Pernicka
Бронзов нож от обект 3 (Резюме) 434
Райко Краус, Ернст Перницка
10.2. Chipped-stone assemblages 435
Maria Gurova
Кремъчни ансамбли (Резюме) 465
Мария Гюрова
10.3. Archaeozoological analysis of the animal remains 466
Nadezhda Karastoyanova
Археозоологичен анализ на животински останки (Резюме) 478
Надежда Карастоянова
10.4. Human remains from a pit at site 5 479
Victoria Russeva
Човешки костни останки от яма на обект 5 (Резюме) 481
Виктория Русева
11. Conclusions / Заключение 483
11.1. Novgrad I project 483
Lyudmil Vagalinski
Проект Новград I 483
Людмил Вагалински
11.2. The mouth of the Yantra with the Tash Bair ridge – an important crystallisation and crossing point in the history of settlement on the eastern Balkan peninsula 484
Sven Conrad, Raiko Krauß
Устието на р. Янтра при Таш баир – значим селищен център през вековете и преходен пункт на Източните Балкани 488
Свен Конрад, Райко Краус
12. Catalogue of the archaeological sites 493
Nadezhda Kecheva, Lyudmil Vagalinski, Sven Conrad, Lyuba Traykova, Silva Sabkova
Каталог на археологическите обекти (Резюме) 658
Надежда Кечева, Людмил Вагалински, Свен Конрад, Люба Трайкова, Силва Събкова
13. References / Използвана литература 661

AFFILATIONS OF THE AUTHORS IN ALPHABETICAL ORDER

Andreas López del Olmo, M.Sc.
Department of Earth and Environmental Sciences
Division of Geography and Tourism
KU Leuven
Celestijnenlaan 200E
B-3001 Leuven (Heverlee)
lopezandreas@hotmail.com

Burkart Ullrich, Dipl.-Geophys.
Eastern Atlas GmbH & Co. KG
69 Berliner St.
D-13189 Berlin
Germany
b.ullrich@eastern-atlas.de
ORCID: 0000-0001-7619-6810

Ernst Pernicka, Prof. Dr.
Senior Professor University of Tübingen
Scientific Director
Curt-Engelhorn-Zentrum Archäometrie gGmbH
D6, 3
68159 Mannheim
Germany
ernst.pernicka@ceza.de
ORCID ID: 0000-0003-4746-9239

Gert Verstraeten, Prof. Dr.
Department of Earth and Environmental Sciences
Division of Geography and Tourism
KU Leuven
Celestijnenlaan 200E
B-3001 Leuven (Heverlee)
Belgium
gert.verstraeten@kuleuven.be
ORCID: 0000-0002-6529-7381

Henning Zoellner, Dipl.-Geophys.
Eastern Atlas GmbH & Co. KG
69 Berliner St.
D-13189 Berlin
Germany
h.zoellner@eastern-atlas.de

Lyuba Traykova, Assist. Prof. Dr.
Department of Antiquity
National Archaeological Institute with Museum
Bulgarian Academy of Sciences
2 Saborna St.
BG-1000 Sofia
Bulgaria
latraykova@gmail.com
ORCID 0000-0002-5185-6816

Lyudmil Vagalinski, Prof. Dr.
Department of Antiquity
National Archaeological Institute with Museum
Bulgarian Academy of Sciences
2 Saborna St.
BG-1000 Sofia
Bulgaria
lfvagalinski@gmail.com
ORCID 0000-0002-2870-0688

Maria Gurova, Assoc. Prof. Dr.
Department of Prehistory
National Archaeological Institute with Museum
Bulgarian Academy of Sciences
2 Saborna St.
BG-1000 Sofia
Bulgaria
maria.gurova@naim.bg
ORCID: 0000-0002-2702-2117

Nadezhda Karastoyanova, Assist. Prof. Dr.
Department of Palaeontology and Mineralogy
National Museum of Natural History
Bulgarian Academy of Science
1 Tsar Osvoboditel Blvd.
BG-1000 Sofia
Bulgaria
Department of Interdisciplinary Research and Archaeological Map of Bulgaria
National Archaeological Institute with Museum
Bulgarian Academy of Sciences
2 Saborna St.
BG-1000 Sofia
Bulgaria
n_karastoyanova@nmnhs.com
ORCID 0000-0001-6032-4873

Nadezhda Kecheva, Assist. Prof. Dr.
Department of Interdisciplinary Research and Archaeological Map of Bulgaria
National Archaeological Institute with Museum
Bulgarian Academy of Sciences
2 Saborna St.
BG-1000 Sofia
Bulgaria
nadezhda.kecheva@naim.bg
n.kecheva@gmail.com
ORCID: 0000-0002-0128-1129

Nikolaas Noorda, M. A.
Noorda Noorda Archaeological Assistance
Boven Oosterdiep 119a
NL-9641 JP Veendam
The Netherlands
np_noorda99@hotmail.com
ORCID: 0000-0002-8331-0762

Nils Broothaerts, Dr.
Department of Earth and Environmental Sciences, Division of Geography and Tourism
KU Leuven
Celestijnenlaan 200E
B-3001 Leuven
Belgium
Thomas More University of Applied Science
Zandpoortvest 60
B-2800 Mechelen
Belgium
nils.broothaerts@thomasmore.be
ORCID: 0000-0002-8605-9657

Petar Zidarov
Institute for Prehistory, Early History and Medieval Archaeology
Eberhard Karls University Tübingen
Schloss Hohentübingen
Burgsteige 11
D-72070 Tübingen
Germany
petar.zidarov@gmail.com
ORCID: 0000-0001-9968-7786

Raiko Krauß, Prof. Dr.
Institute for Prehistory, Early History and Medieval Archaeology
Eberhard Karls University Tübingen
Schloss Hohentübingen
Burgsteige 11
D-72070 Tübingen
Germany
raiko.krauss@uni-tuebingen.de
ORCID: 0000-0003-0342-5648

Silva Sabkova, Assist. Prof. Dr.
Department of Interdisciplinary Research and Archaeological Map of Bulgaria
National Archaeological Institute with Museum
Bulgarian Academy of Sciences
2 Saborna St.
BG-1000 Sofia
Bulgaria
s.s.sabkova@gmail.com
ORCID 0000-0002-3673-1716

Sven Conrad, Dr.
Institute for Prehistory, Early History and Medieval Archaeology
Eberhard Karls University Tübingen
Schloss Hohentübingen
Burgsteige 11
D-72070 Tübingen
Germany
sven.conrad@uni-tuebingen.de
ORCID: 0000-0003-0072-6605

Victoria Russeva, Assoc. Prof. Dr.
Department of Anthropology and Anatomy
Institute of Experimental Morphology, Pathology and Anthropology with Museum
Bulgarian Academy of Sciences
Acad. Georgi Bonchev St., Bl. 25
BG-1113 Sofia
Bulgaria
victoria_russeva@yahoo.com
ORCID 0000-0001-8998-6782

LIST OF FIGURES

2. HISTORY OF RESEARCH AND AIMS OF THE PROJECT

Sven Conrad, Raiko Krauß

Fig. 1. Aerial view of Iatrus from the northeast (spring 2000) (figure by S. Conrad)

Fig. 2. Map of archaeological sites (without burial mounds) in the working area registered between 1997 and 2001 (figure by S. Conrad)

Fig. 3. Map of burial mounds in the working area registered between 1997 and 2001 (figure by S. Conrad)

Fig. 4. Satellite picture of 2012 of the mouth of the Yantra River and its surrounding area (Google Earth): At the Tash Bair to the west, the medieval rampart (site 1; see arrow) and the quarter-circle double ditch (site 3; see arrow) at the south slope are very good visible. To the east, the old Yantra meanders stand out very well. The village of Novgrad is situated on the eastern terrace (figure by S. Conrad, on the base of a Google Earth satellite image)

Fig. 5. Satellite picture of 2018 with similar image section like fig. 4 (Google Earth). The ditch which cuts the spur of the Tash Bair (site 4; see arrow) is visible as a dark green line (figure by S. Conrad)

3. ENVIRONMENTAL CONDITIONS IN THE STUDY AREA

Andreas López del Olmo, Raiko Krauß, Sven Conrad

Fig. 1. SRTM DEM of South-Eastern Europe (spatial resolution of 30 m). The most important mountain ranges, rivers, plains, and the Yantra River basin are indicated (processing of DEM Europe, Danube EU-Hydro from ArcGIS online) (figure by A. López del Olmo)

Fig. 2. Section of the geomorphological map of Central-North Bulgaria and South Romania (section 607–520 km along the Danube), with the study area indicated by the red rectangle (adapted from Evlogiev, Enciu 2001). 1 – Pliocene denudation surface (PDS); 2 – Old erosion-accumulation level (OEAL); 3 – Old abrasion-accumulation level (OAAL); 4 – Six-layer loess terrace (T6); 5 – Five-layer loess terrace (T5); 6 – Four-layer loess terrace (T4); 7 – Three-layer loess terrace (T3); 8 – Two-layer loess terrace (T2); 9 – Single-layer loess terrace (T1); 10 – Low flooded terrace (To); 11 – Erosion slopes with gulches; B – boreholes; O – outcrop; O4 – Karamanovo; O5 –Vardim; O6 – Bosilkovtsi

Fig. 3. Section of the geological map of Bulgaria K-35-16 (Byala) for the study area, scale 1:100 000 (adapted from Филипов 1992). aQh – alluvial deposits (river-bed and flood-plain deposits), aQp3 – upper Pleistocene alluvial deposits of 1st and 2nd terraces above the flood plain, eQp2-3 – loess cover, bsN1 -N2 – the Byala Slatina formation (sands with interbeds and lenses of pebble and clays of Pontian-Pliocene age), IN1 -N2 – the Aidemir and Sarpovo formation, consisting of white to rusty sands or green -grey sandy banded clays,tK1 – the Trambesh Formation (marls with interbeds of limestones and sandstones of Aptian age), rsK1 – the Ruse Formation (Aoolitic, organogenic and detrital limestones of Aptian age)

Fig. 4. Soil map for the study area, scale 1:400 000 (adapted from Койнов et al. 1968)

Fig. 5. Different recognised soil horizons in a typical chernozem soil. With left a calcareous chernozem (Epicalcic Chernozem Siltic) and right a leached chernozem soil (Endocalcic Chernozem Siltic) (Shishkov, Kolev 2014c)

Fig. 6. Morphostructural zones in the Yantra River basin with: zone A representing the Danubian Plain (or Moesian Platform), zone B1 the Fore-Balkan (or Pre-Balkan) and zone B2 the Balkan mountain ridge (or the Balkans) (processing of DEM Europe from ArcGIS online, based on Nedkov et al. 2007; Nikolova, Nikolov 2011, processed by A. López del Olmo)

Fig. 7. Land cover map of 2018 for the Yantra River basin with pixel resolution of 100 m (CORINE land cover data from Copernicus, 2018, processed by A. López del Olmo)

Fig. 8. Main ridge of the Balkan mountain range (Kupena peak, 2169 m) in morphostructural zone B2 in Central Bulgaria (Stoyanov, Gachev, 2012)

Fig. 9. Yantra River at Veliko Tarnovo in morphostructural zone B1 (figure by A. López del Olmo)

Fig. 10. Left picture shows the characteristic undulating relief of the Danubian Plain in morphostructural zone A, near Beltsov, Northern Bulgaria. Right picture visualises the Lower Yantra River, incised in the Mesozoic-Neogene limestone plateau at about 5 km stream upwards of the confluence of the Yantra with the Danube (figure by A. López del Olmo)

Fig. 11. Modelled annual distribution of the monthly average discharge (Qavg), for reference period 1961–1998 and the monthly average maximum discharge (Qmax), for reference period 1961–1988 for the Yantra outlet (adapted from Nikolova, Nikolov 2011)

4. PALAEO-RIVER COURSE RECONSTRUCTION IN THE FLOODPLAIN OF THE YANTRA RIVER, NORTH-CENTRAL BULGARIA

Andreas López del Olmo, Gert Verstraeten, Nils Brothaerts

Fig. 1. A) Georeferenced satellite image of the study area (processing of Google earth imagery). B) LIDAR DTM for the study area (pixel resolution of 1 m). Area of fieldwork is indicated by the black rectangles. The current river channel (blue), the most recent active meander (yellow) and the embankments (red) are indicated as well (figure by A. López del Olmo)

Fig. 2. Panorama picture across the study area, taken from the south, looking in a northward direction (composition of 4 pictures, taken by S. Conrad, spring 2019)

Fig. 3. Panorama view across the study area from Tash Bair (south-eastward direction, during late winter 2018). Withered reed vegetation is growing in former palaeo-meanders (composition of two pictures, taken by S. Conrad, 2018)

Fig. 4. A) Recent river course changes of the Lower Yantra River, depicted on a SRTM DEM (resolution 30m). B) SRTM DEM of the Yantra River basin (resolution 30 m). The black rectangle indicates the Lower Yantra in the Yantra basin (processing of SRTM data provided by USGS, figure by A. López del Olmo)

Fig. 5. Left: coring locations (indicated in dark blue), displayed on a DTM of the study area (resolution 1 m). The current river channel is indicated in blue. Top right: localization of the coring transects on a Google Earth satellite image. Bottom right: localization of the ERT transects on a Google Earth satellite image (processing of Google Earth imagery and LIDAR DTM, figure by A. López del Olmo)

Fig. 6. ERT profile 2. High resistivity values are indicated by the colour range orange through to purple. Low resistivity values are indicated by the dark blue through to light blue colour range. The black box indicates the validated depth of the profile from the corings. The black lines indicate low resistivity values, which indicate potential former river meanders. The interpretation of the coring transect, corresponding to this ERT profile is shown in figure 12 (figure by A. López del Olmo)

Fig. 7. ERT profile 3. High resistivity values are indicated by colour range orange through to purple. Low resistivity values are indicated by the dark blue through to light blue colour range. The black box indicates the validated depth of the profile from the corings. The black lines indicate low resistivity values, which indicate potential former river meanders. The interpretation of the coring transect, corresponding to approximately the first 800 m of this ERT profile is shown in figure 13 (figure by A. López del Olmo)

Fig. 8. Detailed cross-section of the alluvial plain along transect 1 east of the entrance of the SW-meander. The position of ^{14}C-sample 1 is visualised (figure by A. López del Olmo)

Fig. 9. Cross-section of the alluvial plain along transect 1 south. The position of ^{14}C-sample 2 is visualised (figure by A. López del Olmo)

Fig. 10. Cross-section of the alluvial plain along transect 2 (figure by A. López del Olmo)

Fig. 11. Cross-section of the alluvial plain along transect 4. The positions of ^{14}C-samples 3–5 are visualised (figure by A. López del Olmo)

Fig. 12. Cross-section of the alluvial plain along transect 7. The positions of ^{14}C-samples 6; 7 are visualised (figure by A. López del Olmo)

Fig. 13. Cross-section of the alluvial plain along transect 8. The positions of ^{14}C-samples 8; 9 are visualised (figure by A. López del Olmo)

Fig. 14. Cross-section of the alluvial plain along transect 9. The positions of ^{14}C-samples 10–12 are visualised (figure by A. López del Olmo)

Fig. 15. Cross-section of the alluvial plain along transect 10. The position of ^{14}C-sample 13 is visualised (figure by A. López del Olmo)

Fig. 16. Visualisation of former locations where the Yantra River entered the study area on top of a DTM. The inset shows a Google Earth image of the entire study area (processing of LIDAR DTM) (figure by A. López del Olmo)

Fig. 17. Localization of the SW-meander, the middle meander and the northern meander valleys, the current Yantra River channel and the coring transects on top of a LIDAR DTM (processing of LIDAR DTM) (figure by A. López del Olmo)

Fig. 18. Reconstruction of the river activity of the Yantra in the study area, from the current river channel in figure 18,1 to the scenario proposed in figure 18,6a. figure 18,7 indicates that reconstructions for the Early and Middle Holocene become impossible. Figures 18,8–10 indicate probable locations of Late Glacial palaeo-meanders. For some time periods more scenarios are plausible, they are indicated by the letter 'a'. Note the reduced channel width when channel branching takes place. The base map in all sub-figures is a LIDAR DTM). The corresponding legend for every sub-figure is only visualised in figure 18,0 (figure by A. López del Olmo)

Fig. 19. Map of the corings from site 1 to the Studena Reka valley (T11) (figure by A. López del Olmo)

Fig. 20. Sedimentological interpretation of Tash Bair towards the alluvial plain of the Studena Reka and Yantra rivers (figure by A. López del Olmo)

Fig. 21. The red circle indicates the location of the corings along T1 south where buried archaeological remains were found. The inset shows the location of T1 south in the study area on a Google Earth image (figure by A. López del Olmo)

Fig. 22. Archaeological finds of pottery remains, a blade, and a rounded stone along transect 1 south. Unit of scale: cm (figure by A. López del Olmo)

Fig. 23. Digitisation of points from Tash Bair (left), towards the floodplain (right). The inset shows the location of all coring transects on a Google Earth image (processing of Google Earth imagery and LIDAR DTM) (figure by A. López del Olmo)

Fig. 24. Elevation profile of the digitised points in the gully west of coring transect 2. The two red dots mark the start and endpoint of the gully (figure by A. López del Olmo)

Fig. 25. SW-meander (delineated by the red line) buried by colluvium from the sunken lane. The apparent extent of the colluvial fan is shown by the border between the ploughed field and the wittered reed vegetation (picture: S. Conrad, late winter 2018)

Fig. 26. Localization of the Middle Bronze Age double ditch with its hypothetical circular form, depicted on a DTM. The digitised points to construct the elevation profile (fig. 27) are indicated as well. The Google Earth images show the location of the Bronze Age double ditch, coring transect 4 and the location where panorama figure 28 was taken (processing of LIDAR DTM) (figure by A. López del Olmo)

Fig. 27. Elevation profile from the Bronze Age enclosure towards the floodplain of the Yantra. The locations of the inner ditch, outer ditch and the presumed location of the centre of the enclosure and the mirrored inner and outer ditch are indicated (figure by A. López del Olmo)

Fig. 28. The white polygons indicate the location of three archaeological sites on the Tash Bair hill. Site 1 indicates the location of a Neolithic to Medieval settlement, site 2 a mainly Roman to Late Roman and site 3 of a Middle Bronze Age double ditch. Note the gullies in the crop fields as an indication for erosion on the steeper slopes. The picture is taken in a north-westward direction, see fig. 26 for the exact location (picture: S. Conrad, 2018, early spring 2018)

Fig. 29. Limes fort Iatrus, architectural plan of Period A (ca. 320–360) (after Iatrus-Krivina VI, plan, suppl. 3). The sharply jagged line marks the break-off edge as it was found at the beginning of the excavations in 1958. Due to the backfilling with excavated material, this brim is no longer visible in the terrain

5. METHODOLOGY OF ARCHAEOLOGICAL RESEARCH

5.1. The measurement system

Nadezhda Kecheva, Sven Conrad

Fig. 1. Map with the position of the fixed points at the sites 1–4 on the Tash Bair (figure by S. Conrad)

Fig. 2. Newly set anchor point No. 35 with marking (photo by S. Conrad)

Fig. 3. Fixed point No. 24 on the survey point, which is located on the burial mound site 14 (photo by S. Conrad)

Fig. 4. Measurement with Trimble M3 DR total station (photo by S. Conrad)

Fig. 5. Measurement with GNSS receivers Leica GS08 plus (photo by S. Conrad)

5.2. Field survey methods

Nadezhda Kecheva

Fig. 1. Tash Bair field survey project workflow in 2018 and 2019 (figure by N. Kecheva)

Fig. 2. Fieldwork activities. Team members' movement: a team member marked by a waypoint in a smartphone application at each team stop (1); and a team member recording data on a paper form (2) (figure and photos by N. Kecheva)

Fig. 3. Fieldwork activities. Placing small polygon vertices with the help of a total station (photo by L. Vagalinski)

Fig. 4. Definition of small polygons (grid in green) created by tracks (red lines) and waypoints (red dots) (left) and a polygon (the whole green rectangular) with the grid of small polygons (grid in cyan) (right) (figure by N. Kecheva)

Fig. 5. Fieldwalkers direction of movement, filled in paper form, spatial location and attributes of polygons and small polygons in GIS (figure by N. Kecheva)

Fig. 6. Paper form used for field recording of environmental and artefact data (scan by N. Kecheva)

Fig. 7. Total pick up paper form for field recording data for stones, pieces of daub, tiles and bricks (photo by L. Traykova)

Fig. 8. Total pick up paper form for post-processing of all pottery fragments (two pages). The same paper form was used for post-processing of collected diagnostic pottery fragments per polygon (photos by S. Conrad)

5.5. Sampling

Sven Conrad

Fig. 1. Sample flotation near the archaeological base in the village of Novgrad (photo by S. Conrad)

6. THE GEOPHYSICAL PROSPECTIONS. METHODS AND RESULTS

6.1. Geophysical prospections at sites 1 and 3–5

Burkart Ullrich, Nikolaas Noorda, Henning Zoellner

Fig. 1. Map with the magnetometer survey areas (blue) and the resistivity transects (red). Base maps: OpenTopoMap (figure by B. Ullrich, N. Noorda, H. Zoellner)

Fig. 2. The LEA-MAX system with 10 gradiometer probes and GNSS-positioning at site 4 in between the trees of the apricot plantation (photo by N. Noorda)

Fig. 3. Magnetometer survey data at site 1 (figure by B. Ullrich, N. Noorda, H. Zoellner)

Fig. 4. Interpretation of magnetic data at site 1 (figure by B. Ullrich, N. Noorda, H. Zoellner)

Fig. 5. Resistivity survey along transect at site 1 (figure by B. Ullrich, N. Noorda, H. Zoellner)

Fig. 6. Magnetometer survey data at sites 3 and 5 (figure by B. Ullrich, N. Noorda, H. Zoellner)

Fig. 7. Interpretation of magnetic data at sites 3 and 5 (figure by B. Ullrich, N. Noorda, H. Zoellner)

Fig. 8. Magnetometer survey data at site 4 (figure by B. Ullrich, N. Noorda, H. Zoellner)

Fig. 9. Interpretation of magnetic data at site 4 (figure by B. Ullrich, N. Noorda, H. Zoellner)

Fig. 10. Resistivity survey along transect at site 4 (figure by B. Ullrich, N. Noorda, H. Zoellner)

6.2. Geomagnetic survey at site 2

Petar Zidarov

Fig. 1. Tash Bair, site 2. Location and extent of magnetic surveys carried by J. Tirpák (2001, green) and P. Zidarov (2019, blue) on topographic map with original scale 1:5000 (source: Geoportal of the Ministry of Regional Development and Public Works – http://gis.mrrb.government.bg/)

Fig. 2. Novgrad, Tash Bair, site 2. Survey in progress in the areas to the S/SW from the field track (photo by S. Conrad)

Fig. 3. Tash Bair, site 2 (2019). Vertical magnetic gradient map. Instrument: caesium magnetometer G-858, grid density 0.30 × 0.30 m, dynamics -5/5nT, greyscale (surveyed and assembled by P. Zidarov)

Fig. 4. Tash Bair site 2. Magnetic map of the Slovak team on LiDAR DTM, scale 1:2000 (Bartík et al. 2000) (georeferenced and enhanced (increased contrast) by N. Kecheva and P. Zidarov)

Fig. 5. Tash Bair, site 2 (2019). Vertical magnetic gradient map. Instrument: caesium magnetometer G-858, grid density 0.30 × 0.30 m, dynamics -5/5nT, greyscale (surveyed and assembled by P. Zidarov)

Fig. 6. Tash Bair, site 2 (2019). Vertical magnetic gradient map and tentative interpretation. Instrument: caesium magnetometer G-858, grid density 0.30 × 0.30 m, dynamics -1/1nT, highest values (surveyed and assembled by P. Zidarov)

Fig. 7. Tash Bair, site 2 (2019). Tentative interpretation of vertical magnetic gradient map from 2019 on LiDAR DTM, scale 1:2000 (figure by P. Zidarov)

6.3. Two ER T profiles through the ditches on site 3
Gert Verstraeten

Fig. 1. Location of the two ERT profiles measured at Tash Bair in September 2018. The southern profile is ERT TB01, the northern one ERT TB02 (figure by S. Conrad)

Fig. 2. Inversion result of ERT profile TB01 (figure by G. Verstraeten)

Fig. 3. Inversion result of ERT profile TB02 (figure by G. Verstraeten)

7. THE INTENSIVE FIELD SURVEYS AT THE TASH BAIR LOCALITY AND IN ITS SURROUNDINGS
Nadezhda Kecheva, Lyudmil Vagalinski, Lyuba Traykova, Silva Sabkova

Fig. 1. Focus area in the lands of Novgrad and Karamanovo villages, Tsenovo municipality, Ruse district, and Vardim village, Svishtov municipality, Veliko Tarnovo district, between the left banks of Yantra and Studena Reka rivers, background map: hillshade derived from ASTER Global DEM version 2 (figure by N. Kecheva)

Fig. 2. Recorded archaeological sites in the region: in AIS AKB (red triangles), during the extensive field surveys in 1997–2001 (green squares), and a background map: hillshade derived from ASTER Global DEM version 2 (figure by N. Kecheva)

Fig. 3. Area covered during field surveys in 2018 (in white), in 2019 (in grey) and total pick up in 2018 (in purple), background maps: hillshade derived from ASTER Global DEM version 2 (larger area) and hillshade derived from airborne laser scanning data (smaller area) (figure by N. Kecheva)

Fig. 4. Area covered during field surveys in 2018 (in white), in 2019 (in grey), recorded archaeological site scatters (in black) and recorded archaeological site centres with field number sites IDs (from 1 to 38) – habitation sites – in red dots; mortuary sites – in yellow dots; road – in green dot. In the lower left corner, a pie chart shows the percentage of the recorded sites with different types of function and a background map: hillshade derived from airborne laser scanning data (figure by N. Kecheva)

Fig. 5. Concentrations of quantities of handmade and wheelmade pottery fragments, pieces of daub, tiles and bricks, and stones counted on the surface visualised by dot density quantitative descriptive statistics in GIS (1 dot equals 4 artefacts). Recorded archaeological site scatters (in black), recorded archaeological site centres with field number sites IDs (from 1 to 38) – habitation sites – in red dots; mortuary sites – in yellow dots; road – in green dot. In the upper part, a pie chart shows the percentage of the recorded site chronologies and a background map: hillshade derived from airborne laser scanning data (figure by N. Kecheva)

Fig. 6. Spatial distribution of Late Neolithic pottery fragments collected from polygons (in cyan). Area covered during field surveys in 2018 and 2019 (in thin black polygons), recorded archaeological site scatters (in thick black polygons), recorded archaeological site centres with field number sites IDs (from 1 to 38) – habitation sites – in red dots; mortuary sites – in yellow dots; road – in green dot, and a background map: hillshade derived from airborne laser scanning data (figure by N. Kecheva)

Fig. 7. Spatial distribution of Bronze and Bronze/Iron Age pottery fragments collected from polygons (in cyan). Area covered during field surveys in 2018 and 2019 (in thin black polygons), recorded archaeological site scatters (in thick black polygons), recorded archaeological site centres with field number sites IDs (from 1 to 38) – habitation sites – in red dots; mortuary sites – in yellow dots; road – in green dot, and a background map: hillshade derived from airborne laser scanning data (figure by N. Kecheva)

Fig. 8. Spatial distribution of Early Iron Age pottery fragments collected from polygons (in cyan). Area covered during field surveys in 2018 and 2019 (in thin black polygons), recorded archaeological site scatters (in thick black polygons), recorded archaeological site centres with field number sites IDs (from 1 to 38) – habitation sites – in red dots; mortuary sites – in yellow dots; road – in green dot, and a background map: hillshade derived from airborne laser scanning data (figure by N. Kecheva)

Fig. 9. Spatial distribution of Late Iron Age pottery fragments collected from polygons (in cyan). Area covered during field surveys in 2018 and 2019 (in thin black polygons), recorded archaeological site scatters (in thick black polygons), recorded archaeological site centres with field number sites IDs (from 1 to 38) – habitation sites – in red dots; mortuary sites – in yellow dots; road – in green dot, and a background map: hillshade derived from airborne laser scanning data (figure by N. Kecheva)

Fig. 10. Spatial distribution of Roman pottery fragments collected from polygons (in cyan). Area covered during field surveys in 2018 and 2019 (in thin black polygons), recorded archaeological site scatters (in thick black polygons), recorded archaeological site centres with field number sites IDs (from 1 to 38) – habitation sites – in

red dots; mortuary sites – in yellow dots; road – in green dot, and a background map: hillshade derived from airborne laser scanning data (figure by N. Kecheva)

Fig. 11. Spatial distribution of Late Antique pottery fragments collected from polygons (in cyan). Area covered during field surveys in 2018 and 2019 (in thin black polygons), recorded archaeological site scatters (in thick black polygons), recorded archaeological site centres with field number sites IDs (from 1 to 38) – habitation sites – in red dots; mortuary sites – in yellow dots; road – in green dot, and a background map: hillshade derived from airborne laser scanning data (figure by N. Kecheva)

Fig. 12. Spatial distribution of Early Medieval pottery fragments collected from polygons (in cyan). Area covered during field surveys in 2018 and 2019 (in thin black polygons), recorded archaeological site scatters (in thick black polygons), recorded archaeological site centres with field number sites IDs (from 1 to 38) – habitation sites – in red dots; mortuary sites – in yellow dots; road – in green dot, and a background map: hillshade derived from airborne laser scanning data (figure by N. Kecheva)

Fig. 13. Spatial distribution of recorded burial mounds (in yellow dots) divided into three mound necropolises (in purple ellipses). Area covered during field surveys in 2018 and 2019 (in thin black polygons), recorded archaeological site scatters (in thick black polygons), recorded archaeological site centres with field number sites IDs (from 1 to 38) – habitation sites – in red dots; mortuary sites – in yellow dots; road – in green dot, and a background map: soviet headquarters topographic maps from the 1980s in scale 1:50 000 (figure by N. Kecheva)

Fig. 14. Part of the possible Roman road between Novae and Iatrus. 1. Aerial photos from 1944–1945 with visible road route; 2. Aerial photos from 1970 with visible road route; 3 Airborne laser scanning data with visible road route; 4. Satellite imagery from Google Earth from 4th of March 2012 with visible road route (figure by N. Kecheva)

Fig. 15. Total pick up field survey conducted on part of site 1 area in 2018 (in purple) and in 2001 (in yellow), and a background map: hillshade derived from airborne laser scanning data (figure by N. Kecheva)

Fig. 16. Total pick up data from 2018 visualised in GIS. Pie charts showing the spatial distribution of all collected and counted pieces of daub and tiles (left map). Pie charts showing the spatial distribution of all collected and post-processed pottery fragments from the Late Neolithic, Early Iron Age, Late Iron Age, Roman period, Late Antiquity and Early Middle Ages (right map), and a background map: geophysical survey data from 2018 (figure by N. Kecheva)

Fig. 17. Total pick up data from 2018 visualised in GIS. 1. Pie charts showing the spatial distribution of all collected and post-processed Late Neolithic pottery fragments. 2. Pie charts showing the spatial distribution of all collected and post-processed Early Iron Age pottery fragments. 3. Pie charts showing the spatial distribution of all collected and post-processed Late Iron Age pottery fragments. 4. Pie charts showing the spatial distribution of all collected and post-processed Roman pottery fragments. 5. Pie charts showing the spatial distribution of all collected and post-processed Late Antique pottery fragments. 6. Pie charts showing the spatial distribution of all collected and post-processed Early Medieval pottery fragments, and a background map: geophysical survey data from 2018 (figure by N. Kecheva)

8. ARCHAEOLOGICAL EXCAVATIONS

8.1. The Late Neolithic ditches at site 1 (trench 1.2)

Raiko Krauß, Sven Conrad

Fig. 1. Site 1 (cutout). Map of geomagnetic anomalies (see contributions by B. Ullrich et al., fig. 3) with the excavation trenches (figure by S. Conrad)

Fig. 2. Trench 1.2. Planum 2 at niv. 29.46 m with feature 1.2.5 (view from the west) (figure by Lea Valcov)

Fig. 3. Trench 1.2. Planum 3 at niv. 29.30 m with feature 1.2.5 (view from the the west) (figure by Lea Valcov)

Fig. 4. Trench 1.2. Feature 1.2.6, profile (view from the north) (figure by S. Conrad)

Fig. 5. Trench 1.2. Part of the eastern profile. Early Medieval ditch 1.2.5 which cuts the prehistoric ditch 1.2.6 (figure by S. Conrad)

Fig. 6. Trench 1.2, planum 4. Part of ft. 1.2.4 (view from the west). In the eastern corner (up left), part of the separating loess stripe and a very small section of the parallel ditch 1.2.7/8 (figure by S. Conrad)

Fig. 7. Trench 1.2. Reconstructed overall plan of the features (summarised from planum 3 and 4) (figure by S. Conrad)

Fig. 8. Trench 1.2. Overall plan projected onto the geomagnetic plan (figure by S. Conrad)

Fig. 9. Trench 1.2. W- and N-profile, obtained from SfM photo combination (M. Offermann). Legend: 1 – colluvium; 2 – shifted rampart(?); 3 – ancient surface; 4 – earthenwall(?); 5 – disturbed area; 6 – Late

Neolithic ditch (feature 1.2.4); 7 – Late Neolithic ditch (feature 1.2.7/8); 8 – Early Medieval ditch (feature 1.2.5) (interpretation by R. Krauß and S. Conrad)

8.2. Bronze Age

8.2.1. The inner ditch of the enclosure in trench 3.6

Lyudmil Vagalinski, Lyuba Traykova, Nadezhda Kecheva

Fig. 1. Site 3, geophysical survey results in 2018 (cf. the contributions by B. Ullrich et al., chapter 6.1) and location of the trenches in 2018 (figure by N. Kecheva)

Fig. 2. The ditch in trench 3.6, level ▼58.32 m (photo by S. Conrad)

Fig. 3. The ditch in trench 3.6, level ▼58.03 m (photo by L. Vagalinski)

Fig. 4. The bottom of the ditch in trench 3.6 (photo by L. Vagalinski)

Fig. 5. The pit 3.6.1 (photo by L. Vagalinski)

Fig. 6. The pit 3.6.1, SE quarter (photo by L. Traykova)

Fig. 7. The pit 3.6.1, animal bone at the bottom (photo by L. Traykova)

Fig. 8. The pit 3.6.1, bottom (photo by L. Traykova)

Fig. 9. The pit 3.6.1 in the northern cross-section of the trench No. 3.6 (photo by L. Vagalinski)

Fig. 10. Site 3. Trench 3.6, northern section: 1 – Sterile: yellowish-brown loess; 2 – Ditch – phase 1; 3 – Burnt strip and phase 1 ditch filling: loess and humus soil with scattered handmade pottery fragments dated to the Bronze Age, scattered charcoals, pieces of burnt clay; 3a – A strip of burnt clay situated at a distance of 1.50 m from the north section: it marks the phase 1 ditch bottom; 4 – Stone cladding of the phase 2 ditch bottom: crushed stones/limestone, the larger slab-shaped ones are arranged at the edges of the bottom of the ditch, following its curve; in the middle between these two faces two large horizontal slab-shaped stones and many smaller stones are placed. The bottom of the ditch is narrowed in this way, but we cannot distinguish the contour of the ditch in height during phase 2; 5 – Natural filling of the ditch after its usage: dark brown loess full of humus soil with scattered charcoals, handmade pottery fragments from BA, EIA, and LIA; small crushed stones; animal bones; scattered pieces of burnt clay; 6 – Pit, which contains: 10–15 undiagnostic handmade pottery fragments dated to the Bronze Age, a large animal bone, a large crushed stone, dark brown layer loess full of humus soil; 7 – Probable ground level of (6) and of the ditch; 8 – Strongly full of humus soil, dark brown, a loose layer which contained: handmade pottery fragments from BA, wheelmade pottery fragments from LIA and Roman period, tile fragments from the Hellenistic period; animal bones; small crushed stones; a large amount of rotten vegetation. The layer had been deposited on the slope descending from north to south. It had been strongly disturbed by bioturbation. Bioturbation was also recorded in (5) but in less quantity; 9 – Ploughzone layer, light brown loess full of humus soil, strongly disturbed by vegetation roots and bioturbations. It contained: pottery fragments from EBA, LIA, Antiquity and modern age; modern iron hinge; 10 – Bioturbation (drawing and interpretation by L. Vagalinski, L. Traykova, N. Kecheva)

Fig. 11. Site near Pietrele, Romania (after Hansen et al. 2017, 98, Abb. 126)

Fig. 12. Site near Bikovo village (after Hristova 2018, 348, fig. 1)

Fig. 13. Site near Polski Gradets village (after Ников, Георгиева 2018, 79, обр. 1)

Fig. 14. Site near Polski Gradets village (after Ников, Георгиева 2019, 86, обр. 1)

8.2.2. The structure in trenches 3.2–5

Lyudmil Vagalinski, Lyuba Traykova

Fig. 1. Site 3, geophysical survey results in 2018 (cf. the contributions by B. Ullrich et al., chapter 6.1) and location of the trenches in 2018 (figure by N. Kecheva)

Fig. 2. Trench 3.2, northeast cross-section (photo by L. Vagalinski)

Fig. 3. Trench 3.3, level ▼63.38 m (photo by S. Conrad)

Fig. 4. Site 3. Trench 3.2, northwestern and northeastern sections: 1 – Sterile loess, light brown in colour; 2 – Slipped down the slope burnt remains of a Bronze Age dwelling: scattered pieces of burnt wood (charcoals); crushed stones in different sizes mainly recorded on the ground level; few handmade pottery fragments; pieces of burnt mudbrick as well as unburnt/decomposed mudbrick; pieces of burnt floor daub with traces of wattle fence; many holes resulted from bioturbation some of which mixed artefacts from layer (2) to layer (1). No animal bones were recorded. Brown layer. There is humus soil in it. 3 – Loose, humus soil, ploughzone, dark brown (drawing and interpretation by L. Vagalinski, L. Traykova)

Fig. 5. Trenches 3.2 and 3.3, northeast cross-section (photo by S. Conrad)

8.2.3. The pit in trench 3.1

Sven Conrad, Raiko Kraus

Fig. 1. Site 3. View from the northeast (SfM model by P. Kluge and M. Offermann)

Fig. 2. Site 3. Geomagnetic map with the boundaries of the trenches (figure by S. Conrad)

Fig. 3. Feature 3.1.1, planum 1. Vertical picture taken from an UAV (figure by P. Kluge)

Fig. 4. Trench 3.1, planum 1. Overall plan of the pit 3.1.1 (with completion). The numbered markings indicate the measured finds of larger ceramic pieces in the course of the excavation (see chapter 9.1, table 9); the unnumbered markings relate to animal bone finds (figure by S. Conrad)

Fig. 5. Feature 3.1.1, quadr. A. Orthophoto of planum 2 (niv. 61.21) obtained from a SfM model (figure by M. Offermann)

Fig. 6. Feature 3.1.1, quadr. A. Planum 2 (niv. 61.21) with socketed pottery fragments and bones of layer b. Detail (from northeast) (photo by M. Offermann)

Fig. 7. Feature 3.1.1. Negative of the pit, view from the east (photo by M. Offermann)

Fig. 8. Feature 3.1.1, profile between quadr. A and B. View from the east (photo by S. Conrad)

Fig. 9. Feature 3.1.1., profile between quadr. A and B (redrawing by S. Conrad after original drawing by J. Becher). a – pale yellowish grey, yellowish spotted; b – pale grey, ochre grey mixed; with charcoal, ash, bones; c – light yellowish-grey, slightly denser than a; d – (lateral fall) yellowish pale grey; e – sterile loess, with animal dens

Fig. 10. Feature 3.1.1., north profile at the trench boundary (view from the south) (photo by M. Offermann)

8.3. Late Iron Age

8.3.1. The Late Iron Age ditch in trench 1.1

Lyudmil Vagalinski, Lyuba Traykova, Nadezhda Kecheva

Fig. 1. Site 1, geophysical survey results in 2018 (cf. the contributions by B. Ullrich et al., chapter 6.1) and location of the trenches in 2019 (figure by N. Kecheva)

Fig. 2. Trench 1.1-E, level ▼26.76 m (photo by Lea Valcov)

Fig. 3. Trench 1.1-E, NE corner, level ▼26.76 m (photo by S. Conrad)

Fig. 4. Trench 1.1-E, NE corner, level ▼26.67 m (photo by Lea Valcov)

Fig. 5. Trench 1.1-E, NE corner, level ▼26.60 m (photo by Lea Valcov)

Fig. 6. Trench 1.1-E, NE corner, level ▼26.00 m (photo by Lea Valcov)

Fig. 7. Trench 1.1-W, level ▼27.21 m (photo by Lea Valcov)

Fig. 8. Trench 1.1-W, level ▼26.78 m (photo by Lea Valcov)

Fig. 9. Plan of the ditches in trench No. 1.1 (drawing by S. Conrad, adapted by L. Traykova)

Fig. 10. Site 1. Trench 1.1-W, western cross-section: 1 – Loose and full of humus soil, greyish-brown layer – ploughzone. It contains pottery fragments. Pits of unrooted trees from an orchard are visible; 2 – Light brown loess, very dense layer, formed by erosion; it contained small pottery fragments, single charcoals, small pieces of burned clay, single small stones; 3 – Dark grey full of humus layer, but not as much as layer No. 1. It contained small pottery fragments, single small stones, small and scattered pieces of burned clay, lots of animal holes; 6 – Sterile yellowish-brown loess; 7 – Fill of earlier ditch with direction E–W, cut by the Early Medieval ditch. It contained ash strips, Late Neolithic pottery fragments, yellowish-brown loess lumps fallen from the ditch sides, single small stones; 9 – Early Medieval surface from which the ditch N-S was dug. It is almost the same as the surface of the other ditch probably because of the constant significant erosion (drawing and interpretation by L. Vagalinski, L. Traykova)

Fig. 11. Site 1. Trench 1.1-E, eastern cross-section: 1 – Loose and full of humus soil, greyish-brown layer – ploughzone. It contains pottery fragments. Pits of unrooted trees from an orchard are visible; 2 – Light brown loess, very dense layer, formed by erosion; it contained small pottery fragments, single charcoals, small pieces of burned clay, single small stones; 3 – Dark grey full of humus layer, but not as much as layer No. 1. It contained small pottery fragments, single small stones, small and scattered pieces of burned clay, lots of animal holes; 6 – Sterile yellowish-brown loess; 7 – Fill of earlier ditch with direction E–W, cut by the Early Medieval ditch. It contained ash strips, Late Neolithic pottery fragments, yellowish-brown loess lumps fallen from the ditch sides, single small stones, one flint; 8 – modern pit, loose and humus greyish-brown soil; 9 – Early Medieval surface from which the ditch N-S was dug. It is almost the same as the surface of the other ditch probably because of the constant significant erosion (drawing and interpretation by L. Vagalinski, L. Traykova)

Fig. 12. Site 1. Trench 1.1, northern cross-section: 1 – loose and full of humus soil, greyish-brown layer – ploughzone. It contains pottery fragments. Pits of unrooted trees from an orchard are visible; 2 – Light brown

loess, very dense layer, formed by erosion; it contained small pottery fragments, single charcoals, small pieces of burned clay, single small stones; 3 – Dark grey full of humus layer, but not as much as layer No. 1. It contained small pottery fragments, single small stones, small and scattered pieces of burned clay, lots of animal holes; 4 – Fill of the Early Medieval ditch, brownish-black dense layer; it contained pottery fragments, medium- to small-size stones, single animal bones, single lumps of loess, scattered charcoals, single small pieces of burned clay, single animal holes. The artefacts cluster in the lower part of the ditch, close to the bottom, pottery fragments and stones are larger than the ones in the upper layers. In the northern section of trench No. 1.1-W there were strips of fallen loess lumps from the eastern side of the Early Medieval ditch; 6 – Sterile yellowish-brown loess; 7 – Fill of earlier ditch with direction E–W, cut by the Early Medieval ditch. It contained ash strips, Late Neolithic pottery fragments, yellowish-brown loess lumps fallen from the ditch sides, single small stones, one flint; 9 – Early Medieval surface from which the ditch N-S was dug. It is almost the same as the surface of the other ditch probably because of the constant significant erosion (drawing and interpretation by L. Vagalinski, L. Traykova)

Fig. 13. Mound 39 near Sveshtari village, Isperih municipality, eastern profile of S9 with the ditch F91 (after Гергова et al. 2018, 124, обр. 2)

Fig. 14. Mound 39 near Sveshtari village, Isperih municipality, general plan of the excavated areas of the central part of sanctuary (after Гергова et al. 2020, 500, обр. 2)

Fig. 15. Site near Knyazhevo village, Topolovgrad municipality, the ditch at the western part of the site (Sq. A11) – VI mechanical layer (after Агре, Дичев 2017, 166, обр. 1)

Fig. 16. Sketch of the fortress Kale Karaach near Brestak village, Silistra district (after K. Škorpil cited in Торбатов 2010, 155, обр. 1.б)

Fig. 17. Plan of the earthen fortification in the locality Domuz azman near Brestnitsa village, Dobrich district (after Торбатов 2010, 158, обр. 4.а)

8.3.2. The Early Roman pits 5.1.2 and 5.1.6

Sven Conrad

Fig. 1. View from site 3 in south-easterly direction on site 5 with the trench 5.1/2 under work (photo by S. Conrad)

Fig. 2. Position of the trench 5.1/2 in relationship to the geomagnetically mapped area on site (figure by S. Conrad)

Fig. 3. Planum 1 of trench 5.1/2. View from the north (photo by S. Conrad)

Fig. 4. Excavation map of trench 5.1/2 (without excluded features) (figure by S. Conrad)

Fig. 5. Feature 5.1.2. Profile (view from the north) (photo by S. Conrad)

Fig. 6. Feature 5.1.2. Redrawing of the profile (redrawing by S. Conrad after original drawing by J. Becher); a – pale brown; loamy weakly humous; pieces of daub and charcoal. b – brown, with some yellowish spots; loamy, mixed with humous; pieces of daub. c – dark grey, spotty; loamy-sandy, humous. d – yellowish, with grey-brown spots; loamy (native; alluvial). e – brown; loamy-sandy (native; alluvial)

Fig. 7. Feature 5.1.6. Profile (view from the northwest) (photo by S. Conrad)

Fig. 8. Feature 5.1.6. Redrawing of the profile (redrawing by S. Conrad after original drawing by J. Becher); a – dark greyish brown; humous, loamy (arable layer). b – greyish brown, slightly pale and yellowish mixed; loamy; some daub pieces and small spots of limestone. c – greyish brown; loamy; some daub pieces and very few small spots of limestone. d – dark brown; loamy humous. e – yellowish, with grey-brown spots; loamy (native; alluvial)

8.3.3. The grave in pit 5.1.5

Lyudmil Vagalinski, Lyuba Traykova, Nadezhda Kecheva

Fig. 1. Site 5, geophysical survey results in 2018 (cf. the contributions by B. Ullrich et al., chapter 6.1) and location of the trench 5.1 in 2018 (figure by N. Kecheva)

Fig. 2. Plan of the pits in trench 5.1 (drawing by S. Conrad, adapted by L. Traykova)

Fig. 3. Trench 5.1, level ▼20.68 m (photo by S. Conrad)

Fig. 4. The pit 5.1.5, level ▼19.75 m (photo by N. Kecheva)

Fig. 5. Extended area of the pit 5.1.5 (photo by N. Kecheva)

Fig. 6. Northeastern quarter, extended area of the pit 5.1.5, level ▼19.89 m (photo by N. Kecheva)

Fig. 7. Northeastern quarter, extended area of the pit 5.1.5, level ▼19.69 m (photo by N. Kecheva)

Fig. 8. Northern half, extended area of the pit 5.1.5 (photo by N. Kecheva)

Fig. 9. Site 5. Trench 5.1, southern section: 1 – Light brown clay, sterile, with single white inclusions (soft stones with sizes under 1 × 1 cm) and black vertical strips from vegetation roots. A lot of bioturbations; 2 – Light brown clay, probable river deposit (it contains shells from mussels and small snails), with a large number of white inclusions some of which mark concentrations; black vertical strips from vegetation roots; separate pieces of burnt clay (with sizes under 0.5 × 0.5 cm). A lot of bioturbations; 3 – Pit 5.1.5, brown colour; it contained single handmade pottery fragments, small pieces of burnt clay (with sizes under 0.5 × 0.5 cm), bones. A lot of bioturbations; 4 – A recording level of pit 5.1.5; 5 – Dark brown layer, ploughzone, it contains: handmade and wheelmade pottery fragments; animal bones; 5a – Light brown dense layer that contains household Roman pottery fragments dated to the period of the second half of 1st–2nd c. The same fragments were found in layer (5) (drawing and interpretation by L. Traykova, N. Kecheva, L. Vagalinski)

Fig. 10. Amphorae type Hr II-1 after Borislavova 2018 (photo by L. Vagalinski)

Fig. 11. Trench 5.2, southern half of the pit 5.1.5 (photo by L. Traykova)

Fig. 12. Trench 5.2, southern half of the pit 5.1.5, level ▼20.56 m (photo by L. Traykova)

Fig. 13. The pit 5.1.5 in trenches 5.1 and 5.2 (photo by L. Traykova)

Fig. 14. Pit 5.1.5, the human skull (photo by N. Kecheva)

Fig. 15. Pit 5.1.5, the human skeleton under the pottery (photo by N. Kecheva)

Fig. 16. Pit 5.1.5, the human skeleton (photo by N. Kecheva)

Fig. 17. Pit 5.1.5, the human skeleton before and after removing the pottery (drawing by L. Traykova)

Fig. 18. Female burial on the pottery kiln's grate of pottery kiln near Krivina village, Tsenovo municipality (after Vagalinski 2011a, 222, fig. 4)

Fig. 19. Pit with a human skeleton (C6) near Gorni Dabnik village, Dolni Dabnik municipality (after Тонкова, Маджаров 2020, 516, обр. 2. 4)

8.4. The Early Medieval fortifications in trenches 1.1 and 1.2

Lyudmil Vagalinski, Lyuba Traykova, Nadezhda Kecheva

Fig. 1. Site 1, geophysical survey results in 2018 (cf. the contributions by B. Ullrich et al., chapter 6.1) and location of the trenches in 2019 (figure by N. Kecheva)

Fig. 2. Trench 1.1-E, level ▼26.76 m (photo by Lea Valcov)

Fig. 3. Trench 1.1-E, level ▼26.44 m (photo by Lea Valcov)

Fig. 4. Trench 1.1-E, bottom of the ditch in NW corner level ▼24.36 m (photo by L. Vagalinski)

Fig. 5. Trench 1.1-E, bottom of the ditch in NW corner level ▼24.36 m (photo by S. Conrad)

Fig. 6. Trench 1.1-W, level ▼26.78 m (photo by Lea Valcov)

Fig. 7. Trench 1.1-W, level ▼26.71 m (photo by S. Conrad)

Fig. 8. Trench 1.1-W, level ▼26.66 m (photo by S. Conrad)

Fig. 9. Trench 1.1-W, level ▼26.58 m (photo by Lea Valcov)

Fig. 10. Trench 1.1-W, bottom of the ditch in NE corner level ▼24.35 m (photo by L. Vagalinski)

Fig. 11. Plan of the ditches in trench 1.1 (drawing by S. Conrad, adapted by L. Traykova)

Fig. 12. Site 1. Trench 1.1, northern section: 1 – Loose and full of humus soil, greyish-brown layer – ploughzone. It contained pottery fragments. Pits of unrooted trees from an orchard were visible; 2 – Light brown loess, very dense layer, formed by erosion; it contained small pottery fragments, single charcoals, small pieces of burnt clay, single small stones; 3 – Dark grey full of humus layer, but not as much as layer No. 1. It contained small pottery fragments, single small stones, small and scattered pieces of burnt clay, lots of bioturbations; 4 – Fill of the Early Medieval ditch, brownish-black dense layer; it contained pottery fragments, medium- to small-size stones, single animal bones, single lumps of loess, scattered charcoals, single small pieces of burnt clay, single bioturbations. The artefacts cluster in the lower part of the ditch, close to the bottom, pottery fragments and stones were larger than those in the upper layers. In the northern section of trench No. 1.1/W there were strips of fallen loess lumps from the eastern side of the Early Medieval ditch; 6 – Sterile yellowish-brown loess; 7 – The fill of the earlier ditch with direction E–W, cut by the Early Medieval ditch. It contained ash strips, Late Neolithic pottery fragments, yellowish-brown loess lumps fallen from the ditch sides, single small stones, one flint; 9 – Early Medieval surface from which the ditch N-S was dug. It is almost the same as the surface of the other ditch probably because of the constant significant erosion (drawing and interpretation by L. Vagalinski, L. Traykova)

Fig. 13. Site 1. Trench 1.1, southern section: 1 – Loose and full of humus soil, greyish-brown layer – ploughzone. It contained pottery fragments. Pits of unrooted trees from an orchard were visible; 2 – Light brown loess, very dense layer, formed by erosion; it contained small pottery fragments, single charcoals, small pieces of

burnt clay, single small stones; 3 – Dark grey full of humus layer, but not as much as layer No. 1. It contained small pottery fragments, single small stones, small and scattered pieces of burnt clay, lots of bioturbations; 4 – The fill of the Early Medieval ditch, brownish-black dense layer; it contained pottery fragments, medium- to small-size stones, single animal bones, single lumps of loess, scattered charcoals, single small pieces of burnt clay, single bioturbations. The artefacts clustered in the lower part of the ditch, close to the bottom, pottery fragments and stones were larger than those in the upper layers. In the northern section of trench No. 1.1/W there were strips of fallen loess lumps from the eastern side of the Early Medieval ditch; 6 – Sterile yellowish-brown loess; 9 – Early Medieval surface from which the ditch N-S was dug (drawing and interpretation by L. Vagalinski, L. Traykova)

Fig. 14. Site 1. Trench 1.1-E, western section: 1 – Loose and full of humus soil, greyish-brown layer – ploughzone. It contained pottery fragments. Pits of unrooted trees from an orchard were visible; 2 – Light brown loess, very dense layer, formed by erosion; it contained small pottery fragments, single charcoals, small pieces of burnt clay, single small stones; 3 – Dark grey full of humus layer, but not as much as layer No. 1. It contained small pottery fragments, single small stones, small and scattered pieces of burnt clay, lots of bioturbations; 4 – The fill of the Early Medieval ditch, brownish-black dense layer; it contained pottery fragments, medium- to small-size stones, single animal bones, single lumps of loess, scattered charcoals, single small pieces of burnt clay, single bioturbations. The artefacts clustered in the lower part of the ditch, close to the bottom, pottery fragments and stones were larger than those in the upper layers. In the northern section of trench No. 1.1/W there were strips of fallen loess lumps from the eastern side of the Early Medieval ditch; 5 – A passage/path through the ditch – sterile yellowish-brown loess; 6 – Sterile yellowish-brown loess; 9 – Early Medieval surface from which the ditch N-S was dug (drawing and interpretation by L. Vagalinski, L. Traykova)

Fig. 15. Site 1. Trench 1.1-W, eastern section: 1 – Loose and full of humus soil, greyish-brown layer – ploughzone. It contained pottery fragments. Pits of unrooted trees from an orchard were visible; 2 – Light brown loess, very dense layer, formed by erosion; it contained small pottery fragments, single charcoals, small pieces of burnt clay, single small stones; 3 – Dark grey full of humus layer, but not as much as layer No. 1. It contained small pottery fragments, single small stones, small and scattered pieces of burnt clay, lots of bioturbations; 4 – The fill of the Early Medieval ditch, brownish-black dense layer; it contained pottery fragments, medium- to small-size stones, single animal bones, single lumps of loess, scattered charcoals, single small pieces of burnt clay, single bioturbations. The artefacts clustered in the lower part of the ditch, close to the bottom, pottery fragments and stones are larger than those in the upper layers. In the northern section of trench No. 1.1/W there were strips of fallen loess lumps from the eastern side of the Early Medieval ditch; 5 – A passage/path through the ditch – sterile yellowish-brown loess; 6 – Sterile yellowish-brown loess; 9 – Early Medieval surface from which the ditch N-S was dug (drawing and interpretation by L. Vagalinski, L. Traykova)

Fig. 16. Trench 1.2, level ▼29.46 m (photo by S. Conrad)

Fig. 17. Plan of the features in trench 1.2 (drawing by S. Conrad, adapted by L. Traykova)

Fig. 18. Trench 1.2, level ▼29.30 m (photo by Lea Valcov)

Fig. 19. Trench 1.2, the bottom of the ditch 1.2.5, level ▼26.94 m (photo by S. Conrad)

Fig. 20. Trench 1.2, western cross-section and the bottom of the ditch 1.2.5, level ▼26.94 m (photo by L. Vagalinski)

Fig. 21. Trench 1.2, eastern cross-section and the bottom of the ditch 1.2.5, level ▼26.94 m (photo by L. Vagalinski)

Fig. 22. Site 1. Trench 1.2, eastern section: 1 – Loose and full of humus soil, greyish-brown layer – ploughzone. It contained pottery fragments. Pits of unrooted trees from an orchard were visible; 2 – Light brown loess, very dense layer, formed by erosion; it contained small pottery fragments, single charcoals, small pieces of burnt clay, single small stones; 3 – Dark grey full of humus layer, but not as much as layer No. 1. It contained small pottery fragments, single small stones, small and scattered pieces of burnt clay, lots of bioturbations; 4 – The ditch was older than the Early Medieval ditch which it was cut by it, light brown dense layer. It contained Late Neolithic pottery fragments, animal bones, scattered charcoals, single pieces of yellowish-brown loess fallen from the sides of the ditch, single pieces of burnt clay, single traces of bioturbation; 4a – Layer/fill of the older ditch, light brown layer. It contained Late Neolithic pottery fragments, loess pieces fallen from the sides of the ditch, scattered charcoals, pieces of burnt clay. Probably (4) and (4a) are part of the same double ditch; 5 – Early Medieval ditch, greyish-brown dense filling. It contained pottery fragments, animal bones, single charcoals, single pieces of yellowish-brown loess fallen from the sides of the ditch; 6 – Sterile yellowish-brown loess (drawing and interpretation by L. Vagalinski, L. Traykova)

Fig. 23. Site 1. Trench 1.2, western section: 1 – Loose and full of humus soil, greyish-brown layer – ploughzone. It contained pottery fragments. Pits of unrooted trees from an orchard were visible; 2 – Light brown loess, very dense layer, formed by erosion; it contained small pottery fragments, single charcoals, small pieces of burnt clay, single small stones; 3 – Dark grey full of humus layer, but not as much as layer No. 1. It contained small pottery fragments, single small stones, small and scattered pieces of burnt clay, lots of bioturbations; 4a – Layer/fill of the older ditch, light brown layer. It contained Late Neolithic pottery fragments, loess pieces fallen from the sides of the ditch, scattered charcoals, pieces of burnt clay. 5 – Early Medieval ditch, greyish-brown dense filling. It contained pottery fragments, animal bones, single charcoals, single pieces of yellowish-brown loess fallen from the sides of the ditch; 6 – Sterile yellowish-brown loess (drawing and interpretation by L. Vagalinski, L. Traykova)

9. POTTERY AND SMALL FINDS

9.1. The pottery finds (with catalogue)

9.1.1. Prehistoric pottery

Raiko Krauß

Fig. 1. Chronology of the prehistoric periods in the Eastern Balkan region (by R. Krauß)

Fig. 2. Gauss Monte Carlo Wiggle Matching of stratified radiocarbon samples from Bronze Age features at site 3 (by R. Krauß)

9.1.2. Late Iron Age to Medieval pottery

Sven Conrad

Fig. 3. Chronological framework of the historical periods of the Eastern Balkans and the adjacent regions (by S. Conrad)

9.1.3. Pottery statistics from the excavations of different features

Sven Conrad, Raiko Krauß

Fig. 4. Trench 1.1-W/E, north profile (combined), and trench 1.1-W, west profile. Legend: 1a – Shifted rampart (feature 1.1.5); 1b – Shifted rampart (features 1.1.1; 1.1.5); 2 – Gateway of the Early Medieval fortress; 3 – Ancient surface; 4 – Gateway surface; 5 – Modern colluvium; 6 – Post-Medieval surface with colluvium; 7a – Late Iron Age ditch (feature 1.1.15); 7b – Late Iron Age ditch (feature 1.1.6); 8a – Early Medieval ditch (feature 1.1.13); 8b – Early Medieval ditch (feature 1.1.7) (by the authors using an orthophoto obtained from a SfM model by M. Offermann)

Fig. 5. Trench 1.1-W/E, planum 3 (niv. 26.78–26.76 m). Interpretation of features: 1.1.1, 1.1.5 – eroded material of the secondarily shifted Early Medieval rampart; 1.1.2, 1.1.5 – top layer of the filling of the Early Medieval ditch; 1.1.4 – colluvium; 1.1.6 – earlier ditch (Late Iron Age) (by S. Conrad using an orthophoto obtained from a SfM model by M. Offermann)

Fig. 6. Trench 1.1-W/E, planum 4 (niv. 26.58–26.53 m). Interpretation of features: 1.1.7/13 and 1.1.8/14 – ditch heads at the doorway of the medieval fortification; 1.1.6/15 – earlier ditch (Late Iron Age); 1.1.9 – colluvium (transition to the sterile loess); 1.1.11 – concentration of finds in the doorway of the Early Medieval fortification (partially sunken in the sterile loess) (by S. Conrad using an orthophoto obtained from a SfM model by M. Offermann)

Fig. 7. Trench 1.1-W/E, planum 5 (26.38–26.44 m). Interpretation of features: 1.1.7/13 and 1.1.8/14 – ditch heads at the doorway of the Early Medieval fortification; 1.1.6/15 – earlier ditch (Late Iron Age); 1.1.12 – pit (not dated); 1.1.16 – post hole (?; Early Medieval); 1.1.17 – pit (not dated) (by S. Conrad using an orthophoto obtained from a SfM model by M. Offermann)

Fig. 8. Feature 1.1.15. Pottery of the Late Iron Age (selection) (by S. Conrad)

Fig. 9. Feature 1.1.7/13. Early Medieval pottery (niv. 25.17–24.56 m) (by S. Conrad)

Fig. 10. Feature 1.1.7/13. Early Medieval pottery (niv. 27.35–25.17 m) (by S. Conrad)

Fig. 11. Feature 1.2.5, north profile of the longitudinal section. Orthophoto obtained from a SfM model (by M. Offermann)

Fig. 12. Feature 1.2.5. Early Medieval pottery (niv. 27.35–26.94 m) (by S. Conrad)

Fig. 13. Feature 1.2.5. Early Medieval pottery (niv. 28.89–27.49 m) (by S. Conrad)

Fig. 14. Trench 3.6, north profile. Stratigraphical distribution of the pottery finds (by the authors using an orthophoto obtained from a SfM model by M. Offermann). Legend: 1 – (Prehistory) / Bronze Age; 2 –

(Prehistory) / Middle Bronze Age / Bronze Age; 3 – (Prehistory); 4 – (Prehistory) / Bronze Age / Late Iron Age; 5 – (Prehistory) / Bronze Age / Early Iron Age / Late Iron Age; 6 – (Prehistory) / Late Iron Age; 7 – (Prehistory) / Early Iron Age / Late Iron Age; 8 – Late Iron Age; 9 – (Prehistory); 10 – (Prehistory) / Late Bronze Age; 11 – (Prehistory) / Middle Bronze Age / Bronze Age / Late Iron Age / Late Roman period; 12 – (Prehistory) / Middle Bronze Age / Late Bronze Age / Late Iron Age /Roman period / Late Roman period; 13 – (Prehistory) / Middle Bronze Age / Late Iron Age / Late Roman period; 14 – (Prehistory) / Middle Bronze Age / Late Bronze Age / Late Iron Age / Late Roman period; 15 – Pit 3.1.1: (Prehistory) / Middle Bronze Age / Bronze Age

Fig. 15. Trench 3.6. Late Roman pottery sherds found in the upper filling of the ditch (selection) (by S. Conrad)

Fig. 16. Trench 3.6. Late Roman roof tile fragments from the upper filling of ditch (by S. Conrad)

Fig. 17. Feature 3.2.1, northeast profile. Orthophoto obtained from a SfM model (by M. Offermann)

Fig. 18. Feature 3.2.1, northeast profile. Drawing (by S. Conrad and S. Roller). a – plough layer; greyish brown, humous. b – light grey, yellowish mixed, slightly humous, homogeneous; some charcoal and burnt clay pieces; single small stones. c – like b, but bigger pieces of burnt clay (house masonry) and wood; small, middle and large stones. d – natural ground (yellowish loess)

Fig. 19. Feature 5.1.2. Pottery (niv. 20.68–20.28 m) (by S. Conrad)

Fig. 20. Feature 5.1.5 (trench 5.2). Pottery from the filling of the pit (selection) (niv. 20.56–20.49 m) (by S. Conrad)

Fig. 21. Feature 5.1.5 (trench 5.1). Pottery from the filling of the pit (selection) (niv. 20.70–20.56 m) (by S. Conrad)

Fig. 22. Feature 5.1.6. Pottery (selection) (by S. Conrad)

9.2. SMALL FINDS (WITH CATALOGUE)

9.2.1. Small finds from prehistory

Raiko Krauß

Fig. 1. Examples for hafting of stone axes (a) and stone adzes (b); a (left): collection of the Institute for Prehistory, Early History and Medieval Archaeology in Tübingen, b (right): Keefer 1993, 98

Fig. 2. Use of wood and antlers to make axe or adze shafts with or without intermediate chucks (Stöckli et al. 1995, 161, Abb. 96)

Fig. 3. Manufacturing of hammer stones (Hahn 1991, Abb. 91)

Fig. 4. Roman slinger in the Dacian War. Detail of a relief from Trajan's Column

Fig. 5. Neolithic tokens made from pottery fragments. Ovcharovo-Gorata (after Krauß 2014, Abb. 106)

Fig. 6. Early Iron Age clay ceramic stamps of the Basarabi group (different scale) (Ailincăi et al. 2004, Fig. 8)

9.2.2. Small finds from Antiquity and Early Middle Ages

Lyuba Traykova

Fig. 1. Glass bracelets: a – after Karwowski 2004, 23, Tafel 17. 228, 229; b – after Zerobin 2017, Taf. 6.11

Fig. 2. Ceramic stamps: a – after Лука 2006, 168, обр. 7; b – after Димитрова-Милчева 2008, 143, обр. 29; c – Nagy, 220, fig. 25

Fig. 3. Ceramic loom weights (after Cholakov 2015, 135, fig. 6. 1)

Fig. 4. Gravestone stele with the Roman numeral 30 in ligature (after Conrad 2004, 223; Tafel 120.3)

Fig. 5. Stone loom weights: a – after Cholakov 2015, 133, fig. 5. 11–13; b – after Трайкова, Тагарева 2021

Fig. 6. Graphic reconstruction of part of a horse bridle (drawing by L. Traykova)

Fig. 7. Iron bridles (after Йотов 2004, табло LXVII. 729, 730, табло LXVIII. 732, 734)

Fig. 8. Bronze bell (after Andreeva, Atanasov 2020, 482, cat. No. 389)

LIST OF TABLES

4. PALAEO-RIVER COURSE RECONSTRUCTION IN THE FLOODPLAIN OF THE YANTRA RIVER, NORTH-CENTRAL BULGARIA

Andreas López del Olmo, Gert Verstraeten, Nils Brothaerts

Table 1. Summary of changes in river length, sinuosity and slope between the current river channel and the river course active until the 1950s

Table 2. Admixtures of the lithogenitic units

Table 3. Abandoned channel and floodplain sediment accumulation rates. Floodplain accumulation rates are indicated with an asterisk *

Table 4. Coring ID and depth of the corresponding archaeological layer. The coring locations are given in decimal degrees (DD)

Table 5. Overview of radiocarbon dated samples. The first part of the sample ID indicates along what transect the sample was taken (Tx, with x being a number from 1 to 10), then at which coring (Cx, with x being a number between 3 and 29). The number after the underscore equals the depth of the sample below the surface (cm). The conventional ^{14}C age gives the measured radiocarbon age of the samples in years before present ± one standard deviation. Calibrated calendar ages are given in years before present and in AD "Anno Domini" or BC "Before Christ", rounded to ten. OxCal online with IntCal13 atmospheric curve was used for calibration

Table 6. Lithogenetic units, key of the interpretation figures

5. METHODOLOGY OF ARCHAEOLOGICAL RESEARCH

5.1. The measurement system

Nadezhda Kecheva, Sven Conrad

Table 1. Table with point No., easting (X), northing (Y) in WGS 1984 UTM 35N coordinate system, height in Baltic coordinate system

5.2. Field survey methods

Nadezhda Kecheva

Table 1. Covered Area ESRI shapefile/feature class attributes list description

Table 2. Attributes list description of post-processed chronologies of collected diagnostic pottery fragments from the field surveys per polygon

Table 3. Total pick up attributes list description of post-processed stones, pieces of daub, tiles and bricks per small polygon

Table 4. Total pick up attributes list description with post-processed pottery fragments chronologies and fabrics per small polygon

7. THE INTENSIVE FIELD SURVEYS AT THE TASH BAIR LOCALITY AND IN ITS SURROUNDINGS

Nadezhda Kecheva, Lyudmil Vagalinski, Lyuba Traykova, Silva Sabkova

Table. 1. The chronological periods used in Bulgarian archaeology with their names in Bulgarian and in English and their start and end

8. ARCHAEOLOGICAL EXCAVATIONS

8.2. Bronze Age

8.2.2. The structure in trenches 3.2–5

Lyudmil Vagalinski, Lyuba Traykova

Table 1. Results of the quantitative analysis of the alloy (Eurotest-Control EAD, accredited laboratory on ISO / IEC 17025, a certificate for of approval on ISO 9001 by LRQA)
Table 2. Results of the quantitative analysis of the corrosion product (Eurotest-Control EAD, accredited laboratory on ISO / IEC 17025, a certificate for of approval on ISO 9001 by LRQA)

9. POTTERY AND SMALL FINDS
9.1. The pottery finds (with catalogue)
9.1.1. Prehistoric pottery
Raiko Krauß
Table 1. Fabrics (ware groups) of the prehistoric pottery

9.1.2. Late Iron Age to Medieval pottery
Sven Conrad
Table 2. Fabrics (ware groups) of the pottery from the Late Iron Age to the Ottoman period

9.1.3. Pottery statistics from the excavations of different features
Sven Conrad, Raiko Krauß
Table 3. Features 1.2.4/6 and 1.2.7/8; detailed pottery finds statistics (part 1)
Table 3. Features 1.2.4/6 and 1.2.7/8; detailed pottery finds statistics (part 2)
Table 4. Trench 1.1-E. Feature 1.1.6, pottery statistics
Table 5. Trench 1.1-W. Feature 1.1.15, pottery statistics
Table 6. Trench 1.1-E. Feature 1.1.7 (NW ditch), pottery statistics
Table 7. Trench 1.1-W. Feature 1.1.13 (NE ditch), pottery statistics
Table 8. Trench 1.2. Feature 1.2.5 (EMA ditch), pottery statistics
Table 9. Ditch in trench 3.6. Pottery statistics according to the excavated layers
Table 10. Feature 3.2.1, pottery statistics according to the excavated layers
Table 11. Feature 3.1.1/2. Pottery statistics according to excavated layers including the single finds measured. Layer a: niv. 61.68 m (planum 1) – ca. 61.40 m; layer b: ca. 61.40 m – ca. 61.25 m; layer c: ca. 61.25–60.98 m
Table 12. Statistics of pottery finds from features 5.1.2, 5.1.5 and 5.1.6
Table 13. Radiocarbon data from northern Bulgaria (radiocarbon data from Tash Bair is between Nos. 158–182)

LIST OF PLATES

9. Pottery and small finds

9.1. The pottery finds (with catalogue)

Catalogue and plates of the pottery finds

Plate 1. Site 1, survey: Late Neolithic pottery (P1/001–P1/015)

Plate 2. Site 1, survey: Late Neolithic pottery (P1/016–P1/031)

Plate 3. Site 1, survey: Late Neolithic pottery (P1/032–P1/044)

Plate 4. Site 1, survey: Late Neolithic pottery (P1/045–P1/059)

Plate 5. Site 1, survey: Late Neolithic pottery (P1/060–P1/073)

Plate 6. Site 1, survey: Bronze Age pottery (P1/074–P1/086)

Plate 7. Site 1, survey: Early Iron Age pottery (P1/087–P1/098)

Plate 8. Site 1, survey: Early Iron Age pottery (P1/099–P1/113)

Plate 9. Site 1, survey: Early Iron Age pottery (P1/114–P1/125)

Plate 10. Site 1, survey: Late Iron Age pottery (P1/126–P1/139)

Plate 11. Site 1, survey: Pottery of the Roman period (P1/140–P1/147)

Plate 12. Site 1, survey: Pottery of the Roman period (P1/148–P1/157); Late Roman pottery (P1/158–P1/162)

Plate 13. Site 1, survey: Early Medieval pottery (P1/163–P1/172)

Plate 14. Site 1, excavations: Late Neolithic pottery (P1/173–P1/181)

Plate 15. Site 1, excavations (trench 1.1-W/E, features 1.1.6/15): Late Neolithic pottery (P1/172–P1/187)

Plate 16. Site 1, excavation (trench 1.1-W/E, features 1.1.6/15): Late Neolithic pottery (P1/188–P1/197)

Plate 17. Site 1, excavation (trench 1.1-W/E, features 1.1.6/15): Late Neolithic pottery (P1/198–P1/204); Late Iron Age pottery (P1/205)

Plate 18. Site 1, excavation (trench 1.1-W/E, features 1.1.7/13): Late Neolithic pottery (P1/206–P1/207); Late Iron Age pottery (P1/208–P1/209); Early Medieval pottery (P1/210–P1/211)

Plate 19. Site 1, excavation (trench 1.1-W/E, features 1.1.2–4): Late Neolithic pottery (P1/212–P1/221)

Plate 20. Site 1, excavations (trench 1.1-W/E, features 1.1.2–4): Bronze Age pottery (P1/222); Late Iron Age pottery (P1/223); Early Medieval pottery (P1/224–P1/225). – Site 1, excavations (trench 1.1-E, feature 1.1.9): Bronze Age pottery (P1/226); Early Iron Age pottery (P1/227). – Site 1, excavations (trench 1.1-W, feature 1.1.11): Late Neolithic pottery (P1/228–P1/230). – Site 1, excavations (trench 1.1-W, feature 1.1.16): Early Iron Age pottery (P1/231)

Plate 21. Site 1, excavations (trench 1.2, feature 1.2.4/6): Late Neolithic pottery (P1/232–P1/241)

Plate 22. Site 1, excavations (trench 1.2, feature 1.2.4/6): Chalcolithic pottery (P1/242). –Site 1, excavations (trench 1.2, feature 1.2.7/8): Late Neolithic pottery (P1/243–P1/248). – Site 1, excavations (feature 1.2.5): Late Neolithic pottery (P1/249–P1/250); Bronze Age pottery (P1/251)

Plate 23. Site 2, survey: Late Neolithic pottery (P2/001); Roman pottery (P2/002–010)

Plate 24. Site 2, survey: Roman pottery (P2/011–P2/019); Late Roman pottery (P2/020–P2/021)

Plate 25. Site 3, survey: Early Iron Age pottery (P3/001) – Site 3, excavations (feature 3.6): Bronze Age pottery (P3/002–008)

Plate 26. Site 3, excavations (feature 3.6): Bronze Age pottery (P3/009–P3/017)

Plate 27. Site 3, excavations (feature 3.6): Late Iron Age pottery (P3/018); Late Roman pottery (P3/019–P3/021). – Site 3, excavations (feature 3.6.1): Bronze Age pottery (P3/022–P3/023). – Site 3, excavations (feature 3.2.1): Bronze Age pottery (P3/024–026)

Plate 28. Site 3, excavations (feature 3.1.1/2): Bronze Age pottery (P3/027–P3/036)

Plate 29. Site 3, excavations (feature 3.1.1/2): Bronze Age pottery (P3/037–P3/047)

Plate 30. Site 4, survey: Late Iron Age pottery (P4/001). – Site 5, survey: Early Iron Age pottery (P5/001); Late Iron Age (– Early Roman) pottery (P5/002–P5/006); Roman pottery (P5/007–P5/009)

Plate 31. Site 5, excavations: Roman pottery (P5/010–P5/014)

Plate 32. Site 5, excavations: Roman pottery (P5/015–P5/018)

Plate 33. Site 5, excavations: Roman pottery (P5/019–P5/026)
Plate 34. Site 12, survey: Roman pottery (P12/001–P12/009); Late Roman pottery (P12/010–P12/011)
Plate 35. Site 17, survey: Early Iron Age pottery (P17/001–P17/002); Late Iron Age pottery (P17/003–P17/004). – Site 18, survey: Late Iron Age pottery (P18/001–P18/007)
Plate 36. Site 18, survey: Roman pottery (P18/008–P18/018)
Plate 37. Site 19, survey: Early Iron Age pottery (P19/001–P19/003); Late Iron Age pottery (P19/004–P19/011)
Plate 38. Site 19, survey: Early Medieval pottery (P19/012–P19/014). – Site 20, survey: Early Medieval pottery (P19/001). – Site 21, survey: Early Iron Age pottery (P21/001); Early Medieval pottery (P21/002–P21/005)
Plate 39. Site 24, survey: Early Iron Age pottery (P24/001–P24/006); Late Iron Age pottery (P24/007–P24/008). – Site 25, survey: Late Iron Age pottery (P25/001)
Plate 40. Site 34, survey: Late Iron Age pottery (P34/001); Early Medieval pottery (P34/002–P34/003). – Site 37, survey: Early Medieval pottery (P37/001)

9.2. Small finds (with catalogue)

9.2.1. Small finds from prehistory

Raiko Krauß

Catalogue and plates of the small finds from prehistory
Plate 1. SF 01–08 – small finds from site 1, field survey (figure by R. Krauß)
Plate 2. SF 09–15 – small finds from site 1, field survey (figure by R. Krauß)
Plate 3. SF 16–22 – small finds from site 1, field survey (figure by R. Krauß)
Plate 4. SF 35–43 – small finds from site 1, excavations (figure by R. Krauß)
Plate 5. SF 44–45 – small finds from site 1, excavations; SF 53 – small find from site 3, excavations; SF 60–61 – small finds from site 18, field survey; SF 62–63 – small finds from site 19, field survey; SF 70 – small find from site 24, field survey (figure by R. Krauß)

9.2.2. Small finds from Antiquity and Early Middle Ages

Lyuba Traykova

Catalogue and plates of the small finds from Antiquity and Early Middle Ages
Plate 6. SF 23–26 – small finds from site 1, field survey (figure by L. Traykova)
Plate 7. SF 27–29 – small finds from site 1, field survey (figure by L. Traykova)
Plate 8. SF 30–31 – small finds from site 1, field survey (figure by L. Traykova)
Plate 9. SF 32–33 – small finds from site 1, field survey (figure by L. Traykova)
Plate 10. SF 34 – small find from site 1, stray find (figure by L. Traykova)
Plate 11. SF 46–50 – small finds from site 1, excavations (figure by L. Traykova)
Plate 12. SF 51–52 – small finds from site 2, field survey (figure by L. Traykova)
Plate 13. SF 54–55 – small finds from site 3, excavations (figure by L. Traykova)
Plate 14. SF 56–57 – small finds from site 5, field survey; SF 58–59 – small finds from site 5, excavations (figure by L. Traykova)
Plate 15. SF 64–66 – small finds from site 19, field survey (figure by L. Traykova)
Plate 16. SF 67–68 – small finds from site 22, field survey; SF 69 – small find north of site 22, field survey; SF 71 – small find from site 27, field survey (figure by L. Traykova)

1. PREFACE

Sven Conrad, Raiko Krauß, Lyudmil Vagalinski

The Bulgarian-German collaboration in archaeological research at the confluence of the Yantra and the Danube has a long and established tradition. In 1958 the first excavation campaign in the late antique fort *Iatrus* was started by a joint team consisting of archaeologists from the National Archaeological Institute with Museum of the Bulgarian Academy of Sciences, Sofia (NAIM–BAS) and the Institute for Greco-Roman Antiquity at the German Academy of Sciences Berlin of the GDR (later: Central Institute for Ancient History and Archaeology of the Academy of Sciences). The excavations continued until 1981 and provided fundamental knowledge not only about the history of the fort, but also about the whole Limes on the Lower Danube.

After the political changes of 1989/90, the joint excavations resumed in 1992 and continued until 2000. The German partnership was now with the Roman-Germanic Commission Frankfurt a.M. of the German Archaeological Institute (RGK). The excavations in the fort were an important factor in regional life among the population and those responsible for the regional administration, therefore, despite the sometimes difficult conditions in the period of upheaval during the 1990s, we received great support. The good personal connections that had grown over the years also contributed to this.

The contractual conditions between the Bulgarian and German sides also enabled research in the area around the *Iatrus* fort, which was implemented at the RGK between 1997 and 2001 via a project funded by the German Research Foundation (DFG). The main part of the interdisciplinary research consisted of extensive field inspections, with which a comprehensive idea of the settlement history of the region could be obtained for the first time. In 2002, limited excavations were conducted on some selected sites in the vicinity of *Iatrus*, and the last work in the documentation of the finds was carried out in 2004. Lyudmil Vagalinski continued the excavations on the Early Roman lime kiln near Krivina until 2007.

The ongoing research now opens its third chapter in the Bulgarian-German research at the mouth of the Yantra River, with which we have entered the seventh decade since the research began. The Institute for Prehistory, Early History and Medieval Archaeology at the University of Tübingen is now acting as a contractual partner on the German side.

The previous research had already established that the important sites at the Tash Bair play a key role in understanding the settlement system at the mouth of the Yantra. New possibilities in archaeological exploration, such as improved access to satellite images and large-scale geomagnetic mappings, allowed the research to expand to areas which were previously difficult to access. The DFG was also convinced of the scientific importance of the project and approved extensive funding for an initial period of three years (applicant: Sven Conrad; project No. 388543935 / CO-288 / 2-1). The NAIM–BAS unreservedly supported the resumption of the joint research work, so that the work could start with a survey campaign in March 2018. A total of two surveys and two excavation campaigns, as well as one finds processing campaign were carried out by September 2020.

This volume contains the results and finds of the intensive field surveys and the targeted excavations that were carried out during the first research phase from 2018 to 2020, including pottery and small finds as well as the results of the interdisciplinary investigations. For several reasons, the results of the research on archaeobotanical remains will be published in the next volume.

The reader will notice some contradicting opinions and differences in the interpretations in the individual contributions. Some of these can be traced back to the current state of research, so we have decided not to clear them up for the time being and allow the reader to form their own opinion. The

second research phase, which already began in 2021 and will continue until 2024, offers the opportunity to clarify a number of these problems.

Several colleagues and students were involved in the field research during the first phase of the project. In addition to the three editors and Lyuba Traykova (vice-head of the field work) and Nadezhda Kecheva (NAIM–BAS) were also members of the joint Bulgarian-German team; Silva Sabkova (NAIM–BAS) took part in the 2018 campaigns.

In the summer campaigns of 2018 and 2019, Andreas López del Olmo, Gert Verstraeten and Nils Broothaerts from the Geographical Institute of the KU Leuven carried out geomorphological studies in the Yantra lowlands and at the Tash Bair. They were supported by Johanna Gille-Petzoldt and Joachim López del Olmo. The results formed the basis for a master's thesis successfully completed in 2020 by Andreas López del Olmo.

Victoria Russeva (Institute of Experimental Morphology, Pathology and Anthropology with Museum of the Bulgarian Academy of Science) supported the excavation and salvage of the grave on site 5 and gave an initial on-site expertise. Other substantial contributions to this volume were made by Maria Gurova through her processing of flint tools, and by Nadezhda Karastoyanova through processing of animal bones. The Bronze Age knife was examined in the Curt-Engelhorn-Centre of Archaeometry in Mannheim and by the accredited laboratory Eurotest-control EAD in Sofia.

The following students took part in the research campaigns: Julia Becher (University of Tübingen), Judith Berning (State Academy of Fine Arts Stuttgart), Lea Valcov (University of Tübingen), Boris Borisov (University of Veliko Tarnovo), Philipp Kluge, Martin Offermann, Samantha Petrella, Stephan Roller and Jonas Sprißler (University of Tübingen). During the campaign in summer 2019, Luca Valcov (Dudeştii Vechi / Timişoara) took part in the excavation work.

The following colleagues visited the excavations or examined the finds: Stefan Aleksandrov and excavation team (NAIM–BAS), Canay Alpagut, Lennart Brandtstätter (University of Tübingen), Gerda Sommer-von Bülow (Berlin), Peti Donevski (Svishtov), Deyan Dragoev (Regional Historical Museum Ruse), Piotr Dyczek (University of Warsaw), Nikolay Nenov (Regional Historical Museum Ruse), Agnieszka Tomas and excavation team, Janusz Recław (University of Warsaw) and Varbin Varbanov (Regional Historical Museum Ruse).

Ceramic drawings were made by Achim Frey (Tübingen) and Doncho Karakolev (Ruse) as well as by Julia Becher and Jonas Sprißler. The processing of the ceramic drawings and the setting of the illustration plates was in the hands of Jonas Sprißler (University of Tübingen). The restoration work was carried out by Maria Taseva (NAIM–BAS).

Catalina Labra-Odde (based in Melbourne) took over the English copy editing and proofreading of chapters 1–4; 5.1; 5.3.2; 5.4.; 5.5; 6; 8.1; 8.2.3; 8.3.2; 9.1; 9.2.1; 10; 11.2). The translation in English of all other chapters was done by Nadezhda Kecheva (NAIM–BAS), and its proofreading was carried out by the British colleague Amber Roy (Newcastle University, UK).

Christel Bock (University of Tübingen), Tsvetanka Starcheva and Anton Nikov (both NAIM–BAS) took care of the financial reports, which are essential for such a project, with their well-known reliability.

We received extensive support from the administration of the municipality of Tsenovo under Mayor Dr Petar Petrov and his deputy Vanya Ignatova as well as by the Mayor's office Novgrad under Mayoress Diana Kopcheva. In the warm welcome and the high level of commitment of the workers and inhabitants from various villages in the community, we felt the connectedness that has grown through our many years of activity in the region, and which has not insignificantly contributed to the success of the project.

We thank all for their support!

УВОД

Свен Конрад, Райко Краус, Людмил Вагалински

Българо-германското сътрудничество по археологическите проучвания в района около устието на р. Янтра при вливането ѝ в Дунав има дълга и утвърдена традиция. През 1958 г. започва първата кампания от разкопки в късноантичната крепост „Ятрус“ от съвместен екип, съставен от археолози от Националния археологически институт с музей при Българската академия на науките в София (НАИМ – БАН) и Института за гръко-римска древност към Академия на науките на ГДР в Берлин (по-късно Централен институт за древна история и археология към Академията на науките). Разкопките продължават до 1981 г. и дават фундаментални знания не само за историята на крепостта, но и за целия лимес по долното течение на Дунав.

След политическите промени през 1989/90 г. съвместните разкопки са възобновени през 1992 г. и продължават до 2000 г. Германското партньорство вече е с Римско-германската комисия във Франкфурт на Майн към Германския археологически институт (РГК). Разкопките в крепостта „Ятрус“ са важен фактор в регионалния живот сред населението и отговорните за регионалната администрация, поради което, въпреки понякога трудните условия в периода на сътресения през 90-те години, получихме голяма подкрепа. За това допринесоха и добрите лични връзки, които се бяха създали през годините.

Договорните условия между българската и германската страна дадоха възможност и за изследвания в района на крепостта „Ятрус“, които бяха осъществени между 1997 и 2001 г. чрез проект към РГК, финансиран от Германската фондация за научни изследвания (Deutsche Forschungsgemeinschaft – DFG). Основната част от интердисциплинарното изследване се състоеше в мащабни теренни обхождания, с които за първи път можеше да се получи цялостна представа за историята на заселването на региона. През 2002 г. са проведени ограничени разкопки на някои избрани обекти в околностите на „Ятрус“, а последните работи по документирането на находките бяха извършени през 2004 г. Людмил Вагалински продължава разкопките на ранноримски пещи за изпичане на вар край Кривина до 2007 г.

Продължаващите изследвания сега отварят своята трета глава в българо-германските проучвания при устието на р. Янтра, с които навлязохме в седмото десетилетие от началото на проучванията. Институтът за праистория, ранна история и средновековна археология към Университета в Тюбинген сега действа като договорен партньор от германска страна.

Още при предишните изследвания беше установено, че важните обекти при местността Таш баир играят ключова роля за разбирането на селищната система по устието на р. Янтра. Новите методи в археологията, като например подобреният достъп до сателитни изображения и широкомащабни геомагнитни карти, позволиха изследванията да се разширят до райони, които преди това са били труднодостъпни. DFG също беше убедена в научната значимост на проекта и одобри широко финансиране за първоначален период от три години (заявител Свен Конрад; проект № 388543935 / CO-288/2-1). НАИМ – БАН безрезервно подкрепи възобновяването на съвместната изследователска работа, за да може тя да започне с проучвателна кампания през март 2018 г. До септември 2020 г. бяха проведени общо пет кампании: две за теренни издирвания, две за археологически разкопки и една за обработка на находките.

Настоящият том съдържа резултатите и описание на находките от теренните издирвания и археологическите разкопки, които бяха проведени по време на първия етап на проучванията от 2018 до 2020 г., включително керамика и малки находки, както и резултатите от интердисциплинарните проучвания. По няколко причини резултатите от проучванията на археоботаничните останки ще бъдат публикувани в следващия том.

Читателят ще забележи някои противоречиви мнения и различия в интерпретациите в отделните приноси. Някои от тях могат да бъдат проследени до сегашното състояние на изследванията, затова решихме засега да не ги изясняваме и да дадем възможност на читателя да си състави собствено мнение. Вторият етап на изследванията, който започна през 2021 г. и ще продължи до 2024 г., дава възможност да се изяснят редица от тези проблеми.

Няколко колеги и студенти участваха в теренните проучвания по време на първата фаза на проекта. Освен трите редактори, Люба Трайкова (заместник-ръководител на теренната работа) и Надежда Кечева (НАИМ – БАН) бяха членове на съвместния българо-германски екип; Силва Събкова (НАИМ – БАН) взе участие в кампаниите през 2018 г.

През летните кампании на 2018 г. и 2019 г. Андреас Лопес дел Олмо, Херт Верстраетен и Нилс Бротхаертс от Географския институт на университета в Льовен (Белгия) извършиха геоморфоложки проучвания в низината на р. Янтра и на Таш баир. Те бяха подкрепени от Йохана Гиле-Пецолд и Йоахим Лопес дел Олмо. Резултатите са в основата на магистърска теза, успешно защитена през 2020 г. от Андреас Лопес дел Олмо.

Виктория Русева (Институт по експериментална морфология, патология и антропология с музей при БАН) подкрепи разкопките и спасителните дейности на гроба на обект 5 и направи първоначална експертиза на място. Други съществени приноси към този том са направени от Мария Гюрова чрез обработката на кремъчните артефакти и от Надежда Карастоянова чрез обработката на животинските кости. Един бронзов нож беше изследван в Центъра по археометрия „Курт Енгелхорн“ в Манхайм и в акредитирана лаборатория Евротест-контрол ЕАД в София.

В изследователските кампании взеха участие следните студенти: Юлия Бехер (Университет Тюбинген), Юдит Бернинг (Държавна академия за изящни изкуства, Щутгарт), Леа Вълков (Университет Тюбинген), Борис Борисов (Великотърновски университет), Филип Клуге, Мартин Оферман, Саманта Петрела, Щефан Ролер и Йонас Шприслер (Университет Тюбинген). По време на кампанията през лятото на 2019 г. в разкопките се включи и Лука Вълков (Стар Бешенов / Тимишоара / Румъния).

Следните колеги посетиха разкопките или проучиха находки: Стефан Александров с екип (НАИМ – БАН), Джанай Алпагут, Ленарт Брандщетер (Университет Тюбинген), Герда Зомер-фон Бюлов (Берлин), Пети Доневски (Свищов), Деян Драгоев (Регионален исторически музей – Русе), Пьотр Дичек (Варшавски университет), Николай Ненов (Регионален исторически музей – Русе), Агнешка Томаш с екип, Януш Рецлав (Варшавски университет) и Вървин Върбанов (Регионален исторически музей – Русе).

Рисунките на керамиката са направени от Ахим Фрай (Тюбинген) и Дончо Караколев (Русе), както и от Юлия Бехер и Йонас Шприслер. Обработката на керамичните рисунки и поставянето на таблата е дело на Йонас Шприслер (Университет Тюбинген). Реставрационните дейности бяха извършени от Мария Тасева (НАИМ – БАН).

Каталина Лабра-Оде (Мелбърн, Австралия) пое редактирането и коректурата на английски език на глави 1-4; 5.1; 5.3.2; 5.4.; 5.5; 6; 8.1; 8.2.3; 8.3.2; 9.1; 9.2.1; 10; 11.2). Преводът на английски език на всички останали глави е направен от Надежда Кечева (НАИМ – БАН), а коректурата му е извършена от Амбър Рой (Университет на Нюкасъл, Великобритания).

За финансовите отчети, които са от съществено значение за подобен проект, се погрижиха с известната си надеждност Кристел Бок (Университет Тюбинген), Цветанка Старчева и Антон Ников (и двамата от НАИМ – БАН).

Получихме широка подкрепа от администрацията на община Ценово под ръководството на кмета д-р Петър Петров и неговата заместничка Ваня Игнатова, както и от кметство Новград под ръководството на кмета Диана Копчева. Топлото отношение и високата ангажираност на работниците и жителите на различните села в общността ни накараха да почувстваме силната връзка, изградена и развила се по време на дългогодишната ни дейност в региона, която допринесе немалко за успеха на проекта.

Благодарим на всички за тяхната подкрепа!

2. HISTORY OF RESEARCH AND AIMS OF THE PROJECT

Sven Conrad, Raiko Krauß

2.1. EXCAVATIONS IN THE LATE ROMAN LIMES FORT OF IATRUS 1958–2000

The Bulgarian-German research collaboration at the confluence of the Yantra River into the Danube has a tradition that goes back to 1958. This is also when excavations in the Late Roman fort of Iatrus began as a joint project of the National Archaeological Institute with Museum of the Bulgarian Academy of Sciences and the Institute for Greco-Roman Antiquity of the Academy of Sciences of the GDR up until 1981 (von Bülow, Wachtel 2015, 203–207). These excavations resumed in 1992 and continued until 2000, this time led by the Roman-Germanic Commission Frankfurt a.M. of the German Archaeological Institute (fig. 1).



Fig. 1. Aerial view of Iatrus from the northeast (spring 2000) (figure by S. Conrad)

Approximately 40% of the former fort area was excavated; the publication of the results, which represents an important point of reference in the exploration of the Late Roman Limes, is now complete (Iatrus-Krivina I–VI; summarised: von Bülow 1994). The results of the investigations in the fort are exemplary of 4th and 6th century Late Roman and Early Byzantine limes. Nevertheless, some conclusions are still under discussion (Vagalinski 2003; Wachtel 2015, 253 f.; von Bülow, Wachtel 2015; Vagalinski 2016). The history of the occupation and the architecture of the fort (built by Constantine the Great to strengthen the limes in a strategic position at the mouth of the Yantra), can be divided into four periods:

– Period A (approx. 320–360 AD): Construction of the fort in the scheme of Late Roman military architecture of Diocletian-Constantine style. The fort was occupied by a regular military unit. Abandonment and extensive demolition of the interior;

– Period B/C (after 360 AD to about the middle of the 5th century AD): Construction of two *horrea* in the course of Valentinian II's campaigns and resettlement, probably by *foederati*. Construction of the first Christian basilica. Partial destruction and abandonment of the *horrea* at the beginning of the 5th century and subsequent densification with small-scale buildings. This process may have been a result of the settling of the strongly civilized *foederati*. By the middle of the 5th century, the fort had been destroyed, most likely during a series of invasions from the Huns;

– Period D1 (approx. 480 AD – approx. 520 AD): re-occupation and repair of the fort under Emperor Anastasius. Unstructured architecture in the interior. Again, destruction of the fort;

– Per. D2 (approx. 520 AD – approx. 600 AD): Large, massive church building as the most important building under Justinian I. Few, poorly founded interior structures speak for a very simple, predominantly civil character of the settlement. Destruction and abandonment of the fort during the invasions from the Slavs and Avars at the turn of the 6th and 7th century.

In the late 7th century, an Early Slavic settlement was established in the castle ruins, which later developed into a fortified settlement of the First Bulgarian Kingdom.

In addition to the investigations in Iatrus, the Bulgarian-Polish teams have been running extensive excavations in the legionary camp of Novae since 1960. These excavations are situated east of Svishtov, approximately 20 km upstream the Danube from the mouth of the Yantra River (Dyczek 2008). The camp was most likely established shortly after the organisation of Moesia as an independent province under the leadership of a *legatus Augusti* in 44 AD (Boteva 2012). During the Late Roman and Early Byzantine times, certain parallels in the development of Novae and Iatrus can be seen.

2.2. DIACHRONIC RESEARCH ON THE ARCHAEOLOGICAL LANDSCAPE AT THE LOWER YANTRA FROM 1997 TO 2002

Until the 1990s, research outside of the fort of Iatrus was not part of the official research programme and therefore not possible. Consequently, up until this point only fragmentary knowledge was available about the hinterland of the limes, as well as about the prehistoric and Early Medieval settlement on the lower reaches of the Yantra (predominantly based on two preliminary site catalogues) (Стефанов 1956; Дремсизова-Нелчинова, Иванов 1983).

To embed the Iatrus fort and the legionary camp Novae in the surrounding settlement landscape, an interdisciplinary research project was initiated between 1998 and 2001, funded by the German Research Foundation (lead by G. v. Bülow; realisation and local management by S. Conrad). The extensive field surveys were supplemented by limited geophysical investigations and aerial photographs, with the focus initially on the period between the Late Iron Age and Medieval times. Due to the very good conditions of the findings, the project was extended to include finds from the prehistoric periods, these were processed and published in a PhD thesis by R. Krauß (2006a).

In 2002, several excavation trenches were carried out on Roman and Late Roman sites in the vicinity of Iatrus. The results provide initial indications of the settlement around the Iatrus fort from the Roman Empire, Late Roman and the Early Middle Ages. For the first time, there is a diachronic settlement history for a region on the Lower Danube from the Neolithic to the Early Modern period. This research area is some of the best researched amongst the regions of the Lower Danube (Conrad, Stanchev 2002; Conrad 2006; Krauß 2006a; Vagalinski 2011a; 2011b; Iatrus-Krivina, vol. VII [in prep.]) (fig. 2; 3).

Based on the findings of the field surveys on the Lower Yantra, a working group from the Geographical Institute of the Catholic University of Leuven (Belgium) carried out geomorphological investigations in the Batinsko dere, east of the Yantra valley in 2012. The exemplary results of the predictive modelling and on the erosion processes in the loess area are presented in two Master's theses (Verhasselt 2013; Scheere 2013).

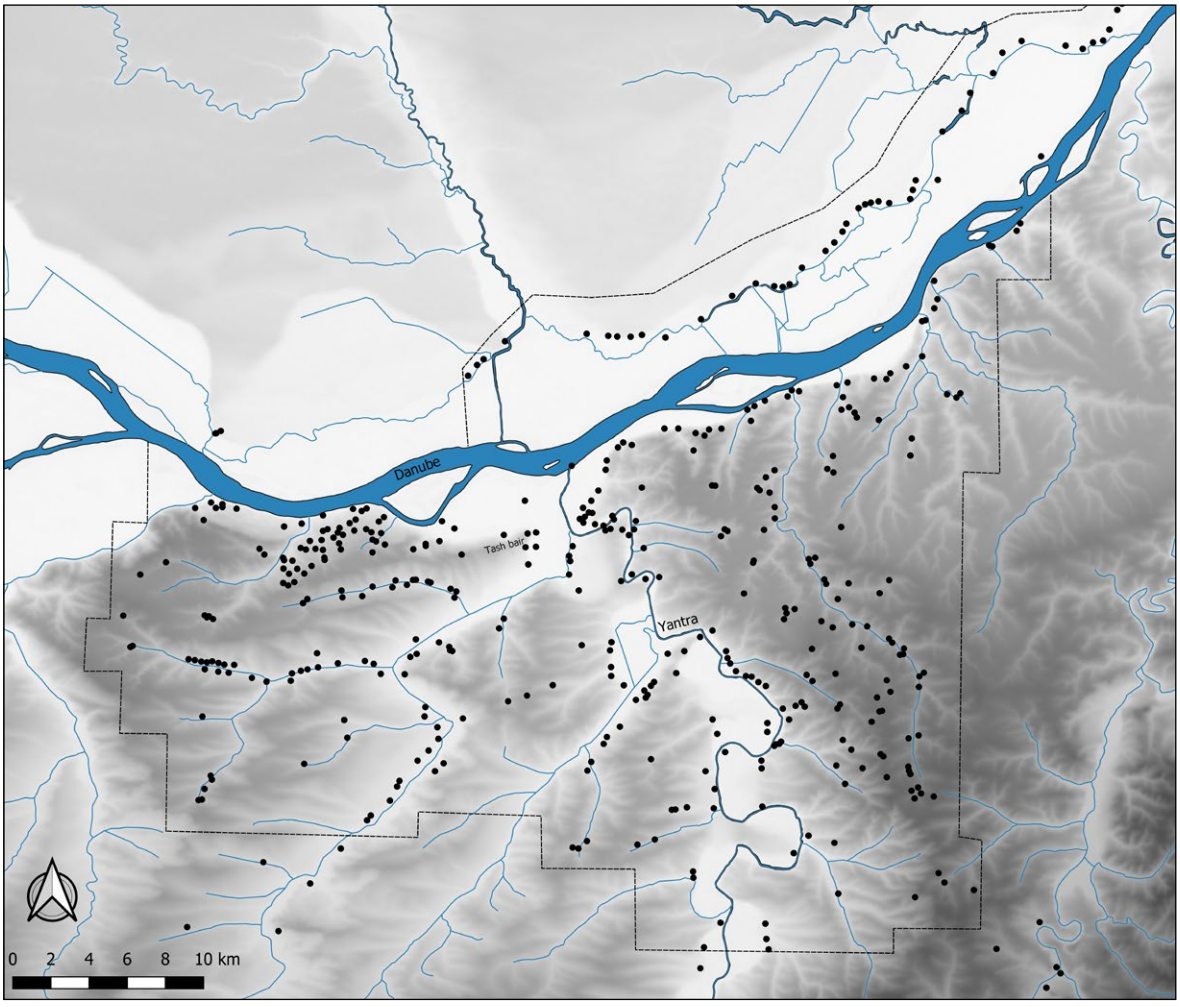


Fig. 2. Map of archaeological sites (without burial mounds) in the working area registered between 1997 and 2001 (figure by S. Conrad)

2.3. A SHORT OUTLINE OF THE SETTLEMENT HISTORY AT THE LOWER YANTRA AND BEYOND

The region was certainly already settled during the Palaeolithic, indicated by individual artefact finds (Kowal, Kozłowski 2011). Significant traces from the Upper Palaeolithic next to our research area can only be found in the Wallachian territory north of the Danube (Ciornei 2017). For the Early Neolithic in our research area, the preserved remains are limited to a few locations in higher terrain (150 m above sea level). They show connections to the known sites on the middle course of the Yantra and Kamchiya area (Krauß 2006a, 217–219). These can be considered the oldest agricultural settlements in the Eastern Balkans to date. Radiocarbon dates are now available for all these sites, which indicate the beginning of the Neolithisation process in the 61st century BC (Krauß 2014, 280–294; Marinova, Krauß 2014, 183–184). At least at the Koprivets and Borovo-Chakmak tepe sites, the settlement continuity extends into the Late Neolithic.

The settlement activity intensified during this time, and sites can thus also be found in the river plains both in the lowlands of the Yantra and the Danube, as well as in the Batinsko dere. During this period, which can be narrowed down to the second half of the 6th millennium BC using just a few radiocarbon dates from the Kachitsa and Hotnitsa-Orlovka sites. The first larger settlement of the Vădastra culture arises on the site to be examined on the southern slope of Tash Bair, at the confluence of Balgaroslivovsko dere with the Yantra, southwest of Novgrad (Krauß 2006a, 219–222). This settlement is remarkable since the Vădastra phenomenon has its main distribution in Wallachia and is only documented

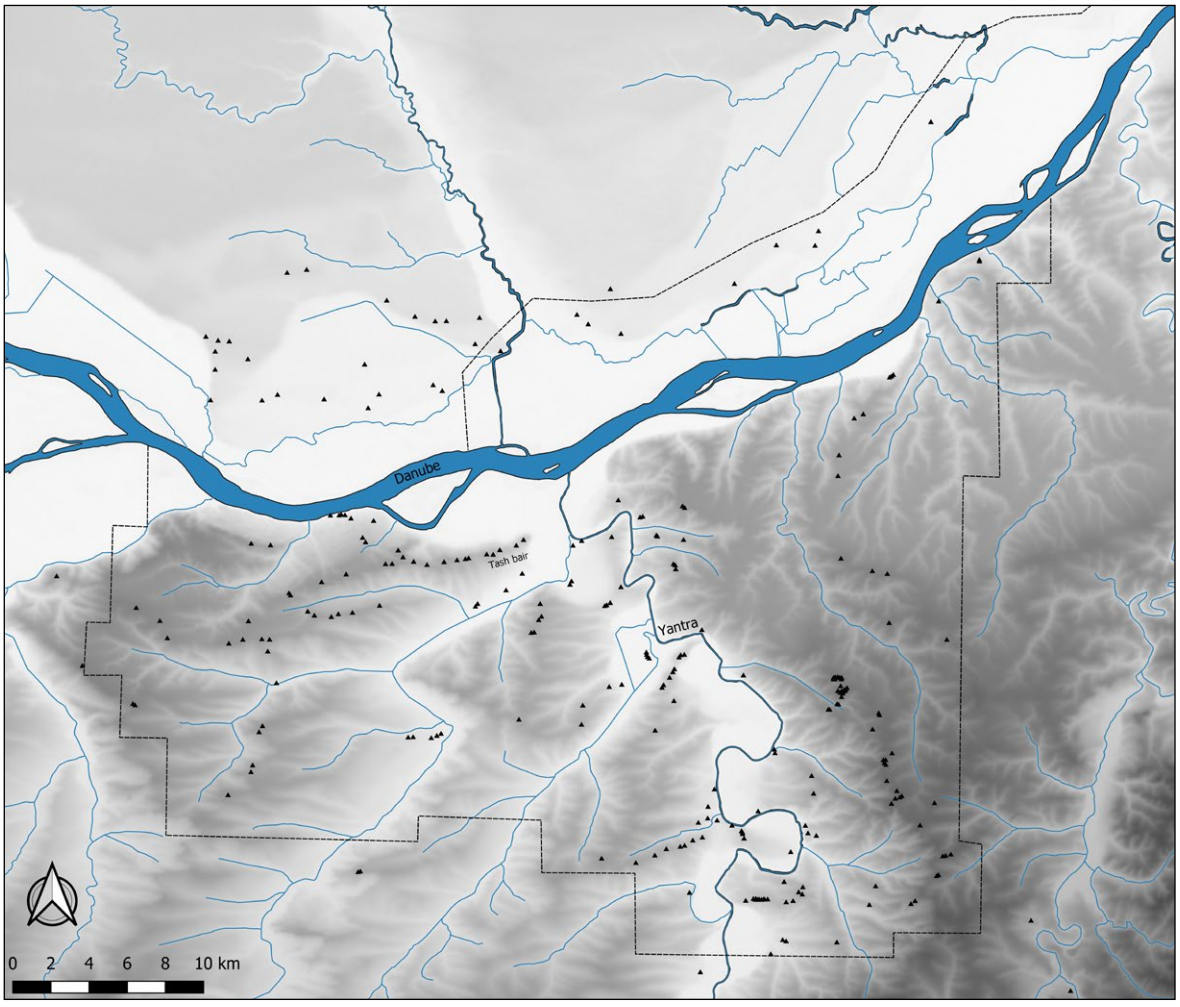


Fig. 3. Map of burial mounds in the working area registered between 1997 and 2001 (figure by S. Conrad)

in very few places south of the Danube (Christescu 1932; Gaul 1940; Naidenova 2005). For northern Bulgaria, the Kachitsa group as a northern variant of the Karanovo IV culture is more characteristic of this period. During the Chalcolithic, the region is rather marginal in relation to the prosperous tell settlements of the Kamchiya area and the settlement microregions in the catchment area of the Rusenski Lom. This could be related to the resource situation in the Yantra area, due to the intensively exploited flint deposits of the Ludogorie area to the east, and the gold-bearing rivers in northern Bulgaria draining east into the Black Sea. With the tell settlements of Pet Kladentsi-Manastira, Pet Kladentsi reservoir, Koprivets, Volovo-Dermenyolu and Borovo-Chakmaktepe, only the extreme western extension of a larger concentration of tell settlements in the catchment area of the Rusenski Lom has been recorded (Krauß 2006a, 223–227).

The Early Bronze Age settlement shows a different geographical distribution compared to the Neolithic-Chalcolithic settlement, as it lies along the small streams near the Danube. Of supra-regional importance is a small group of graves near Batin, which together with the long-known burial ground of Zimnicea on the Romanian bank of the Danube (Alexandrescu 1974) is an eponym for the development of the Bronze Age in the entire area of the Lower Danube. The settlements of this period are comparatively difficult to detect and were largely unknown until the systematic field surveys along the Yantra. It is noticeable that the Early Bronze Age sites were also found in the vicinity of less fertile soils, which could indicate that agriculture is less important in the increase of animal husbandry (Krauß 2006a, 228–229). In the Middle and Late Bronze Age, a settlement pattern began to emerge along the Yantra, which can be considered characteristic of the later prehistory of the region up until the Roman

fortification of the Danube Limes. Settlement (especially in the area east of the Yantra) increased, and in addition to a few central settlement sites, smaller settlements, as well as several burial sites appeared in their vicinity for the first time (Krauß 2006a, 231–233). Typical for this period, around the second half of the 2nd millennium BC, are large metal hoards. In the wider area around the Yantra, the hoard of Ovcha Mogila with a Mycenaean horned sword (Krauß 2005) and one depot with several gold objects recently discovered east of Svishtov (Alexandrov et al. 2018a) are worth mentioning.

With a relatively low number of sites, two settlement microregions near Byala and Svishtov could be identified for the Early Iron Age. These are grouped around two hill settlements that were perhaps already fortified at that time (Krauß 2006a, 235–239 fig. 125). In the vicinity of the newly discovered site at Byala (Kaleto), which oversees an important Yantra ford, signs of a hierarchical settlement landscape can already be seen. Material from the Basarabi culture which can be dated to the 8th and 7th century BC comes from several sites. Similar to the Late Neolithic Vădastra material, Basarabi finds have only been found sporadically south of the Danube (Vulpe 1965; 1986; Conrad, Krauß 2020).

The number of sites continued to grow in the outgoing Early Iron Age and the beginning of the Late Iron Age; the settlement spreads to the west over the Yantra into the wider, fertile side valleys. The settlement pattern described above was essential for the following period of the Late Iron Age. The fortified hilltop settlements of Svishtov and Byala, to which the better-researched fortification at Zimnicea on the northern bank of the Danube (Alexandrescu 1980; Măgureanu 2011; Spânu 2014) must be assigned, show some characteristics for classification as central places with surrounding unfortified smaller settlements (Conrad 2006, 312–315).

Hr. Popov (Попов 2002) presents in his study on the Iron Age fortifications in Bulgaria and Illyria, signs of a protourban development for this period. He states that there is insufficient research both for the fortified centres and in particular for the surrounding flat settlements. This also applies to our research area at the lower course of the Yantra. Presently, it cannot be decided whether the fortifications of Byala and Svishtov could be complex centres or subordinate fortified settlements with some central local functions within a tribal society (cf. Gringmuth-Dallmer 1999). Their assignment to a specific Thracian tribe remains uncertain for the time being, as the Yantra roughly marks the border between the territories of the Getes-Krobyzoi and the smaller Usdikenian group which can be reconstructed from the written sources (Danov 1976, 130–131; Stoyanov 2000; Stoyanov et al. 2006). The influence of the Odrysian Kingdom in the 5th–4th century BC to these northern tribes cannot be clearly defined.

The settlement structure of a fortified hilltop and open flat settlements identified for the research area show clear parallels with the extensive settlement belt of ancient civilisations surrounding the Mediterranean world. This settlement pattern has been intensively researched in the last decades, especially for the Celtic world, but also for the Iberian Peninsula, initially based on the middle and late Latène Age *oppida* (see e.g. Buchsenschutz 1981; Fichtl 2005; 2012), then intensified for the Late Hallstatt and Early La Tène chieftain seats ('Fuerstensitze') (Krausse, Steffen 2008; Krausse, Beilharz 2010). As the example of the fortification of Sboryanovo and its surrounding near Isperih (Helis) show (Stoyanov 2000; Стоянов 2006), a similar settlement structure may be assumed in all northern Bulgaria, as well as in southern Romania during the Late Iron Age (Spânu 2019).

The settlement development of the younger phase of the Late Iron Age, (i.e., the period from the 2nd century BC until the beginning of Roman rule on the lower Danube in the first half of the 1st century AD) could only be partially clarified thus far. The Celtic migration at 279/278 BC caused considerable destruction in the areas south of the Balkans but may also have led to upheavals along the Danube (Strobel 1996, 153–174). The image of a disastrous collapse and permanent population decline, which appears as a sparse population between the rivers Osam and Yantra, is likely a reflection of insufficient research (Danov 1975/6; 1979, 47–57; Tomas 2017b). For example, D. Spânu (2014, 110–120; 2016) recognises that the fortification of Zimnicea on the left bank of the Danube may have suffered a certain decrease in settlement during the middle section of the Late Iron Age; however, there does not seem to have been a *hiatus*.

As we already mentioned above the Novae legionary camp near Svishtov was very likely set up after the organisation of Moesia as an independent province in 44 AD. The further expansion of the limes east of the Yantra in the Flavian period is only recognisable at a few sites. The systematic settlement only began after the end of the Dacian wars of Traian (101–106) (Iatrus-Krivina, vol. VII [in prep.]). The river Yantra is said to have demarcated the Roman province of Moesia from the customs district of Ripa Thraciae after 44 AD for a few decades. However, the presumed Early Imperial fort at the mouth of the Yantra has not yet been proven (cf. von Bülow, Wachtel 2015, 209).

A more detailed chronological differentiation is not possible based on the surface finds collected thus far. Therefore, the summarised settlement pattern obtained for the Roman Empire in the research area most likely corresponds to the 3rd and first half of the 4th century. A dense network of suburban *villae,* that required central planning, form a significant settlement agglomeration around the legionary camp of Novae. Land plots were most likely provided for veterans in the course of their *honesta missio* (Conrad 2006, 321–324). In recent years the investigations on the settlement structure in the vicinity of the legionary camp have intensified (Tomas 2016; 2017a).

In rural areas, villages (*vici*) occupy favourable places in open areas and valley sections, especially west of the Yantra. They are situated in greater distances to each other, approximately 6–8 km apart. It is not known whether they performed administrative tasks and thus had a central local function of the middle level within the area. The space on the valley borders and around water sources is mainly occupied by *villae*. The settlement pattern is similar to the situation in the territory of Nicopolis ad Istrum, located approximately 50 km to the south (Poulter 2004; 2007a; 2007b; 2019).

The rural area of the research area was apparently not significantly affected by the Gothic incursions in the second half of the 3rd century. Thus, after the stabilisation of the limes, the settlement network continued to densify during the 4th century. However, the Second Gothic War (376–382) and invasions of the Huns in the first half of the 5th century led to an almost complete abandonment of the rural settlement area. At the same time, the density of buildings in the fort Iatrus and the extension of the extramural settlement were increasing (Conrad 2006, 318–319). Iatrus was finally abandoned and completely destroyed shortly before the middle of the 5th century.

Under Emperor Anastasius, the Limes along the Lower Danube was restored at the end of the 5th century. However, the depopulation of the rural area could not be reversed. There was no stable settlement and supply base north of the Balkan Mountains. The emperors Anastasius and Justinian I tried to stop the decline of agriculture and thus of tax revenues through legislative measures (Curta 2006, 44 f.), which, according to our research, does not appear to have been very successful. During the invasions of the Slavs and Avars, the Danube limes and the areas north of the Balkan Mountains finally had to be abandoned at the turn of the 6th and 7th century.

From the second half of the 7th century, a dense network of Early Medieval settlements developed in the research area. It shows a hierarchical structure which consists of open settlements and fortifications of different sizes and with different purposes. Among these there a earth-and-wood ramparts and fortified settlements in former limes fortifications. Numerous very small settlements seem to indicate a (semi-) nomadic way of life. Regarding the Early Medieval settlements in our research area, up until now only the Early Medieval settlement of Iatrus (Wendel 1986) and the multi-phase site of Starmen have been examined in more detail (Hensel 1980; Михайлов et al. 1982).

The Byzantine conquest of the First Bulgarian Kingdom at the beginning of the 11th century once again caused a complete collapse of the social order and the settlement structure. The withdrawal of the Byzantines behind the Balkan Mountains created a power vacuum that favoured the subsequent incursions of the Pechenegs and other steppe peoples and probably had an even more devastating effect.

The origins of today's settlement system, with relatively few and far apart villages, goes back to the Late Medieval period i.e., the time of the Second Bulgarian Kingdom (end of 12th–14th century).



Fig. 4. Satellite picture of 2012 of the mouth of the Yantra River and its surrounding area (Google Earth): At the Tash Bair to the west, the medieval rampart (site 1; see arrow) and the quarter-circle double ditch (site 3; see arrow) at the south slope are very good visible. To the east, the old Yantra meanders stand out very well. The village of Novgrad is situated on the eastern terrace (figure by S. Conrad, on the base of a Google Earth satellite image)

2.4. THE AIMS OF THE RESEARCH PROJECT AT THE TASH BAIR

In the course of the landscape archaeological research on the Lower Yantra 1997–2001, the lack of intensively explored sites apart from the limes fortifications became increasingly noticeable and a hindrance to the detailed description of the settlement processes. There were only a few reference points to classify the results. One of the few find areas that could be explored more intensively was an extensive, multi-periodically settled site on the southern lower slope of the Tash Bair, on the western edge of the Yantra mouth plain. On the one hand, it was especially remarkable due to its overall size and the richness of finds from the L ate Neolithic, Bronze and Iron Ages; and Roman period; as well as the Early Middle Ages. The latter is characterised by a 200 × 200 m rampart which is still visible on the surface today. On the other hand, the site occupied an outstanding location near the old meander of the Yantra and the old confluence of the Studena Reka stream.

During previous investigations in 2001, a section of this site could be explored with geomagnetic prospections on 2.5 ha and a grid survey on 5,37 ha. It could be stated that the site held a key position in the prehistoric and early historical settlement systems on the Lower Yantra as well as in the culture transfer across the Danube (Krauß 2006a, 146–157). Other sites that have only recently been discovered in satellite images are also part of this complex find area. This includes a site with a double quarter-circle ditch (site 3) and a ditch that separates the spur of the Tash Bair from the ridge itself (fig. 4; 5).

Certainly, this concentration of sites at Tash Bair did not accidentally emerge on the striking ridge of the Tash Bair. In the approximately 20 km long section between Svishtov and the Yantra estuary, the



Fig. 5. Satellite picture of 2018 with similar image section like fig. 4 (Google Earth). The ditch which cuts the spur of the Tash Bair (site 4; see arrow) is visible as a dark green line (figure by S. Conrad)

Danube reaches the southernmost point of its overall course. The high terrace of the Danube protruding on the north bank of the Danube near Zimnicea close to the main arm facilitates crossing at this point. The Romans paid special attention to the geostrategic importance of this section of the river by setting up the Novae legionary camp near Svishtov. However, as the sources report, this could not prevent the crossing of at least part of the Gothic troops under Kniva in the year 250 (Kolendo 2008). In 1877, the Russian army chose this point as the most suitable place for translation during the Russo-Turkish War (Lemke 2015, 133–134).

The direct access to the river and the location on the road along the Yantra valley that led to the Balkan passes give the Tash Bair a strategic position at the crossroads of supra-regional exchange and trade. In this context, the ambivalence of the Lower Danube as a transport and communication route, as well as a natural barrier through the ages is worth emphasising. At the same time, this touches on the question of whether the Danube is to be regarded as a border between cultures at certain times and to what extent it was permeable.

Within the framework of the project, the possible position and function of the individual sites in the settlement systems on the Lower Yantra was to be examined, as well as focussing on the questions of continuity and discontinuity. Furthermore, a substantial contribution to the investigation of the Roman Imperial and Late Roman defence systems at the mouth of the Yantra and the classification of the Iatrus fort could be expected.

The investigations at the Tash Bair should be carried out through a combination of different methods, since large-scale excavations are excluded due to resource-technical and logistical reasons, as well as due to the extensive agricultural use (cf. chapter 5 in this volume). A survey and an excavation

campaign were carried out in both 2018 and 2019 headed by L. Vagalinski (L. Traykova as vice-head, both NAIM–BAS) from the Bulgarian side and S. Conrad and R. Krauß from the German side (both Institute for Prehistory and Archaeology of the Middle Ages of the University of Tübingen). In 2020, the finds were finally processed.

During our investigations, the originally intended focus on the period from the pre-Roman Iron Age to the Late Roman period has been significantly expanded. This expansion was due to the gaining of substantial results on basic questions for older and younger periods from the beginning, for example for the Bronze Age and the Early Middle Ages. Furthermore, the research area, which should be limited to the Tash Bair and its immediate vicinity, was extended to the entire southern part of the mouth plain due to a necessary change in the work plan. The intensive survey planned on site 1 could not be carried out because agricultural tillage began in 2019 due to the warm weather already at the end of February. This change made surprising new discoveries about the settlement in the Yantra lowlands possible.

The direct access to the river, which is nowadays cut off by siltation, is assumed to be one of the constitutive reasons for the formation of the site concentration at Tash Bair. Investigations of the landscape and river history carried out in the area of the Yantra mouth plain by specialists of geomorphology from the KU Leuven (Belgium) should therefore contribute to the reconstruction of the former environmental conditions and help gain a better understanding of the choice and development of settlement sites on the Lower Yantra. In the course of the project, the interdisciplinary range of methods proved to be suitable for investigating the multifactorial causes for the formation and demise of the extensive site complex at Tash Bair.

ИСТОРИЯ НА ПРОУЧВАНИЯТА И ЦЕЛИ НА ПРОЕКТА

Свен Конрад, Райко Краус

(Резюме)

Българо-немското изследователско сътрудничество в района около устието на р. Янтра започва през 1958 г. Тогава започват разкопките в късноримския кастел „Ятрус“ като съвместен проект на Националния археологически институт с музей (Българска академия на науките) и Института за гръко-римска античност (Академия на науките на ГДР), които продължават до 1981 г. Тези разкопки се възобновяват през 1992 г. и продължават до 2000 г. с Римско-германската комисия (във Франкфурт на Майн) на Немския археологически институт като немски партньор. Приблизително 40% от площта на кастела е разкопана. Налице са многобройни немски и български публикации с резултати от археологическото проучване на „Ятрус“. Те са задължително четиво за всеки, който се интересува от историята на Долен Дунав през Късната античност и Ранното средновековие.

За да се разбере мястото на „Ятрус“ и на легионерския лагер „Нове“ (край гр. Свищов) в околния район, в периода 1998 – 2001 г. бе проведен интердисциплинарен изследователски проект, финансиран от Немската изследователска фондация. Извършени бяха мащабни като проучена площ теренни издирвания. Те бяха обогатени с геофизични изследвания и въздушно заснемане. Първоначално фокусът беше върху периода между късната желязна епоха и Средновековието, но добрите резултати наложиха да се включи и най-дългата епоха на човешката история – праисторията. Така стана възможно да се представи историята на един долнодунавски район от неолита до ново време.

В хода на изпълнение на проекта от 1998 – 2001 г. се усети липсата на проучени археологически обекти във вътрешността на избрания район (около устието на Янтра), извън римските укрепления по Дунав. Много перспективен в това отношение е микрорайонът в долния, южен

склон на възвишението Таш баир, в землището на с. Новград. Тук е регистрирано обитаване от късния неолит до Ранното средновековие. Последното е представено и чрез дървено-землено укрепление с размери 200 × 200 м. То е имало непосредствен достъп до реките Студена и Янтра, което му осигурявало стратегически контрол върху пътища, свързвали Дунав и вътрешността на юг към Стара планина. Евентуално детайлно археологическо изследване на този микрорайон би обогатило знанията ни за Дунав като естествена природна граница, но и като важна транспортна връзка за обмен на културни постижения. Новият проект набляга върху функцията на отделните селища в Таш баир през различните епохи. Акцентира се върху въпросите за културно-историческа приемственост и дисконтинуитет. Същевременно се цели обогатяване на информацията за късноримската отбранителна система около устието на Янтра и мястото на „Ятрус“ в нея.

Предвидено беше археологическите проучвания на Таш баир да се извършват чрез комбинация от различни методи, тъй като мащабните разкопки са изключени поради ресурсно-технически и логистични причини, както и поради екстензивното селскостопанско използване. През 2018 и 2019 г. бяха извършени теренни издирвания и разкопки. Находките бяха окончателно обработени през 2020 г.

3. ENVIRONMENTAL CONDITIONS IN THE STUDY AREA

Andreas López del Olmo, Raiko Krauß, Sven Conrad

3.1. REGIONAL SETTING OF THE STUDY AREA

The working area is located approximately in the middle of northern Bulgaria on the Lower Danube, which, coming from the Danube Gorges (Iron Gates), initially crosses the lowlands between the Carpathians and the Balkans in a west-east direction (fig. 1). Over a distance of 471.5 km, it forms both a natural and a geographical border between Bulgaria and Romania (Grecu et al. 2017; ICPDR Bulgaria 2020; Shishkov, Kolev 2014a) by dividing Walachia from the North Bulgarian lowlands.

East of the confluence of the Lom river near Ruse, the Danube turns to the northeast, where it separates the Dobrudzha from Wallachia in the shape of a wide arc. After a sharp turn to the east, the Danube forks into several arms that form a huge river delta flowing into the Black Sea (Enciu 2010; Lóczy 2007).

The working area is located on the western edge of the alluvial plain of the Yantra River, approximately 4.5 km southwest of its confluence with the Danube. Around this point, the Danube reaches the southernmost point of its entire course.

The work area at the Tash Bair is characterised by a remarkable, even unique, geographical situation. A ridge which is part of the northern Bulgarian hill country, runs alongside the Danube and ends in a spur that advances to the northeast into the alluvial plain of the Danube. This ridge is known as the Tash Bair (turkish; 'stone ridge'). The origin of the name, which dates to the time of Ottoman rule, is not yet known. Towards the end of the spur, its height drops from 110 m to 90 m a.s.l. Apart from the narrow land bridge of the ridge, the spur is surrounded on all sides by steep slopes. In the southwest, the Tash Bair is separated by a wide erosion valley, initially long and steep before moderately descending at the south-facing slope towards the Studena Reka valley.

In the alluvial plain of the Yantra, to the east and north of the Tash Bair, partially silted up meanders (palaeo-meanders) are noticeable especially due to the reeds. After entering the plain from the northeast, the current channel of the Yantra turns immediately northward, towards the Danube.

Regarding the modern administrative division, the working area is located in the western part of the boundary of the Novgrad village. Its western border roughly coincides with the border between the Ruse and Veliko Tarnovo regions.

3.2. RECENT GEOLOGICAL TECTONIC EVOLUTION

The modern relief of the Wallachian and Danubian Plain is the result of: the infill of the Dacian Basin between the Late Eocene (34 Ma) and the upper part of the Miocene (5 Ma), slow vertical movements, neotectonic faulting, and river activity (Jipa, Olariu 2009a; Zagorchev 2009). Both Cenozoic Plains are relative recent planation surfaces, developed on top of a rigid Precambian-Paleozoic socle (the Moesian Platform) (Armaş et al. 2019; Evlogiev, Enciu 2001; Haas 2012; Jipa, Olariu 2009b). The Danubian Plain was covered by thin Miocene-Pliocene marine deposits as compared to the thick deposits in the central part of the Wallachian Plain (Tari et al. 1997).

The timing and evolution of the Lower Danube formation is still under debate. According to Olariu et al. (2018) and Jipa (2014), the transition of the Dacian Basin towards a fluvial system dates to 4 Ma. Alternatively, according to Enciu (2010), first fluvial sediments were deposited by

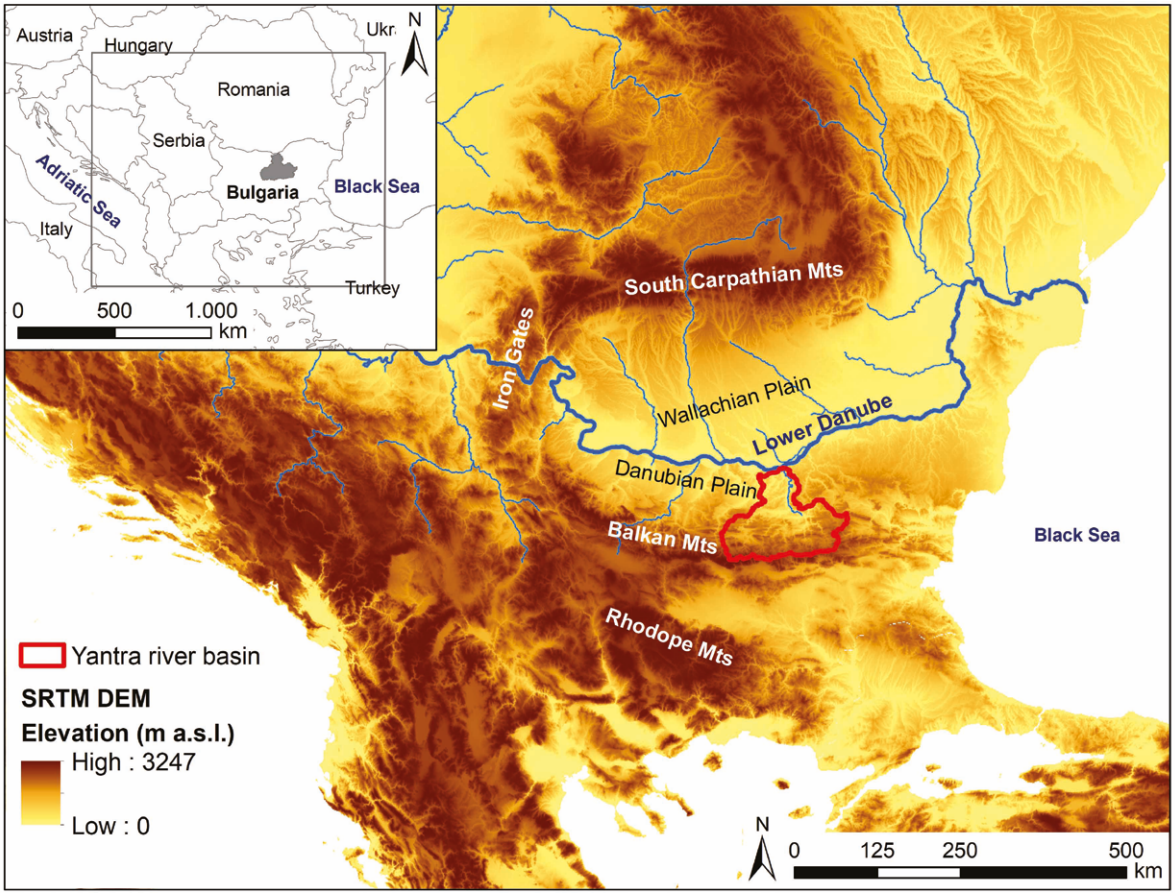


Fig. 1. SRTM DEM of South-Eastern Europe (spatial resolution of 30 m). The most important mountain ranges, rivers, plains, and the Yantra River basin are indicated (processing of DEM Europe, Danube EU-Hydro from ArcGIS online) (figure by A. López del Olmo)

the palaeo-Lower Danube during the Upper Pliocene (2.6 Ma). The gradual infill of the basin, the Wallachian uplift of the South-Western Carpathians and their foreland during the Pleistocene and a global decrease in sea level, associated with a general cooling of the Northern hemisphere around 2.5 Ma led to a withdrawal of the Dacian Basin (Armaş et al. 2019; Enciu 2010). The Danube kept on branching out towards the current location of the Black Sea, while the extent of the Black Sea further retreated (Enciu 2010).

Since the Middle Pleistocene (about 900 ka), climatologically driven aggradation-incision cycles occurred along the Lower Danube. The Danube incised during stadial periods (cold glacial periods) into: the thick layered Late Miocene, Early Pliocene sediments of the Dacian basin in the Wallachian Plain, and into shallow subsurface Paleogene to Mesozoic deposits of the Moesian Platform of the Danubian Plain (Armaş et al. 2019; Enciu 2010; Shishkov, Kolev 2014a).

3.3. GEOMORPHOLOGIC EVOLUTION

As the geomorphological map of Central-North Bulgaria (fig. 2; cf. Evlogiev, Enciu 2001), constructed after the lithostratigraphic investigations between 1998–1999 shows, the relief in the surroundings of the study area varies between 20 – 250 m a.s.l. North of the Danube, the elevation of the relief decreases in a step-like manner from 110 m a.s.l. (20 km north of the Danube) towards 20 m a.s.l. adjacent to the Danube (Evlogiev in prep.; Evlogiev, Enciu 2001).

The contemporary plateaus which surround the study area, were formed during the Pliocene. They are interpreted as the continental Pliocene denudation surface (PDS), located to the south of the Dacian Basin (which occupied the lowest parts of the Wallachian plain until 0.82 Ma) (Evlogiev

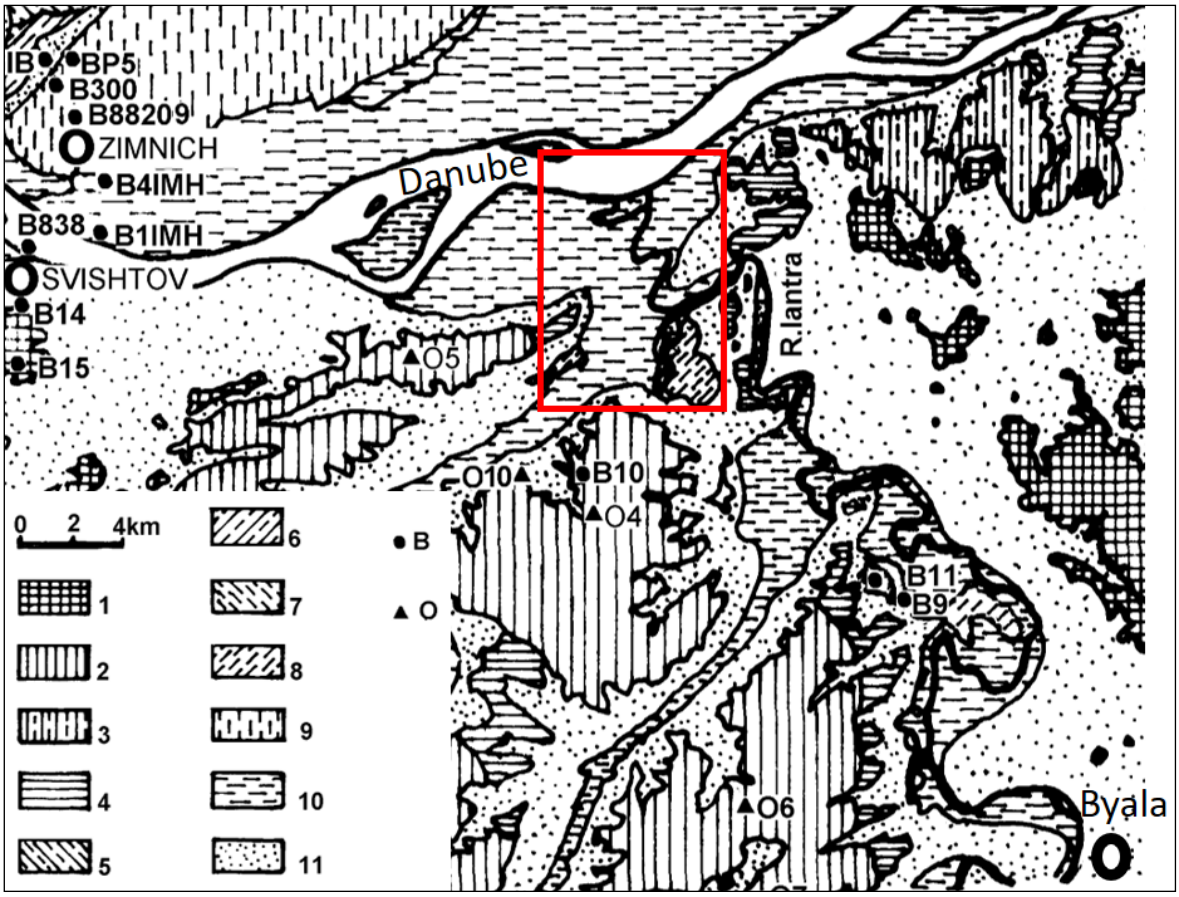


Fig. 2. Section of the geomorphological map of Central-North Bulgaria and South Romania (section 607–520 km along the Danube), with the study area indicated by the red rectangle (adapted from Evlogiev, Enciu 2001). 1 – Pliocene denudation surface (PDS); 2 – Old erosion-accumulation level (OEAL); 3 – Old abrasion-accumulation level (OAAL); 4 – Six-layer loess terrace (T6); 5 – Five-layer loess terrace (T5); 6 – Four-layer loess terrace (T4); 7 – Three-layer loess terrace (T3); 8 – Two-layer loess terrace (T2); 9 – Single-layer loess terrace (T1); 10 – Low flooded terrace (To); 11 – Erosion slopes with gulches; B – boreholes; O – outcrop; O4 – Karamanovo; O5 – Vardim; O6 – Bosilkovtsi

2007). As a result of the Pleistocene ice ages, a thick loess packet consisting of eight loess horizons and seven buried soils were formed on top of the Pliocene denudation surface. Loess packets were deposited during glacial periods (cold and dry) and soils developed during interglacial periods (warmer and wetter periods) (Минков 1968; Evlogiev in prep.). An old erosional-accumulative level (OEAL) was formed at an elevation of 110 m a.s.l. in Cretaceous (marls, clays, sandstones and limestones) and Pliocene (sands and clays) sediments (Evlogiev in prep.; Evlogiev, Enciu 2001). These OEALs are found west and south of the study area (fig. 2).

The climate fluctuations since the Middle Pleistocene (900 ka) have had a particular influence on the water levels of the Black Sea (Krauß 2006a). These changes in Black Sea water levels initiated the development of river terraces along the Danube and its tributaries, through a gradual incision of the rivers in the Pliocene denudation surface. Six former river terraces have been identified at 1–2 m, 5–7 m, 15–18 m, 30–35 m, 55–60 m, and 90–100 m above the current water level (Krauß 2006a and references therein). Terrace formations differ significantly between the Romanian and Bulgarian side of the Danube. Along the Romanian side, terraces T0 (current alluvial plain, located directly adjacent of the Danube), T1, T4, T5 and T6 (most remote river terrace in the area) have been established. The succession from old towards younger river terraces towards the south in Romania indicate a southward migration of the Danube. In Bulgaria only T0, T1 and T2 have been established as Danubian terraces. T5 and T6 have been observed in the valleys of the Yantra, Barata and Osam rivers (Evlogiev, Enciu 2001).

Differential positive neo-tectonic movement (uplift) during the Early to Middle Pleistocene has been deduced from a difference in elevation of the OEAL and T6 between the Romanian and Bulgarian side of the Danube. During the formation of T5, T4, T2, T1 and T0 neo-tectonic movements were uniform on both sides of the Danube (Evlogiev, Enciu 2001).

The study area, indicated by the red rectangle in Fig. 2 comprises the contemporary alluvial plain T0, remnants of the two-layer loess terrace (T2) in the southwest and southeast of the study area and erosion slopes with gulches on the adjacent hill slopes. As seen in figure 2, the area where the fieldwork has been carried out is entirely located in the Holocene alluvial plain (T0).

3.4. SOILS AND GEOLOGY

North Bulgaria represents the southernmost location in Europe where loess (= aeolian silt) was deposited during Pleistocene glaciation periods (Haase et al. 2007; Fitzsimmons et al. 2012). These loess deposits function as important palaeo-environmental records of South-Eastern Europe (Fitzsimmons, Hambach 2014; Jipa 2014). As already mentioned above, they comprise several well preserved palaeo-soil sequences, which reflect glacial-interglacial periods (Fitzsimmons, Hambach 2014; Fitzsimmons et al. 2012; Jipa 2014). The study area is located near the Danube where loess deposits cover Neogene and Cretaceous deposits of the Wallachian and Danubian Plain (fig. 3). The Danube played a primary role in transporting fluvial silts from its headwaters towards the Lower Danube region where it subsequently became a source of fluvial silts which were further transported towards the south through a bimodal NW-NE palaeo-wind direction (Evlogiev 2007; Fitzsimmons, Hambach 2014; Jipa 2014). Y. Evlogiev

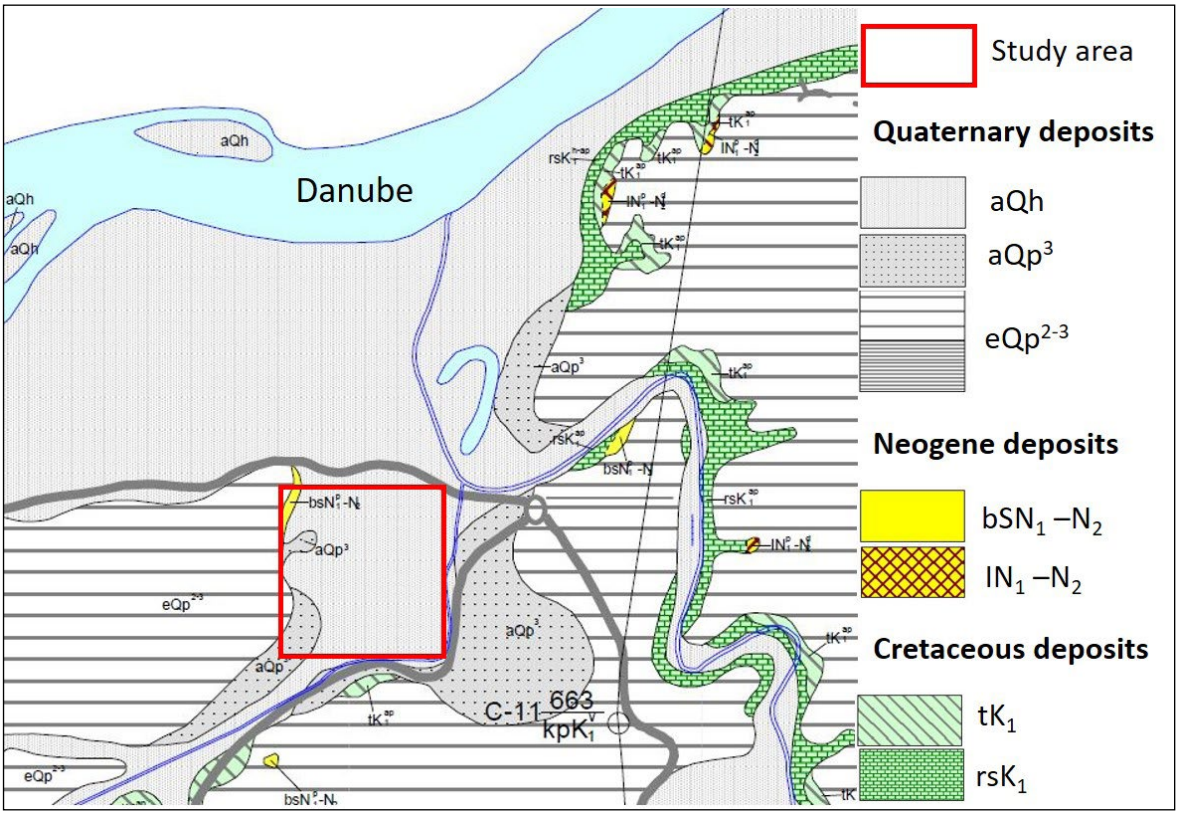


Fig. 3. Section of the geological map of Bulgaria K-35-16 (Byala) for the study area, scale 1:100 000 (adapted from Филипов 1992). aQh – alluvial deposits (river-bed and flood-plain deposits), aQp3 – upper Pleistocene alluvial deposits of 1st and 2nd terraces above the flood plain, eQp2-3 – loess cover, bsN1 -N2 – the Byala Slatina formation (sands with interbeds and lenses of pebble and clays of Pontian-Pliocene age), IN1 -N2 – the Aidemir and Sarpovo formation, consisting of white to rusty sands or green -grey sandy banded clays,tK1 – the Trambesh Formation (marls with interbeds of limestones and sandstones of Aptian age), rsK1 – the Ruse Formation (Aoolitic, organogenic and detrital limestones of Aptian age)

(2007) highlights the role of the paleo-Danube and of the parched Dacian lacustrine fluvial basin. Additionally, the significance of the dry Black Sea continental shelf during glacial periods and more remote regions as important loess deflation areas are also discussed.

Loess deposit thicknesses along the Lower Danube are typically highly variable (Fitzsimmons, Hambach 2014). They are on average 55 m thick near the Danube and diminish to less than 10 m towards the south of morphostructural zone A (Stoyanov, Gachev 2012; Iovita et al. 2014; Jipa 2014; Shishkov, Kolev 2014a; Grecu et al. 2015). Loess deposits are indicated on the geological map of Byala with eQp2-3 (fig. 3) (Филипов 1992).

The main soil type in the Bulgarian Danubian lowlands (morphostructural zone A) are chernozems. They are very fertile and typically develop in the Pleistocene loess deposits (Krauß 2006a, 34–36; Shishkov, Kolev 2014a). Chernozems have a thick A-horizon, a high base saturation (>85%), a good structure and a high water-holding capacity. Main processes in chernozems are humification, leaching and seasonal migration of soluble minerals (Shishkov, Kolev 2014b).

Main developed soil horizons in chernozems are: A, B and C horizon (fig. 5). The A horizon is a homogeneous dark greyish brown horizon with a 40–80 cm thickness where organic matter accumulates. The A horizon often gradually changes into the B horizon. This transition zone is sometimes indicated as the AB horizon. The B horizon is a mineral metamorphic horizon. It has a dark brownish to dark yellowish colour. Sometimes, pseudo-mycelia threads and carbonate like concretions accumulate as secondary carbonate features in the upper part of this layer. The lower part of this horizon has often lesser pseudo mycelia threads and is richer in carbonate concretions. The Ck horizon has a brown to yellowish brown colour. This horizon is considered as parent material with a major accumulation of secondary carbonates and the formation of concretions (Shishkov, Kolev 2014c).

A relevant section of the soil map of Bulgaria (Койнов et al. 1968), scale 1:400.000, is presented in Fig. 4. Most of the soils in the study area are classified as loamy calcareous chernozems (code 1) or eroded chernozems (code 38). Soils in the study area (indicated by the red rectangle) are classified as "alluvial and alluvial-meadow, sandy and loamy" soils (code 31). However, according to the soil map all the soils in the entire study area would be salinised (combination of classification codes 31 and 37). Contrary, according to Krauß (2006a) and Evlogiev (in prep.) only the soils at the confluence of the Studena Reka valley and the alluvial plain of the Yantra are salinised (southwestern part of the study area). This was proved by the geomorphological investigation, where there was a visual indication for

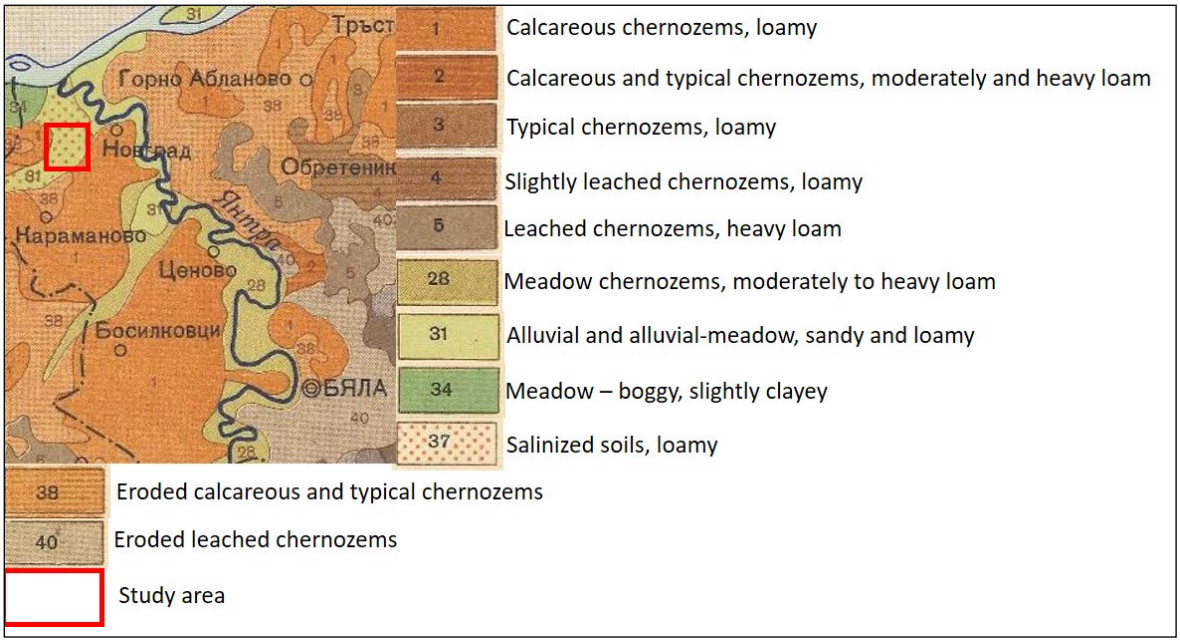


Fig. 4. Soil map for the study area, scale 1:400 000 (adapted from Койнов et al. 1968)

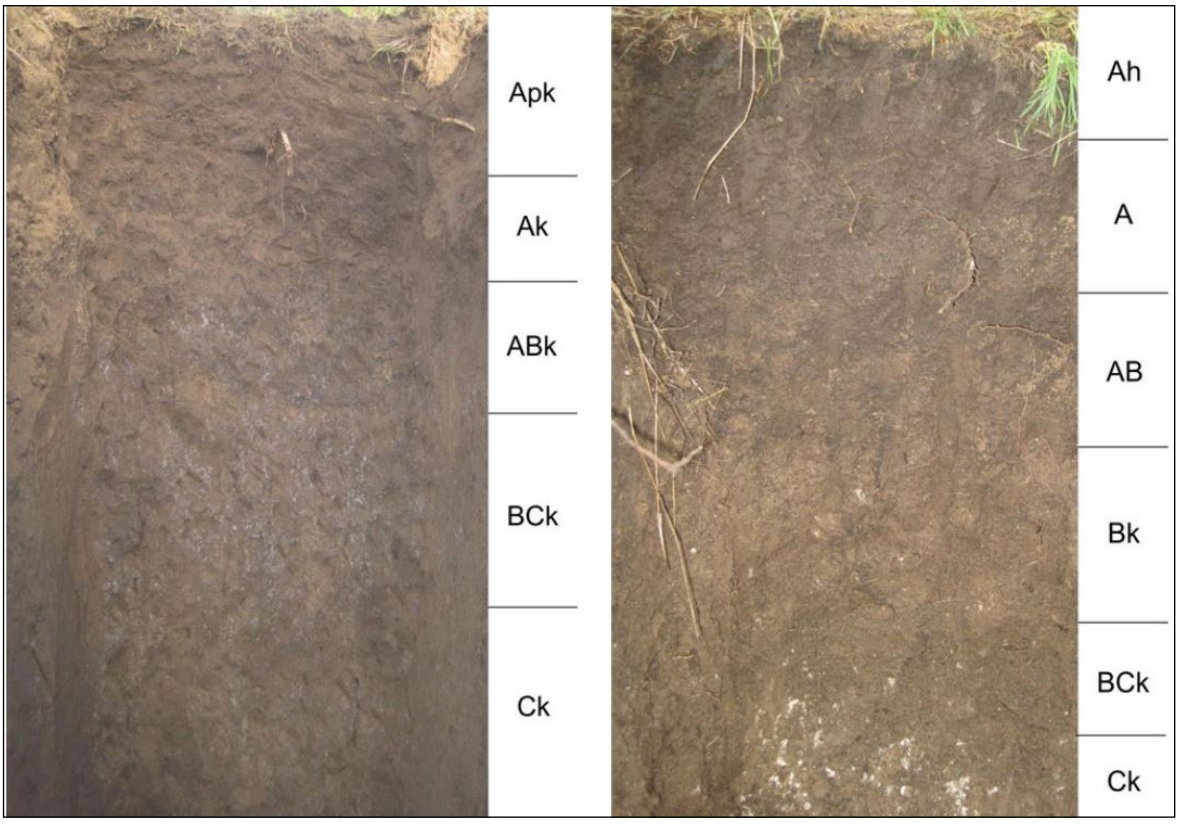


Fig. 5. Different recognised soil horizons in a typical chernozem soil. With left a calcareous chernozem (Epicalcic Chernozem Siltic) and right a leached chernozem soil (Endocalcic Chernozem Siltic) (Shishkov, Kolev 2014c)

high salt concentrations only at coring T1C23 to T1C32 (salt crystals in the upper 3 m of the cores) (cf. the contributions by A. López del Olmo et al., chapter 4).

In any case, the loess cover is very susceptible to erosion processes of all kinds. As was shown in the investigations into the development of the floodplain of the Yantra, the floodplain aggraded up to three meters even before the introduction of agriculture. The processes of erosion have been accelerated by the intensification of agriculture and the decline in forest cover, especially since the Early Iron Age. The increased sediment load of the Yantra and its tributaries was likely responsible for an increase in floodplain aggradation and abandonment of the meanders (cf. the contributions by A. López del Olmo et al., chapter 4).

In 2012, the extent of erosion in the Loess region was investigated in a project that was carried out by a working group of the KU Leuven in the Batinsko dere near Obretenik, i.e. approximately 20 km southeast of our current work area. According to Laura Scheere (2013, 63–64 fig. 28), the soil erosion rate here is between 0.18 ± 0.02 t/ha/year and 3.53 ± 0.4 t/ha/year, which corresponds to an erosion between 12 ± 1,2 mm/1000 years and 235 ± 25 mm/1000 years. Similar values were also found by M. Verhasselt (2013, 67–70). According to these investigations, the erosion accelerated in the Late Iron Age; however, most of the erosion began in the Early Middle Ages.

Deflation processes are an important component of erosion, the extent and impact of which are often underestimated. In particular, the loess regions of northern Bulgaria, including the working area, are threatened by wind erosion (Кукуларов, Нинов 1979; Алексиев 2002, 79).

The study area is located in the alluvial plain of the Yantra. As expected, this area is indicated as alluvial deposits (aQh) in Fig. 3). Upper Pleistocene alluvial deposits of 1st and 2nd terraces above the alluvial plain are situated near the study area, indicated as aQp3 (fig. 3). Due to the incision of the Yantra River in the Danubian Plain since the Middle Pleistocene, outcrops of Neogene sands (bSN1 -N2 and

In1 -N2) and Mesozoic limestone rocks (tk1 and rsK1 formations) occur at the valley borders (fig. 3) (Филипов 1992).

3.5. MORPHOSTRUCTURAL ZONES A-C

The Yantra flows from south to north through three morphostructural zones (fig. 6). Each zone has specific characteristics concerning relief, geology, river morphology and current land cover. The different morphostructural zones strongly affect the river-valley network of the Yantra (Nikolova, Nikolov 2011). Each morphostructural zone has special characteristics in the landscape along the river (fig. 8–10).

The first zone (B2) is located in the most upstream part of the Yantra River, the Balkan Mountains. This zone is characterised by a strong relief with steep slopes and deeply incised rivers (Nikolova, Nikolov 2011; Stoyanov, Gachev 2012). Land cover mainly consisted of forest in 2018 (fig. 7). The river flows through the Fore-Balkans or Pre-Balkans (zone B1). This upland zone is characterised by a moderate mountainous relief. Slopes become gentler and the lower parts of the valley widen (Stoyanov, Gachev 2012). The Pre-Balkans consist of folded Mesozoic rocks, which express the geological structure through ridges which run perpendicular to subsequent river valleys (Embleton 1984). Steep sections are covered with forest, while the flatter valleys are cultivated (fig. 7). Finally, the Yantra flows through the Central Danubian Plain (zone A) (Nedkov et al. 2007; Nikolova, Nikolov 2011; Shishkov, Kolev 2014a). During the Quaternary, tributaries of the Danube incised into the Mesozoic, partly Neogene limestone plateau, resulting in dissected flat ridges and asymmetric large valleys of meandering rivers south of the Danube (Shishkov, Kolev 2014a). In this zone, altitudes range between 18 to 400 m (Embleton 1984). West of the Yantra, land cover in zone A mainly consists of intensively cultivated agricultural land. Some small built-up areas are located in this zone (representing small rural villages) (fig. 7). East of the Yantra, the Mesozoic, partly Neogene limestone plateau changes into a dome-shaped plateau (Embleton 1984; Krauß 2006a; Stoyanov, Gachev 2012). This area is more forested and has less cultivated agricultural land cover, as compared to the area west of the Yantra (fig. 7).

The river basin of the Yantra has a peculiar triangular shape (fig. 6). The southern part of the basin is wide, while it becomes narrower towards the lower river course. The basin morphology, together

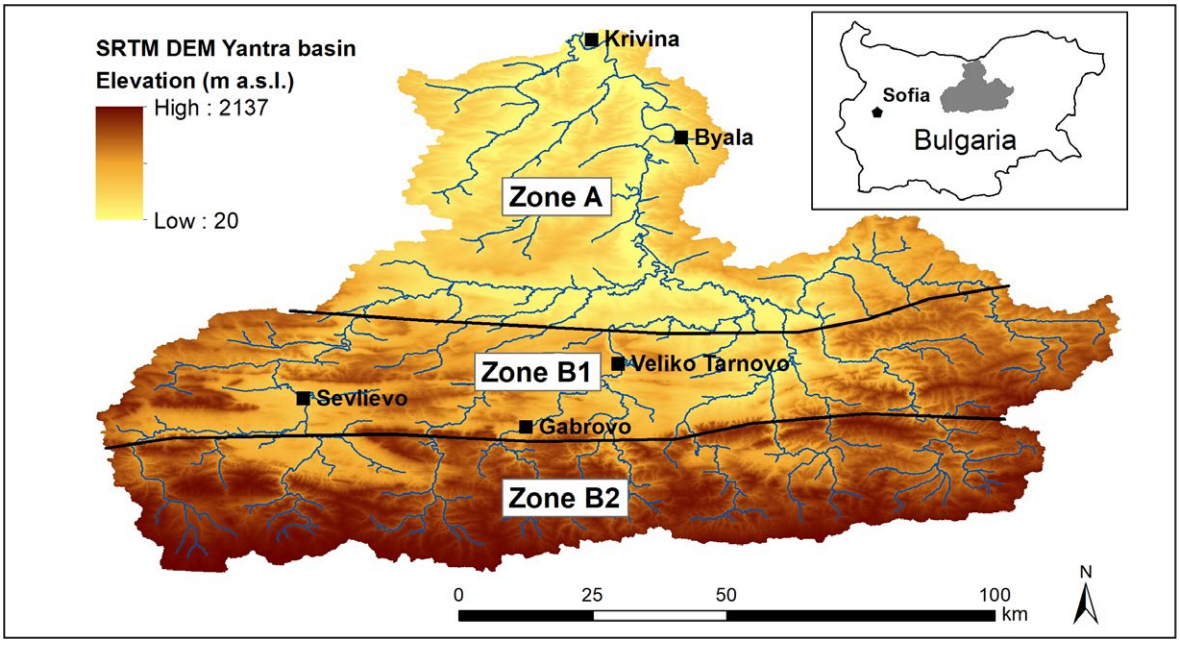


Fig. 6. Morphostructural zones in the Yantra River basin with: zone A representing the Danubian Plain (or Moesian Platform), zone B1 the Fore-Balkan (or Pre-Balkan) and zone B2 the Balkan mountain ridge (or the Balkans) (processing of DEM Europe from ArcGIS online, based on Nedkov et al. 2007; Nikolova, Nikolov 2011, processed by A. López del Olmo)

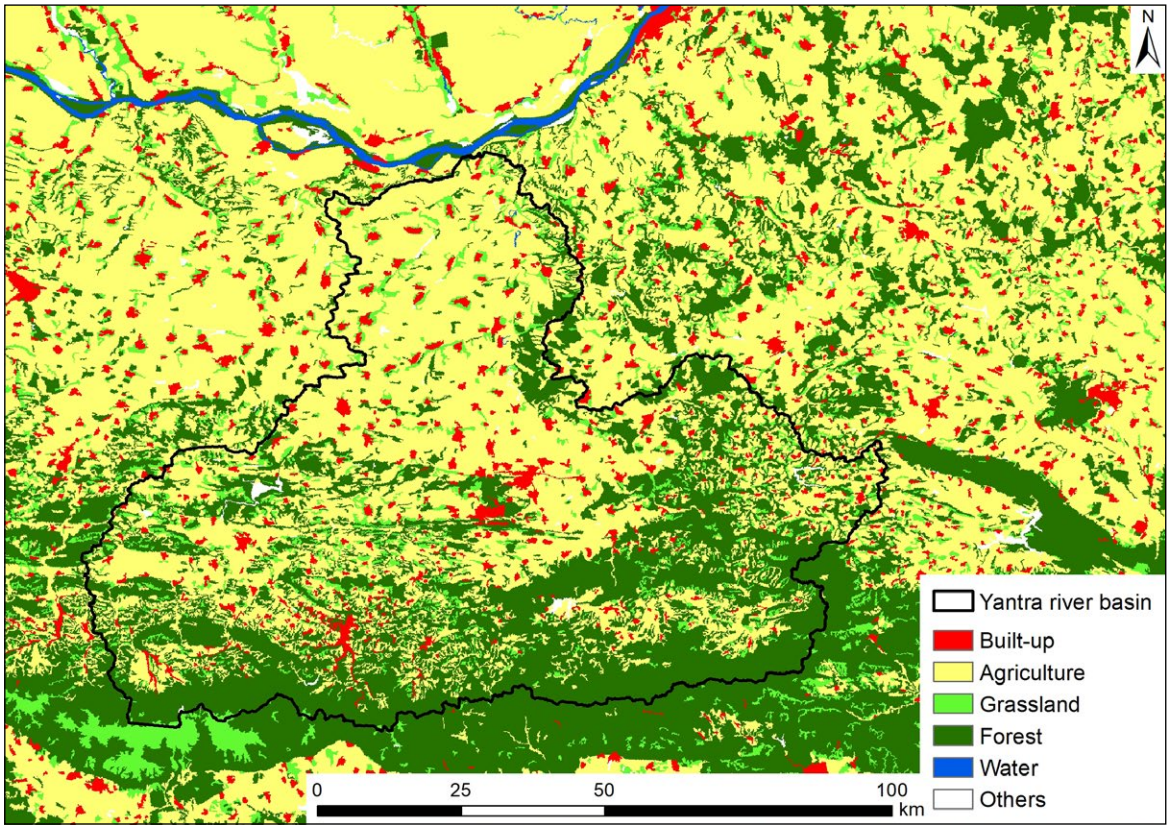


Fig. 7. Land cover map of 2018 for the Yantra River basin with pixel resolution of 100 m (CORINE land cover data from Copernicus, 2018, processed by A. López del Olmo)



Fig. 8. Main ridge of the Balkan mountain range (Kupena peak, 2169 m) in morphostructural zone B2 in Central Bulgaria (Stoyanov, Gachev, 2012)



Fig. 9. Yantra River at Veliko Tarnovo in morphostructural zone B1 (figure by A. López del Olmo)



Fig. 10. Left picture shows the characteristic undulating relief of the Danubian Plain in morphostructural zone A, near Beltsov, Northern Bulgaria. Right picture visualises the Lower Yantra River, incised in the Mesozoic-Neogene limestone plateau at about 5 km stream upwards of the confluence of the Yantra with the Danube (figure by A. López del Olmo)

with the relief, geology, soils, and land cover are conditions which have an influence on surface runoff. Water concentrates in the middle course of the Yantra where it develops considerable power and creates major flood-related hazards (Nedkov et al. 2007; Nikolova, Nikolov 2011).

3.6. HYDROGRAPHIC CONDITIONS IN THE STUDY AREA AND ITS SURROUNDINGS

The Yantra River basin (indicated in red in fig. 1) covers an area of about 7862 km^2, making it the second largest river basin (after the Iskar) in north Bulgaria (ICPDR Flood Protection Expert Group 2009; NEWADA 2012). The source of the Yantra (with coordinates 42° 44' 05" N, 25° 25' 10" E) is located in the Balkan Mountains, at the foot of the mountain peak Hadzhi Dimitar at 1340 m a.s.l.

After 285 km, the Yantra River converges into the Danube at an altitude of 18 m a.s.l., near the village of Krivina. The average river gradient is 4.6‰ for the main river (ICPDR Flood Protection Expert Group 2009; Nikolova, Nikolov 2011). The mean annual discharge at the confluence of the Yantra with the Danube is estimated at 47.1 m^3/s or 49.83 m^3/s by different authors (Bojilova 2017; Nedkov et al. 2007; Nikolova, Nikolov 2011; Popov et al. 2003). From its source, the Yantra runs through three morphostructural zones (fig. 6).

In its course, the Yantra absorbs the water of numerous smaller and some larger tributaries that arise in the surrounding hills or on the edge of the plateaus. The largest tributary is the Rositsa, which flows into the Yantra at the village of Krusheto about 45 km upstream as the crow flies.

Along the Danube and on the middle and lower course of the Yantra, numerous dikes were built, and river straightening was carried out in the 20th century. In addition, the lowlands on both sides of the Danube were traversed by a dense network of channels for drainage, which enabled agricultural use of the area, but influenced the water balance to a considerable extent (Krauß 2006a, 36 f.). At the Yantra confluence area, the wide valley of the Studena Reka connects from the south-westerly direction. Nowadays it is not more than a small stream which is channelled and flows into the Yantra near Novgrad.

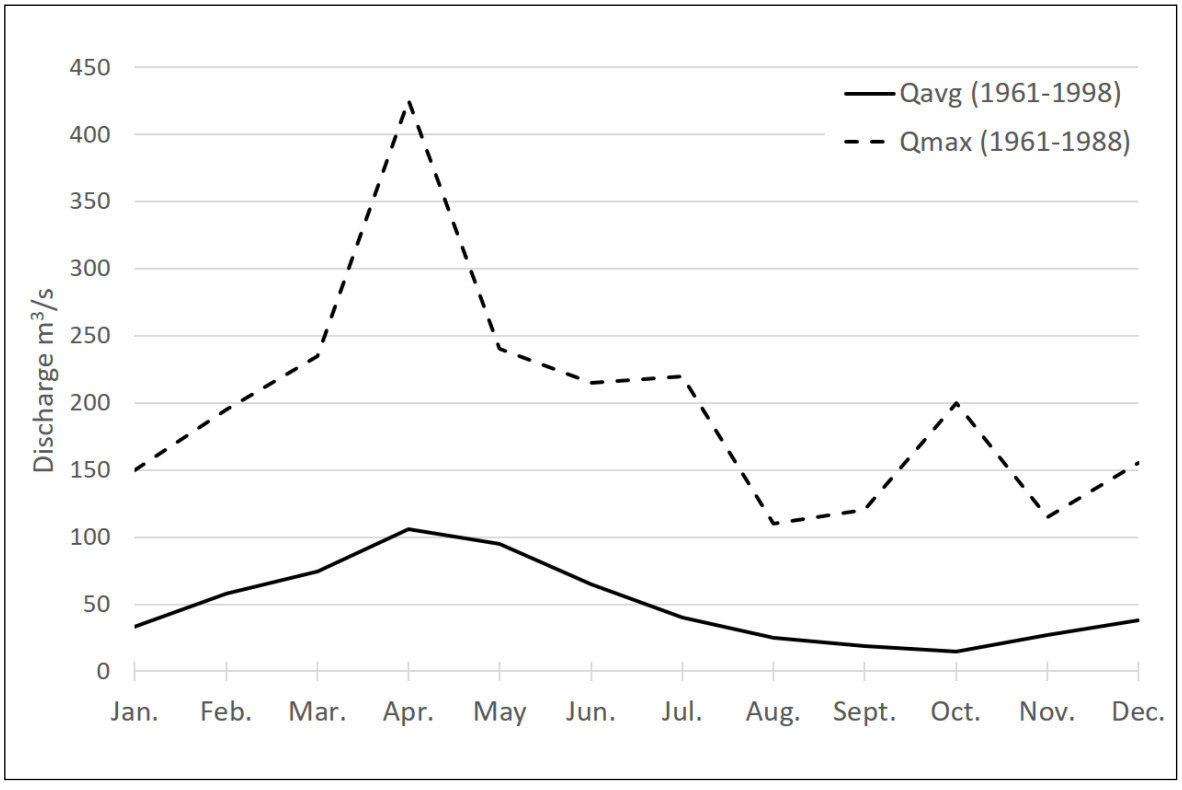


Fig. 11. Modelled annual distribution of the monthly average discharge (Qavg), for reference period 1961–1998 and the monthly average maximum discharge (Qmax), for reference period 1961–1988 for the Yantra outlet (adapted from Nikolova, Nikolov 2011)

Due to a temperate continental climate, monthly average discharges of the Yantra fluctuate strongly between different seasons (fig. 11). Discharges are typically highest in spring, caused by snowmelt in the mountains and simultaneous rainfall events (ICPDR Flood Protection Expert Group 2009). Although discharges are generally low during summer and autumn, intensive convective thunderstorms may cause high discharge events with a short duration (Bojilova 2017). However, typically 50% of the annual outflow of the Yantra is recorded between March and June and even 80 to 85% of the annual outflow is recorded between November and June (Bojilova 2017; ICPDR Flood Protection Expert Group 2009; Nikolova, Nikolov 2011).

The Yantra presumably carried much more water in larger periods of time during the late Holocene, especially during the summer months. It is assumed that the city of Nicopolis ad Istrum was at least temporarily accessible by river barges via the Yantra and Rositsa during Roman times (Krauß 2006a, 37; cf. literature cited there). In the area of Byala, there are still remnants of landing stages from the Early Modern period (N. Nenov, Ruse; *pers. comm.*); the river has not been navigable here for a long time either.

3.7. THE CLIMATE

Current climate

The Danubian Plain is, according to the Köppen-Geiger climate classification, located in a Cfa climate zone. This corresponds to a climate which is: warm temperate, fully humid and has warm summers (Rubel, Kottek 2010). According to other classification systems, the climate in the Danubian Plain is humid continental, with warm summers or classified as a Forest-Steppe climate zone (Tomescu 2000; Howard et al. 2004; Marinova, Atanassova 2006; Peel et al. 2007; Connor et al. 2013; Shishkov, Kolev 2014a). Annual precipitation in the Danubian Plain varies between 450 and 600 mm (Nikolova, Nikolov 2011; Shishkov, Kolev 2014b; Stagl, Hattermann 2015; Fick, Hijmans 2017; Malcheva et. al. 2017). The Danubian Plain is characterised by large temperature fluctuations between the warmest month (on average 24°C in July) and the coldest month (on average -1°C in January). The average annual temperature equals 11.3°C for the reference period 1961–1990 (Nikolova, Nikolov 2011). The annual potential evapotranspiration for the Danubian Plain is estimated between 1001 and 1250 mm (Trabucco, Zomer 2019). Thus, the potential evapotranspiration largely exceeds the annual precipitation.

The climate becomes wetter and cooler towards the south of the Yantra River basin due to the influence of an increasing relief on temperature and precipitation (Niedźwiedź 2012; Shishkov, Kolev 2014a). At Veliko Tarnovo weather station, located in the Fore-Balkans, average annual temperatures decrease to 10.3°C and annual precipitation increases to 750 mm yr^{-1}. Average annual temperatures diminish further to 3.5°C for the West and Central Balkans, while precipitation increases to 1100 mm yr^{-1} (Nikolova, Nikolov 2011).

Late Glacial and Holocene climate periodisation

Detailed climate reconstructions are not available for the study area. Therefore, a general description of the climate during the Late Glacial is provided here. For the historical periods, it is supplemented by results compiled from various publications.

After the cold and dry, stable climate conditions of the Last Glacial Maximum (26–19 ka BP), a gradual deglaciation of the northern ice sheets took place due to a global temperature increasing between 19–14.7 ka BP (Perşoiu 2017). A variable climate prevailed with a general warming trend. However, warmer periods (interstadials) were interrupted by colder periods (stadials). Accelerated deglaciation took place during the warmer and wetter Bølling–Allerød interstadial (14.7 – 12.8 ka BP). This warmer period was followed by a short-lived climate deterioration (cooler and dryer) during the Younger-Dryas stadial (12.8 – 11.7 ka BP). The Younger Dryas is assumed to be the coldest and driest period during the Late Glacial/Holocene transition with a precipitation reduction of 60–65% in the East European Plain compared to present-day values (Velichko et al. 2002; Bell, Walker 2005; Perşoiu 2017).

The onset of the Holocene at 11.7 ka BP is linked to a major change in atmospheric circulation regime, resulting in a temperature rise of 10 ± 4°C (Walker et al. 2019 and references therein). The

8.2 ka BP Rapid Climate Change event (RCC) forms the boundary between Lower/Early and Middle Holocene. Although the RCC was only a short-lived event of a maximum of 400 years, it caused the most extreme climate anomaly during the Holocene, with a global cooling of about 5°C and a drought in the Near East (Weninger et al. 2006; Weninger et al. 2014). Except for the RCC around 8.2 ka BP, the Middle Holocene is marked by a climatic optimum/thermal maximum (Bell, Walker 2005).

The boundary between the Middle and Upper/Late Holocene corresponds with the 4.2 ka BP RCC event. This event reflects climate cooling at higher latitudes (about 1–2°C) and an aridification at mid- to low latitudes (Walker et al. 2012; Walker et al. 2019).

After a temporary warming at the end of the Bronze Age, around 800 BC a cooler climate with more precipitation prevailed (Lamb 1995, 146 f.). A relatively warm phase is generally assumed for the Roman Empire, which lasted until the beginning of the 4th century before a cooler period began again (Neumann 1991, 461; Patzelt 1994). From the beginning of the 3rd century until about 420/30, it is assumed that it was significantly drier than in the time before (Schmidt, Gruhle 2003, 294). This phase of a relatively dry climate lasted in southern Europe until the Early Middle Ages (Lamb 1995, 168) and was probably followed by a warmer and wetter climate during the High and Late Middle Ages (Lamb 1995, 177–185).

The so-called Little Ice Age from the beginning of the 15th to the beginning of the 19th century manifested itself in southern Europe through changeable weather with individual cold winter periods and occasional regional floods (Lamb 1995, 235 f.).

According to research by Ioan G. Petrescu (1957, 26–28), the Lower Danube was frozen over in its lower reaches for a total of 91 winters (out of 115) between 1836 and 1950, with a mean duration of 40 days. However, Hubert H. Lamb (1995, 159) assumes that the Danube was hardly frozen during the Roman Empire due to the milder climate at that time, since the bridge built by Apollodorus of Damascus near Drobeta under Traian would have been destroyed very quickly by the ice. But Lamb here underestimates the extremely stable construction of the bridge piers, and in ancient literature it is repeatedly reported that the Danube was frozen over (Hornstein 1957). A recent report notes the significant reduction in the number and the length of such events (Babić Mladenović et al. 2018, 25–28). Although in our opinion global warming may play a certain role at least in the last two decades, the authors of this report mainly attribute this to the construction of the dams Iron Gate I and Iron Gate II in the years 1964–1972 and 1977–1984, which hold back ice drift and bring warm water from the depths to the surface, delaying or preventing ice formation, particularly on the Danube in SW Romania and NW Bulgaria. Beside this, they mention the thermal and chemical pollution as possible reasons as well.

3.8. FLORA

The work area at Tash Bair and its surroundings offers a representative section of the current state of the flora in the Danubian lowlands. Of the original extensive forest cover, only the remains of oak trees are left on its north slope. In the erosion valley on the southwest side, there is a planted stock of locust trees. These areas cannot be used for agriculture. Other places that are difficult to access are covered with bushes. According to aerial photographs from 1945, the slopes of the Tash Bair mountain spur were completely deforested by that time. They were only terraced and planted with pine trees in the 1950s and 1960s.

All usable areas on the ridge of the Tash Bair and especially on its southern slope are cultivated on a large scale. This also applies to the Yantra lowlands, which are criss-crossed by the reed oxbow lakes of the former active river meanders. The extensive arable land was only created as a result of collectivisation in the 1950s and 1960s and is also formative for today's landscape. However, the currently observed ratio of arable and forest areas is likely not a result of modern agriculture but can probably be traced back to traditional intensive land use (Krauß 2006a, 40; Marinova, Krauß 2014). Pollen studies show the progressive decrease in tree pollen since the beginning of agriculture in the Neolithic (cf. Krauß 2006a, 40–45, with an overview of agricultural cultures and animal husbandry in the prehistory, and the literature cited therein).

СЪСТОЯНИЕ НА ОКОЛНАТА СРЕДА В РАЙОНА НА ИЗСЛЕДВАНЕ

Андреас Лопес дел Олмо, Райко Краус, Свен Конрад

(Резюме)

Районът на това изследване е в Северна България, в непосредствена близост до Дунав. Той се намира на западния край на алувиалната равнина на р. Янтра, на около 4,5 км югозападно от нейното вливане в р. Дунав. Местността Таш баир (от тур. ез. „каменен хълм“) има забележително географско положение. Тя се издига недалеч от долното течение на Дунав, която разделя Влашката низина от севернобългарската хълмиста Дунавска равнина. Последната е разчленена от големи долини на реки, създали хълмист релеф със стръмни склонове. Надморската височина в този регион е в диапазона от 20 до 250 м.

Северна България е най-южното място в Европа, където през плейстоценските периоди на заледяване е отложен льос (= еолианска тиня). Впоследствие тази тиня се пренася на юг чрез вятъра. Дунав играе основна роля в транспортирането на речна тиня – от изворите си към своята делта.

Таш баир попада в район, където льосовите отлагания покриват неогенски и кредни варовикови скали. Дебелината на льосовите отлагания варира от 55 м (край Дунав) до под 10 м в южния край на Дунавската българска равнина. В климатична зона Cfa (топъл, умерен климат) в плейстоценските льосови отлагания се развиват плодородни черноземни почви. Те са много подходящи за селско стопанство, но са и много податливи на ерозионни процеси.

Басейнът на р. Янтра заема площ от около 7862 км^2. След 285-и километър, при с. Кривина, р. Янтра се влива в Дунав на 18 м надморска височина. Средният наклон на реката е 4,6‰. Средният годишен отток при вливането на р. Янтра в Дунав е оценен от различни автори на 47,1 m^3/s или 49,83 m^3/s. По поречието на р. Дунав и по средното и долното течение на р. Янтра са изградени множество диги, а през XX в. е извършено изправяне на коритото на реката в отделни нейни участъци. Терените от двете страни на Дунав са пресечени от гъста мрежа от напоителни канали. Те осигуряват пълноценно селскостопанско използване на района, но оказват негативно влияние върху водния баланс. Поради умереноконтиненталния климат средномесечните вливания в р. Янтра от околни реки се колебаят силно през различните сезони. Те са най-обемни през пролетта заради топенето на снега в планините и съпътстващи ги дъждове. Въпреки че притоците са обикновено слаби през лятото и есента, интензивни дъждовни бури по това време причиняват кратковременно, но рязко покачване нивото на р. Янтра.

Климатичните условия около реката варират значително. В Дунавската равнина (близо до вливането на р. Янтра в Дунав) средната температура е 11,3°C, а годишните валежи варират между 450 – 600 mm. В района на изворите на Янтра (в Централна Стара планина) климатът е значително по-хладен и влажен. Средната температура там е 3,5°C, а годишните валежи нарастват до 1100 mm.

Таш баир и околността разполагат с представителна извадка от съвременната флора в Дунавската равнина. От някогашната гора по северния склон на хълма са запазени малки групи от дъбови дървета. Поленов анализ разкрива непрекъснато намаляване на прашец на дървета от началото на земеделието през неолита до наши дни. Според въздушни снимки от 1945 г. всички подходящи за земеделие площи и дори стръмните части от склоновете на Таш баир били напълно обезлесени. Днес районът е обект на интензивно земеделие, но стръмните склонове на Таш баир са терасирани и засадени с бор.

4. PALAEO-RIVER COURSE RECONSTRUCTION IN THE FLOODPLAIN OF THE YANTRA RIVER, NORTH-CENTRAL BULGARIA

Andreas López del Olmo, Gert Verstraeten, Nils Brothaerts

4.1. INTRODUCTION

Fresh water is crucial for human survival, like for many other animals (Kummu et al. 2011). Since ancient times, a close relationship exists between river streams and human societies (Evlogiev (in prep.); Krauß 2006a; Gurova, Bonsall 2014b; Krauß et al. 2014; Fang, Jawitz 2019). River systems across the world have been utilised by human societies as a source of drinkable water and food, for transport, delimitations of territories, and others (Kummu et al. 2011; Fang, Jawitz 2019). On the other hand, hazards and threats are associated with this close relationship. Rivers are able to transform into devastating features, flooding low laying areas and destroying everything in their path, as a result of intensive convective storms or prolonged rainfall events (Gilvear, Jefferies 2012; Fang, Jawitz 2019; ICPDR Bulgaria 2020).

Humans have changed river streams significantly over the past few thousand years. Over the past 200–300 years, modifications of river streams accelerated dramatically. This was both through direct human impact by engineering projects (e.g. dam and embankment constructions, river straightening and channelisation, river diversions via watermills, etc), and through indirect impacts by changing catchment characteristics (e.g. land use changes which disturbed sediment dynamics of river streams) (Gilvear, Jefferies 2012; Taylor 2012). An example of direct impacts is the drainage of wetlands. They have been drained massively since the Middle Ages in favour of agricultural expansion (Buijse et al. 2002; Gilvear, Jefferies 2012). The Danube, as the second longest river in Europe, has had around 80% of its length regulated, resulting in a loss of about 80% of its wetlands over the last 150 years. The drainage of the wetlands, in favour of arable land, had a severe impact on the occurrence of catastrophic floods and on pollution in the river basin (Lóczy 2007; Csagoly et al. 2016; ICPDR Wetlands 2020).

To date, little is known about the relationship between river activity and human settling behaviour throughout history in North Central Bulgaria. Besides a single case study at Lake Gorgana in South Romania, which aims to elucidate human-environment interactions (Benecke et al. 2013; Nowacki et al. 2019a), remarkably few palaeoecological and palaeohydrological studies are focussing on the Danubian region (Howard et al. 2004; Lazarova (in prep.); Benecke et al. 2013; Bonsall et al. 2015). Apart from a few studies (e.g. by Howard et al. 2004; Kasse et al. 2010; Rădoane et al. 2015) on respectively the Teleorman river in Romania, the Tisza river in Hungary and the Siret river in Romania, no palaeohydrological studies have been published for this region. Therefore, the aim of this chapter is to contribute to filling the gap in palaeohydrological studies in Eastern Europe (the Danubian lowlands), which is for this discipline a scientifically understudied region (Benecke et al. 2013; Bonsall et al. 2015). Furthermore, the evolution of the Yantra River course with time will be considered in an archaeological perspective, to integrate palaeohydrological and archaeological expertise.

The objective of this contribution is to disentangle the complicated history of the Yantra River courses since the Last Glacial Maximum, and to reveal the former river dynamics and the processes which have shaped the alluvial plain of the Yantra River for a study area of approximately 4 km^2, near the village of Novgrad in northern Bulgaria. This study aims to elucidate the relationship between

former river meander activity and human settling behaviour in the alluvial plain of the Yantra during the Holocene. Moreover, the role of fluvial activity in the development of some important sites at the Tash Bair hill will be studied.

To reveal the history of the Yantra River courses, data collected on sedimentological properties of the subsurface, together with ^{14}C AMS dating of suitable samples, will be used in support of a topographical analysis. The general research aims of this study are to find out:

– how the alluvial plain west of Novgrad developed since the Last Glacial Maximum,
– which palaeo-meanders were active during what time period,
– and to which controlling factors can change in river dynamics be attributed.

4.2. STUDY AREA

In this paper, the 'study area' will refer to the area where fieldwork was conducted during the summer of 2018 and 2019 (cf. the contributions by N. Kecheva et al., chapter 7). The area to the south of the road connecting Novgrad with Svishtov, indicated with the black rectangle in figure 1A delineates the study area (at about 43°36'00" N and 25°33'30" E). It is located in North-Central Bulgaria nearby the confluence of the rivers Yantra and Danube between the village of Novgrad and Tash Bair hill. The considered floodplain area (at an altitude of about 20 m a.s.l.) is surrounded by hills rising up to about 200 m a.s.l., except to the north of the floodplain (fig. 1B). The Holocene alluvial plain is sharply delineated with respect to the Pleistocene river terraces and the older dissected Mesosoic, Neogene plateau remnants (clearly visible in figure 1B) (Shishkov, Kolev, 2014a). The Yantra enters the study area from an entrenched valley in the east and converges into the Danube at an elevation of 18 m a.s.l. near the village of Krivina in the Northern part of the map (fig. 1B). A general description concerning geology, climate and facts about the Yantra can be found in the contributions by A. López del Olmo et al. chapter 3.

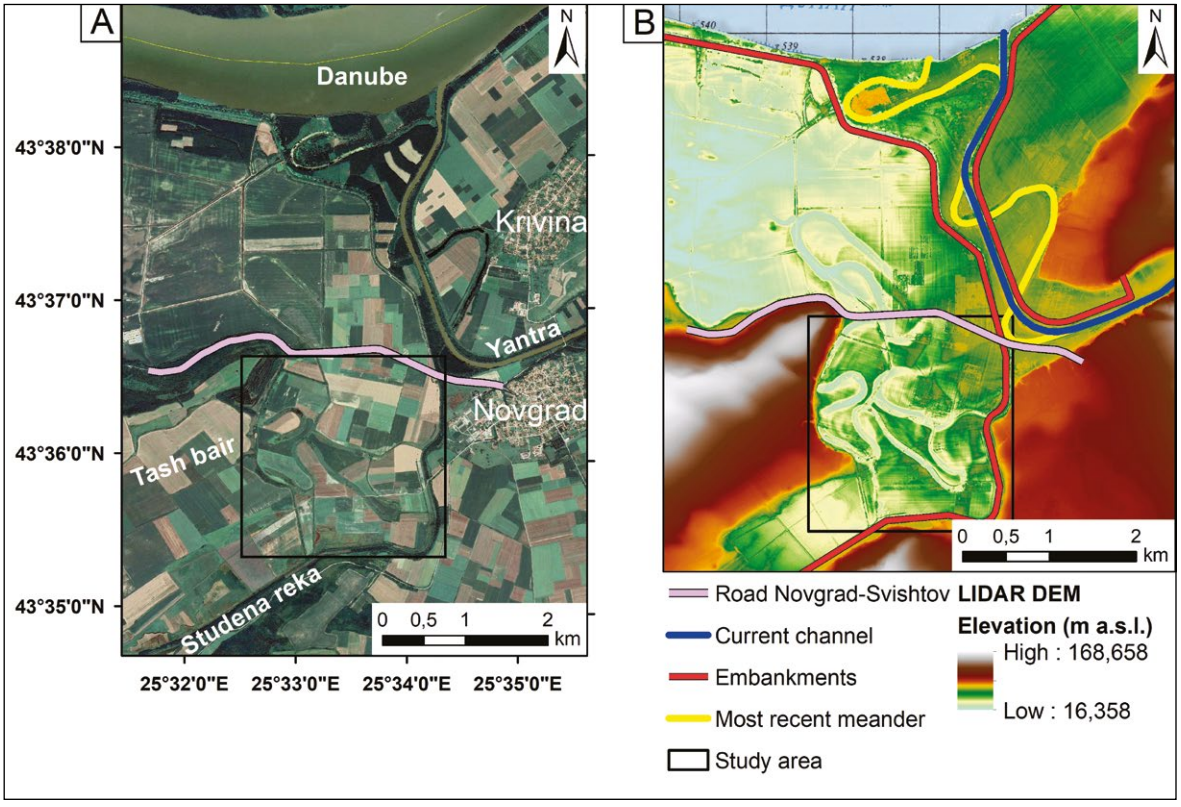


Fig. 1. A) Georeferenced satellite image of the study area (processing of Google earth imagery). B) LIDAR DTM for the study area (pixel resolution of 1 m). Area of fieldwork is indicated by the black rectangles. The current river channel (blue), the most recent active meander (yellow) and the embankments (red) are indicated as well (figure by A. López del Olmo)

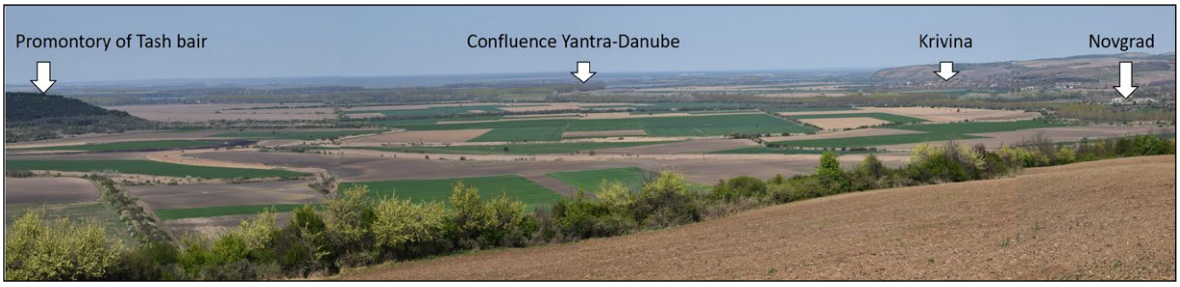


Fig. 2. Panorama picture across the study area, taken from the south, looking in a northward direction (composition of 4 pictures, taken by S. Conrad, spring 2019)



Fig. 3. Panorama view across the study area from Tash Bair (south-eastward direction, during late winter 2018). Withered reed vegetation is growing in former palaeo-meanders (composition of two pictures, taken by S. Conrad, 2018)

A satellite image of the surroundings (fig. 1A) reveals current land use (mainly arable land), the location of two villages (Novgrad and Krivina), former river meanders (palaeo-meanders) in the southwestern quadrant of the image. The location of Tash Bair hill, the Studena Reka River, the Yantra River and the Danube are indicated likewise.

Figures 2 and 3 visualise the study area, each from a different perspective. The first panorama picture is taken from the hill to the south of the study area. It shows the general morphology of the alluvial plain. The villages Krivina and Novgrad are indicated on the panorama picture, as well as the confluence of the Yantra with the Danube, in order to facilitate the orientation across the study area. The second panorama picture is taken during late winter from the Tash Bair hill in a south-eastward direction. Palaeo-meanders become apparent through the withered reed vegetation, growing in these former river meanders.

4.3. ANTHROPOGENIC MODIFICATIONS AT THE LOWER YANTRA RIVER COURSE

Recently, the lower reach of the Yantra River has changed dramatically. An attempt was made to investigate and quantify these changes, by comparing the most recent natural meandering river course (active until the 1950s) with its current straightened course, including river length, slope and sinuosity. The sinuosity (degree of meandering) of both river courses was calculated as the ratio of the river course length to the valley length (Arcement, Schneider 1989; Rosgen 1994; van den Berg 1995). A high sinuosity is expected for rivers with a wide valley and rivers which carry relatively large suspended loads (Bridge 1985; Rosgen 1994; Candel et al. 2017). Both river courses were digitised in Google Earth. The analysis covers the river section from the point where the two main Yantra River branches converge, up to the confluence of the Yantra with the Danube as shown in figure 4.

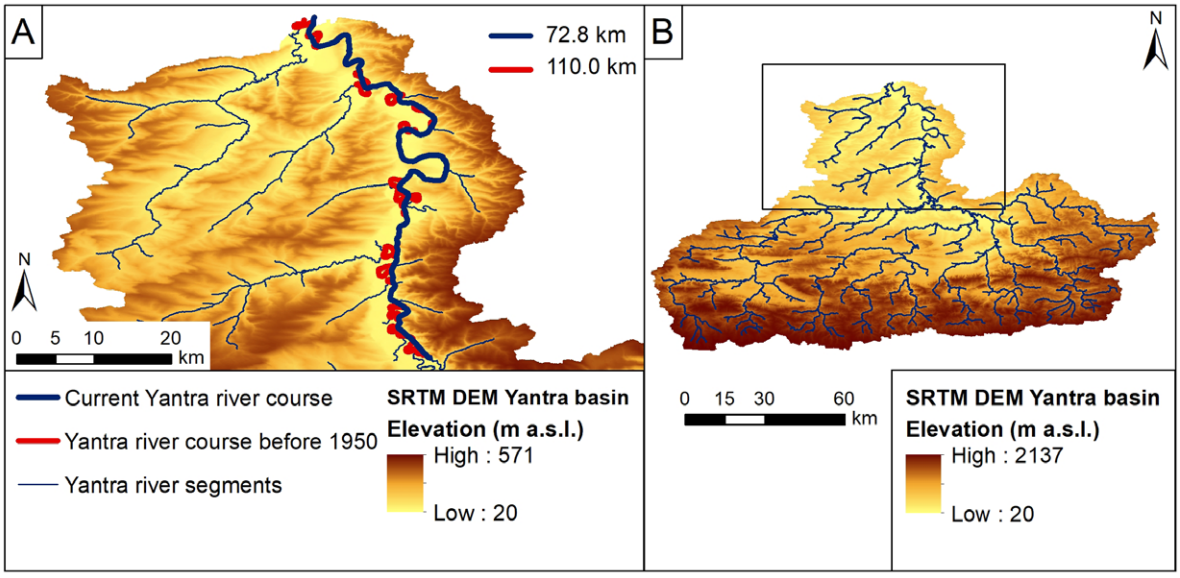


Fig. 4. A) Recent river course changes of the Lower Yantra River, depicted on a SRTM DEM (resolution 30m). B) SRTM DEM of the Yantra River basin (resolution 30 m). The black rectangle indicates the Lower Yantra in the Yantra basin (processing of SRTM data provided by USGS, figure by A. López del Olmo)

4.3.1. Significant changes of river characteristics

The fluvial landscape of the Lower Yantra has changed dramatically. Meanders have been cut-off, channels straightened, and wetlands have massively been drained. Figure 4A visualises the result of the digitisation of the current Lower Yantra stream (in blue) and the most recently active natural meandering river stream until the 1950s (in red). In less than one century the Lower Yantra lost about one third of its length as a consequence of channel straightening, resulting in changes in channel slope and river sinuosity. Consequently, these changes altered key characteristics of the river such as water storage capacity, velocity of the stream, sediment dynamics and changed the hydrograph and probably increased peak discharges (Nedkov et al. 2007; Nikolova, Nikolov 2011). The results of changes in river length, sinuosity and channel slope are summarised in table 1.

Table 1. Summary of changes in river length, sinuosity and slope between the current river channel and the river course active until the 1950s

	Lower Yantra until 1950s	Current Lower Yantra	Lower Yantra valley
Length (km)	110.0	72.8	68.7
Sinuosity	1.60	1.06	/
Slope (m/m)	$2.18*10^{-4}$	$3.30*10^{-4}$	$3.49*10^{-4}$

4.3.2. Major construction works at the confluence of the Yantra with the Danube

The fluvial landscape, at the confluence of the Yantra with the Danube, changed dramatically from the 1920s onwards. In the 1920s and 1930s, the Studena Reka River was channelised and became diverted to the southern and eastern edge of the alluvial plain. This intervention is not very well documented, apart from the mentions in the publications of the finds that were unearthed during the channelisation of the river at the contemporary numbered sites as 21; 24 (Миков 1933; Стефанов 1974; Krauß 2006a, No. 45).

Major construction works took place to drain the floodplain and to protect the area against inundations caused by the Yantra and Danube and in favour of the expansion of arable land in the floodplains. Most far-reaching interventions were carried out after the Second World War by the new political system between 1958 and 1964 (Димитров 1969, 171–173). The naturally meandering part

of the Lower Yantra was straightened and channelised, embankments were constructed, and entire floodplain areas were drained (Krauß 2006a; Sven Conrad, 2020, personal communication). Major human interventions at the confluence of the Yantra with the Danube are indicated in figure 1B.

4.4. GEOMORPHOLOGY OF THE FLOODPLAIN

4.4.1. Materials and methods

4.4.1.1. Topographical analysis

Recently, a pilot project "Aerial surveying of the terrain and preparation of a digital terrain model of the floodplain at the Bulgarian bank of the Danube river" was successfully completed (DANUBE FLOODRISK 2009–2012 Project (Басейнова дирекция „Дунавски район" 2013) for the Bulgarian Ministry of Environment and Water. The resulting DTM, with a pixel resolution of 1 m, made it possible to identify areas which are prone to flooding. In addition, it provides a very precise image of the topography of the alluvial plain of the Yantra at its confluence with the Danube.

The DTM is used for several analyses in the alluvial plain of the Yantra west of Novgrad. Firstly, to extract elevation values for the coring locations. Secondly, to construct sedimentological coring profiles. Thirdly, to investigate the morphology of the gully which connects the floodplain of the Yantra with the Tash Bair hill next to coring transect 2. Finally, the LIDAR DTM was an important element to investigate the evolution of the Bronze Age enclosure on Tash Bair (section 4.6.4).

4.4.1.2. Fieldwork: data collection

Two consecutive fieldwork campaigns were performed during the summer of 2018 and 2019 in order to reconstruct the former river dynamics of the Yantra in the study area. In total, 3 Electric Resistivity Tomography (ERT) profiles and 166 sediment corings were conducted in the study area of

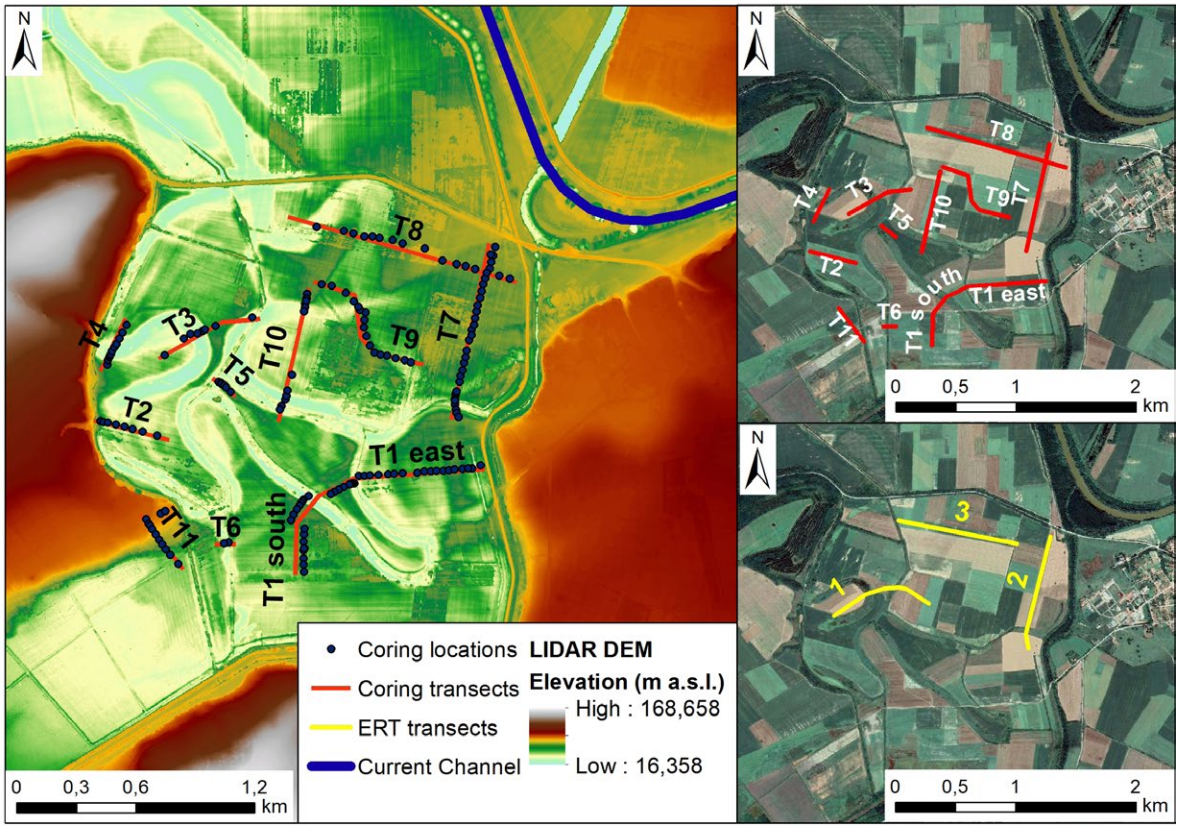


Fig. 5. Left: coring locations (indicated in dark blue), displayed on a DTM of the study area (resolution 1 m). The current river channel is indicated in blue. Top right: localization of the coring transects on a Google Earth satellite image. Bottom right: localization of the ERT transects on a Google Earth satellite image (processing of Google Earth imagery and LIDAR DTM, figure by A. López del Olmo)

approximately 4 km^2 along 11 coring transects (fig. 5). The position of the transects and sediment corings of 2018 and 2019 were determined by a Garmin handheld GPS (with a precision of 3 m). A summary of all coring locations and a map with all coring names displayed on a DTM can be found in the master paper of A. López del Olmo (2020), respectively in Appendix 1 & 2.

ERT is a geophysical technique used to characterise sub-surface materials in terms of their electrical properties. Variations in electrical resistivity correlate with variations in lithology or grain size, water saturation, fluid conductivity, porosity and permeability, and is used in this study to map and identify sedimentary facies in the river valley. Clayey sediments have typically low resistivity values. Contrary, coarser sediments have typically higher resistivity values. 2D profiles were created making use of a model application which converts the detected apparent resistivity values by iteratively modelling until the best model output is reached (Degryse et al., 2015). Sediment corings were made along the ERT profiles to facilitate the interpretations of the ERT profiles.

Sediment corings were performed with an Edelman and a Gouge auger. Corings were made along transects across the river valley, with a coring spacing of 10–50 m, in order to obtain a complete and representative picture of the fluvial architecture (Houben 2007). For each coring, a detailed sedimentological field description was made, with a vertical resolution of 5 cm for the Edelman profile and 1 cm for the Gouge profile. This description includes sediment texture (based on the USDA Soil Texture Triangle) determined by palpation, and information about the colour and inclusions (such as gravel, plant material and artefacts).

4.4.1.3. Lithogenetic units

To facilitate the systematic identification and interpretation of the sedimentological core profiles, interpretation figures were constructed for every coring transect, based on the fluvial architecture concept proposed by Houben (2007) or Huisink (2000), applied by e.g. Broothaerts et al. (2014), Candel et al. (2018), Notebaert et al. (2011). The fluvial architecture concept would enhance the geomorphological understanding of depositional river environments. Differences in sediment texture, structure, geometry and location in the floodplain would foster the interpretation of past alluviation (Houben 2007).

As proposed by Houben (2007), adjustments of the specific facies (or units) in the fluvial architecture approach are needed for every single case study. This case study was conducted in North Bulgaria, in another climate zone and with another geological context as compared to the study of Houben (2007). Therefore, slightly different fluvial architectural lithogenetic units were proposed in this study, to characterise the fluvial architecture.

4.4.1.4. Radiocarbon sample dating

In total, 13 strategically positioned samples were selected for radiocarbon dating from the 170 samples collected. The selected samples were sieved over a 500 μm mesh. Next, particles larger than 500 μm were examined through a light microscope, for seeds or other datable material. Radiocarbon dating of the samples (five bulk samples, four samples containing seeds, two wood and two bark samples) were executed by the Royal Institute for Cultural Heritage in Brussels (KIK–IRPA 2020) (cf. table 5).

Preferably, seeds and pieces of bark are selected for radiocarbon dating (Tornqvist et al., 1992). Sufficiently large samples were selected, ensuring that the minimum limit for ^{14}C analysis of 0.5 mg of carbon per sample was exceeded. Samples containing more than 1 mg of carbon are preferred, because they would yield the most accurate and precise results, with a narrower confidence interval, improving the accuracy of the reconstruction of the Yantra River courses (KIK–IRPA 2020).

Radiocarbon dating allows the calculation of average sediment accumulation rates in the floodplain and within abandoned river channels. Samples located in channel infills provide information about the upper age of the moment of channel abandonment. Samples located in overbank deposits provide information about net sediment accumulation for a given time period (Notebaert et al., 2011). Sediment accumulation rates in former channel infills were calculated at transect 4, 7 and 8 (fig. 5) by dividing the sediment thickness by the time period since channel abandonment. In addition, sediment accumulation rates in the floodplain were calculated at transect 1 south and 9 (fig. 5).

4.4.2. Results

4.4.2.1. Electrical Resistivity Tomography profiles (ERT)

The results of two ERT profiles, made in the summer of 2018 are shown in figures 6 and 7. The black boxes in the figures indicate the depth reached with sediment corings to validate the ERT profiles and will therefore only be part of the discussed results. Relatively low resistivity values, delineated by black lines, are an indication for former river channel infill deposits.

Figure 6 shows ERT profile 2, located along coring transect 7, oriented north-south in the alluvial plain (fig. 5). General high resistivity values are measured along this profile, with a peak in surface resistivity between 480–620 m distance along the profile. Four locations with slightly lower resistivity values are indicated in the figure, respectively around 25–95 m, 370–480 m, 720–800 m and 840–880 m distance along the profile.

Figure 7 shows ERT profile 3, located along coring transect 8, oriented east-west in the alluvial plain (fig. 5). General high resistivity values are measured in the upper parts of the profile between 0–290 m, 430–575 m and 780–860 m distance along the profile. Four zones with low resistivity values are indicated on the figure, respectively around 190 m, 290–430 m, 575–690 m and 890–940 m distance along the profile.

4.4.2.2. Radiocarbon dating

Table 5 gives an overview of the samples which have been dated in order to put the Yantra River course evolution in a temporal context. Appendix 3 in A. López del Olmo (2020) shows the location and the corresponding age of the samples on a map. The sample numbers are indicated on the interpretation figures (figs. 8–15).

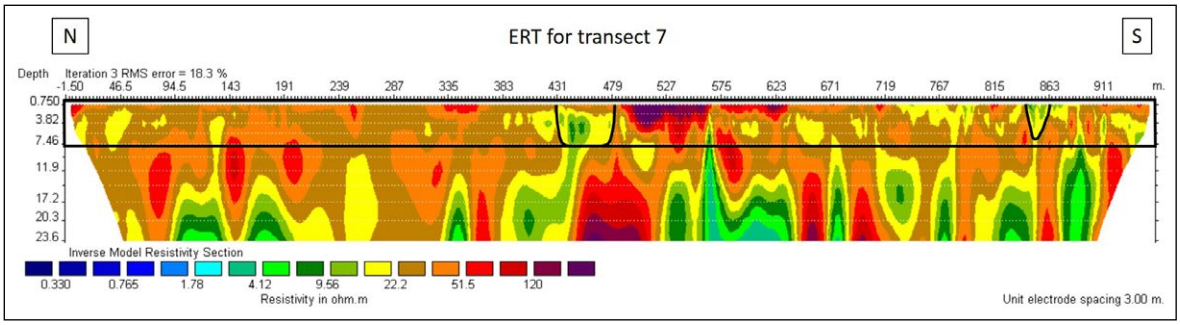


Fig. 6. ERT profile 2. High resistivity values are indicated by the colour range orange through to purple. Low resistivity values are indicated by the dark blue through to light blue colour range. The black box indicates the validated depth of the profile from the corings. The black lines indicate low resistivity values, which indicate potential former river meanders. The interpretation of the coring transect, corresponding to this ERT profile is shown in figure 12 (figure by A. López del Olmo)

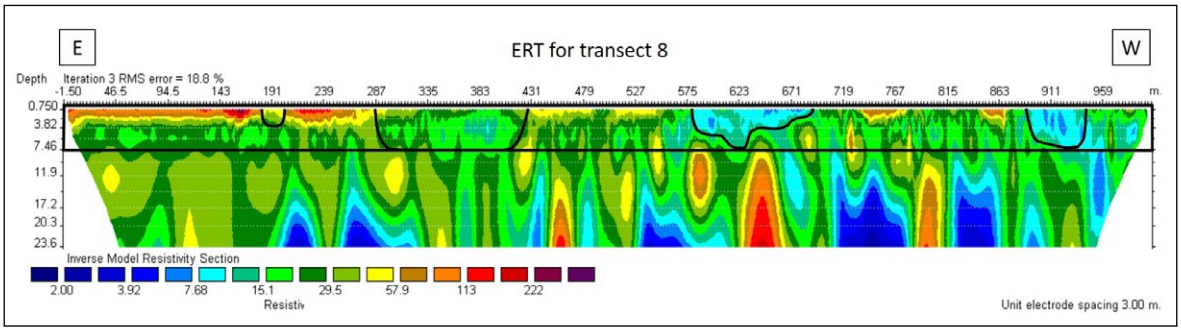


Fig. 7. ERT profile 3. High resistivity values are indicated by colour range orange through to purple. Low resistivity values are indicated by the dark blue through to light blue colour range. The black box indicates the validated depth of the profile from the corings. The black lines indicate low resistivity values, which indicate potential former river meanders. The interpretation of the coring transect, corresponding to approximately the first 800 m of this ERT profile is shown in figure 13 (figure by A. López del Olmo)

4.4.2.3. Interpretation of sedimentological core profiles

All sedimentological core profiles (created in RStudio) can be found in Appendix 4 in the master thesis of A. López del Olmo (2020), with a description in section 5.2.1. of the master thesis.

The results obtained from these sedimentological core profiles form the base of the interpretation figures. All interpretation figures of the floodplains architecture can be found in section 5.5 in López del Olmo (2020). In the next section, the concept of fluvial architecture is introduced. Next, the most relevant sedimentological interpretation profiles will be discussed.

4.4.2.4. Fluvial architecture

Different lithogenetic units have been distinguished for the purpose of this study, based on sedimentological properties of the floodplain deposits of the Yantra River in the study area. The characteristic lithogenetic units are summarised in table 6. Table 2 lists admixtures, specifying additional properties occurring in parts of the major lithogenetic units. The lithogenetic units and admixtures in both tables form the key to understanding the figures of the sedimentological core profiles, visualised in figures 8–15. Question marks in some figures indicate locations where the core spacing was too coarse to deduce the fluvial architecture.

Table 2. Admixtures of the lithogenitic units

Admixtures	Explanation
A	Enriched with nodules/concretions
B	Enriched with vitreous crystals
C	Enriched with shells
D	Enriched with human artefacts
O	Organic enriched A-horizon

An overview of the characteristics of each lithogenetic unit is given below:

Unit 1 consists of organic rich deposits which have a dark grey to black colour. Organic rich material is typically located in cut-off meander channels. These former active channels formed local depressions in the landscape where water concentrates and stagnates, almost all year round, forming oxbow lakes. This increases the preservation potential for organic material. Unit 1 is very often enriched with small white freshwater shells (admixture A).

Unit 2 is also typically found in cut-off meanders of former active river channels. Texture types are clayey and sediment colours vary from dark brown at the top to grey at the bottom of the profile, caused by reduction processes below the water table. Unlike unit 1, unit 2 contains barely to no organic material.

Unit 3 is typically found in cut-off meanders of former active river channels (equal to unit 2). This unit consists however of different sediment textures, namely fine sand-clay sequences. Clay and sand layers are often sharply delineated from each other. Similar to unit 2, unit 3 does not contain much organic material.

Unit 4 is typically found at the bottom of a river channel. Deposits consist of coarse sand to fine gravel, pointing to high energetic fluvial systems at these locations (Notebaert et al., 2011). Corings get typically stuck at this unit.

Unit 5 contains both levee and point bar deposits. Levees are typically found on both sides along a river channel. Point bars are typically found in inner-bends of river meanders. Levee deposits typically become coarser with depth from loamy sediment textures at the top, to sand at the bottom. Point bar deposits have a sandy sediment texture.

Unit 6 forms basically the rest of the alluvial plain. Sediments of unit 6 are deposited outside a river channel during flooding events. Only sediments which have been carried in suspension are found in overbank deposits, ranging from loamy to clay textures.

Unit 7 consists of deposits which are a result of the erosion and transport towards the alluvial plain of loess deposits (unit 9) on the surrounding hillslopes. This explains the typical silt-loam texture of the colluvial sediments and their location at the foot of steep slopes (e.g. at coring transect 2, figure 10). Note that we do not consider micro colluvial deposits in the alluvial plain as colluvial deposits, due to their limited distribution (e.g. nowadays local in-channel colluvial sediments are being deposited due to tillage erosion caused by recent agricultural practices on the former active river channel sidewalls). An example of such small-scale colluvium deposits, due to tillage erosion, is visible in figure 8 at core C11, indicated as unit O.

Unit 8 is distinguished by its higher elevation and the clear development of a soil profile, in comparison to the rest of the alluvial plain. Sediment textures range from clay to sand.

Unit 9 represents aeolian loess deposits, mostly consisting of silt fraction.

4.4.2.5. Interpretation figures

Figures 8–11 are sedimentological interpretation figures which have one thing in common; they all cross the same former river channel (the SW-meander, fig. 17).

Figure 8 shows the sedimentological interpretation figure of coring transect 1 east, located in the SE part of the study area (fig. 5). The interpretation figure reveals a former river channel, which has been filled with successive clayey (unit 2), sandy (unit 5), peaty (unit 1C) and again clayey (unit 2) deposits. The ^{14}C dating result of sample 1 suggests that this former river channel was abandoned before 550–400 calBC. The most recent river, which occupied this channel was about 40 m wide.

The interpretation figure of coring transect 1 south (fig. 9) reveals a large part of the subsurface of the southern part of the floodplain within the study area (fig. 5). This remote part of the floodplain is characterised by a horizon, rich in salt and calcium carbonate concretions (unit 6A). A clear A-horizon was able to develop, suggesting a rather stable surface (recently, not frequently covered with fluvial sediments) in this part of the floodplain. Moreover, traces of human occupation have been found in core C19–C22, C24. Even an entire horizon with traces of human occupation (a cultural layer) is located about 3 m below the contemporary surface.

Coring transect 1 south crosses the same river channel as coring transect 1 east. The river channel has a length of about 1.5 km between both transects. The floodplain elevation is comparable in both figures. However, the river channel crossed by coring transect 1 south is filled with fewer sediments, compared to the former channel at coring transect 1 east. Also, the sediment fingerprint of both former channel infill deposits differ between both locations. Similar for both locations, peaty deposits are located near the current surface elevation.

Figure 10 visualises the sedimentological interpretation figure for coring transect 2, located in the floodplain, near to Tash Bair hill (fig. 5). The sediment signature of coring 1 (unit 4, 2, 7 and 1) reveals a former river channel which has been filled with sediments. Remarkable is the high surface elevation above the former channel. The former channel is filled with a vast amount of colluvial sediments (unit 7), which originate from Tash Bair hill. Also, some human related artefacts (unit D) have been observed in the colluvial deposits.

Figure 11 shows the sedimentological interpretation of coring transect 4, also located in the floodplain, near the Tash Bair hill (fig. 5). The topography reveals a wide river channel of about 100 m width. Sedimentological information from core C4–C8 reveal that the most recent active river was only occupying 40–60 m in this wider channel. To the edges of the wider channel, in-channel point bar sediments were deposited (unit 5). Hence, the most recent river underfits in a much wider and older former river channel. This most recent active river channel was, according to the dating results, abandoned between 320–200 calBC and 970–1050 calAD. According to the geological map of the region, at least corings 1–3 are located in an Upper Pleistocene terrace (Филипов 1992). The sediment signature of core C1–C3 differ substantially from the sediments in core C9–C11, suggesting a different origin.

Figure 12 represents the sedimentological interpretation figure for a long coring transect (coring transect 7, fig. 5). As the topography is rather flat along this transect, former river channels can only be

revealed, based on the sedimentological fingerprint in every coring. This revealed a former river channel between core C23 and C25, which was abandoned before 20–140 calAD. Subsequently, the former channel was filled with sediments of unit 3, 2, 1C and 6. Sandy deposits (unit 5) confine this wide former channel. These levees can be interpreted to be older because a clear A-horizon (unit O) was able to develop. More recently, the topography was flattened by overbank deposits (unit 6) originating from the new location of the Yantra River channel. Most overbank deposits were deposited in the northern half of the transect. Another former river channel is located at C3 and C14. Unfortunately, no dating results are available to place this river channel abandonment in a temporal perspective.

The interpretation of coring transect 8 (fig. 13) is difficult due to a less dense coring spacing in the northern part of the study area (fig. 5). Nevertheless, three former river channels can be identified. The northern meander (fig. 17) passes transect 8 twice, once at C5 and once at C3, C13, C14. In between, a higher elevated area can be distinguished with a thickly developed A-horizon, pointing to its stability during the past centuries. The identified channel in the east is covered with recent overbank deposits (unit 6), similar to the observations in the northern part of coring transect 7. Unfortunately, no datable material was found at the bottom of this channel to place the abandonment of this channel in a temporal perspective.

Sedimentological interpretation figure 14 visualises the interpretation of the cores along coring transect 9 in the middle of the study area (fig. 5). A very deep former river channel, located at core C9 was filled with unit 3, 1C and 2 during the past approx. 2000 years. Another (filled with unit 3, 2 and 1C) former river channel is located between core C11–C14. Sample 11 is probably located too deep in unit 4 to represent the actual moment of channel abandonment.

The last interpretation figure within the floodplain visualises the interpretation of the cores along coring transect 10 (fig. 15). The middle meander is crossed twice by transect 10 (fig. 17). The middle meander in the north of the transect is almost completely levelled while the same channel is still much more

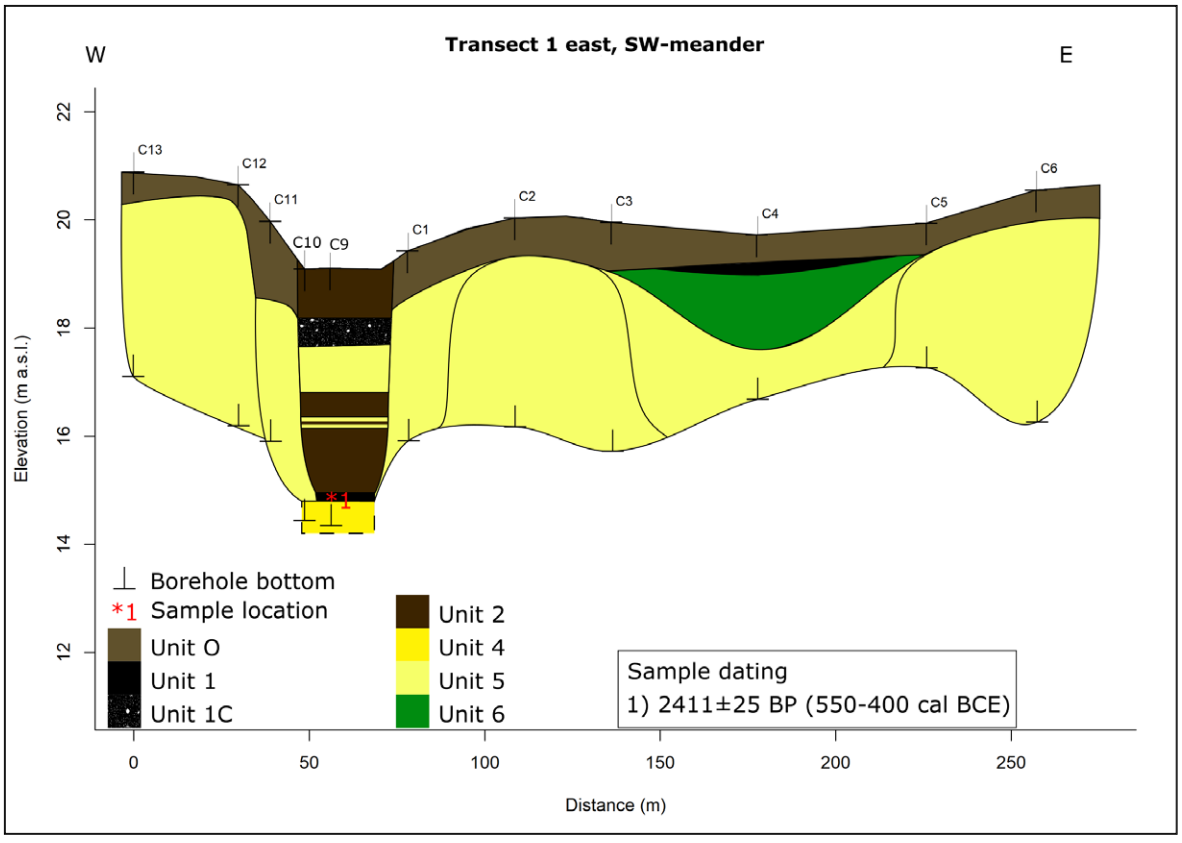


Fig. 8. Detailed cross-section of the alluvial plain along transect 1 east of the entrance of the SW-meander. The position of ^{14}C-sample 1 is visualised (figure by A. López del Olmo)

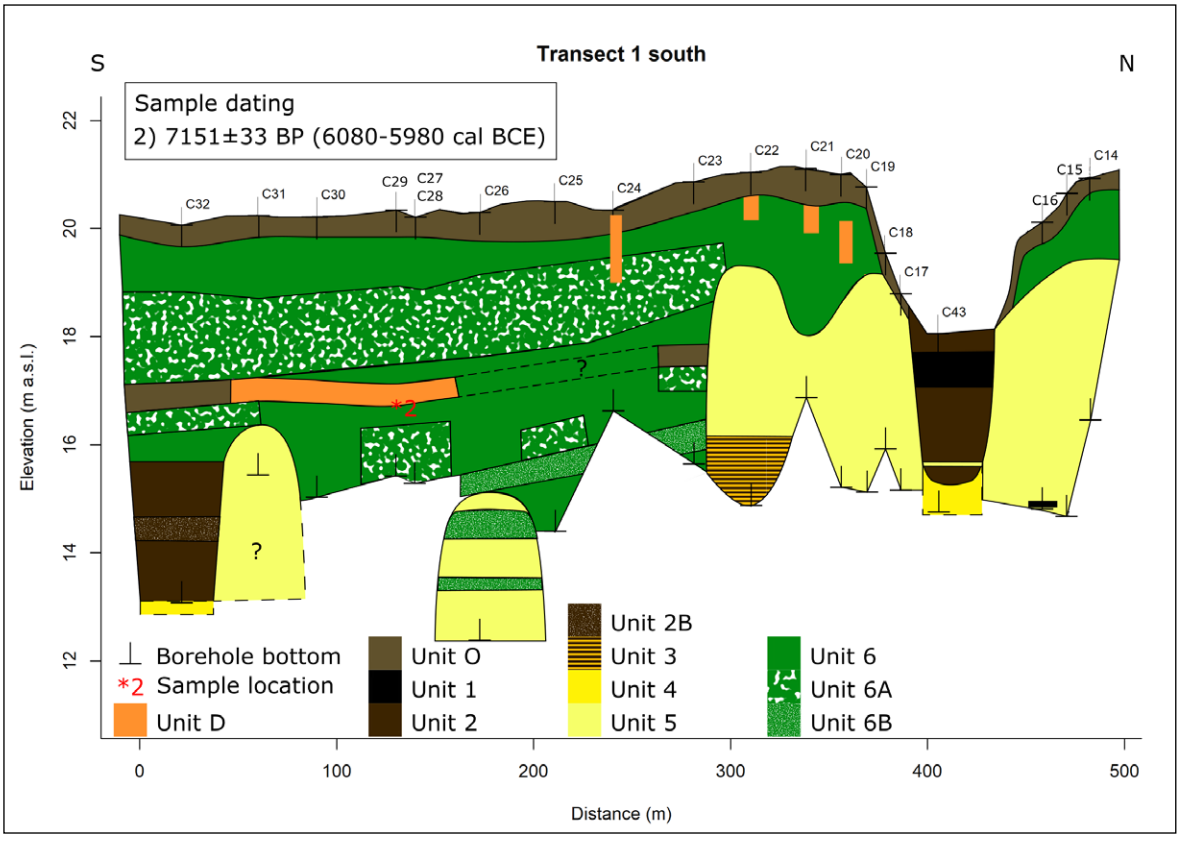


Fig. 9. Cross-section of the alluvial plain along transect 1 south. The position of ^{14}C-sample 2 is visualised (figure by A. López del Olmo)

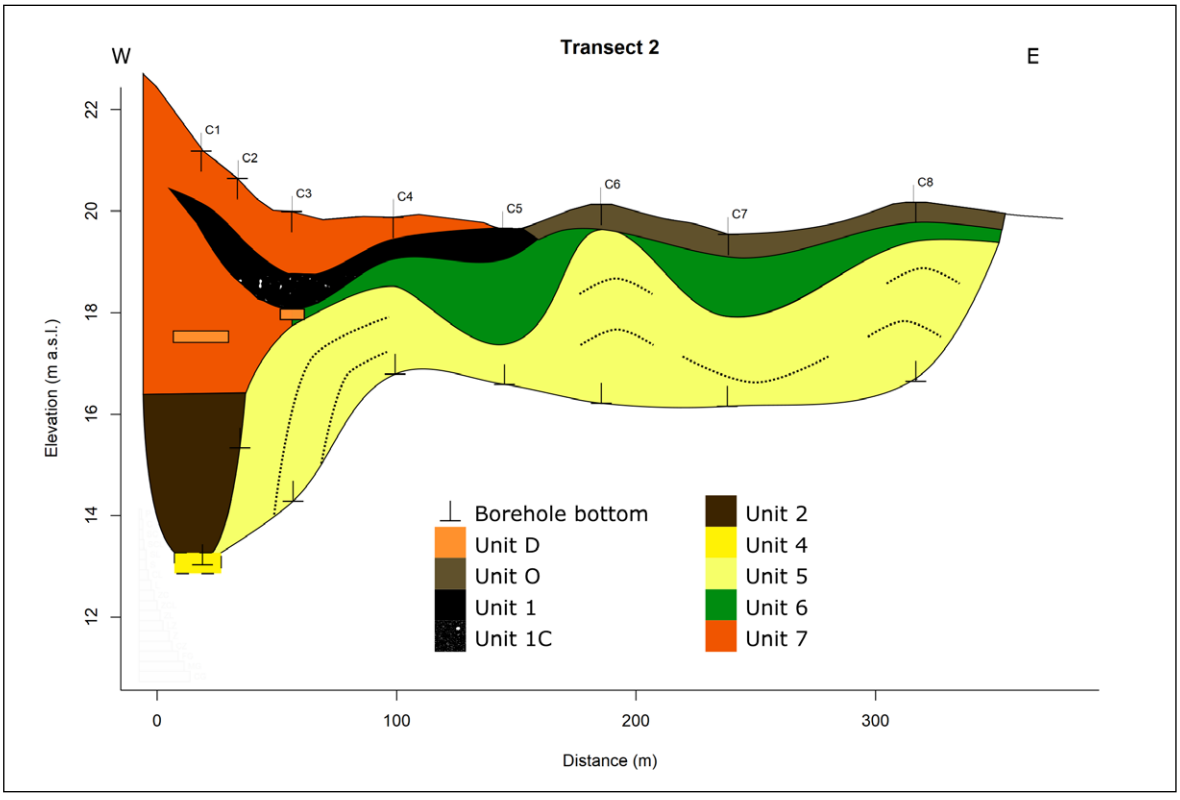


Fig. 10. Cross-section of the alluvial plain along transect 2 (figure by A. López del Olmo)

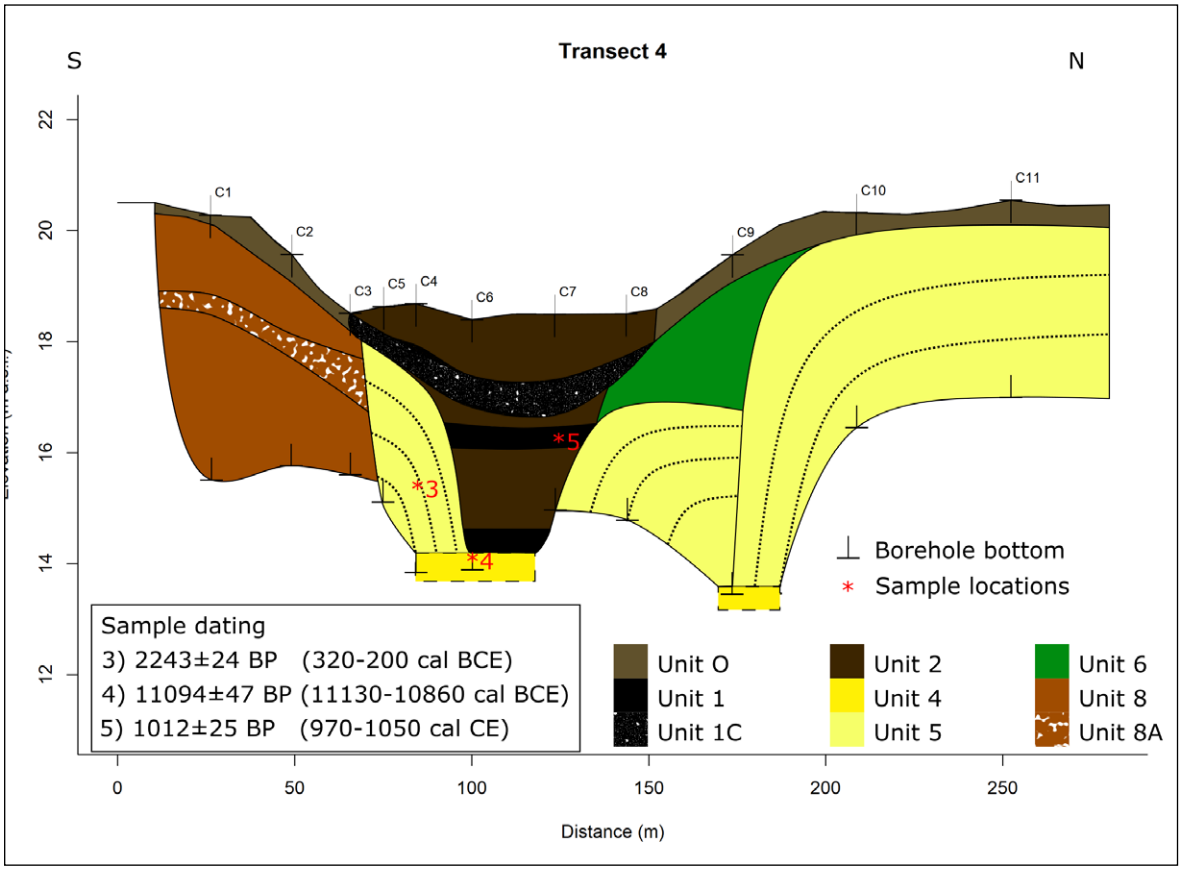


Fig. 11. Cross-section of the alluvial plain along transect 4. The positions of ^{14}C-samples 3–5 are visualised (figure by A. López del Olmo)

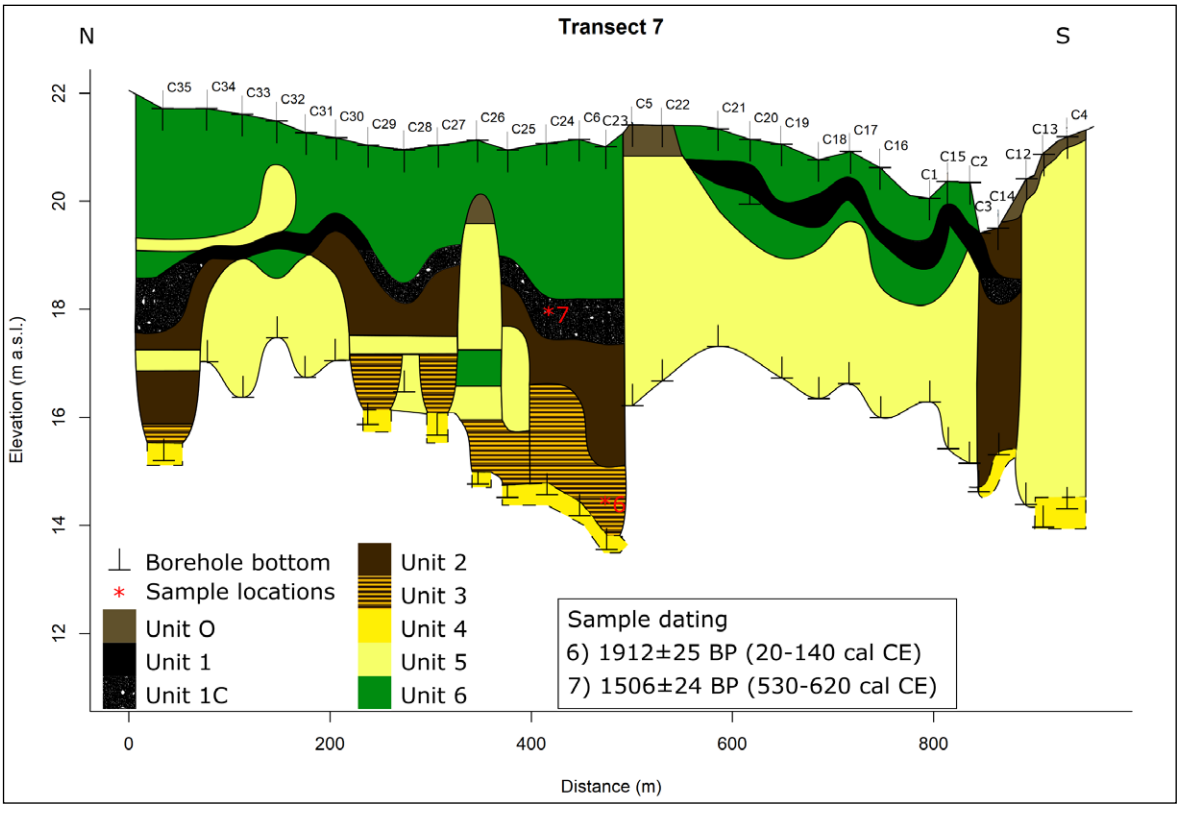


Fig. 12. Cross-section of the alluvial plain along transect 7. The positions of ^{14}C-samples 6; 7 are visualised (figure by A. López del Olmo)

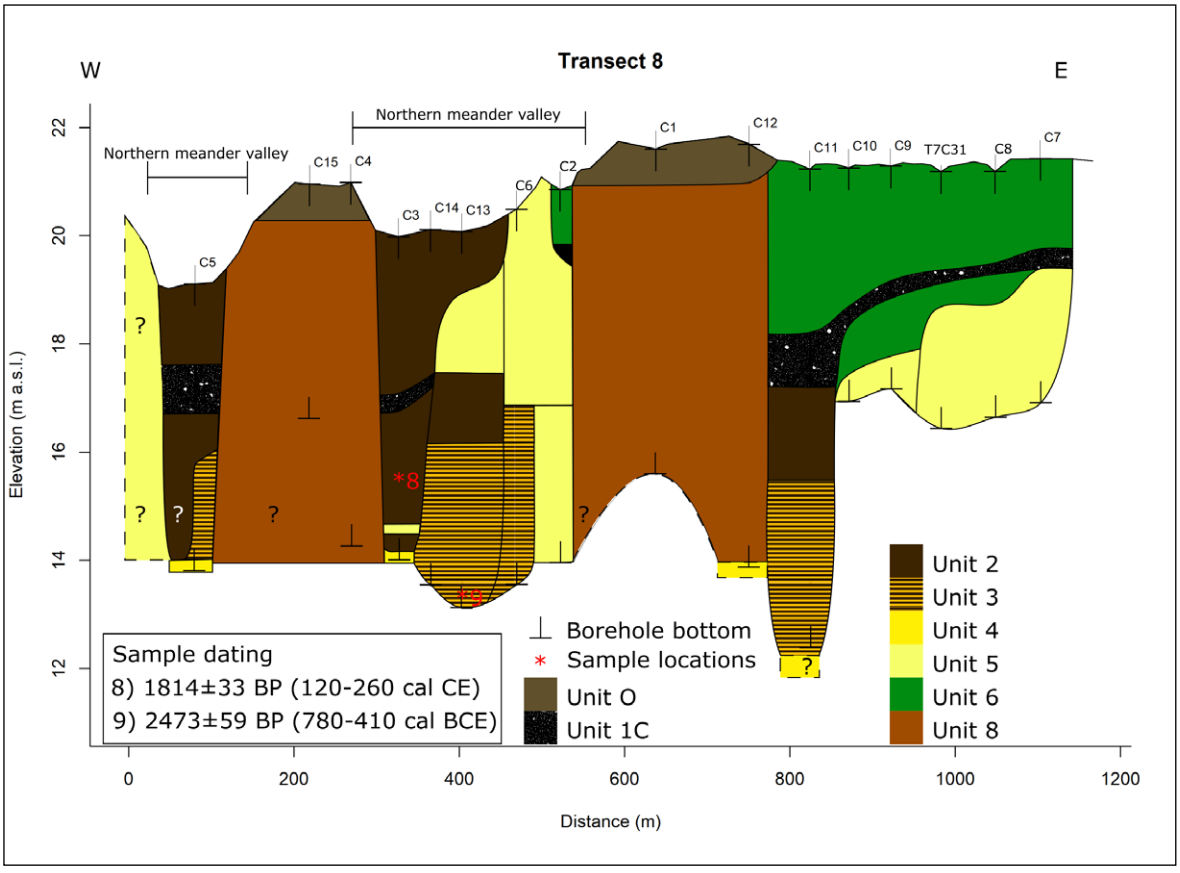


Fig. 13. Cross-section of the alluvial plain along transect 8. The positions of ^{14}C-samples 8; 9 are visualised (figure by A. López del Olmo)

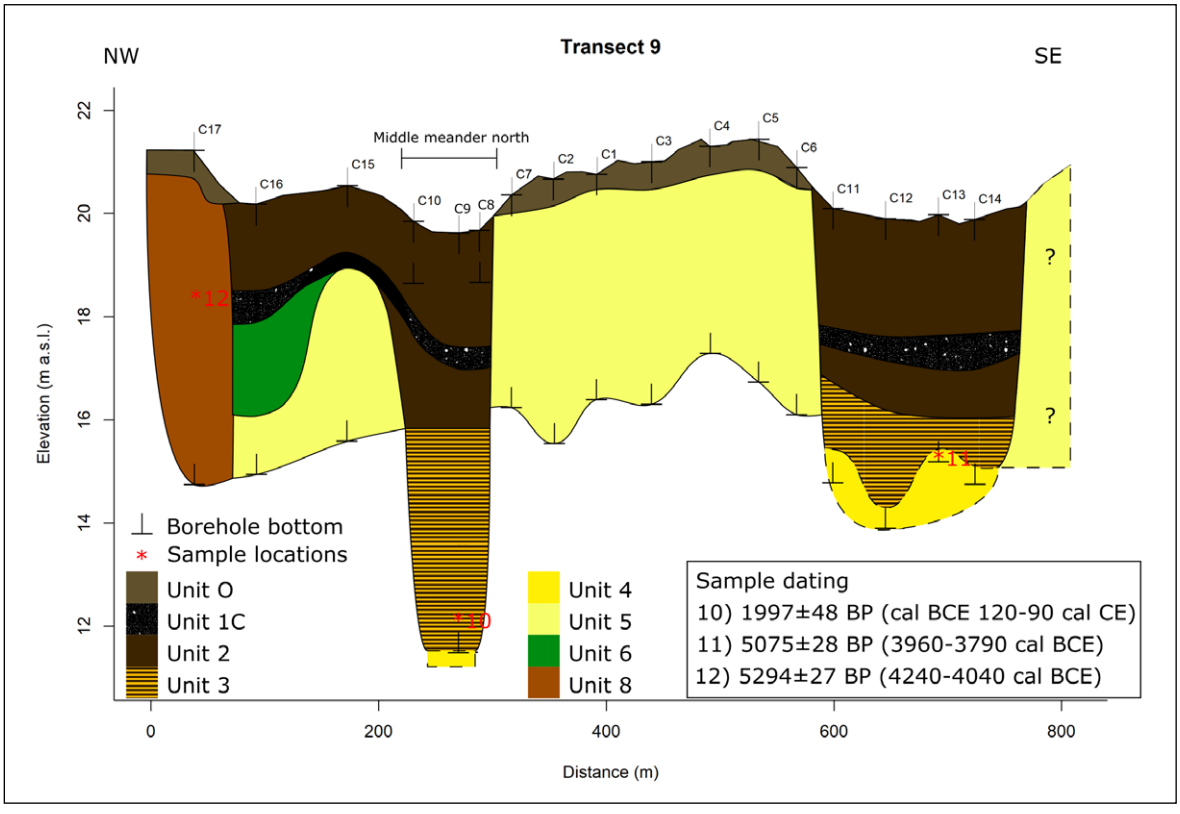


Fig. 14. Cross-section of the alluvial plain along transect 9. The positions of ^{14}C-samples 10–12 are visualised (figure by A. López del Olmo)

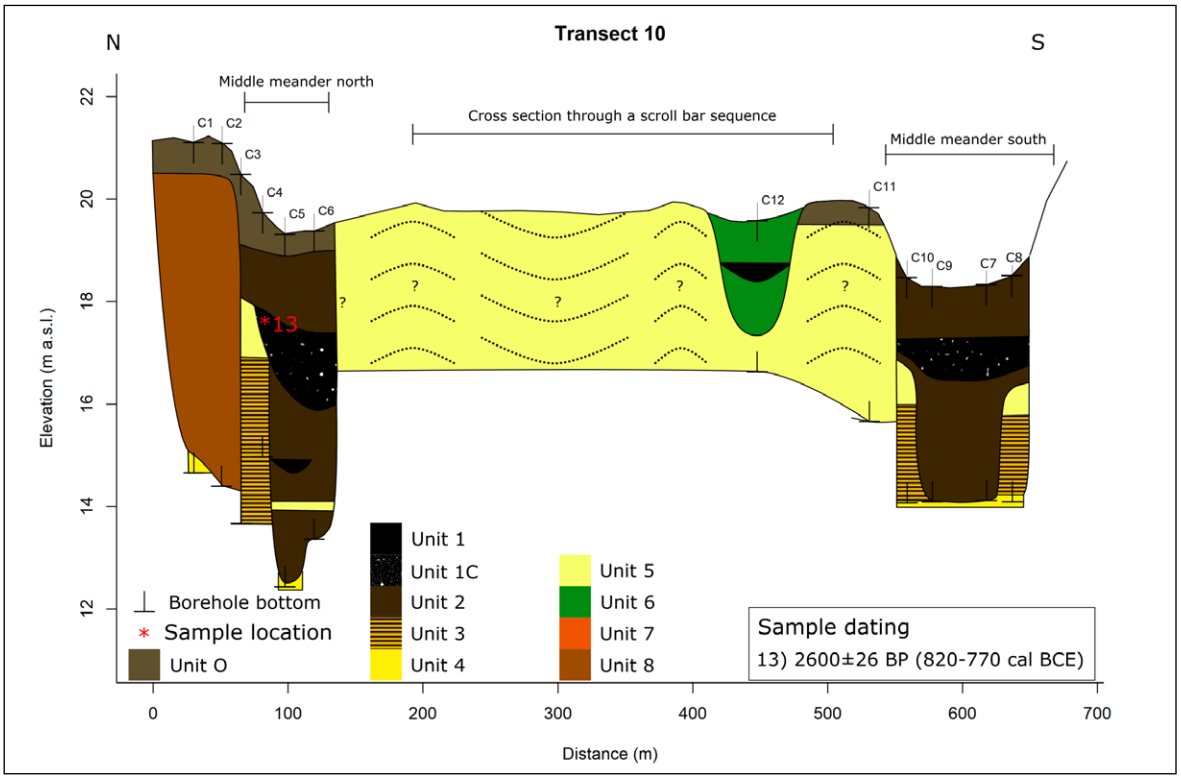


Fig. 15. Cross-section of the alluvial plain along transect 10. The position of ^{14}C-sample 13 is visualised (figure by A. López del Olmo)

visible along the southern part of the transect. Also, a clear difference in channel bottom elevation can be observed in the figure. Although only two corings were performed in the area between the two former river channels, a scroll bar sequence can be derived based on a topographical and visual analysis (fig. 5).

4.4.2.6. Sediment accumulation rates

A summary of sediment accumulation rates, based on radiocarbon dating, is shown in table 3. Floodplain sediment accumulation rates equal 0.45 mm yr^{-1} at T1C29 and T9C19 over a time period of respectively 8050 and 6150 years. Average abandoned channel infill rates range between 2.24 and 6.58 mm yr^{-1}. At T7C23 a distinction is made between early and late sedimentation accumulation rates in one abandoned river channel. The average sediment accumulation rate equals 6.58 mm yr^{-1} for the lower 329 cm of the channel infill. The average sediment accumulation rate for the upper 325 cm of the abandoned channel infill equals 2.24 mm yr^{-1}.

Table 3. Abandoned channel and floodplain sediment accumulation rates. Floodplain accumulation rates are indicated with an asterisk *

Location	Sediment accumulation depth (cm)	Time period of sedimentation (yr)	Average sedimentation rate (mm yr^{-1})
T1C29*	360	8050	0.45
T4C7	226	1000	2.26
T7C24	325	1450	2.24
T7C23	654	1950	3.35
T7C23	329	500	6.58
T8C3	430	1850	2.32
T9C17*	280	6150	0.46

4.5. EVOLUTION OF PALAEO-RIVER COURSES

4.5.1. Identification of palaeo-channels

In order to unravel the evolution of the activity of the palaeo-meanders within the study area, two issues are discussed successively. First, possible palaeo-channel entrances towards the study area need to be identified (section 4.5.1.1.). Second, the main meander valleys need to be distinguished (section 4.5.1.2.).

4.5.1.1. Palaeo-channels entering the study area

Three potential river entrances towards the study area have been identified (fig. 16), based on the analysis of sedimentological coring profile 7 (fig. 12), ERT profile 2 (fig. 6) and a topographical analysis of the LIDAR DTM (fig. 1B).

Entrance 1 is topographically the most straightforward location where the Yantra entered the study area in the past. Figure 12 clearly demonstrates a negative anomaly in the topography at C3 and C14 (indication of a former channel which has not entirely been filled yet with sediments). Additionally, the results of the ERT profile (fig. 6) suggest that this location might have been a former river channel entrance towards the study area. This is confirmed by the sedimentological fingerprint of core C3 and C14 (a thick clay packet above a coarse sand layer at the bottom of the former river channel).

Based on the topography, it was suggested that entrance 2 might have been another former river entrance. However, no sedimentological evidence was found during the fieldwork to support this. In addition, the corresponding ERT profile only indicate superficial lower ERT values instead of a deep homogenous layer. Therefore, this entrance cannot be interpreted as one of the most recently active former channels. This entrance is probably older and was only partially filled with sediments, resulting in the negative topographical anomaly in the contemporary relief. Entrance 2 will not be included in our reconstruction, due to a lack of sedimentological evidence and a lack of dating results in support of a recent river entrance.

Entrance 3 is located in the middle of coring transect 7, between core C23 and C25. This entrance is not visible anymore in the contemporary relief. However, the ERT profile and sediment cores reveal that there must have been a rather recent river entrance.

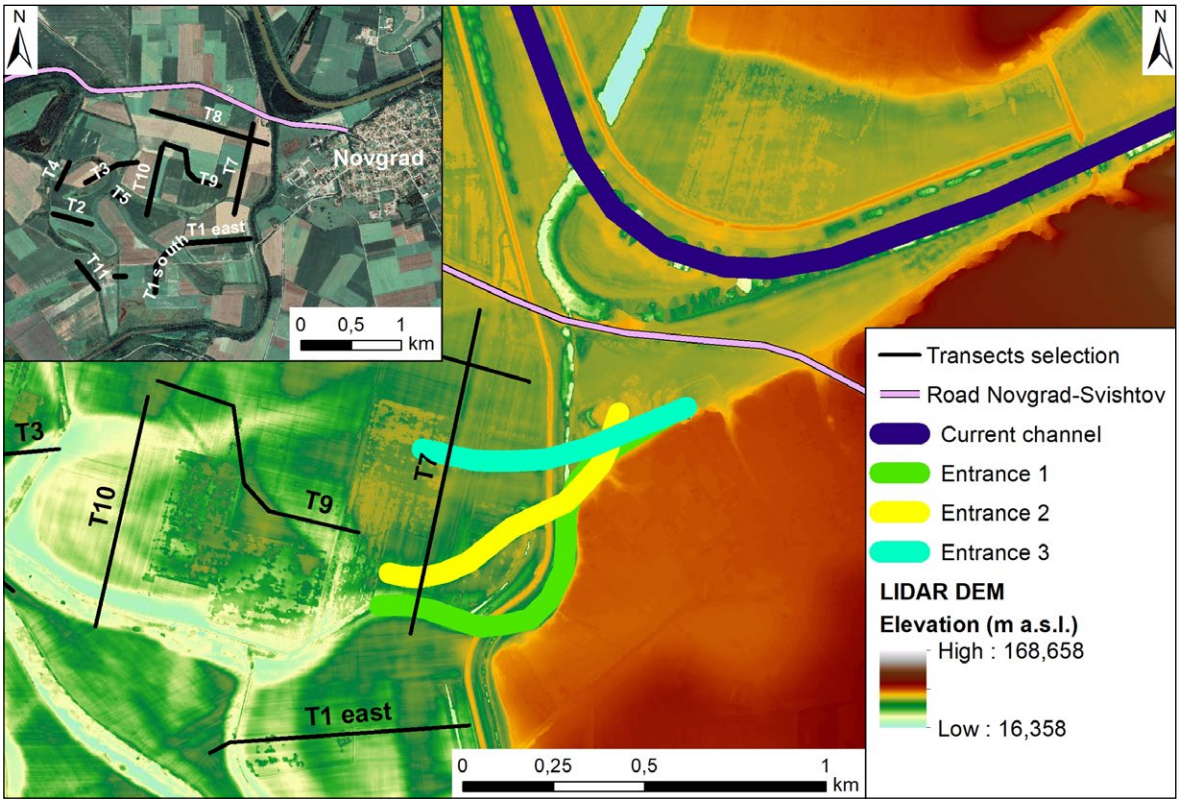


Fig. 16. Visualisation of former locations where the Yantra River entered the study area on top of a DTM. The inset shows a Google Earth image of the entire study area (processing of LIDAR DTM) (figure by A. López del Olmo)

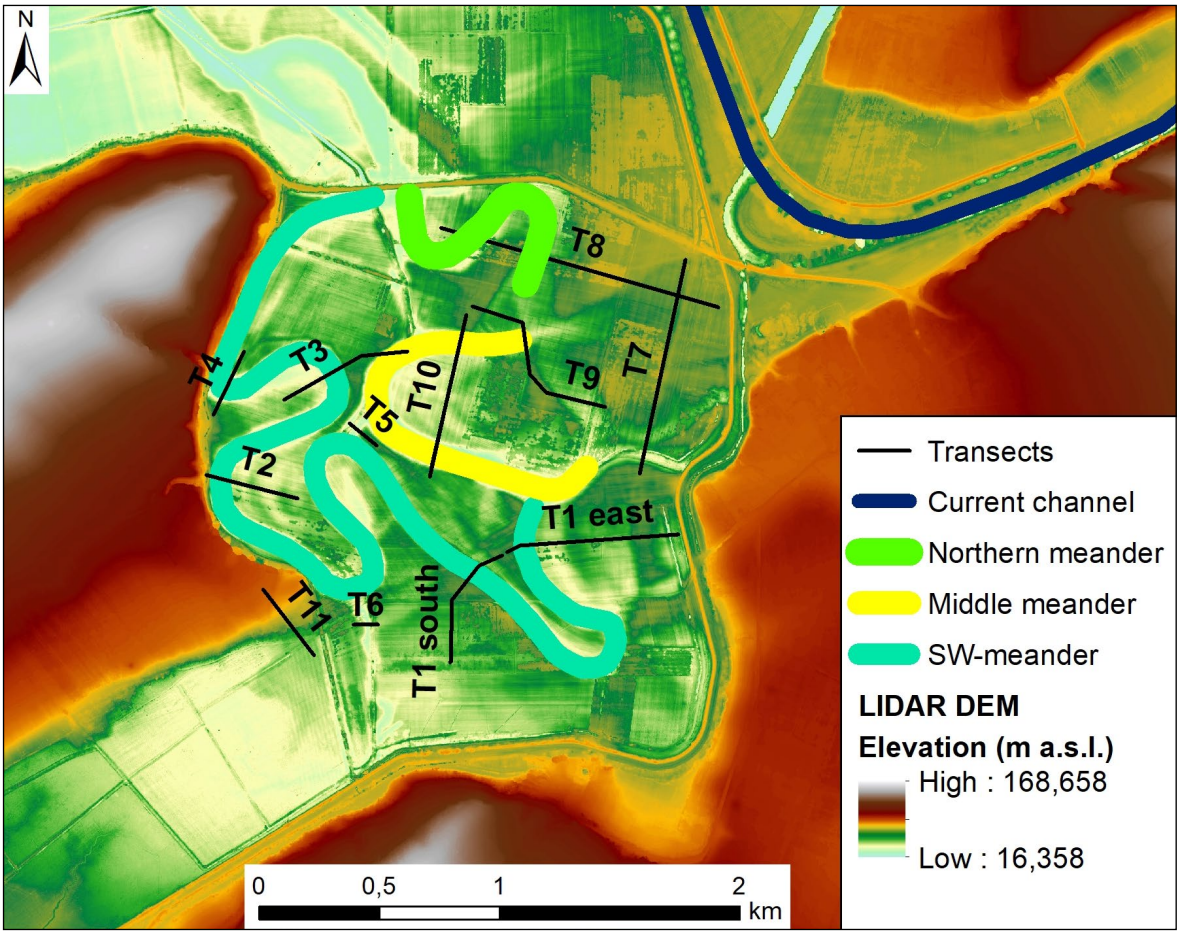


Fig. 17. Localization of the SW-meander, the middle meander and the northern meander valleys, the current Yantra River channel and the coring transects on top of a LIDAR DTM (processing of LIDAR DTM) (figure by A. López del Olmo)

The interpretation figure of coring transect 7 (fig. 12) illustrates two potential additional former river channels, crossing coring transect 7 to the north of entrance 3. First one between core C27 and C29, and second one at core C35. These two additional channels are not included in the reconstruction because there is not enough evidence to support these. Moreover, based on their location in the alluvial plain, both channels are more likely to be an outlet rather than an entrance.

4.5.1.2. Main meander branches

Three main meander valleys can be identified within the study area (the northern-, the middle- and the SW-meander), see figure 17. Note that these three names specifically refer to the wide valleys, characterised by a lower elevation in the contemporary topography and not to a certain former river channel within these valleys.

4.5.2. Palaeo-river course reconstruction

4.5.2.1. Abandonment contradiction of the SW-meander

The evolution of the southwestern meander (SW-meander) is examined along coring transects 1 east and south, transect 2, 3 and 4 (abbreviated as T1, T2, T3 and T4 in fig. 5).

In total, four samples (sample 1, 3, 4 and 5, table 5) have been dated in the SW-meander. One at the beginning of the SW-meander at coring transect 1 east (core C9), and three at coring transect 4. Sample 1 is located directly on top of the presumed channel bottom (fig. 8). It can be considered as the first moment of channel abandonment of the SW-meander. Based on sample 1, the SW-meander was abandoned between 550–400 calBC (86.1% confidence level).

Sample 3 reflects the age of an accreted point bar, which is exceptionally located in the outer bend of a meander (fig. 11). The acquired age of 320–200 calBC (69.2 % confidence level), indicates the moment when the SW-meander must still have been active, because the sample was subsequently covered by 2 m of sediments which are typically deposited by active rivers. Taking the stratigraphic position of sample 1 and 3 into account, the dating results of these samples contradict each other.

Sample 4 yields another remarkable result. It has an age between 11130–10860 calBC (95.4% confidence level). This result suggests that a palaeo-channel was active during the Late Glacial period and was abandoned at the onset of the Younger Dryas stadial. Not much is known about the exact river course nor its evolution. Nevertheless, the channel bottom elevation would have been similar to the more recent river channel in the SW-meander. It can be argued that the palaeo-meander was reoccupied by the Yantra during the Holocene, to abandon the SW-meander again, gradually from 550–400 calBC to 320–200 calBC. The radiocarbon dating result of sample 5 (970–1050 calAD, 91.9% confidence level) provides an ultimate age when river activity completely ceased. Moreover, the channel had filled already halfway with sediments, in particular organic rich sediments by that time (fig. 11).

4.5.2.2. Floodplain aggradation at coring transect 1 south

Soil formation (pedogenesis) is a slow process, taking place over hundreds to thousands of years, depending on the physio-climatological circumstances (Reading 1996; Evlogiev (in prep.); Chapman 2012). Along coring transect 1 south (fig. 5), to the south of the SW-meander, an A-horizon was able to develop in the floodplain, pointing to a limited sediment input over a considerable time period (Reading 1996). The dating result at coring transect 1 east has shown that the SW-meander was abandoned around 740–400 calBC. This resulted probably in a sharp decrease of overbank deposits, terminating floodplain aggradation, allowing soil formation to become the dominant process in this part of the floodplain (Reading 1996).

Radiocarbon dating of an organic rich bulk sample, located at a depth of 360 cm at T1C29 (sample 2, table 5, fig. 9) yields a radiocarbon age of 6080–5980 calBC (95.4% confidence level). From this, an average floodplain accumulation rate of 0.45 mm yr^{-1} is calculated (table 3). Previously, it is concluded that floodplain accumulation in this area of the floodplain ceased after the abandonment of the SW-meander at 740–400 calBC. Therefore, it is appropriate to subtract the time period since the abandonment of the SW-meander from the total time span and to recalculate the sediment accumulation rate for the period when the SW-meander was most likely active. This results in a floodplain aggradation rate of 0.65 mm yr^{-1}.

4.5.2.3. Abandonment of the middle meander

The middle meander (fig. 17) is the widest and clearest palaeo-meander, visible on the DTM in the study area (fig. 5). Sedimentological evidence (deposition of unit 5 sediments in the middle of the channel infill) from coring transect 1 (fig. 8) illustrates that the middle meander must have remained active after the abandonment and partial infill of the SW-meander. The attempt to date the abandonment of the middle meander yielded contradicting ages. Sample 10 is located 64 cm above the interpreted former channel bottom (fig. 14). It yields a calibrated radiocarbon age between 120 BC–90 AD (91.7% confidence level). At coring transect 10, the organic rich layer (sample 13, fig. 15), which is also observed in core C9 of transect 9 (fig. 14) is suspected to be younger, because it is stratigraphically located above the layer which has been dated by sample 10. However, sample 13 yields an older age (820–770 calBC, 95.4% confidence level). This is unexpected and makes interpretations difficult. Additional cores at coring transect 9 and/or additional radiocarbon dates might solve this apparent contradiction in the future.

4.5.2.4. Middle meander reactivation history

The southern part of the middle meander provides the ideal conditions to study the geometry of the middle meander due to the recent, almost entire, clearance of the reed vegetation in the former channel. Moreover, coring transect 10 (T10 in fig. 5) crosses the middle meander perpendicularly. The sedimentological fingerprints of core C7, C8, C9 and C10 (as interpreted in fig. 15) reveal the geometry of the former river channel. It shows that the most recently active river channel did not occupy the entire width of the valley of the middle meander south (i.e. underfitting river channel). The width of the

most recently active channel equal to less than 80 m. This, in contrast to the bankfull middle meander channel width of about 120 m. This wide channel is probably a remnant of Late Glacial river activity in the study area (when the Yantra River was characterised by large-scale meanders) formed under different climatological circumstances than today (Kasse et al. 2010; Perșoiu, Rădoane 2017; Perşoiu et al. 2017; Vandenberghe, Sidorchuk 2020).

Figure 15 visualises the interpretation of the remarkable differences between the sediments found in core C8 and C10, compared to core C7 and C9. Core C8 and C10 are both located near the sidewalls of the wide middle meander. The lower part of the sediment core reveals a clay-sand sequence infill of about 150 cm thickness. Clay minerals only deposit in stagnant water (Taylor 2012). Therefore, the middle meander must have been abandoned, however still well connected with an active river channel over a certain time period in order to be able to deposit sand layers as well. Afterwards, the channel must have been reactivated.

Two observations support the idea that this reactivation took place. First, a packet of 50 cm of sand has been found on top of this clay-sand sequence (fig. 15). Sand is only being deposited by river streams with enough energy (Taylor 2012). This indicates that a river must have reoccupied the formerly formed middle meander channel. Second, the two middle cores reveal a vast clay packet of about 400 cm thickness in contrast to both cores near the side walls where roughly only the upper 200 cm consist of clay sediments. Both sediment sequences (i.e. the sand-clay sequence and the pure clay packet) can be interpreted as accretionary sediment deposits. However, their sediment signature reveal that they must have been deposited in different energetic river environments. The pure clay and the clay-sand sequence can be interpreted as deposits in a cut-off meander, while the sandy deposits on top of the clay-sand sequence in C8 and C10 can be interpreted as bar/levee deposits at both sides of the channel. These were probably deposited after the reactivation of the middle meander. The reactivation of the middle meander created the incision of a new channel into the clay-sand sequence, erasing the sand-clay sequence between core C7 and C9. After the recent abandonment of the study area between calBC 80–140 calAD, the channel was filled again with a vast clay packet.

Unfortunately, no radiocarbon dating results are available for the middle meander south. Nonetheless, its temporal evolution can be reconstructed, based on the dating results in the SW-meander and the information acquired through the fieldwork. Based on the sandy deposits, identified in the channel infill at the entrance of the SW-meander at coring transect 1 east (fig. 8), it can be argued that the middle meander must have been active for a certain time period after the abandonment of the SW-meander at coring transect 1 east. A packet of about 80 cm thick sandy deposits has been identified in the channel infill (T1C9). This type of sediments can only be related to the activity of the middle meander. With the current information, it can be suggested that this must have occurred between 740–400 calBC (the abandonment of the SW meander east, sample 1) and calBC 80–140 calAD (the abandonment of entrance 3, see section 4.5.2.6.). The dating result of sample 10 (calBC 120–90 calAD, 91,7% confidence level) supports the assumption that the middle meander abandoned during the same time period as the northern meander and the channel passing entrance 3.

4.5.2.5. Changes in the northern meander ultimately leading to channel abandonment

Major changes (channel abandonment, reactivations and shifts of river courses) within the northern meander valley during the Iron Age are deduced from the sedimentological information along coring transect 8 (fig. 13) and the radiocarbon dating results of samples 8 and 9 (table 5). In addition, an increase over time of the elevation of the river channel bottom is observed.

It can be assumed that this wide valley formed as a result of the activity of multiple river channels which successively occupied only a part of the wide valley. The study of the infill of the sediments in this wide valley can provide a treasure of information provided that coring spacing is small and the lateral migration of the river course minimal (as such the preservation of the fluvial sediment deposits is maximal).

The most recently active channel within the northern meander crosses coring transect 8 at core C3 and probably C5 (i.e. in the westernmost part of the wide valley). It was probably less than 60 m wide

i.e. clearly underfitted in the wide northern meander valley. The dated seeds located 150 cm above the former channel bottom yield a calibrated radiocarbon date between 120–330 calAD (95.4% confidence level). When the sediment accumulation rate of the upper 430 cm of channel infill deposits at T8C3 is used to extrapolate the moment of channel abandonment, it is estimated at about 650 years earlier. This would correspond to a channel abandonment between 530–320 calBC. This is probably a misleading extrapolation. It can be argued that the extrapolation at T8C3 made a major underestimation of the age of channel abandonment. The calculated sediment accumulation rates at river entrance 3 (T7C23 and T7C24, table 3) demonstrate that the average sediment accumulation of the deepest half (329 cm) of the channel infill is about three times higher than the average sediment accumulation rate of the upper half (325 cm) (table 3). This is in accordance with the general theory that channels are being filled most rapidly during the initial phase of channel abandonment (Citterio, Piégay 2009). Furthermore, the sandy layers in the lower 50 cm of channel infill at T8C3 indicate a high initial fluvial activity during the first phase of abandonment (Sedláček et al. 2016). Therefore, channel abandonment at T8C3 is re-extrapolated, making use of a sediment accumulation of 7 mm yr^{-1} (about three times the average rate of the upper 430 cm). This results in a channel abandonment between calBC 95–105 calAD.

4.5.2.6. Abandonment of channel at entrance 3

Radiocarbon dated sample 6 and 7 (table 5) provide information about the abandonment of the former river channel at entrance 3 and its average sediment infill rate during two time periods. Although the samples were taken about 60 meters apart from each other, they can be considered as if they came from one coring because both are located in the same former channel infill (fig. 12). The radiocarbon age of sample 6 indicates that the river passing through entrance 3 abandoned its channel before 20–140 calAD (95,4% confidence level), as the dated piece of wood was located 63 cm above the former river bed (table 5, coring T7C23 in figure 12). The former channel was filled half-way by 530–620 calAD (86.8% confidence level).

Sample 6 is located at a depth of 654 cm, and sample 7 is located at a depth of 325 cm. From the difference in radiocarbon dating and sample depth, an average sediment accumulation rate of 6.58 mm yr^{-1} has been calculated for the lower 329 cm of the cut-off meander infill (table 3). If this average sediment accumulation rate is extrapolated for the underlaying 63 cm, channel abandonment will have occurred maximum 100 years earlier. From the theory, it is expected that the initial infill rate of the abandoned channel is substantially higher (Citterio, Piégay 2009). In addition, it can be argued that the new channel avulsion was not directly, entirely established. It probably took several decades before the channel was abandoned completely (Bridge 1985; Erkens et al. 2009). Therefore, initial sedimentation at entrance 3 probably exceeds the average channel infill rate of 6.58 mm yr^{-1}. Consequently, calBC 80–40 calAD can be considered a lower age for the abandonment of entrance 3. In conclusion, channel entrance 3 was most likely abandoned in a time interval between calBC 80–140 calAD. This time interval corresponds to the extrapolated age of the abandonment of the river channel in the northern meander (calBC 95–105 calAD). Consequently, it can be suggested that the ultimate palaeo-river in the study area was flowing through entrance 3, directly towards the northern meander where it left the study area.

4.5.2.7. Abandonment of the study area

Based on the fact that the all radiocarbon ages in other channel infills indicate an earlier channel abandonment (e.g. sample 1, 3, 6, 8, 9, 10 and 11; table 5), it is assumed that the abandonment of entrance 3 (fig. 16) between calBC 80–140 calAD (i.e. the transition from the Late Iron Age to the Early Roman times) coincides with the formation of a new channel avulsion to the north. Hence, calBC 80–140 calAD can be seen as the moment when the Yantra River ultimately abandoned the study area. In other words, no permanent river activity of the Yantra took place within the study area in approximately the last 1900 years.

4.5.2.8. River course scenarios

Most plausible river course scenarios are developed making use of the results of the fieldwork, radiocarbon dating and the interpretation of the current topography of the alluvial plain, retrieved from the detailed DTM produced by LIDAR. Figure 18 visualises the reconstructed river courses starting with

the present situation (fig. 18,1), and extending back in time until the Late Glacial period (fig. 18,10). In addition, the presumed time period in which the channel was active is displayed within the figure. In some cases, several scenarios have been developed for the same time period. Multiple scenarios for one-time period are indicated with a lower-case letter.

Figure 18,0 shows the topography of the entire area, from the entrenched Yantra channel in the eastern part of the sub-figure to the confluence of the Yantra with the Danube in the north.

Figure 18,1 shows the most recently active human-made river channel of the Yantra. Until the 1950s, the Yantra had a natural meandering patter. The location of this river course is indicated in yellow in figure 18,2. The channel in figure 18,3 probably formed during Early Roman times. This channel avulsion is interpreted as the cause for the final abandonment of the floodplain within the study area between calBC 80–140 calAD. Figure 18,4 visualises the location of the most recently active river channel in the study area. It is inferred that the activity of this channel ceased between calBC 80–140 calAD.

Channel branching in the study area (i.e. occupation of two river channels during the same time period) can be hypothesised to meet the apparent dating contradiction in the SW-meander. Corresponding hypothesised river courses are proposed in figures 18,4a.5a. Scenarios 4a and 5a are highly speculative. The hypothetical branch may either have been active in time period 4, or in time period 5, or may have remained active during both periods. Based on the available results, neither scenario can be assumed more likely. The branching may have been a short-lived event but may also have persisted for a longer period of time.

The transition from figure18,5 to figure 18,4 indicates that the channel figure 18,4 formed due to meander migration, resulting in a meander breach. With the current information, the exact moment of meander breaching cannot be reconstructed. Sedimentological evidence, from the in-channel deposits at coring transect 1 east, indicates that the middle meander must have remained active after the abandonment of the SW-meander until the abandonment of the study area (i.e. between the 8th–5th c. BC and the 1st c. BC – 1st c. AD).

The more than 3 m thick clayey sediment deposits, south of the SW-meander are considered to be the result of floodplain aggradation since the Middle Holocene. The aggradation of the floodplain might be an indication of prolonged river activity of the SW-meander (fig. 18,6 or 18,6a), from 6080–5980 calBC until 740–400 calBC. It is however unknown whether the SW-meander was the continuation of a channel which entered the study area via entrance 1 (fig. 18,6a) or via entrance 3 (fig. 18,6). The curvature of the channel in figure 18,6a looks more probable than the one in figure 18,6. This would imply that the river channel shifted from entrance 1 to entrance 3 between the transition from figure 18,6 towards figure 18,5.

The lack of comprehensive evidence, due to reactivations of channels and only partial preservation of former river channels, hampers the reconstruction of former river courses further back in the past and makes reconstructions highly speculative. Hence, this study cannot present reliable reconstructions for the Yantra River in the study area for the Lower to the beginning of the Middle Holocene (fig. 18,7).

The identification of wide, 'overfitting' river valleys, occupied by underfitting Upper Holocene palaeo-river courses give rise to the hypothesis that remnants of large Late Glacial meander bends are still observable in the study area (e.g. the middle meander and SW-meander, see fig. 18,8–10). However, this topic will not be further elaborated due to a lack of dating results.

4.5.3. Indications for indirect-anthropogenic impact on the Yantra

Unequivocally, the Yantra River has dramatically been modified in recent times by direct human impact (e.g. channel straitening, floodplain drainage), similar to other studied areas in the Lower Danube region (Buijse et al. 2002; Lóczy 2007; Benecke et al. 2013; Constantinescu et al. 2015; Csagoly et al. 2016; Nowacki et al. 2019b). It remains however unclear what the exact impact of human activities was on e.g. floodplain aggradation.

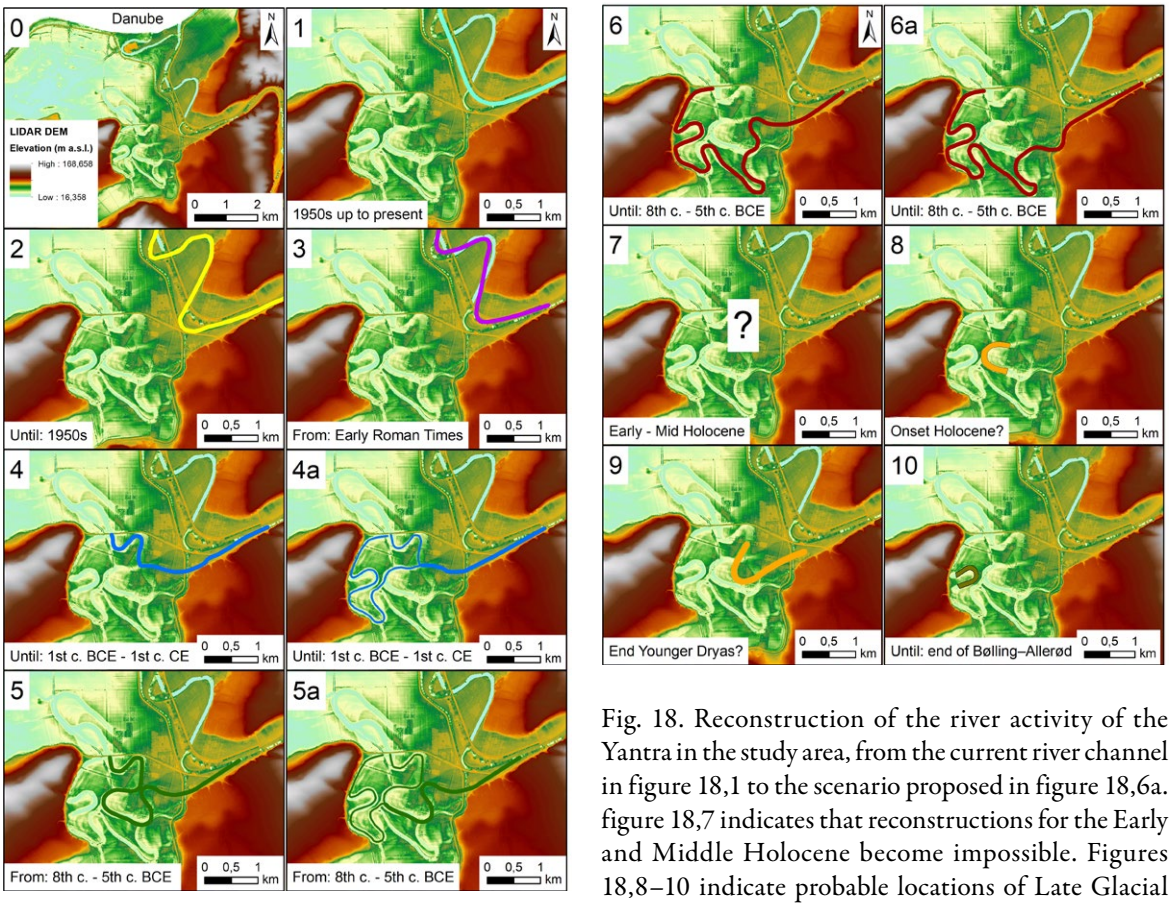


Fig. 18. Reconstruction of the river activity of the Yantra in the study area, from the current river channel in figure 18,1 to the scenario proposed in figure 18,6a. figure 18,7 indicates that reconstructions for the Early and Middle Holocene become impossible. Figures 18,8–10 indicate probable locations of Late Glacial palaeo-meanders. For some time periods more scenarios are plausible, they are indicated by the letter 'a'. Note the reduced channel width when channel branching takes place. The base map in all sub-figures is a LIDAR DTM). The corresponding legend for every sub-figure is only visualised in figure 18,0 (figure by A. López del Olmo)

In West and Central Europe, a distinct evolution from natural to human-dominated floodplains is established in several catchments. The natural state of the floodplains was characterised by peat growth which was subsequently covered by silty overbank deposits. This process is related to an increase in human impact in the river catchments, more specifically, an increase in soil erosion on the hill slopes, caused by agricultural activities. This resulted in an increase of the suspended sediment load of the rivers, which subsequently ceased peat growth and caused vertical floodplain aggradation by silty overbank deposits. Several authors point at the exceedance of a certain threshold of human impact and the connectivity of hillslopes with the alluvial plain as important factors to explain the discrepancy between the timing of the start of human impact and the response of a river system (Lang et al. 2003; Erkens et al. 2009; Notebaert, Verstraeten 2010; Notebaert et al. 2011; Houben et al. 2012; Broothaerts et al. 2013, 2014). Contrary to floodplains in the lowlands of West and Central Europe, no marshy environments or buried black floodplain soils have been observed in the floodplain of the Yantra within the study area (except for former channel infills in cut-off meanders). Therefore, the start of human impact on floodplain development cannot be derived from the transition of peat growth to clastic overbank deposits.

However, combining the fieldwork of this study, with topographic information from the LIDAR DTM, results in information about floodplain aggradation over time as an indication of external impact on floodplain development.

In section 4.5.2.7. it is concluded that the Yantra abandoned the study area between calBC 80–140 calAD. Consequently, overbank deposits diminished significantly in this area of the floodplain since approximately 2000 yr. The LIDAR DTM (fig. 18,0) reveals a markable higher elevation of the north-

eastern part of the floodplain near the most recently active, natural meandering channel (active during the past 2000 yrs). If a flat floodplain elevation is assumed for the floodplain 2000 yrs ago, it can be inferred from the LIDAR DTM (fig. 18,0) that the floodplain aggradated up to 3 m near the active channel. The aggradation of 3 m clastic overbank deposits must have occurred within the past 2000 yrs.

The Danubian Plain is an excellent region for agriculture due to its extremely fertile soils (cf. the contributions by A. López del Olmo et al., chapter 3). It can be expected that early human settlers started to clear the natural forest steppe vegetation (established during the Atlantic climate optimum) in favour of agricultural land (Lazarova (in prep.). Palynological analyses by M. Lazarova (in prep.) revealed that the reduction in forest pollen at the end of the Subboreal coincided with an increase in all anthropogenic indicator pollen. M. Verhasselt (2013) modelled that the human impact on the landcover in the northernmost part of the Lower Yantra was limited until the end of the Iron Age but increased sharply at the onset of the Roman period. This increased human impact might be the cause for the floodplain aggradation of up to 3 m close to the most recent, naturally meandering channel. This would imply that erosion processes on the undulating loess plateau caused a major increase in sediment delivery towards the incised Yantra River.

However, section 4.5.2.2. demonstrated that major floodplain aggradation (3.6 m) took place in the study area already a long time before humans started to have a major impact on the landcover through agricultural practices (Evlogiev (in prep.); Verhasselt 2013). A further floodplain aggradation of 3.6 m took place in a time period between 6080–5980 and 740–400 calBC in the southernmost part of the study area. This explains the beginning of the extensive scattering of the surface finds from the Early Iron Age here. In addition, sample 12 (table 5; fig. 14) indicates a floodplain aggradation of 2.8 m between 4240–4040 calBC and calBC 80–140 calAD (i.e. abandonment of the study area) in the middle of the floodplain. These findings might be explained in two ways: either, human activity had already impacted the suspended load of the Yantra River earlier, causing the early floodplain aggradation (this would be in contrast with observations in West and Central Europe), or, the floodplain of the Yantra in the study area aggradated due to natural external perturbations of the river system, caused by e.g. climate change, tectonic movement, base level changes related to the Black Sea level.

4.5.3.1. Base level changes due to subsidence in the Lower Danube region

The study area is located in a relatively active seismic region (Stoyanov, Gachev, 2012). Although the Lower Danube is located in a subsidence region, Krauß (2006) does not expect major adaptations of the Yantra River, resulting from tectonic movements within the Holocene (Enciu 2010; Perşoiu 2017). A recent study of Armaş et al. (2019) measured vertical GPS vectors velocities of ~2 mm yr^{-1} (subsidence) to the east of Ruse. The subsidence of that area might lower the base level of the Lower Danube, which results in theory in channel incision. This contradicts with the observed floodplain aggradation in the study area since ca. 6000 calBC. Therefore, tectonic movement (subsidence) in the Lower Danube region can be considered a controlling factor with minor impact on the Holocene river dynamics of the Yantra.

4.5.3.2. Base level changes caused by Black Sea level changes

The level of the Black Sea is another factor controlling the base level of the Lower Danube and thus indirectly the base level of the Lower Yantra (Erkens et al. 2009). After the reconnection of the Mediterranean and Black Sea around 9500 calBP (i.e. 7550 calBC), the level of the Black Sea increased between 60–130 m due to rapid transgression (Bahr et al. 2006; Lóczy 2007; Benecke et al. 2013; Starkel et al. 2015; Perşoiu 2017). The Black Sea transgression influenced the base level of the Lower Danube substantially during the Early and Middle Holocene. Resulting in a base level increase and floodplain aggradation of the Yantra. This may explain why no Early Holocene river channels have been identified in the study area. It also corresponds to observations in the Teleorman river (Howard et al. 2004).

After ca. 5200 calBP (i.e. 3250 calBC), the Black Sea level became relatively stable (Lóczy 2007). Therefore, it can be expected that the base level of the Lower Danube as related to the Black Sea level did not affect the Lower Yantra over the last ca. 5000 years. The floodplain aggradation of 3.6 meter in the southernmost part of the study area between 6080–5980 and 740–400 calBC (section 4.5.2.2)

can be interpreted as the result of the transgression of the Black Sea. Contrary, the more recent, doubled floodplain aggradation rate cannot be explained by the transgression of the Black Sea and was therefore most likely caused by another controlling factor.

4.5.3.3. Natural versus anthropogenic floodplain aggradation

According to A.J. Howard et al. (2004) and J. Evlogiev (in prep.), floodplain accumulation started in South Romania and North Bulgaria around 2500–2400 yr BP, and might be related to increased erosion processes caused by agriculture (Evlogiev (in prep.). P. Houben et al. (2012) argue that anthropogenic floodplain aggradation started in Germany around 2200 ± 200 calBP, despite the much earlier start of agriculture in the loess areas (around 7000 calBP). This would imply that the overbank deposits in the southernmost part of the study area (0.65 mm yr^{-1} for the time period 6080–5980 calBC to 740–400 calBC (at T1C29)) were deposited under natural conditions. Hence, the natural average floodplain aggradation rate can be assumed to be 0.65 mm yr^{-1}.

Over the last 2000 years, 3 m of floodplain aggradation occurred near the most recently active channel in the north-east of the study area, if it is assumed that the floodplain had a rather flat relief 2000 years ago, and floodplain aggradation ceased in the most remote parts of the floodplain after the abandonment of the study area. Hence, the average floodplain aggradation rate in this part must have been 1.5 mm yr^{-1} over the past 2000 years, which roughly doubles the assumed natural floodplain aggradation of 0.65 mm yr^{-1}. This remarkable increase points towards the influence of enhanced erosion processes in the Yantra basin during the last 2000 years, causing the natural floodplain aggradation to increase.

Although rough trends in floodplain aggradation have been revealed in this study, it is recommended that additional sediment corings are performed in the floodplain of the Yantra, near the most recent active river channel (i.e. outside the study area), to provide field verification for the visual LIDAR DTM analysis.

Furthermore, it is virtually impossible to disentangle the importance of tectonic subsidence and climate variability in causing changes in the river catchment during the Holocene, as compared to stronger signals (e.g. anthropogenic impact, base level control by the level of the Black Sea). In addition, it is difficult to link river course changes to Holocene climate variability due to the absence of climatological reconstructions for the central part of the Lower Danube region. Nevertheless, this study provides evidence that shows that the floodplain in the study area was in a natural aggradation phase between 6000–5980 calBC to 740–400 calBC. While the indirect impact of humans increased and caused the floodplain to accrete faster during the past 2000 years.

4.6. EXEMPLARY GEOMORPHOLOGICAL INVESTIGATIONS ON ARCHAEOLOGICAL SITES

4.6.1. Sedimentological coring profile: from Tash Bair towards Studena Reka valley

The interpretation figure of the sediment corings (fig. 20), performed on the southern slopes of Tash Bair (near archaeological site 1, fig. 28) is located along coring transect 11 (fig. 5; 19). This investigation continues and extends former investigations at this site (cf. Krauß 2006a, 148–149 fig. 52; 53)

Corings along the upper part of the transect (C1–C5) show a typical development of a Chernozem soil profile, developing in aeolian loess deposits. The flatter part in the profile (between C6 and C7) is according to the geological map of Late Glacial origin (Филипов 1992). A distinct sediment signature can be observed in C6 and C7, compared to the other cores. Core C8, C9 and C10 are located in the Holocene alluvial plain of the natural confluence area of the Studena Reka and the Yantra. A relative thin A-horizon can be observed in these cores, compared to the thick A-horizon developed on Tash Bair hill. The thinner A-horizon in the floodplain is an indication for a younger soil in the floodplain, compared to the soil at Tash Bair.

In addition, figure 20 reveals human impact on Tash Bair in two ways: Firstly, cores show a clear disturbance of the soil profile (e.g. at C3) or human artefacts were found in the sediments (e.g. at C1,

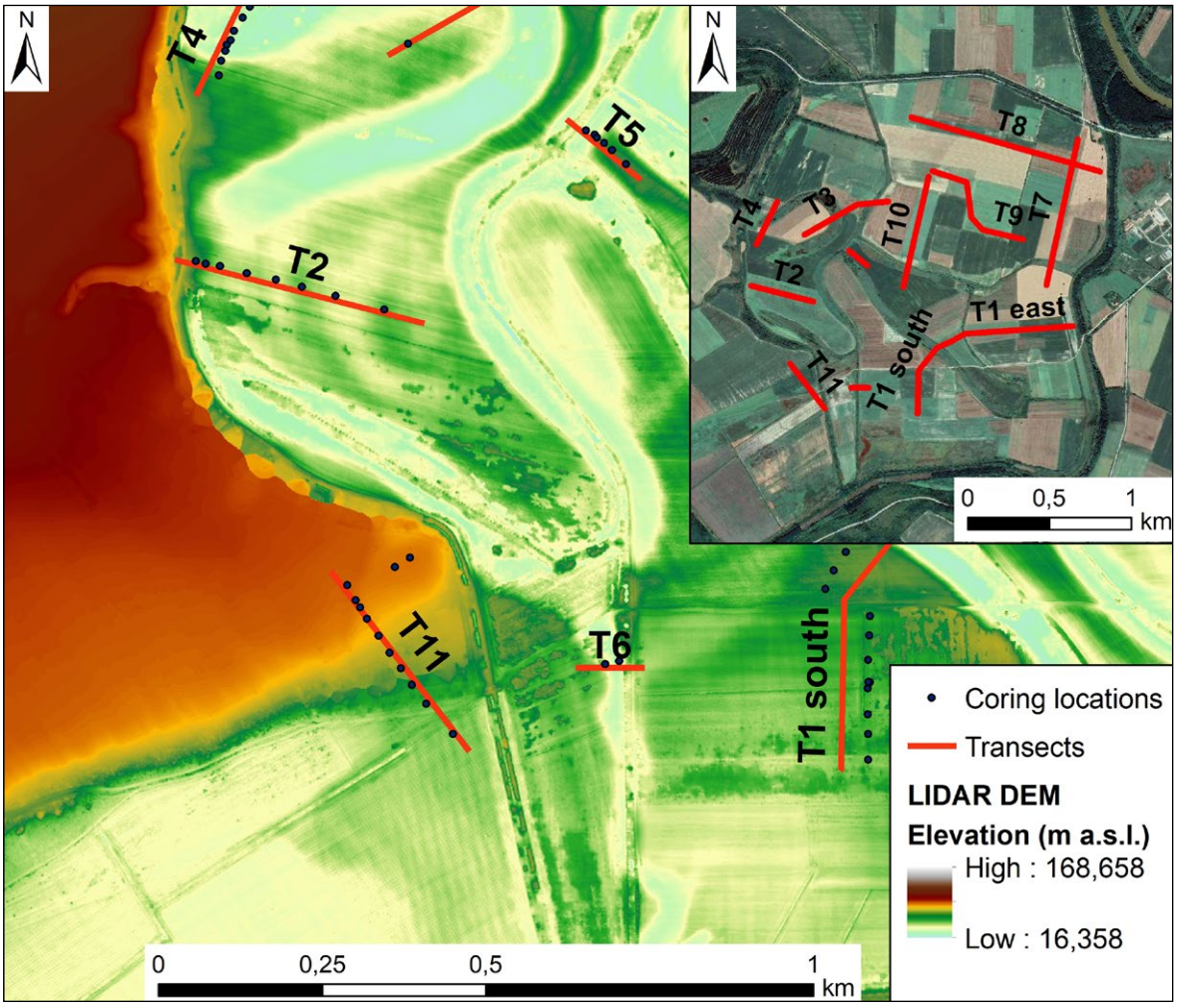


Fig. 19. Map of the corings from site 1 to the Studena Reka valley (T11) (figure by A. López del Olmo)

5, 7, 8 and 9), Secondly, core C6, located at the foot of Tash Bair shows a significant thicker A-horizon (unit O), compared to the other cores (respectively 130 cm at the foot and 100 cm on the hillslope). Relative recent soil erosion processes caused by agriculture are likely to have transported a part of the thick A-horizon from Tash Bair towards the foot of the hill and covered an archaeological horizon there. However, except at C2, the erosion at this part of the hillslope of Tash Bair seems to be limited, probably as a result of the rather gentle slope of about 3.5%.

4.6.2. Traces of a buried Neolithic site within the floodplain

Human artefacts (e.g. burned pottery, a blade, cereal seeds, animal bones and fish bones) were discovered by chance during the fieldwork in core 27 along coring transect 1 south (fig. 21). Additional cores in the surroundings (core C28, C29) provided more human artefacts. They come from a continuous human disturbed layer (a cultural layer), located at a depth between 310 and 360 cm. It was discovered between core C27 and C31, over a distance of about 80 m (fig. 22). Coring IDs, the depth of the archaeological layer and the coordinates of the cores are shown in table 4.

Radiocarbon dated sample 2, located at T1C29 (360 cm depth) does not only provide information about floodplain sediment accumulation rates (section 4.5.2.2. and 4.5.3.3.). It also provides a temporal reference frame for the identified human disturbed soil horizon. The sample was located at the bottom of this layer. As such, it provides a lower age for the cultural layer.

It is hypothesised that the darker grey layer, identified in core C23, C27–C32 (fig. 9) can be interpreted as a buried A-horizon, formed during a period when overbank deposits from the Yantra were

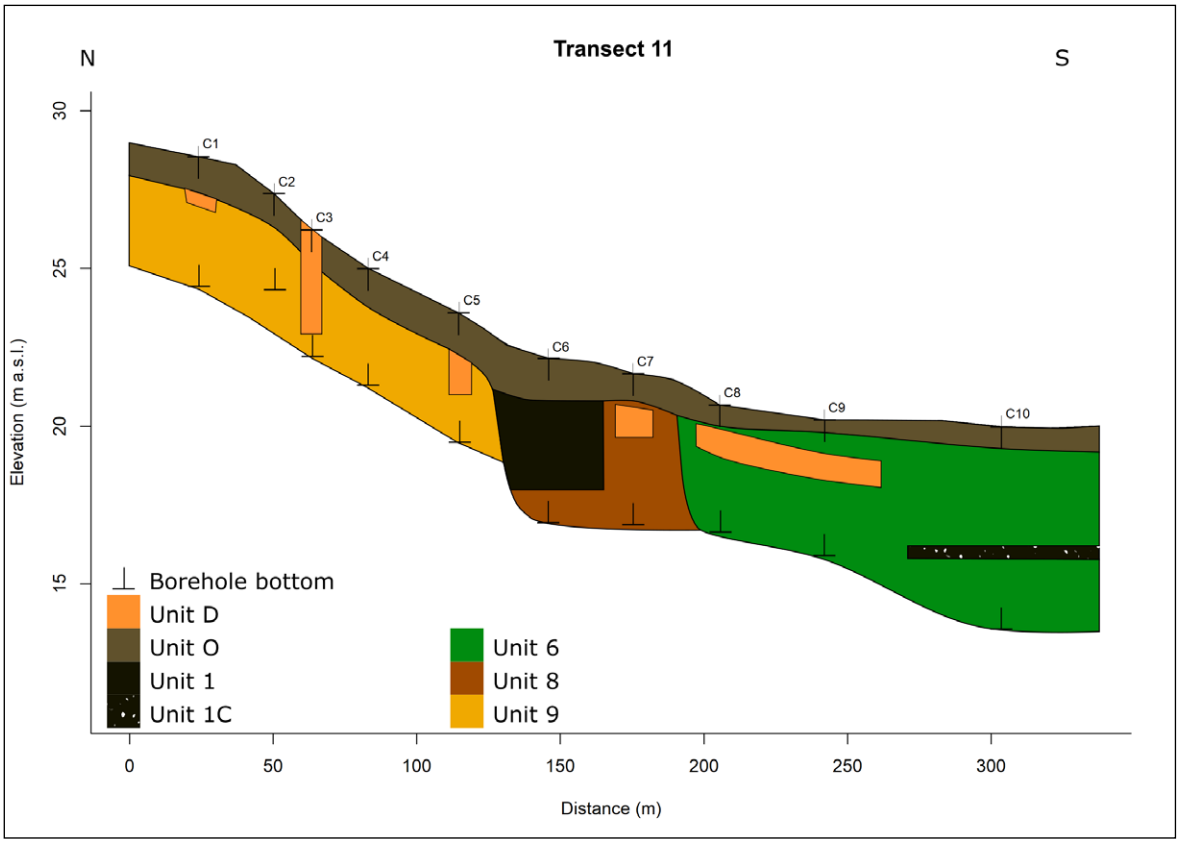


Fig. 20. Sedimentological interpretation of Tash Bair towards the alluvial plain of the Studena Reka and Yantra rivers (figure by A. López del Olmo)

limited in this area of the floodplain (i.e. the SW-meander was probably not active during this period). According to the dating of the sample, Early Neolithic farmers could have settled at this location of the floodplain. To date, no artefacts dating back to Early Neolithic times have been found at the confluence of the Yantra with the Danube.

The fragment of a silex knife (fig. 22), found at T1C27 at a depth of 330 cm, originates from a common tool and is too small for precise dating. It can be attributed to the period between 6000 and 3000 BC only (Raiko Krauß, 2020, personal communication).

During the fieldwork campaign of 2019, evidence was found to assume that the cultural layer, discovered in the floodplain of the Yantra, obviously dates back to one of the earliest moments of neolithization in the study area. Further research into this Early Neolithic archaeological layer might be an opportunity for future archaeological research in the area.

Firstly, it would be adequate to explore the entire extent of the site in the floodplain of the Yantra. Secondly, this case might be an opportunity to investigate seasonal settlement occupations. For example, did the settlers have a settlement in the floodplain, nearby a direct water source during summer and did they migrate towards Tash Bair e.g. during spring floods? Thirdly, additional dating of short living material, i.e. osteological remains of domestic animals or humans, will be crucial to place the cultural layer in a correct and narrower temporal time frame. This would provide direct information about human occupation, while this study provides indirect evidence through radiocarbon dating of an organic rich bulk sample at the bottom of the cultural layer.

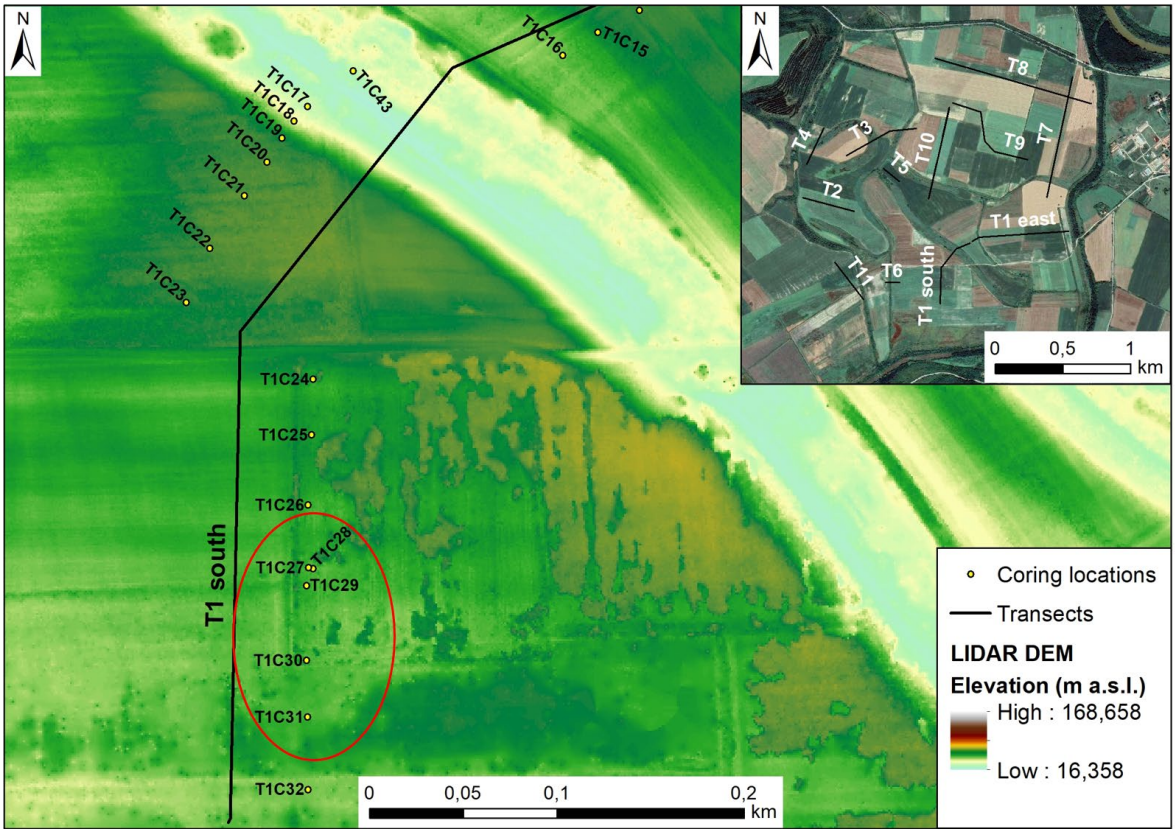


Fig. 21. The red circle indicates the location of the corings along T1 south where buried archaeological remains were found. The inset shows the location of T1 south in the study area on a Google Earth image (figure by A. López del Olmo)



Fig. 22. Archaeological finds of pottery remains, a blade, and a rounded stone along transect 1 south. Unit of scale: cm (figure by A. López del Olmo)

Table 4. Coring ID and depth of the corresponding archaeological layer. The coring locations are given in decimal degrees (DD)

Coring ID along coring transect 1 south	Depth of archaeological layer (cm below the surface)	Coordinates (DD)
C27	320–350	25,557438°E 43,594392°N
C28	310–340	25,557466°E 43,594388°N
C29	330–365	25,557428°E 43,594306°N
C30	310–360	25,557435°E 43,593945°N
C31	325–345	25,557488°E 43,593674°N

4.6.3. Tash Bair connected with the floodplain by a sunken lane

The LIDAR DTM and a Google Earth image of the study area reveal a remarkable gully, west of coring transect 2. This gully is rather deeply incised in the hill side of Tash Bair and has an unnatural deflection to the southwest. The gully was digitised making use of point locations (fig. 23). The corresponding coordinates and extracted elevation values were used to construct a 2D profile which reveals the elevation profile of the gully.

The length profile of the gully (fig. 23) west of coring transect 2 has a fairly moderate decline from Tash Bair towards the alluvial plain. The gully covers a height difference of about 20.5 m over a

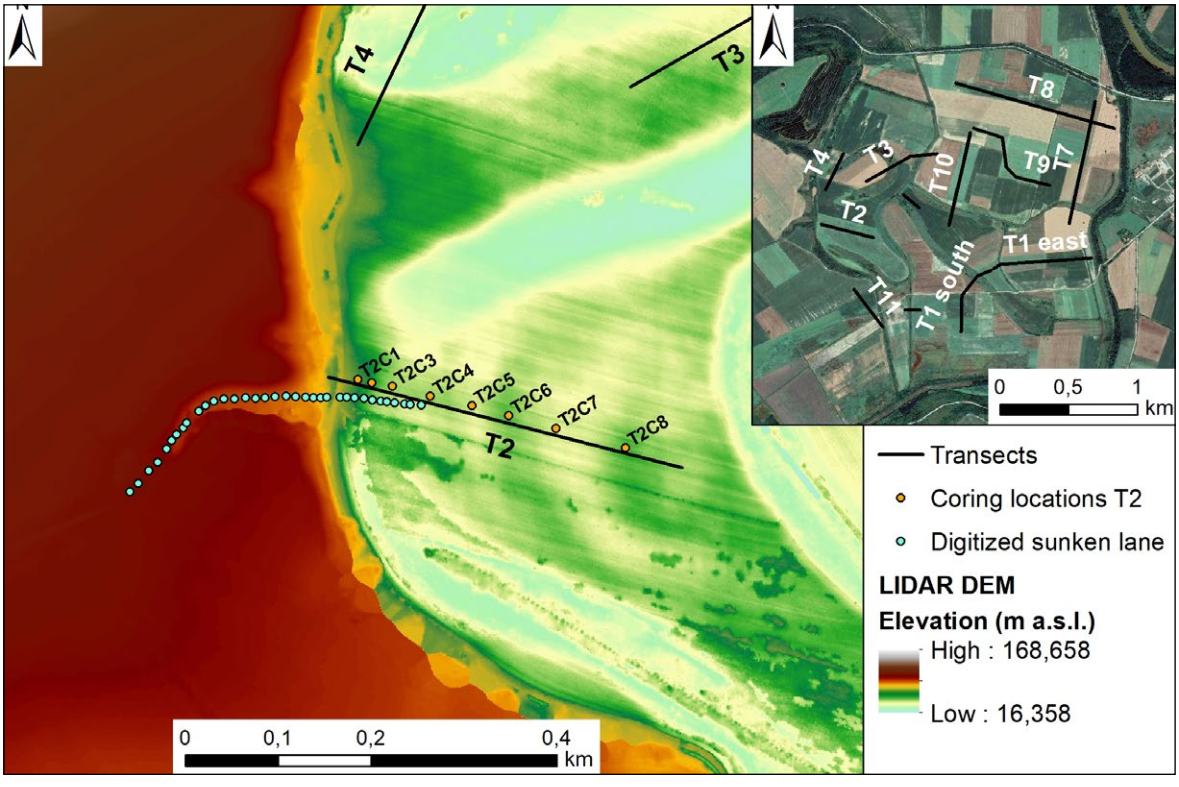


Fig. 23. Digitisation of points from Tash Bair (left), towards the floodplain (right). The inset shows the location of all coring transects on a Google Earth image (processing of Google Earth imagery and LIDAR DTM) (figure by A. López del Olmo)

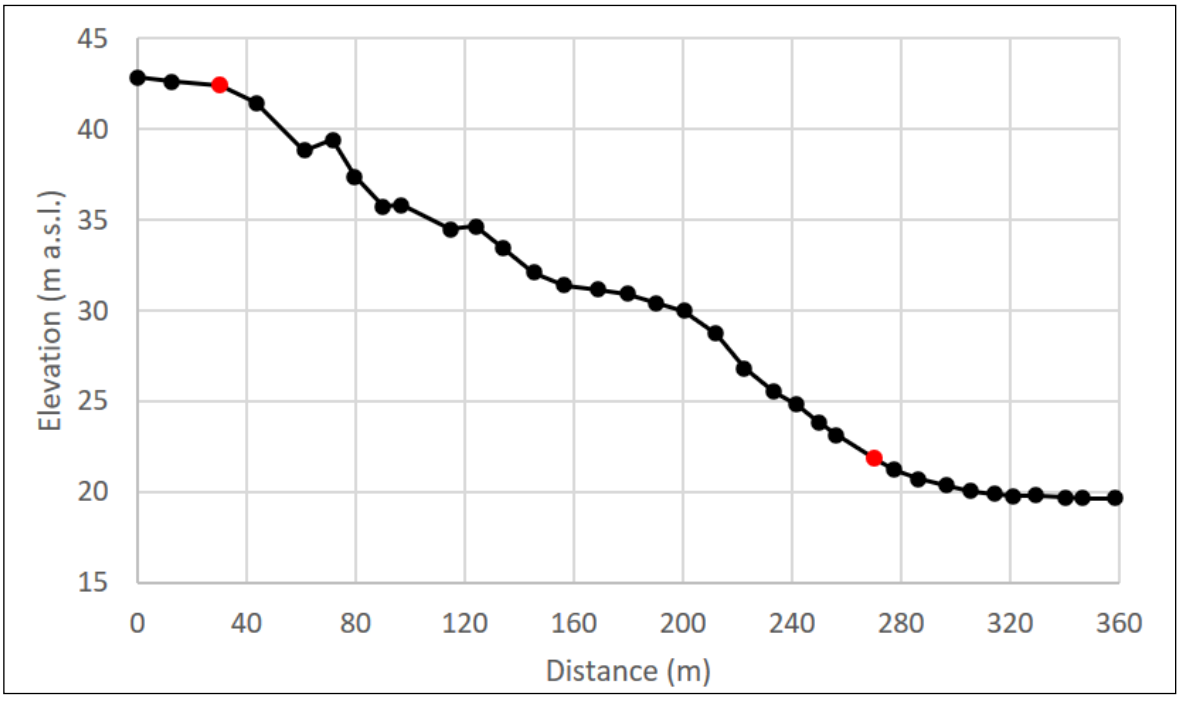


Fig. 24. Elevation profile of the digitised points in the gully west of coring transect 2. The two red dots mark the start and endpoint of the gully (figure by A. López del Olmo)

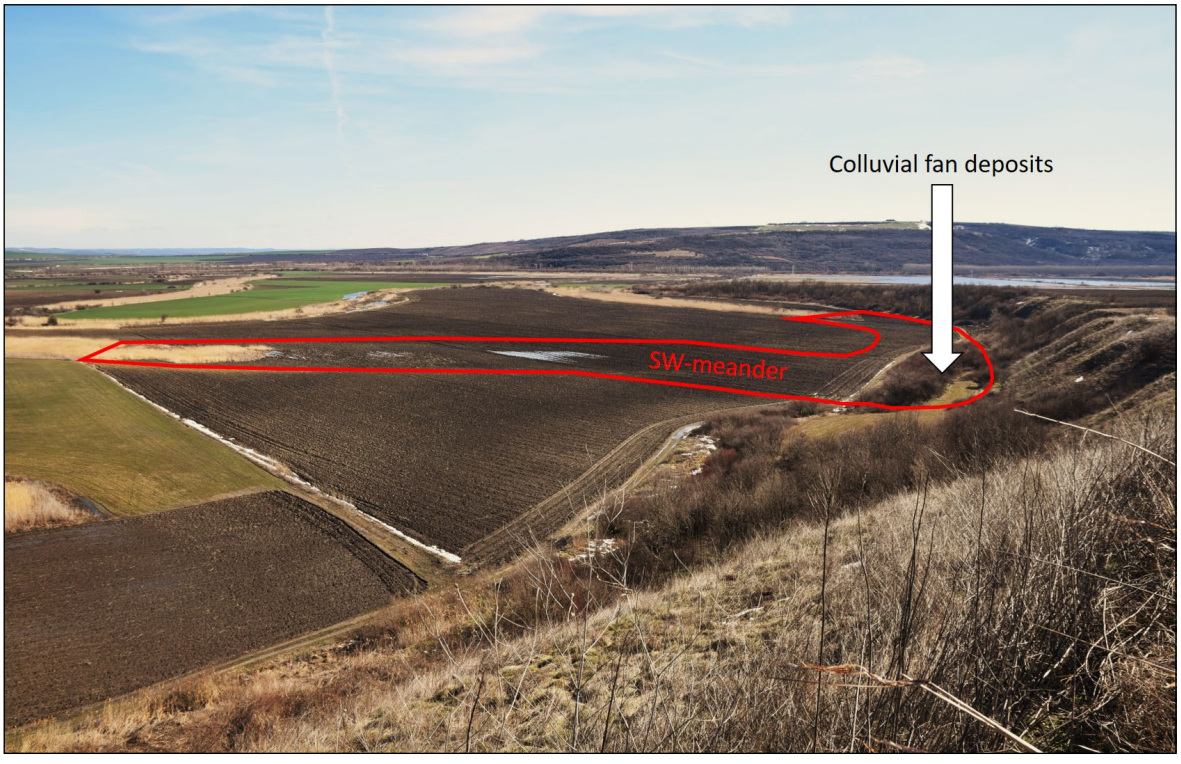


Fig. 25. SW-meander (delineated by the red line) buried by colluvium from the sunken lane. The apparent extent of the colluvial fan is shown by the border between the ploughed field and the wittered reed vegetation (picture: S. Conrad, late winter 2018)

distance of 240 m. The average slope within the gully (indicated by the two red dots) is about 5°. Near flat surfaces are visible at the plateau on the middle slope of the Tash Bair and on the floodplain.

Nowadays, the former river channel of the SW-meander is not visible at coring transect 2 due to the deposition of a vast amount of colluvial sediments (fig. 25). This in contrast to locations further away

from the apex of the gully, where withered reed vegetation grows in the lower elevated (wetter) parts of the former river channel. The interpretation figure of coring transect 2 (fig. 10) reveals a major colluvial fan deposit on top of the former SW-meander channel. About 790 cm of sediments have been deposited at T2C1 since the channel was abandoned about 2000 years ago. Sediment core C1 is not located at the apex of the gully. Hence, this core does not represent the maximal colluvial sediment thickness. It can be assumed that the colluvial sediment thickness is thicker at the apex of the gully. Outside the former river channel sediment deposits will be less thick. However, sediment thickness and the exact extent of the colluvial fan was not investigated in this research.

The results of the LIDAR DTM analysis (fig. 24) show that the gully has almost a linear slope of 5°. In addition, the western end of the gully bends towards the south, turning away from the area with the steepest hillslope. Taking the multiperiodic archaeological finds on Tash Bair into account, it can be assumed that the gully is actually a sunken lane. Sunken lanes are permanent, gully-like features in the landscape which (partially) have an anthropogenic origin. They are common geomorphic features in the west- and central loess belt, mainly formed by passage of people, animals, vehicles and the action of water and gravity (De Geeter et al. 2020). Furthermore, they can act as important features in the connectivity between hillslopes and valleys (Boardman 2013).

Although the sunken lane is overgrown nowadays, it can be assumed that it might have played an important role in connecting the alluvial plain with the settlements on Tash Bair. Furthermore, the sunken lane might have served as an important access and transportation route as they did at many other places (cf. for West and Central Europe De Geeter et al. 2020).

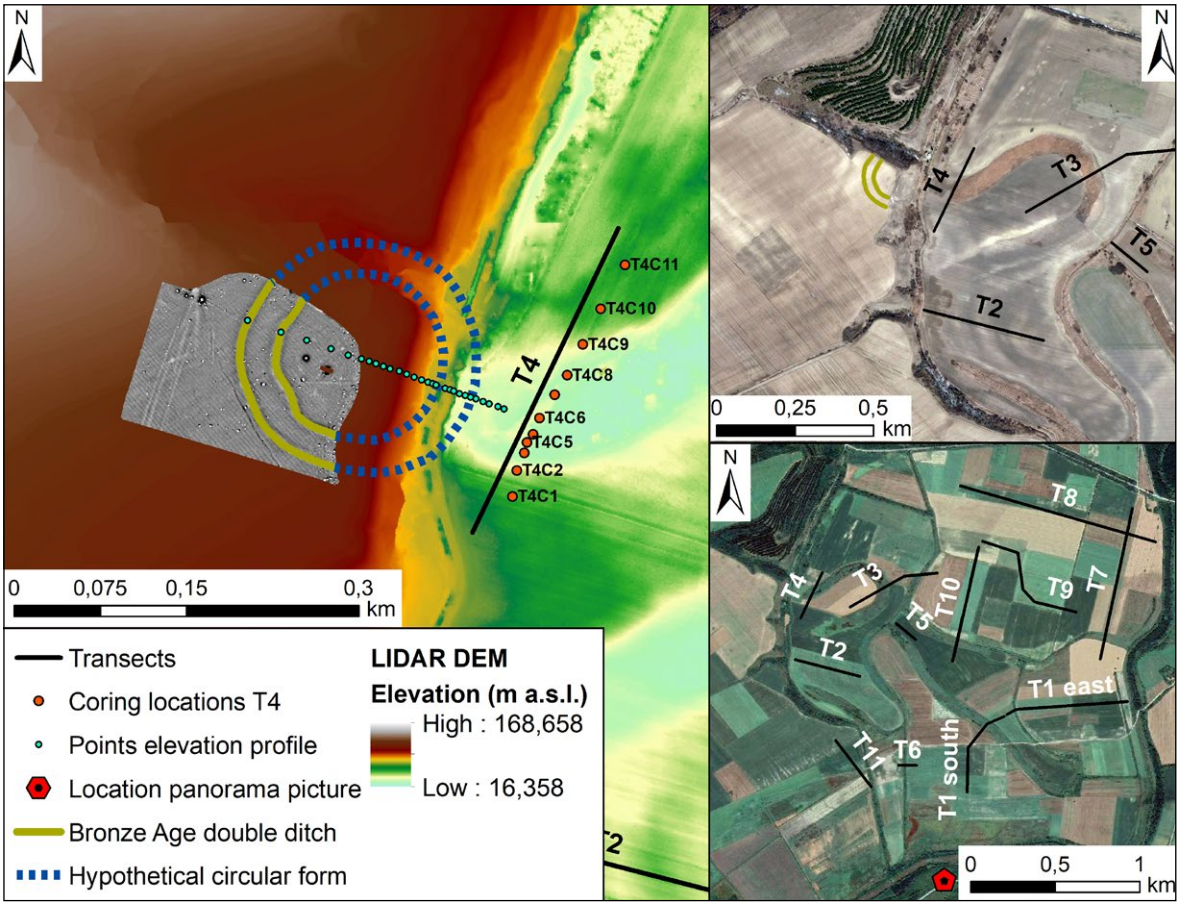


Fig. 26. Localization of the Middle Bronze Age double ditch with its hypothetical circular form, depicted on a DTM. The digitised points to construct the elevation profile (fig. 27) are indicated as well. The Google Earth images show the location of the Bronze Age double ditch, coring transect 4 and the location where panorama figure 28 was taken (processing of LIDAR DTM) (figure by A. López del Olmo)

4.6.4. The Bronze Age double ditch (site 3) and its possible reconstruction

Satellite imagery and a geomagnetic survey, together with a subsequent archaeological excavation in 2018 at Tash Bair revealed a quarter of a circular double ditch on the eastern part of hill, before it steeply descends (with a rather linear slope around 35°) towards the floodplain of the Yantra (fig. 26) (see the contributions by L. Vagalinski et al., chapter 8.2.1; Вагалински et al. 2019). A height difference of 38 m between Tash Bair and the alluvial plain of the Yantra is covered over a distance of only 54 m. Figure 27 shows the elevation profile established from the digitised points visualised in figure 26. At least the inner ditch originates from the Middle Bronze Age (20th–19th c. BC). Finds in the filling indicate that it was reused during the Late Iron Age (5th–1st c. BC) and the Late Roman period (5th c. AD). Based on Middle Bronze Age circular ditches, consideration is being given to reconstruct the complex at Tash Bair as a circular enclosure. In this case, a large part of the monument would be lost (fig. 26).

In assumption of this case, the location of the outer and inner ditch and the presumed centre of the enclosure are indicated on the graph (fig. 27). If a symmetric round enclosure is assumed, the remaining location of the inner and outer ditch could be mirrored to determine the location of the disappeared inner and outer ditch. The mirrored location of the inner and outer ditch is also indicated on the graph. These points are respectively located at 67 and 97 m from the current slope head. Before the topography completely flattens in the former river channel, a clear colluvial deposit with an extent of about 30 m and a thickness of 3 m is recognised at the foot of the hill slope.

The riddle is: when and how did three quarter of the protection ditches of the Bronze Age enclosure disappear? The northern part of the double ditch was probably eroded by the large gully to the north of the site (visible on the LIDAR DTM and on the Google Earth image, fig. 26). The levelling of the former channel at the foot of the gully indicates that major gully erosion (responsible for the supposed vanishing of the northern part of the enclosure) took place after the abandonment of the SW-meander about 2000 years ago. Gully erosion was probably caused by intensive agricultural practices during Roman times or even more recently, because of the transformation of small fields to large parcels and the introduction of new crops during the collectivisation period after 1950 (Krauß 2006a; Sedláček et al. 2016 and references therein).

What happened with the eastern part of the Bronze Age enclosure is less certain and leads to two hypotheses. The first is that the eastern part of the enclosure was probably prone to erosion processes caused by the river and/or hillslope processes. This hypothesis suggests that the circular reconstruction of the enclosure (about 100 m of the east side of Tash Bair) was eroded between today and the foundation of the enclosure. An alternative hypothesis, is that the Bronze Age settlers constructed a more or less semi-circular-, instead of the common circular enclosure (with the use of the promontory like situation and the natural barrier i.e. a 35° sloping cliff towards the alluvial plain of the Yantra as protection).

The time period in which an active river could erode Tash Bair is 500 to 1500 years (i.e. after the construction between 20th–13th c. BC, until the abandonment of the SW-meander 8th–5th c. BC). Although river activity is demonstrated around 390–200 calBC in the SW-meander, sedimentological information proves that in that period the river was not capable to erode its outer meander bend, probably due to a reduced discharge, caused by channel branching as proposed in section 4.5.2.8.

Hence, to remove 100 m in a time interval of 500 to 1500 years, erosion by scouring and/or mass failure of the outer bend of the Yantra meander at Tash Bair must have occurred at a cliff retreat rate of 67 to 200 mm yr^{-1}. Rivers would erode annually about 0.1 to 1% of the width of their channel (Kummu et al. 2008; De Rose, Basher 2011). If this holds true for the Yantra River, Tash Bair would have been eroded at a rate between 60–600 mm yr^{-1}. In other words, adopting average bank erosion rates can explain how the eastern part of Tash Bair vanished. However, this comparison might be invalid because Tash Bair is a rather massive hill, compared to riverbanks. Hence, erosion rates should be compared with similar cases. This is however virtually impossible due to a lack of similar cases where erosion rates of loess cliffs, by highly sinuous rivers with a low channel gradient, are presented.

Although coastal processes are different from fluvial processes, a comparable setting can be found at the Bulgarian loess cliffs at the Black Sea coast. Average coastal loess cliff retreat rates equal 300 mm yr^{-1} (Stanchev et al. 2013).

Another insight comes from the excavations at the fortress of Iatrus at the eastern edge of the Yantra floodplain. According to the missing north-western fortress wall and a large part of the inner architecture, it is suggested that about 50–60 m of the Pleistocene river terrace (where the fortress was built on, fig. 29) eroded by indirect fluvial activity (mass failure due to annual flooding of the floodplain) in a time period of less than 1400 years (Sven Conrad, 2020, personal communication). The vanished part of the fortress is comparable with the missing part at the Tash Bair, over a similar time interval. However, the erosion rate of the Pleistocene river terrace at Iatrus is not directly comparable with the cliff erosion at the Tash Bair for two reasons. Firstly, the considered river terrace where Iatrus is built on is merely 10–12 m above the floodplain while the cliff of Tash Bair is about 30 m high. As the rate of channel migration depends on bank height, it is expected that the hillslope of Tash Bair erodes slower than the river terrace at Iatrus (Hickin, Nanson 1984; Brooks 2003). Secondly, only a small part of Iatrus was exerted by direct erosion of the river but annual flooding of the floodplain would have caused the erosion of the Pleistocene river terrace while the river meander at Tash Bair probably scoured the cliff.

Based on average bank erosion rates, cliff erosion rates at the Black Sea and the Pleistocene river terrace erosion at Iatrus, the hypothesis that fluvial erosion – mainly flooding – caused the vanishing of the eastern 100 m of Tash Bair would seem acceptable. From very old eyewitnesses report, the entire floodplain used to be regularly flooded over long periods of time. The water backed up to the level of Karamanovo in the valley of the Studena Reka. This backwater was very often caused by piled ice floes in the Danube. According to the report by Georgi Georgiev (Krivina), this happened for the last time in the winter of 1941/42.

However, based on additional research, it is not expected that fluvial erosion alone could cause the vanishment of half of a full circle Bronze Age enclosure on Tash Bair for two reasons. Firstly, a visual inspection of the curvature of the entire eastern hillside of Tash Bair does not reveal significantly more erosion at locations where the outer bend of a meander meets the hill like near coring transect 4 (fig. 26). In other words, the cliff is not more eroded near coring transect 4, as compared to the rest of the cliff. Secondly, the result of radiocarbon dated sample 4, illustrates that the SW-meander, at coring transect 4 was already located at a similar position at the onset of the Younger Dryas (13080–12810 calBP). In addition, in the geological map of the study area (see Филипов 1992), the higher elevated area between coring transects 2, 3 and 4 is indicated as Upper Pleistocene alluvial deposits of the 1st and 2nd terrace above the floodplain. This suggests that the SW-meander had already a similar river course next to Tash Bair during the Late Glacial up to the abandonment of the SW-meander at the onset of the Younger Dryas. Hence, it can be assumed that the currently observed wide channel geometry (at coring transect 4) was established during the Bølling–Allerød interstadial, when large-scale meanders were active. The SW-meander was probably reactivated by a less capable, underfitting river stream, from the Middle Holocene until the Late Iron Age. Consequently, this river stream did not have the power to erode the side wall of Tash Bair. As the competence of a river to erode its sidewall is related to, amongst others, discharge and channel slope, it is expected that this competence was rather low for the Yantra, being a relatively small channel with a very low channel slope, reoccupying the much wider Late Glacial SW-meander channel (Nanson, Hickin, 1983, Hickin, Nanson 1984; Lawler 1995; van den Berg 1995; Lawler et al. 1999; Brooks 2003; Kleinhans, van den Berg 2011).

If the Yantra River would have scoured the cliff significantly at the enclosure, a clear curve would have been visible in the current side wall of Tash Bair between the section next to the Upper Pleistocene terrace and the section where the river was scouring the cliff. However, this is not observable. A visual inspection of the Google Earth image or LIDAR DTM (fig. 26) does not reveal substantially more erosion of the side wall at the location of the Middle Bronze Age double ditch adjacent to coring transect 4 as compared to

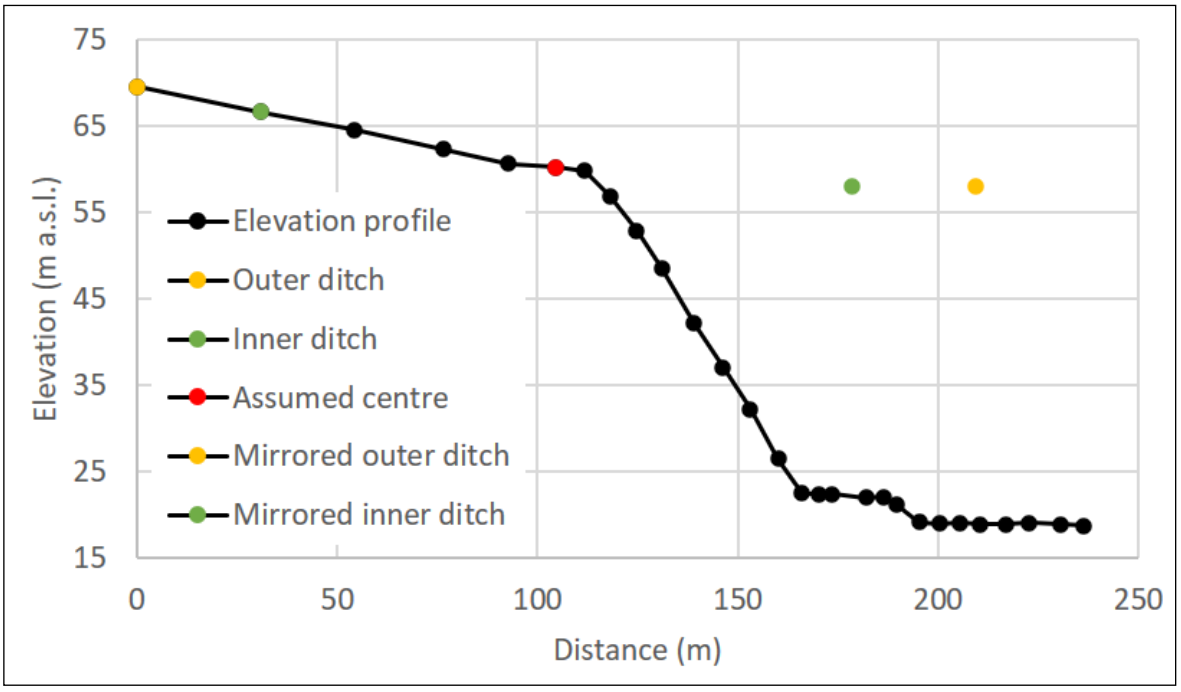


Fig. 27. Elevation profile from the Bronze Age enclosure towards the floodplain of the Yantra. The locations of the inner ditch, outer ditch and the presumed location of the centre of the enclosure and the mirrored inner and outer ditch are indicated (figure by A. López del Olmo)

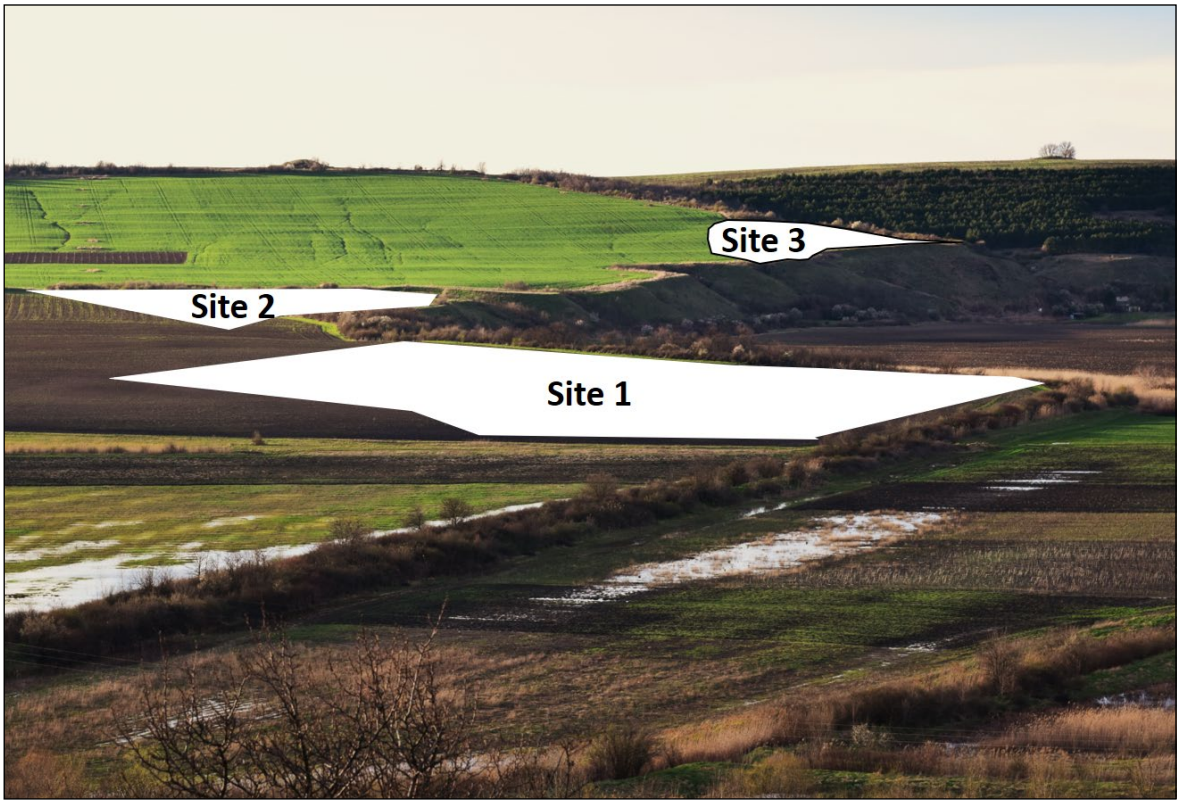


Fig. 28. The white polygons indicate the location of three archaeological sites on the Tash Bair hill. Site 1 indicates the location of a Neolithic to Medieval settlement, site 2 a mainly Roman to Late Roman and site 3 of a Middle Bronze Age double ditch. Note the gullies in the crop fields as an indication for erosion on the steeper slopes. The picture is taken in a north-westward direction see Fig. 26 for the exact location (picture: S. Conrad, 2018, early spring 2018)

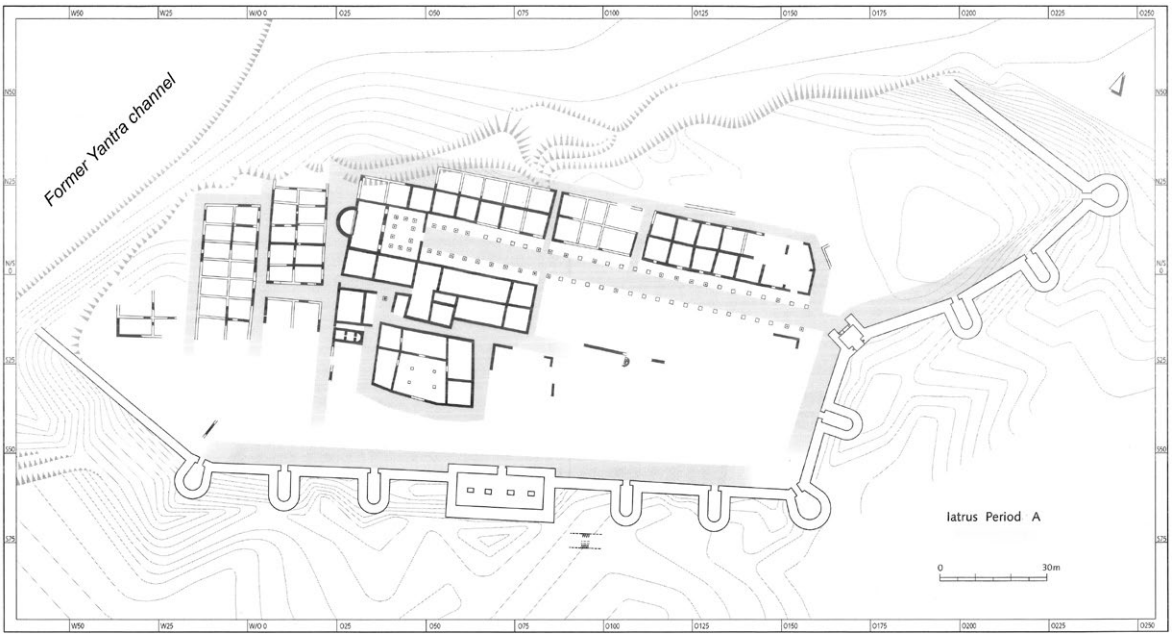


Fig. 29. Limes fort Iatrus, architectural plan of Period A (ca. 320–360) (after Iatrus-Krivina VI, plan, suppl. 3). The sharply jagged line marks the break-off edge as it was found at the beginning of the excavations in 1958. Due to the backfilling with excavated material, this brim is no longer visible in the terrain

other parts of the side wall. Contrary, the curvature of the east side of the Tash Bair hill is rather straight, only interrupted by gullies. This indicates that the eastern side of the Tash Bair hill was rather little subject to fluvial erosion by the less capable river stream in the SW-meander since the Younger Dryas.

Another option is that hillslope processes (e.g. mass failure, similar to the Pleistocene river terrace at Iatrus) were responsible for the removal of the eastern part of the double ditch. If active scouring of Tash Bair by the river is assumed, the sidewall would probably have had a vertical cliff. The slope of the cliff would evolve over time towards a gentler slope after the abandonment of the SW-meander. This process alone could explain 54 m of cliff head retreat since the abandonment of the SW-meander about 2000 years ago. This option can however be refuted, based on figure 27. This figure shows that the sediment volume, stored at the foot of the hill is insufficient to explain the transition from a straight cliff towards the current hill slope. This implies that hillslope processes over the previous 2000 years are unlikely to have caused the disappearance of half of the double ditch.

Hence, it seems unlikely that hillslope processes nor erosion alone by the Yantra River were capable to remove about 100 meters of the east side of the Tash Bair hill since the Middle Bronze Age. In summary, it can be said that on the basis of our investigations, the erosion by the river alone should not have been sufficient for such a large erosion to justify a reconstruction as a circular enclosure. On the other hand, since cliff erosion caused by the floods is difficult to estimate, but in the case of Iatrus it has led to considerable destruction over the centuries under similar conditions, this cannot be ruled out.

4.7. CONCLUSION

The main objective of this geomorphological research was to disentangle the complicated history of the Yantra River courses since the Last Glacial Maximum and to reveal the former river dynamics and the processes which have shaped the alluvial plain of the Yantra for a study area near the village of Novgrad. Sedimentological information of 166 corings, sub-surface information from 3 ERT profiles, radiocarbon dates of 13 samples and a topographical analysis (based on a LIDAR DTM) made it possible to reveal important insights of the fluvial history of the Yantra. The results contribute to ongoing joint Bulgarian-German archaeological research at the Tash Bair hill and its surroundings near the confluence of the Yantra with the Danube.

Concerning the history of the Yantra River courses since the Last Glacial Maximum, it is demonstrated that river channels were formed, abandoned, and reactivated since the Late Glacial, which complicated the reconstruction of former river courses. Therefore, river course scenarios should be considered with prudence. Although only two remnants of large-scale Late Glacial meanders have been identified, it is substantiated that two phases of large-scale meandering occurred during the Late Glacial. Additional research is required to gain more insights in the shape, extent and exact timing of the activity of large-scale Late Glacial meanders in the study area.

Similar to the study of A.J. Howard et al. (2004), this study was not able to reconstruct earlier river courses of the Yantra during the Lower Holocene. It is assumed that the SW-meander was reactivated as the main river channel of the Yantra during the Middle Holocene until 740–400 calBC. It is proposed that one channel avulsion between calBC 80–140 calAD (i.e. the transition from the Late Iron Age to the Early Roman times) was responsible for the abandonment of the study area, in favour of a northward channel deflection. Furthermore, it is proposed that the Yantra had a rather stable course during ca. the last 2000 years, until major construction works impeded the natural meandering river by channel straightening and the construction of embankments from the beginning of the 20th c. These major infrastructure works resulted in a shortening of the overall river length by almost 40 km, on a reach of 110 km.

Continuous floodplain aggradation took place during the Middle and Upper Holocene, with an average sediment accumulation rate of 0.65 mm yr^{-1} between 6080–5980 calBC and 740–400 calBC. This rate doubled in the last 2000 years. Initial floodplain aggradation can be linked to an increase of the base level of the Yantra, related to the base level of the Danube, regulated by the level of the Black Sea which increased drastically at ca. 9500 calBP (reconnection Mediterranean and Black Sea), and continued until ca. 5200 calBP (stabilization of the Black Sea level). The impact of climate change or land subsidence on floodplain aggradation is less obvious.

Recent channel aggradation cannot be attributed to changes in the level of the Black Sea. They can however be attributed to an increased human impact, which enhanced erosion processes, caused by land use changes in the river basin, comparable to studies in North and Central Europe (Lang et al., 2003; Erkens et al., 2009; Notebaert, Verstraeten, 2010; Notebaert et al., 2011; Houben et al., 2012; Broothaerts et al., 2013, 2014).

During our investigation, amongst others the potential reconstruction of site 3 as a typical circular Bronze Age enclosure was discussed. According to our results, the river was not able to cause such an amount of erosion to justify this reconstruction. But since the influence of the river flooding is difficult to estimate, such a reconstruction cannot be excluded, especially in regarding the case of Iatrus.

Furthermore, an important archaeological discovery was done during the fieldwork. A cultural layer, containing remains of fish bones, cereals, pieces of daub and a piece of a stone blade, covered by a sediment packet of more than 3 m was identified in the southern part of the floodplain. This cultural layer seems to be one of the first discovered traces of human activity during the Early Neolithic at the confluence of the Yantra with the Danube. It is considered an unexpected and unique result of the field work that merits further research.

Acknowledgements

This research was made possible by a transdisciplinary collaboration between a joint Bulgarian-German archaeological research team from the National Archaeological Institute with Museum at the Bulgarian Academy of Sciences with the Institute of Prehistory and Archaeology of the Middle Ages of the Eberhard Karls University of Tübingen (Germany) and the Division of Geography & Tourism from the KU Leuven (Belgium). Moreover, the authors thank all people who were involved during the fieldwork. In particular, the three workmen (Vesko, Miroslav and Sashko), assistance from Johanna Gille and Joachim López and supervision by Gert Verstraeten and Nils Broothaerts.

Table 5. Overview of radiocarbon dated samples. The first part of the sample ID indicates along what transect the sample was taken (Tx, with x being a number from 1 to 10), then at which coring (Cx, with x being a number between 3 and 29). The number after the underscore equals the depth of the sample below the surface (cm). The conventional ^{14}C age gives the measured radiocarbon age of the samples in years before present ± one standard deviation. Calibrated calendar ages are given in years before present and in AD "Anno Domini" or BC "Before Christ", rounded to ten. OxCal online with IntCal13 atmospheric curve was used for calibration

Sample nr.	Coordinates (DD)	Sample ID & depth (cm)	Lab ID	Conventional ^{14}C age BP ($\pm 1\sigma$)	Calendar age calBP (confidence level)	Calendar age calAD/BC (confidence level)	Stratigraphic position	Dated material
1	25,560516°E 43,597393°N	T1C9_430	RICH-28052	2411±25	2680–2640 (8,0%) 2610–2600 (1,3%) 2500–2350 (86,1%)	BC 740–690 (8,0%) BC 660–650 (1,3%) BC 550–400 (86,1%)	Organic rich layer of 6 cm thick, directly on top of a coarse sand layer (interpreted as the former river channel bottom).	Piece of bark
2	25,557428°E 43,594306°N	T1C29_360	RICH-28447	7151±33	8025–7930 (95,4%)	BC 6075–5980 (95,4%)	At the bottom of a human disturbed, organic enriched layer of clayey overbank deposits in a distal floodplain.	Bulk
3	25,545155°E 43,603061°N	T4C4_332	RICH-28436	2243±24	2340–2290 (26,2%) 2270–2150 (69,2%)	BC 390–340 (26,2%) BC 320–200 (69,2%)	In a sandy-loam deposit (interpreted as an in-channel point bar deposit in an abandoned river channel).	Piece of bark
4	25,545223°E 43,603193°N	T4C6_420	RICH-28078	11094±47	13080–12810 (95,4%)	BC 11130–10860 (95,4%)	Upper part of an organic rich coarse sand layer (interpreted as the former river channel bottom).	Bulk
5	25,545379°E 43,603376°N	T4C7_226	RICH-28438	1012±25	980–900 (91,9%) 850–830 (3,5%)	AD 970–1050 (91,9%) AD 1100–1120 (3,5%)	In a clayey, peaty abandoned channel infill layer.	Seeds

Sample nr.	Coordinates (DD)	Sample ID & depth (cm)	Lab ID	Conventional ^{14}C age BP ($\pm 1\sigma$)	Calendar age calBP (confidence level)	Calendar age calAD/BC (confidence level)	Stratigraphic position	Dated material
6	25,567671°E 43,604455°N	T7C23_654	RICH-28048	1912±25	1930–1810 (95,4%)	AD 20–140 (95,4%)	In a clay-sand sequence (63 cm above a fine gravel layer, interpreted as the former river channel bottom).	Piece of wood
7	25,567879°E 43,604971°N	T7C24_325	RICH-28448	1506±24	1520–1460 (8,7%) 1420–1330 (86,8%)	AD 430–490 (8,7%) AD 530–620 (86,8%)	In the middle of a 65 cm thick organic and shell enriched clay layer (interpreted as the infill of an oxbow lake).	Bulk
8	25,560873°E 43,608610°N	T8C3_430	RICH-26700	1814±33	1830–1690 (86,2%) 1680–1620 (9,2%)	AD 120–260 (86,2%) AD 270–330 (9,2%)	In a clay packet of an abandoned channel fill (150 cm above a coarse sand layer, interpreted as the former river channel bottom).	Seeds
9	25,561842°E 43,608562°N	T8C13_683	RICH-28437	2473±59	2730–2360 (95,4%)	BC 780–410 (95,4%)	In a sand-clay sequence (interpreted as an abandoned channel fill).	Silene and Carex seeds
10	25,560579°E 43,605420°N	T9C9_747	RICH-28439	1997±48	2110–2080 (2,0%) 2070– 1860 (91,7%) 1850– 1820 (1,7%)	BC 160– 130 (2,0%) BC 120– 90 AD (91,7%) AD 100– 130 (1,7%)	In a sand-clay sequence, interpreted as an abandoned channel fill (64 cm above a coarse sand layer, interpreted as the former river channel bottom).	Seeds
11	25,563531°E 43,603014°N	T9C13_467	RICH-28435	5075±27	5910–5740 (95.4%)	BC 3960–3790 (95,4%)	Top 20 cm of a coarse sand layer (interpreted as the former river channel bottom).	Wood
12	25,558250°E 43,606415°N	T9C17_280	RICH-28446	5294±28	6190–5990 (95,4%)	BC 4240–4040 (95,4%)	In a terrace deposit	Bulk

Sample nr.	Coordinates (DD)	Sample ID & depth (cm)	Lab ID	Conventional ^{14}C age BP (±1σ)	Calendar age calBP (confidence level)	Calendar age calAD/BC (confidence level)	Stratigraphic position	Dated material
13	25,557233°E 43,605498°N	T10C4_215	RICH-28068	2600±26	2760–2720 (95,4%)	BC 820–770 (95,4%)	In the middle of an organic and shell enriched layer in an abandoned channel fill (shallow open water deposits)	Bulk

Table 6. Lithogenetic units, key of the interpretation figures

Colour indication	Lithogenetic units	Sediment texture characteristics	Deposition locations	Interpreted deposition environment
	Unit 1	Organic material	Low elevated locations in the floodplain	Marshy floodplain
	Unit 1C	Enrichment with freshwater shells		
	Unit 2	Clay	Abandoned river channels	Abandoned river channel
	Unit 3	Clay-sand layer sequence	Frequently flooded abandoned river channels	Abandoned river channel
	Unit 4	Coarse sand to fine gravel	At the bottom of channels	In-channel deposits
	Unit 5	Loam to coarse sand (fining-up sequence)	Elongated ridges along river channels	Levee and point bar deposits
	Unit 6	Clay to loam	Higher elevated areas in the floodplain	Overbank deposits
	Unit 6A	Enrichment of concretions/ nodules		
	Unit 6B	Enrichment of vitreous crystals		
	Unit 7	Loam to silt	At the foot of a steep slope	Colluvial deposits
	Unit 8	Compact clayey, loamy to sandy sediments	Higher elevated depositional floodplain remnants which do not match the current river activity	River terrace
	Unit 9	Aeolian silt loam (Loess)	Surfaces exposed during the Late Glacial period, beyond the alluvial plain.	Cold and dry steppe environments
	Unit D	Enriched with anthropogenic artefacts	In the alluvial plain, on hillslopes, mostly near the current surface	

Colour indication	Lithogenetic units	Sediment texture characteristics	Deposition locations	Interpreted deposition environment
	Unit O	A-horizon	Forms in the upper 40 up to 80 cm of the soil profile	

РЕКОНСТРУКЦИЯ НА ПАЛЕОРЕЧНОТО ТЕЧЕНИЕ В ЗАЛИВНАТА НИЗИНА НА Р. ЯНТРА, ЦЕНТРАЛНА СЕВЕРНА БЪЛГАРИЯ

Андреас Лопес дел Олмо, Херт Верстраетен, Нилс Бротхаертс

(Резюме)

Основната цел на това геоморфоложко изследване е да се изясни сложната история на теченията на р. Янтра след LGM (последен глациален максимум), като се проследи древната динамика на реката и на процесите, които са оформили нейната алувиална равнина в изследваната площ от приблизително 4 км^2 близо до с. Новград в Северна България. Седиментоложка информация от 166 сондажа, направени с ръчен свредел, подповърхностна информация от 3 ERT (томография на електрическо съпротивление) профила, както и радиовъглеродно датиране (^{14}C AMS) на 13 проби и топографски анализ (базиран на цифров модел на терена от въздушно лазерно сканиране – LIDAR DTM) осигуриха нужните научни данни за търсените изводи. Настоящото проучване изяснява и връзката между развитието на речните меандри и реакцията на хората на този природен процес през холоцена.

Установи се, че югозападният меандър на Янтра бил нейно основно корито от средния холоцен до 740 – 400 calBC. Изглежда, че друго корито, датиращо от 80 calBC – 140 calAD (т.е. преходът от късната желязна епоха към Ранната римска империя), причинило изместване на реката на север и североизток вместо първоначалната посока към Таш баир. Промяната предизвикала изоставяне на изследвания микрорайон в полза на терена източно от р. Янтра. Вероятно тя определила и местоположението на късноримския кастел „Ятрус“. Изглежда, че реката е поддържала стабилно течение през следващите векове, докато нейното корито било променено в началото на XX в. чрез изкуствени канали и диги. Така дължината на цялата река била скъсена с почти 40 км. Човешката намеса променила драстично течението на Янтра, което се е развивало по естествен път през холоцена.

Непрекъсната аградация (отлагания) на заливните низини протичала през средния и горния холоцен. Средната скорост на натрупване на седименти била от 0,65 mm yr^{-1} между 6080 – 5980 calBC и 740 – 400 calBC. Тази скорост се удвоила през последните 2000 години. Първоначалната аградация на заливната низина може да се свърже с повишаване на базовото ниво на р. Янтра, свързано с основното ниво на Дунав, влияещо се от това на Черно море. Последното се повишило рязко в периода от около 9500 calBP (след свързването на Средиземно с Черно море) до около 5200 calBP (стабилизиране на нивото на Черно море). Климатични или геоложки промени оказали малко въздействие върху процеса на алувиация при заливните тераси. Неотдавнашната аградация на коритото на речните меандри не се дължи на амплитуди в нивото на Черно море. Тя била причинена от засилено човешко въздействие (земеделие), което ускорило ерозионните процеси. Същата зависимост е установена в Северна и Централна Европа.

Беше обсъдена потенциална реконструкция на обект 3 като типично кръгло заграждение (рондел) от бронзовата епоха. Според нашите резултати самата река не била в състояние да причини такава мащабна ерозия на площта му на високата тераса. Все пак тази възможност не е напълно изключена, имайки предвид частичното разрушаване на късноримския кастел „Ятрус“ от реката и от наводнения.

В южната част на заливания терен разпознахме културен пласт, покрит с дебел над 3 м утаечен слой. Първият съдържа рибени кости, зърнени храни, парчета мазнина и фрагмент от кремъчно острие. Датировката на органични проби от пласта е около 6000 г. пр. Хр. Изглежда, че разполагаме със следа от човешко присъствие в района през ранния неолит. Нужно е да се проучи допълнително този терен, за да се установи дали става въпрос за сезонни заселвания. Датирането на костни останки от домашни животни и/или хора от същия културен пласт ще уточни настоящата хронология, която е направена чрез изследване с радиовъглеродния метод на богата на органика насипна проба, взета от долния край на въпросния пласт.

5. METHODOLOGY OF ARCHAEOLOGICAL RESEARCH

5.1. THE MEASUREMENT SYSTEM

Nadezhda Kecheva, Sven Conrad

The measurement systems used during field and geophysical surveys and archaeological excavations in the project included a combination of different techniques according to the different objectives. The establishment of a fixed-point grid at the beginning of the project work was one of the most important prerequisites for the subsequent implementation of the interdisciplinary research

During field surveys of 2018 and 2019 each team member carried handheld GNSS receiver (usually a smartphone with special mobile applications or a handheld Garmin GPS receiver) with estimated accuracies between 3 to 5 m in open areas (cf. the contributions by N. Kecheva, chapter 5.2). They were used for tracking fieldwork activities and creating waypoints.

In the peripheral areas of sites 1–4, which are untouched by agricultural activity, a total of 38 control points were set in visible and easily retrievable locations in the spring of 2018 (fig. 1). As a rule, a 40 cm long marking pipe designed for surveying work was hammered into the ground and a plastic pipe measuring mark was placed on it. To protect against damage, the upper edges of the pipe measuring

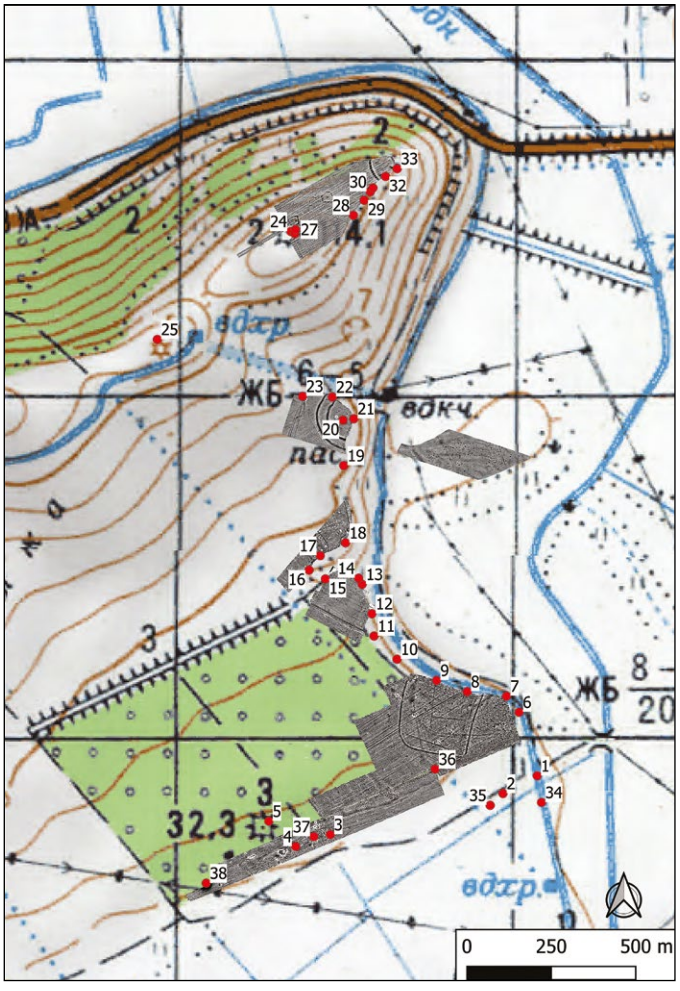


Fig. 1. Map with the position of the fixed points at the sites 1–4 on the Tash Bair (figure by S. Conrad)



Fig. 2. Newly set anchor point No. 35 with marking (photo by S. Conrad)



Fig. 3. Fixed point No. 24 on the survey point, which is located on the burial mound site 14 (photo by S. Conrad)

marks were placed approximately 15–20 cm below the surface of the earth and were covered with earth between the work campaigns. The points were marked with a stone next to it and a stake nearby. In addition, prominent trees nearby were given a colour symbol (fig. 2). In individual cases, fixed objects such as the foundation of a bridge railing or the old fixed point on the burial mound site 24 were used to define fixed points (fig. 3).

During the geophysical surveys conducted in the spring of 2018 by geophysicists from the company Eastern Atlas, Berlin, two GNSS receivers Forsberg ReAct with embedded NovAtel OEM6 technology were used. The collected data was post-processed to a centimetre accuracy using RINEX data from Belene and Ruse reference stations ordered from SmartNetBG company. The exact positioning of the geomagnetic mapping enabled the precise placement of excavation trenches.

The geophysicists measured the control points X and Y coordinates in World Geodetic System (WGS) 1984 in Universal Transverse Mercator (UTM) projection, zone 35N (table 1). Baltic vertical coordinate system was used for measuring height. Temporary control points were used for total pick up tracing on site 1 and recording of three-dimensional measurement of archaeological excavations in 2018 and 2019.

During the spring of 2018 the small polygonal grid of the intensive field-by-field surveys (total pick up) (cf. the contributions by N. Kecheva, chapter 5.2) was traced on the surface of site 1 using a Trimble M3 DR total station. The deviation that arises from the original measurement of the corner points with handheld GNSS devices could be neglected for this purpose.

In most cases, a Trimble M3 DR total station (fig. 4) was used for measurement during the archaeological fieldwork activities, for example for the three-dimensional (X, Y and Z) measurement of archaeological structures and finds as part of the excavation recording methods. Two GNSS receivers Leica GS08 plus (fig. 5) were used for the excavation work in 2018 and two GNSS receivers CHCNav



Fig. 4. Measurement with Trimble M3 DR total station (photo by S. Conrad)



Fig. 5. Measurement with GNSS receivers Leica GS08 plus (photo by S. Conrad)

i70 in 2019. The collected data measurements were daily downloaded in .csv and .xml formats then added and used in GIS software and Agisoft Metashape photogrammetric software.

Based on the control points set at the edge of the sites, temporary points were additionally set around the excavation trenches during the excavation work. The temporary points were recorded using Trimble M3 DR total station in a list together with a description of the position and photos of the situation.

Table 1. Table with point No., easting (X), northing (Y) in WGS 1984 UTM 35N coordinate system, height in Baltic coordinate system

Point No.	Easting (m)	Northing (m)	Height (m)
1	382980.640	4827819.130	23.350
2	382879.080	4827766.690	21.390
3	382367.710	4827645.150	22.180
4	382265.060	4827609.610	22.090
5	382185.550	4827684.870	33.320
6	382926.810	4828007.360	23.500
7	382889.770	4828054.900	26.080
8	382773.210	4828068.300	30.390
9	382682.500	4828101.600	32.770
10	382565.320	4828164.180	35.330
11	382497.210	4828232.900	37.320
12	382491.000	4828298.920	38.190
13	382462.020	4828385.970	40.490
14	382451.470	4828404.100	40.790
15	382353.040	4828402.100	42.550
16	382304.780	4828428.020	44.330
17	382337.870	4828470.760	44.020
18	382412.850	4828508.730	42.900
19	382407.350	4828737.530	52.990
20	382405.230	4828872.060	63.020
21	382437.310	4828876.080	60.730
22	382373.690	4828940.340	66.180
23	382285.290	4828942.650	74.410
24	382250.800	4829430.480	115.230
25	381855.190	4829110.880	117.110
26	382262.660	4829424.240	112.380
27	382264.280	4829435.850	112.390
28	382436.010	4829478.350	102.130
29	382467.880	4829523.220	100.110
30	382486.190	4829547.780	98.460
31	382493.980	4829559.410	97.900
32	382531.440	4829593.370	94.010
33	382565.780	4829616.270	90.700
34	382993.513	4827740.272	22.083
35	382841.209	4827731.755	20.825
36	382677.956	4827838.898	24.208
37	382318.751	4827639.046	21.372
38	381999.960	4827501.322	23.282

СИСТЕМИ ЗА ИЗМЕРВАНЕ И ДОКУМЕНТИРАНЕ
Надежда Кечева, Свен Конрад

(Резюме)

Системите, използвани за измерване и документиране при теренните издирвания, геофизичните проучвания и археологическите разкопки, включват комбинация от различни технологии според различните цели.

При теренните издирвания през 2018 и 2019 г. всеки член на екипа носеше ръчен GNSS приемник (обикновено смартфон със специални мобилни приложения или ръчен GPS приемник) с точност между 3 и 5 м на открити пространства. Те са използвани за създаване на тракове и точки.

През пролетта на 2018 г. в периферията на обекти 1 до 4, извън обработваемите площи, 38 контролни точки са стабилно поставени на 0,15 – 0,20 м под повърхността. При геофизичните проучвания през пролетта на 2018 г., извършени от компанията Eastern Atlas, Берлин, два GNSS приемника са използвани за събиране на данни. Тези данни са допълнително обработени до достигане на сантиметрова точност с помощта на RINEX данни от референтни станции в Белене и Русе, получени от компания SmartNetBG. Контролните точки са измерени от геофизиците с проектирани координати в WGS 1984 UTM 35 N и височина – в Балтийска координатна система.

През пролетта на 2018 г. малките полигони на обект 1, на които е направено пълно събиране на артефакти (total pick up), са трасирани на повърхността с помощта на тотална станция Trimble M3 DR.

По време на археологическите разкопки за документиране на X, Y и Z координати са използвани: тотална станция Trimble M3 DR (през 2018 и 2019 г.), два GNSS приемника Leica GS08 plus (през 2018 г.) и два GNSS приемника CHCNav i70 (през 2019 г.). Събраните данни бяха ежедневно сваляни в .csv и .xml разширения и после добавяни и използвани в ГИС софтуер и във фотограметричен софтуер Agisoft Metashape.

5.2. FIELD SURVEY METHODS
Nadezhda Kecheva

5.2.1. Introduction

The recording of archaeological monuments and artefacts began with archaeological pedestrian field surveys[1]. Recording methods have been a subject of many publications since the 1960s and different theoretical movements, approaches and landscapes have since developed a vast amount of diverse methods. Site-based field surveys used for recording archaeological sites raise the need for a definition of "an archaeological site" (also called just "a site") (Dunnell 1992, 22–26). There is no one-and-only definition accepted, furthermore, they vary between visible monuments (Orton 2000, 140–147) to quantification of artefacts (Plog et al. 1978, 387). The difficulty in defining "a site" especially in different chronological periods was the basis for the development of the siteless field survey approach, i.e. where the most detailed level – the artefact – is the centre for the fieldwork activities (Dunnell 1992, 33–36). One of the major differences lies in the term *intensity* – recording the intensity of artefacts, intensity of the distance between team members, and intensity of area covered. Siteless surveys became very popular[2] mostly in the Mediterranean where background noise

1 History of archaeological field surveys and different methods and approaches are systemized in Кечева (in press)-a.

2 For more information on different projects: (Lewarch and O'Brien 1981, 325–328; Wilkinson 1982; Dunnell and Dancey 1983; Gaffney et al. 1985; Cherry et al. 1988; Stoddart and Whitehead 1991; Wandsnider and Camilli 1992; Tainter 1998; Kuna 2000, 31–32; Caraher et al. 2006, 7–10; Richards 2008; De Haas 2012; Given et al. 2013; Bintliff 2000; Schofield 1991).

of small amounts of artefacts is distributed everywhere (Cherry 1983, 395). Hidden prehistoric landscapes is another concept in the Mediterranean region where small quantities of prehistoric artefacts compared to younger ones are recorded on the surface because of different reasons (Bintliff et al. 1999; Bintliff 2011).

According to the planned area, covered surveys are usually defined as small-scale (covering a small territory) and large-scale (covering a large territory) surveys (Lock and Molyneaux 2006, 5).

Many of the contemporary projects use a combination of the approaches according to the regional characteristics, level of intensity of coverage, artefact types and chronologies. Places with a high concentration of artefacts with different chronologies are usually defined as "a site" (Banning 2002, 18). Recording artefact amount is a common practice during field surveys. Sometimes the intensity changes survey methods – usually published as regional and intra-site surveys (Bintliff 2013). The more detailed level of area covered intensity, i.e. distance of 10–15 m between fieldwalkers, has developed vastly in recent years and has been helped by the high levels and easy access of information technologies for both desktop and mobile usage.

5.2.2. A brief history of the development of archaeological field surveys in Bulgaria

Archaeological pedestrian field surveys for site discovering and recording have a long history in Bulgaria. Starting as exploratory travels in the beginning – the first half of the 20th century[3], they developed through purposive and extensive approaches in the 1960s–1980s[4] up to full-coverage field surveys by the end of 1970s[5] and with a high level of intensity by the beginning of the 21st century[6]. A number of publications emerged as a result of the different types of surveys. More recently a combination of different methods has been used in regards to the project objectives and different landscape characteristics.

5.2.3. The recent development of archaeological field surveys in Bulgaria

The archaeological pedestrian field surveys in Bulgaria have been an integral part of the archaeological information system "Archaeological Map of Bulgaria" (AIS AKB)[7]. AIS AKB is an archaeological information system of *'sites and monuments'* type at a national level (Нехризов 2014). It contains information about archaeological sites from the Palaeolithic Period to the Bulgarian National Revival period from across the whole country territory. Thus, most of the fieldwork activities in Bulgaria have been site-orientated. In the last 10 years, the above-mentioned intensive surveys for full-coverage of territory flourished. A new approach was adopted dependent on the usage of desktop and mobile Geographic Information Systems (GIS) applications. Some of the pilot applications were used during the Tundzha Regional Archaeological Project in Kazanlak and Tundzha regions (Ross et al. 2018). It became popular amongst Bulgarian archaeologists conducting fieldwork activities at a regional scale (Нехризов 2018) as well as during rescue field surveys on gas and road infrastructures (Tzvetkova et al. 2012; Kecheva 2019). AIS AKB has gradually changed from a typical site-oriented information system to a more offsite and siteless system where different standardised archaeological and environmental data is collected on the field per a unit marked with the help of GNSS receivers by tracks and waypoints (Kecheva 2019, Кечева (in press)-b).

---

3 Some of the published materials for archaeological map: (Шкорпил 1914, Мутафчиев 1915; Попов 1925; Шкорпил 1925; Шкорпил 1926; Велков 1927; Миков 1933; Стефанов 1956; Цончев 1963).

4 Some of the expeditions: (Венедиков and Фол 1976; Фол 1982; Георгиева et al. 1983).

5 Full-coverage survey expeditions in Southwestern Bulgaria in 1978–1982 (Домарадски 2001; Śliwa and Domaradzki 1983; Гергова 2009; Кулов 2009, 16–17; Domaradzki 1982; Ostrowski 2005).

6 History and contemporary development of archaeological field surveys in Bulgaria are systemized in Кечева (in press)-a.

7 In Bulgarian "*Arheologicheska karta na Bulgaria*" and that is why abbreviation AIS AKB is widely used.

5.2.4. Field survey methods in Tash Bair

During the spring of 2018 and 2019 for a total amount of 23 working days in the field, the Bulgarian-German team conducted archaeological field surveys in Tash Bair area. The small-scale survey is focused in the following workflow (fig. 1).

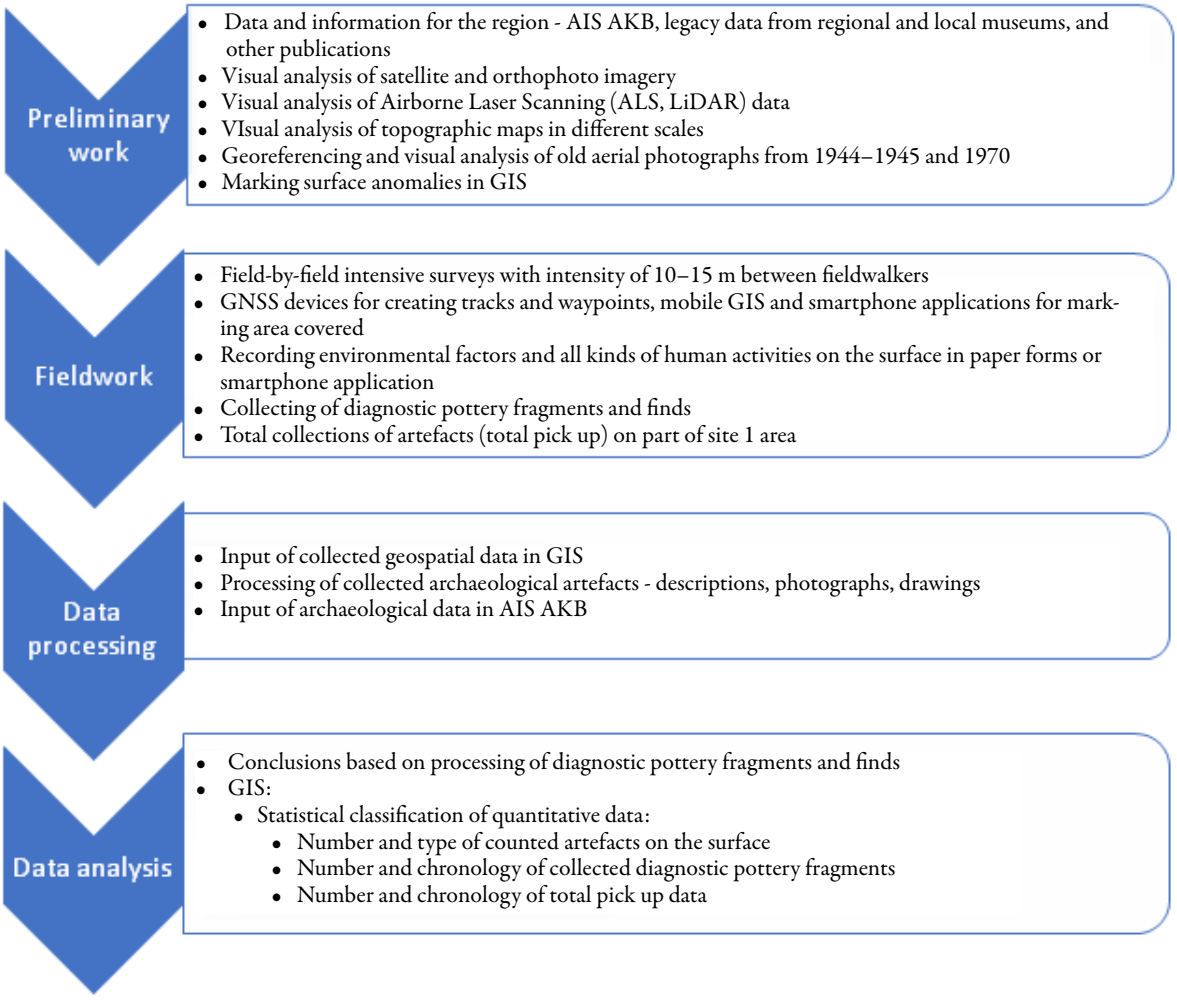


Fig. 1. Tash Bair field survey project workflow in 2018 and 2019 (figure by N. Kecheva)

5.2.4.1. Preliminary work

One of the project objectives was focused on establishing settlement changes in the Tash Bair locality. The focus was an area of about 20 km^2.

Raster data was collected from:

• Topographic maps in different scales: 1:50 000[8] and 1:5000[9];

• Google and Bing satellite imagery[10];

• Orthophoto imagery[11];

• Old aerial military photographs[12] from years 1944–1945 and 1970 that were additionally georeferenced;

8 Soviet headquarters maps from the 1980s, available as WMS.

9 Bulgarian maps created by the Geodesy, cartography and cadaster agency, constantly updating, available as WMS.

10 Available as WMS.

11 Available at Geodesy, cartography and cadaster agency website: https://kais.cadastre.bg/bg/Map.

12 Ordered from the Military Geographic Service from the Geoportal of Ministry of Defense.

• Airborne laser scanning data[13] – digital terrain and surface models – DTM and DSM with a horizontal resolution of 1 m as well as analytical hillshades derived from them;

• ASTER GDEM, version 2[14] , digital elevation model and a hillshade derived from it.

Vector data was collected[15] for:

• Administrative units of Bulgaria[16];

• Soils[17];

• Susceptibility to soil erosion[18];

• Geology[19].

Additional vector data and information were gathered from:

• AIS AKB for the current administrative units;

• Legacy data from regional and local museums – both published (Стефанов 1956; Стефанов 1974; Дремсизова-Нелчинова, Иванов 1983) and unpublished information.

Additional data was provided by S. Conrad and the Bulgarian-German expeditions from 1997–2001 (Вагалински et al. 2001a; Вагалински et al. 2001b; Станчев 2002; Conrad 2006; Krauß 2006a).

5.2.4.2. Fieldwork

Since the area that was in the focus of the project objectives was about 20 km^2, the most appropriate methods were a combination of the field-by-field method resulting in full-coverage of a region area, with an intensity of 10–15 m between the fieldwalkers[20], and a site-based approach. This means that sites were recorded in two ways:

1. Visible sites – visible by the naked eye above or below the surface, i.e. burial mounds, ramparts, ditches, etc.; site scatters were defined by the extent of the visible remains of the sites;

2. Invisible sites – invisible by the naked eye, based on quantitative analysis in GIS of concentrations of recorded artefacts on the surface, i.e. quantities of pottery fragments, pieces of daub, tiles and bricks, etc.; site scatters were defined by the extent of higher concentrations per polygons/units of recorded artefacts on the surface.

Sampling methods that were used included:

• Collection of diagnostic artefacts used in inter- and intra-site surveys – applied in all areas covered;

• Total collection of artefacts used in intra-site surveys – applied only to part of the area of one of the recorded sites.

The suitable and accepted definition of "a site" for the project and compatible with the Archaeological Map of Bulgaria concept was: *a topographic place in space where people in different chronological periods have been doing different types of permanent or periodical activities*.

5.2.4.2.1. The intensive field-by-field survey approach, a type of inter-site survey

The area covered consisted of large agriculture fields yearly ploughed. Fieldwalkers directions were compliant with the field boundaries and ploughed furrows. The team members purposefully chose areas with visibility above 80%[21] for a better comparison of the results. The distance between

---

13 Gathered through DANUBE FLOODRISK 2009–2012 Project (Басейнова дирекция „Дунавски район" 2013) and provided by the Ministry of Environment and Water to NAIM-BAS for non-commercial use.

14 (NASA/METI/AIST/Japan Space systems and U.S./Japan ASTER Science Team. ASTER Global Digital Elevation Model [Data set]. NASA EOSDIS Land Processes DAAC 2009).

15 JICA geodatabase (Басейнова дирекция „Източнобеломорски район". Изследване за интегрирано управление на водите в Република България, юни 2006 – март 2008 2018) and provided by the Ministry of Environment and Water to NAIM-BAS for non-commercial use.

16 Updated by current data from National Statistical Institute.

17 1:400 000 scale.

18 1:100 000 scale.

19 1:500 000 scale, a digitized vector version of the Geological Map of Bulgaria from 1989.

20 Also called "team members".

21 This visibility class covers areas that were ploughed or covered with crops with height of approximately 10–15 cm. In rare cases fields with surface visibility less than 80% were covered.

fieldwalkers varied between 10–15 m[22]. The area covered was marked by tracks on the field with GNSS receivers.

A *two-level* of intensity was recorded:

1. Units of an area of between approximately 10–1700 m^2 (a mean of 167 m^2) within the polygons named *small polygons*[23] with all observed artefacts on the surface counted while walking;

2. Units of an area of between approximately 500–20 000 m^2 (a mean of 5200 m^2) named *polygons*, with recorded specific attributes[24] including diagnostic artefacts collected while walking.

The fieldwork included the following activities:

• 5 to 6 team members with different responsibilities:

All team members carried a personal handheld GNSS receiver (usually a smartphone[25] or a handheld Garmin GPS receiver both with accuracy between 3–5 m in open areas) turned on and collecting automatically waypoints for creating a track of each team member movements;

o One of the team members was responsible for organising the other fieldwalkers direction and speed of movement, purposefully marking waypoints and taking photos when necessary;

o One of the team members was responsible for recording on a paper form the data observed by all fieldwalkers;

o One of the team members was responsible for collecting the diagnostic artefacts in a plastic bag with a note of the current date and polygon ID.

• After each 10–15 m every team member stopped and shouted artefact type and number that they counted on the surface;

• While one of the team members recorded this data on a paper form, another one marked each team stop with a waypoint in a smartphone application (fig. 2);

• At the end of each polygon, the team members gathered together and decided which diagnostic artefacts would be collected for further processing.

The paper form included standardised attributes collected for each polygon (fig. 5, 6). They included data for:

• polygon ID[26];
• date;
• fieldwalkers order from left to right;
• environmental predefined standardised data for:
  o land use;
  o land cover;
  o visibility;
  o the strategy of field surveys.
  artefact type and quantity data for small polygons within the polygon:
  o pottery artefacts:
  o handmade;
  o wheelmade.
  o pieces of daub;
  o tiles and bricks;
  o stones;
  o flints.

22 In rare cases a distance of 15–30 m was used.

23 Small polygons ID was formed from a combination of: polygon ID; initials of first name and family name of the particular team member; and their consecutive length in the polygon.

24 Polygon ID started at 1 in the beginning of the project.

25 Android smartphone applications that were used: OruxMaps (https://www.oruxmaps.com/cs/en/), SW Maps (http://swmaps.softwel.com.np/) and Mapit GIS (https://mapitgis.com/) with WMS capabilities.

26 Polygon ID started at 1 in the beginning of the project.



Fig. 2. Fieldwork activities. Team members' movement: a team member marked by a waypoint in a smartphone application at each team stop (1); and a team member recording data on a paper form (2) (figure and photos by N. Kecheva)



Fig. 3. Fieldwork activities. Placing small polygon vertices with the help of a total station (photo by L. Vagalinski)

• additional notes.

The specific attributes were recorded for the polygons. The quantities of polygon artefact types and counts is a sum of the type and count of these amounts collected for the small polygons (fig. 5). Polygons were created for all areas covered while small polygons – only in places where artefacts were observed on the surface.

5.2.4.2.2. The 'window' (total pick up) method, a type of intra-site survey

A total collection of all artefacts within an artificially predefined area or *small windows* (circles, squares) spread across a site is sometimes used by surveyors with different purposes (Bintliff 2013, 198). *All* artefacts are collected, weighed, counted and analysed. This method has its advantages[27] and disadvantages[28] (Bintliff 2013, 198).

A total pick up was conducted on part of the site 1 area. The 'windows' used were the small polygons within 5 polygons. The small polygons vertices, generated automatically by GIS software, were placed on the field with the help of a total station (fig. 3). All artefacts were collected per 123 small polygons. Pottery fragments were taken for further analysis, while pieces of daub, tiles and bricks, and stones were weighed and counted on the field (fig. 7). This data was filled in an attribute table (table 3), while a specific paper form for pottery processing was used[29] (fig. 8), and a specific attribute table was developed for describing all collected pottery fragments from the total pick up (table 4). Based on the same attribute field, "small_poly_ID", these two tables could be related to the attribute table in GIS.

5.2.4.3. Data processing

Data processing included:

• Processing of collected and recorded digital and paper data in GIS software[30];

• Analysis of collected artefacts per polygons;

• Site defining;

• Data input in AIS AKB.

Back in the base all collected and recorded data on the field was loaded and filled in desktop GIS software. Imported GNSS tracks and waypoints were the basis from which the polygons and small polygons were created (fig. 4). ESRI shapefile/feature class with the same attributes in the attribute

27 If the large amount of undiagnostic artefacts is processed and analysed correctly, it could point out to spatial distribution of artefacts with different chronologies.

28 It is a time-consuming method resulting in high percentage of undiagnostic artefacts.

29 With contributions by S. Conrad who post-processed the collected pottery fragments.

30 ESRI ArcGIS 10.4 and QGIS software were used with WGS 1984 UTM zone 35N projected coordinate system.

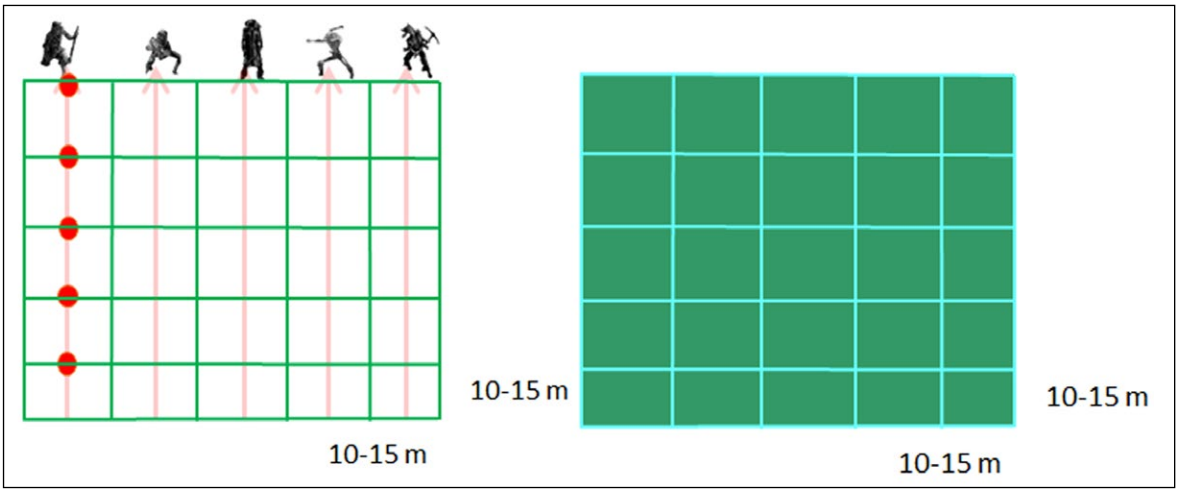


Fig. 4. Definition of small polygons (grid in green) created by tracks (red lines) and waypoints (red dots) (left) and a polygon (the whole green rectangular) with the grid of small polygons (grid in cyan) (right) (figure by N. Kecheva)

table (fig. 5, table 1), and a specific paper form for pottery processing were used[31] (fig. 8). Chronologies of collected diagnostic pottery fragments were recorded in another attribute table (table 2). The two attribute tables were related in GIS through the same field, "polygonID".

5.2.2.4.4. Data analysis

A text focused on field survey data analysis is included in the contributions by N. Kecheva et al., chapter *7 "The intensive field surveys at the Tash Bair locality and in its surroundings"*.

5.2.5. Conclusion

During the Tash Bair project, a combined field survey approach was used regarding the regional and environmental characteristics, project objectives, the requirements of AIS AKB and the current stage of development of information technologies. Both the field-by-field survey approach and total pick up method were conducted. Mobile and desktop GIS applications were used for collecting and processing data. Recording of standardised environmental and artefact data on fields with a minimum of 80% surface visibility gave the possibility of thorough observation of the distribution of traces of human activities in the past.

31 With contributions by S. Conrad who post-processed the collected pottery fragments.

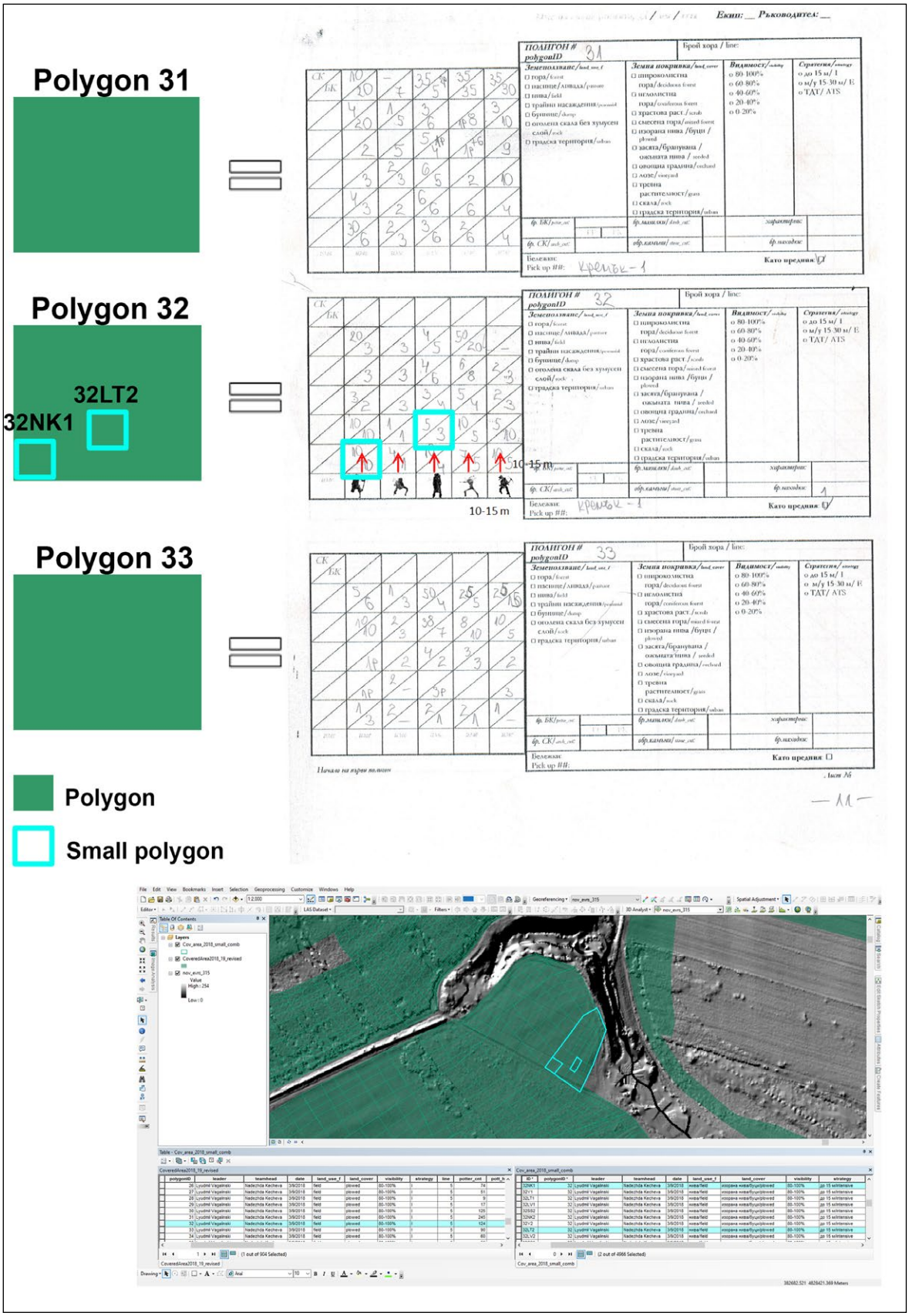


Fig. 5. Fieldwalkers direction of movement, filled in paper form, spatial location and attributes of polygons and small polygons in GIS (figure by N. Kecheva)

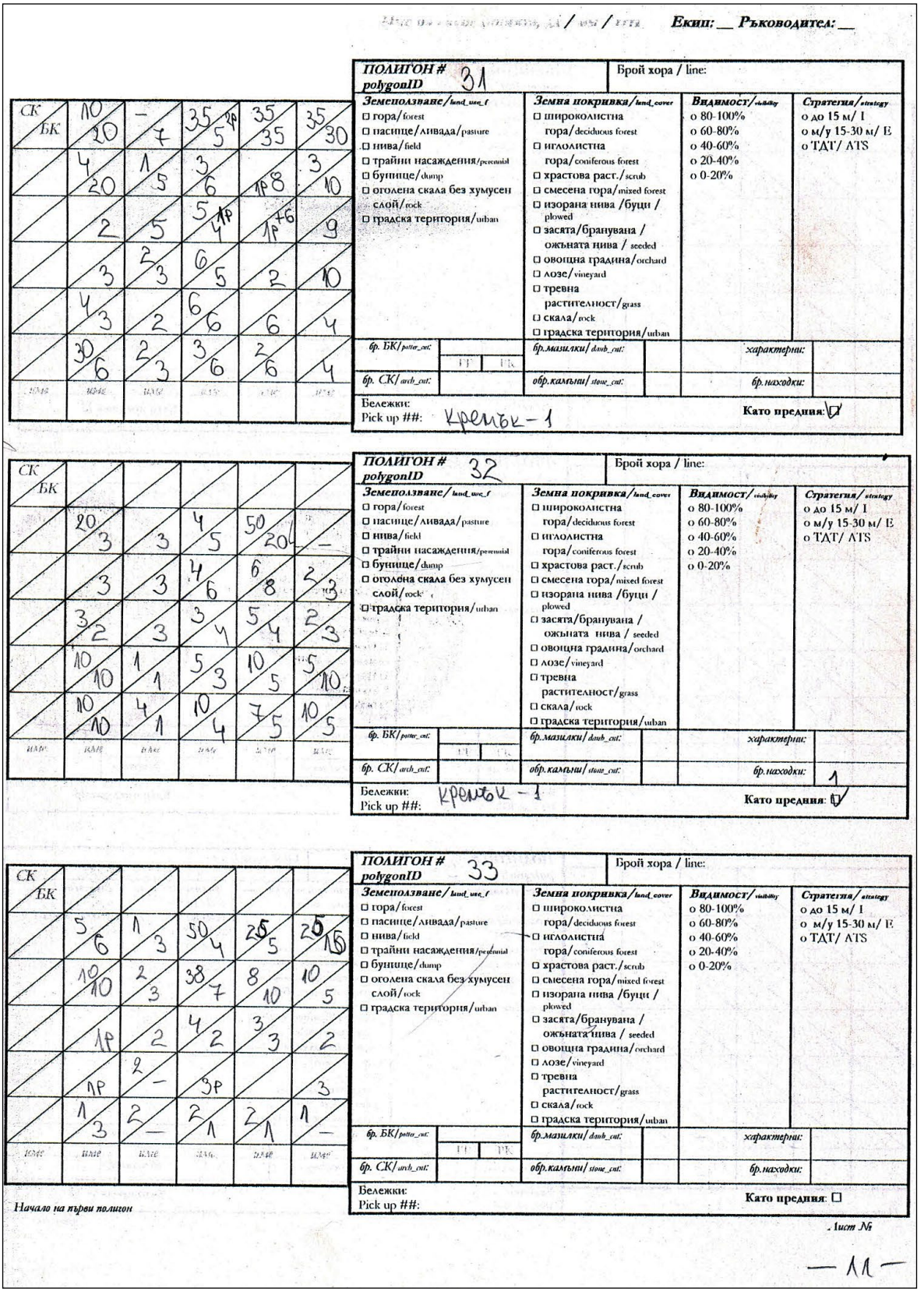
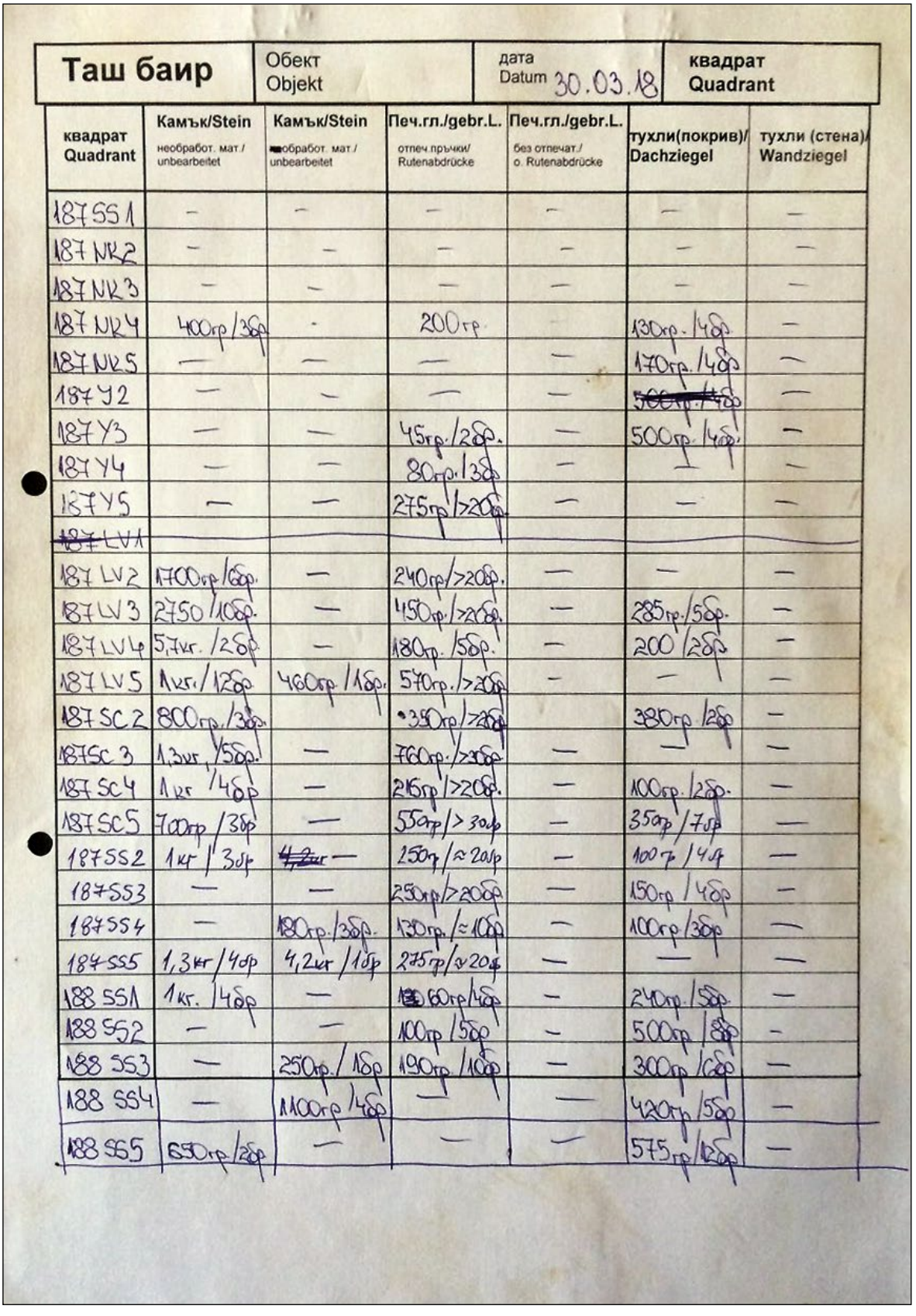


Fig. 6. Paper form used for field recording of environmental and artefact data (scan by N. Kecheva)



Таш баир	Обект Objekt	дата Datum 30.03.18	квадрат Quadrant

квадрат Quadrant	Камък/Stein необработ. мат./ unbearbeitet	Камък/Stein обработ. мат./ unbearbeitet	Печ.гл./gebr.L. отпеч.пръчки/ Rutenabdrücke	Печ.гл./gebr.L. без отпечат./ o. Rutenabdrücke	тухли(покрив)/ Dachziegel	тухли (стена)/ Wandziegel
187 SS1	–	–	–	–	–	–
187 NK2	–	–	–	–	–	–
187 NK3	–	–	–	–	–	–
187 NK4	400гр/3бр	·	200гр		130гр./4бр	–
187 NK5	–	–	–	–	170гр./4бр	–
187 Y2	–	–	–	–	~~500гр./4бр~~	–
187 Y3	–	–	45гр./2бр.	–	500гр./4бр.	–
187 Y4	–	–	80гр./3бр	–		–
187 Y5	–	–	275гр/>20бр	–	–	–
~~187 LV1~~						
187 LV2	1700гр/6бр.	–	240гр/>20бр.	–	–	–
187 LV3	2750/10бр.	–	450гр./>20бр.	–	285гр./5бр.	–
187 LV4	5,7кг./28бр	–	180гр./5бр.	–	200/2бр	–
187 LV5	1кг./12бр	460гр./1бр.	570гр./>20бр	–	–	–
187 SC2	800гр./3бр.		350гр/>20бр		380гр./2бр	–
187SC3	1,3кг./5бр.	–	760гр./>30бр	–	–	–
187 SC4	1кг/4бр	–	215гр/>20бр.	–	100гр./2бр.	–
187 SC5	700гр/3бр	–	55гр/>30бр	–	35гр/7бр	–
187SS2	1кг/3бр	~~4,2кг~~ –	250гр/≈20бр	–	100гр/4бр	–
187SS3	–	–	250гр/>20бр	–	150гр/4бр	–
187SS4	–	180гр./3бр.	130гр./≈10бр	–	100гр/3бр	–
184SS5	1,3кг/4бр	4,2кг/1бр	275гр/≈20бр	–	–	–
188 SS1	1кг./4бр	–	60гр/4бр	–	240гр./5бр	–
188 SS2	–	–	100гр/5бр	–	500гр/8бр	–
188 SS3	–	250гр./1бр	190гр/10бр	–	300гр/6бр	–
188 SS4	–	1100гр/4бр	–	–	420гр/5бр	–
188 SS5	650гр/2бр	–	–	–	575гр/2бр	–

Fig. 7. Total pick up paper form for field recording data for stones, pieces of daub, tiles and bricks (photo by L. Traykova)

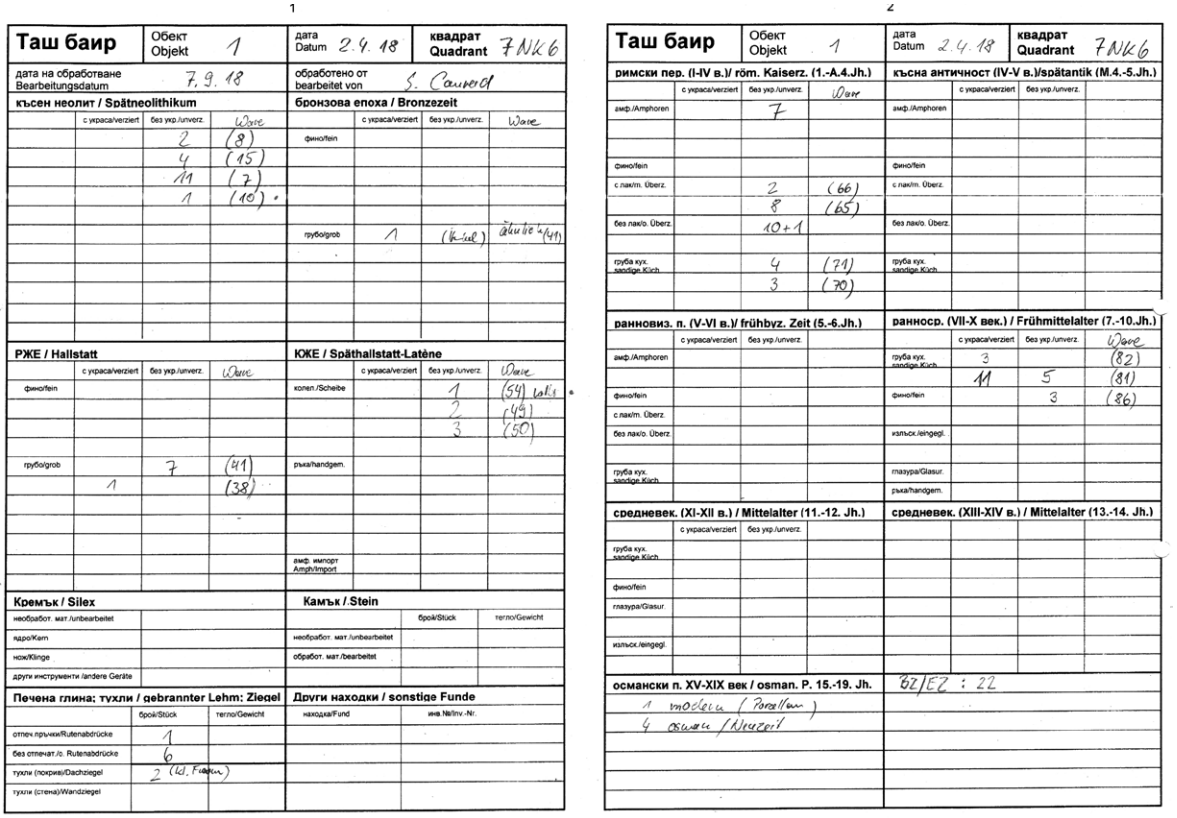


Fig. 8. Total pick up paper form for post-processing of all pottery fragments (two pages). The same paper form was used for post-processing of collected diagnostic pottery fragments per polygon (photos by S. Conrad)

Table 1. Covered Area ESRI shapefile/feature class attributes list description

Attribute Name	*Data Type*	Description	
polygonID	*Long Integer*	Consecutive number of polygon (1, 2, 3, etc.)	
leader	*Text*	Text, name of leader of the field surveys who was responsible for the permission	
teamhead	*Text*	Text, name of team leader on the field, responsible for the fieldwork	
line	*Short Integer*	Integer, number of fieldwalkers in a line	
date	*Date*	Current date from a calendar	
land_use_f	*Domain (in ESRI ArcGIS)* *Value Map (in QGIS)*	Standardized predefined attribute: **land use**	
		Code	**Description (in Bulgarian/English)**
		field	нива/field
		perennial	трайни насаждения/perennial
		pasture	пасище/ливада/pasture
		forest	гора/forest
		dump	бунище/dump
		rock	скала/rock
		urban	градска територия/urban

Attribute Name	*Data Type*	Description	
land_cover	*Domain (in ESRI ArcGIS)* *Value Map (in QGIS)*	Standardised predefined attribute: **land cover**	
		Code	**Description (in Bulgarian/English)**
		plowed	изорана нива/буци/plowed
		seeded	засята/бранувана/ожъната нива/seeded
		orchard	овощна градина/orchard
		vineyard	лозе/vineyard
		grass	тревна растителност/grass
		deciduous forest	широколистна гора/deciduous forest
		coniferous forest	иглолистна гора/coniferous forest
		scrub	храстова растителност/scrub
		mixed forest	смесена гора/mixed forest
		rock	скала/rock
		urban	градска територия/urban
visibility	*Domain (in ESRI ArcGIS)* *Value Map (in QGIS)*	Standardised predefined attribute: surface **visibility** classes depending on the land cover	
		Code	**Description**
		0-20%	0-20%
		20-40%	20-40%
		40-60%	40-60%
		60-80%	60-80%
		80-100%	80-100%
strategy	*Domain (in ESRI ArcGIS)* *Value Map (in QGIS)*	Standardised predefined attribute: **strategy** of the particular field survey, distance between field walkers in the polygon:	
		Code	**Description (in Bulgarian/English)**
		I	до 15 м/intensive
		E	м/у 15-30 м/extensive;
		ATS	в труднодостъпен терен/adverse terrain survey (in mountain or hilly area where team members walk in a column)
potter_cnt	*Short Integer*	Number, **total amount of all pottery fragments** observed and counted from the team members in the current polygon (it is the sum of the amounts of pottery fragments observed and counted in the small polygons)	
pott_hand	*Short Integer*	Number, amount of **handmade pottery fragments** observed and counted from the team members in the current polygon (it is the sum of the amounts of handmade pottery fragments observed and counted in the small polygons)	
pott_wheel	*Short Integer*	Number, amount of **wheelmade pottery fragments** observed and counted from the team members in the current polygon (it is the sum of the amounts of wheelmade pottery fragments observed and counted in the small polygons)	
daub_cnt	*Short Integer*	Number, **total amount of pieces of daub** observed and counted from the team members in the current polygon (it is the sum of the amounts of pieces of daub observed and counted in the small polygons)	

Attribute Name	*Data Type*	Description
arch_cnt	*Short Integer*	Number, **total amount of tiles and bricks fragments** observed and counted from the team members in the current polygon (it is the sum of the amounts of tiles and bricks fragments observed and counted in the small polygons)
stone_cnt	*Short Integer*	Number, **total amount of stones** observed and counted from the team members in the current polygon (it is the sum of the amounts of stones observed and counted in the small polygons)
flint_cnt	*Short Integer*	Number, **total amount of flints (silex)** observed and counted from the team members in the current polygon (it is the sum of the amounts of flints observed and counted in the small polygons)
notes	*Text*	Text, notes for the current polygon *(i.e. finds encountered, slag, millstones, and other observations)*
SHAPE_ Length	*Double*	*Perimeter of a polygon or a small polygon (in m); automatically calculation*
SHAPE_Area	*Double*	*Area of a polygon or a small polygon (in m²); automatically calculation*
small_polyID	*Text*	Only for small polygons: Small polygons ID was formed from a combination of: polygon ID, initials of first name and family name of the particular team member and their consecutive length in the polygon

Table 2. Attributes list description of post-processed chronologies of collected diagnostic pottery fragments from the field surveys per polygon

Attribute Name	Data Type	Description per polygon
polygonID	*Long integer*	Polygon ID started at 1 in the beginning of the project
LN_2018_19	*Short integer*	A sum of Late Neolithic pottery in 2018 and 2019
BA_2018_19	*Short integer*	A sum of Bronze Age pottery in 2018 and 2019
EBA_2018_19	*Short integer*	A sum of Early Bronze Age pottery in 2018 and 2019
BA_IA_2018_19	*Short integer*	A sum of Bronze and Iron Age pottery (common, not exactly datable) in 2018 and 2019
IA_2018_19	*Short integer*	A sum of Iron Age pottery in 2018 and 2019
EIA_2018_19	*Short integer*	A sum of Early Iron Age pottery in 2018 and 2019
LIA_2018_19	*Short integer*	A sum of Late Iron Age pottery in 2018 and 2019
RP_II_IV_2018_19	*Short integer*	A sum of Roman pottery (2nd – middle of 4th c.) in 2018 and 2019
LRP_IV_V_2018_19	*Short integer*	A sum of *Late Antiquity* pottery (middle of 4th–5th c.) in 2018 and 2019, in the catalogue of the pottery it is labelled as LRP
EByz_V_VI_2018_19	*Short integer*	A sum of Early Byzantine pottery (5th–6th c.) in 2018 and 2019
EMA_VII_X_2018_19	*Short integer*	A sum of Early Medieval pottery (7th–10th c.) in 2018 and 2019
BP_XI_XII_2018_19	*Short integer*	A sum of Medieval pottery of the Byzantine period (11th–12th c.) in 2018 and 2019
HMA_XIII_ XIV_2018_19	*Short integer*	A sum of High Medieval pottery (13th–14th c.) in 2018 and 2019

Attribute Name	Data Type	Description per polygon
Ottoman_2018_19	*Short integer*	A sum of Ottoman pottery in 2018 and 2019
Renaissance_2018_19	*Short integer*	A sum of Bulgarian National Revival period pottery in 2018 and 2019
Other_finds_2018_19	*Short integer*	A sum of other finds in 2018 and 2019
Modern_2018_19	*Short integer*	A sum of modern pottery in 2018 and 2019

Table 3. Total pick up attributes list description of post-processed stones, pieces of daub, tiles and bricks per small polygon

Attribute Name	*Data Type*	Description
small_poly_ID	*Text*	Small polygons ID was formed from a combination of: polygon ID, initials of first name and family name of the particular team member and their consecutive length in the polygon
Stone_unchopped_kg	*Short integer*	Kilograms of unchopped stones
Stone_uchopped_cnt	*Short integer*	Number of unchopped stones
Stone_chopped_kg	*Short integer*	Kilograms of chopped stones
Stone_chopped_cnt	*Short integer*	Number of chopped stones
Daub_with_sticks_kg	*Short integer*	Kilograms of pieces of daub with traces of sticks
Daub_with_sticks_cnt	*Short integer*	Number of pieces of daub with traces of sticks
Daub_without_sticks_kg	*Short integer*	Kilograms of pieces of daub without traces of sticks
Daub_without_sticks_cnt	*Short integer*	Number of pieces of daub without traces of sticks
Tiles_kg	*Short integer*	Kilograms of pieces of tiles
Tiles_cnt	*Short integer*	Number of pieces of tiles
Bricks_kg	*Short integer*	Kilograms of pieces of bricks
Bricks_cnt	*Short integer*	Number of pieces of bricks

Table 4. Total pick up attributes list description with post-processed pottery fragments chronologies and fabrics per small polygon

Attribute Name	*Data Type*	Description
small_poly_ID	*Text*	Small polygons ID was formed from a combination of: polygon ID, initials of first name and family name of the particular team member and their consecutive length in the polygon
Prehistory	*Short integer*	Pottery fragments belonging to prehistory in general
LN	*Short integer*	Late Neolithic
LNfineNOdec	*Short integer*	Late Neolithic, fine fabric, no decoration
LNfineDec	*Short integer*	Late Neolithic, fine fabric, with decoration
LNgrossNOdec	*Short integer*	Late Neolithic, coarse fabric, no decoration
LNgrossDec	*Short integer*	Late Neolithic, coarse fabric, with decoration
LN_ALL	*Short integer*	A sum of all Late Neolithic pottery fragments

Attribute Name	*Data Type*	Description
Eneolithic	*Short integer*	Eneolithic/Chalcolithic
BA	*Short integer*	Bronze Age (common ware, without chronol. specification)
EBA_MBA	*Short integer*	Early Bronze Age and Middle Bronze Age
LBA	*Short integer*	Late Bronze Age
BA_ALL	*Short integer*	A sum of all Bronze Age pottery fragments
BA_IA	*Short integer*	Bronze Age or Iron Age
IA	*Short integer*	Iron Age
EIA	*Short integer*	Early Iron Age
EIAfineNOdec	*Short integer*	Early Iron Age, fine fabric, no decoration
EIAfineDec	*Short integer*	Early Iron Age, fine fabric, with decoration
EIAgrossNOdec	*Short integer*	Early Iron Age, coarse fabric, no decoration
EIAgrossDec	*Short integer*	Early Iron Age, coarse fabric, with decoration
EIA_ALL	*Short integer*	A sum of all Early Iron Age pottery fragments
LIA6_1_ImpAmph	*Short integer*	Late Iron Age (6th–1st c. BC) imported amphorae
LIA6_1wheel	*Short integer*	Late Iron Age (6th–1st c. BC), wheelmade
LIA6_1_ALL	*Short integer*	A sum of all Late Iron Age (6th – 1st c. BC) pottery fragments
LIA2_1	*Short integer*	Late Iron Age (2nd–1st c. BC)
LIA2_1wheel	*Short integer*	Late Iron Age (2nd–1st c. BC), wheelmade
LIA2_1_ALL	*Short integer*	A sum of all Late Iron Age (2nd–1st c. BC) pottery fragments
RP2_mid4	*Short integer*	Roman period (2nd – middle of 4th c.)
RP2_mid4Amph_Imp	*Short integer*	Roman period (2nd – middle of 4th c.) imported amphorae
RP2_mid4fine	*Short integer*	Roman period (2nd – middle of 4th c.), fine fabric
RP2_mid4gross	*Short integer*	Roman period (2nd – middle of 4th c.), coarse fabric
RP2_mid4_ALL	*Short integer*	A sum of all Roman period (2nd – middle of 4th c.) pottery fragments
LAmid4_mid5	*Short integer*	Late Antiquity (middle of 4th – middle of 5th c.)
LAmid4_mid5Amph_Imp	*Short integer*	Late Antiquity (middle of 4th – middle of 5th c.), imported amphorae
LAmid4_mid5fine	*Short integer*	Late Antiquity (middle of 4th – middle of 5th c.), fine fabric
LAmid4_mid5gross	*Short integer*	Late Antiquity (middle of 4th – middle of 5th c.), coarse fabric
LAmid4_mid5_ALL	*Short integer*	A sum of all Late Antiquity (middle of 4th – middle of 5th c.) pottery fragments
Early_Byz_mid5_6	*Short integer*	Early Byzantine (middle of 5th–6th c.)
EM	*Short integer*	Early Medieval
EMfine	*Short integer*	Early Medieval, fine fabric
EMgross	*Short integer*	Early Medieval, coarse fabric (wheelmade)
EMglaze	*Short integer*	Early Medieval, with glaze
EMhand	*Short integer*	Early Medieval, handmade
EM_ALL	*Short integer*	A sum of all Early Medieval pottery fragments
MA_11_12c	*Short integer*	Middle Ages (11th–12th c.)

МЕТОДИ ПРИ ТЕРЕННИТЕ ИЗДИРВАНИЯ

Надежда Кечева

(Резюме)

По време на терените издирвания през 2018 и 2019 г. в района на Таш баир са използвани утвърдени в световната, европейската и българската археология недеструктивни методи с приложение на географски информационни системи (ГИС) при събирането на стандартизирани археологически и друг вид данни. В последните 10 години в България голяма част от научните и спасителните проекти, фокусирани върху теренни издирвания, са провеждани по подобен начин. Процесът включва няколко етапа: предварителна / кабинетна работа, теренна работа, обработка и анализ на събраните данни.

Предварителната работа включва събирането в ГИС софтуер на растерни и векторни данни на площ от около 20 км^2 около района на Таш баир. Допълнителни данни са събрани от литературни източници, местни музеи, както и от автоматизираната информационна система „Археологическа карта на България“ (АИС АКБ).

Теренната работа е извършена чрез интензивни теренни издирвания с разстояние между участниците 10 – 15 м и маркиране в ГИС на покритата територия. Отделните концентрации на преброени артефакти на повърхността впоследствие са обособени в отделни археологически обекти. Приетото определение за „археологически обект“ в проекта съвпада с дефиницията в АИС АКБ, а именно: топографско място в пространството, където хора през различни хронологически периоди са извършвали различни видове постоянни или периодични дейности. При теренната работа интензивността на покриване на територия е разделена на две нива: полигони (маркирани площни единици между 500 и 20 000 м^2 със специфични атрибути, между които и събраните диагностични артефакти) и малки полигони (маркирани площни единици между 10 и 1700 м^2 със специфични атрибути с всички преброени артефакти на повърхността). Специфични атрибути за всеки полигон / малък полигон са отбелязвани на хартиен формуляр, а полигоните са маркирани чрез тракове от членовете на екипа с точност между 3 и 5 м от ГИС приложения за смартфон или ръчни GPS приемници. Атрибутите на полигоните включват: номер, дата, земеползване, земна покривка, видимост, стратегия, вид и количество преброени артефакти, допълнителни бележки. Методът на събиране на всички археологически артефакти (т. нар. total pick up) е приложен частично на обект 1.

Обработката на данни включва въвеждане на събраните на терен данни в ГИС софтуер, анализ на събраните артефакти във всеки полигон, определяне границите на археологическите обекти, въвеждане на данните в АИС АКБ. Анализът на тези данни по определените вид и хронология на обектите е представен в глава 7.

При изпълнението на проекта в района на Таш баир е използван комбиниран подход при терените издирвания според характеристиките на региона и околната среда, целите на проекта, дефинираните изисквания в АИС АКБ и съвременното състояние на развитието на информационните технологии.

5.3. ARCHAEOLOGICAL EXCAVATION METHODS

5.3.1. Archaeological excavation methods

Lyudmil Vagalinski, Lyuba Traykova

Preliminary investigations. Preparatory work carried out to establish settlement changes in the Tash Bair locality included several stages. The first work stage was focused on gathering publications and data from AIS AKB for the region – both legacy (Стефанов 1956; Стефанов 1974; Дремсизова-Нелчинова, Иванов 1983) and more contemporary publications (Вагалински et al. 2001a; Вагалински et al. 2001b; Conrad and Stančev 2002; Станчев 2002; Conrad 2006; Krauß 2006a). The next stage included an intensive field-by-field full coverage survey with GIS applications to record field data (cf. the contributions by N. Kecheva, chapter 5.2). Recording of archaeological sites was followed by a geophysical survey of some of the sites (cf. the contributions by B. Ullrich et al., chapter 6.1).

Objectives. Analysis of field survey data and the geophysical results were used to choose the locations for the trenches for archaeological excavations. The coordinates of the trenches were created in GIS in the WGS 1984 UTM Zone 35N coordinate system. GNSS receivers Leica in 2018 and CHCNav i70 in 2019 were used to trace the trenches on the ground surface. The main objectives of the archaeological excavations were to determine the feature types excavated in the trenches and the chronological periods in which they were formed.

Conditions for conducting archaeological excavations. The fulfilment of the set objectives and the successful conduct of the research depended on additional factors. Such factors determined the volume of work that could be performed, respectively what area could be studied, the deadlines, access to the team and worker resources, as well as the possibility of using machines for excavations. Machines were used only to remove the surface ploughzone layer (about 0.4 m) in trenches 1.1 and 1.2. The execution time also depended on the climatic conditions and the peculiarities of the terrain (relief, surface type). The sites where the archaeological excavations were conducted were located in plough zones. This required prior coordination with the users of these areas. An important condition was to specify when these areas were free of crops as well as to establish the appropriate season for outdoor work. The planning of the terms for the archaeological excavations occurred a few months before the beginning of the fieldwork activities.

Archaeological excavations methods. The stratigraphic method was the main method used for the archaeological excavations (Николов 1995, 17, 18 and works cited). This archaeological method is borrowed from the geological sciences. It is based on the successive formation of layers and the principle that the upper layer is younger than the lower. Layers could be disturbed by later phenomena and events. Archaeological stratigraphy traces the layers formed primarily as a result of human activity.

The horizontal arbitrary levels were removed with a 0.2 – 0.3 m thickness and the recorded artefacts were separated. The division of the recorded artefacts into horizontal arbitrary levels complemented the information gained from their subsequent processing. After analysis and dating the artefacts were assigned to the actual stratigraphic layers. The application of this approach shows good results in cases when the stratigraphic layer is not distinguished during the fieldwork activities. The archaeological excavations in the Tash Bair locality covered mostly dug features. Non *in situ* remains of a dwelling in trenches 3.2–5 was the exception (cf. the contributions by L. Vagalinski., L. Traykova, chapter 8.2.2). Stratigraphic layers were difficult to distinguish in the soil from the fill of the dug features. The soil colour was not the criterion; looking at soil colour alone could be misleading. Complex analysis based on three basic characteristics – colour, content and density – was used to determine the presence of a separate stratigraphic layer or feature. When these characteristics were of a similar nature, the recognition of stratigraphic layers was difficult. In such cases, the recorded and analysed artefacts divided into arbitrary levels were used to confirm or reject the assumptions about the differentiation of a stratigraphic unit.

After the removal of each layer, the presence or absence of archaeological features recognized in the plan or sections of the trench was analysed. All the features recognized in the plan and sections were documented by photographing and if it was necessary by graphic drawings. When recognising the dug features, a cross-section was created. The fill of the section was removed through arbitrary levels until it was completely excavated. The purpose of these partial excavations was to determine whether there were different layers in the fill which would indicate different stages of filling of the feature. Distinguishing between these stages helped us to more accurately date and interpret the features. When recording the intersection of different features, the artefacts were separated from one another within each arbitrary level.

In order to optimize performance and meet deadlines, the study area in trench 3.6 was reduced (cf. the contributions by L. Vagalinski et al., chapter 8.2.1). This approach was applied to the study of features dug into the sterile layer. Work ceased on the sections of the trenches when a sterile layer had been reached. This made the job easier without losing scientific information. All the features were studied until they were completely excavated and a sterile layer has been reached.

After the completion of the excavation work, the stratigraphic sections of the excavated trenches were graphically recorded. The graphic recording contained a description and interpretation of the layers and features within. The processing of the excavated artefacts and its comparison with the stratigraphic sections significantly helped the interpretation and more precise dating of the studied features. This comparison was used to check the correct interpretation of the stratigraphy reflected in the graphical documentation of the sections in the trenches. The two processes, graphic documentation and processing of artefacts, were employed. They took place at different times and independently of each other. The combination of the data obtained from these two processes was the basis of the conclusions reached. In this way, the chronology of the stratigraphic layers and features was determined.

Results of applied methods. The final results achieved after the archaeological excavations are the criterion for whether the applied methods for fieldwork were appropriate.

The division of the recorded artefacts into horizontal arbitrary levels and their distribution to the respective stratigraphic layers complemented the volume of data obtained.

In this manner, the information about the ditch in trench 3.6 was enriched. The time of its construction, the long period of its maintenance and use, and the period of its abandonment were all established. According to the stratigraphy of the sections in the trench, it is assumed that there was probably a rampart on the eastern, inner side of the trench (cf. the contributions by L. Vagalinski et al., chapter 8.2.1). The refinement of the chronology at all stages from the construction to the abandonment of the ditch is a result of the applied methods in the conducted archaeological excavations.

A similar example of a good selection of the applied methods is the two Early Medieval ditches studied in trenches 1.1 and 1.2. The stratigraphic distribution of the pottery fragments in the two ditches allowed the assumption that they probably marked two phases in the use of the Early Medieval earthwork fort (cf. the contributions by L. Vagalinski et al., chapter 8.4).

The application of these methods in the study of pit 5.1.5 also led to optimal results. The stratigraphic distribution of the pottery fragments contributed significantly to its dating and interpretation (cf. the contributions by L. Vagalinski et al., chapter 8.3.3).

As noted above, during the archaeological investigations in the Tash Bair locality dug features were mostly excavated. Exploring such dug-in features by excavating their fill as a single context would lead to a loss of information. Without the division of the artefacts into horizontal arbitrary levels, it would not have been possible to distribute them stratigraphically.

МЕТОДИ ПРИ АРХЕОЛОГИЧЕСКИТЕ РАЗКОПКИ

Людмил Вагалински, Люба Трайкова

(Резюме)

Основният метод, приложен в археологическото проучване, е стратиграфският. Този метод в археологията е зает от науката геология, базиран на последователното образуване на пластове и на принципа, че горният пласт е по-млад от долния. Пластовете могат да бъдат нарушени от по-късни във времето явления и събития. Археологическата стратиграфия проследява пластовете, образувани в резултат преди всичко от човешка дейност.

Работихме с отнемане на хоризонтални механични пластове с дебелина 0,20 – 0,30 м, с отделяне на подемния материал. Той се подлага на последваща обработка и се разпределя към реалните стратиграфски пластове.

Прилагането на този подход показва добри резултати в случаите, когато при теренната работа не е разграничен стратиграфски пласт. Проведените археологически разкопки в м. Таш баир обхванаха предимно вкопани структури.

Комплексният анализ е основан на три основни характеристики – цвят, съдържание и плътност, и определя наличието на отделен стратиграфски пласт или структура.

Документирахме всички структури, очертани в план и в разрез, с фотозаснемане, а при нужда и графично. При разпознаване на вкопана структура правехме напречен разрез. Отнемахме нейния пълнеж по направения разрез отново чрез механични пластове до пълното му изчерпване. Целта на това частично проучване беше да установим дали има различни етапи на запълване. Разграничаването на различни етапи на запълване ни помогна за по-прецизното датиране и интерпретация на структурите. При установяване на пресичане на различни структури отделяхме подемния материал на всяка от тях в рамките на всеки механичен пласт.

Проучихме всички структури до пълното им изчерпване в рамките на заложените сондажи и достигане на стерилен пласт. След приключването на изкопната работа заснехме графично стратиграфските разрези на изкопаните сондажи. Графичното заснемане задължително съдържа описание и интерпретация на пластовете и структурите, нанесени в него. Обработването на подемния материал и съпоставянето му със стратиграфските разрези подпомогна в значителна степен интерпретирането и по-прецизното датиране на проучените структури.

Обединяването на получените данни от тези два процеса е в основата на достигнатите изводи.

Постигнатите крайни резултати след извършването на археологическите разкопки са критерий дали приложените методи за теренна работа са целесъобразни.

Разделянето на подемния материал по хоризонтални механични пластове и неговото разпределяне към съответните стратиграфски пластове допълни обема на получените данни. Прилагането на тези методи при проучването също доведе до оптимални резултати при проучването на сондажи 1.1, 1.2, 3.6 и яма 5.1.5.

Проучването на вкопаните структури чрез изчерпването на техния пълнеж като единен контекст щеше да доведе до загуба на информация. Без разделянето на подемния материал по хоризонтални механични пластове не би било възможно той да бъде разпределен стратиграфски.

5.3.2. Archaeological excavation methods for the trenches 1.2, 3.1 and 5.1

Sven Conrad

The mapping of the geomagnetic measurements was the basis for the positioning of the archaeological trenches. They were targeted to selected locations that, in accordance with the project aims, promised the highest possible information about the site and archaeological structures of outstanding importance. Another important criterion was the expected information about the stratigraphic relationships between the main archaeological structures on the site. At site 5, the trenches could not be set in the area of geomagnetic mapping because of the permanent crop. They were placed close to a concentration of features but still within the limits of the scatter indicated by the surface finds.

The corner coordinates of the trenches were determined in the GIS and staked out in the field using the total station (planum 0). The excavations in sections 1.2, 3.1 and 5.1 were carried out according to the generally applicable standards (see Archäologische Ausgrabungen 1999). Therefore, these excavations were primarily done in natural layers (Harris 1989, 29–81; Gersbach 1998, 32–43; Linke 1998, chapter 16.5; Carver 1999, 157–164). Due to the very different character of the archaeological structures, no uniform excavation method could be used for the excavations. If necessary, a combined method of excavation in natural layers and arbitrary levels was used.

In the 2018 excavation season, the arable layer within trenches 3.1 and 5.1/2 was manually removed. After reaching the natural subsurface, the natural ground was cleaned with trowels. The emerging features were documented as planum 1. According to the excavation method for natural layers, the investigation of the small features (pits; post holes) was carried out in the negative, with documentation of a transverse profile. Since it was not possible to completely separate the filling layers in pit 3.1.1 during the excavation process, single find measurement of a large part of the finds was carried out. This later enabled a reconstruction of the distribution of the finds within the feature. Unmeasured finds were labelled with the number of the layer and/or the upper and lower level.

During the excavations at site 1 in 2019 the arable land was removed with an excavator including trench 1.2. The planum 1 which still covered parts of the colluvium within the medieval earthen wall fortification was cleaned with trowels and then documented. In the further course of the excavations, colluvial deposits and extended structures of unclear character and limitation (niveau levels, ditches) were mostly excavated in arbitrary levels (see Linke 1998a; Gersbach 1998, 29–31), with a consequent documentation of plana and profiles. The decision about the thickness of the respective removal (up to 20 cm) and the use of tool (spade, trowel) was made according to the respective diagnostic situation. Further plana were documented according to planum 1. Depending on the situation, individual features were examined in negative excavation.

The plana were cleaned with trowels; a vacuum cleaner was also used during the 2019 excavation season. The documentation of the plana consisted of measurements, photography and descriptions. Features, trench borderlines and important levelling data of the respective planum were recorded during the measurements. The use of the Photomast MK2 high tripod proved its worth in the 2019 excavation season for taking the planum photos.

Profiles of individual features were recorded through photographs, drawings on a 1:20 scale and descriptions (see Linke 1998b; 1998c; Gersbach 1998, 53–76). Larger, hard-to-reach features were documented by a series of photos, from which a SfM model was created for the overall profile (see below).

Features were given a three-part numbering consisting of: a number for the site, a number for the trench, and a consecutive number for the feature at the respective site. For each feature a report sheet was created with the descriptions of plans, profiles and observations during the excavation. In addition, a detailed excavation diary was kept in which the excavation progress, coordinates, levelling data and observations during the excavation were recorded.

After the excavations had been completed and the profiles had been cleaned and smoothed in the respective section, they were graphically documented and described. Due to the depth of the trenches

and their narrow width, in most cases it was not possible to capture the large profiles in one photo and at a suitable angle. In these cases, the profiles were documented by a series of overlapping photos, from which a 3D model was generated using the Agisoft Metashape program. This in turn formed the basis for obtaining orthophotos of the respective profiles.

At present, these orthophotos are not yet approved by the Bulgarian guidelines for excavation documentation as an equally valid method to the production of field drawings made at a uniform scale. For this reason, in this publication the orthophotos are not placed alongside the interpreted field drawings but are instead published in connection with the pottery statistics (cf. contributions by S. Conrad, R. Krauß, chapter 9.1).

МЕТОДИ ПРИ АРХЕОЛОГИЧЕСКИТЕ РАЗКОПКИ НА СОНДАЖИ 1.2, 3.1 И 5.1

Свен Конрад

(Резюме)

Картирането на геомагнитните измервания е основата на позиционирането на археологическите сондажи. Те бяха насочени към избрани места, които, в съответствие с целите на проекта, обещаваха възможно най-висока информация за обекта и археологическите структури от изключителна важност. Друг важен критерий беше очакваната информация за стратиграфските връзки между основните археологически структури на обекта.

Ъгловите координати на сондажите са определени в ГИС и са заложени на полето с помощта на тотална станция (план 0). Тези разкопки са извършвани предимно в естествени пластове.

Поради много различния характер на археологическите структури не може да се използва единен метод на проучване при разкопките. При необходимост е използван комбиниран метод на изкопни работи в естествени пластове и произволни/изкуствени нива.

При археологическите разкопки през 2018 г. обработваемият слой в рамките на сондажите 3.1 и 5.1/2 беше ръчно отстранен. Очертаващите се структури са документирани като план 1. Съгласно метода на разкопките по естествени пластове изследването на малките структури (ями, дупки за стълбове) е извършено в негатив, с документиране на напречен профил.

В яма 3.1.1 са извършени индивидуални измервания на голяма част от находките.

При разкопките на обект 1 през 2019 г. орницата е премахната с багер. В колувиалните отлагания и разширените структури с неясен характер и ограничение (нива, ровове) са разкопавани предимно на произволни/изкуствени нива. Профилите на отделните структури бяха документирани чрез снимки, чертежи в мащаб 1:20 и описания.

Обектите получиха номерация от три части, състояща се от номер за обекта, номер на сондажа и последователен номер за структура на съответния обект.

Профилите бяха графично документирани и описани. Големите профили бяха документирани чрез серия от припокриващи се снимки, от които беше генериран 3D модел с помощта на програмата Agisoft Metashape.

Понастоящем тези ортоснимки все още не са одобрени от българските изисквания за теренна археологическа документация като еднакво валиден метод за изработване на полеви чертежи, направени в еднакъв мащаб. Поради тази причина в тази публикация ортоснимките не се поставят редом с интерпретираните полеви чертежи, а вместо това се публикуват във връзка със статистиката на керамиката.

5.4. FIND RECORDING

5.4.1. Recording of pottery finds, silex and animal bones

Sven Conrad

During the excavation in arbitrary layers, pottery fragments, flint pieces and animal bones were collected as part of this defined layer and labelled accordingly. The levelling of the upper and lower limits of the removed layers were determined on site.

In the case of special features (3.1.1; 1.1.6; 1.1.11), individual three-dimensional measurements of the find position of some of the pottery sherds and bones were carried out in order to be able to determine their distribution in the features and their limits.

After washing and drying, the finds were sorted according to the appropriate categories. While animal bones and flint finds were handed over to the respective specialists for processing (cf. the contributions for the animal bones by N. Karastoyanova, chapter 10.3, and for the flints by M. Gurova, chapter 10.2), the pottery and small finds were recorded and processed at the excavation base on site.

The prehistoric ceramic finds were first assigned macroscopically to one of the periods documented at the respective site and recorded in a database and tables. Specific types of fabrics were also identified within the cultural-historical units based on the research between 1997 and 2001. Diagnostic fragments were photographed, drawn, and then described in the form of a catalogue.

The statistical recording of the pottery finds from the Late Iron Age to the Middle Ages was carried out using the same recording sheets and protocol applied for the processing of the survey finds (cf. the contributions by N. Kecheva, chapter 5.2).

These statistics formed the basis for the find statistics for individual features. Based on the earlier research between 1997 and 2001, an overview of the existing fabrics was compiled, on the basis of which the ceramic fragments were determined. Pencil drawings on a scale of 1: 1 were made of characteristic and well-preserved fragments, i.e. rim fragments or fragments with special decorations. After the pencil drawings had been converted into Indian ink, they were further processed on the computer. In the case of expressive fragments, photos were integrated into the profile drawing (cf. the contributions by S. Conrad, R. Kraußß, chapter 9.1).

ДОКУМЕНТИРАНЕ НА КЕРАМИЧНИ НАХОДКИ, КРЕМЪЦИ И ЖИВОТИНСКИ КОСТИ

Свен Конрад

(Резюме)

По време на разкопките в механични слоеве фрагменти от керамика, кремъци и животински кости са събрани от всеки слой и съответно етикетирани. На място се определя подравняването на горната и долната граница на отстранените слоеве.

При специални структури (3.1.1; 1.1.6; 1.1.11) е извършено частично индивидуално измерване на керамични находки и кости, за да може да се определи тяхното разпространение в структурите и техните граници.

Праисторическите керамични находки първо са причислени макроскопски към един от периодите, документирани на съответния обект, и преброени в база данни и таблици. В рамките на културно-историческите единици бяха идентифицирани и специфични видове материали въз основа на изследванията между 1997 и 2001 г. Диагностичните фрагменти бяха заснети и нарисувани и след това описани под формата на каталог.

Статистическата регистрация на керамичните находки от късната желязна епоха до Средновековието е извършена със същите записни листове по начин, съпоставим с обработката на на-

ходките от теренните издирвания (вж. приноса на Н. Кечева, глава 5.2). Тази статистика формира основата за статистическа оценка на отделни структури. Въз основа на по-ранните изследвания между 1997 и 2001 г. е съставен преглед на съществуващите керамични материали, въз основа на който са определени керамичните фрагменти. Рисунките с молив в мащаб 1:1 са направени от характерни и добре запазени фрагменти, т.е. фрагменти от устия или фрагменти със специална украса.

5.4.2. Small find recording
Lyuba Traykova

Finds recorded during field surveys have been labelled with the following data: date of discovery; short description; place of discovery – Polygon ID and a site number – Site ID.

Finds recorded during excavations have been labelled with the following data: date of discovery; short description; place of discovery – Site ID. The coordinates of the finds found *in situ* before removal were taken with the help of GNSS receivers Leica in 2018 and CHCNav i70 in 2019, using WGS 1984 UTM Zone 35N coordinate system. The coordinates of the finds found in the excavated soil were labelled with an arbitrary level or exact depth and with coordinates relative to two of the angles of the respective trenches. For the discovered finds, their labels indicate the date of discovery, a brief description, and the place of discovery – Site ID and an arbitrary level.

ДОКУМЕНТИРАНЕ НА МАЛКИ НАХОДКИ
Люба Трайкова

(Резюме)

Находките, открити по време на теренните издирвания, притежават етикет със следната информация: дата на откриване; кратко описание; място на откриване – Polygon ID и принадлежност към обект – Site ID.

Находките, открити по време на археологическите разкопки, притежават етикет със следната информация: дата на откриване; кратко описание; място на откриване – Site ID; координатите на находките, открити на място, преди да бъдат изкопани, са взети с помощта на GNSS приемници Leica за сондажите, които проучихме през 2018 г. и с CHCNav i70 GNSS за тези, проучени през 2019 г. Те са в координатна система WGS 1984 UTM 35N. Координатите на находките, открити във вече изкопаната пръст, съдържат механичен пласт или точна дълбочина и координати спрямо два от ъглите на съответния сондаж; за находките, открити в събрания подемен материал, в етикета се отбелязва дата на откриване, кратко описание, място на откриване – Site ID и принадлежност към механичен пласт.

5.5. SAMPLING
Sven Conrad

With the resources and processing options available, it was not possible to take samples of all sediment layers and features during the excavations systematically. No archaeobotanist was present at the excavation sites. Exemplary samples for the extraction of archaeobotanical material were taken under the supervision of the trench supervisor, specifically from sealed layers and level deposits as well as from backfilling of clearly definable features. A total of 48 samples were obtained during the two

excavation campaigns. Due to the possibilities and resources available, in most cases these are random samples from the corresponding structures.

The soil samples collected were usually around 10 litres. If the amount of sediment to be sampled was smaller and if it was taken from drilling samples, the amount was correspondingly lower.

During the flotation process, which was carried out with a simple installation near the excavation base (fig. 1), two special sieves, one on top of the other, with mesh sizes of 1 and 2 mm were used. For this purpose, the samples were generously soaked in a large bucket by a semi-skilled assistant or a team member, stirring carefully, and then placed on the sieves in portions and rinsed out by hand. The fractions from the two sieves were dried separately. The botanical material was then manually separated out from the rest of the heavy fraction (located in the 2 mm sieve) by a team member. The respective 1 mm and 2 mm fractions of the botanical material were recorded in a list and packaged. From the remaining heavy fraction, further finds (ceramics, flint, daub) were sorted out and assigned to the respective find category. The heavy fraction was kept in exceptional cases only.

In addition, during the 2018 excavation season, a total of 20 separate charcoal samples were taken from the features 3.1.1 and 3.2.1 for a determination.

Acknowledgements

Sample flotation was performed by Danka Angelova (Novgrad), Julia Becher and Lea Valcov (both University of Tübingen).

The sieves were provided by Cornelius Fischer, Institute of Resource Ecology, Department of Reactive Transport Leipzig of the Helmholtz-Zentrum Dresden-Rossendorf.

Many thanks to all for their support.



Fig. 1. Sample flotation near the archaeological base in the village of Novgrad (photo by S. Conrad)

ВЗИМАНЕ НА ПРОБИ

Свен Конрад

(Резюме)

С наличните ресурси и възможности за обработка не беше възможно систематично да се вземат проби от всички слоеве и характеристики на седиментите по време на разкопките. На местата на разкопките не е присъствал специалист по археоботаника. Примерни проби за извличане на археоботанически материал бяха взимани под наблюдението на археолог от запечатан слой и нивелирни отлагания, както и от седимента на ясно дефинирани структури. По време на двете теренни кампании са получени общо 48 проби.

Изтегленото количество обикновено беше около 10 л. Ако количеството на седимента, от който трябва да се вземе проба, е по-малко и ако е взета от проби от сонда, количеството е съответно по-малко.

По време на процеса на флотация, който се извършваше с обикновена инсталация близо до археологическата база в с. Новград, бяха използвани две специални сита, едно върху друго, с размери на отворите 1 и 2 мм. След това ботаническият материал беше сортиран от член на екипа на око от тежката фракция, разположена в 2 мм сито. Съответните 1 мм и 2 мм фракции от ботаническия материал бяха записани в списък и опаковани.

6. THE GEOPHYSICAL PROSPECTIONS. METHODS AND RESULTS

6.1. GEOPHYSICAL PROSPECTIONS AT SITES 1 AND 3–5

Burkart Ullrich, Nikolaas Noorda, Henning Zoellner

6.1.1. Introduction

Within the research project entitled "The strategic position of the southernmost point of the Danube from the Early Iron Age until the end of the Roman Limes", large scale magnetometer surveys and additional resistivity surveys were conducted by Eastern Atlas. The project focuses on settlement dynamics in prehistory at different scales (Conrad 2006) at Tash Bair near the village of Novgrad, Bulgaria (fig. 1). Tash Bair refers to the east-west running ridge with a long south slope on the western bank of the Yantra River. From prior surveys, it is known that there are archaeological sites dating to the Pre-Roman Iron Age here (Krauß 2006a, No. 48). Aerial photos point to fortifications, which can probably be assigned to this period as well but are not investigated in detail as of yet. Within this framework, geophysical surveys were both applied to gain additional information at a landscape and more detailed scale.

Within this context a large-scale magnetometer survey was conducted on four archaeological sites covering approx. 30 ha in total. The conditions for the magnetic survey were excellent, despite occasional difficulties due to bad weather. The slight topography and the large open fields allowed a very efficient magnetometer survey with the mobile LEA-MAX system. Additionally, electrical resistivity tomography (ERT) transects were measured to gain additional data from specific magnetically detected anomalies

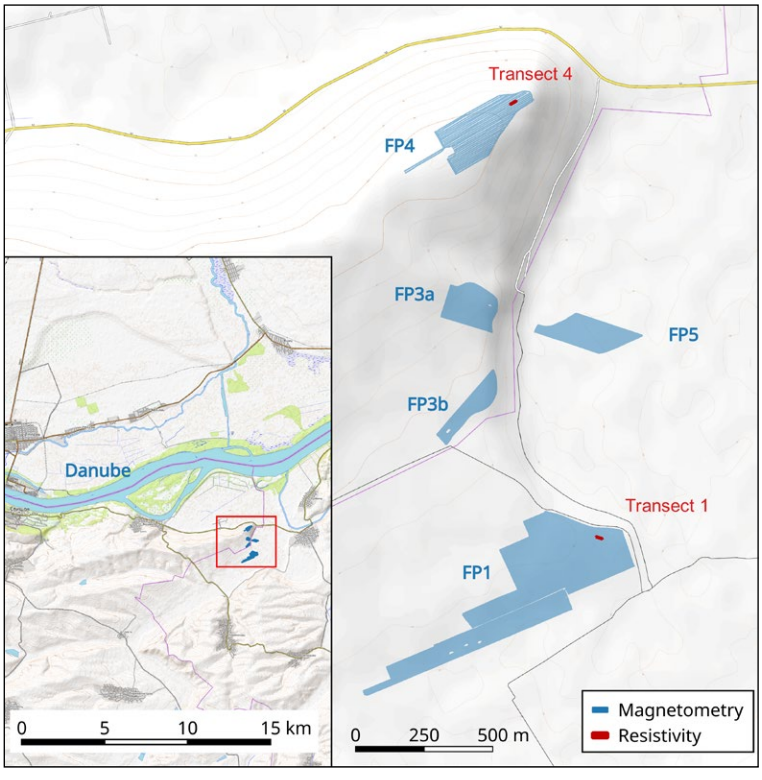


Fig. 1. Map with the magnetometer survey areas (blue) and the resistivity transects (red). Base maps: OpenTopoMap (figure by B. Ullrich, N. Noorda, H. Zoellner)

at two sites. The geophysical surveys were performed by Henning Zöllner (Geophysicist, Eastern Atlas, Germany) and Nikolaas Noorda (Archaeologist, NAA – Noorda Archaeological Assistance, NL) during a one-week campaign in March 2018.

6.1.2. Methodology and conducted surveys

The objective of a magnetometer survey is the identification and description of spatial changes (anomalies) in the magnetic field. At archaeological sites, anomalies occur as a consequence of the contrast between the magnetic properties of archaeological features and their surroundings. Both are mainly composed of natural materials, such as rock or soil. In soils, the highest magnetic susceptibility values are observed with ferromagnetic or ferrimagnetic minerals such as iron oxides, magnetite and maghemite. These minerals occur in a wide range of natural rock. Typically, dark, basic igneous rocks possess a higher susceptibility than acid igneous rocks. The latter, in turn, have a higher susceptibility than sedimentary rocks (Breiner 1999, 8). Furthermore, these minerals occur ubiquitously in soft soil, forming microscopically small grains. There are several explanations of their origin and concentration in soil, in particular, these aspects can be attributed to heat and the effects of microbes and bacteria. In soils with rich organic content, iron oxides with low magnetisation can be transformed into magnetite and maghemite under the influence of fire in reducing conditions (Le Borgne 1955). Microbes populating rich organic deposits can sufficiently change soil conditions to support the conversion of weakly magnetised iron oxides into more magnetic forms (Linford 2004). Furthermore, magnetotactic bacteria are able to produce intracellular crystalline magnetite that remains in the soil after the death of the bacteria (Fassbinder et al. 1990).



Fig. 2. The LEA-MAX system with 10 gradiometer probes and GNSS-positioning at site 4 in between the trees of the apricot plantation (photo by N. Noorda)

For the magnetometer surveys at Tash Bair, the convertible system LEA developed by Eastern Atlas was used, mainly in the ATV Mode, pulled by a light quad bike (fig. 2). The LEA-MAX system used includes an array of ten Foerster fluxgate gradiometer probes mounted on a light and foldable cart, the LEA-D2 data recording device, and several independently working positioning systems, i.e. differential GNSS and an odometer. The Foerster FEREX CON 650 fluxgate gradiometer probes register the vertical gradient of the Z-component of the Earth Magnetic Field with an accuracy better than 0.2 nT (nanotesla). The gradient is measured as the difference between two vertically arranged fluxgate sensors (at a distance of 650 mm from each other) inside the probes. The reading of the probes is given as the difference between the Z-components of the magnetic field from the lower sensor minus those of the upper sensor. Hence a positive difference, resulting in positive amplitudes, is given in the case of an enhanced magnetisation of objects near the surface. The measured difference is insensitive

to the various time changes of the external magnetic field, which occur as daily, diurnal, or short-term variations.

During measurements the magnetic data of each sensor in the array are registered along straight profiles of any length. The point distance in profile direction is defined by the sample rate, set at the registration unit, and the speed at which the system is moving. At the end of each profile, the raw data are decoded and normalised. To decode registered-time-series data to georeferenced data, the GNSS positions and/or the wheel markers from the odometer are used. The standard decoding process uses a polynomial fit to calculate the long-term sensor variations. The residual data show local variations (anomalies) of the gradient of the Z-component while sensor drift and regional field effects are suppressed.

At Tash Bair five single areas located at the northeast tip of the spur over the Yantra and specific areas further south were investigated (fig. 1), namely:

– an area of 5.1 ha at site 4 on top of the spur in the north;
– further south an area of 3.0 ha at site 5;
– two areas in the north and south at site 3, named 3a and 3b with 2.6 and 2.8 ha respectively, and;
– a large open field in the south of site 1, covering 17.5 ha.

In total an area of 30 ha was investigated by means of magnetometry.

The data positioning for the magnetic survey was realised by means of a differential GNSS using two GNSS receivers in base and rover configuration with a relative accuracy of ±2 cm. The coordinate system used during magnetic measurements was WGS84 / UTM zone 35. For the correction of the base position, GNSS raw data was logged. Subsequently, the position of the base was corrected using correction data provided by the Bulgarian provider SMARTNET, achieved from the GNSS station Belene, situated approximately 40 km west of the survey area. With the correction the positioning of the geophysical data achieves an absolute accuracy of about ±2 cm.

The additional electric resistivity tomography measurements (ERT) were conducted along two transects to evaluate depth and structure of detected linear magnetic anomalies. The transect ERT1 at site 1 was positioned perpendicular over an oblong positive magnetic anomaly located in the north-east of site 1, while the transect ERT4 at the site 4 was situated across the arc anomaly in the northeastern part of site 4.

Subsurface structures can be detected through electrical resistivity investigations if a measurable contrast exists between the resistivity of the target and its surroundings. Mainly solid materials, such as stone walls and foundations or solid rock (e.g. bedrock) can be visualised since they maintain a higher level of resistivity compared to the lower resistivity levels of loose materials with a higher pore volume, such as backfills of ditches and pits. Under average conditions, the pore space of the materials is saturated or partly saturated, contributing significantly to the electrical conductivity of the ground. This means that daily and seasonal variations could have a strong influence on the obtained resistivity distribution of structures near the surface. Furthermore, the measurement of the bulk resistivity depends on this electrical conductivity of minerals in the solid phase. So, a minor amount of clay minerals can considerably increase the measured bulk conductivity.

For the resistivity measurements, an electric current I is generated into the ground between two current electrodes A and B. At the surface the potential difference ΔU of the resulting electrical field is measured between two other electrodes M and N. Depending on the measured parameters, current I and voltage U, as well as the positions of the four active electrodes, the measured resistivity is called the apparent resistivity (valid for a homogeneous ground). The resistivity distribution for the naturally inhomogeneous ground has to be calculated by an inversion process from the measured data.

For the 2d-ERT surveys at Tash Bair, the multi-electrode resistivity meter GeoTom (Geolog, Starnberg, Fig. 5, above, right) with 50 electrodes was used. The position of the transects was determined by the results of the magnetometer survey. Two profiles were measured in the northeastern corners of their respective research areas, 1 and 4. The resistivity measurements were provided along profiles of 24.5 m length with an electrode distances of 0.5 m. The position of the first and the last electrode of the

profiles and the altitude of few electrodes in-between were measured by GNSS. For the data inversion the software package Boundless Electrical Resistivity Tomography (BERT) (Rücker et al. 2006) was used.

6.1.3. Results of the geophysical survey and archaeological interpretation

The results of the magnetometer surveys at Tash Bair are presented in two maps for each site, showing the magnetic data and their preliminary interpretation. The magnetometer data are plotted on a greyscale in a dynamic range of ±3 nT. According to our definition, the positive maximum is plotted as black, while the negative minimum is white. The preliminary archaeological interpretation reflects aspects of the subsurface archaeological context, (sub)surface conditions at the site related to geology and soil formation processes, as well as potential modern-day impacts. Therefore, the magnetic data images were thoroughly examined for anomalies corresponding to three main categories: archaeological, natural geological, or recent features. Attributing magnetic anomalies to distinct subsurface structures can be ambiguous for several reasons. As is stated in the known "equivalence principle" in the field of potential theory, different objects in relation to their depth below the ground, their volume and magnetic moment may produce the same anomaly measured at the surface. Furthermore, a superposition of anomalies originated by features from different categories and classes is always to be expected. For example, archaeological features like pits and ditches might overlap with the natural soil formations in which they are embedded, or they might be covered by recent or archaeological relevant objects with an enhanced remanent magnetisation caused by heating, like metal debris from agricultural machines or burnt bricks. For the interpretation of the magnetic data at Tash Bair, single anomalies were distinguished by means of their shape, amplitudes, and polarisation. Anomalies interpreted as being of archaeological relevance are assigned to the classes: pits, ditches, walls, kilns and burnt materials, and debris. Anomalies interpreted as non-archaeological are assigned to recent disturbances or geological formation and geomorphological processes. Furthermore, unspecified anomalies are marked. The main results of this interpretation are discussed below according to the sites.

Figures 3 and 4 show the results of the magnetometer surveys for site 1. Large parts of the magnetic data are characterised by southwest-northeast oriented plough lines. Further recent disturbances are produced by a water pipeline and related metal installations, running from northeast to southwest, and a power pylon in the most southwestern edge. The most conspicuous archaeological features are interpreted as infilled ditches that form a rectangular enclosure of 200 m × 220 m, recognisable as positive anomalies with amplitudes of up to +5 nT and a width of approximately 3.5 m in the northeastern part of the surveyed area. Parallel wall features are visible on the eastern and the western side inside these rectangular enclosures as positive linear anomalies, probably originated from limestone structures or palisade remains. Some of the most significant linear anomalies are of similar orientation in the east-west and north-south overlay. In the eastern part of the surveyed area a large number of single pits is interpreted. These anomalies are concentrated in the north and in the east of the covered area. Few anomalies with very high amplitudes are likely related to kilns or pits, filled with remanent material, and may point to metal workshop areas. Furthermore, several weak linear anomalies are marked in the central area. These point to foundation ditches or rectangular structures with a slightly different orientation compared to the large anomalies of the enclosure ditches. In the southwest of the surveyed area only a stripe with a width of 70 m to 140 m was covered, which hinder a clear delimitation of large scale archaeologically relevant anomalies. The most southwestern stripe contains a group of several burial mounds. Their location in the map is recognisable as gaps in the magnetic data. Nearby scattered dipole anomalies with very high amplitudes are concentrated. They may point to recent scrap metal, but also an archaeological interpretation as burnt bricks could be feasible.

Figure 5 shows the location and the result of the resistivity survey at transect 1 at site 1. The transect was placed over a ditch-like structure visible in the magnetic data (red line on magnetic map) located at the ploughed field. The data area presented in a vertical cross-section of the 2d-resistivity distribution. The section shows a very low resistivity contrast levels due to the high clay content in the loess and the



Fig. 3. Magnetometer survey data at site 1 (figure by B. Ullrich, N. Noorda, H. Zoellner)

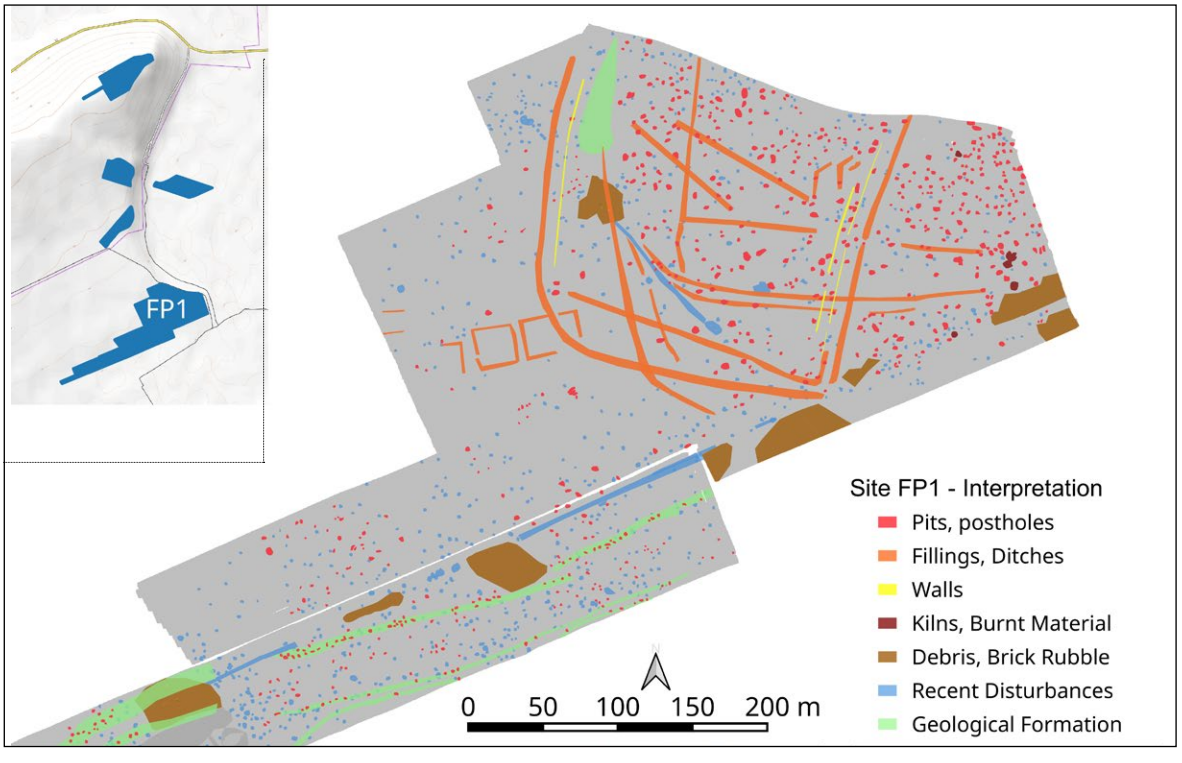


Fig. 4. Interpretation of magnetic data at site 1 (figure by B. Ullrich, N. Noorda, H. Zoellner)

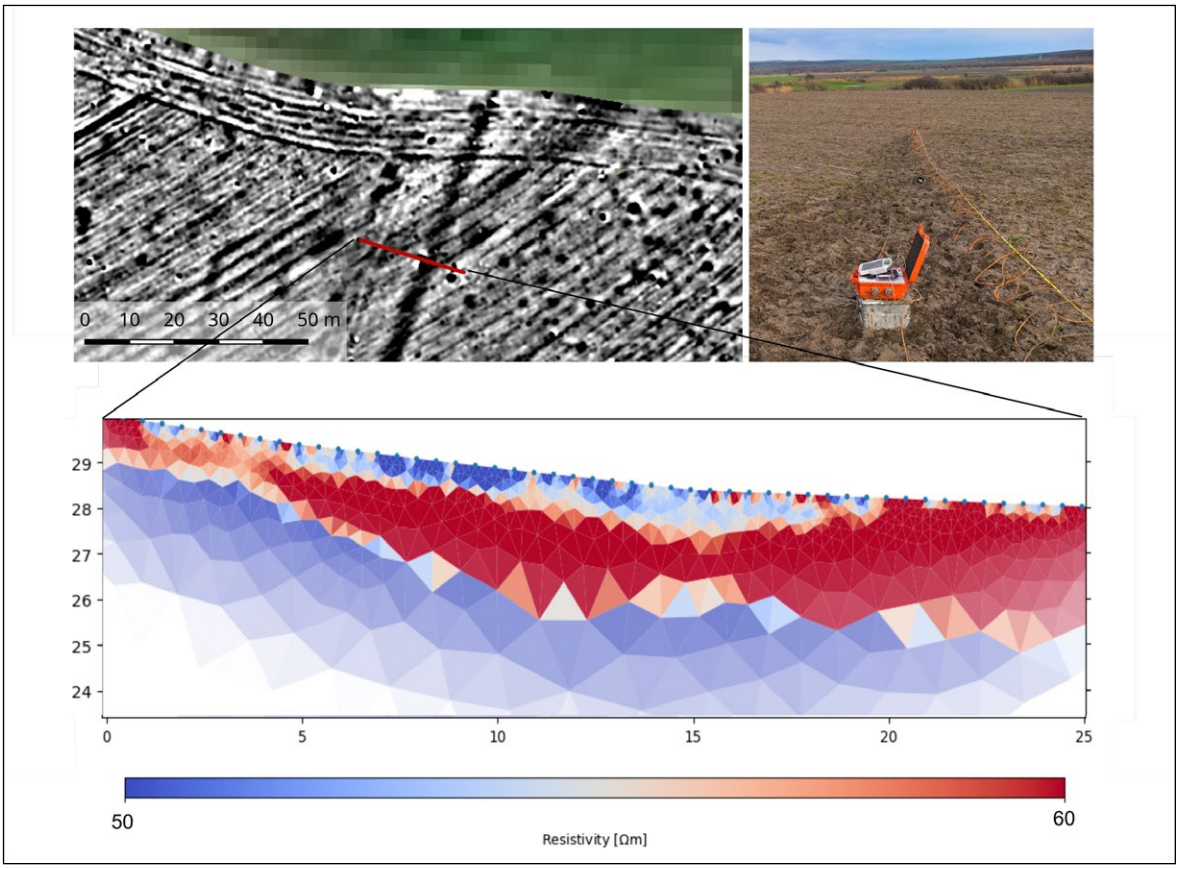


Fig. 5. Resistivity survey along transect at site 1 (figure by B. Ullrich, N. Noorda, H. Zoellner)

high water saturation of the pore space during the measurements. The 2d-data, presented in a very narrow range from 50 to 60 Ωm, show a layered model of the resistivity distribution. Near the surface, variations occur because of surface effects related to the micro topography. A low resistivity layer with varying depths is visible on top of a layer with enhanced values. The low-resistivity layer reaches a maximum depth of approximately 1 m between 13 m and 15 m along the transect. This layer with slightly reduced values most likely corresponds to the infills of ditches. In conclusion, only shallow ditch remains can be expected from the resistivity survey. Archaeological excavation near the gate approximately 50 m to the south revealed a medieval ditch up to a depth of 4.5 m (cf. the contributions by L. Vagalinski et al., chapter 8.4). The resistivity section did not reflect that depth, because of the high saturation of both, the infilled material and the surrounding soil. Also, this could be due to the depression in this part caused by erosion.

Figures 6 and 7 show the results for the central survey for area 3 and 5. The magnetic data for the northern area (named 3a) show two main ditches, delimiting the eastern promontory above the river plain. A quarter circle is visible as a positive anomaly with a width of about 4 m over a length of more than 200 m. Inside this, at a distance of 30 m, another linear anomaly, with a width of 5 m, indicates an additional enclosure system. In comparison, this linear anomaly, recognisable for over more than 150 m, shows a curved course. Inside the enclosures, few pits or other archaeological features can weakly be derived from the magnetic data. Additional linear anomalies show an orientation towards the passage of a hollow way in the northwest of the surveyed area. They are mainly attributed to recent features, likely roads or pathways.

The data from the southern area, named 3b contains several single and linear anomalies of varying characteristics. Recent disturbances are produced by single dipole anomalies interpreted as scrap metal and linear anomalies in orientation of the plough lines. Very similar linear anomalies are interpreted as geological formations, e.g. in the case of the anomaly parallel to the edge of the terrain in the northeast, or as a ditch feature in case of the alignment of positive anomalies (interpreted as pits) in the southwest. A large dipole anomaly in the south may point to a recent origin (pipe trench) of this linear feature too.



Fig. 6. Magnetometer survey data at sites 3 and 5 (figure by B. Ullrich, N. Noorda, H. Zoellner)

The most notable archaeologically relevant anomalies are a sequence of southwest-northeast oriented ditches and a continuation towards northwest. These anomalies point to a larger structure, probably an enclosure or ditch system, which could not be covered completely.

The magnetic data at site 5 cover an area of 115 m width and up to 300 m in length of an elevated area in a meander loop of the Yantra River plain. Interestingly, the data contain several hundred single anomalies with a positive amplitude, which are mainly assigned to archaeological features. More than 400 distinct single positive anomalies are interpreted as pits. They are concentrated in the central and in the eastern part of the area. Most striking are four enlarged anomalies with high amplitudes between 10 und 50 nT, interpreted as archaeological features containing burnt material, probably kilns or waste pits. These are likely related to metal workshops located in the wet lowlands with potential bog ore deposits. Several northwest-southeast oriented linear anomalies of unclear origin are visible in the data. These traces might have originated from refilled irrigation trenches or recent used paths.

The magnetic data from site 4 in Figure 8 show gaps of approximately 1 m width along the southwest-northeast oriented rows of fruit trees belonging to the orchard (see also fig. 2). Furthermore, lines from ploughing and older plantations result in a high background noise of the magnetic data. Nevertheless, the data allow a clear distinction of three recognised main features (fig. 9). The northeastern promontory is delimited by a positive anomaly of 6 m wide, assigned to a continuous ditch over 70 m. Inside the delimited area few pits, recent metal and geological anomalies are interpreted. Most noticeable are two semi-rectangular structures, recognisable by positive linear anomalies, marked as ditches. The central one, measuring 30 × 30 m, encloses an area of approximately 700 m² by round and linear ditches. A positive anomaly in the centre is marked as a pit. Additional pits and pit alignments are marked west

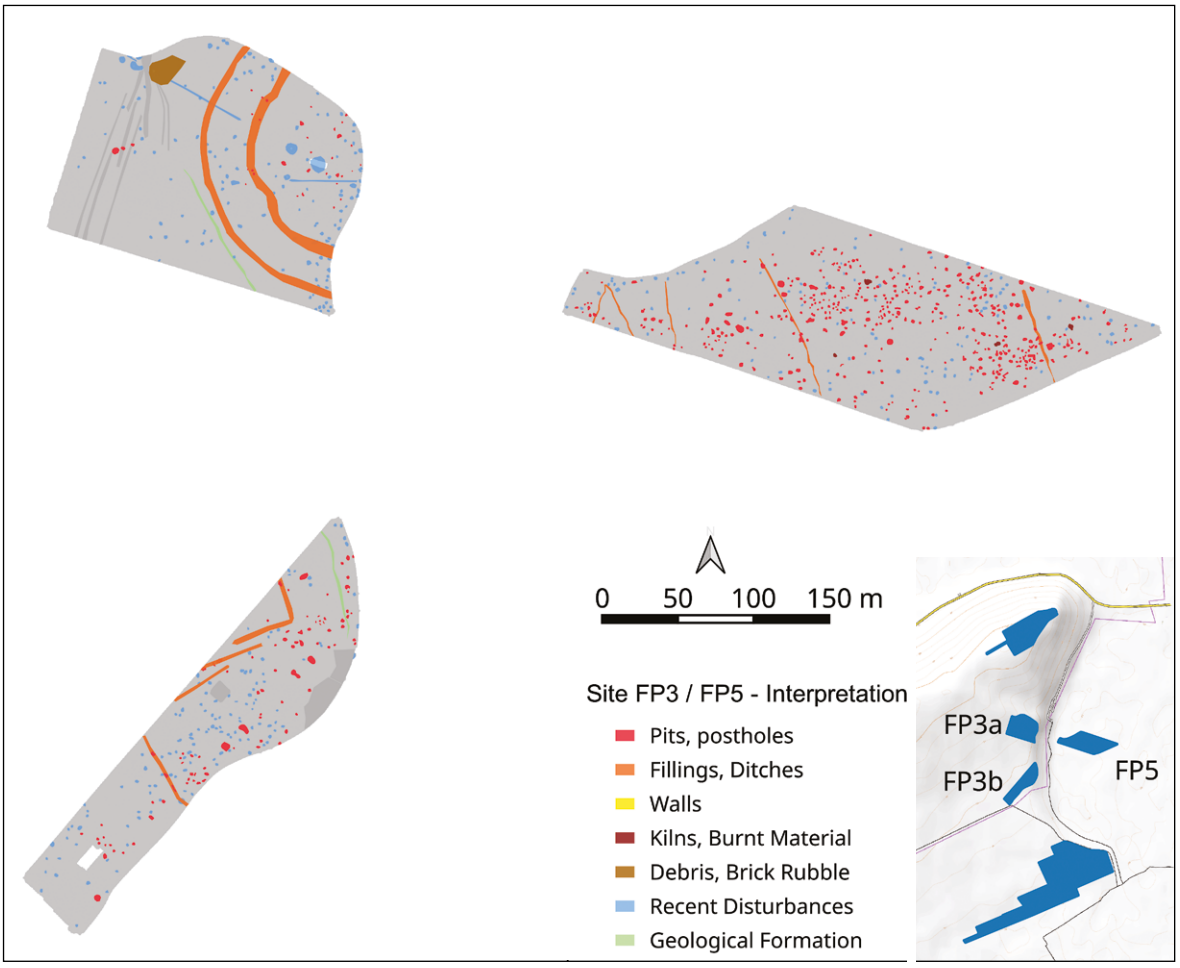


Fig. 7. Interpretation of magnetic data at sites 3 and 5 (figure by B. Ullrich, N. Noorda, H. Zoellner)



Fig. 8. Magnetometer survey data at site 4 (figure by B. Ullrich, N. Noorda, H. Zoellner)

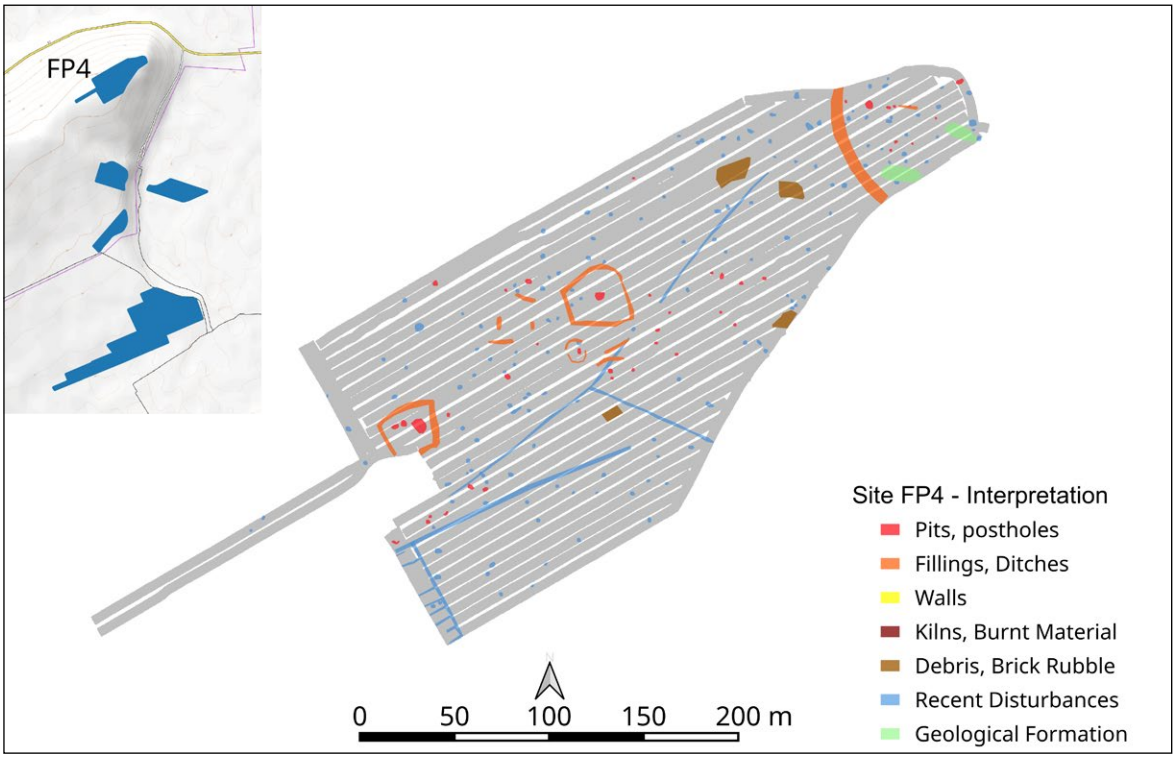


Fig. 9. Interpretation of magnetic data at site 4 (figure by B. Ullrich, N. Noorda, H. Zoellner)

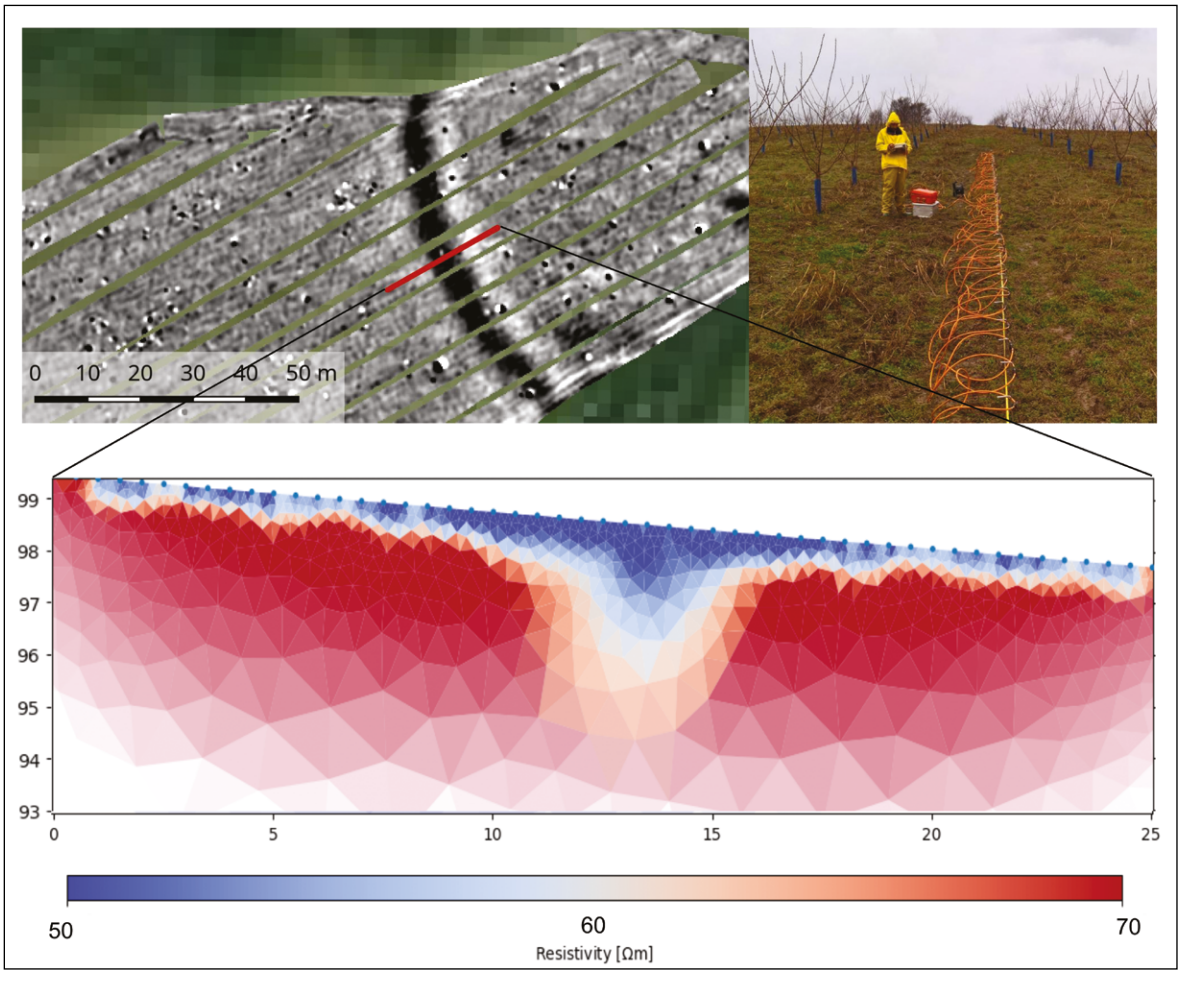


Fig. 10. Resistivity survey along transect at site 4 (figure by B. Ullrich, N. Noorda, H. Zoellner)

and south of this structure. Among them an oval enclosure of 8 × 12 m in the south of the main structure is notable. The second structure expands over 30 × 25 m and is directly attached in the northeast to the burial mound. The enclosed area is nearly 500 m². Inside, a dipole anomaly with a very high amplitude of +500 nT is detected, which could be caused by a recent iron object but also by an object of archaeological relevance of burnt material, due to the prominent location inside the enclosure. Nearby two additional anomalies are interpreted as pits. Furthermore, several very straight linear anomalies with a positive amplitude are marked as recent in origin. They could be caused by small pipe trenches. Three enlarged concentrations of dipole anomalies in between the northeastern ditch and the central rectangular structure are interpreted as areas with debris.

The results of the additional resistivity survey at transect 4 is shown in Figure 10 in a vertical cross-section of the 2d-resistivity distribution. This profile is situated in the fruit orchard and covers the oblong anomaly visible in the magnetic map. The anomaly, possibly indicating the filling of a former ditch, is clearly visible in the model section between 12 m and 16 m along the profile. The depth of the supposed ditch can be estimated to approx. 2.5 m, assuming 60 Ωm as threshold for the resistivity of the infill. The relative high resistivity at greater depth is caused by underlying natural soils. A drilling well resulted in a depth of 3 m below the surface, which matched the result of the resistivity survey (cf. the contributions by N. Kecheva et al., chapter 12, site 4).

The results of the prospection on different archaeological sites at the Tash Bair show the huge potential of non-destructive geophysical surveys for archaeological prospecting in the widely open river landscapes of the Danube and its tributaries. In particular, magnetic prospection with mobile multi-channel arrays can not only be used to explore individual archaeological sites but can also reveal traces of an entire archaeological landscape preserved in the ground. Thus, bringing archaeological field research to a new level, with regard to the spatial and temporal completeness of the information before planned excavations are conducted.

ГЕОФИЗИЧНИ ПРОУЧВАНИЯ НА ОБЕКТИ 1 И 3 – 5

Буркарт Улрих, Николаас Ноорда, Хеннинг Цьолнер

(Резюме)

Геофизичните проучвания са извършени от фирмата Eastern Atlas, Берлин, в м. Таш баир близо до с. Новград, Северна България. Теренът лежи на западния бряг на р. Янтра.

В четири археологически обекта от различни епохи е проведено геомагнитно и електросъпротивително изследване. При първото е приложена системата LEA-MAX с десет паралелни градиометрични сензора и RTK-GNSS. Използвано е ATV, което позволи да се проучи значителна площ от около 30 ха.

Получените геомагнитни данни бяха изследвани в ГИС. Близо 3000 единични магнитни аномалии бяха пренасочени като многоъгълник и разпределени в три основни категории: археологически, природно-геоложки и съвременни структури. Най-изявените магнитни аномалии са причинени от укрепителни ровове. На най-южния обект 1 са регистрирани застъпващи се ровове, което показва дълготрайно обитаване на терена (многопластов археологически обект).

Извършени бяха и 2D-съпротивителни изследвания за определяне на формата и дълбочината на ровове в две избрани зони.

Резултатите от геофизичните проучвания предоставят отлична база данни за по-нататъшен анализ на пространствената организация на древните селища в местността, както и за успешни целеви разкопки.

6.2. GEOMAGNETIC SURVEY AT SITE 2

Petar Zidarov

6.2.1. Introduction

Concentrations of shattered roof tiles, amphorae, and tableware found on a field surface after ploughing, disclose the location of a settlement inhabited during the Roman and Late Roman periods, on a high terrace close to the confluence of river Yantra and the Danube (Вагалински et al. 2020b). This study documents the extent and spatial organisation of this prospective archaeological site referred to as Tash Bair Site 2, using geophysical prospection (cf. the contributions by N. Kecheva et al., chapter 12). It is located on a promontory above an old meander of Studena Reka River, inaccessible from the north and the east due to its steep slopes (fig. 1), but offers a good vantage point to the valleys of Studena Reka River and the Yantra River. On the surface, no special barriers or fortifications are noticed, neither to the west, nor along the very edge of the terrace in the northern and southern direction. Geophysical surveys and excavations from 2018 and 2019, as well as dense habitation on the Tash Bair and its southern slope during several periods, document its lasting topographic attractiveness throughout several millennia (Krauß 2006a, 146–155; Вагалински et al. 2019; 2020a; 2020b and contributions in this volume). Immediately north of the site, the existence of a sunken lane, which would have allowed access from the east, was apparent from the geomorphological investigations (cf. the contributions by A. López del Olmo et al., chapter 4).

Its geological foundation is made of tens of meters of loess, while the uppermost soil layer is composed of chernozem with carbonate inclusions (Krauß 2006a, 146 with references to unpublished data by N. Ninov). Both soil varieties have mainly paramagnetic properties, which are extremely favourable for recording even the weakest magnetic disturbances for characterising the expected archaeological structures. This is unequivocally documented during previous geophysical campaigns along the edge of the same terrace and determined the method of choice during this one (Вагалински et al. 2019; cf. the contributions by B. Ullrich et al., chapter 6.1).

The first geophysical survey in this area was carried out in 2001 by a team of geophysicists led by Prof. Dr. Ján Tirpák from the Archaeological Institute in Nitra, Slovakia. The magnetic survey area encompassed 2 hectares (100x200 m) and revealed some notable point-like and linear patterns of enhanced magnetic values extending beyond the survey borders. However, the missing local datum points hindered the exact location of these observations (Bartík et al. 2000). Therefore, a new survey undertaken in 2019 was performed in order to: (a) capture the entire area of site 2 in detail, (b) accurately locate settlement structures, and (c) establish their location relative to modern terrain topography. The identification of identical point-shaped and linear signals among the results of this and the previous study allowed the accurate georeferencing of the data from the 2001 magnetic map, which partly extend beyond the limits of the current study (fig. 1; 3; 4).

6.2.2. Methods

The magnetic measurements were taken with a G858 caesium magnetometer in vertical gradient mode along parallel profiles set in one-meter distance, using the boundaries of the arable fields as a baseline (fig. 2). The orientation of the measurements was carried out by laying a supporting square grid with a 40 m side. Its corners were marked with wooden pegs placed with a total station and georeferenced by means of datum points set with a GNSS receiver. Between the corners of the grid in the east/west direction, geodetic measuring tapes were placed, and a pair of assistants moved a line marked every 5 m across the measuring tapes to guide the operator. The two sensors are set at 0.30m and 0.90 m above ground respectively recording both the total magnetic field as well as its vertical gradient. The measurements were carried out in a continuous measurement mode along the profiles at a tact of 10 measurements per second. Thus, the ground measurement density is 100 × 15 cm, but during the software processing it was interpolated to 33 × 33 and 16.5 × 16.5 cm. The adjacent profiles have an opposite direction of measurement, which has some effect on the visualisation of the data.

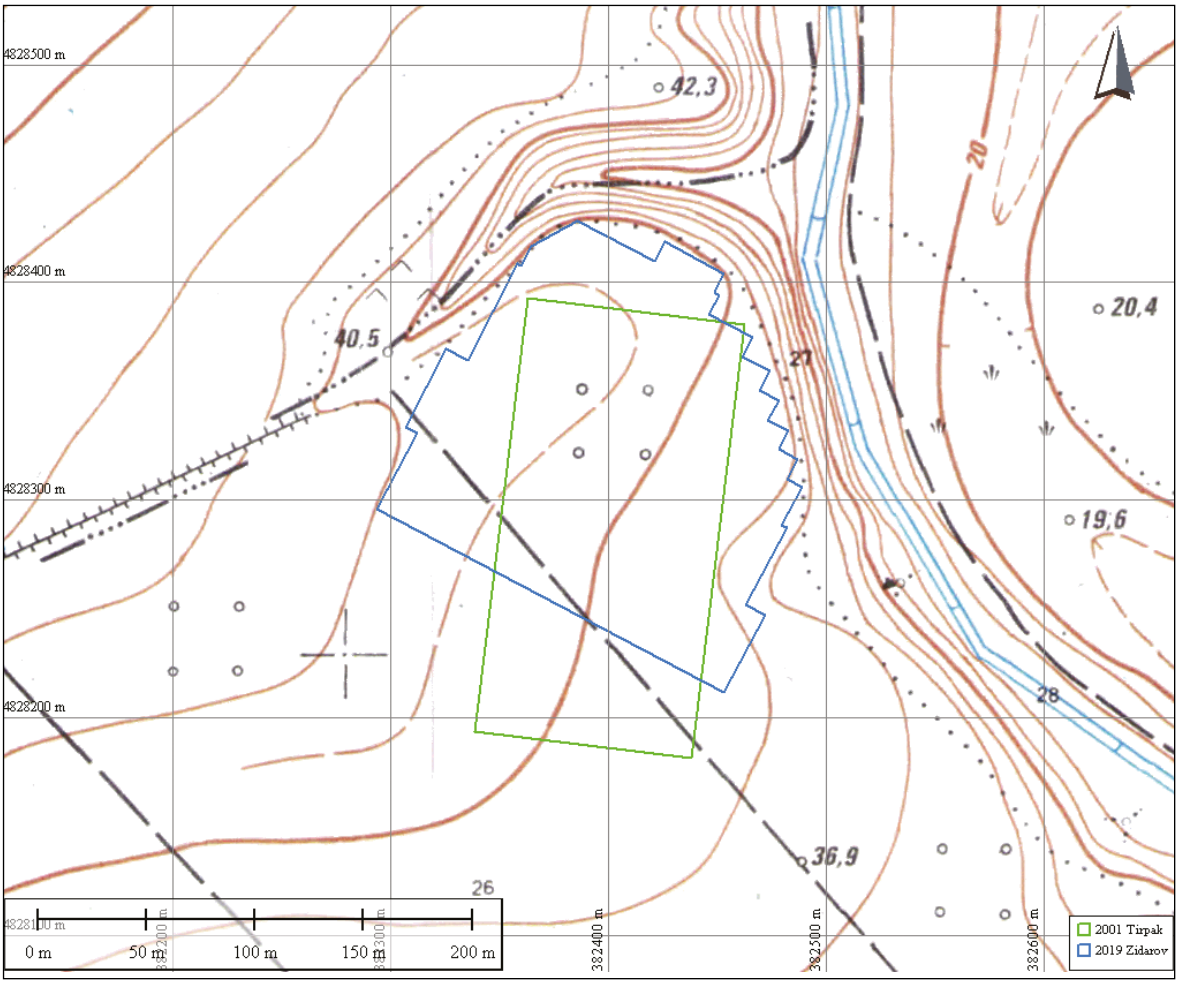


Fig. 1. Tash bair, site 2. Location and extent of magnetic surveys carried by J. Tirpák (2001, green) and P. Zidarov (2019, blue) on topographic map with original scale 1:5000 (source: Geoportal of the Ministry of Regional Development and Public Works – http://gis.mrrb.government.bg/)

The zigzags of some linear anomalies located across the profiles, as well as striping (alternating white and dark stripes) due to the so-called heading errors is exacerbated by the parallel flow of the plough marks (fig. 3; 5; 6).

The magnetic data were integrated into a GIS-based project including georeferenced raster images of the topography of the terrain in scale 1:5000 (fig. 1), digital altitude model obtained by LiDAR measurement (figs. 4–7), a cadastre with orientation of the boundaries of the properties in the area, as well as satellite images used for ground-truthing of the geophysical data.

6.2.3. Measurement and processing

In the course of the field work, 238,351-point measurements covering an area of 2630 m^2 or 2.63 ha were collected. During software data processing the measured values are processed and interpolated to a pixel density of 16.5 × 16.5 cm. The filtered values of the magnetic intensity of the vertical component of the local magnetic field are reduced first to +/- 5nT (fig. 3) and even to +/- 1nT (fig. 6). The distribution of the obtained values is symmetrical, with a standard deviation of 1.63 nT, and with mean and median values of 0.03 and 0.05 nT, respectively.

The data were analysed by visual inspection, focusing on linear alignments and geometric patterns using different values of the data and colour palettes. This was done both in the context of the survey polygon, and against the spatial context of the site topography and the orientation of the ploughing marks. Maximum contrast was used to outline the contours of potential buildings. The lineaments with a rectangular shape,



Fig. 2. Novgrad, Tash bair, site 2. Survey in progress in the areas to the S/SW from the field track (photo by: S. Conrad)

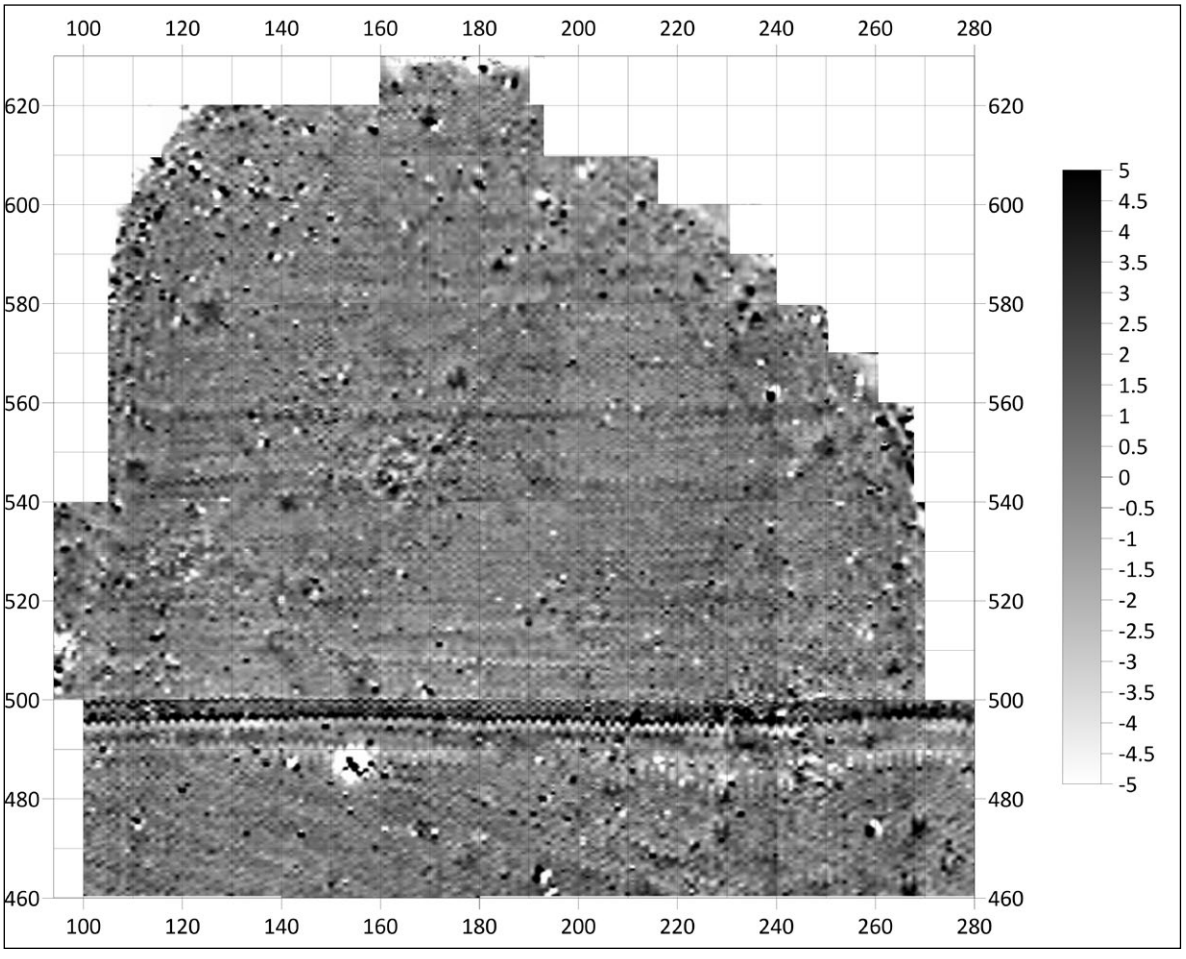


Fig. 3. Tash bair, site 2 (2019). Vertical magnetic gradient map. Instrument: caesium magnetometer G-858, grid density 0.30 × 0.30 m, dynamics -5/5nT, greyscale (surveyed and assembled by P. Zidarov)

which could be interpreted as the foundations of buildings are also outlined (fig. 6; 7). The newly obtained data are also compared with data from previous geophysical measurements, which were analysed separately by enhancing the contrast of black-and-white visualisation imposed on the terrain model (fig. 4).

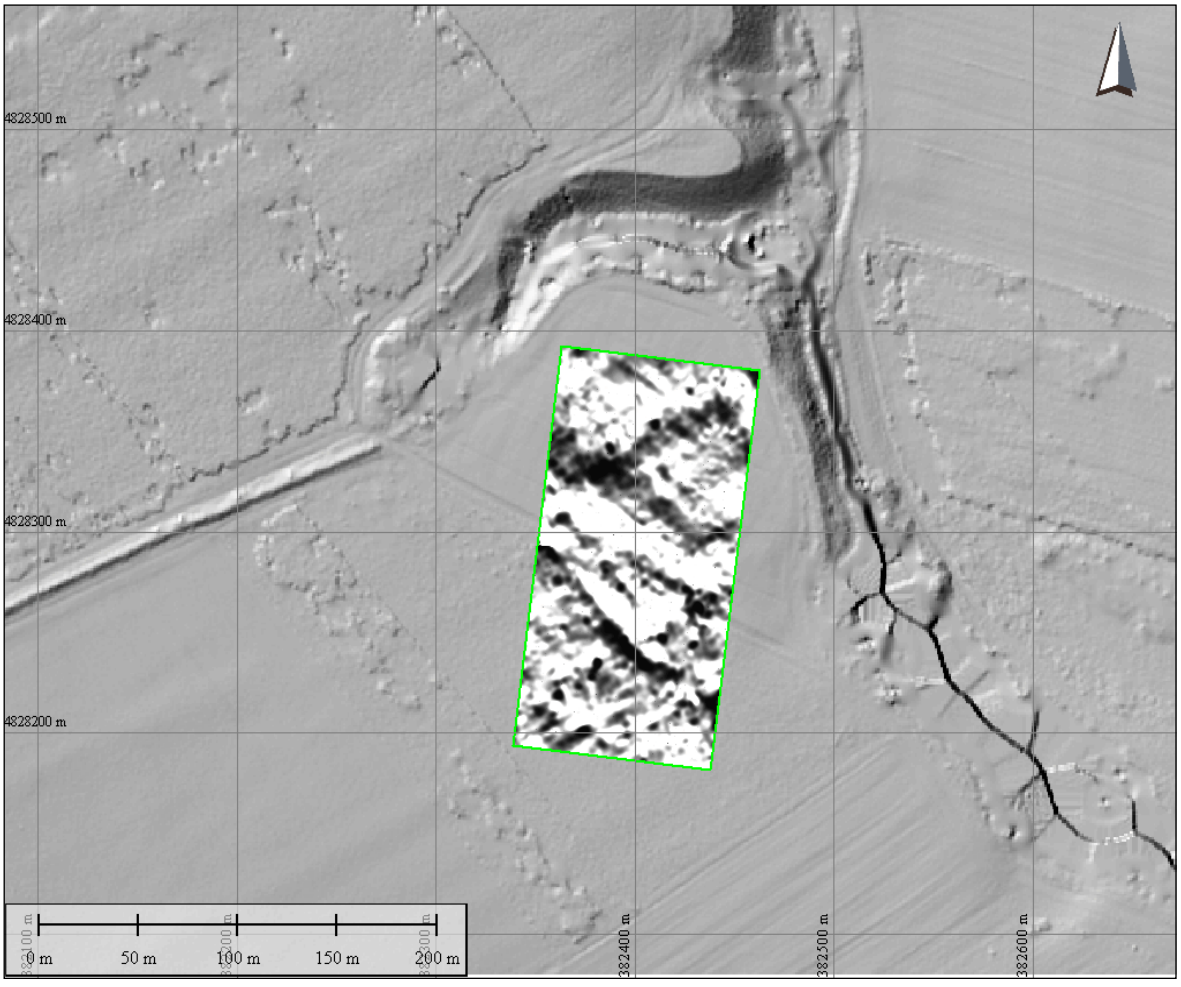


Fig. 4. Tash bair site 2. Magnetic map of the Slovak team on LiDAR DTM, scale 1:2000 (Bartík et al. 2000) (georeferenced and enhanced (increased contrast) by N. Kecheva and P. Zidarov)

6.2.4. Interpretation of the results

The interpretation of magnetic maps is organised according to geometric patterns, starting from the brightest and clearest signals to the weaker signals and uncertain reconstructions.

1. Linear features (plough marks and road) – at first glance the magnetic map (fig. 3) is dominated by linear "features" located parallel to the baseline of the measured area. Along the southern edge of the survey perimeter these linear signals are located also perpendicular to the profiles measured. This corresponds exactly to the changing orientation of the ploughing furrows on either side of the field track, documented both on the LiDAR and on satellite imagery. The clearest linear signal is produced by the same field track, located parallel to the 500N line in the local survey grid (fig. 2; 3) and separating the two neighbouring field plots especially with its northern boundary, which was probably repeatedly ploughed deeper.

2. Dipoles (iron objects) – most of the measured area and especially its peripheral zones are dotted with highly-contrasting signals (dipoles), usually marking the location of ferromagnetic (iron) objects. The brightest dipole signal is localised around 155E / 490N (fig. 3). The enhanced values in its centre (black) among the contrastingly low values around it is consistent with the magnetic signature of a vertically placed iron object (bar, tube) or a concrete post reinforced with iron bars.

3. Monopoles (pits or hearths) – some point-shaped signals mostly located in the northern part of the measured area are identified as round areas with enhanced magnetic values, resembling black circles. If they are of anthropogenic origin, they can be correlated with and interpreted as large pits or as zones with thermoremanent magnetism resulting from the burning of a strong fire. Their clear identification on

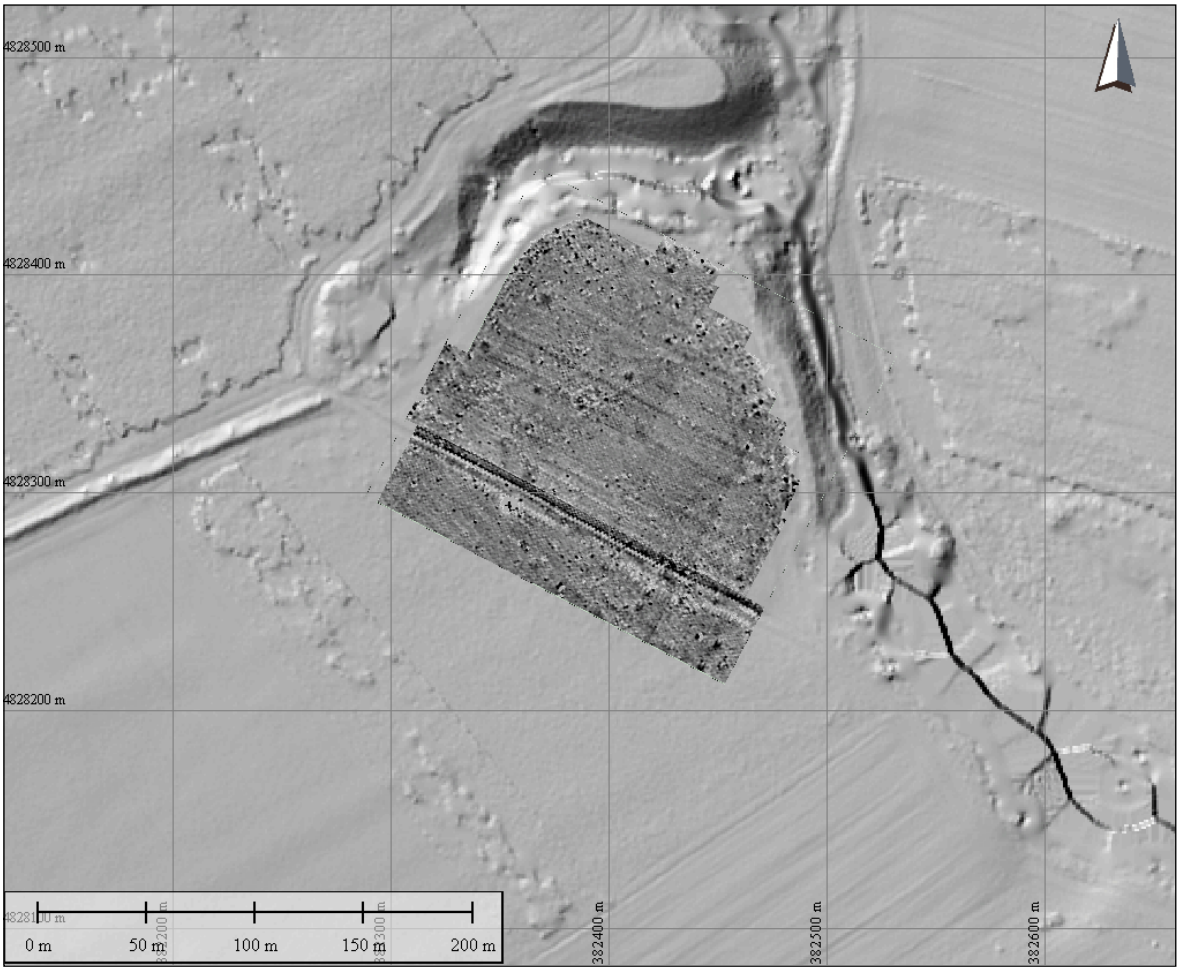


Fig. 5. Tash bair, site 2 (2019). Vertical magnetic gradient map. Instrument: caesium magnetometer G-858, grid density 0.30 × 0.30 m, dynamics -5/5nT, greyscale (surveyed and assembled by P. Zidarov)

both magnetograms from 2001 (fig. 4) and 2019 (fig. 3) allowed their exact correlation and georeferencing of the results of the Slovak team.

4. Polygons (architectural remains) – a number of intersecting linear correlations can be distinguished at different degrees of contrast visualisation. Some resemble the ground plan of buildings especially if at least two intersect at right angles that do not coincide with the direction of the abovementioned plough-marks or the field track. One notable exception is what looks like potentially the largest building with its trapezoidal plan.

Some of the most distinct linear correlations of enhanced magnetic values, intersect with each other and form a trapezoidal shape, generally locked between 170–250E and 520–590N and outlined with thick line of Figures 6; 7. With an average side length of 50–60 m, they enclose an area amounting to approximately 2800 m^2. Given its size, shape and the concentration of Roman tiles, fragments of amphora tare and red-slipped table ware on its surface, the area looks like a good match to the ground plan of *villae rusticae* from the Roman era. A review of most excavated monuments of this kind in Bulgaria, shows that the trapezoidal plan is rather characteristic of the Late RomanPeriod – especially during the 3rd and 4th century (Диничев 1997, 68–73).

At the western corner of this trapezoid-like structure, there is a small rectangular structure about 15 × 10 m in size with a similar orientation. Massive walls seem to be emerging, suggesting a fortification, i.e. a tower-like construction. It remains unclear for the time being whether there is a connection to the trapezoidal enclosure.

Northwest of the described area – generally between 120–140E and 530–560N, there is a distinct right angle, open to the north/north-west – with approximate dimensions 30 × 10 m. If it marks the

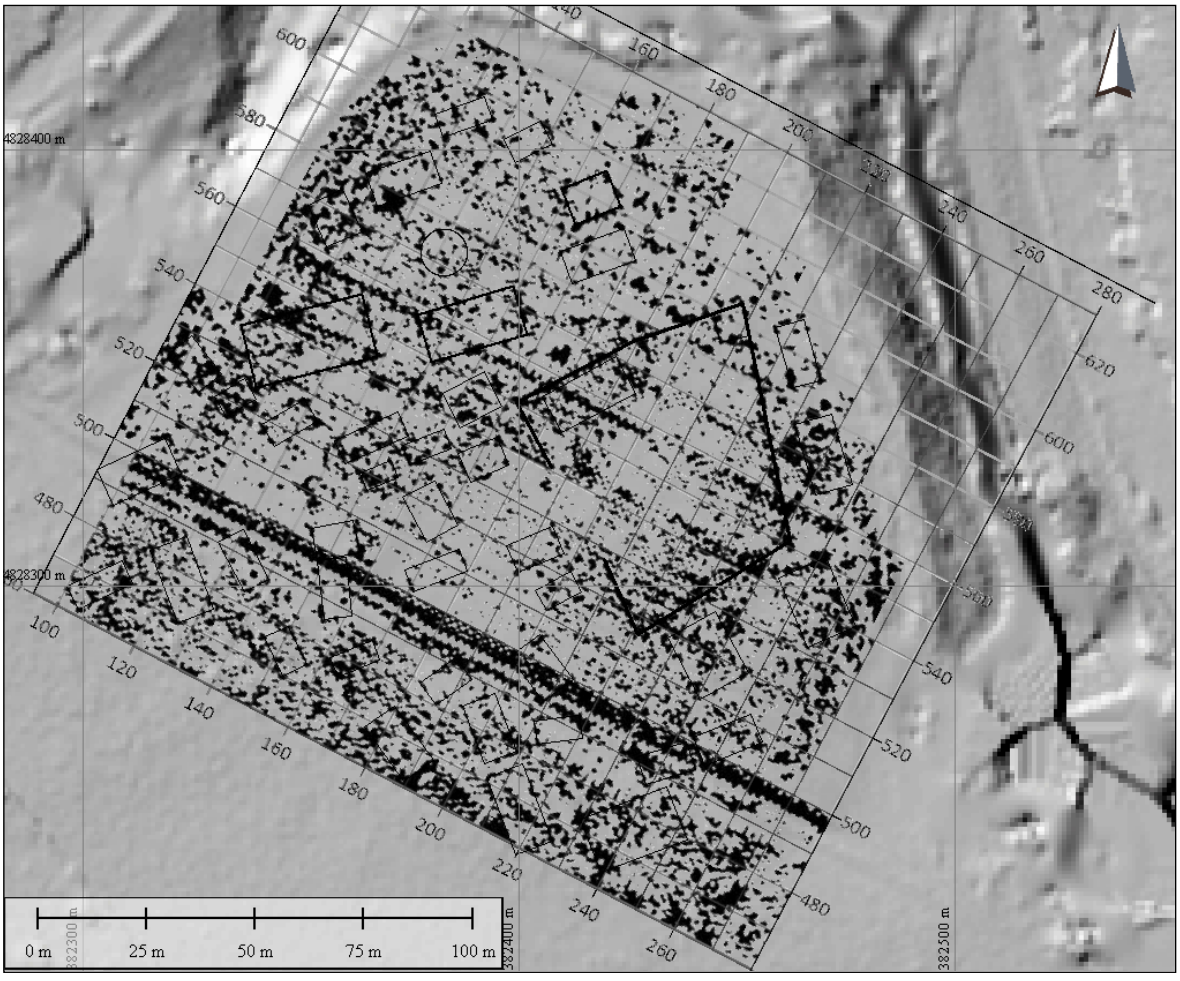


Fig. 6. Tash bair, site 2 (2019). Vertical magnetic gradient map and tentative interpretation. Instrument: caesium magnetometer G-858, grid density 0.30 × 0.30 m, dynamics -1/1nT, highest values (surveyed and assembled by P. Zidarov)

foundations of two intersecting walls, by ancient standards, this would correspond to the size of a public or storage building. Other linear correlations with enhanced magnetic values, reminiscent of rectangular ground plans with long sides extending over 10 m could be recognised to the east of this large building. In the proposed interpretations (fig. 6; 7), they are outlined with solid black lines.

Finally, a closer look at the highest values (approx. 1nT) of the most contrasting magnetic map (fig. 6) led me to connect groups of points that seemed to align and intersect at mutually parallel and perpendicular lines, some of which could be connected in rectangles measuring between 30–60 m^2. It is not always clear whether the subparallel alignments that could be interpreted as wall foundations belonged to one building or another. Therefore, I marked this level of interpretation with the thinnest possible lines. Even though they do not match the signals on the 2001 magnetogram, I find it useful to offer this possibility of interpretation, as such correlations would correspond perfectly to the expected area of medium-sized residential buildings from antiquity. It is noteworthy, that most of them seem to correspond to the orientation of the trapezoidal enclosure but are lacking any common orthogonal or radial settlement plan. If the reconstruction of their layout is correct, then it should be assumed that such a lack of centralised planning would characterise an organic development postdating the Roman period at the site.

6.2.5. Conclusion

The resulting map of the vertical gradient of the magnetic field obtained in 2019 points to a likely identification of an architectural complex with a trapezoidal shape and an area of about 2,800 m^2. This is accompanied by one or three buildings with an enclosed area exceeding 300 m^2 each. The possible

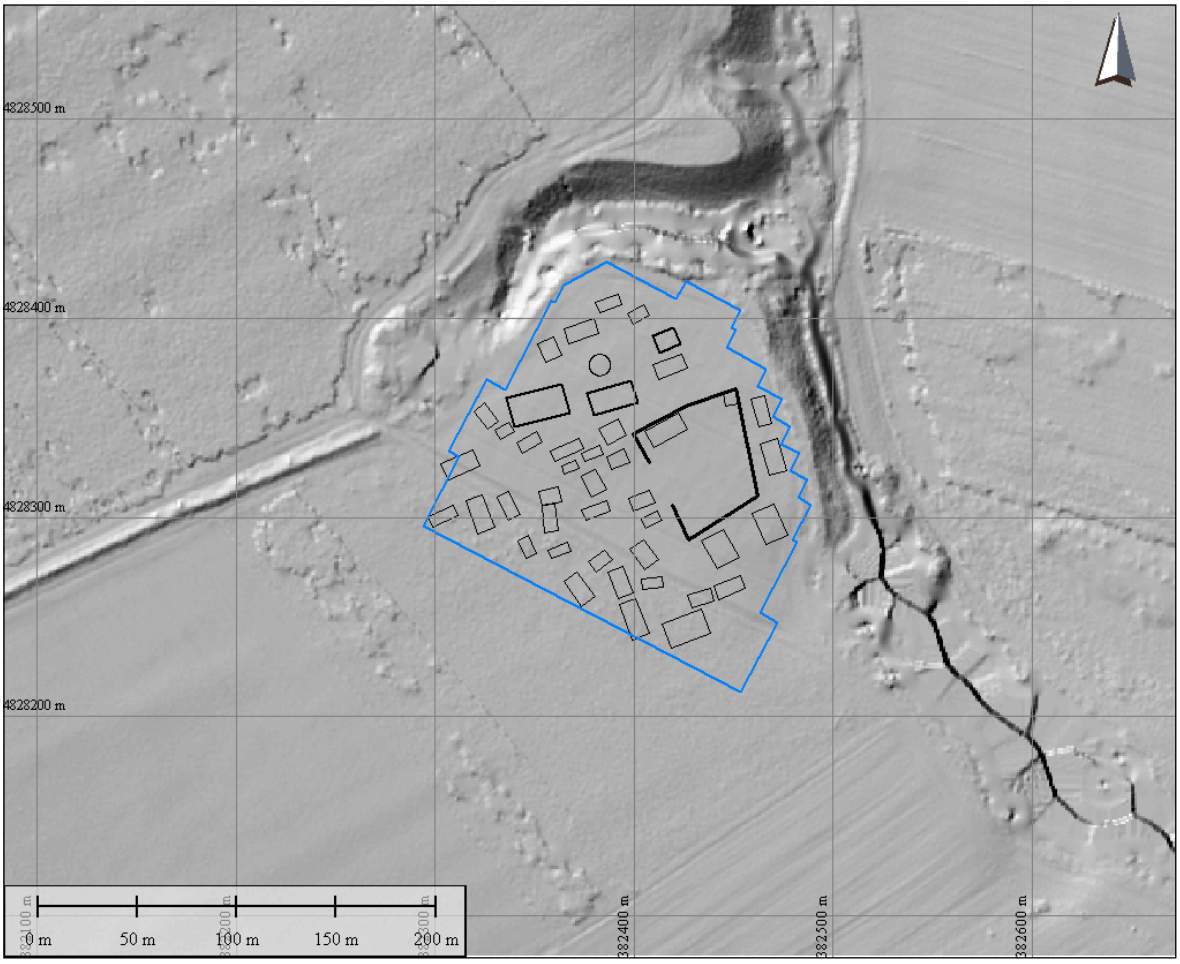


Fig. 7. Tash bair, site 2 (2019). Tentative interpretation of vertical magnetic gradient map from 2019 on LiDAR DTM, scale 1:2000 (figure by P. Zidarov)

interpretation of the first is a villa rustica, while the dimensions of the accompanying structures correspond to the dimensions of public buildings such as granaries from the Late Roman and Late Antique periods. The georeferencing and revision of the data from the previous 2001 survey, indicate similarities between the size and the outlines of the "villa" measured with two different magnetometers over the last 18 years of intensive agricultural activities.

Due to the lack of correlation between the reconstructed smaller building foundations based on weaker amplitudes of magnetic values from the two surveys (2001 and 2019), definite conclusions cannot be drawn. Other signals that are unambiguously represented in the results of both surveys have the shape of circular areas with enhanced magnetic values (large black dots on the magnetogram). Three of them are aligned along the "north wall of the villa" suggesting their contemporaneity, while the rest are located without any obvious order. Their shape and characteristics are consistent with large pits, fireplaces or column fundaments made of imported volcanic or metamorphic rock.

Regardless of the differences in the interpretation of the weaker signals, it is notable that the considerably robust indications for the presence and exact outlines of several large representative buildings from the Late Roman or Late Antique periods, correlate well with the surface concentrations of broken tiles, amphorae and tableware, and underlines their potential for future field research.

Acknowledgements

The success of the field research and the optimal pace for its implementation is primarily due to the extremely collegial attitude of all members of the team directed by L. Vagalinski (NAIM–BAS) and S. Conrad (University of Tübingen). The measurements with a GNSS receiver needed for georeferencing

of the local grid were performed by N. Kecheva (NAIM–BAS), who also provided 3D terrain model based on LiDAR scanning and georeferenced the magnetograms of the Slovak team.

ГЕОМАГНИТНИ ПРОУЧВАНИЯ НА ОБЕКТ 2

Петър Зидаров

(Резюме)

Изследването представя резултатите от геофизично измерване, извършено от автора през 2019 г. С помощта на цезиев магнитометър G858 е измерена площ с размер 2,63 ха. Резултатите отчасти дублират, но и допълват тези от предишно измерване в района, извършено от Ян Тирпак от Института по археология в гр. Нитра (Словакия) през 2001 г. Те са наложени върху топографски карти, както и върху височинен модел, получен от данни от LiDAR.

Сред главните резултати от геофизичните проучвания може да се открояят трапецовидни очертания със страни 50 – 60 м, заграждащи площ от около 2800 м^2, разположена в централната част на проучената територия. Наличието на римска керамика в орницата и сравнението с пространствените характеристики на сгради от същото време позволява с голяма доза увереност да интерпретираме този обект като останки от римска вила рустика. Анекс с квадратна форма и размери 15 × 10 м до западния ъгъл на това съоръжение напомня на основата на кула. Успоредно на северната страна на „вилата“ се наблюдава и редица от три точкови аномалии със завишени стойности на магнитното поле. Те могат да се дължат на контраста в магнитните свойства на почвата, който би се получил вследствие на термореманентен магнетизъм, в случай че на тези места е горял силен огън (напр. пещи за керамика) или при запълване на големи ями с органика и по-силно намагнитена почва от повърхността. Още пò на север и северозапад се наблюдават няколко линейни аномалии, отново сключващи прави ъгли. Ако допуснем, че те маркират ъгли на масивни сгради, чрез интерполация на липсващите части може да се реконструират основите на три сгради с размери 30 × 10 м, т.е. всяка с около 300 м^2 застроена площ. Това би отговаряло на размерите на обществени сгради или в конкретния контекст – по-скоро на складове за зърно или друга търговска продукция. Около вилата се наблюдават и множество линейни аномалии, отличаващи се със значително по-слабо контрастни стойности. Това предполага много по-голяма несигурност при интерпретацията им. Затова и на графичните реконструкции са очертани с много тънки линии. Ако предложената интерпретация е вярна, на това място може да се очаква откриването и на останките на непланомерно застроено селище от по-късен период. В заключение, дори и не всички интерпретации да се потвърдят, податките за наличие на масивни сгради на местата с най-висока концентрация на римска керамика на повърхността подсказват, че изследваната територия потенциално ще предложи добре запазени архитектурни паметници при евентуално бъдещо проучване чрез разкопки.

6.3. TWO ERT PROFILES THROUGH THE DITCHES ON SITE 3

Gert Verstraeten

In 2018, two electrical resistivity tomography (ERT) 2D profiles were measured at site 3 to investigate the quarter-circular double ditches, clearly visible in the geomagnetic mapping (cf. the contributions by B. Ullrich et al., chapter 6.1) (fig. 1). The profiles were positioned near the excavation trench 3.6 on the inner ditch, approx. 12 m to the south. The measurements were carried out with an ABEM SAS Terrameter, each with a 1 m electrode spacing and in compliance with the Wenner-Schlumberger protocol. The two parallel profiles are separated 3 m from each other and run WSW – ENE across (for location, see fig. 1). They have a total length of 79 m. Profile TB01 is located south of

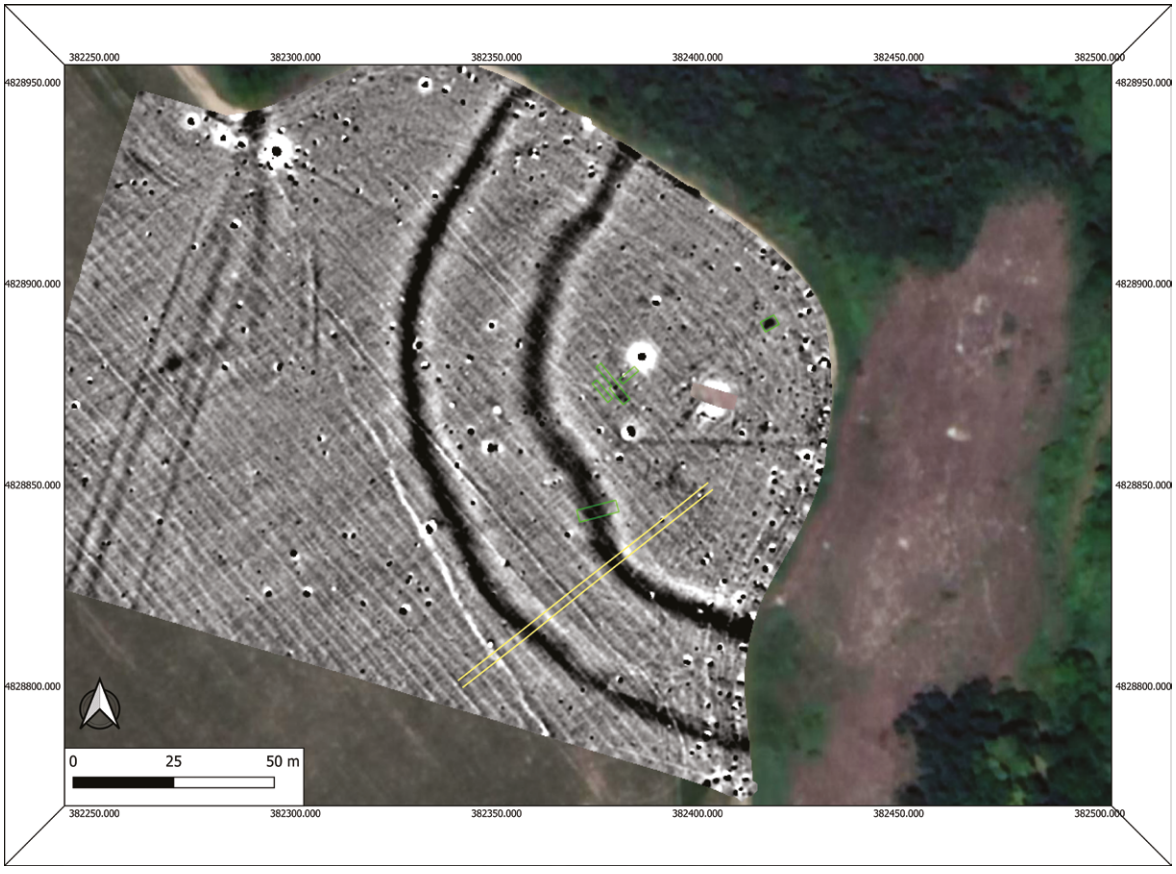


Fig. 1. Location of the two ERT profiles measured at Tash bair in September 2018. The southern profile is ERT TB01, the northern one ERT TB02 (figure by S. Conrad)

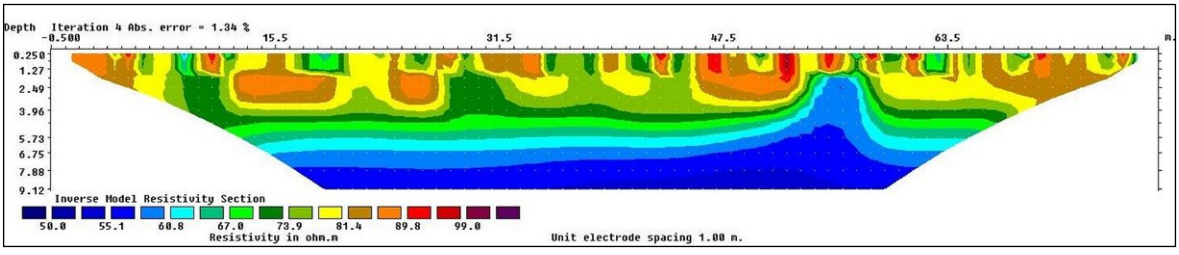


Fig. 2. Inversion result of ERT profile TB01 (figure by G. Verstraeten)

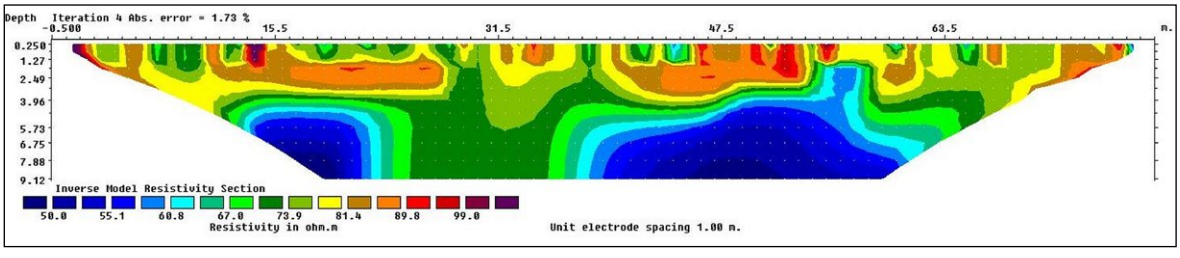


Fig. 3. Inversion result of ERT profile TB02 (figure by G. Verstraeten)

profile TB02. The resistivity data measure apparent resistivities and were inverted to resistivity values using RESD2INV software. Inversion continues until the mean error between measured and simulated apparent resistivity values are below a predefined threshold. For both profiles, errors are below 2% after four model iterations. The resultant modelled resistivity profiles are shown in figures 2 and 3.

Both profiles show overall higher resistivity values (70–90 ohm.m) in the upper 3 m, whereas at depths of 6 to 9 m typical resistivity values are in the order of 50–60 ohm.m. As the measuring protocol

utilised typically detects gradient transitions, it can be suggested that in reality the transition from one layer to the other is more abrupt (can be placed somewhere between 4 and 5 m depth). Since coring information at this depth is lacking, it remains difficult to come up with a final explanation. Lower resistivity values most probably point to the transition from the loess cover to Neogene clays or Cretaceous marls which locally outcrop on steep valley benches to the East of the site. A striking feature is the rise of the lower resistivity values at a distance of 55–58 m from the start of the profile up to a depth of only 2 m below the surface.

In the upper 2 m, large variability in resistivity values can be observed, which is quite common when the surface is very dry as was the case during the measurements. Nevertheless, some patterns emerge from both profiles. Between 10 and 25 m, as well as between 40–45 and 55 m, slightly higher resistivity values (75–100 Ohm.m) are observed, in particular at depths of 1.5 to 2.5 m. According to the mapping of the geomagnetic results, the ditches are situated approx. between 17 and 24 m (outer ditch) and 45–53 m (inner ditch) (from WSW), within these areas of higher resistivity. Especially in TB02, areas of high resistivity correspond with the position of the ditches. The visualised depths of 2.5 to 3 m do not reach the real depths of the ditches established by excavations and coring (inner ditch: 4.38 m; outer ditch 3.10), which can be explained by the dry surface layers. This can also be due to the Wenner-Schlumberger protocol applied, which typically produces gradient instead of abrupt transitions, making the exact location of the transition more uncertain.

Higher values at shallow depth are also seen near the start of each profile, as well as beyond 67 m on profile ERT TB 01 and from 71 m on profile ERT TB02. The latter feature can probably be associated with a weak, widespread anomaly that can be seen in the mapping of the geomagnetic survey. Between these areas, slightly lower resistivity values are observed (60–80 Ohm.m), and in particular, the higher values at 1.5–2.5 m depth are absent. Subtle variation in resistivity in loess-like deposits can point to difference in soil moisture condition and/or to moderate changes in soil texture.

ДВА ERT ПРОФИЛА ПРЕЗ РОВОВЕТЕ НА ОБЕКТ 3

Херт Верстраетен

(Резюме)

През 2018 г. на обект 3 бяха измерени два 2D профила на електрическа съпротивителна томография (ERT) за изследване на двойните ровове, ясно видими в геомагнитното картографиране. Профилите са позиционирани в близост до сондаж 3.6 към вътрешния ров, около 12 м на юг.

В горните 2 м може да се наблюдава голяма променливост в стойностите на съпротивлението, което е доста често срещано, когато повърхността е много суха, както беше по време на измерванията. Въпреки това някои модели се появяват и от двата профила. Между 10 и 25 м, както и между 40 – 45 и 55 м се наблюдават малко по-високи стойности на съпротивление (75 – 100 Ohm.m), особено на дълбочини от 1,5 до 2,5 м. Според картирането на геомагнитните резултати рововете са разположени на приблизително 17 – 24 м (външен ров) и 45 – 53 м (вътрешен ров) (от запад – югозапад) в тези области с по-високо съпротивление. Особено в TB02 зони с високо съпротивление съответстват на позицията на рововете. Визуализираните дълбочини от 2,5 до 3 м не достигат реалните дълбочини на рововете, установени от изкопи и ядро от сондиране със свредел (вътрешен ров 4,38 м; външен ров 3,10 м), което може да се обясни със сухите повърхностни слоеве.

По-високи стойности на малка дълбочина също се виждат близо до началото на всеки профил, както и над 67 м на профил ERT TB 01 и от 71 м на профил ERT TB02. Последната характеристика вероятно може да бъде свързана със слаба, широко разпространена аномалия, която може да се види при картографирането на геомагнитното изследване.

7. THE INTENSIVE FIELD SURVEYS AT THE TASH BAIR LOCALITY AND IN ITS SURROUNDINGS

Nadezhda Kecheva, Lyudmil Vagalinski, Lyuba Traykova, Silva Sabkova[1]

7.1. INTRODUCTION

The intensive field surveys at the Tash Bair locality and in its immediate surroundings were a major part of the non-destructive approach of the project. They were conducted in March and April of the 2018 and 2019 project campaigns by an international team of members: L. Vagalinski, S. Conrad, L. Traykova, N. Kecheva, S. Sabkova, B. Borisov, L. Breuer and J. Sprißler (Вагалински et al. 2019; Вагалински et al. 2020b). One of the project objectives was focused on establishing settlement changes in Tash Bair locality, North Bulgaria, close to the estuary of Yantra River in the Danube (Dunav). The focus area was about 20 km^2 situated in the lands of Novgrad and Karamanovo villages, Tsenovo municipality, Ruse district, and Vardim village, Svishtov municipality, Veliko Tarnovo district. Most of the area is bordered by the left bank of the contemporary channel of Yantra River and the left bank of its left tributary – the contemporary channel of Studena Reka River (fig. 1).

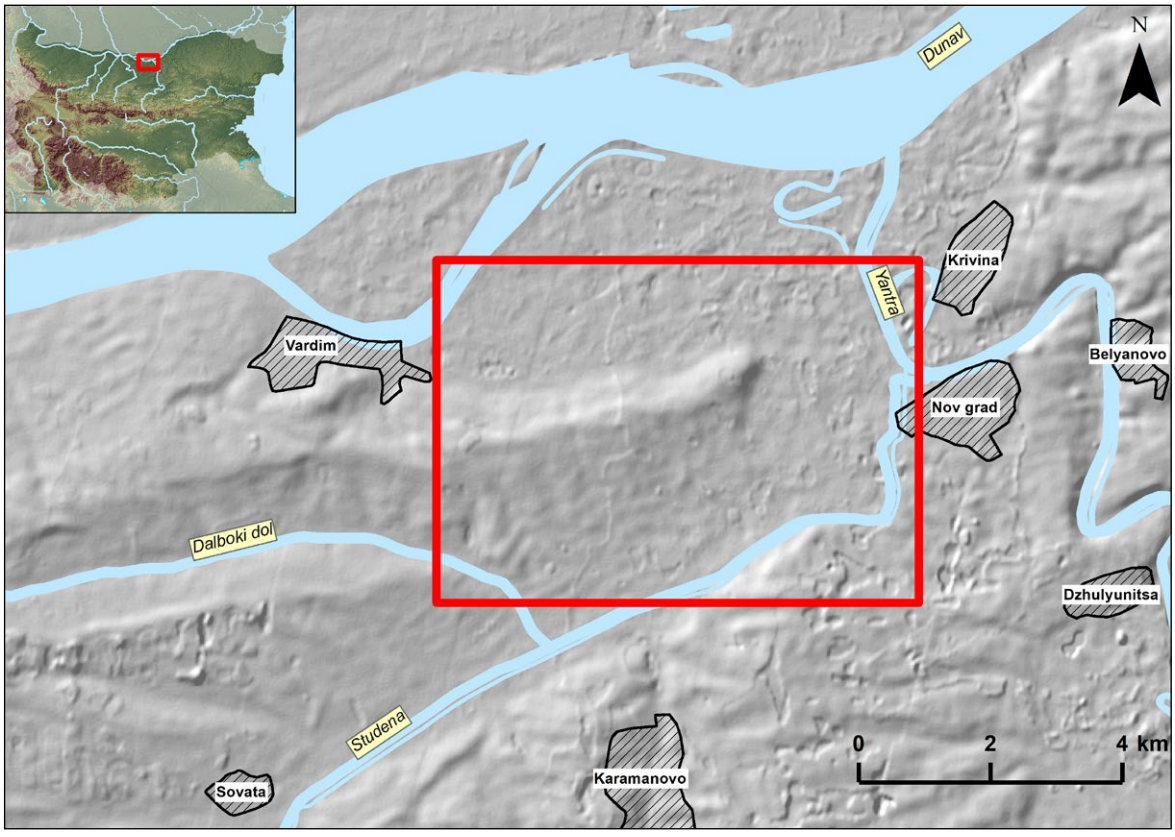


Fig. 1. Focus area in the lands of Novgrad and Karamanovo villages, Tsenovo municipality, Ruse district, and Vardim village, Svishtov municipality, Veliko Tarnovo district, between the left banks of Yantra and Studena Reka rivers, background map: hillshade derived from ASTER Global DEM version 2 (figure by N. Kecheva)

1 With contributions by S. Conrad for the post-processing of the collected pottery fragments.

The field survey methods that were used are explicitly described in the contributions by N. Kecheva, chapter *5.2 Field survey methods*. Conclusions are drawn based mainly on data gathered through non-destructive methods[2]:

• Recorded sites specifics fully described in the archaeological site catalogue of the volume (cf. the contributions by N. Kecheva et al., chapter 12);

• Post-processed diagnostic pottery fragments described in the pottery catalogue (cf. chapter 9.1 and chapter 12, table 1);

• Post-processed small/exceptional/rare finds recorded in different sites described in the small finds catalogue (cf. chapter 9.2);

• Conducted geophysical surveys on sites 1, 2, 3, 4 and 5 (cf. chapter 6).

In the years 1997–2001 the Tash Bair locality and its immediate surroundings were extensively surveyed as part of a large-survey project focused on the archaeological survey on the Lower Danube (Вагалински et al. 2001a; Вагалински et al. 2001b; Conrad and Stančev 2002; Conrad 2006; Krauß 2006a). The project was part of a collaboration between the National Archaeological Institute with Museum at the Bulgarian Academy of Sciences, the Romano-Germanic Commission and the Regional Historical Museum – Ruse, and it was financed by the German Research Foundation (Conrad, Stančev 2002, 673). The non-destructive fieldwork activities in the project included: field surveys, limited geophysical prospection, a site specific grid survey ('window' method or total pick up), aerial photography, palynological and soil analyses (Conrad 2006, 309). A large-scale extensive field survey in the territory between Svishtov and Ruse towns along the Lower Danube was conducted during seven campaigns on an area of approximately 1200 km^2. More than 600 archaeological sites were recorded. Only a small amount of them were already registered in the "Archaeological Map of Bulgaria" information system (AIS AKB)[3] (fig. 2). Another aspect of the field survey in 2001 was the total pick up conducted on part of the site 1 area near Novgrad village (site 48 based on the numeration of 2001) (Krauß 2006a, 171–175). The detailed results of the post-processing of the collected artefacts are published in the dissertation of R. Krauß (Krauß 2006a, 173–175).

The small-scale survey conducted in 2018–2019 followed the established methods for field-by-field intensive survey approach as a type of inter-site survey with an area covered of 4.71 km^2 – 0.74 km^2 in 2018 and 3.97 km^2 in 2019 (fig. 3). Only fields with surface visibility above 80% were covered by fieldwalking which included ploughed areas and areas covered with an approximate 10–15 cm height of seeded crops. A total collection of artefacts (total pick up) was conducted as a type of intra-site survey within part of site 1 with an area of 2.27 ha (fig. 3).

The suitable and accepted definition of "an archaeological site" for the project and which is compatible with the Archaeological Map of Bulgaria concept was: *a topographic place in space where people in different chronological periods have been doing different types of permanent and/or periodical activities*. Site scatters were recorded in two ways according to their traces on the surface: as visible and as invisible sites. Burial mounds, ramparts and ditches fall within the visible sites. All the other scatters were defined based on quantitative analysis, in GIS, of amounts of counted artefacts on the surface.

Conclusions based on surface data were drawn only for the intensively covered areas in 2018 and 2019. Older legacy published unstratified data was included when it was relevant for the surveyed area (Стефанов 1956; Стефанов 1974; Дремсизова-Нелчинова, Иванов 1983).

2 Only partial information for the excavations in 2018 and 2019 is included.

3 For none of the newly recorded sites in 1997–2001 registration cards were created, and their data was not included in AIS AKB. A forthcoming full publication of S. Conrad is going to make the data available for scientists.

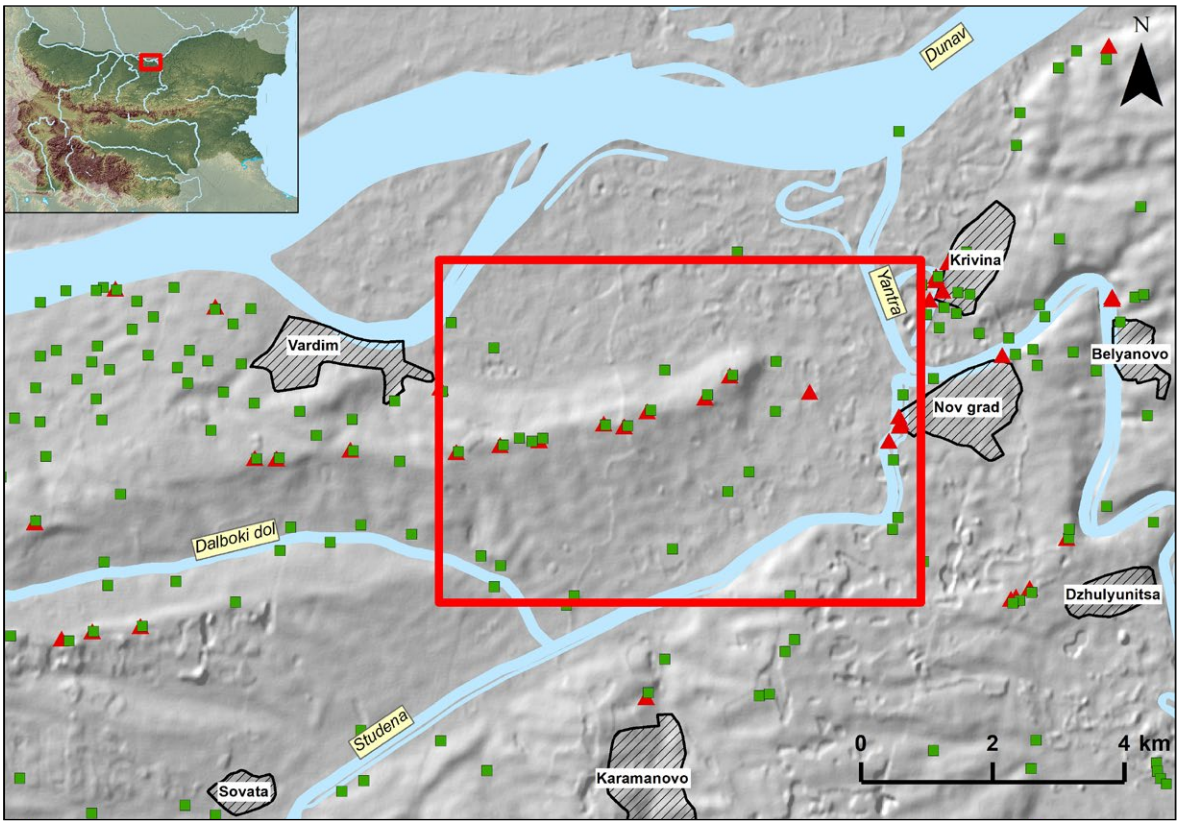


Fig. 2. Recorded archaeological sites in the region: in AIS AKB (red triangles), during the extensive field surveys in 1997–2001 (green squares), and a background map: hillshade derived from ASTER Global DEM version 2 (figure by N. Kecheva)

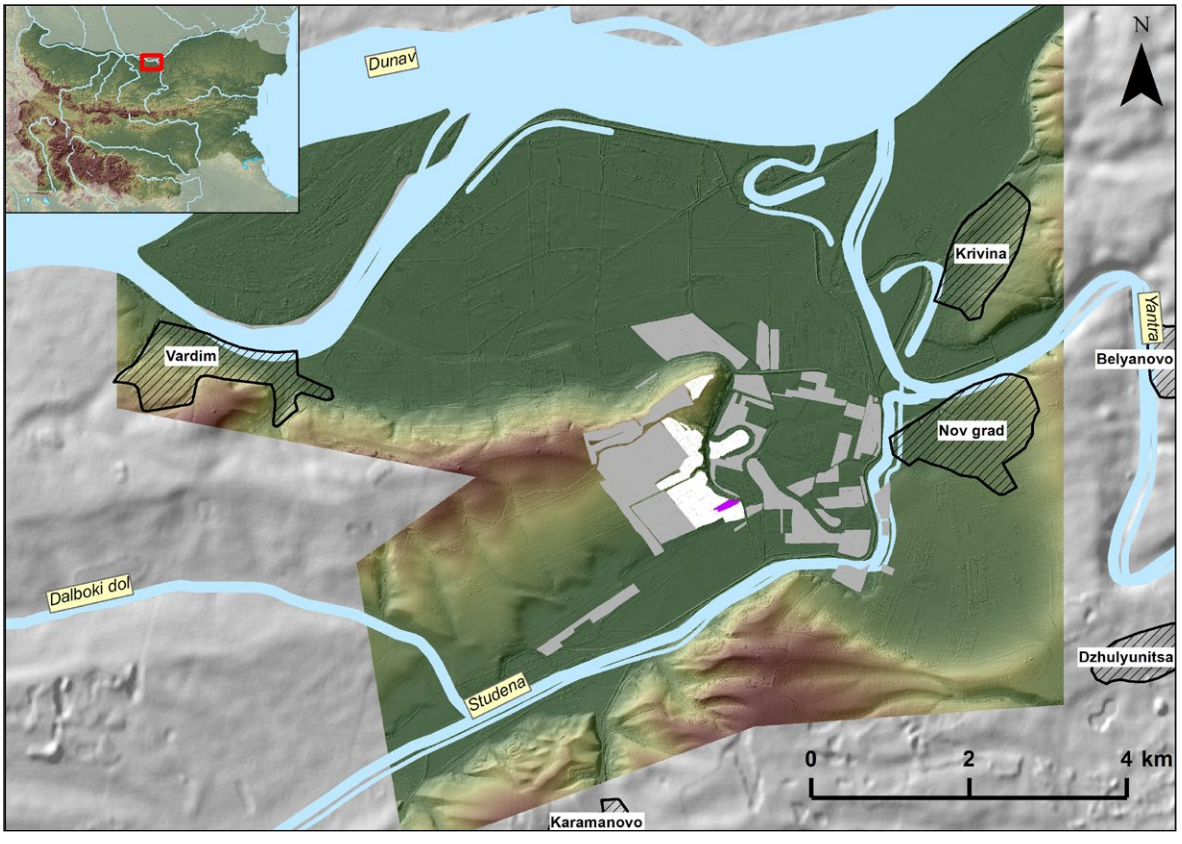


Fig. 3. Area covered during field surveys in 2018 (in white), in 2019 (in grey) and total pick up in 2018 (in purple), background maps: hillshade derived from ASTER Global DEM version 2 (larger area) and hillshade derived from airborne laser scanning data (smaller area) (figure by N. Kecheva)

7.2. CHRONOLOGICAL PERIODS IN BULGARIAN ARCHAEOLOGY

Table 1 below shows the chronological periods used in Bulgarian archaeology with their names in Bulgarian and English, and their start and end. The absolute dates for prehistoric periods are approximate. This terminology is used in this chapter[4].

Table. 1. The chronological periods used in Bulgarian archaeology with their names in Bulgarian and in English and their start and end

Chronological periods in Bulgaria (in BG)	Chronological periods in Bulgaria (in EN)	Start	End
Неолит	Neolithic	6300 BC	4900 BC
Ранен неолит	Early Neolithic	6300 BC	5500 BC
Среден неолит	Middle Neolithic	5500 BC	5200 BC
Късен неолит	Late Neolithic	5200 BC	4900 BC
Халколит	Chalcolithic	4900 BC	3800 BC
Ранен халколит	Early Chalcolithic	4900 BC	4600 BC
Късен халколит	Late Chalcolithic	4600 BC	3800 BC
Преходен период между халколит и бронзова епоха	Transitional period between Chalcolithic and Bronze Age	3800 BC	3200 BC
Бронзова епоха	Bronze Age (BA)	3200 BC	1200 BC
Ранен бронзов период	Early Bronze Age (EBA)	3200 BC	2200 BC
Среден бронзов период	Middle Bronze Age (MBA)	2200 BC	1600 BC
Късен бронзов период	Late Bronze Age (LBA)	1600 BC	1200 BC
Желязна епоха	Iron Age (IA)	1200 BC	end of 1st c. BC
Ранен железен период	Early Iron Age (EIA)	1200 BC	500 BC
Късен железен период	Late Iron Age (LIA)	500 BC	end of 1st c. BC
Класическа епоха	Classical period	500 BC	end of 4th c. BC
Елинистическа епоха	Hellenistic period	end of 4th c. BC	end of 1st c. BC
Римска епоха	Roman period	1st c. AD	4th c.
Ранен римски период	Early Roman period	1st c. AD	mid 3rd c.
Късен римски период	Late Roman period	mid 3rd c.	4th c.
Късна античност	Late Antiquity	4th c.	beginning of 7th c.
Средновековие	Medieval period / Middle Ages	beginning of 7th c.	mid 18th c.
Ранно средновековие	Early Medieval period / Early Middle Ages	beginning of 7th c.	beginning of 11th c. .
Византийски период	Byzantine period	beginning of 11th c.	end of 12th c.
Зряло средновековие	High Medieval period / High Middle Ages	end of 12th c.	end of 14th c.
Късно средновековие	Late Medieval / Ottoman period	15th c.	mid 18th c.
Възраждане	Bulgarian Renaissance / Bulgarian National Revival period	mid 18th c.	end of 19th c.
Съвременна епоха	Contemporary	end of 19th c.	today

4 This terminology is also used in part of chapter 8 and the archaeological site catalogue (cf. the contributions by N. Kecheva et al., chapter 12). For some differences in the terminology and chronology used in the pottery catalogue cee chapter 9.1.

7.3. TASH BAIR LOCALITY AND ITS SURROUNDINGS

The field surveys in 2018 and 2019 covered an area of 4.71 km^2. This area included:

• Tash Bair and part of Karaman Bair ridge localities;

• The southern slopes of Tash Bair and Karaman Bair ridge localities;

• Partially the northern slope of Tash Bair ridge locality.

The territory between the Tash Bair ridge locality and the left bank of the channelled Studena Reka River – between the old meanders of Yantra River. These lowlands are part of the larger Vardim – Novgrad lowlands that were often flooded at the beginning of the 20th c., and that is why an embankment of the right bank of the Danube and the left banks of the Yantra and Studena Reka rivers was constructed in the period 1928–1931 (Стефанов 1974, 251–252);

• Part of the right bank of the channelled Studena Reka River;

• Part of the lowlands that are situated immediately on the southern foot of Tash Bair and Karaman Bair ridge locality to the transition to the left bank of the channelled Studena Reka River.

The forest areas on the northern and southern steep slopes of Tash Bair ridge as well as certain agricultural fields in the lowlands were not accessible due to the crops and the ongoing cultivation of the fields.

Tash Bair locality and its surroundings geomorphological situation is further analysed in chapter 4 (cf. the contributions by A. López del Olmo et al.).

7.4. FIELD SURVEYS DATA ANALYSIS

This part of the paper presents the analysis of field-by-field intensive surveys data and 'window' (total pick up) data. The post-processed diagnostic artefact data is further analysed in GIS.

7.4.1. Field-by-field intensive surveys data analysis

Field-by-field intensive surveys data analysis is based on:

• Small-scale field-by-field intensive surveys in deliberately chosen areas with surface visibility above 80%;

• Artefacts counted on the surface including handmade and wheelmade pottery fragments, tiles and bricks, pieces of daub, chipped-stone artefacts (flints), small/exceptional/rare finds;

• Site chronologies according to collected **diagnostic** pottery fragments and small/exceptional/rare finds (stone tools, millstones, loom weights, spindle whorls, chipped-stone artefacts) per polygon;

• Inter- and intra-site scatter classification (where it was possible).

Site scatters were classified with different types of function as:

• Habitation sites:

  o Settlements: settlements were defined based on the presence of pottery fragments mixed with pieces of daub, tiles and bricks, stones;

  o Sites with undefined function: defined based only on the presence of pottery fragments.

• Mortuary sites: burial mounds, mound necropolises, other traces of burials;

• Roads: visible on satellite/orthophoto imagery, recorded stone scatters on the surface.

As part of the inter-site survey, no offsites were classified. Only units with single artefacts were taken into account for the overall picture of the microregion.

Thirty-eight[5] archaeological sites are defined. Seventeen sites are classified as habitation sites, 20 as mortuary sites (burial mounds and mound necropolises) and one as an ancient road (fig. 4). Habitation site areas varied between 1.4 and 20 ha while mortuary site areas were between 0.01 and 0.4 ha. The ancient road most visible length is 2.54 km.

5 Including site 38 traces of which were discovered at a depth of 2.80 and 3.60 m below the surface level (cf. the contributions by N. Kecheva et al., chapter 12, site 38).

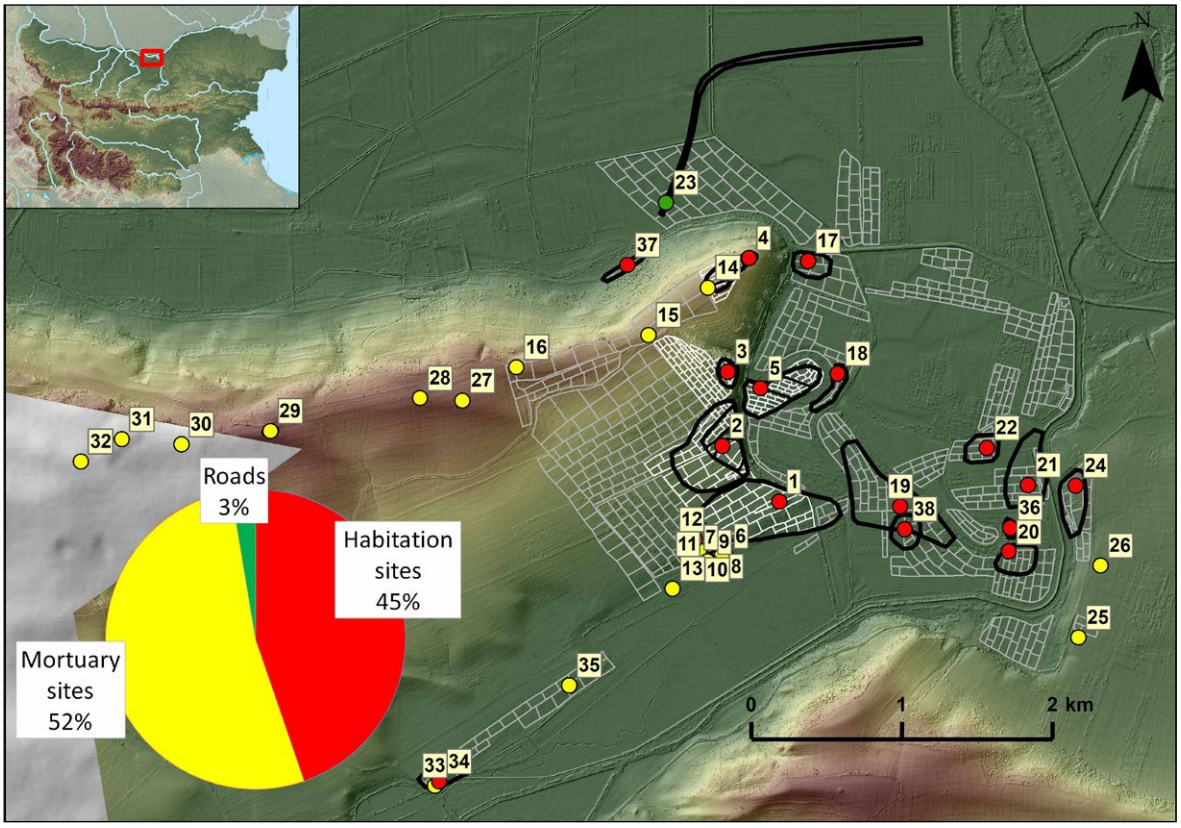


Fig. 4. Area covered during field surveys in 2018 (in white), in 2019 (in grey), recorded archaeological site scatters (in black) and recorded archaeological site centres with field number sites IDs (from 1 to 38) – habitation sites – in red dots; mortuary sites – in yellow dots; road – in green dot. In the lower left corner, a pie chart shows the percentage of the recorded sites with different types of function and a background map: hillshade derived from airborne laser scanning data (figure by N. Kecheva)

Habitation sites are part of the so-called 'invisible' sites. They were identified based on quantitative analysis in GIS of higher concentrations of recorded artefacts on the surface, i.e. quantities of both handmade and wheelmade pottery fragments, pieces of daub, tiles and bricks, stones (fig. 5).

Traces from the Late Neolithic to the Ottoman period were recorded on the area covered. Usually, more than one chronological period was found on one site; their percentage varies between 1 and 20% (fig. 5).

All[6] prehistoric artefact quantities and distribution suggest they could fall in the definitions of the *hidden prehistoric landscapes* concept which is well-published in the intensive survey of the Mediterranean region (Bintliff et al. 1999; Bintliff 2011).

At this stage of the research, no Palaeolithic and Mesolithic traces were found[7].

7.4.1.1. Habitation sites and sites with undefined function

7.4.1.1.1. Late Neolithic

The core drilling samples for the geomorphological investigations, in 2019, in the southern part of Yantra lowlands found a cultural layer dated approximately 6080–5980 calBC which was buried under approximately 3 m thick colluvium. Further investigation will clarify whether it could be associated with a Neolithic settlement (cf. the contributions by A. López del Olmo et al., chapter 4). It is defined as site 38.

Late Neolithic artefacts on the surface are recorded in high concentrations in the southernmost lower parts of the Tash Bair ridge (site 1) (fig. 6). This site was recorded in the 1997–2001 field campaigns (Krauß 2006a, 173–174). The most significant artefact concentration was in the NE part of the site where

6 Excluding areas with Late Neolithic and Early Iron Age artefacts with high concentration of artefacts on the surface.

7 The artefacts recorded on the surface of site 4 are mostly chipped-stone, but the analysis by M. Gurova does not show certainty for their chronology (cf. the contributions by M. Gurova, chapter 10.2).

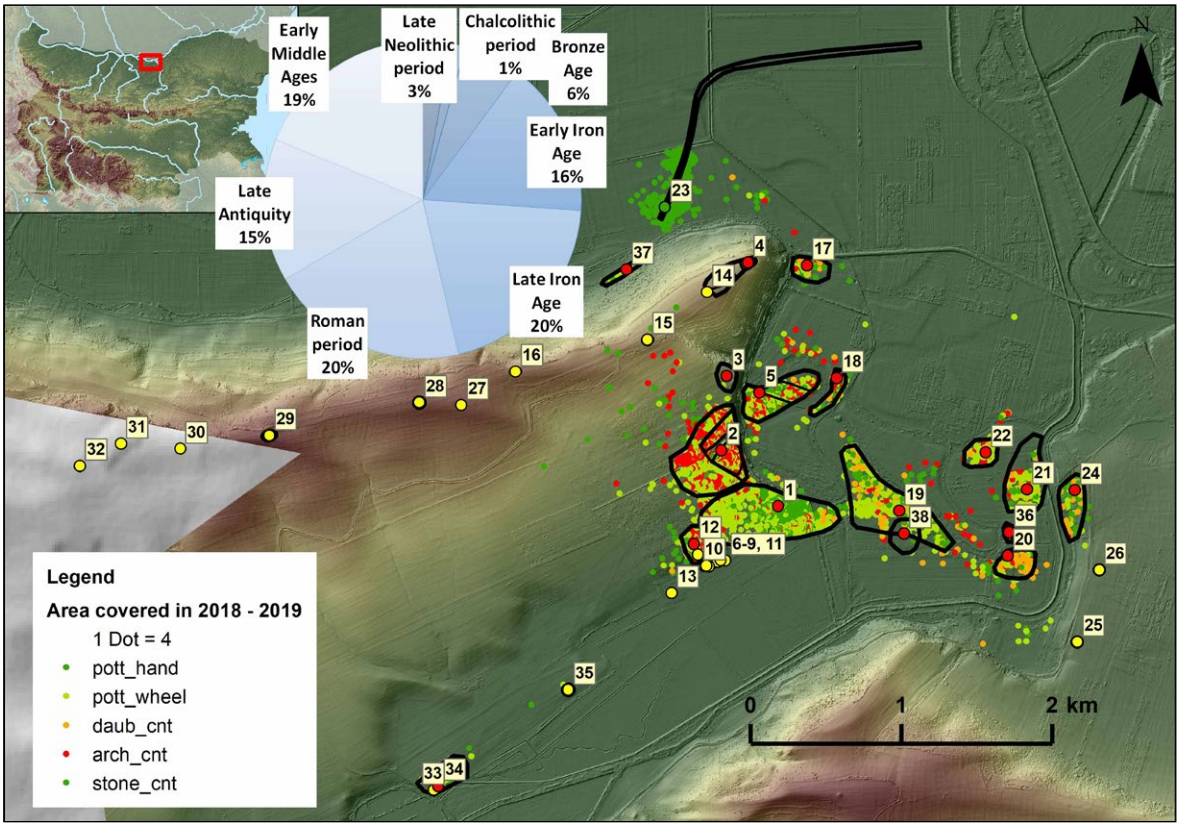


Fig. 5. Concentrations of quantities of handmade and wheelmade pottery fragments, pieces of daub, tiles and bricks, and stones counted on the surface visualised by dot density quantitative descriptive statistics in GIS (1 dot equals 4 artefacts). Recorded archaeological site scatters (in black), recorded archaeological site centres with field number sites IDs (from 1 to 38) – habitation sites – in red dots; mortuary sites – in yellow dots; road – in green dot. In the upper part, a pie chart shows the percentage of the recorded site chronologies and a background map: hillshade derived from airborne laser scanning data (figure by N. Kecheva)

the rampart is visible above the surface. The soil from the ditch that was used in the rampart destroyed Late Neolithic features and brought to the surface Late Neolithic artefacts. According to the scattered artefacts, the area of habitation was at least 7 ha which is clearly larger than the average habitation site (a settlement) (fig. 6). The results of geophysical surveys and the excavations in 2019 also suggested that part of the Late Neolithic site area was surrounded by a ditch (cf. the contributions by B. Ullrich et al., chapter 6.1, and R. Krauß, S. Conrad, chapter 8.1).

The high concentration of artefacts on the surface included pottery fragments, pieces of daub, and other finds that were diagnostic of a settlement (cf. the contributions by R. Krauß, S. Conrad, chapter 8.1). Based on this it could be assumed that large Late Neolithic settlement(s?) existed on site 1 at the Tash Bair. Three radiocarbon dates were obtained from animal bones from the excavations in 2019 of the ditch in trench 1.2 dating to the 51st/50th century calBC (cf. the contributions by R. Krauß, chapter 9.1.1).

Artefacts from the cultural groups Vădastra, Boian, Hamangia and the local North Bulgarian Late Neolithic (Kachitsa, Polyanitsa) came from the surface and the filling of the younger features at the site (cf. the contributions by R. Krauß, S. Conrad, chapter 8.1 and R. Krauß, chapter 9.1.1). It remains unclear whether they occurred simultaneously or whether they belong to different Late Neolithic habitation phases.

Single artefacts from the Late Neolithic were collected as diagnostic on the area of site 2 which was situated on the middle part of the ridge. A much smaller amount of handmade pottery fragments was counted on the surface; these artefacts could be indicative of some periodical activities/burial practices in that area.

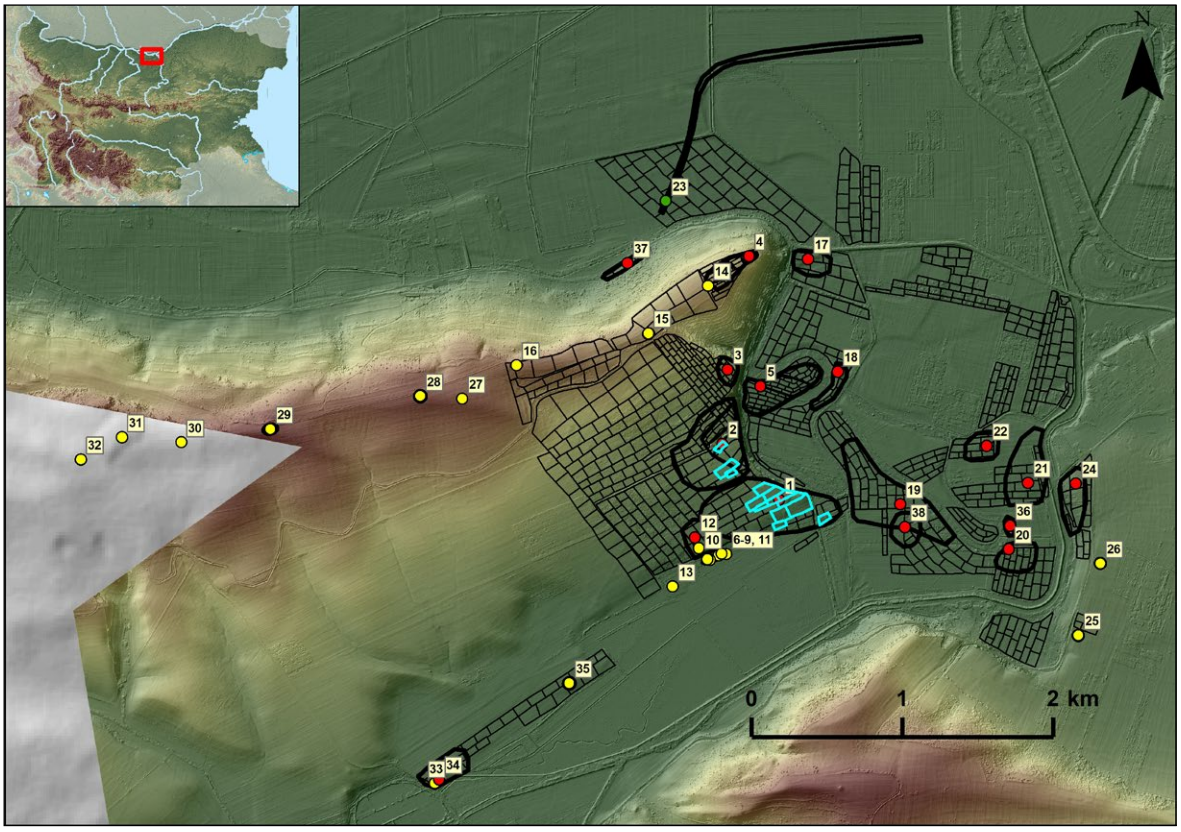


Fig. 6. Spatial distribution of Late Neolithic pottery fragments collected from polygons (in cyan). Area covered during field surveys in 2018 and 2019 (in thin black polygons), recorded archaeological site scatters (in thick black polygons), recorded archaeological site centres with field number sites IDs (from 1 to 38) – habitation sites – in red dots; mortuary sites – in yellow dots; road – in green dot, and a background map: hillshade derived from airborne laser scanning data (figure by N. Kecheva)

7.4.1.1.2. Chalcolithic

Only five pottery fragments dated to the Chalcolithic were recorded during the 2018 and 2019 total pick up field surveys on part of site 1. The excavations on site 1 in trench 1.2 revealed one pottery fragment (P 1/242) dated to the Chalcolithic. This fragment could be classified chronologically using a radiocarbon date obtained by an animal bone from the same layer for activities in approximately 4470–4310 calBC (cf. the contributions by R. Krauß, chapter 9.1.1). However, since there are not enough diagnostic Chalcolithic survey data, no assumptions could be made about the size of the possible site[8]. It could be assumed that the chalcolithic artefacts belonged to the *hidden prehistoric landscapes* concept known from the intensive surveys in the Mediterranean region (Bintliff et al. 1999; Bintliff 2011).

7.4.1.1.3. Bronze Age

Field surveys in 2018 and 2019 revealed a small amount of diagnostic Bronze Age artefacts. They were recorded mainly in the site 1 area because of the total pick up collected data[9]. Single mostly undiagnostic fragments were found on sites 2, 3 and 17. Some Bronze/Iron Age pottery fragments were recorded on site 4 and site 5 area (fig. 7). No diagnostic Early, Middle or Late Bronze Age artefacts were recorded on the surface.

The geophysical survey and the excavations of site 3 revealed traces of parallel ditches and other features belonging to the Bronze Age (MBA and LBA based on excavated pottery fragments and radiocarbon dates obtained by animal bones and a single piece of charcoal) (cf. chapter 8.2, chapter 9.1.1). Surface traces of the Bronze Age on site 3 were very scarce probably because of constant soil erosion and

8 Fieldwork results in 1997–2001 suggest for a chalcolithic site in the same area (Krauß 2006a, site 48b, 308).
9 Fieldwork results in 1997–2001 suggest for a Bronze Age site in the same area (Krauß 2006a, site 48c, 308).

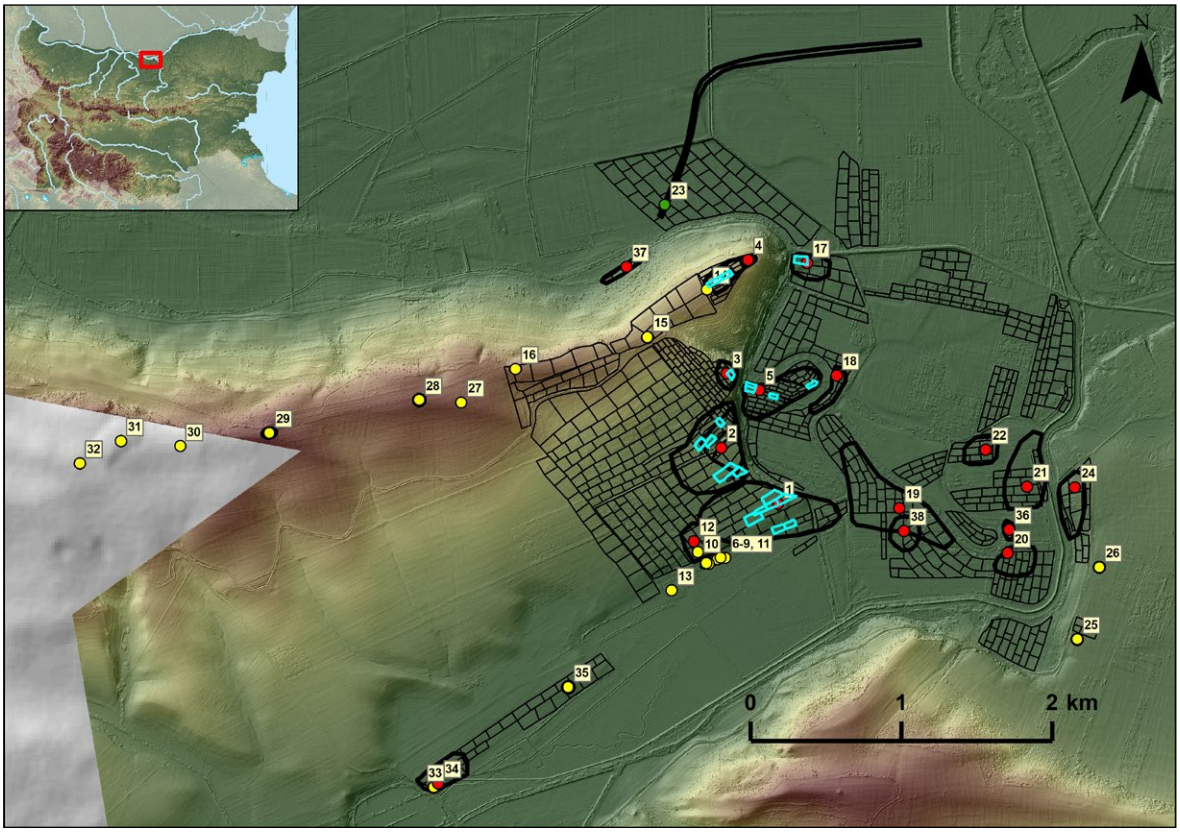


Fig. 7. Spatial distribution of Bronze and Bronze/Iron Age pottery fragments collected from polygons (in cyan). Area covered during field surveys in 2018 and 2019 (in thin black polygons), recorded archaeological site scatters (in thick black polygons), recorded archaeological site centres with field number sites IDs (from 1 to 38) – habitation sites – in red dots; mortuary sites – in yellow dots; road – in green dot, and a background map: hillshade derived from airborne laser scanning data (figure by N. Kecheva)

the following destruction of upper levels of the features. It could be assumed that the parallel ditches had originally been concentric – a probable full enclosure – with destroyed northern and eastern parts through the erosion processes (cf. the contributions by A. López del Olmo et al., chapter 4). Similar assumptions could be made for the ditch recorded on site 4 where not only erosion processes could have affected the full enclosure but also human activities, such as the artificial terracing from the north, east and south.

Excluding site 5 and site 17 all the other sites with traces of Bronze Age artefacts were situated on the southern slope of Tash Bair ridge. With the exception of site 3, the Bronze Age artefacts did not suggest a habitation, features or other types of activities. It is not unusual to find such traces in the immediate vicinities of the Bronze Age site 3. The sporadic Bronze Age finds in the western part of Yantra lowlands next to the steep slopes of the eastern part of Tash Bair ridge could be the result of erosion from site 3 (resulting in presence of fragments on site 5) and site 4 (resulting in presence of fragments on site 17). The assumption that no Bronze Age inhabitation is visible on the surface of Yantra lowlands between Tash Bair ridge and the left bank of the channelled Studena Reka River is supported by the publication of S. Stefanov (Стефанов 1974). It mentions that many Bronze (Early and Late) Bronze Age artefacts have been found on the right high bank of Studena Reka River, 1 km SW from the Novgrad village, at a height of between 3 to 5 m above the lowlands (Стефанов 1974, 252).

The occupation of the higher parts of the surveyed area during the Bronze Age was proven by the partial excavations of site 3. Otherwise, the Bronze Age artefacts could also be part of the hidden prehistoric landscapes in the Mediterranean region (Bintliff et al. 1999; Bintliff 2011). Whether the current surface of the lowlands or some landscape below colluvium deposits were used for permanent occupation or periodical activities during the Bronze Age is difficult to say at this stage of the surveys.

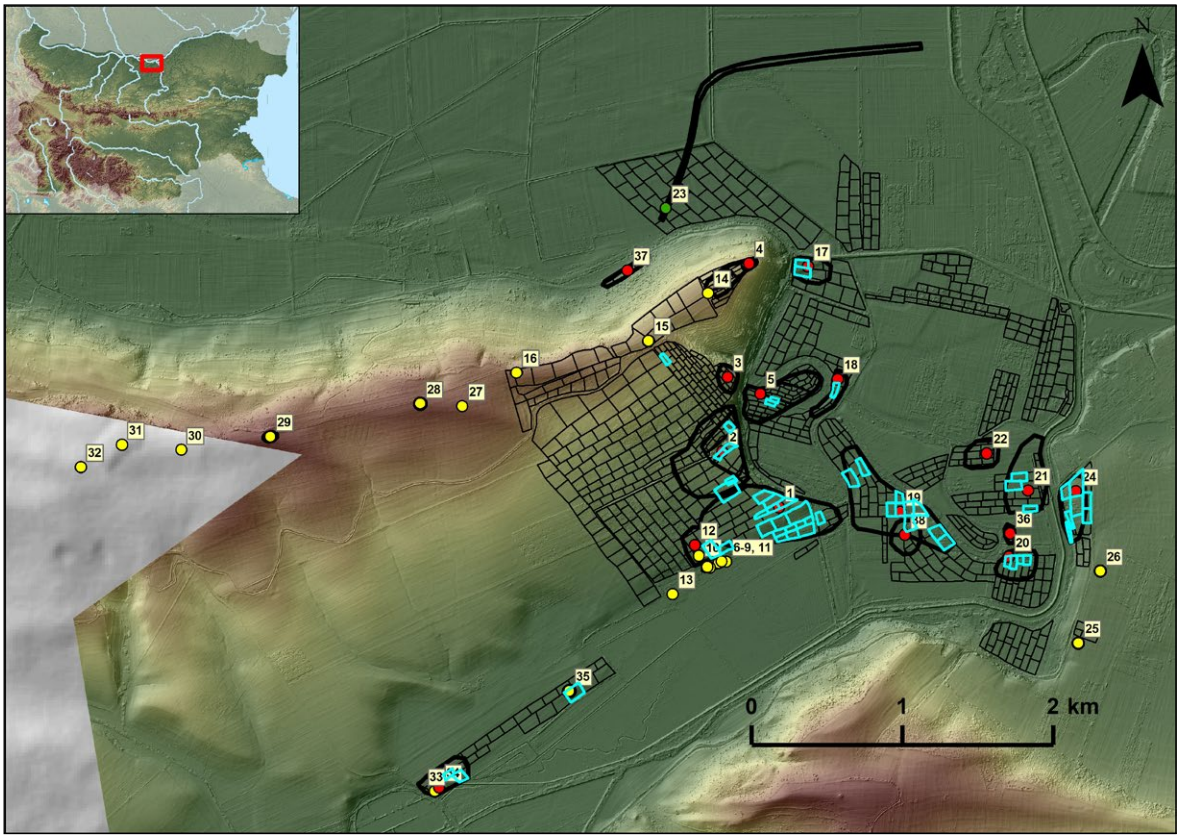


Fig. 8. Spatial distribution of Early Iron Age pottery fragments collected from polygons (in cyan). Area covered during field surveys in 2018 and 2019 (in thin black polygons), recorded archaeological site scatters (in thick black polygons), recorded archaeological site centres with field number sites IDs (from 1 to 38) – habitation sites – in red dots; mortuary sites – in yellow dots; road – in green dot, and a background map: hillshade derived from airborne laser scanning data (figure by N. Kecheva)

7.4.1.1.4. Early Iron Age

The Early Iron Age (EIA) was vastly recorded during the field surveys in 2018 and 2019 (fig. 8). The diagnostic artefacts belong mainly to Basarabi culture (8th–7th c. BC). The earlier phase of the EIA is not recorded with certainty. This is the reason why conclusions were drawn mainly for the period 8th–7th c. BC. Traces of EIA were recorded on 11 sites.

The largest habitation site (a probable settlement) in the EIA was recorded at site 1[10]. Its area is estimated to be around 10 ha. Until recently no geophysically detected features could be associated with the finds from the EIA. Traces of EIA artefacts were also recorded on other sites on the southern slope of Tash Bair ridge – site 2 and site 12. Some EIA pottery fragments were recorded in the backfilling of the inner ditch above the Bronze Age layers on site 3. The function of the enclosure remained unknown during that time.

EIA artefacts with high concentrations which signify habitation places were recorded in the Yantra lowlands. They fell within the defined sites (from north to south) – 17, 5, 18, 19, 21 and 20. At site 20, traces of a dwelling connected to the EIA were recorded with a high concentration of pieces of daub and pottery fragments across an area of 600 m^2 (polygon 554). Three other traces of dwellings were recorded, but it was difficult to identify a certain chronological period.

Traces of EIA habitation could be assumed at sites 21 and 24 situated on the low left and the high right bank of the channelled Studena Reka River. Somewhere in or in the immediate vicinity of the site

10 Fieldwork results in 1997–2001 suggest for an Early Iron Age site in the same area (Krauß 2006a, site 48d, 308).

24 area, S. Stefanov published traces for an EIA settlement and EIA burials – both inhumation and cremation (Стефанов 1974, 277–285).

EIA artefacts were also recorded at site 34 in the SW foot of the Tash Bair ridge part of the area covered.

The significant amount of diagnostic artefacts in the surveyed area suggest a dense inhabitation of the microregion during the Early Iron Age and, especially, its second phase – the Basarabi culture (8th–7th c. BC). Since most of the diagnostic EIA traces belonged to the 8th–7th c. BC, it could be assumed that the sites existed simultaneously – probably some were permanent (i.e. site 1, 19?, 20, 24) and others were occupied periodically (i.e. site 2, 5, 12, 17, 18, 21, 34).

7.4.1.1.5. Late Iron Age

Late Iron Age (LIA) traces were with one of the highest concentrations of artefacts recorded on the surface during 2018 and 2019 field surveys. The LIA was divided into two phases[11] during the post-processing of the pottery according to the collected diagnostic artefacts which included especially grey monochrome wheelmade pottery: 6th–5th, 5th–4th (3rd) c. BC and 2nd–1st c. BC.

Continuity between the second phase of EIA (8th–7th c. BC) and the beginning of the first phase of LIA (6th–5th c. BC), based on collected diagnostic pottery fragments, could be assumed for the areas of sites 1, 19 and 24 which could also be identified as EIA–LIA habitation sites.

LIA surface artefacts were recorded at sites 1, 12, 2, 4, on the southern slope of Tash Bair ridge, site 37 on the northern slope of Tash Bair ridge, from north to south sites in the Yantra lowlands 17, 5,

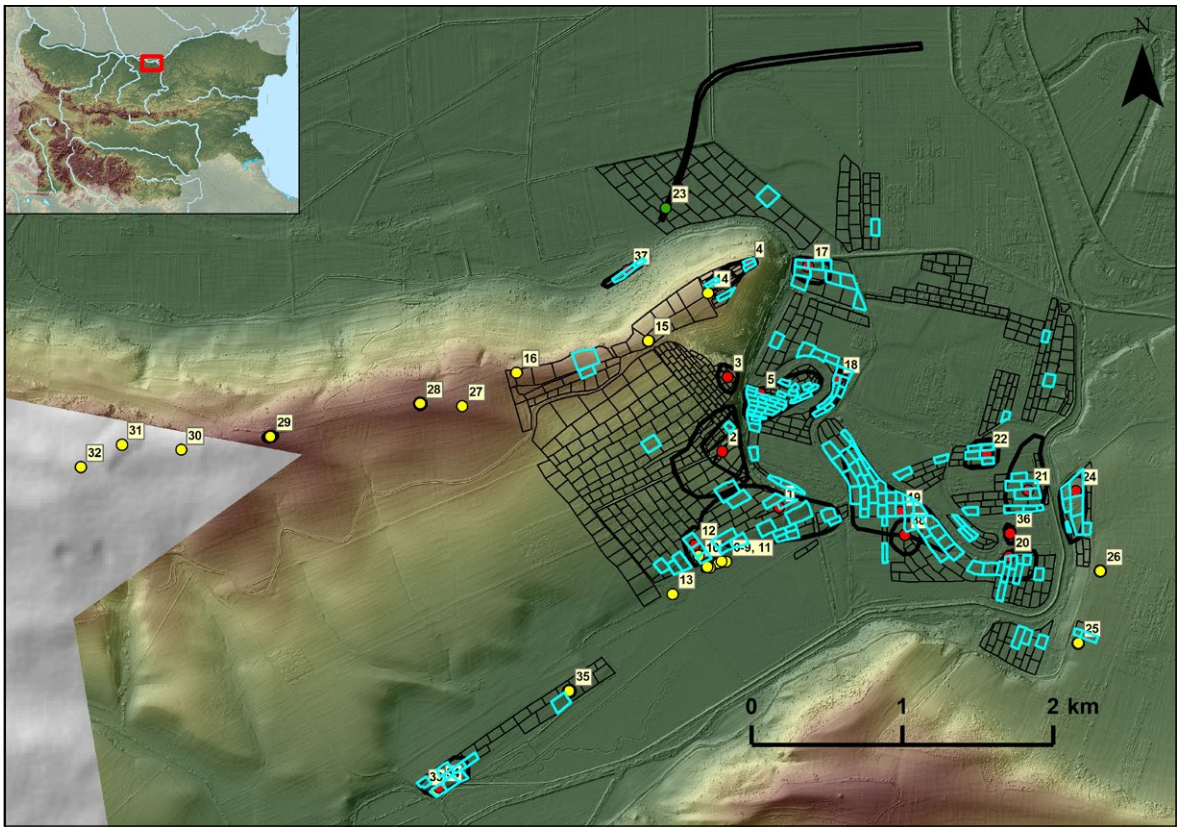


Fig. 9. Spatial distribution of Late Iron Age pottery fragments collected from polygons (in cyan). Area covered during field surveys in 2018 and 2019 (in thin black polygons), recorded archaeological site scatters (in thick black polygons), recorded archaeological site centres with field number sites IDs (from 1 to 38) – habitation sites – in red dots; mortuary sites – in yellow dots; road – in green dot, and a background map: hillshade derived from airborne laser scanning data (figure by N. Kecheva)

11 Corresponding approximately to Classical and Hellenistic period.

18, 19, 22, 21, 20 and site 34 in the SW part of the area covered (fig. 9). Other LIA single diagnostic artefacts were also recorded in different polygons in both the Tash Bair ridge and Yantra lowlands.

Site 1 also showed traces of a significant amount of LIA artefacts. The partial excavations of a possible LIA ditch (5th–3rd c. BC) visible on the geophysical survey emphasised that this must have been a place with more special functions than just a habitation site (cf. the contributions by L. Vagalinski et al., chapter 8.3.1). The second phase of LIA was also recorded during the field survey of the site 1 area. No approximate LIA site area could be estimated.

Several LIA finds were recorded in the inner ditch of site 3 which can very likely be dated from the 5th to 3rd c. BC (cf. the contributions by L. Vagalinski et al., chapter 8.2.1). Although no relevant excavation or surface finds have so far been found in the enclosed area; the site was likely used again for a previously unknown purpose.

Site 4 on the highest part of Tash Bair ridge is a place where among the very few surface finds only artefacts from the second phase has been identified thus far. Results of future partial archaeological excavations are needed to clarify the exact chronology and function of the site.

Both phases of the LIA were recorded based on collected diagnostic artefacts from two sites in the Yantra lowlands: sites 5 and 18. They are both assumed to be of undefined function for this period. The partial excavations on site 5 showed the presence of pits dated to the Late Iron Age – Early Roman period (cf. the contributions by L. Vagalinski et al., chapter 8.3.2). The contemporary surface of site 24 on the higher right bank of the channelled Studena Reka River also showed traces of both LIA phases. The publication for the same territory signified the presence of LIA artefacts (Стефанов 1974, 285–291).

7.4.1.1.6. Roman period

A lot of traces across the whole surveyed area which dated to the Roman period (Early Roman period – 1st c. AD to the middle of 3rd c. AD and Late Roman period – middle of 3rd c. to 4th c.) were recorded during the 2018 and 2019 field surveys (fig. 10).

The southern slope of Tash Bair ridge was densely inhabited during the Roman period: sites 1, 2, 12 and some additional polygons near these sites. The excavations of site 3 revealed some Roman period artefacts (a Roman tile and a bronze bell with cat. No. SF 54) in the upper layer of the inner ditch filling, but the extent and the purpose of the site during that period remains uncertain (cf. the contributions by L. Vagalinski et al., chapter 8.2.1). The main site in the Roman period on the southern slope of Tash Bair ridge was site 2. Its surface was covered mainly with artefacts from that period including concentrations of tiles and bricks signifying the existence of dwellings/buildings. Based on the data of the geophysical surveys it could be assumed that either a Roman *villa rustica* or a Roman *village*[12] with adjacent dwellings existed at that location (cf. the contributions by P. Zidarov, chapter 6.2). The artefacts found at site 2 dated to between 1st c. and the second half of the 4th c. which suggests a continuation between Early and Late Roman period inhabitation. The nearest site which was partially excavated and interpreted as a *villa rustica* is situated 1 km to the east of Vardim village, approximately 4.5 km NW from site 2 (Динчев 1997, 25–26).

Sites 1 and 12 also included the presence of Roman artefacts. No geophysical anomalies could be associated with the Roman remains on site 1. At site 12 two remains of probable dwellings with a higher concentration of tiles and bricks were recorded.

In the Yantra lowlands, traces of Roman artefacts were recorded on sites 17, 5, 18, 19, 22, 21, 20, partially at site 24 on the right bank of the channelled Studena Reka River and at site 34. Places with higher concentrations of tiles and brick were recorded at sites 18 and 19. The coin of Emperor Claudius (41–54) found at site 19 (cat. No. SF 65) was rather erased, which shows that it was in circulation for a long time. The discovery of this Early Roman Imperial coin could be further evidence of an Early Roman presence in this area.

12 The authors do not exclude the possibility of a Roman village since most of the time it is difficult to differentiate remains of villages and *villae rusticae* (Динчев 1997, 14).

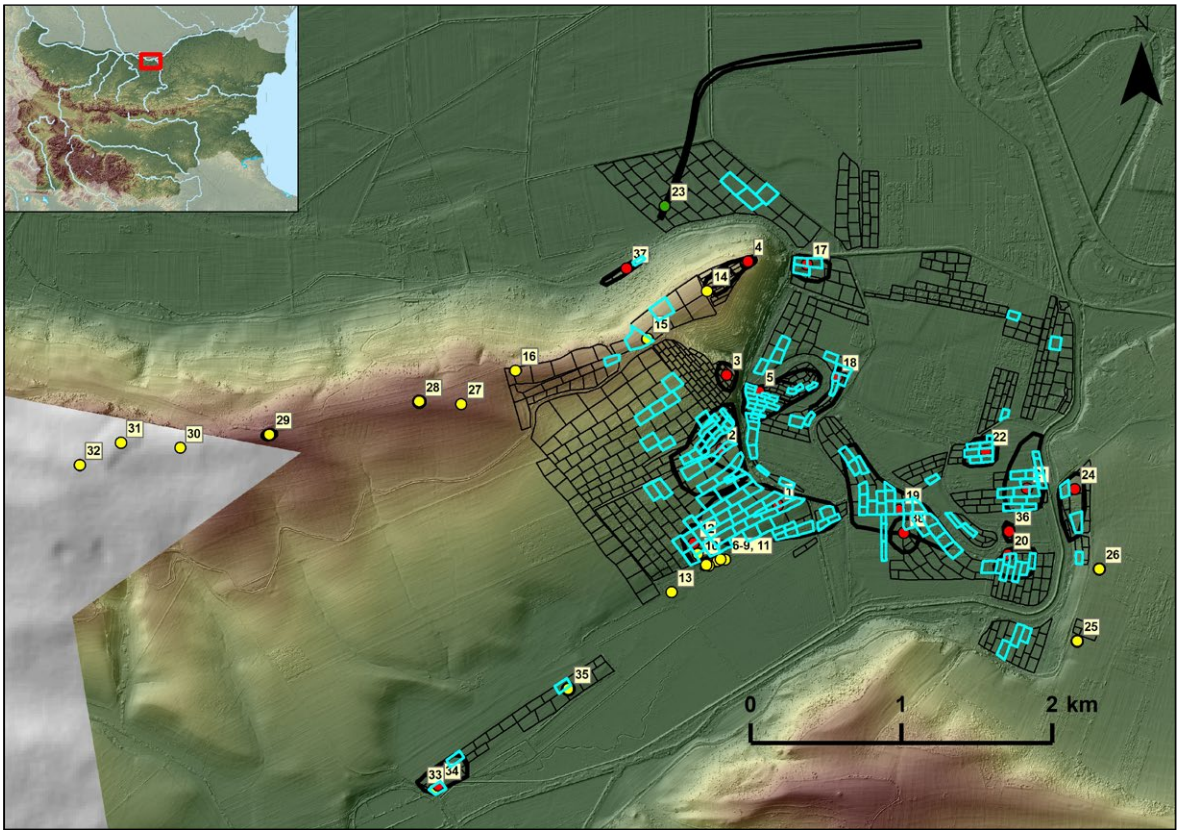


Fig. 10. Spatial distribution of Roman pottery fragments collected from polygons (in cyan). Area covered during field surveys in 2018 and 2019 (in thin black polygons), recorded archaeological site scatters (in thick black polygons), recorded archaeological site centres with field number sites IDs (from 1 to 38) – habitation sites – in red dots; mortuary sites – in yellow dots; road – in green dot, and a background map: hillshade derived from airborne laser scanning data (figure by N. Kecheva)

The partial excavations on site 5 show the presence of pits dated to the Late Iron Age – Early Roman period (cf. the contributions by L. Vagalinski et al., chapter 8.3.2).

Single Roman artefacts found in some polygons outside differentiated sites could be evidence of land usage for agricultural purposes.

The Tash Bair ridge and Yantra lowlands are situated at a distance between 2 and 5 km SW from *Iatrus*, close to the Danube, therefore it was not surprising that this area was densely occupied in the Roman period.

7.4.1.1.7. Late Antiquity

Artefacts dating to the beginning of the Late Antiquity (4th–5th c.) were recorded in small amounts during 2018 and 2019 field surveys of both the southern slope of the Tash Bair ridge and the Yantra lowlands (fig. 11). The northern part of site 2, the eastern part of site 1 and site 12 surfaces produced such pottery fragments[13]. Traces of such artefacts were also recorded at sites 17, 5, 18, 19, 22, 20, and 34.

Traces of two Late Antique dwellings, dated by a Justin II (565–578) coin, were found during the channelling of the right bank of Studena Reka River near the mill of Novgrad village (Стефанов 1974, 291–293). The field surveys in 2018 and 2019 did not reveal any artefacts dated to the period 6th – the beginning of the 7th c.

13 They are assigned as "Late Roman pottery" (end of 4th – 1st half of 5th c.) in the pottery catalogue (cf. the contributions by S. Conrad, chapter 9.1.2).

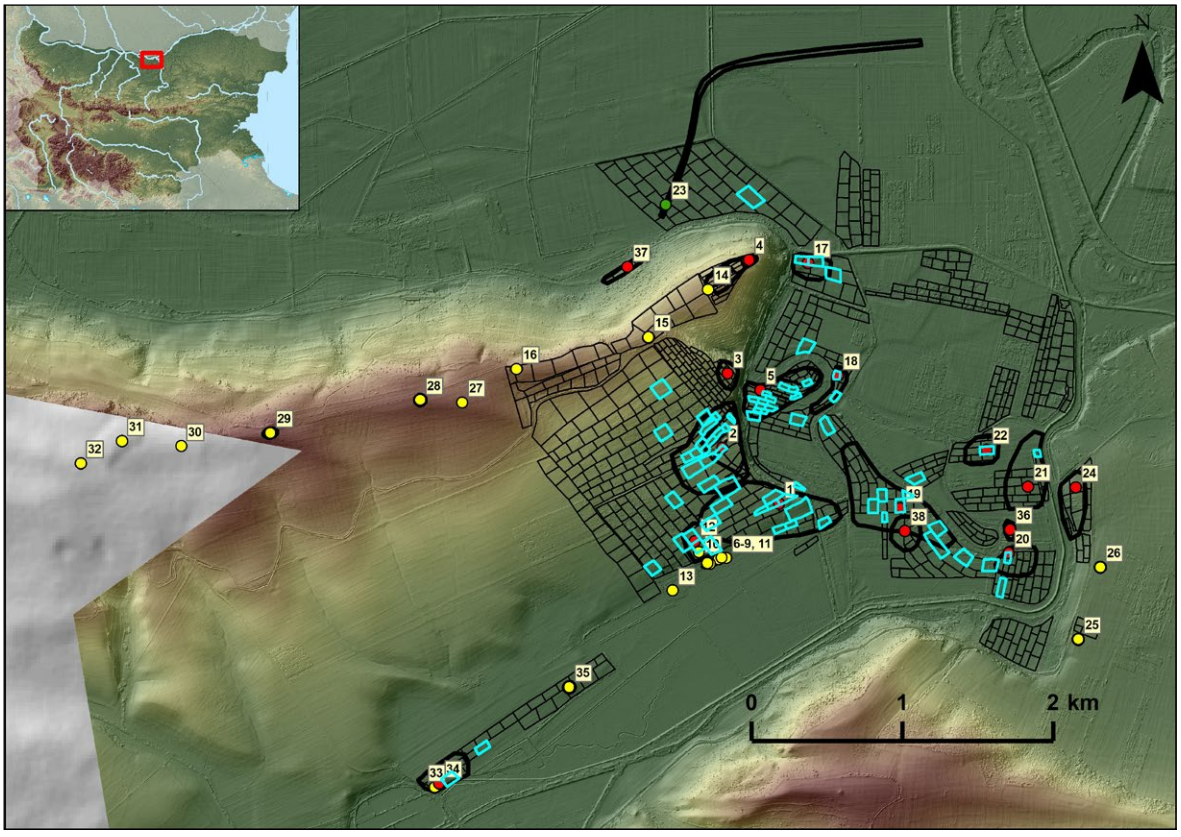


Fig. 11. Spatial distribution of Late Antique pottery fragments collected from polygons (in cyan). Area covered during field surveys in 2018 and 2019 (in thin black polygons), recorded archaeological site scatters (in thick black polygons), recorded archaeological site centres with field number sites IDs (from 1 to 38) – habitation sites – in red dots; mortuary sites – in yellow dots; road – in green dot, and a background map: hillshade derived from airborne laser scanning data (figure by N. Kecheva)

7.4.1.1.8. Early Middle Ages

Early Middle Ages artefacts were densely recorded during the field surveys in 2018 and 2019 (fig. 12). The earthwork fortification at site 1 consisted of a rampart and a ditch with an approximate area of 4 ha which was interpreted as an Early Medieval fort (cf. the contributions by L. Vagalinski et al., chapter 8.4) and is the assumed Early Medieval centre of the surveyed area. The geophysical surveys and the partial excavations revealed part of two ditches and a possible entrance for the fort from the east (cf. the contributions by B. Ullrich et al., chapter 6.1, and L. Vagalinski et al., chapter 8.4). Early Middle Ages artefacts were recorded across the entire surface of sites 1 and 12, while single artefacts were found on site 2.

Early Medieval artefacts were recorded at site 37 on the lowest part of the northern slope of the Tash Bair ridge as well as at site 34 in the SW part of the area covered. The surface of the Yantra lowlands between the old meanders also revealed Early Middle Age artefacts from sites 17, 5, 18, 19, 22, 21, and 20. No traces of dwellings from that period were identified because of their characteristics – dug or semi-dug dwellings with stone bases and no durable upper parts and ceilings.

Early Middle Ages artefacts were recorded on the surface of site 24 on the higher right bank of the channelled Studena Reka River. The publications show that many traces of metal and pottery artefacts were found on the same higher right bank of the river during the digging for its channelling (Стефанов 1974, 296–309).

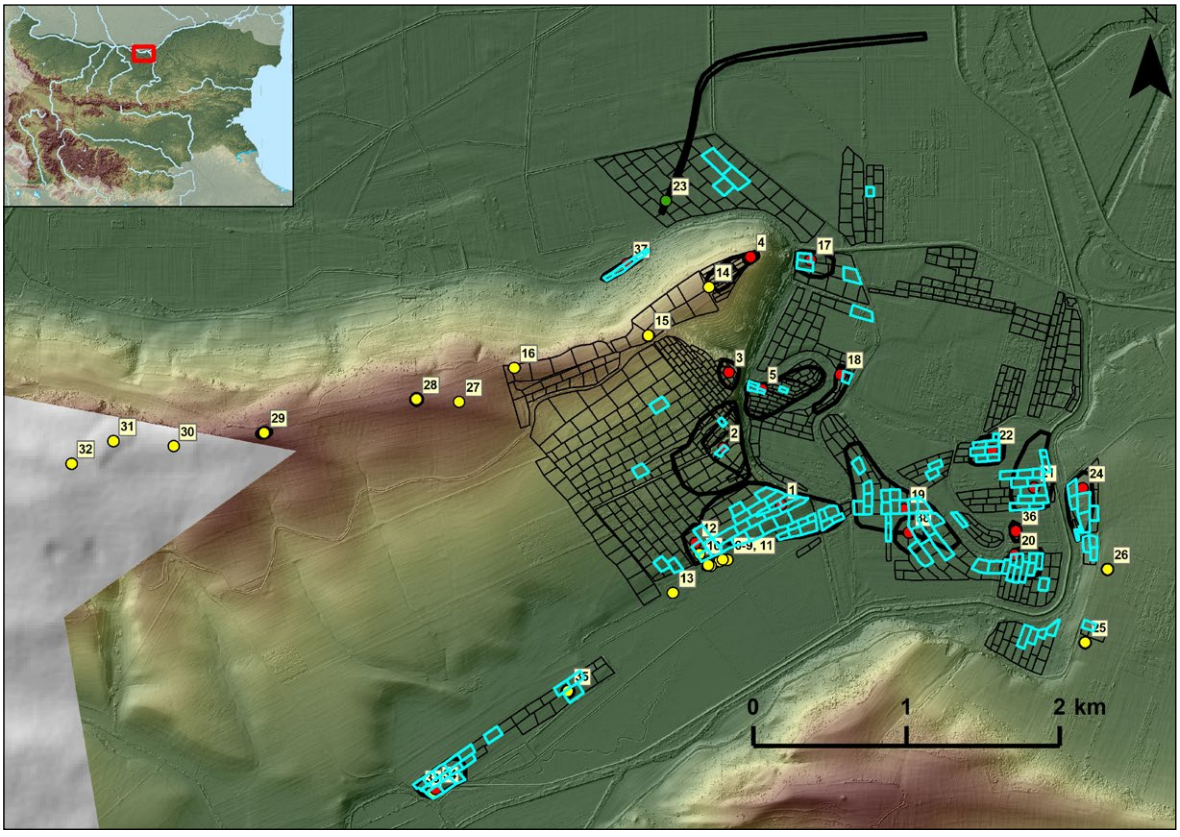


Fig. 12. Spatial distribution of Early Medieval pottery fragments collected from polygons (in cyan). Area covered during field surveys in 2018 and 2019 (in thin black polygons), recorded archaeological site scatters (in thick black polygons), recorded archaeological site centres with field number sites IDs (from 1 to 38) – habitation sites – in red dots; mortuary sites – in yellow dots; road – in green dot, and a background map: hillshade derived from airborne laser scanning data (figure by N. Kecheva)

7.4.1.1.9. High Middle Ages, Ottoman period and Bulgarian National Revival period

No significant concentration of remains of the High Middle Ages, Ottoman period and Bulgarian National Revival period were recorded during the field surveys in 2018 and 2019. The traces were scattered all over the area studied. For this reason, no habitation site could be connected with these three periods.

7.4.1.2. Mortuary sites – burial mounds, mound necropolises, other traces of burials

Burial mounds are regarded as visible sites, and they are often marked on topographic maps with different scales. One quick look on a topographic map with a scale of 1:50 000 shows that the region is full of the specific labels used to identify mounds. They are situated mostly on the top of the ridges, but some are also found on lower slopes of ridges and even on transitions to the lowlands. Most of them have already been described in older publications (Стефанов 1956; Conrad 2006) as well as in AIS AKB. Their visibility above the surface is one of the reasons why almost all of them are partially destroyed through either looting and/or machine ploughing.

Twenty mounds were recorded during the field surveys in 2018 and 2019. They are interpreted as part of mortuary sites. Twenty burial mounds were divided into three mound necropolises according to their locations (fig. 13). Their contemporary heights varied between 0.50 and 4.50 m. They were scattered across the area except for the Yantra lowlands between its old meanders. It is difficult to assume the exact habitation sites to which these mounds belong.

Nine mounds were situated on the top of the Tash Bair and Karaman Bair ridges, reaching up to the contemporary road between Vardim and Karamanovo villages. They follow the direction of the ridges from east to west (sites 14–16; 27–32). The distances between adjacent mounds varied between 300 m and 900 m. The visible mounds on the field and topographic maps continued in a westerly

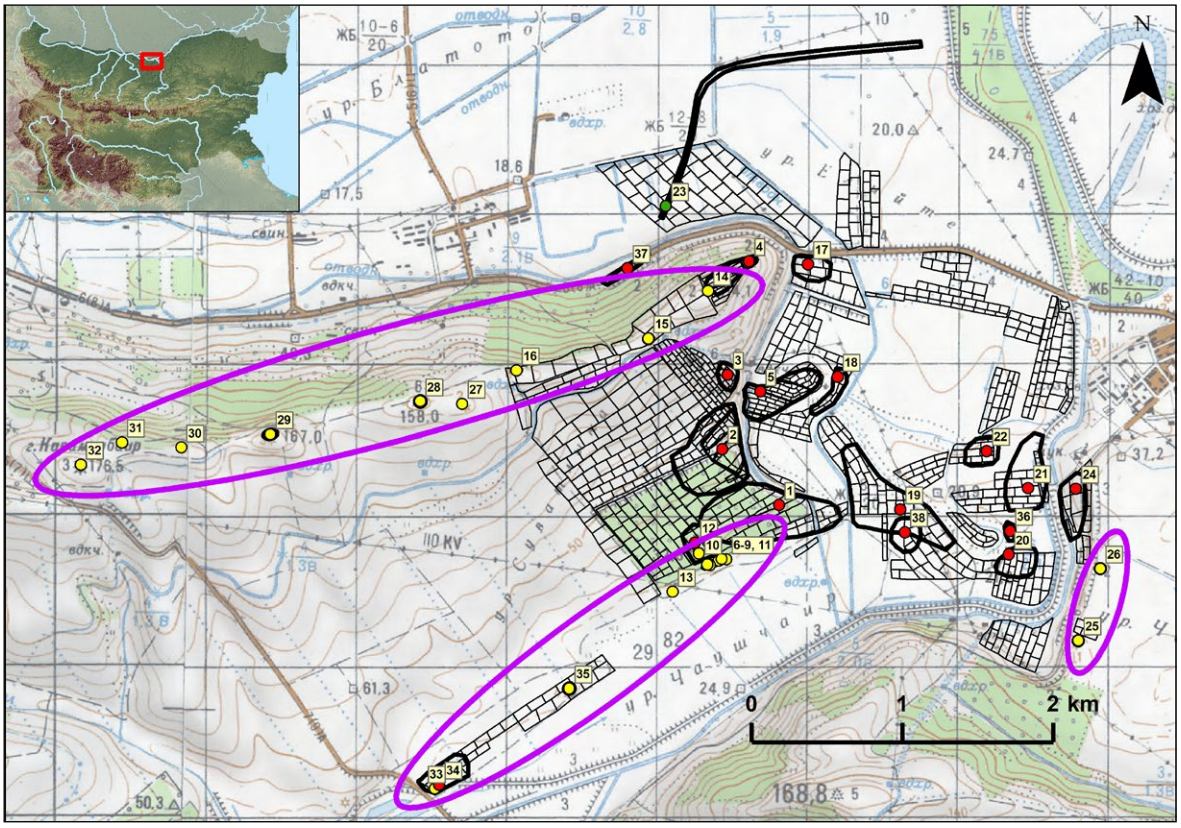


Fig. 13. Spatial distribution of recorded burial mounds (in yellow dots) divided into three mound necropolises (in purple ellipses). Area covered during field surveys in 2018 and 2019 (in thin black polygons), recorded archaeological site scatters (in thick black polygons), recorded archaeological site centres with field number sites IDs (from 1 to 38) – habitation sites – in red dots; mortuary sites – in yellow dots; road – in green dot, and a background map: soviet headquarters topographic maps from the 1980s in scale 1:50 000 (figure by N. Kecheva)

direction, but these were not recorded during this project. Three of the burial mounds were partially destroyed by machine ploughing and most mounds showed evidence of looter trenches. On four of the mounds, artefacts were found, such as a pottery fragment from the Roman period which was recorded at site 15. While, at site 27 human bones, horse tooth and a fragment of an iron knife (cat. No. SF 71) were recorded in looters' trenches; it is questionable whether this burial was either secondary or primary. At site 29 three LIA pottery fragments were found and one LIA pottery fragment was also discovered at site 31.

Another nine mounds were situated on the lower slopes of the Tash Bair and Karaman Bair ridges, where the lowlands transition to the channelled Studena Reka River (sites 6–11, 13, 33, 35). They follow a NE – SW direction. Burial mounds were recorded up to the contemporary road between the Vardim and Karamanovo villages. The distances between adjacent mounds varied between 50 m and 1100 m. Sites 33 and 35 were mounds that had been ploughed at some time, and most of the other site areas were also partially destroyed either by looting, past agricultural activities or animal dens. Some Early Medieval pottery fragments were recorded on the surface of site 35, but they could not be connected with the site.

The other two recorded mounds were situated on a high terrace on the right channelled bank of Studena Reka River (sites 25 and 26). Their direction was north-south, the distance between them was 500 m and both were destroyed by machine ploughing. At site 26, traces of burned daub were found with several pottery fragments dated to the LIA and Early Medieval period. They were very likely not connected to the chronology of the mound.

Other traces of burial places (probable flat graves/necropolises) were also recorded during the field surveys. These included several human bones between the areas of sites 1 and 2. Several scattered

human bones were also found during the excavations on site 1, trench 1.1. They were not *in situ*, and at this point, they could not be assigned to a particular chronological period. The geophysical surveys do not show clear traces of flat graves/necropolises, but such could be assumed on the areas of site 4 and near sites 6–9, 11 and 13.

7.4.1.3. Ancient road

Traces of a road were recorded during the field surveys in 2019 (site 23) (Вагалински et al. 2020b, 19–20). They were interpreted as part of the remains of the Roman road between *Novae* and *Iatrus*. The traces of road were recorded first in 2000 and partially excavated with a trench situated approximately 0.9 km north of the asphalt road at the foot of the Tash Bair ridge, near the building of a former electrical transformer (Вагалински et al. 2001b, 81; Conrad, Stančev 2002, 676 fig. 10–12). Stone padding had been recorded at a depth of 0.30–0.40 m with a width of 5.30 m. The pottery fragments that were found during the partial excavations dated in 4th – the beginning of the 5th c. The road remains were not traceable on the right bank of Yantra River in the immediate vicinity of *Iatrus* probably because they had been destroyed by the river (Вагалински et al. 2001b, 81).

Road remains are visible as a linear anomaly with different lengths in SW to NE-E direction on different raster data in GIS: georeferenced aerial photographs from 1944–1945, georeferenced aerial photographs from 1970, analytical hillshade, and satellite imagery from 4th of March 2012 (fig. 14).

A high concentration of small- and middle-sized stones were recorded on the surface across a length of 0.50 km with a direction SW – NE (fig. 5). In the polygons near the linear anomaly single wheelmade pottery fragments dating to Antiquity were recorded which suggested temporary activities in the region.

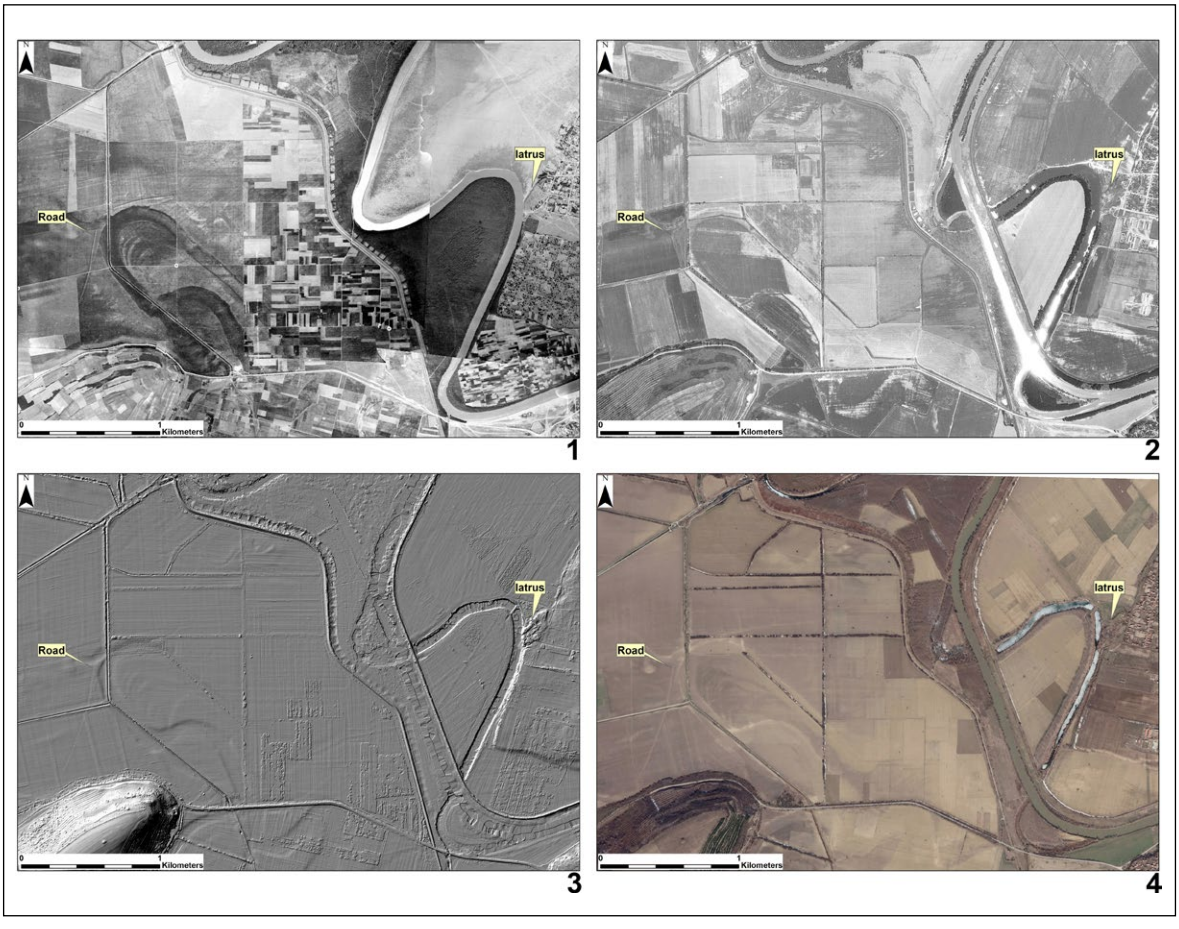


Fig. 14. Part of the possible Roman road between Novae and Iatrus. 1. Aerial photos from 1944–1945 with visible road route; 2. Aerial photos from 1970 with visible road route; 3 Airborne laser scanning data with visible road route; 4. Satellite imagery from Google Earth from 4th of March 2012 with visible road route (figure by N. Kecheva)

7.4.2. Total pick up data analysis

A total pick up, famous in the publications as a type of intra-site survey or 'window' method (Bintliff 2013), was conducted on part of the site 1 area in 2018 (fig. 15). On part of the same area a total pick up with different grid square sizes and orientation was conducted in 2001 (Krauß 2006a, 171–175). It covered an area of 5.37 ha with 537 grid squares 10 × 10 m^2 (Krauß 2006a, 172) (fig. 15). This data is not compared to the data gathered in 2018.

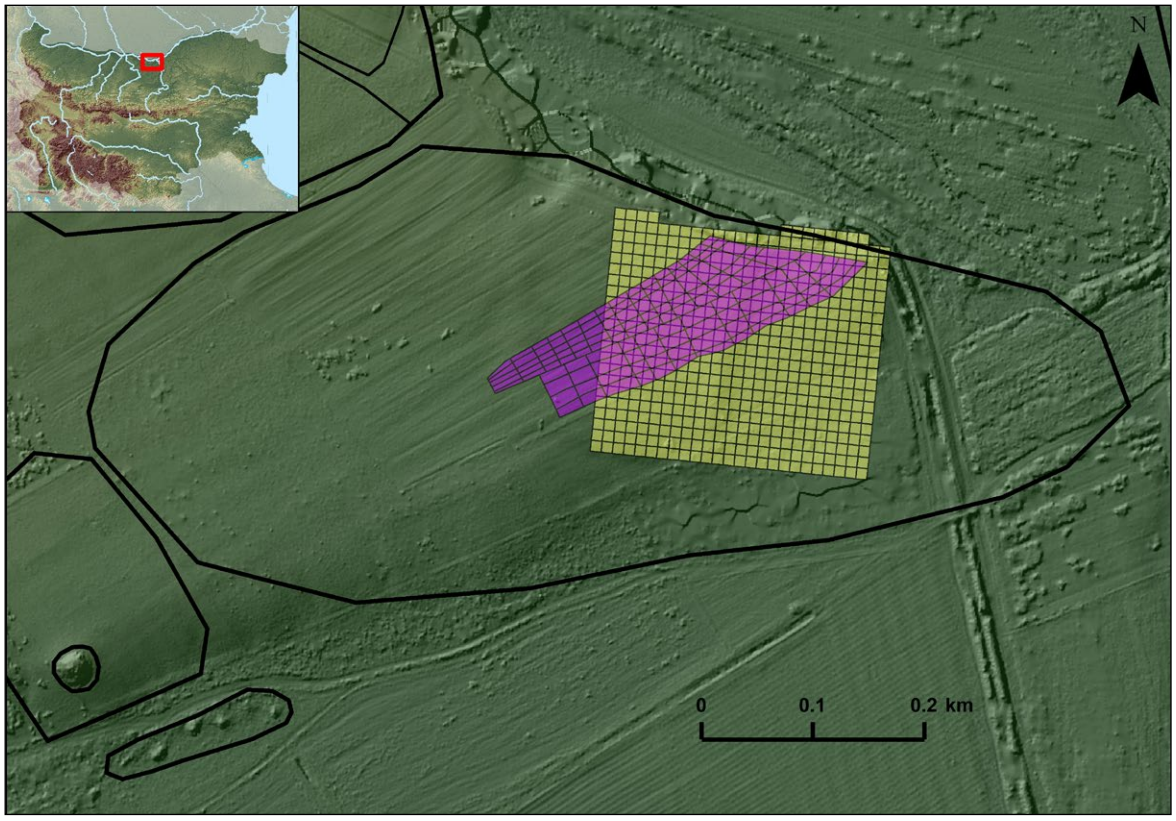


Fig. 15. Total pick up field survey conducted on part of site 1 area in 2018 (in purple) and in 2001 (in yellow), and a background map: hillshade derived from airborne laser scanning data (figure by N. Kecheva)

The total collection of artefacts in 2018 covered a ploughed area of 2.27 ha – five polygons with IDs 187, 188, 189, 7 and 8 divided into 123 small polygons with a mean area of each of 185 m^2. The area was situated diagonally in the middle of the earthwork fortification with a direction of 65°–245°. Pottery fragments were taken for further analysis, while pieces of daub, tiles and bricks, and stones were weighed and counted on the field. Total pick up data analysis is based on the spatial distribution of post-processed artefacts.

The pottery fragments with higher amounts belonged to the Late Neolithic, EIA, LIA, Roman, and Early Medieval period (fig. 16, right map). Small amounts of Chalcolithic and Bronze Age pottery fragments were also collected from the total pick up area.

The spatial distribution of artefacts suggesting traces of dwellings, such as quantities of pieces of daub and tiles, showed a presence of horizontal stratigraphy (fig. 16, left map). Three places with a higher concentration of pieces of daub were marked, in the N, NE and S part of the total pick up area, while the concentration of tiles was visible in the W part (fig. 16, left map). The three places of pieces of daub concentrations correlate with higher amounts of Late Neolithic pottery fragments (fig. 17.1). The higher amounts of EIA pottery fragments correlate with the concentrations of pieces of daub in the NE and the S part (fig. 17.2). LIA pottery fragments had smaller quantities and they partially correlate with the N and NE places of pieces of daub concentrations (fig. 17.3). The high quantity and concentrations of Roman pottery fragments correlate with the higher amount of fragments of tiles collected in the W part

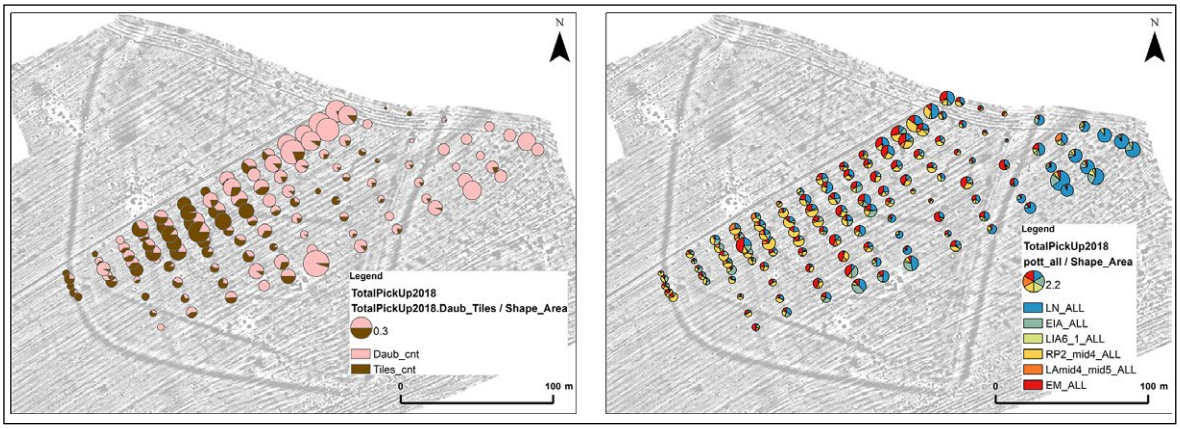


Fig. 16. Total pick up data from 2018 visualised in GIS. Pie charts showing the spatial distribution of all collected and counted pieces of daub and tiles (left map). Pie charts showing the spatial distribution of all collected and post-processed pottery fragments from the Late Neolithic, Early Iron Age, Late Iron Age, Roman period, Late Antiquity and Early Middle Ages (right map), and a background map: geophysical survey data from 2018 (figure by N. Kecheva)

(fig. 17.4). An interesting observation is that other Roman pottery fragments with higher concentrations correlate with the N area where there are also a higher concentration of pieces of daub and lower tile concentrations. The pottery fragments with high concentrations from Late Antiquity correlate with the higher amount of fragments of tiles collected in the W part (fig. 17.5). The Early Medieval pottery fragments show higher concentrations in the N part, and additional high quantities were recorded in the W, S and NE part – all in the fortified area (fig. 17.6).

The analysis shows that traces of Late Neolithic dwellings/features can be assumed in the NE, N and S part of the total pick up area. EIA traces can be assumed in the NE, W and S part while Roman dwellings are thought to be in the W and N part of the total pick up area (fig. 16 and 17). The geophysical survey reveals anomalies with circular shapes in these areas, some of which can be interpreted as traces of features *in situ*. It is difficult to make assumptions for the spatial distribution of features for the other periods.

7.5. CONCLUSION

The field-by-field intensive surveys data analysis shows some significant points:

• Neolithic is *terminus post quem* and EIA is a probable *terminus ante quem* for colluvium deposits in the Yantra lowlands situated between the Tash Bair ridge from the west and the left bank of the channelled Studena Reka River from the east across an area of approximate 4 km^2;

• Hidden landscapes for some of the prehistoric habitation traces;

• Significant habitation of the Yantra lowlands in EIA, LIA, Roman period, Late Antiquity and Early Middle Ages across an area of approximate 2 km^2;

• Significant habitation of the southern slope of Tash Bair ridge in Late Neolithic, EIA, Roman period and Early Middle Ages;

• Traces of LIA and Late Antiquity activity on the southern slope of Tash Bair ridge;

• Habitation of the slope on the high terrace at the eastern edge of the Yantra lowlands in EIA, LIA, Roman period and Early Middle Ages.

The above-mentioned points show that the same topographic places in this microregion have been used for habitation throughout the Iron Age, Roman period and Early Middle Ages.

The total pick up intra-site survey amount of added value over the intensive field-by-field surveys is often explored in the literature (especially for the Mediterranean region) (Bintliff 2013). Many factors are important for its success some of which include specific project requirements, surface conditions, enough time and money, etc. In the case of Tash Bair the total pick up survey on part of the site 1 area, the added

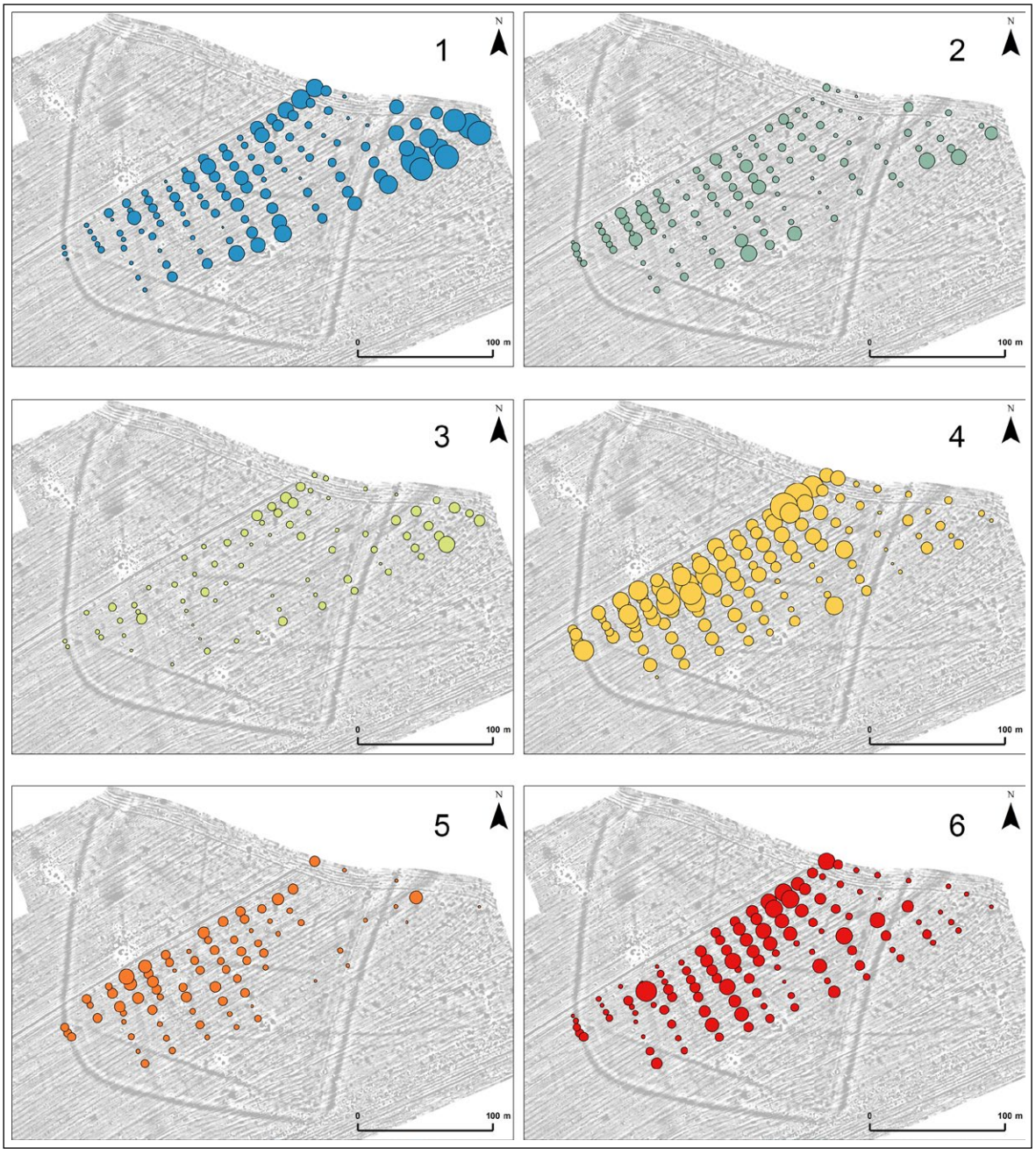


Fig. 17. Total pick up data from 2018 visualised in GIS. 1. Pie charts showing the spatial distribution of all collected and post-processed Late Neolithic pottery fragments. 2. Pie charts showing the spatial distribution of all collected and post-processed Early Iron Age pottery fragments. 3. Pie charts showing the spatial distribution of all collected and post-processed Late Iron Age pottery fragments. 4. Pie charts showing the spatial distribution of all collected and post-processed Roman pottery fragments. 5. Pie charts showing the spatial distribution of all collected and post-processed Late Antique pottery fragments. 6. Pie charts showing the spatial distribution of all collected and post-processed Early Medieval pottery fragments, and a background map: geophysical survey data from 2018 (figure by N. Kecheva)

value of the total pick up includes the collection of Chalcolithic pottery fragments, more Bronze Age artefacts and a possible horizontal distribution of habitation traces in different chronological periods. A total pick up of the whole site area will give more interesting results, but it should not be conducted more than once since it requires the collection of all artefacts from the visible part of the ploughzone which could cause the site to "disappear" further on the surface.

ИНТЕНЗИВНИ ТЕРЕННИ ИЗДИРВАНИЯ В РАЙОНА НА ТАШ БАИР

Надежда Кечева, Людмил Вагалински, Люба Трайкова, Силва Събкова[14]

(Резюме)

Интензивните теренни издирвания в района на рида Таш баир и неговите околности са основна част от недеструктивните проучвания на проекта. Те са извършени през месеците март и април на 2018 и 2019 г. Една от поставените цели е установяването на промените в селищната система в района на Таш баир близо до устието на р. Янтра. Фокусът е насочен към територия с площ около 20 км^2 в землищата на селата Новград и Караманово, общ. Ценово, обл. Русе и с. Вардим, общ. Свищов, обл. Велико Търново. По-голямата част от площта е оградена от изток и югоизток от левия бряг на съвременното корито на р. Янтра и левия бряг на нейния ляв приток – съвременното корито на Студена река.

При проведените интензивни теренни издирвания е покрита територия от 4,71 км^2 – 0,74 км^2 през 2018 г. и 3,97 км^2 през 2019 г. Обходени са терени с видимост на повърхността над 80%, в които попадат изорани, бранувани площи или такива, покрити с 0,10 – 0,15 м поникнали житни култури. Пълно събиране на всички артефакти от повърхността (т. нар. total pick up) е извършено на 22,7 ха площ от територията на обект 1. Подробно описание на използваните методи при интензивните теренни издирвания е представено в глава 5.2.

Приетото определение за „археологически обект“ в проекта съвпада с дефиницията в АИС АКБ, а именно: топографско място в пространството, където хора през различни хронологически периоди са извършвали различни видове постоянни и / или периодични дейности. Границите на обектите са определяни в зависимост от останките по повърхността, като са разделени на видими или невидими обекти. Надгробни могили, валове и ровове спадат към видимите обекти. Всички останали граници са определяни въз основа на количествен анализ в ГИС на преброените артефакти на повърхността. Изводите са направени единствено за интензивно проучената територия през 2018 и 2019 г.

Покритите 4,71 км^2 през 2018 и 2019 г. включват: ридовете Таш баир и част от Караман баир, както и техните южни склонове, част от северния склон на Таш баир, част от десния бряг на канализираната Студена река и низината между Таш баир и левия бряг на канализираната Студена река, която е разположена между старите меандри на р. Янтра. Тази територия е част от по-голямата низина Вардим – Новград, често наводнявана през началото на XX в. и по тази причина оградена с дига от юг и изток. Геоморфологията на изследваната територия е допълнително анализирана в глава 4.

Анализът на събраните данни при интензивните теренни издирвания е базиран на: покритата територия с видимост на повърхността над 80%; преброените на терен артефакти, които включват битова керамика (керамични фрагменти, изработени на ръка и на грънчарско колело), строителна керамика (керемиди и тухли), късове мазилка, кремъци, единични находки; събраните по полигони диагностични керамични фрагменти и находки (каменни сечива, хромели, тежести за стан, прешлени за вретено, кремъци). Регистрираните обекти са класифицирани въз основа на предполагаеми различни функции като: обекти със следи от обитаване (селищни обекти с останки от битова и строителна керамика, късове мазилка и камъни и обекти с неопределена функция с останки единствено от битова керамика); обекти със следи от погребения (надгробни могили, могилни некрополи и други следи от погребения); пътища (видими на сателитни и ортофото изображения и регистрирани на повърхността с разпръснати камъни).

Регистрирани са 38 археологически обекта, класифицирани като обекти със следи от обитаване (17 бр.), обекти със следи от погребения (20 бр.) и един античен път. Площта на

14 С принос от С. Конрад при обработката на събраните керамични фрагменти.

регистрираните селищни обекти и обекти с неопределена функция варира между 1,4 и 20 ха. Низината около старите меандри на р. Янтра е гъсто заселена през ранния и късния железен период, римския период, Късната античност и Ранното средновековие. Южните склонове на Таш баир са обитавани през късния неолит, ранния железен период, римския период и Ранното средновековие. Там се откриват и следи от бронзова епоха, късен железен период и Късна античност. На цялата покрита територия са регистрирани единични артефакти от Зрялото средновековие (XIII – XIV в.). При геоморфологичните проучвания са установени следи от културен пласт около старите меандри на р. Янтра на дълбочина между 2,80 и 3,60 м от съвременната повърхност, който е датиран 6080 – 5980 calBC. Това показва, че в ниските части, западно – югозападно от с. Новград, наноси с дебелина над 3 м са се натрупали след неолита и преди началото на ранния железен период.

Пълното събиране на всички артефакти от повърхността, извършено на 22,7 ха от територията на обект 1, показва превес на битовата керамика от късния неолит, ранния и късния железен период, римския период и Ранното средновековие. Пространственото разпределение на артефакти, свидетелстващи за вероятни следи от постройки, като късове мазилка, строителна керамика и камъни, показват, че структури от късния неолит могат да бъдат регистрирани в североизточната, северната и южната част от територията, следи от ранния железен период са установени в североизточната, западната и южната част, докато останки от евентуални римски постройки се предполагат в западната и северната част от територията на total pick up.

8. ARCHAEOLOGICAL EXCAVATIONS

8.1. THE LATE NEOLITHIC DITCHES AT SITE 1 (TRENCH 1.2)

Raiko Krauß, Sven Conrad

8.1.1. Preliminary remarks

The site 1 in our site catalogue has already been registered as an archaeological findspot by Stefan Stefanov (Стефанов 1956, 46). Throughout our surveys from 1997–2001, the settlement pattern, which previously mainly concerned the Roman occupancy, could be expanded considerably. Since then, we have known that this section of the Tash Bair in particular was settled from the Late Neolithic until the Early Middle Ages. Based on these observations, the project presented here was initiated with the aim of achieving a chronological resolution of the various materials found during the surveys.

On the Tash Bair and its surroundings, site 1 has the greatest extent (total 6.4 ha), and most intense find density from numerous periods. The site is situated on a moderately inclined slope, at the confluence of the Studena Reka in the lowlands of the river Yantra near its confluence with the Danube (cf. the contributions by N. Kecheva et al., chapters 7 and 12).

The geomagnetic surveys revealed numerous anomalies, including several linear structures of large dimensions (cf. the contributions by B. Ullrich et al., chapter 6.1). These are likely related to ditch systems from different chronological periods. The site is dominated by the mighty, almost square ramparts, which had already been discovered during earlier research and ascribed to the Early Middle Ages. This is the only structure that has been relatively reliably dated without excavation.

During the 2019 summer campaign investigations, three trenches (1.1-E, 1.1-W, 1.2) were placed at the intersections of larger linear structures, which promised a high level of information based on stratigraphic observations and finds (fig. 1).

8.1.2. Stratigraphy

The rectangular, NNE-SSW-oriented trench 1.2 with a size of 7 × 3.40 m, was positioned at a right angle over a striking, relatively wide linear structure (fig. 1). This structure runs in a straight line in a WNW-ESE direction and can be followed in the geomagnetic map over a distance of approx. 182 m. On both ends, it seems to 'disappear' in a slightly arched course under the earth rampart of the Early Medieval quarter. Initially, it was hypothetically addressed as a possible Roman ditch.

In the area of trench 1.2, a much less recognisable, slightly curved linear structure crosses this strong linear anomaly at an obtuse angle. In comparison to the large structure, it has an obviously different character. This feature runs roughly in a straight line from the section in NNW direction for approx. 155 m and ends in a depression caused by erosion. In the SE direction, it turns after approx. 40 m in ESE direction and can be followed for another 100 m before it 'disappears' at the foot of the slope. Here, it is very likely covered by the colluvium.

At the beginning of the excavations, the ploughed surface layer and the upper part of the light greyish-brown, slightly humous colluvium were removed with an excavator to a depth of approx. 0.60 m below the surface (niv. 30.49 m). The trench was then cleaned to the first planum at niv. 29.91 m and did not reveal any structures. During further step-by-step, manual removal of the colluvium, no archaeological structures were discovered, apart from individual tree pits, which may indicate the use of the area as an orchard several decades ago. A mixed spectrum of ceramic finds was recovered from the colluvium. Furthermore, a comb-like stamp from the Early Iron Age was found (cat. No. SF 45).

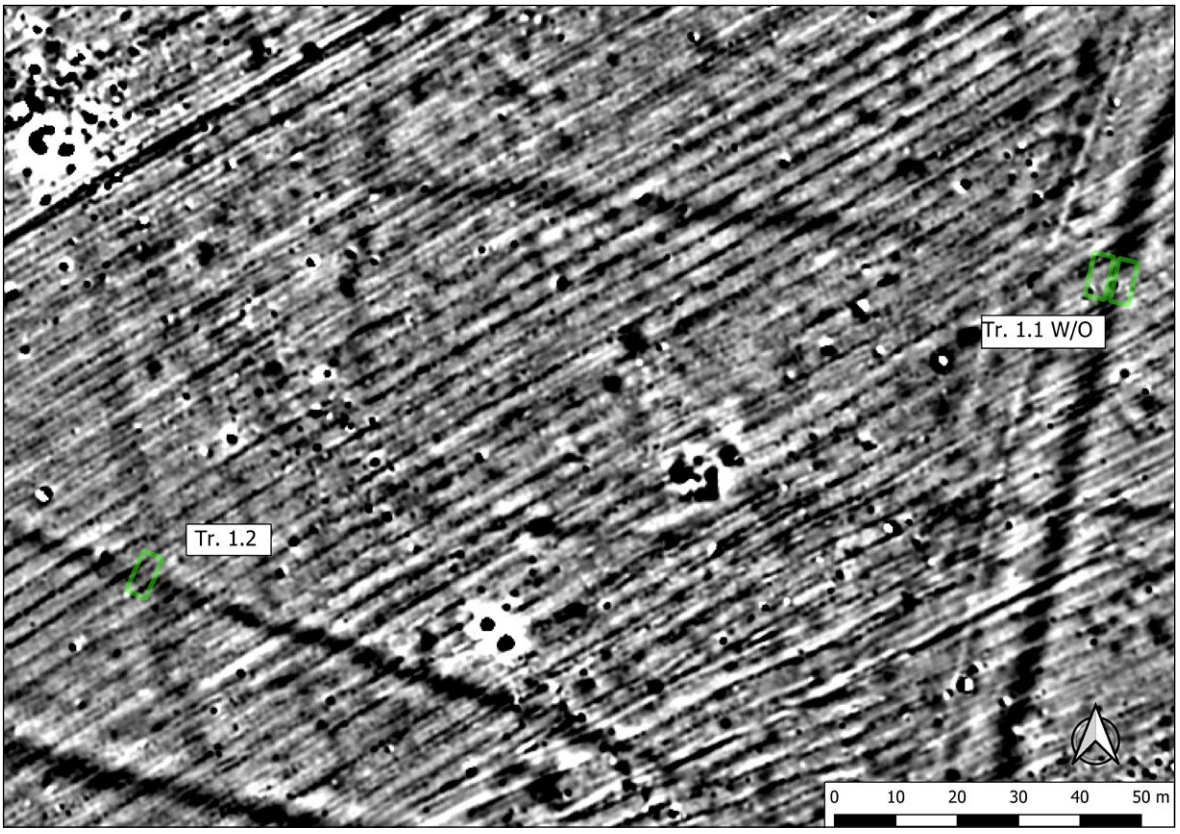


Fig. 1. Site 1 (cutout). Map of geomagnetic anomalies (see contributions by B. Ullrich et al., fig. 3) with the excavation trenches (figure by S. Conrad)

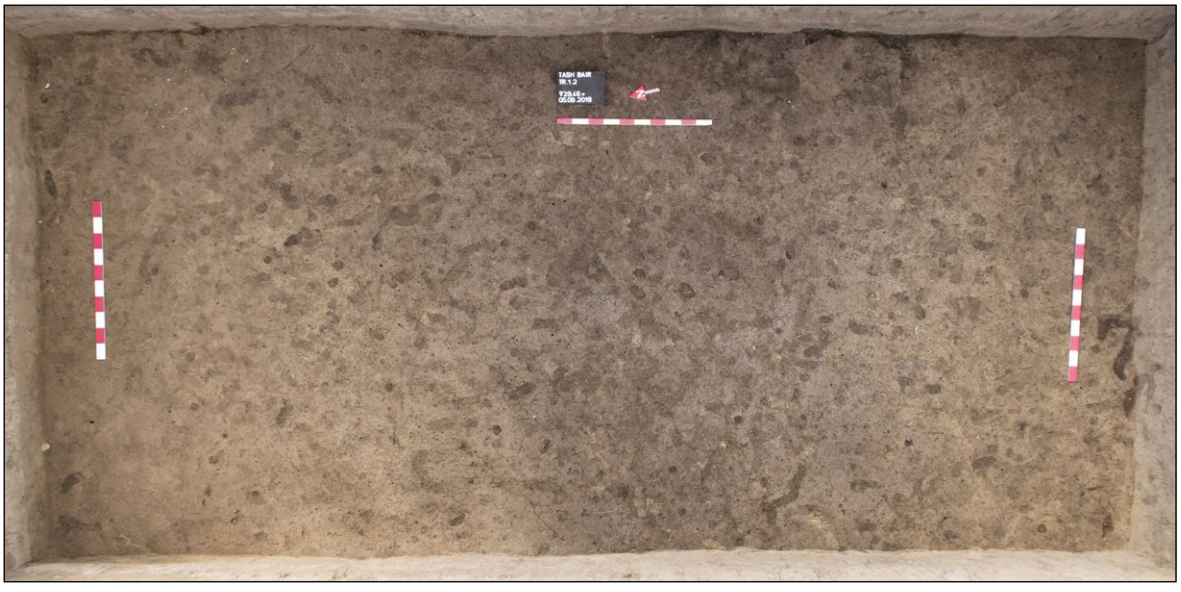


Fig. 2. Trench 1.2. Planum 2 at niv. 29.46 m with feature 1.2.5 (view from the west) (figure by Lea Valcov)

In planum 2 at niv. 29.46 m (fig. 2), i.e. approx. 1.03 m below the surface, the large ditch structure 1.2.5 was initially recognised as having a vague dark discoloration. It was only in the later analysis of the profiles that it was recognised that the planum in its northern part also included a flat, wall-like structure made of light-coloured loess that ran approximately east-west (fig. 2; 9). It seems to precede the medieval ditch stratigraphically, but in any case, lies above the Late Neolithic ditches. The exact dating and purpose of this supposed wall structure is not possible to define thus far. The spectrum of finds of



Fig. 3. Trench 1.2. Planum 3 at niv. 29.30 m with feature 1.2.5 (view from the the west) (figure by Lea Valcov)

the mostly fragmented ceramics from this level ranged from the Late Neolithic, Bronze and Iron Ages, to individual finds from the Roman and Late Roman periods, as well as from the Early Middle Ages. After removing parts of this layer, the ditch 1.2.5 could then be clearly delineated in planum 3 (level 29.30 m) as a 2.70 to 2.82 m wide structure with a dark brown colour (fig. 3; 7). This feature, 1.2.5, which finally turned out to be part of the Early Medieval fortification, was excavated and documented in the negative (cf. the contributions by L. Vagalinski et al., chapter 8.4).

Further features were indistinctly discernible N and S of feature 1.2.5. The feature 1.2.6 observed on the southern edge of 1.2.5 was partially documented (width 2,39 m) by a profile that was not vertically oriented to its outer edges (fig. 4; 5). It shows the western part of a relatively flat depression (maximum depth 0.85 m below pl. 3) with a flat bottom that slopes slightly to the east. Despite the massive disruptions from animal dens, it can be seen that the western edge was tiered. Two layers can be distinguished in the filling: in the lower part an approx. 0.48 m thick yellow-greyish pale brown and yellowish speckled, humous layer, on top of which lies a greyish brown and up to 0.37 m thick, humous layer.

To the N of feature 1.2.5, the trench was divided, and the western part of the section with a width of 1.70 m was further excavated. The northern continuation (finding 1.2.4) of feature 1.2.6 including its eastern boundary was documented in planum 4 (fig. 6). At the same time, another feature emerged in the NE corner of this section which could be identified as a parallel ditch to feature 1.2.4/6 by a final extension, without its eastern edge being able to be recorded. This feature was named 1.2.7/8.

Based on the documented sections of features 1.2.4/6 and 1.2.7/8, the overall plan was reconstructed (fig. 7). There are two parallel ditches which are approx. 0.85 m apart (fig. 8). The western ditch 1.2.4/6 is approx. 2.60 m wide; the width of the eastern ditch 1.2.7/8 could not be determined by the excavations. If one takes the total width of about 6.20 m (determined from the geomagnetic plan), the eastern ditch could be considered to be a similar width to the western ditch. The preserved depth of 1.2.4/6 under planum 4 is approximately 0.60 m, of 1.2.7.8 approximately 0.70–0.75 m.

The excavation results also enable a more extensive interpretation of the geomagnetic mapping. An approx. 75 m long broadening of this NNW-SSE running linear anomaly covered by Tr. 1.2 starts approx. from the curve in the SE. It can be explained with the construction of a double ditch at least in this area.



Fig. 4. Trench 1.2. Feature 1.2.6, profile (view from the north) (figure by S. Conrad)



Fig. 5. Trench 1.2. Part of the eastern profile. Early Medieval ditch 1.2.5 which cuts the prehistoric ditch 1.2.6 (figure by S. Conrad)



Fig. 6. Trench 1.2, planum 4. Part of ft. 1.2.4 (view from the west). In the eastern corner (up left), part of the separating loess stripe and a very small section of the parallel ditch 1.2.7/8 (figure by S. Conrad)

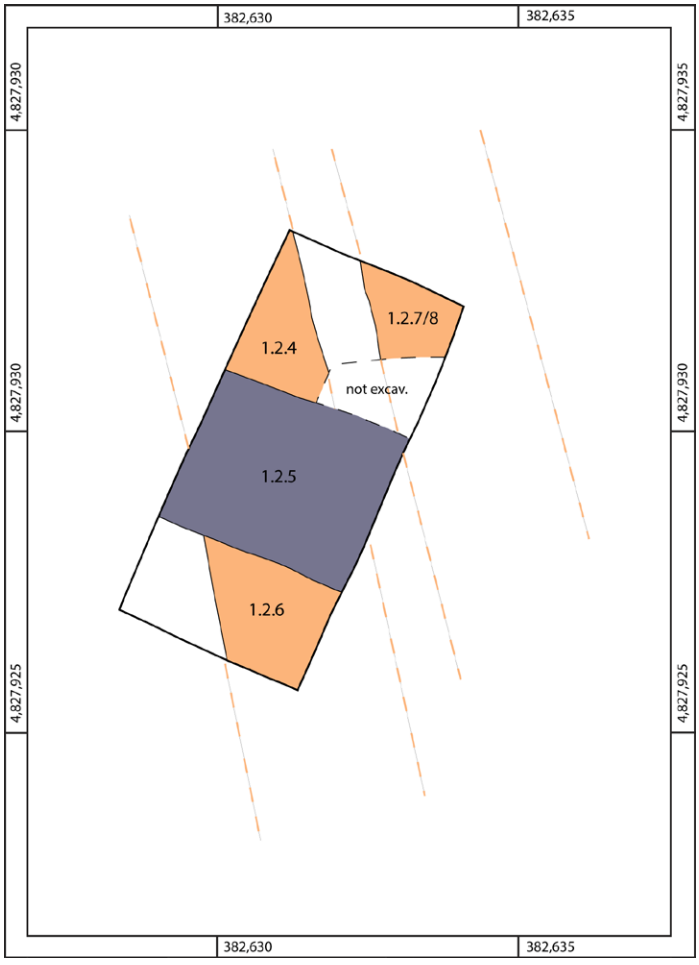


Fig. 7. Trench 1.2. Reconstructed overall plan of the features (summarised from planum 3 and 4) (figure by S. Conrad)

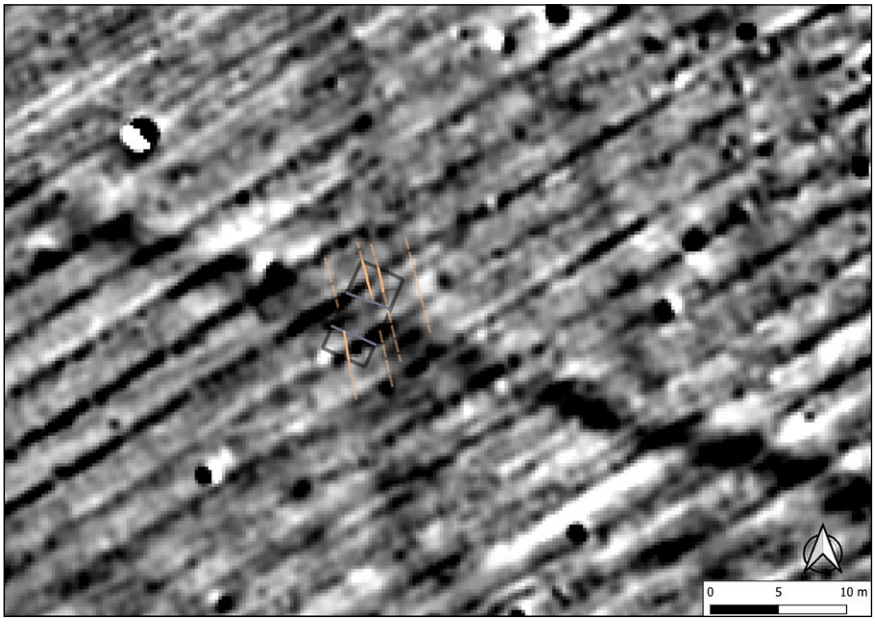


Fig. 8. Trench 1.2. Overall plan projected onto the geomagnetic plan (figure by S. Conrad)

The NW and SE adjoining sections appear to be significantly narrower, which cannot be explained at present. It could be a single ditch, overlapping of two ditches, or decreased visibility of the anomalies.

The profiles at the trench edges were all oriented at an oblique angle to the feature boundaries of trenches 1.2.4/6 and 1.2.7/8. Nevertheless, the information provided about their shape and stratigraphy was sufficiently reliable. Both ditches are approx. 1.10 m deep under the overlying level layer and have trough-shaped cross-sections with a bottom that curves slightly downwards. The western ditch 1.2.4/6 was likely tiered throughout on its western exterior (see above fig. 4).

At its bottom, feature 1.2.7/8 has a 6–8 cm thick humous soil layer brown in colour (fig. 9). This indicates that the ditch had been left open for a considerable amount of time. In the overlying silvery-brown, clayey mixed backfill, numerous ceramic sherds recognisable in the profile are embedded. Feature 1.2.4 has a backfill that differs from that of the ditch section 1.2.6 to the south (fig. 9). On the bottom, there is a thick, dark brown, humous fill covered by a light grey layer that may fit to trench 1.2.7/8.

The stratigraphic relationship between the two ditches could not be clarified by the trench, as the upper area of the separating loess strip and also the entire upper area of the ditch backfills are considerably disturbed by animal dens.

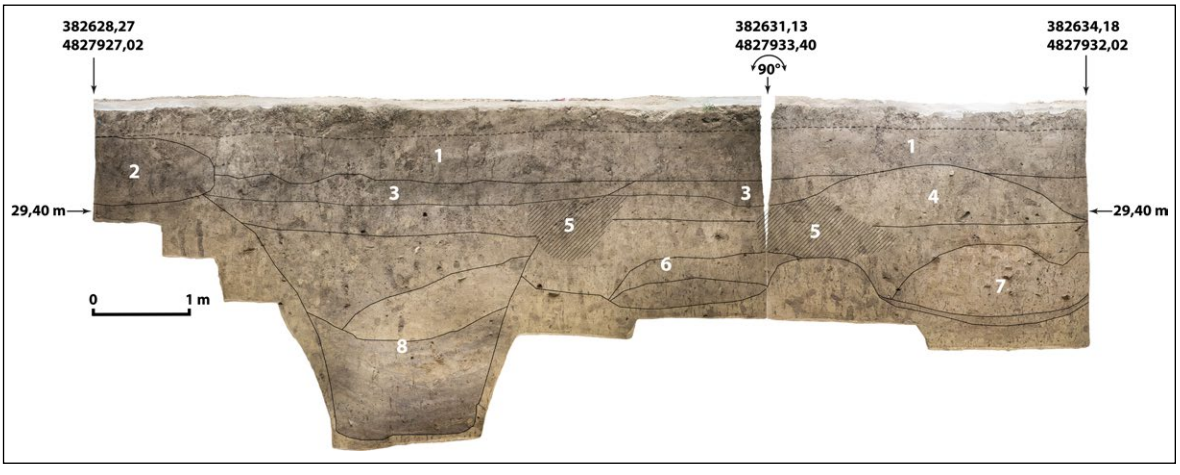


Fig. 9. Trench 1.2. W- and N-profile, obtained from SfM photo combination (M. Offermann). Legend: 1 – colluvium; 2 – shifted rampart(?); 3 – ancient surface; 4 – earthenwall(?); 5 – disturbed area; 6 – Late Neolithic ditch (feature 1.2.4); 7 – Late Neolithic ditch (feature 1.2.7/8); 8 – Early Medieval ditch (feature 1.2.5) (interpretation by R. Krauß and S. Conrad)

8.1.3. Dating

Ditches are one of the most typical structures of prehistoric settlements. As early as the beginning of the Neolithic, certain areas of settlements were marked by ditches or the entire settlement was surrounded by them. In this respect, ditches can also be expected at the Tash Bair in connection with the very large Late Neolithic settlement. From the excavation work thus far, only a very small section of one of these ditches has been uncovered, the structure of which contributes little to its dating. Furthermore, in addition to the curved course of the ditch, only two other criteria speak for a Late Neolithic dating. In the lowest, undisturbed filling layers of the ditch, almost exclusively Late Neolithic finds were uncovered (cf. the contributions by S. Conrad, R. Krauß, chapter 9.1). The few ceramic fragments from later periods, all very small in size, could have easily entered through animal passages. Finally, we have four radiocarbon dates on animal bones which give us an important clue for the early history of the backfilling of this trench. Three of these dates are statistically identical and lie in the chronological segment of the Bulgarian Late Neolithic, the 52nd–51st century BC (cf. Görsdorf, Bojadžiev 1996). Another date lies in the area of the Bulgarian Late Chalcolithic, the 45th–44th century BC. The finds from the ditch can be assigned to these two periods (cf. the contributions by S. Conrad, R. Krauß, chapter 9.1).

According to the results of the field surveys, the ditch enclosed essential parts of the Late Neolithic settlement. Of this enclosed area, about 4 hectares are still preserved (cf. the contributions by N. Kecheva et al., chapters 7 and 12).

8.1.4. Interpretation

The structure of the ditch as it is visible in the geomagnetic plan differs from that of the more recent ditches because of its curved shape. Both due to the stratigraphic overlay and due to the extensive lack of more recent finds, it can be assumed that this is a structure that is related to the massive Late Neolithic settlement on the site. Examples for Neolithic settlement ditches can be seen at Aşağı Pınar (Özdoğan 2011), Yabalkovo (Roodenberg et al. 2014), Golyamo Delchevo (Тодорова et al. 1975) and Ovcharovo-Gorata (Krauß 2014). It would be too easy to see only obstacles to approach in these ditches (cf. Todorova 1982, 18–20). Many of these run through the settlements or end abruptly so they would not have been used for fortification. Other interpretations have also been put forward, for example as enclosures for the cattle pasture or as delimitation for various settlement areas (Petrasch 2012; Řídký, Daněček 2012; Kuzma, Tirpák 2012). The passages of the Neolithic ditches are often oriented according to astronomically significant cardinal directions, which is why they were also assigned a function as a calendar, to determine the time or as an aid for astronomical sky observation (Schlosser 2012; Meinike 2012; Zotti 2012). Often burials can also be found in these ditches, which also indicate a ritual use. An extreme case is the Early Neolithic ditch at Herxheim in the German province of Palatinate (Zeeb-Lanz 2010; 2016), where hundreds of human bodies, some of which were cut up like slaughtered animals, were found. In Central Europe, ditch works also occur spatially isolated from settlements. A ritual function is often revealed in these free-standing structures. For the settlement ditches of the Late Neolithic in the Balkans, a fortification function is becoming more apparent. This is expressed through the fact that the ditches either completely enclose the settlements or they secure topographical sections that allow access to the settlement. We recently published a selection of the Late Neolithic settlement fortifications (Čohadžiev, Krauß 2019). In this we were able to show that these Late Neolithic installations developed into real castles a little later, during the Chalcolithic era.

The prehistoric ditch at Tash Bair would also fit in well into this category. Whether the ditch completely encloses the Late Neolithic settlement cannot be recognised from the geomagnetic measurements alone. In any case, the core of the settlement seems to be within the ditch. The discovery of chalcolithic sherds in the upper filling of the ditch could indicate that the structure remained open for a very long time[1].

1 The excavations in 2022 uncovered numerous other Late Neolithic and Early Chalcolithic features at site 1. The results will be published in the next volume.

КЪСНОНЕОЛИТНИ РОВОВЕ НА ОБЕКТ 1 (СОНДАЖ 1.2)

Райко Краус, Свен Конрад

(Резюме)

Обект 1 е разположен на умерено наклонен склон при вливането на Студена река в р. Янтра в близост до устието на последната. Той е с най-голяма площ (приблизително 6,4 ха) и гъстота на находките сред регистрираните обекти в местността.

Геомагнитните проучвания разкриха множество аномалии, включително няколко линейни структури с големи размери. Перпендикулярно спрямо една от тях заложихме сондаж 1.2 с размери 7 × 3,40 м. Въпросната аномалия се проследява на геомагнитната карта на дължина от 182 м. В рамките на сондажа попада втора, по-слаба аномалия, сключваща тъп ъгъл с предходната.

Разкопките в сондажа установиха, че голямата аномалия принадлежи на ранносредновековен отбранителен ров. Той пресича двоен късноеолитен ров. Датирането на двете структури е постигнато чрез стратиграфския метод и чрез керамичните находки. Праисторическата принадлежи на голямо синхронно селище на същия обект 1. Неолитни ровове са известни от обекти при Ашагъ Пънар, Ябълково, Голямо Делчево и Овчарово-Гората. Някои ровове не са отбранителни, защото преминават през самото селище или завършват по начин, който обезсмисля фортификационно предназначение. Такива биха могли да служат като загражденията за добитък или като разграничаване на селищни зони. Все пак известните ровове от късния неолит на Балканите сякаш са отбранителни, съдейки по разположението им спрямо синхронни селища. Праисторическият ров на Таш баир се вписва в тази характеристика. Без разкопки не можем да определим дали е ограждал цялото селище, или само неговото ядро.

Ровът е останал отворен дълго време, защото в горната част на пълнежа му намерихме малко халколитна керамика.

8.2. BRONZE AGE

Several Bronze Age features were excavated on site 3 (cf. the contributions by N. Kecheva et al., chapter 12). Six trenches were placed based on the results of the geophysical survey of 2018 (cf. the contributions by B. Ullrich et al., chapter 6.1). A pit was fully excavated in trench 3.1 (cf. the contributions by S. Conrad, R. Krauß, chapter 8.2.3). Burnt dwelling remains, not *in situ*, and which had slipped down the slope into a fold of the terrain were fully excavated in trenches 3.2–5 (cf. the contributions by L. Vagalinski, L. Traykova, chapter 8.2.2). Part of an inner ditch in trench 3.6 was also excavated. This feature was located based on the geophysical results showing two concentric ditches at a distance of about 30 m from each other (cf. the contributions by L. Vagalinski et al., chapter 8.2.1).

8.2.1. The inner ditch of the enclosure in trench 3.6

Lyudmil Vagalinski, Lyuba Traykova, Nadezhda Kecheva

Description. The team (L. Vagalinski, S. Conrad, L. Traykova, N. Kecheva, S. Sabkova, B. Borisov) excavated the inner ditch of the enclosure in trench 3.6 from 6th – 22nd of September 2018 (Вагалински и др. 2019, 84). The location of trench 3.6 was decided based on the presence of recorded geophysical anomalies within site 3, visible as two concentric ditches at a distance of approximately 30 m from each other. They encircle the western part of the terrace whose eastern periphery is a steep slope with more than a 40 m difference in height (fig. 1).

The trench area was 30 m^2, with dimensions 10 m along the east-west axis and 3 m along the north-south axis. It was perpendicular to the inner ditch and its lower/southern half. The modern surface

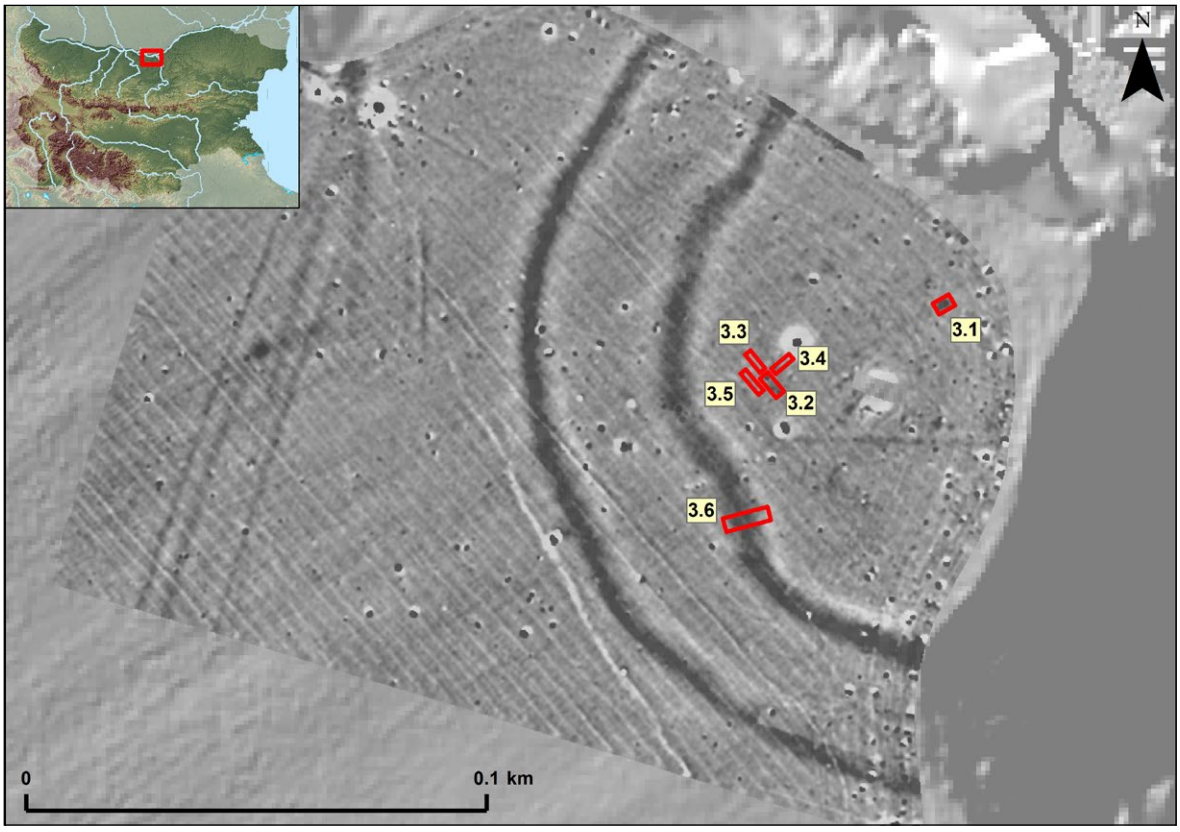


Fig. 1. Site 3, geophysical survey results in 2018 (cf. the contributions by B. Ullrich et al., chapter 6.1) and location of the trenches in 2018 (figure by N. Kecheva)

sloped from north to south and from west to east. The lowest point of the southeastern corner of the trench was ▼61.38 m. Coordinates of the trench corners were measured with GNSS receivers and the work was carried out with arbitrary levels. The first arbitrary level measured ▼61.33 m. The excavated trench area was reduced so that the investigation could be completed in accordance with the project deadlines. They continued only in the northern half of the trench with dimensions along the north-south axis of 1.5 m from ▼60.37 m in depth. Only the western ditch border was visible after the removal of an arbitrary layer (▼60.72–60.37 m). The eastern ditch border was distinguished after the removal of the arbitrary layer (▼60.12–59.87 m). The borders were not clearly visible, probably because the ditch sides had been constantly washed out, and thus additional soil from the surrounding area was added to the ditch filling. The cross section had an irregular trapezoidal form, the ditch was about 7.5 m wide in its uppermost visible level, its depth was approximately 3 m, and its bottom was approximately 2 m wide. It was visible in the northern trench section which meant that the eastern side of the trench appeared steeper and staircase-shaped, while the western side descended and narrowed more smoothly. Relatively large crushed limestones were excavated at ▼58.32 m (fig. 2). The larger slab-shaped stones were arranged at the edges of the ditch bottom following its curve; most of them were vertically placed. Large, slab-shaped stones lay horizontally in the middle between the two stone faces. A lot of small crushed stones were also arranged between the larger ones. The stones did not reach the eastern or western ditch sides (fig. 3) and it was observed that they were not lying down on the bottom of the first ditch (fig. 4). The ditch bottom was reached at a level of ▼57.49 m. A thin strip of burnt clay and charcoals with a length of about 1 m was visible on the southern section of the northern half of the trench at a level of ▼57.67 m. This strip marked the collapsed remains on the ditch bottom which was dug into the sterile sediment.

Pit 3.6.1. We recorded a pit in the northeastern corner of the trench at ▼60.72 m. It was situated to the east of the excavated ditch and was cut by the northern section of the trench (fig. 5). Its borders in plan and section were deeply disturbed by bioturbation. The investigation of pit 3.6.1 began with the excavation of its northeastern quarter (fig. 6), followed by its northwestern quarter. The pit diameter in



Fig. 2. The ditch in trench 3.6, level ▼58.32 m (photo by S. Conrad)



Fig. 3. The ditch in trench 3.6, level ▼58.03 m (photo by L. Vagalinski)

its uppermost part on the northern section was 1.02 m and it narrowed towards its bottom. Its shape was very regular and it is possible that there was a food storage vessel inside. The pit contained humus soil, a greyish-brown layer, and large crushed stone in the middle. Finds from the pit included a large animal bone from cattle on its bottom (fig. 7) and several handmade pottery fragments dated to the Bronze Age, including 1 rim and 1 shoulder with the base of a handle part of a biconical vessel. The cut of the pit was in the yellow sterile loess at a depth of 0.91 m from the recording level ▼60.72 m to the bottom at ▼59.81 m (figs. 8, 9). The pit position relative to the ditch location indicates that the pit was positioned within the berm between the assumed rampart and the ditch. The level from which the pit was dug could not be distinguished nor could its relation to it. It could be assumed that the pit was younger than the ditch so it is less likely that the pit and the ditch were built at the same time. Another indication for its



Fig. 4. The bottom of the ditch in trench 3.6 (photo by L. Vagalinski)



Fig. 5. The pit 3.6.1 (photo by L. Vagalinski)



Fig. 6. The pit 3.6.1, SE quarter (photo by L. Traykova)



Fig. 7. The pit 3.6.1, animal bone at the bottom (photo by L. Traykova)

younger timing is its stratigraphic position. The recorded level of the pit in plan (▼60.72 m) was much higher than the recorded level of the eastern border of the ditch (▼59.87 m). This difference of about 0.85 m demonstrates that the ditch and the pit were dug from different ancient surfaces. However, for some time, the ditch and the pit functioned simultaneously.

Analysis and dating. The ditch stratigraphy shows the stages of its construction, usage and filling (fig. 10). The first ditch excavation probably did not include bottom and side strengthening. Since it



Fig. 8. The pit 3.6.1, bottom (photo by L. Traykova)



Fig. 9. The pit 3.6.1 in the northern cross-section of the trench No. 3.6 (photo by L. Vagalinski)

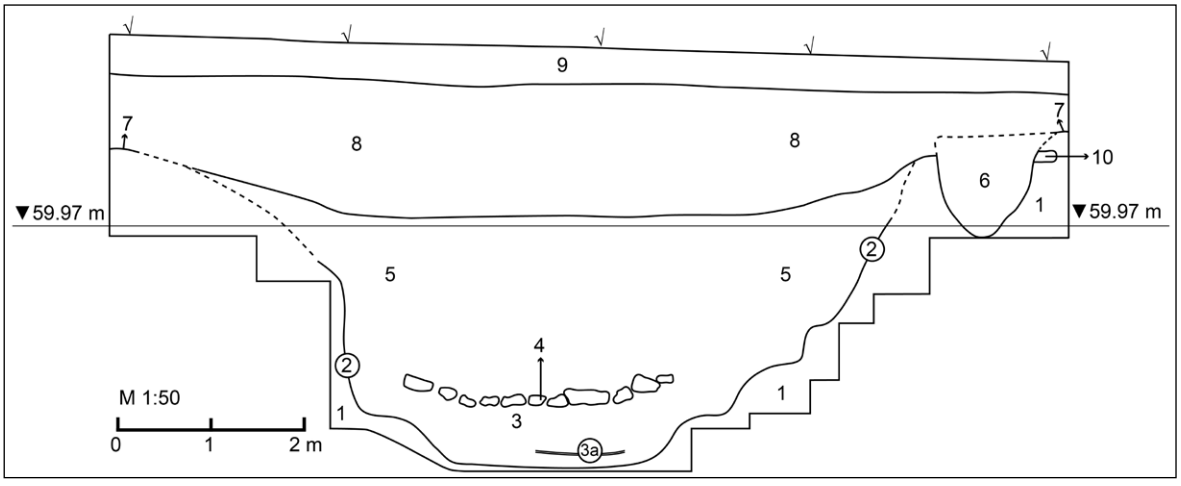


Fig. 10. Site 3. Trench 3.6, northern section: 1 – Sterile: yellowish-brown loess; 2 – Ditch – phase 1; 3 – Burnt strip and phase 1 ditch filling: loess and humus soil with scattered handmade pottery fragments dated to the Bronze Age, scattered charcoals, pieces of burnt clay; 3a – A strip of burnt clay situated at a distance of 1.50 m from the north section: it marks the phase 1 ditch bottom; 4 – Stone cladding of the phase 2 ditch bottom: crushed stones/limestone, the larger slab-shaped ones are arranged at the edges of the bottom of the ditch, following its curve; in the middle between these two faces two large horizontal slab-shaped stones and many smaller stones are placed. The bottom of the ditch is narrowed in this way, but we cannot distinguish the contour of the ditch in height during phase 2; 5 – Natural filling of the ditch after its usage: dark brown loess full of humus soil with scattered charcoals, handmade pottery fragments from BA, EIA, and LIA; small crushed stones; animal bones; scattered pieces of burnt clay; 6 – Pit, which contains: 10–15 undiagnostic handmade pottery fragments dated to the Bronze Age, a large animal bone, a large crushed stone, dark brown layer loess full of humus soil; 7 – Probable ground level of (6) and of the ditch; 8 – Strongly full of humus soil, dark brown, a loose layer which contained: handmade pottery fragments from BA, wheelmade pottery fragments from LIA and Roman period, tile fragments from the Hellenistic period; animal bones; small crushed stones; a large amount of rotten vegetation. The layer had been deposited on the slope descending from north to south. It had been strongly disturbed by bioturbation. Bioturbation was also recorded in (5) but in less quantity; 9 – Ploughzone layer, light brown loess full of humus soil, strongly disturbed by vegetation roots and bioturbations. It contained: pottery fragments from EBA, LIA, Antiquity and modern age; modern iron hinge; 10 – Bioturbation (drawing and interpretation by L. Vagalinski, L. Traykova, N. Kecheva)

is dug into loess with low values of bulk density (Евлогиев, Евстатиев 2007, 94, fig. 2, 97), the ditch sides would not have been stable enough. A cultural layer lay on the bottom of the ditch containing scattered charcoals, small pieces of burnt clay, handmade pottery fragments, cattle and pig bones (cf. the contributions by N. Karastoyanova, chapter 10.3). The stone cladding was placed above this layer and strengthened the lower part of the ditch after it had been used for some time. Thus, the ditch had two functional phases.

The eastern ditch side was internal to the space that was fenced. Most likely, the steps in this eastern side facilitated the removal of the excavated soil during the construction of the ditch, as well as its periodic cleaning from fallen soil. We assume that with the excavated soil a rampart was built on the inner, eastern side of the ditch.

A cattle bone was discovered situated on the ditch bottom, associated with its first functional phase, and under the stone cladding dating to its second functional phase. The radiocarbon dating of the piece refers to a point in 2040–1840 calBC (cf. chapter 9.1, fig. 2, table 13, No. 166). This gives a *terminus ante quem* for the ditch digging and a *terminus post quem* for the strengthening of its bottom with stones. It looks that both functional phases fall within the beginning of the Middle Bronze Age. A second animal bone found on the bottom of the ditch from its second functional phase has a similar ^{14}C date – sample TB3, 2010–1770 calBC (cf. chapter 9.1, fig. 2, table 13, No. 167). This supports the first date and shows that the two construction phases of the ditch fall across a relatively short period of time. The second sample belongs to a chronologically mixed layer containing pottery fragments dated to the Bronze Age and the beginning of the Late Iron Age (cf. chapter 9.1, table 9). This stratigraphic situation shows that the ditch had been maintained/cleaned for about 1300–1500 years up to the middle of the 1st millennium BC. Pottery fragments dating to the Early Iron Age (cf. chapter 9.1, table 9) were found as well as one dated to the Late Iron Age (cf. chapter 9.1, table 9). Radiocarbon dating of an animal bone and charcoal within the enclosed area by the ditch indicates a Late Bronze Age usage inside the ditch – respectively 1450–1290 calBC and 1350–1110 calBC (cf. chapter 9.1, fig. 2, table 13, Nos. 170 and 173).

The stratigraphic position of the pottery fragments in the ditch filling points to the hypothesis that it had been maintained up to the middle of the 1st millennium BC. There were no stratigraphic observations that the ditch had been restored in the middle of the 1st millennium BC; such a restoration would have been disturbed its original outline. No later human intervention could be observed in the well-preserved lower part of the ditch (fig. 10).

By Late Antiquity, the ditch was almost filled; it contained tile fragments, household pottery fragments and two small finds (cat. Nos. SF 24, 25) in the uppermost layer of the ditch filling. The uppermost layer thickness was about 1.5 m and consisted of a dark, humus soil, saturated with rotten organic material. In this layer, we also found several bones of a domestic pig (cf. the contributions by N. Karastoyanova, chapter 10.3). This layer was distinguished in all stratigraphic trench sections except the eastern one. A possible explanation for this is the presence of a defensive rampart on the eastern, inner side of the ditch. This rampart likely stopped the sliding of soil containing organic material. The ditch had become a landfill for humus soil only after it was no longer used, i.e. after the Early Iron Age.

Parallels and interpretation. The ditch had parallels in partially excavated archaeological sites on the left bank of the Danube, in Southern Romania, as well as in Southern Thrace, in Southern Bulgaria.

In Pietrele, Romania, an oval-shaped feature with a diameter between 130 and 170 m was recognised on an aerial photograph and geomagnetically surveyed (Hansen et al. 2017). A ditch was partially excavated that was 10 m wide at its upper part and 3 m wide at the bottom. The artefacts in the ditch fill were dated to the Tei culture and radiocarbon dating provided a range of 1400–1300 BC, i.e. in the Late Bronze Age. This enclosed area is interpreted as a settlement (Hansen et al. 2017, 98, Abb. 126, 99, Abb. 127, 98–103) (fig. 11).

A ritual complex, enclosed by a ditch with an inner diameter of 46 × 34 m and a maximum depth of 2.34 m, was excavated near Bikovo village, Sliven municipality, Southern Bulgaria (Hristova 2018, 348–349). The ditch cross section in different parts had an irregular U-shape or trapezoidal shape. A



Fig. 11. Site near Pietrele, Romania (after Hansen et al. 2017, 98, Abb. 126)



Fig. 12. Site near Bikovo village (after Hristova 2018, 348, fig. 1)

channel with a rectangular cross section had formed on the bottom. The whole inner side of the ditch was clad by middle-sized and large-sized slab-shaped and other stones. Radiocarbon dating provided ranges of 2031–1889 BC and 1748–1618 BC, i.e. Middle Bronze Age (Hristova 2018, 349, 351) (fig. 12).

Three concentric ditches around the southwestern periphery of a small hill were also excavated near Polski Gradets village, Radnevo municipality, Southern Bulgaria (Ников, Георгиева 2018; Ников,

Георгиева 2019). The outer ditch had a diameter of 175 m, a depth between 0.6–2 m and a width of 1–1.5 m. Its cross section was U-shaped or trapezoidal. There was a 2 m wide entrance recorded in the southwestern part and a stone wall was built alongside the eastern/inner side of the ditch. A second stone wall was built in the ditch alongside its long axis. The inner ditch had a diameter of 127 m, a depth of 2 m, a width of between 2–3 m and a trapezoidal cross section. There was an entrance 1.4 m wide recorded in the southern part. The site was inhabited from the end of the Early Bronze Age I / Early Bronze Age II until the transition Early Bronze Age II/Middle Bronze Age. The inner and probably the middle ditch also dated to the Early Bronze Age II, but it is not clear when the outer ditch was dug. The archaeological features that date to the transition Early Bronze Age II/Middle Bronze Age were mostly situated on and between the middle and the inner ditch when they had already been filled in. They were rarely situated between the middle and the outer ditch (Ников, Георгиева 2018, 78, 79, обр. 1) (fig. 13). During the investigation of the northeastern part of the hill, parts of the middle and the outer ditch were excavated and thirty metres of the inner ditch was investigated. Its width varied between 2.20–2.50 m, while its depth varied between 1.35 to 1.70 m. The cross section was trapezoidal with a very narrow lower part and an uneven bottom. Artefacts found in the ditch dated to the Early Bronze Age. Forty-two metres of the middle ditch were investigated. Its width varied between 2–4.30 m, while its depth varied between 1.25 to 2.90 m. The cross section was trapezoidal with a very narrow lower part and an uneven bottom. All artefacts found in the ditch date to the Early Bronze Age.

Entrances to the enclosed area were recorded in two places. The front side of the two entrances was similarly shaped: stones found *in situ* were arranged in an oval following the shape of the arched ends of the ditch. Remains of two stone walls with defensive purposes were also excavated. One of them was built by different sized stones alongside the inner side of the ditch. Some of them were found to be sliding down along the ditch edge. According to the way they fell, researchers suppose it was destroyed by a natural disaster. The huge stones of this construction remained in place, and the smaller and medium ones were used for the construction of a new wall with a width of 0.40 to 0.60 m. It was erected inside the already partially filled ditch, near its outer side. The small preserved height suggests a superstructure of mudbrick or wood. The construction of the two walls is later than the construction of the ditch. Their remains were visible almost along the entire route of the middle ditch in this part of the site. The demolition of the first and the erection of the second wall mark the last stage of the creation and usage of the middle ditch (Ников, Георгиева 2019, 85, 86, обр. 1, 87) (fig. 14).

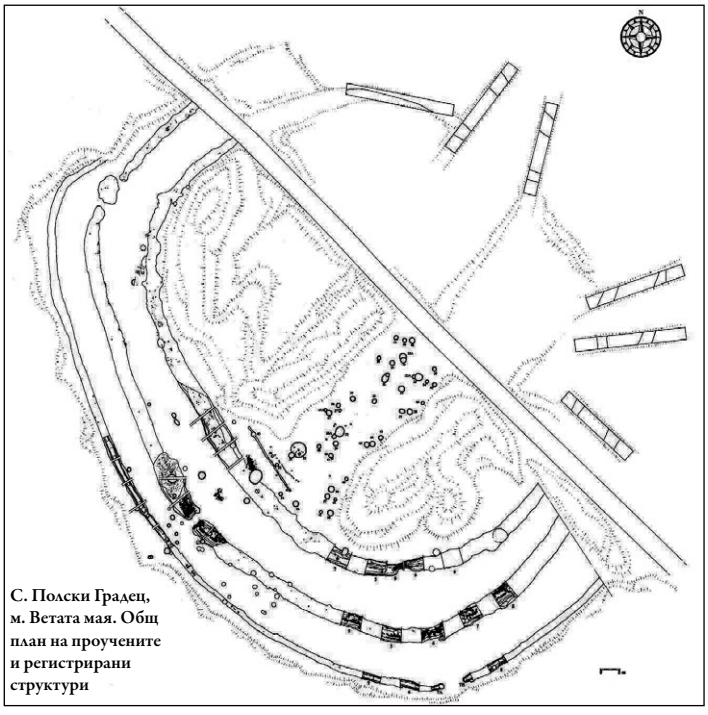


Fig. 13. Site near Polski Gradets village (after Ников, Георгиева 2018, 79, обр. 1)



Fig. 14. Site near Polski Gradets village (after Ников, Георгиева 2019, 86, обр. 1)

The partially excavated area of the ditch in trench 3.6 and of the enclosed area (trenches 3.2–5) do not provide sufficient data to determine with arguments whether the enclosed area was a settlement or a ritual place. Only a quarter of the enclosure survived due to severe erosion or other environmental factors, as such, it was not clear whether the encircled area was an approximately round shape. It could be supposed that the two ditches were largely synchronous because they were parallel to each other although reliable statements about this can only be given by further excavations of the other ditch. They could be part of a defensive structure created during the Middle Bronze Age. It enriches the current archaeological information about circular enclosures from the Bronze Age in the Lower Danube region of south-eastern Europe.

ВЪТРЕШЕН РОВ НА ОГРАДЕНА ПЛОЩ В СОНДАЖ 3.6

Людмил Вагалински, Люба Трайкова, Надежда Кечева

(Резюме)

Описание. Сондаж 3.6 е заложен с цел проучване на геофизична аномалия в рамките на обект 3, изразена като два концентрични рова на разстояние от около 30 м един от друг. Те затварят западната част от тераса, чиято източна периферия завършва със стръмно спускащ се скат с денивелация над 40 м (fig. 1). Общата площ на сондажа е 30 м^2, с размери 10 м по оста изток – запад и 3 м по оста север – юг. Той е перпендикулярен на вътрешния ров в неговата долна/южна половина. Теренът е с наклон от север на юг и от запад на изток. Ограниченият срок на проекта наложи площта на сондажа да бъде намалена наполовина, за да успеем да довършим проучването. След очертаването на западната граница на рова на ▼60,37 м се работи само в северната половина на сондажа, чийто размер по оста север – юг стана 1,5 м.

Границите не са ясно различими, защото най-вероятно стените на рова са се обрушвали и са се добавили към неговия пълнеж от околния терен. Напречният разрез е с неправилна

трапецовидна форма. В най-горната си част от нивото на разграничаване ровът е широк около 7,5 м, дълбочината му е около 3 м, а дъното е широко около 2 м. В северния профил на сондажа се вижда, че източната страна на рова е по-стръмна и оформена стъпаловидно, докато западната се спуска и стеснява по-плавно. На ▼58,32 м бяха разкрити сравнително големи ломени камъни варовик (fig. 2). По-големите плочести камъни са подредени по краищата и дъното на рова, следвайки неговата извивка; повечето от тях са поставени вертикално. Множество малки ломени камъни са подредени между големите. Камъните не достигат до източната и западната стена на рова (fig. 3). Установихме, че те не лежат и на първоначалното дъно на рова (fig. 4). Дъното беше достигнато на ▼57,49 м. В южния профил на северната половина на сондажа на ▼57,67 м се очерта тънка ивица от горяла глина и въгленчета с дължина около 1 м. Тази ивици бележи паднали деструкции на дъното на рова, който е вкопан в стерилна глина.

Яма 3.6.1. В североизточния ъгъл на сондажа, на ▼60,72 м, източно от проучения ров регистрирахме яма, прерязана от северния профил (fig. 5). Проучването започна с изчерпването на нейната североизточна четвърт (fig. 6), а след това беше изчерпана и северозападната четвърт. Диаметърът в горната част на ямата по северния профил е 1,02 м, надолу се стеснява. Ямата има много правилна форма и вероятно в нея е имало съд за съхранение на храна. Ямата съдържаше хумусизирана сиво-кафява пръст; голям ломен камък в средата; голяма животинска кост от едър добитък на дъното (fig. 7); няколко фрагмента битова керамика от бронзовата епоха, изработени на ръка. Вкопана е в жълтия стерилен льос на дълбочина 0,91 м от нивото на регистриране (figs. 8, 9). Позицията на ямата спрямо рова показва, че тя попада в рамките на бермата между предполагаемия вал и рова. Не успяхме да разграничим сигурно от какво ниво е вкопана ямата и как тя се съотнася към нивото, от което е вкопан ровът. Може да се предположи, че ямата е по-млада от рова. По-малко вероятно е ямата и ровът да са изградени едновременно. Друг довод, че ямата е заварила рова, е нейната стратиграфска позиция. Нивото на разграничаване на ямата в план (▼60,72 м) е значително по-високо от нивото на разграничаване на източната граница на рова (▼59,87 м). Тази разлика от около 0,85 м означава, че ровът и ямата са вкопани от различни дневни повърхности. В някакъв период от време ровът и ямата са функционирали едновременно.

Анализ и датировка. Стратиграфията на рова показва етапите от неговото изкопаване, използване и запълване (fig. 10). Първоначалното изграждане на рова най-вероятно не е включвало укрепване на дъното и стените. Тъй като е вкопан в льос, който има ниски стойности на обемната плътност (Евлогиев, Евстатиев 2007, 94, фиг. 2, 97), стените на рова не са били достатъчно стабилни. Върху дъното на рова лежи културен пласт, съдържащ разнесени въглени, малки късове отухлена глина, битова керамика, изработена на ръка и кости от говедо и домашна свиня (вж. приноса на Н. Карастоянова, глава 10.3). Каменната облицовка е положена над този пласт. Тя укрепва долната част на рова, след като той е бил използван известно време. Така ровът има две фази на функциониране.

Източната стена на рова е вътрешна спрямо пространството, което е било оградено. Най-вероятно стъпалата в тази източна стена улеснявали изнасянето на изкопаната пръст при изграждането на рова, както и неговото периодично почистване от нападала земна маса. Предполагаме, че с изкопаната пръст бил натрупан вал от вътрешната източна стена на рова.

Кост от говедо, открито на дъното на рова от неговата първа фаза и под каменната облицовка от втората му фаза, е датирана радиовъглеродно в 2040 – 1840 calBC (вж. глава 9.1, fig. 2, table 13, № 166). Тази датировка е *terminus ante quem* за изграждането на рова и *terminus post quem* за укрепването с камъни на неговото дъно. Изглежда и двете фази попадат в началото на средния бронзов период. Втора животинска кост, лежаща върху дъното на рова от втората му фаза, има много близка датировка 2010 – 1770 calBC (вж. глава 9.1, fig. 2, table 13, № 167), която подкрепя първата и показва, че двете строителни фази на рова попадат в сравнително кратък интервал от време. Втората проба принадлежи на хронологически смесен пласт, съдържащ керамика от бронзовата епоха до началото на късния железен период. Тази стратиграфска

ситуация разкрива, че ровът бил поддържан/почистван в продължение на около 1300 – 1500 години до средата на I хил. пр. Хр.

Радиовъглеродното датиране на животинска кост и въглен в рамките на защитената от рова площ ги отнася към късния бронзов период – съответно в 1450 – 1290 calBC и 1350 – 1110 calBC (вж. глава 9.1, fig. 2, table 13, №№ 170 и 173).

Стратиграфското разпределение на керамиката в рова насочва към хипотеза, че той бил поддържан до средата на I хил. пр. Хр. Липсват стратиграфски данни, че ровът е бил възстановен в средата на I хил. пр. Хр. Не се забелязва по-късна човешка намеса в добре запазената долна част на рова (fig. 10).

До Късната античност ровът вече бил почти запълнен – фрагменти от керемиди, битова керамика, както и две малки находки (кат. №№ SF 24, 25) от това време намерихме в най-горния пласт от пълнежа на рова. Този пласт съдържа тъмна хумусизирана пръст, наситена с изгнила органична маса, разграничава се във всички стратиграфски профили на сондажа с изключение на източния. Възможно обяснение за това е наличието на отбранителен вал от източната, вътрешна страна на рова. Вероятно този вал спирал свличането на пръст, съдържаща органичен материал. Ровът се превърнал в депо за хумусизирана пръст едва след като вече не бил използван/поддържан, т.е. след ранния железен период.

Паралели и интерпретация. Ровът има аналози в проучвани археологически обекти на левия бряг на Дунав, в Южна Румъния, както и в Южна Тракия в рамките на Южна България. В Pietrele, Южна Румъния, е проучен ров. Материалът от запълнителя е отнесен към археологическата култура Тей, а радиовъглеродното му датиране показва 1400 – 1300 г. пр. Хр., т.е. късен бронзов период. Оградената площ е интерпретирана като селище (Hansen et al. 2017, 98, Abb. 126, 99, Abb. 127, 98 – 103) (fig. 11). Край с. Биково, общ. Сливен, в Южна България е проучен ритуален комплекс, ограден с ров. Цялата вътрешна страна на рова е облицована с плочести и неоформени камъни със средни и големи размери. Резултатите от радиовъглеродното датиране показват 2031 – 1889 BC и 1748 – 1618 BC, т.е. среден бронзов период (Hristova 2018, 349, fig. 1, 351) (fig. 12). При с. Полски Градец, общ. Раднево, Южна България, около ниско възвишение са проучени три концентрични рова около югозападната периферия на възвишението. Външният има прекъсване за вход в южната част, широко 5 м. Средният ров има прекъсване за вход в югозападната част, широко 2 м. Покрай източната/вътрешна страна на рова бил изграден зид от необработени камъни. Втори каменен градеж бил издигнат вътре в рова по неговата надлъжна ос. Вътрешният ров има прекъсване за вход в южната част, широко 1,4 м. Обектът бил обитаван от края на ранен бронзов период 1 / началото на ранен бронзов период 2 до края на ранен бронзов период 3 / среден бронзов период. Вътрешният и вероятно средният ров са отнесени към ранен бронзов период 2. Не е изяснено кога е изкопан външният ров. Археологическите структури, датирани в края на ранен бронзов период 2 / среден бронзов период, били изградени върху и между средния и вътрешния ров, когато вече били запълнени, и по-рядко били издигани между средния и външния ров (Ников, Георгиева 2018, 78, 79, обр. 1) (fig. 13). При проучването на североизточната периферия на възвишението са разкопани сектори от средния и вътрешния ров. Откритите в двата рова материали са от ранния бронзов период (Ников, Георгиева 2019, 85, 86, обр. 1, 87) (fig. 14).

Ограничените като площ разкопки както на рова в сондаж 3.6, така и в защитената площ (сондажи 3.2 – 5) не дават достатъчно данни да се определи аргументирано дали оградената площ е селище, или ритуално място. Не е ясно дали защитената площ е била с приблизително кръгла форма, от която до днес е оцеляла едва една четвърт поради силна ерозия. Предполагаме, че двата рова са синхронни, защото са успоредни. Вероятно те са били част от отбранително съоръжение, създадено през средния бронзов период. То обогатява досегашната археологическа информация за фортификация през бронзовата епоха в Долнодунавския регион на Югоизточна Европа.

8.2.2. The structure in trenches 3.2–5

Lyudmil Vagalinski, Lyuba Traykova

Description. The team (L. Vagalinski, S. Conrad, L. Traykova, N. Kecheva, S. Sabkova and German students) excavated the structure in trenches 3.2–5 between 21st of August and 14th of September 2018 (Вагалински и др. 2019, 84). Trench 3.2 was placed because of the presence of a geophysical anomaly within site 3, visible as three oval negative features with a diameter less than 1 m. The anomaly was situated within the area enclosed by two concentric ditches (fig. 1).

The trench area was 12.65 m^2, with dimensions 5.50 m along the northwestern-southeastern axis and 2.30 m along the northeastern-southwestern axis. The surface had a clear slope from north to south. Remains of a burnt dwelling with handmade pottery fragments dated to the Bronze Age, burnt pieces of floor and wall daub, charcoals and scattered crushed stones were excavated (fig. 2).

A bronze knife was found in the destroyed remains of the structure (cat No. SF 53). The amount of tin in the alloy of the knife indicates that it was additionally added to the alloy and that the knife was made of tin bronze[2]. A non-destructive scanning using an electron microscope was performed on the find – an energy-dispersive system captures X-ray photons where each element has a place in the spectrum and its quantity is determined according to the peak in the spectrometer. The permissible deviation in the corrosion product was 1–5%, and in the metal itself – 0.2–0.5%.

Quantitative analysis of the alloy: aluminium (Al) is missing, which is normal for the composition of the alloy in Antiquity; modern alloy includes the addition of Al. The amount of tin (Sn) in the alloy indicates its deliberate addition, there was also a small amount of lead (Pb) and probably also part of the

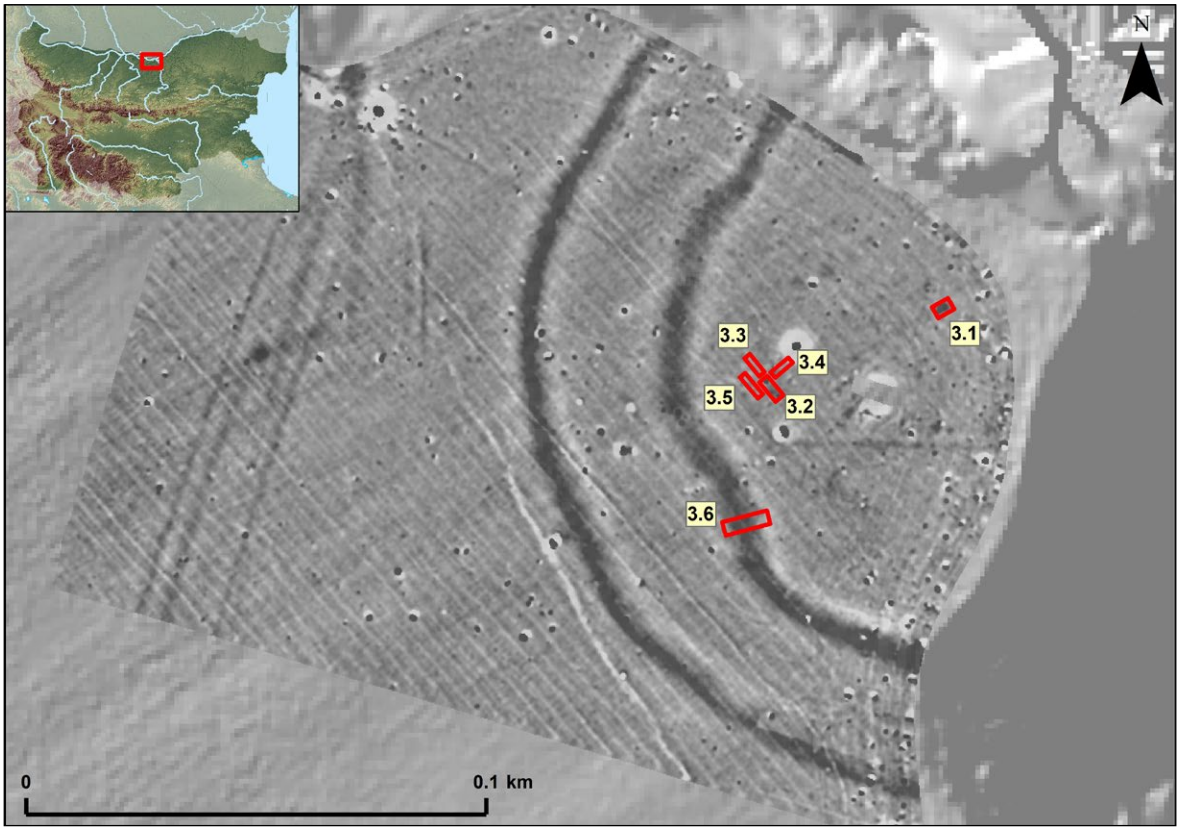


Fig. 1. Site 3, geophysical survey results in 2018 (cf. the contributions by B. Ullrich et al., chapter 6.1) and location of the trenches in 2018 (figure by N. Kecheva)

2 The analysis was done by Eurotest-control EAD (accredited laboratory on ISO / IEC 17025, a certificate for of approval on ISO 9001 by LRQA).



Fig. 2. Trench 3.2, northeast cross-section (photo by L. Vagalinski)

tin ore. The presence of arsenic (As) and nickel (Ni) are also in small amounts and thus were not added to the ore but were probably naturally found in copper ore. Iron (Fe) and silicon (Si) was at the limit of detection and they were also not deliberately added to the alloy. It is possible that these elements sunk into the metal due to corrosion (table 1).

Table 1. Results of the quantitative analysis of the alloy (Eurotest-Control EAD, accredited laboratory on ISO / IEC 17025, a certificate for of approval on ISO 9001 by LRQA)

Elt	XRay	Int	Error	K	Kratio	W%	A%	ZAF
Al	Ka	0.0	0.0000	0.0000	0.0000	0.00	0.00	0.3018
Si	Ka	4.6	8.2149	0.0010	0.0010	0.22	0.53	0.4303
Cl	Ka	7.0	8.2149	0.0000	0.0000	0.00	0.00	0.7559
Mn	Ka	0.0	0.0000	0.0000	0.0000	0.00	0.00	1.0962
Fe	Ka	0.7	0.9485	0.0005	0.0005	0.04	0.05	1.1943
Co	Ka	1.2	0.9485	0.0000	0.0000	0.00	0.00	1.2708
Ni	Ka	7.7	0.9485	0.0071	0.0070	0.64	0.73	1.0949
Cu	Ka	812.5	0.9485	0.8940	0.8824	87.57	92.35	1.0067
As	La	1.2	8.2149	0.0006	0.0006	0.24	0.21	0.2455
Sn	La	123.4	8.2149	0.0905	0.0893	10.42	5.88	0.8560
Pb	Ma	7.2	8.2149	0.0054	0.0053	0.77	0.25	0.6877
				0.9990	0.9860	99.90	100	

Quantitative analysis of the oxide form of the corrosion product. Two studies were performed (table 2): magnification x50, which covers a larger area of the artefact and shows the presence of more elements; magnification x100, which covers a smaller area, may have a smaller number of detected elements, but their quantity is determined more accurately than those in the study at magnification x50.

Table 2. Results of the quantitative analysis of the corrosion product (Eurotest-Control EAD, accredited laboratory on ISO / IEC 17025, a certificate for of approval on ISO 9001 by LRQA)

Quantitative Results – 50										
Elt	**XRay**	**Int**	**Error**	**K**	**Kratio**	**W%**	**A%**	**ZAF**	**Formula**	**Ox%**
O						26.78	54.92	0.0000		0.00
Al	Ka	16.9	29.4855	0.0154	0.0094	2.61	3.17	0.3584	Al2O3	4.93
Si	Ka	61.1	29.4855	0.0569	0.0346	7.17	8.37	0.4816	SiO2	15.33
S	Ka	4.3	29.4855	0.0048	0.0029	0.43	0.44	0.6763	SO3	1.08
Cl	Ka	10.6	29.4855	0.0128	0.0078	1.06	0.98	0.7359		1.06
K	Ka	5.8	29.4855	0.0082	0.0050	0.57	0.48	0.8714	K2O	0.69
Ca	Ka	19.4	29.4855	0.0296	0.0180	1.92	1.58	0.9342	CaO	2.69
Mn	Ka	0.3	2.1129	0.0007	0.0004	0.04	0.02	0.9923	MnO	0.05
Fe	Ka	4.0	2.1129	0.0120	0.0073	0.68	0.40	1.0681	FeO	0.88
Co	Ka	0.2	2.1129	0.0000	0.0000	0.00	0.00	1.1239	CoO	0.00
Ni	Ka	0.3	2.1129	0.0012	0.0007	0.07	0.04	0.9826	NiO	0.09
Cu	Ka	169.2	2.1129	0.8229	0.5001	55.29	28.55	0.9035	CuO	69.21
As	La	2.2	29.4855	0.0048	0.0029	0.98	0.43	0.2988	As2O3	1.30
Sn	La	8.4	29.4855	0.0271	0.0165	2.06	0.57	0.8002	SnO	2.33
Pb	Ma	0.8	29.4855	0.0026	0.0016	0.23	0.04	0.6817	PbO	0.25
				0.9990	0.6071	99.90	100			99.90
Quantitative Results – 100										
Elt	**XRay**	**Int**	**Error**	**K**	**Kratio**	**W%**	**A%**	**ZAF**	**Formula**	**Ox%**
O						23.52	52.59	0.0000		0.00
Al	Ka	14.3	54.5165	0.0052	0.0035	1.05	1.39	0.3336	Al2O3	1.98
Si	Ka	67.2	54.5165	0.0248	0.0168	3.62	4.61	0.4624	SiO2	7.75
S	Ka	9.5	54.5165	0.0042	0.0029	0.42	0.47	0.6805	SO3	1.05
Cl	Ka	24.3	54.5165	0.0117	0.0079	1.06	1.07	0.7429		1.06
K	Ka	6.3	54.5165	0.0035	0.0024	0.27	0.25	0.8830	K2O	0.33
Ca	Ka	41.4	54.5165	0.0251	0.0170	1.78	1.59	0.9501	CaO	2.49
Mn	Ka	0.4	0.7534	0.0004	0.0003	0.03	0.02	1.0320	MnO	0.03
Fe	Ka	6.0	0.7534	0.0070	0.0048	0.42	0.27	1.1217	FeO	0.54
Co	Ka	1.4	0.7534	0.0000	0.0000	0.00	0.00	1.1945	CoO	0.00
Ni	Ka	2.5	0.7534	0.0040	0.0027	0.27	0.16	1.0093	NiO	0.34
Cu	Ka	463.9	0.7534	0.8955	0.6047	65.64	36.96	0.9203	CuO	82.17
As	La	2.4	54.5165	0.0021	0.0014	0.53	0.25	0.2739	As2O3	0.70
Sn	La	11.1	54.5165	0.0142	0.0096	1.18	0.36	0.8118	SnO	1.34
Pb	Ma	0.9	54.5165	0.0011	0.0008	0.11	0.02	0.6862	PbO	0.12
				0.9990	0.6746	99.90	100			99.90



Fig. 3. Trench 3.3, level ▼63.38 m (photo by S. Conrad)

Aluminium (Al), silicon (Si), sulphur (S), chlorine (Cl), potassium (K), calcium (Ca), manganese (Mn) and iron (Fe) fell into the oxide of the soil corrosion product. Nickel (Ni) was present in the alloy and was part of the corrosion product and the copper (Cu) and arsenic (As) were present as oxides. Tin (Sn) and lead (Pb) were absent from the corrosion product as they were removed from the surface layer. There were no significant differences in the number of elements at the two magnifications (x50 and x100). A significant difference observed was the increase in the amount (approximately twice) of silicon (Si) (there is more quartz), which was observed at a magnification of x50. This is normal because a magnification of x50 covers a larger area of the artefact and the amount of deposited clay on the artefact is larger (cf. the contributions by R. Krauß, E. Pernicka, chapter 10.1).

Three more trenches were excavated to determine the area of the dwelling, the remains of which were excavated in trench 3.2 (fig. 1).

Trench 3.3: It was located 1 m northwestern of trench 3.2, its area was 7.5 m^2 and it measured 5 m along the northwestern-southeastern axis and 1.50 along the northeastern-southwestern axis. A small

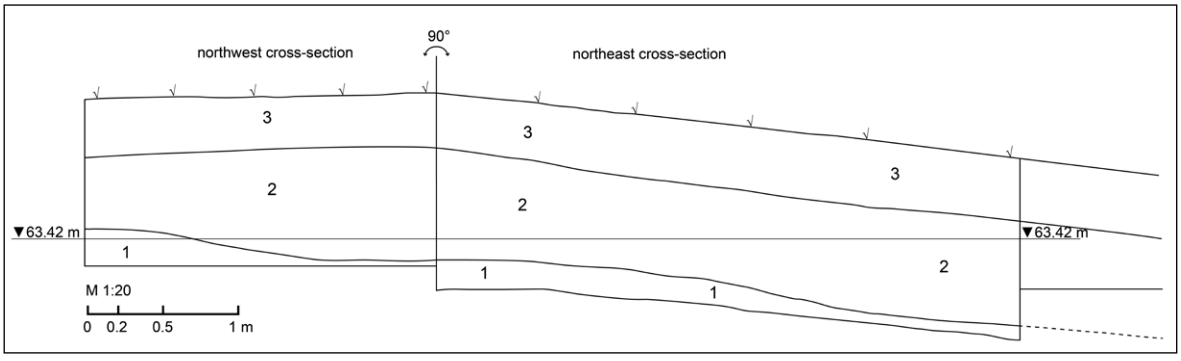


Fig. 4. Site 3. Trench 3.2, northwestern and northeastern sections: 1 – Sterile loess, light brown in colour; 2 – Slipped down the slope burnt remains of a Bronze Age dwelling: scattered pieces of burnt wood (charcoals); crushed stones in different sizes mainly recorded on the ground level; few handmade pottery fragments; pieces of burnt mudbrick as well as unburnt/decomposed mudbrick; pieces of burnt floor daub with traces of wattle fence; many holes resulted from bioturbation some of which mixed artefacts from layer (2) to layer (1). No animal bones were recorded. Brown layer. There is humus soil in it. 3 – Loose, humus soil, ploughzone, dark brown (drawing and interpretation by L. Vagalinski, L. Traykova)



Fig. 5. Trenches 3.2 and 3.3, northeast cross-section (photo by S. Conrad)

number of scattered charcoals, burnt and unburnt clay, small pieces of animal bones, small crushed stones, and several undiagnostic handmade pottery fragments in the southeastern part of the trench were uncovered (fig. 3). Two samples were taken for radiocarbon dating (cf. chapter 9.1, fig. 2, table 13, Nos. 170 and 173). Sample TB5 from an animal bone corresponds with its calibrated date range of 1450–1290 calBC roughly to the archaeological expectation for the Late Bronze Age. The second sample (charcoal) TB4 is even a little younger with 1350–1110 calBC.

Trench 3.4: It was located 1 m northeastern of trench 3.2, its area is 7.5 m^2 and it measured 5 m along the northeastern-southwestern axis and 1.50 along the northwestern-southeastern axis. Finds includes a small number of small charcoals, crushed stones, pieces of burnt clay, handmade (and a small amount – wheel made) pottery fragments in the southwestern part of the trench.

Trench 3.5: It is located 1 m southwestern and parallel to trenches 3.2 and 3.3, its area is 9 m^2 and it measured 6 m along the northwestern-southeastern axis and 1.5 m along the northeastern-southwestern axis. Sterile loess soil was reached after the removal of the ploughzone containing a few small handmade pottery fragments.

No animal bones were found in trenches 3.4 and 3.5.

Analysis: We did not record any traces of artificial terrain levelling for building and inhabitation in trench 3.2. Nor were dwellings *in situ* were preserved, such as traces of timber-framed construction, pits and trenches dug for shaping the walls of the dwelling. The high concentration of large crushed stones lies above, below and in a layer of charcoal, burnt and unburnt daub (fig. 4). No deliberate arrangement of the stones had been recorded anywhere. Moreover, a piece of fibre was found under one of the stones that indicates activity at this feature in the most recent years. All remains follow the slope of the terrain from north to south. The location of these remains in the area of trench 3.2 confirmed the assumption that they were redeposited in a natural fold of the terrain.

The presence of a small number of pottery fragments, charcoals, and small crushed stones in trenches 3.3, 3.4 and 3.5 were recorded only in the adjacent zones of trench 3.2. The section between trenches 3.2 and 3.3 was also excavated. The stratigraphy in the northeastern section of trench 3.3 confirmed the conclusions made for the remains discovered in trench 3.2 (fig. 5). Sterile soil was reached in all trenches. The exact location of the dwelling was not recorded in the trenches that were excavated.

Interpretation: In conclusion, according to the stratigraphic observations the remains of a burnt dwelling from the Bronze Age were excavated; it was found in a secondary position since it had slipped down the slope in a fold of the terrain. The above-mentioned knife and the two ^{14}C dates specify the chronology of the dwelling in the Late Bronze Age. Although tin has been added to metal artefacts in Europe since the end of the 3rd millennium BC, i.e. the beginning of the Middle Bronze Age in Southeastern Europe, tin bronze artefacts appear in Bulgaria in 2nd millennium BC and especially after 1800 BC (Nessel, Pernicka 2018, 135, 139). The results from trenches 3.2–5 support the hypothesis (cf. the contributions by L. Vagalinski et al., chapter 8.2.1) that the enclosed area had been inhabited for a long period during which the two concentric and probably defensive ditches had been systematically maintained.

СТРУКТУРА В СОНДАЖИ 3.2 – 5

Людмил Вагалински, Люба Трайкова

(Резюме)

Описание. Сондаж 3.2 беше заложен с цел проучване на геофизична аномалия в рамките на обект 3, изразена като концентрация от три овални негативни структури с диаметър около и под 1 м. Аномалията попада вътре в оградения от два концентрични рова терен (fig. 1). Общата площ на сондажа е 12,65 м^2; размери 5,50 м по оста северозапад – югоизток и 2,30 м по оста североизток – югозапад. Теренът тук е с изявен наклон от север на юг. В сондажа бяха проучени останки от опожарено жилище с фрагменти битова керамика от бронзовата епоха, изработена на ръка, отухлени глинени замазки и мазилки, въглени и разнесени ломени камъни (fig. 2). Радиовъглеродното датиране на животинска кост и въглен от сондажа ги отнася към късния бронзов период.

В деструкциите беше открито бронзово ножче (кат. № SF 53). Количеството на калая в сплавта показва, че е допълнително добавен към сплавта и ножчето е изработено от калаен бронз[3]. На находката беше направено недеструктивно изследване със сканиращ електронен микроскоп – енергийно-дисперсивна система улавя рентгеновите фотони, всеки елемент има място в спектъра и количеството му се определя според пика в спектрометъра. Допустимото отклонение в корозионния продукт е 1 – 5%, а в самия метал 0,2 – 0,5%.

Количествен анализ на сплавта: алуминий (Al) липсва, което е нормално за състава на сплавта в древността. В съвременната сплав има добавяне на Al; количеството на калая (Sn) показва съзнателно добавяне; количеството на оловото (Pb) е малко и вероятно е част от калаената руда, не е добавено допълнително; арсенът (As) и никелът (Ni) също са в малки количества и вероятно са естествено съдържащи се в медната руда; количеството на желязо (Fe) и силиций (Si) е на границата на откриването и те също не са добавяни съзнателно към сплавта. Възможно е да са попаднали по-дълбоко в метала поради корозията (table 1).

Бяха направени две изследвания за количествен анализ на окисната форма на корозионния продукт: увеличение 50, което обхваща по-голяма площ от предмета и показва наличие на повече елементи; увеличение 100, което обхваща по-малка площ, може да има по-малък брой открити елементи, но количеството им се определя по-точно спрямо изследването при увеличение 50 (table 2) (вж. още приноса на Р. Краус, Е. Перницка, глава 10.1.)

Направихме още няколко сондажа, за да установим площта на жилището, чиито останки бяха разкрити в сондаж 3.2: сондажи 3.3, 3.4 и 3.5. (fig. 1).

Анализ: Никъде в сондаж 3.2 не установихме следи от подравняване на терена с цел застрояване и обитаване. Липсват жилищни структури, запазени на място: следи от носещи

3 Анализът е извършен в Евротест-контрол ЕАД (Акредитирана лаборатория по БДС EN ISO/ IEC 17025, Сертификат за одобрение по ISO 9001 от LRQA).

колове за дървено-глинена конструкция; вкопавания за оформяне стените на жилището. Високата концентрация от големи ломени камъни лежи над, под и в пласт с въглени, горяла и негоряла глина (fig. 4). Никъде не беше установено съзнателно подреждане на камъните. Нещо повече, под един от камъните намерихме парче от изкуствено влакно, използвано след средата на XX век в селското стопанство. Всички останки следват наклона на терена от север на юг. Разположението на тези рушевини в пространството на сондаж 3.2 затвърди предположението, че те са свлечени / преотложени в естествена гънка на терена.

Наличие на малко количество керамика, въглени и малки ломени камъни, които излязоха в сондажи 3.3, 3.4 и 3.5, беше установено само в съседните на сондаж 3.2 зони. Реброто между сондажи 3.2 и 3.3 също беше изкопано. Стратиграфията в североизточния профил на сондаж 3.3 потвърди заключенията, направени за останките, разкрити в сондаж 3.2 (fig. 5). Във всички сондажи беше достигнат стерил. Точното местоположение на жилището не беше локализирано в заложените сондажи.

Интерпретация. Въз основа на стратиграфските ни наблюдения заключаваме, че сме разкрили останки от опожарено жилище от бронзовата епоха. Тези рушевини не са *in situ*, а са се свлекли по склона в гънка на терена. Споменатите по-горе две радиовъглеродни датировки уточняват датировката на жилището в рамките на късния бронзов период. Тези дати са валидни и за бронзовото ножче, което принадлежи на същия археологически контекст. Въпреки че калаят започва да се прилага в метални артефакти в Европа от края на III хил. пр. Хр., т.е. от началото на средния бронзов период в Югоизточна Европа, предмети от калаен бронз се появяват масово в България през II хил. пр. Хр. и особено след 1800 г. пр. Хр. (Nessel, Pernicka 2018, 135, 139). Резултатите от сондажи 3.2 – 5 подкрепят хипотезата ни (вж. Л. Вагалински и др., глава 8.2.1), че въпросната защитена площ е била обитавана дълго, през което време нейните два отбранителни успоредни рова са били системно поддържани / почиствани.

8.2.3. The pit in trench 3.1

Sven Conrad, Raiko Krauß

8.2.3.1. Excavation and stratigraphical observations

At site 3, the geomagnetic mapping shows only a few clearly delimited anomalies or characteristic structures in the area enclosed by a quarter-circular concentric double ditch and the present-day brim (fig. 1). Trench 3.1 with dimensions of 3.95 x 2.70 m was positioned over a small, rounded anomaly in the eastern part of the enclosure. The excavation and the documentation were largely in the hands of Julia Becher and Martin Offermann.

Firstly, the ploughed surface was removed by hand (niv. 61.89–62.37 m) down to planum 1 at the surface of the loess. Only few finds were found here. In planum 1 (niv. 60.91–60.97 m), feature 3.1.1 emerged as an oval, yellowish-grey discoloration, with very blurry boundaries. This feature, with dimensions of SW-NE 2.90 m; SE-NW approx. 2.40 m, was not completely in the trench, i.e. a small part 3.1. was somewhat covered through the northern edge of trench (fig. 3; 4).

The feature was divided with a profile line and the E half of the feature (quadrant A) was excavated in negative first, following the natural layers. The position of a large part of the finds (pottery, bones) was documented by single find measurement (cf. chapter 9.1, table 11). After removing the top layer (a) of the pit filling, which already contained several ceramic fragments, the ashy layer (b) interspersed with charcoal, was found. Several large ceramic and bone fragments were embedded in this layer as well (fig. 5; 6). The later excavation in the western quadrant B showed that the concentration of these finds was essentially limited to the eastern part of the pit, i.e. mainly in quadrant A.



Fig. 1. Site 3. View from the northeast (SfM model by P. Kluge and M. Offermann)



Fig. 2. Site 3. Geomagnetic map with the boundaries of the trenches (figure by S. Conrad)

During the excavation of the bottom layer, large animal dens with removed ceramic fragments were observed, especially in the deeper part of the pit at the north-eastern edge (fig. 4; 7–10). This feature was first given the designation 3.1.2, and later assigned to the main feature. After the documentation of the intermediate profile, quadrant B was excavated according to the sequence of layers. Afterwards, the north profile at the edge of the trench was documented (fig. 10).

Feature 3.1.1. in its southern and middle parts was a relatively shallow pit with a depth below planum 1 (= ca. 0.90 m under the present surface) of about 0.50 m. It had vertical sides and a rounded transition to the bottom. The intermediate profile shows a flat bottom in the southern and middle part and a stepped depression with a deepening of about 0,25 m to the north. Based on the N-profile, a maximum depth of ca. 0.80 m below planum 1 (= ca. 1.20 under the present surface) can be seen at this point (figs. 7–9).

The material, which had laterally fallen inside the pit, shows that it was open for a longer period of time. It was then probably used as a garbage dump. The filling of layer b, heavily interspersed with ash,

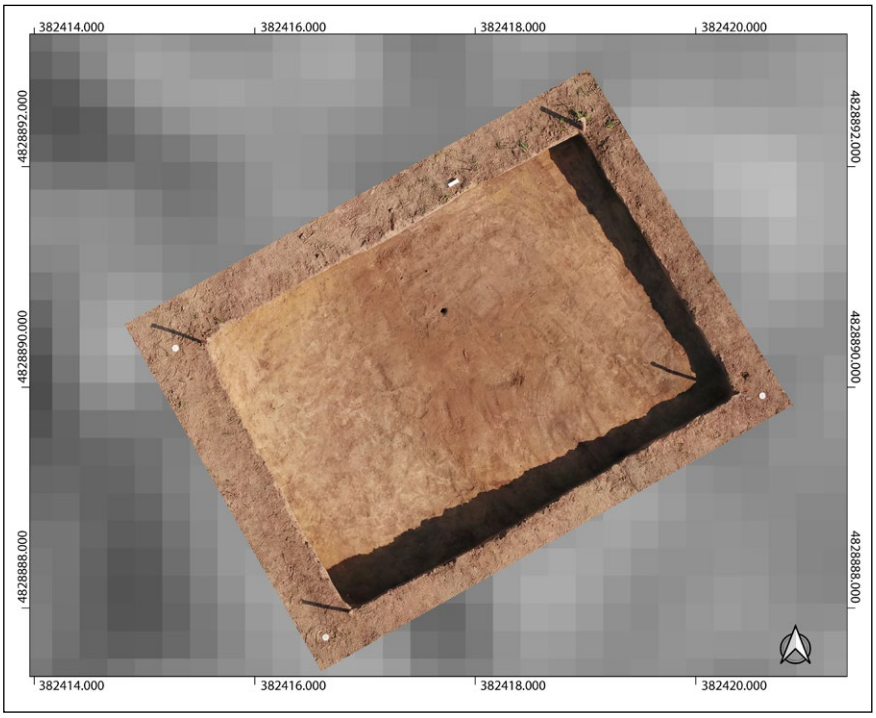


Fig. 3. Feature 3.1.1, planum 1. Vertical picture taken from an UAV (figure by P. Kluge)

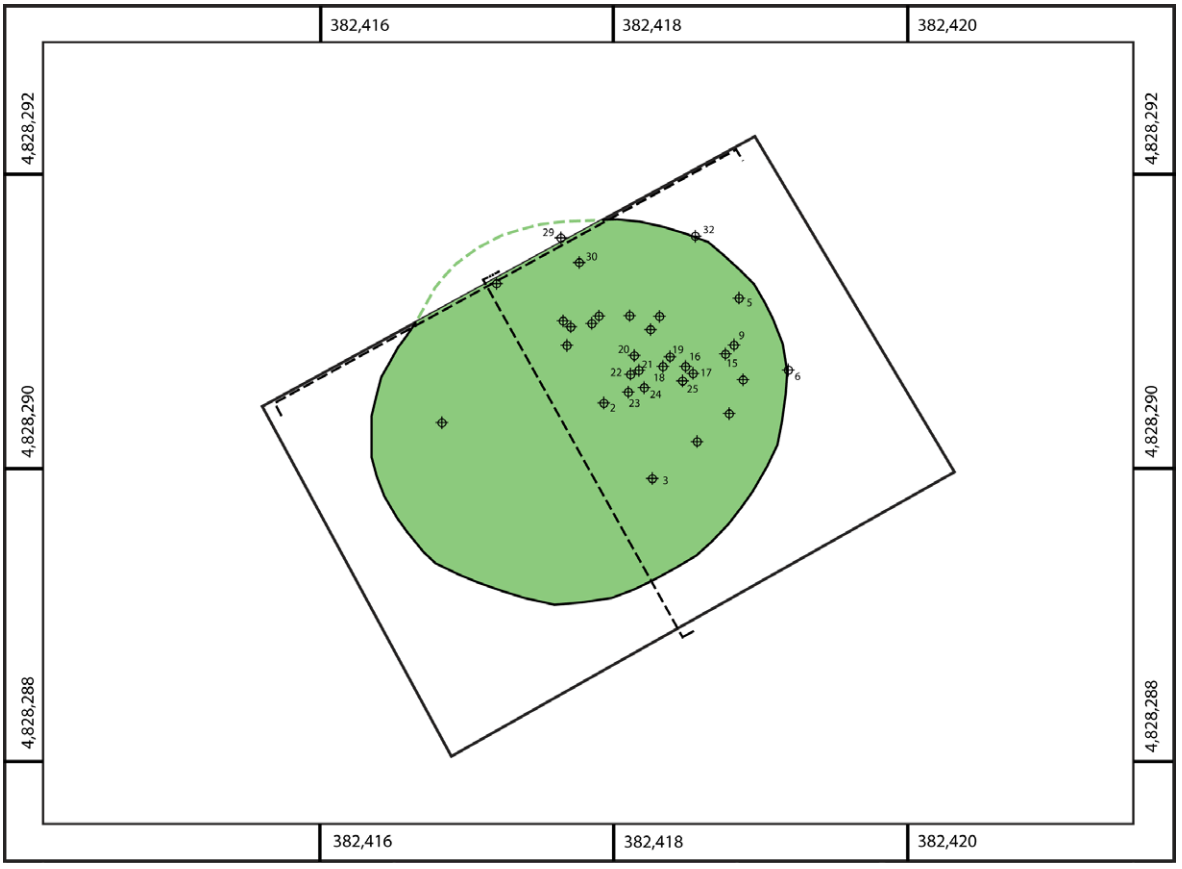


Fig. 4. Trench 3.1, planum 1. Overall plan of the pit 3.1.1 (with completion). The numbered markings indicate the measured finds of larger ceramic pieces in the course of the excavation (see chapter 9.1, table 9); the unnumbered markings relate to animal bone finds (figure by S. Conrad)



Fig. 5. Feature 3.1.1, quadr. A. Orthophoto of planum 2 (niv. 61.21) obtained from a SfM model (figure by M. Offermann)

charcoal and pottery finds, was the last recognisable anthropogenic activity. The uppermost layer, which was sure to be partially absorbed by the ploughed layer, seemed to have been formed by the deposition of material that had eroded up the slope (for the pottery found in the pit, cf. chapter 9.1).

8.2.3.2. Interpretation

The finds consist of mixed material from the Middle and Late Bronze Age, therefore the filling of the pit cannot be older than the Late Bronze Age (cf. chapter 9.1). This is confirmed by the ^{14}C data (cf. chapter 9.1, fig. 2, table 13, Nos. 168, 169, 171, 172).

The original purpose of the pit is unknown. Perhaps it was initially used to extract materials or to keep stocks. In the course of the backfilling, it was finally used as a waste pit. The middle layer b was heavily interspersed with ash and charcoal and contained numerous Late Bronze Age sherds. In addition, some residual pieces from the Middle Bronze Age were found in the overall backfill of the pit.



Fig. 6. Feature 3.1.1, quadr. A. Planum 2 (niv. 61.21) with socketed pottery fragments and bones of layer b. Detail (from northeast) (photo by M. Offermann)



Fig. 7. Feature 3.1.1. Negative of the pit, view from the east (photo by M. Offermann)



Fig. 8. Feature 3.1.1, profile between quadr. A and B. View from the east (photo by S. Conrad)

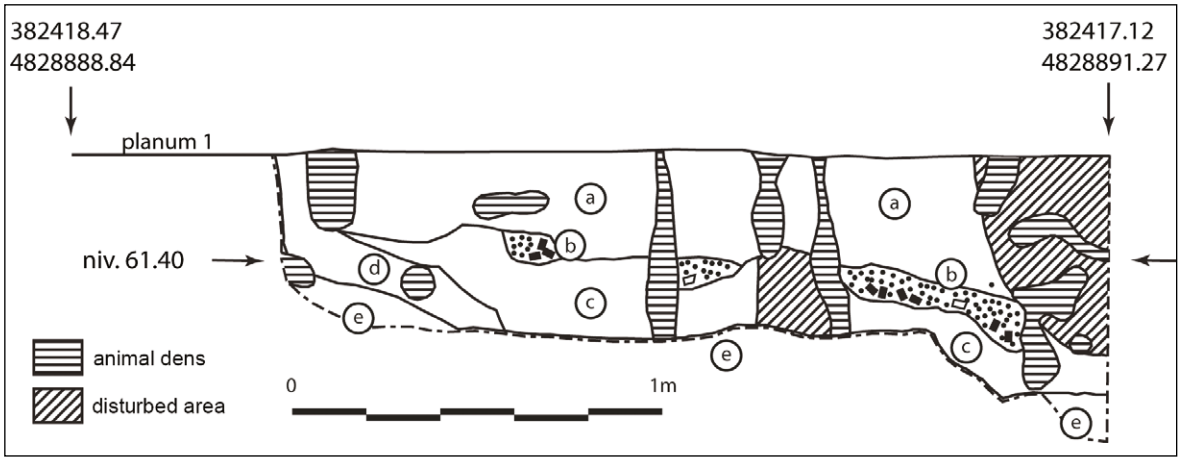


Fig. 9. Feature 3.1.1., profile between quadr. A and B (redrawing by S. Conrad after original drawing by J. Becher). a – pale yellowish grey, yellowish spotted; b – pale grey, ochre grey mixed; with charcoal, ash, bones; c – light yellowish-grey, slightly denser than a; d – (lateral fall) yellowish pale grey; e – sterile loess, with animal dens

ЯМА В СОНДАЖ 3.1

Свен Конрад, Райко Краус

(Резюме)

Геомагнитното проучване очерта неясни аномалии на обект 3 и по-конкретно на площта, ограничена от двоен ров и стръмен съвременен откос. Сондаж 3.1 е с размери 3,95 × 2,70 м и е разположен върху една от тях. Проучена бе яма 3.1.1 с неправилна овална форма и диаметри около 2,90 и 2,40 м. Дъното е сравнително плоско и дълбоко от 0,90 до 1,20 м спрямо съвременната



Fig. 10. Feature 3.1.1., north profile at the trench boundary (view from the south) (photo by M. Offermann)

повърхност. Северният дял на ямата е пресечен от животински дупки и човешки вкопавания. Материалът е смесен и датира от средния и късния бронзов период (вж. глава 9.1). Тази хронология се потвърди от ^{14}C датиране (вж. глава 9.1, fig. 2, table 13, №№ 168, 169, 171, 172).

Предназначението на ямата е несигурно. Може би е била използвана за извличане на строителни материали или за поддържане на продукти. Накрая е служила за изхвърляне на отпадъци.

8.2.4. Bronze Age. Conclusion

Lyudmil Vagalinski, Lyuba Traykova, Nadezhda Kecheva

Features dated to the 2nd millennium BC were excavated at site 3 only, within the middle part of the south-facing slope of the Tash Bair ridge (cf. the contributions by N. Kecheva et al., chapter 12, site 3). Six trenches were located based on the geophysical survey results in 2018 (cf. the contributions by L. Vagalinski et al., chapter 8.2.1, fig. 1). Three features were excavated: two of them within the enclosure – a pit in trench 3.1 (cf. the contributions by S. Conrad, R. Krauß, chapter 8.2.3), the remains of a burnt dwelling in trenches 3.2–5 (cf. the contributions by L. Vagalinski, L. Traykova, chapter 8.2.2), and part of a ditch (enclosure) in trench 3.6 (cf. the contributions by L. Vagalinski et al., chapter 8.2.1).

The finds in the pit consisted of mixed material dated to the Middle and Late Bronze Age, which indicates that the filling of the pit cannot be older than the Late Bronze Age (cf. the contributions by S. Conrad, R. Krauß, chapter 8.2.3), and which was confirmed by the ^{14}C data (cf. the contributions by S. Conrad, R. Krauß, chapter 8.2.3).

According to the stratigraphic observations the remains of a burnt dwelling dating to the Bronze Age were excavated; the building was found situated in a secondary position since it had slipped down the slope in a fold of the terrain (cf. the contributions by L. Vagalinski, L. Traykova, chapter 8.2.2). Finds associated with the dwelling, the bronze knife and the results of radiocarbon dating of two samples suggest chronology was between the 14th and 13th c. BC (cf. the contributions by R. Krauß, E. Pernicka, chapter 10.1).

The stratigraphic observations of the enclosure, excavated in trench 3.6, showed a possibility of two functional phases which occurred across a relatively short period of time (cf. the contributions by L. Vagalinski et al., chapter 8.2.1). According to the samples taken for radiocarbon dating of the enclosure, the ditch was built at the beginning of the 2nd millennium BC. The stratigraphic situation indicates that the ditch had been maintained/cleaned from about 1500–1300 BC up to the middle of the 1st millennium BC. Pottery fragments dating to the Early Iron Age (cf. chapter 9.1, table 9), as well as one dated to the Late Iron Age (cf. chapter 9.1, cat. No. P3/018), were also discovered associated with the enclosure.

The partially excavated area of the ditch, the pit, and the remains of a burnt dwelling in the enclosed area do not provide sufficient data to determine whether the enclosed area was a settlement or a ritual place. Only a quarter of the enclosure survived due to severe erosion or other environmental factors, as such, it was not clear whether the encircled area was an approximately round shape. However, it could be supposed that the two ditches were synchronous because they were parallel to each other. Reliable statements about this can only be given by further excavations of an additional ditch visible in the results of the 2018 geophysical survey. The ditches could be part of a settlement/ritual area created during the beginning of the 2nd millennium BC that had been systematically maintained in later periods. Overall, the geophysical and excavation results enrich the current archaeological information about circular enclosures from the Bronze Age in the Lower Danube region of south-eastern Europe.

БРОНЗОВА ЕПОХА. ЗАКЛЮЧЕНИЕ

Людмил Вагалински, Люба Трайкова, Надежда Кечева

(Резюме)

Структури от средния и късния бронзов период са открити само на обект 3, разположени в средната част на южния склон на рида Таш баир. Частично разкопаната площ на рова (сондаж 3.6), ямата (сондаж 3.1) и останките от опожарено жилище в ограденото пространство (сондажи 3.2 – 5) не дават достатъчно данни, за да се определи дали ограденият участък е бил селище, или ритуално място. Не е ясно дали оградената област е била приблизително кръгла, тъй като само една четвърт е оцеляла поради силна ерозия или от други фактори на околната среда. Предполагаме, че двата рова са синхронни, защото са успоредни един на друг. Надеждни твърдения за това могат да се дадат само от по-нататъшни разкопки на другия ров, видим в резултатите от геофизичното проучване от 2018 г. Те биха могли да бъдат част от отбранителна структура, създадена през средния бронзов период, който е бил систематично поддържан в по-късни периоди. Резултатите от геофизичните изследвания и разкопките обогатяват настоящата археологическа информация за кръгли заграждения от бронзовата епоха в района на Долен Дунав в Югоизточна Европа.

8.3. LATE IRON AGE

Several features dating to the Late Iron Age were uncovered during the excavation at sites 1 and 5 (cf. the contributions by N. Kecheva et al., chapter 12). The trench locations at site 1 were based on the results of the geophysical survey in 2018; linear anomalies (cf. the contributions by B. Ullrich et al., chapter 6.1). The geophysical survey of part of site 5 did not give clear anomalies so two trenches were placed based on the higher surface concentration of artefacts recorded during the field surveys in 2018

(Вагалински et al. 2019, 84). A ditch with a direction east-west was partially excavated in trench 1.1 at site 1, where two of the geophysical anomalies intersected perpendicularly (cf. the contributions by L. Vagalinski et al., chapter 8.3.1). Several pits, including a pit containing a child skeleton, were excavated in trenches 5.1 and 5.2 at site 5 (cf. the contributions by L. Vagalinski et al., chapter 8.3.3).

8.3.1. The Late Iron Age ditch in trench 1.1

Lyudmil Vagalinski, Lyuba Traykova, Nadezhda Kecheva

Description. In the spring of 2018 during field surveys, a rectangular earthwork fort was recorded (Вагалински et al. 2019, 84), measuring 200 × 200 m, in site 1. It is surrounded by a ditch and a rampart visible above the modern surface. The fort was first recorded during field surveys in 1999 (Вагалински et al. 2001a, 77). The team (L. Vagalinski, S. Conrad, L. Traykova, N. Kecheva, R. Krauß and German students) partially excavated this archaeological feature in the period August 28th – September 12th and September 18th – 23rd 2019 (Вагалински et al. 2020a, 1177).

Trench 1.1 was situated on the eastern ditch of the earthwork fort which has a north-south direction. At the same spot, another linear negative anomaly with direction east-west was located according to the results of the geophysical survey in 2018 (cf. the contributions by B. Ullrich et al., chapter 6.1) (fig. 1). The coordinates of the trench were created in GIS in WGS 1984 UTM Zone 35N coordinate system. GNSS receivers CHCNav i70 were used to trace the anomalies on the surface. The trench has an area of 49 m^2 and dimensions of 7 × 7 m. It was divided into two parts: eastern (1.1-E) and western (1.1-W) by a section with 0.9 m in width (fig. 1), and the modern surface was sloping from north to south and from west to east. The artefacts on the eastern ditch surface date to the Middle Ages and most particularly in the Early Middle Ages.

The surface layer of trench 1.1 was the ploughzone (about 0.4 m) and was removed by machines. The excavation continued at depth by hand and was carried out by workers. The excavations continued by removal of arbitrary levels. The first one measured ▼27.25 m in 1.1-E. With the excavation of an arbitrary level ▼27.25–27.00 m in the north-eastern part of the trench a high concentration of large Neolithic pottery fragments mixed with animal bones was recorded. With the excavation of the next arbitrary level ▼27.00–26.76 m in the north-eastern part of the trench Neolithic and Roman pottery fragments were recorded (figs. 2, 3). The artefacts from that corner were collected individually. This north-eastern part of trench 1.1-E was excavated separately with a context number 1.1.6. The concentration of artefacts continued at depth (figs. 4, 5). The borders of this dug feature were visible at level ▼26.00 m as well as at its cross-section by the Early Medieval ditch (fig. 6). With the removal of an arbitrary level ▼25.83–25.39 m the dug feature was completely excavated. Its bottom was recorded at ▼25.48 m. The excavated feature was cut longitudinally by the north section and transversely by the eastern section of trench 1.1-E.

The excavated level after machine work was a depth of ▼27.82 m in 1.1-W. After removing an arbitrary level ▼27.44–27.22 m in the northwestern part of the trench a triangular spot with a light yellow soil colour appeared (fig. 7). It looked like loess, but it contained artefacts that were collected separately from the dark soil in the rest of the trench. This corner was excavated separately and given context number 1.1.15 since it was within a different structure. After finishing the arbitrary level ▼27.22–27.00 m the light yellow strip with a triangular shape in the northwestern corner was enlarged in the eastern and southern directions. At a level of ▼26.78 m, it looked as if sterile soil had reached the northwestern corner (fig. 8). In the north-eastern part of trench 1.1-W and the western side of the Early Medieval ditch a section with different colours was recorded containing larger handmade pottery fragments. It appeared that the Early Medieval ditch cut through older dug feature. At a level of ▼26.38 m in depth, only the sections of the Early Medieval ditch in the northeastern and southeastern parts of 1.1-W were excavated. We continued excavating the northwestern corner from a level of ▼26.38 m in depth. The excavation in this area ended with the removal of an arbitrary level ▼25.77–25.57 m. The bottom of the younger feature was recorded at a level of about ▼25.85 m. Sterile soil was excavated

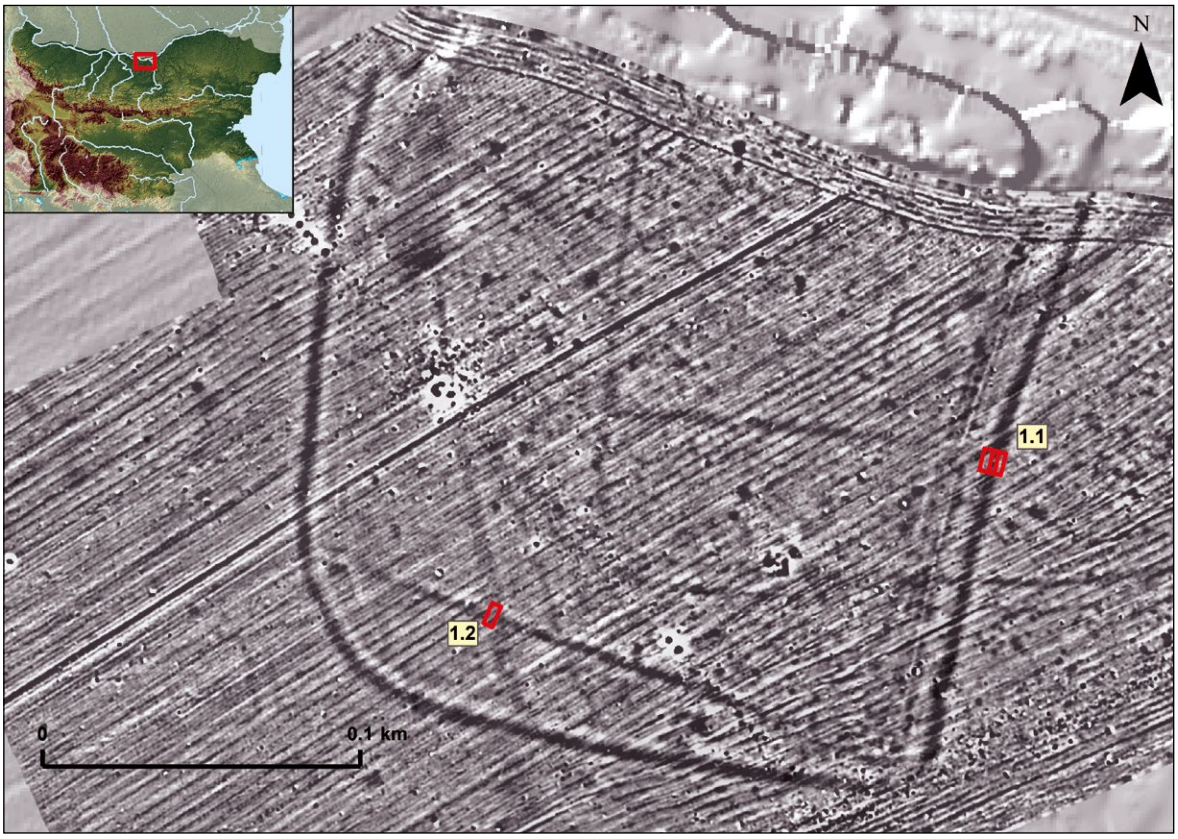


Fig. 1. Site 1, geophysical survey results in 2018 (cf. the contributions by B. Ullrich et al., chapter 6.1) and location of the trenches in 2019 (figure by N. Kecheva)



Fig. 2. Trench 1.1-E, level ▼26.76 m (photo by Lea Valcov)

beneath this level. The excavated feature was cut longitudinally by the north section and transversely by the western section of trench 1.1-W.

Analysis. The excavated features 1.1.6 in the northeastern corner of trench 1.1-E and 1.1.15 in the northwestern corner of trench 1.1-W belong to a ditch with east-west direction (fig. 9).

Wheelmade and handmade pottery fragments were recorded in their fill and especially in the arbitrary levels close to the bottom date this ditch to the Late Iron Age. Few pottery fragments in the



Fig. 3. Trench 1.1-E, NE corner, level ▼26.76 m (photo by S. Conrad)



Fig. 4. Trench 1.1-E, NE corner, level ▼26.67 m (photo by Lea Valcov)



Fig. 5. Trench 1.1-E, NE corner, level ▼26.60 m (photo by Lea Valcov)



Fig. 6. Trench 1.1-E, NE corner, level ▼26.00 m (photo by Lea Valcov)

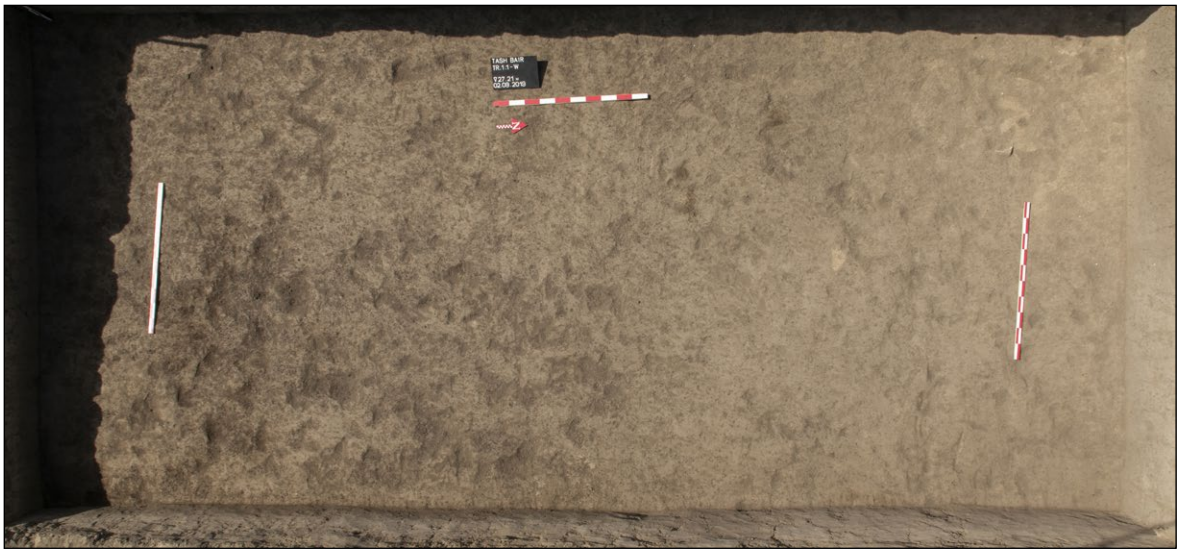


Fig. 7. Trench 1.1-W, level ▼27.21 m (photo by Lea Valcov)

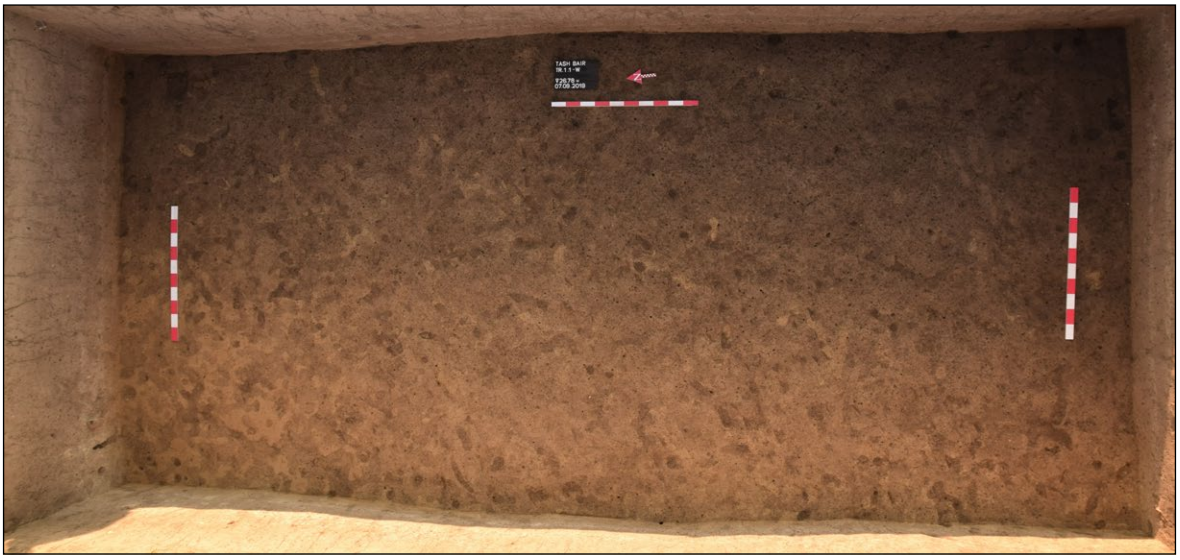


Fig. 8. Trench 1.1-W, level ▼26.78 m (photo by Lea Valcov)

upper layers of the ditch filling could be dated to 2nd–1st c. BC while the rest, which was of a significant amount, were dated to the 5th–3rd c. BC (cf. chapter 9.1). A fragment of a lamp was found that was dated to the last quarter of the 4th c. BC to the third quarter of the 2nd c. BC, but it could be determined for certain whether it was part of the ditch fill (cat. No. SF 47). We assume that the ditch was excavated during the first half of the Late Iron Age. The region is subject to constant strong erosion which prevents the certain recording of the ground level from which the ditch was dug. This is the reason why its depth could not be measured with certainty. According to the eastern section of trench 1.1-E and western section of trench 1.1-W, it could be reasonably assumed that its cross-section was trapezoidal (figs. 10, 11). Since it was cut from the northern section of trench 1.1 (fig. 12) it was not possible to determine its width. The minimum depth, according to the recorded level of the ditch was about 1.30 m, the minimum width at the top was about 2.60 m, and 1.30 m at the bottom (figs. 10, 11).

Parallels and interpretation. Ditches enclosing a rectangular area and dating to the Late Iron Age have been studied north and south of the Balkan Mountains in Bulgaria.

In the Historical and Archaeological Reserve Sboryanovo, near Sveshtari village, Isperih municipality, during a geophysical survey around a mound 39, a negative L-shaped anomaly was recorded.

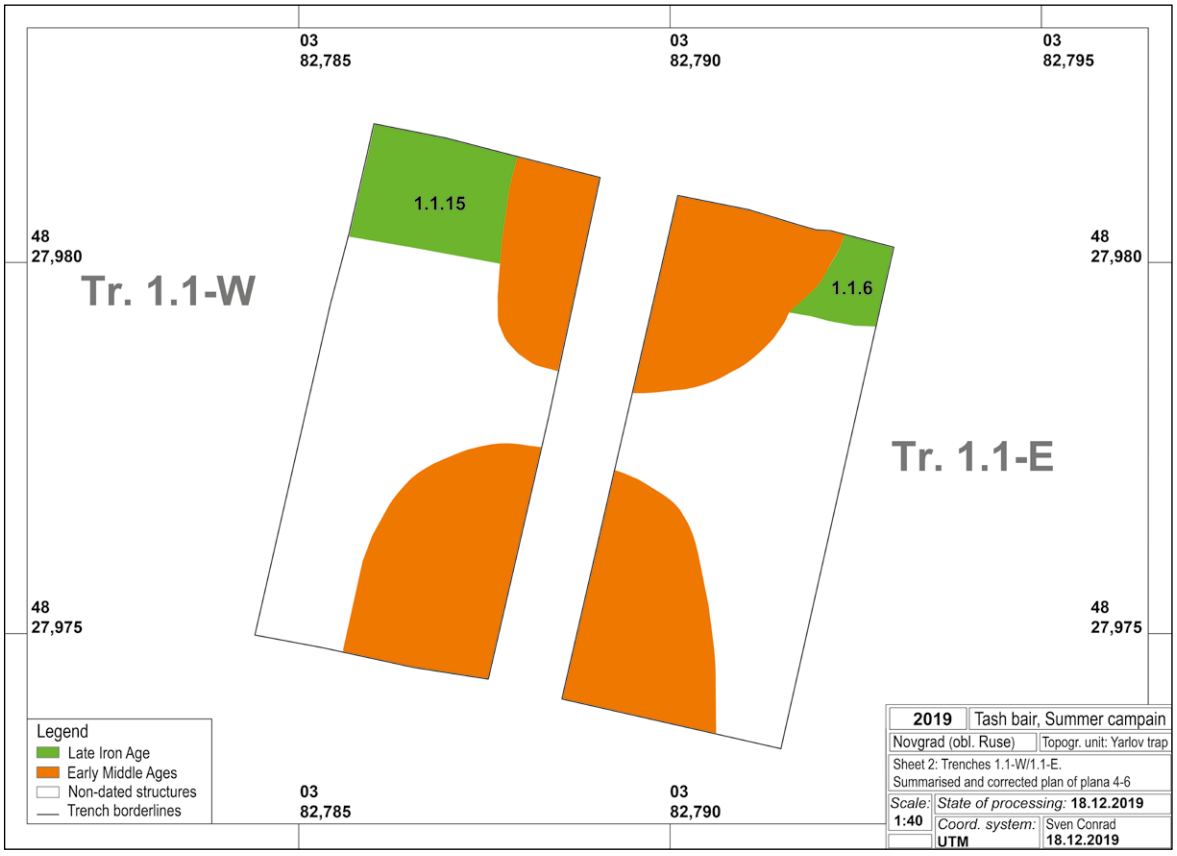


Fig. 9. Plan of the ditches in trench No. 1.1 (drawing by S. Conrad, adapted by L. Traykova)

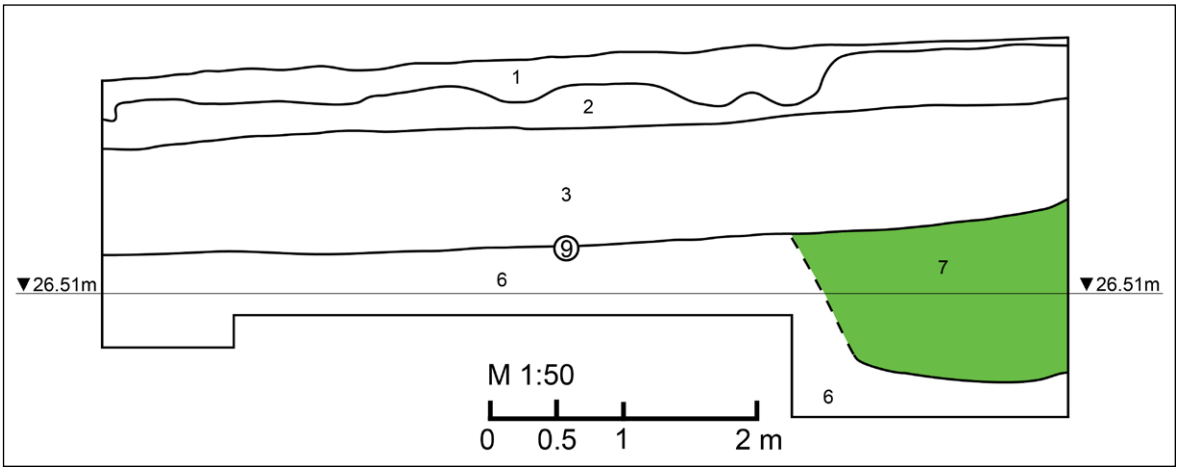


Fig. 10. Site 1. Trench 1.1-W, western cross-section: 1 – Loose and full of humus soil, greyish-brown layer – ploughzone. It contains pottery fragments. Pits of unrooted trees from an orchard are visible; 2 – Light brown loess, very dense layer, formed by erosion; it contained small pottery fragments, single charcoals, small pieces of burned clay, single small stones; 3 – Dark grey full of humus layer, but not as much as layer No. 1. It contained small pottery fragments, single small stones, small and scattered pieces of burned clay, lots of animal holes; 6 – Sterile yellowish-brown loess; 7 – Fill of earlier ditch with direction E–W, cut by the Early Medieval ditch. It contained ash strips, Late Neolithic pottery fragments, yellowish-brown loess lumps fallen from the ditch sides, single small stones; 9 – Early Medieval surface from which the ditch N-S was dug. It is almost the same as the surface of the other ditch probably because of the constant significant erosion (drawing and interpretation by L. Vagalinski, L. Traykova)

After the conducted excavations, a ditch with a rectangular-trapezoidal shape was recorded. It encircled an area of 840 m^2 around mound 39. The ditch has a wide upper part with dimensions between 6 and 10 m. It was funnel-shaped at a depth of about 0.5 from the level of recording. The sides were vertical at depth and the width was 1.90–2.20 m. The bottom was flat and the depth was 1–1.20 m (fig. 13). A probable entrance was recorded in the southern ditch with a width of 5 m. Most of the artefacts found during the excavations were part of the ditch fill. The site is interpreted as a ritual complex dated to around 200 BC. There is also a hypothesis that there was an external duplicating ditch at the southwestern corner of the excavated ditch (Гергова et al. 2017, 215–217; Гергова et al. 2018, 124, обр. 1, 125, обр. 2; Гергова et al. 2020, 500, обр. 1 и 2) (fig. 14).

Near Knyazhevo village, Topolovgrad municipality, an architectural complex under a mound has been excavated. The site is interpreted as "Fortified house of a ruler". Three periods of inhabitation were distinguished: 1st period – from the middle to the third quarter of the 4th c. BC to the first quarter to the 3rd c. BC, which is a period that is associated with the functioning of the house and its burning; 2nd period – second quarter – middle of the 3rd c. BC is associated with metal production; 3rd period – second half of 3rd c. BC is associated with building a mound over the central residential building and performing rituals around it. The building complex was surrounded by a wall and a ditch with a distance of 3 m from each other. The ditch width was 1.35–2.80 m while its depth was 0.55–1.05 m. A thick layer of ash and charcoal was discovered in the area of the southern ditch along a section of about 15 m. The researchers suppose that the probable entrance to the fortified site was located in that area. The entrance consisted of a massive wooden door, and the approach to it across the ditch was made on a wooden ramp. The functions of the ditch were water drainage and channels connected to the ditch have been discovered in the fence wall. A pit dug into the rock, shaped like an overflow to the ditch, was also discovered in front of one of these canals (Агре, Дичев 2017, 166, обр. 1; Агре, Дичев 2019, 140–141; Агре, Дичев 2020, 533–534) (fig. 15).

In Southern Dobrudzha two earthwork forts with a rampart and a ditch dated to the Late Iron Age were recorded. No archaeological excavations have been conducted on these sites. The first fort was located near the old Brestak village (in the lands of Golesh village, Kaynardzha municipality). It had an approximately triangular shape. Two of the sides were naturally protected by steep cliffs, and the third side of the southwest is protected by a rampart and a wide ditch. The surface of the rampart was intentionally burnt to a depth of 0.4 m. It is assumed that its outer side, at least to some extent, was additionally clad

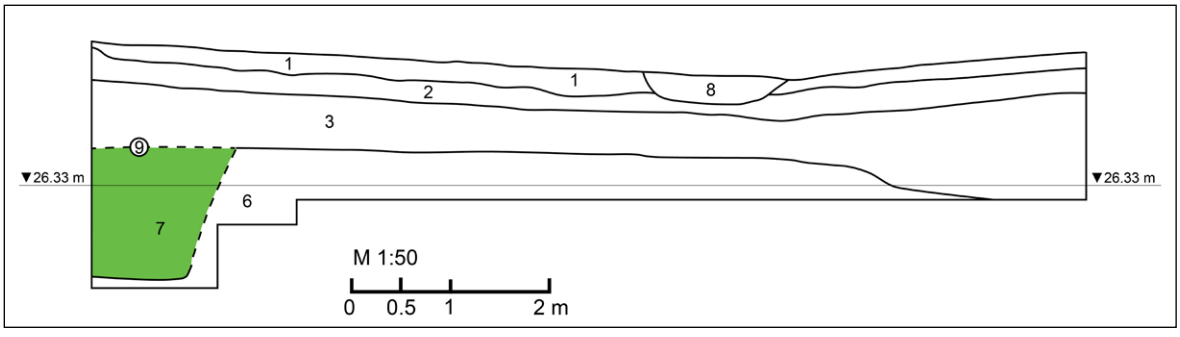


Fig. 11. Site 1. Trench 1.1-E, eastern cross-section: 1 – Loose and full of humus soil, greyish-brown layer – ploughzone. It contains pottery fragments. Pits of unrooted trees from an orchard are visible; 2 – Light brown loess, very dense layer, formed by erosion; it contained small pottery fragments, single charcoals, small pieces of burned clay, single small stones; 3 – Dark grey full of humus layer, but not as much as layer No. 1. It contained small pottery fragments, single small stones, small and scattered pieces of burned clay, lots of animal holes; 6 – Sterile yellowish-brown loess; 7 – Fill of earlier ditch with direction E–W, cut by the Early Medieval ditch. It contained ash strips, Late Neolithic pottery fragments, yellowish-brown loess lumps fallen from the ditch sides, single small stones, one flint; 8 – modern pit, loose and humus greyish-brown soil; 9 – Early Medieval surface from which the ditch N-S was dug. It is almost the same as the surface of the other ditch probably because of the constant significant erosion (drawing and interpretation by L. Vagalinski, L. Traykova)

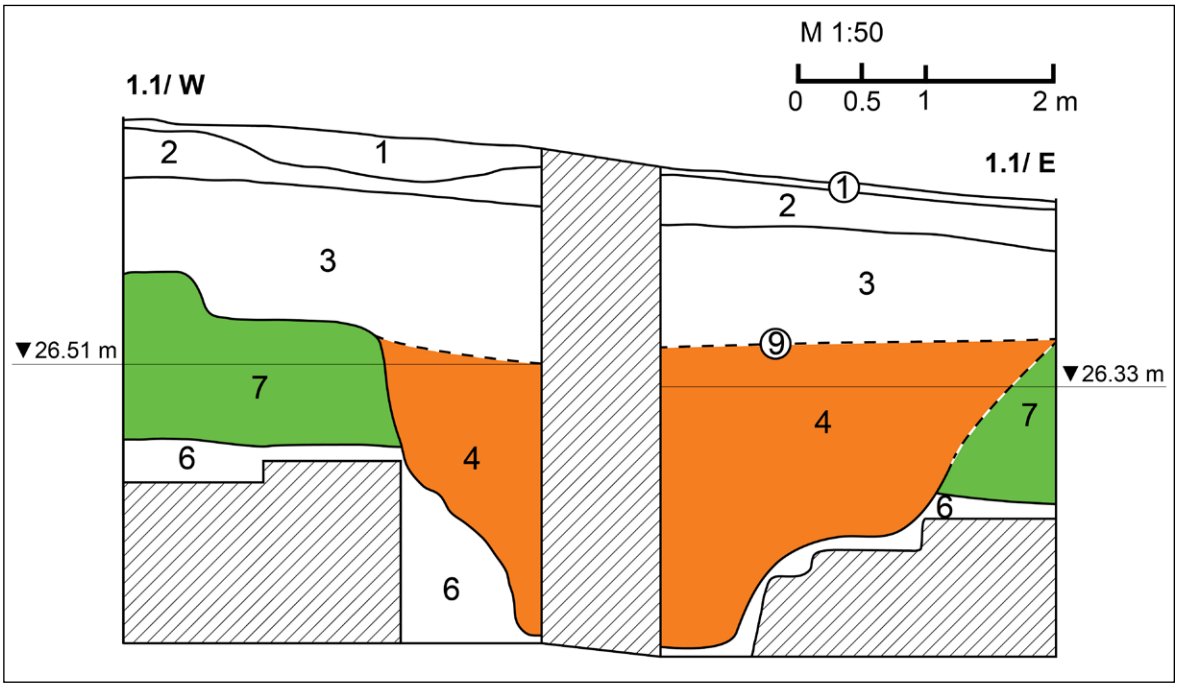


Fig. 12. Site 1. Trench 1.1, northern cross-section: 1 – loose and full of humus soil, greyish-brown layer – ploughzone. It contains pottery fragments. Pits of unrooted trees from an orchard are visible; 2 – Light brown loess, very dense layer, formed by erosion; it contained small pottery fragments, single charcoals, small pieces of burned clay, single small stones; 3 – Dark grey full of humus layer, but not as much as layer No. 1. It contained small pottery fragments, single small stones, small and scattered pieces of burned clay, lots of animal holes; 4 – Fill of the Early Medieval ditch, brownish-black dense layer; it contained pottery fragments, medium- to small-size stones, single animal bones, single lumps of loess, scattered charcoals, single small pieces of burned clay, single animal holes. The artefacts cluster in the lower part of the ditch, close to the bottom, pottery fragments and stones are larger than the ones in the upper layers. In the northern section of trench No. 1.1-W there were strips of fallen loess lumps from the eastern side of the Early Medieval ditch; 6 – Sterile yellowish-brown loess; 7 – Fill of earlier ditch with direction E–W, cut by the Early Medieval ditch. It contained ash strips, Late Neolithic pottery fragments, yellowish-brown loess lumps fallen from the ditch sides, single small stones, one flint; 9 – Early Medieval surface from which the ditch N-S was dug. It is almost the same as the surface of the other ditch probably because of the constant significant erosion (drawing and interpretation by L. Vagalinski, L. Traykova)

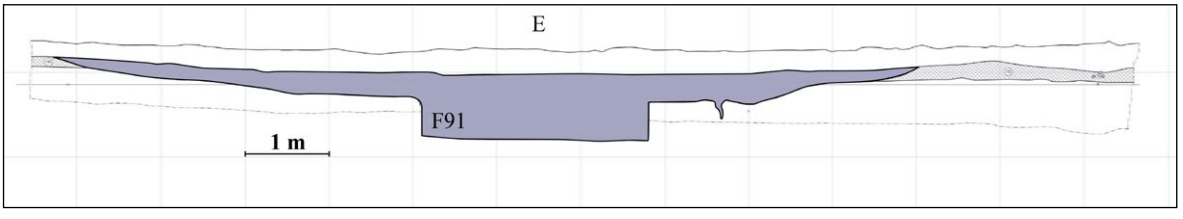


Fig. 13. Mound 39 near Sveshtari village, Isperih municipality, eastern profile of S9 with the ditch F91 (after Герова et al. 2018, 124, обр. 2)

by large flat stones of irregular shape, which were visible in various places in the ditch. The ditch had a trapezoidal cross-section, a depth of about 4.70 m, and the width at the bottom reached 1.2 m (fig. 16). The other fort is located near Brestnitsa village, Tervel municipality. It has an approximately rectangular shape. Three of its sides were naturally protected by steep cliffs. The fourth north-western side was protected by an arched ditch and rampart, and with a protected area are of about 2 ha. The cross-section of the rampart was V-shaped, 10 m wide, and with a visible depth of 1.5 m (fig. 17). According to the observations of the author, both sites lack a berm between the rampart and the ditch (Торбатов 2010, 149–152, 155, обр. 1.6, 156, обр. 2.а, б, 158, обр. 4.а).

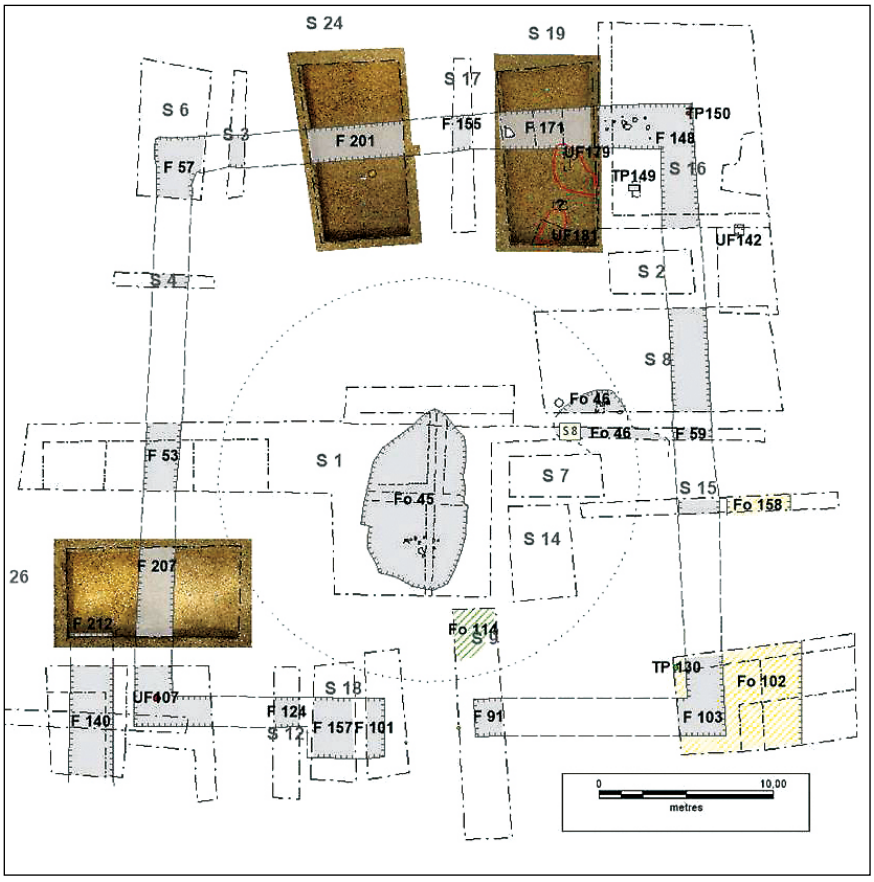


Fig. 14. Mound 39 near Sveshtari village, Isperih municipality, general plan of the excavated areas of the central part of sanctuary (after Гергова et al. 2020, 500, обр. 2)

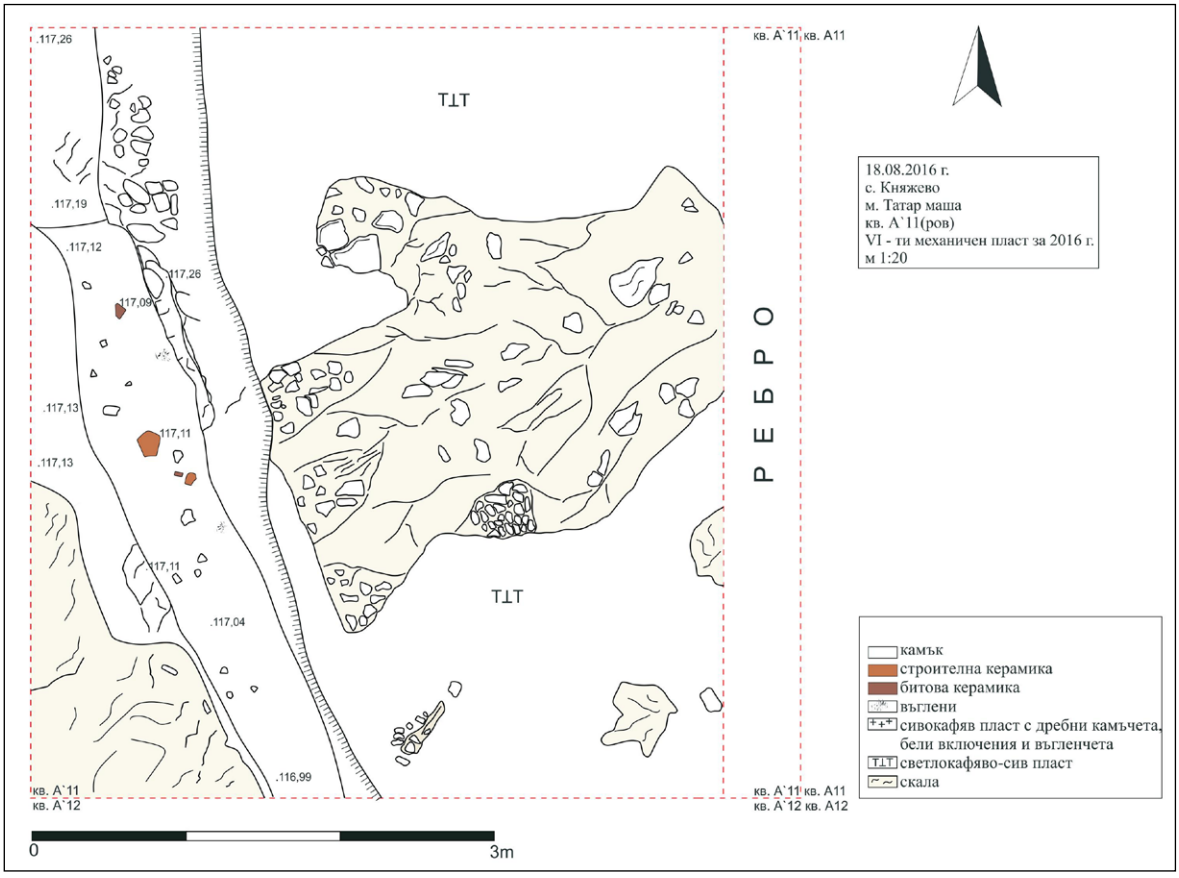


Fig. 15. Site near Knyazhevo village, Topolovgrad municipality, the ditch at the western part of the site (Sq. A11) – VI mechanical layer (after Агре, Дичев 2017, 166, обр. 1)

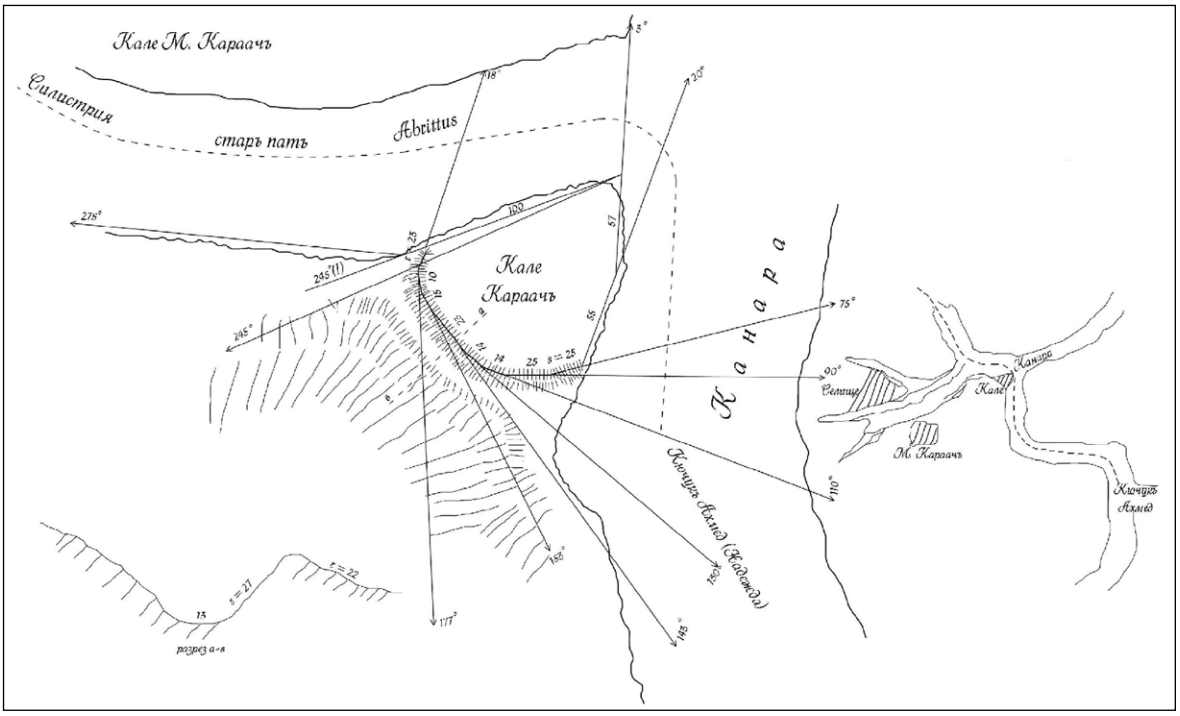


Fig. 16. Sketch of the fortress Kale Karaach near Brestak village, Silistra district (after K. Škorpil cited in Торбатов 2010, 155, обр. 1.б)

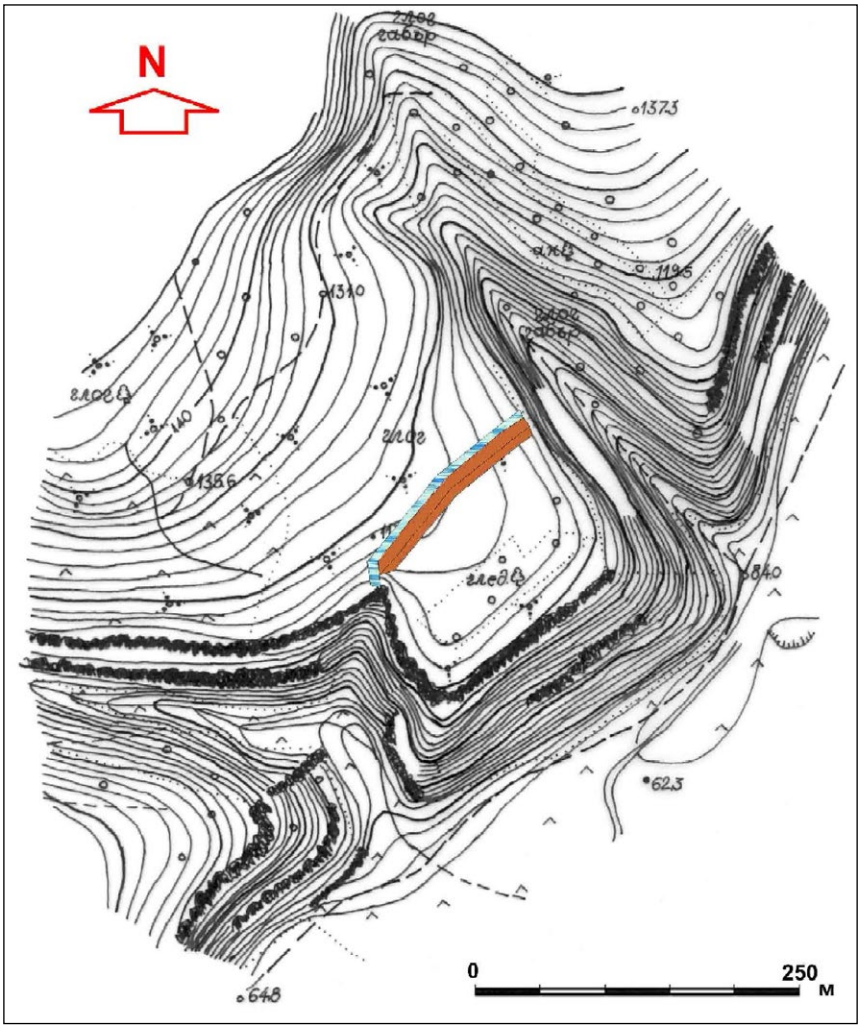


Fig. 17. Plan of the earthen fortification in the locality Domuz azman near Brestnitsa village, Dobrich district (after Торбатов 2010, 158, обр. 4.а)

Due to the limited excavations, there is not enough data to determine the purpose of the ditch in trench 1.1 or to be accurate for the size of the enclosed area. The results of the geophysical survey of site 1 (fig. 1) for this ditch were not definite. A rough right angle recorded in the approximate centre of the Early Medieval earthwork fort suggests that it is the southwestern end of a rectangular or trapezoidal enclosed area. No geophysical anomalies have been recorded to delineate a closed space to the east and north. A possible explanation is that the eastern Early Medieval ditch repeated the route of the older ditch in its northern part. The northern side of the enclosed area may fall under the modern dirt road or it could be located outside the terrain on which a geophysical survey was conducted. Site 1 had been inhabited for a long time during the Late Neolithic, Iron Age, Roman period, Late Antiquity and Early Middle Ages (Вагалински et al. 2019, 84; cf. the contributions by N. Kecheva et al., chapter 12, site 1). It can be assumed that the Late Iron Age ditch protected a settlement with an area of at least 1 ha. It is not clear why the nearby previous earthwork fort was abandoned (cf. the contributions by L. Vagalinski et al., chapter 8.2.1).

РОВ ОТ КЪСНАТА ЖЕЛЯЗНА ЕПОХА В СОНДАЖ 1.1

Людмил Вагалински, Люба Трайкова, Надежда Кечева

(Резюме)

Описание. Сондаж 1.1 е заложен върху източния ров (с направление север – юг) на земленото укрепление, където според резултатите от геофизичното проучване (вж. приноса на Б. Улрих и др., глава 6.1) се пресича перпендикулярно с друга, вкопана линейна аномалия с направление изток – запад (fig. 1). Сондажът е с площ 49 м^2 и размери 7 х 7 м, разделен на източен (1.1-E) и западен (1.1-W) от ребро с широчина 0,9 м (fig. 1). Теренът тук е с наклон от север на юг и от запад на изток. Подемният материал от източния ров на земленото укрепление показва, че той е средновековен от периода на Първата българска държава (681 – 1018 г.).

Повърхностният пласт в сондаж 1.1 от обработваема почва (около 0,40 м) беше отнет със земекопна техника. В дълбочина работата продължи на ръка. В североизточния ъгъл на сондаж 1.1-E разкрихме висока концентрация на подемния материал (figs. 3, 4, 5), който беше отделен. Регистрирахме вкопана структура с номер 1.1.6, която беше проучена отделно.

На ▼26,00 м се очертаха границите на тази вкопана структура в североизточния ъгъл, както и нейното прерязване от ранносредновековния ров (fig. 6). С механичен пласт ▼25,83–25,39 м в североизточния ъгъл беше достигнато дъното на вкопаната структура на ▼25,48 м и стерилът. Проучената структура е прерязана надлъжно от северния профил и напречно от източния профил на сондажа.

В 1.1-W след отнемане на механичен пласт ▼27,44 – 27,22 м в северозападния ъгъл се очерта триъгълно петно със светложълт цвят на пръстта (fig. 7), която прилича на льос, но в нея се съдържат материали, които отделихме от тези в тъмната пръст от останалата част на сондажа. Този ъгъл също се проучи отделно, тъй като се отличава като различна структура в сондажа с номер 1.1.15. Проучването в този участък приключи с механичен пласт ▼25,77 – 25,57 м. Установихме, че дъното на по-ранната структура е на дълбочина около 25,85 м и надолу е стерил. Проучената структура е прерязана надлъжно от северния профил и напречно от западния профил на сондажа.

Анализ. Проучените структури 1.1.6 в североизточния ъгъл на 1.1-E и 1.1.15 в северозападния ъгъл на 1.1-W принадлежат на ров с направление изток – запад (fig. 9).

Керамичните фрагменти, изработени на колело и ръка, открити в неговия пълнеж и главно тези от пластовете близо до дъното, позволяват този ров да се датира в късния железен период. Няколко фрагмента от горната част на запълването на рова могат да се отнесат към

II – I в. пр. Хр.; останалите, които са значително количество, са отнесени към V – III в. пр. Хр. (вж. глава 9.1). Открит е и фрагмент от лампа, който се датира в периода от последната четвърт на IV в. пр. Хр. до третата четвърт на II в. пр. Хр., но не може да се определи със сигурност дали е част от пълнежа на рова (кат. № SF 47). Допускаме, че ровът е изкопан през първата половина на късния железен период. Районът е подложен на постоянна силна ерозия, което възпрепятства сигурното определяне на дневната повърхност, от която е бил вкопан. Това е причина да не може да се измери със сигурност неговата дълбочина. Според източния профил на 1.1-E и западния профил на 1.1-W може с основание да се предположи, че неговото напречно сечение е било трапецовидно (figs. 10, 11). Поради факта, че е прерязан и от северния профил на сондаж 1.1 (fig. 12), не може да се установи каква е неговата широчина. Минималната дълбочина, според нивото на регистриране на рова, е около 1.30 м, минималната широчина в горната част е около 2,60 м, а при дъното около 1,30 м (figs. 10, 11).

Паралели и интерпретация. Ровове, ограждащи правоъгълно пространство, датирани в късния железен период, са проучени северно и южно от Стара планина в рамките на България.

В Историко-археологическият резерват „Сборяново" край с. Свещари, общ. Исперих, след проведените разкопки е разкрит ров с правоъгълно-трапецовидна форма. Той огражда площ от 840 м^2 около могила 39. Оформен е фуниевидно на около 0,5 м от нивото на разкриване, в дълбочина стените са отвесни, а дъното е равно (fig. 13). Обектът е интерпретиран като ритуален комплекс, датиран около 200 г. пр. Хр. Предположено е наличие на външен дублиращ ров при югозападния ъгъл на проучения ров. (Гергова et al. 2017, 215 – 217; Гергова et al. 2018, 124, обр. 1, 125, обр. 2; Гергова et al. 2020, 500, обр. 1 и 2) (fig. 14).

Край с. Княжево, общ. Тополовград, е проучен архитектурен комплекс под могилен насип. Обектът е интерпретиран като „укрепен владетелски дом". Разграничени са три периода на обитаване на мястото. Комплексът от сгради има оградна стена, около която от всички страни има ров, отстоящ на около 3 м от нея. Функциите на рова са били отводнителни за извеждане на атмосферна и битова вода. В оградната стена са разкрити канали, свързани с рова. Пред един от тези канали е разкрита и яма, вкопана в скалата, оформена като преливник към рова. (Агре, Дичев 2017, 166, обр. 1; Агре, Дичев 2019, 140 – 141; Агре, Дичев 2020, 533 – 534) (fig. 15).

В Южна Добруджа са документирани две землени укрепления с вал и ров, датирани в късния железен период. На обектите не са извършвани археологически разкопки. Едното укрепление попада в землището на изселеното през 1965 г. с. Брестак, общ. Кайнарджа. Има приблизително триъгълна форма. Две от страните са естествено защитени от стръмни скали, а третата страна от югозапад е защитена с вал и широк ров. Ровът има трапецовидно напречно сечение (fig. 16). Другото укрепление се намира край обезлюденото с. Брестница, общ. Тервел. Има неправилна правоъгълна форма. Три от страните му са естествено защитени от стръмни скали, а четвъртата северозападна страна е преградена с дъговидно извити навън ров и вал, защитената площ е около 20 дка. Напречното сечение на вала е V-образно (fig. 17). Според наблюденията на автора и при двата обекта липсва берма между вала и рова (Торбатов 2010, 149 – 152, 155, обр. 1.б, 156, обр. 2.а, б, 158, обр. 4.а).

Поради ограничените като площ разкопки не разполагаме с достатъчно данни, за да определим предназначението на рова в сондаж 1.1, нито да заявим размера на ограденото пространство. Резултатите от геофизичното заснемане на обект 1 (fig. 1) по отношение на този ров не са категорични. Регистрираният почти прав ъгъл в приблизителния център на ранносредновековното землено укрепление предполага, че е югозападен край на правоъгълно или трапецовидно оградена площ. Не са регистрирани геофизични аномалии, които да очертаят затворено пространство от изток и от север. Възможно обяснение е, че източният ранносредновековен ров е повторил трасето на по-стария ров в северната си част. Северната страна на ограденатa площ може да попада под съвременния черен път или да се намира извън терена, на

който е направено геофизично изследване. Може да се предположи, че късножелезният ров е защитавал селище с площ поне 10 дка. Не е ясно защо е било изоставено близкото предходно землено укрепление (вж. приноса на Л. Вагалински и др., глава 8.2.1).

8.3.2. The Early Roman pits 5.1.2 and 5.1.6

Sven Conrad

8.3.2.1. Preliminary remarks

The geomagnetically investigated area could not be used for the positioning of the test trench planned at site 5, as it was occupied with a permanent field crop. However, in order to increase the probability of capturing possible structures, the trench was placed at the edge of the adjacent field to the south, i.e. near a loose concentration of anomalies in the western part of the geomagnetic map (fig. 1; 2).

After obtaining permission from the local farmer, the maize growing on this site could be harvested on an 8 × 6 m area. Then, the 6 × 3 m trench was set with an orientation west-north-west - east-south-east and the manual removal of the arable layer (niv. approx. 21.07 m) to planum 1 (level 20.68 m) began. This was carried out in two layers, with some pottery fragments being recovered in the process. Planum 1 was roughly 10 cm below the surface of the alluvial clay, which had not been disturbed by ploughing. After cleaning, six structures 5.1.1–5.1.6 were recognised and documented (fig. 3; 4).

During the further investigation, three features (5.1.1; 5.1.3; 5.1.4) were excluded as archaeological structures because they could be traced back to different disturbances (animal dens and root channels). The other three structures, 5.1.2; 5.1.5 and 5.1.6 (of which the last two were only partially recorded in section) were excavated and documented. After the excavation of a grave in the southern half of the feature 5.1.5, the trench was expanded to the south with dimensions of 2.50 × 1.50 m (trench 5.2).

8.3.2.2. The features 5.1.2 und 5.1.6. Excavation and stratigraphy

Feature 5.1.2 was situated in the western part of the trench. In planum 1, it had a round outline with a diameter of approx. 1.80 m. The feature was largely excavated within its limits, i.e. in the negative. The upper section had an irregular funnel shape down to a depth of 40 cm below planum 1 (niv. 20.30 m), through which the diameter narrowed to 0.95 m. The upper part was followed by a conical shape, which reduced the diameter to approx. 0.60 m at a depth of approx. 1 m (niv. 19.75 m) (fig. 5; 6). The pale brown filling (a) in the upper part of the pit had a downward-bending contour, likely due to the sagging of the material after the lower pit filling was compressed. In the middle part, there was a layer (b) of brown, humous clay with some yellowish spots. In the profile some pottery and daub fragments as well as pieces of charcoal were recognised, as before in planum 1.

The bottom of the pit could not be determined with certainty since the loamy-sandy layer (c) in the lowest part hardly differed in consistency and colour from the adjacent sand layer, which was also due to the increasing moisture with the depth. According to our observations, the feature had a depth of about 1 m under planum 1. Therefore, the bottom was at approximately 19.75 m.

After the profile was documented (down to a depth of 1.08 m below planum 1 = level 19.72 m), the second half of the backfill was removed. Afterwards, the sondage was deepened further into the sandy soil (e) to a level of approximately 19.20 m without further observations being made.

In the backfilling of the pit, in addition to pieces of charcoal and a few daub pieces, only ten relatively small pottery fragments were found (cf. chapter 9.1). There are three fragments of Early Roman amphorae, as well as a fragment of grey wheel-made fabric, and six fragments of handmade ware in the late Iron Age manner. Due to their small size, none of these fragments could be typologically determined.

The unusual shape of the pit and the apparently targeted digging into a water-bearing layer could suggest an interpretation of the feature 5.1.2 as a simple well, especially since the few, very small pottery finds do not support the interpretation of its function as a waste pit.



Fig. 1. View from site 3 in south-easterly direction on site 5 with the trench 5.1/2 under work (photo by S. Conrad)

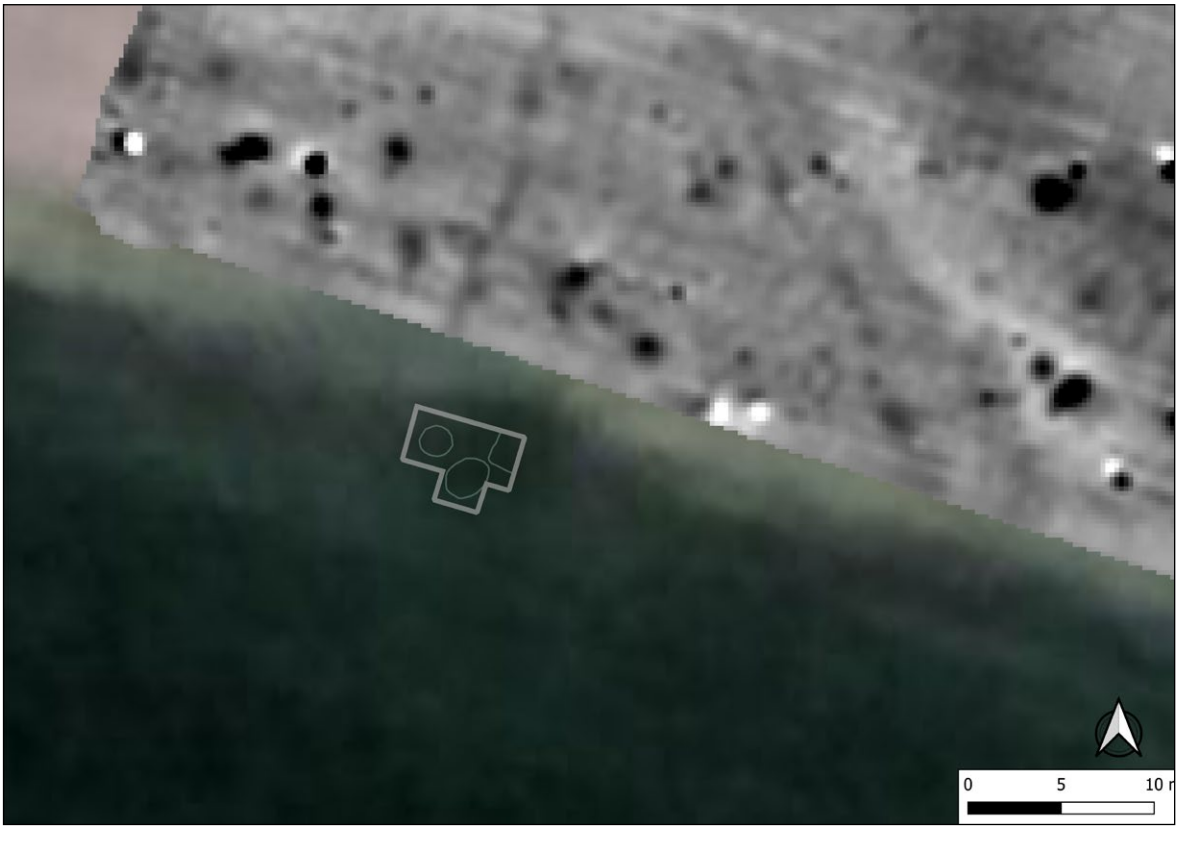


Fig. 2. Position of the trench 5.1/2 in relationship to the geomagnetically mapped area on site (figure by S. Conrad)



Fig. 3. Planum 1 of trench 5.1/2. View from the north (photo by S. Conrad)

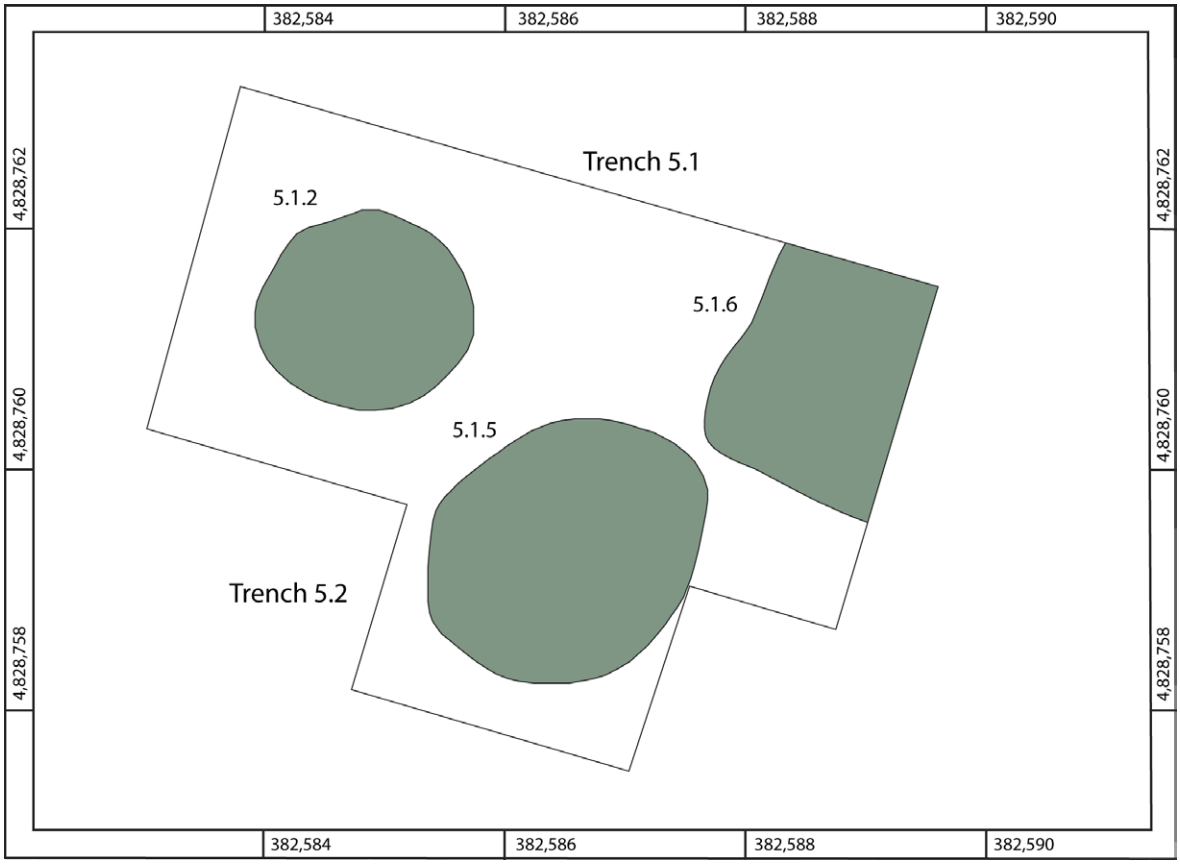


Fig. 4. Excavation map of trench 5.1/2 (without excluded features) (figure by S. Conrad)

Feature 5.1.6. was situated in the northwest corner of section 5.1 but was only partially recorded. The maximum north-south extent of the partial feature was 2.15 m, and the maximum east-west extent was 1.65 m. The feature could have had an approximately rectangular or trapezoidal overall shape (with rounded corners) in accordance with the relatively straight outlines. However, overall size and exact outline are not known.

After the excavation of the entire feature within the trench, the profile at the eastern section boundary was documented. It shows a slightly irregular, funnel-shaped outline with a narrow, slightly rounded bottom. The pit, calculated from the lower edge of the field horizon, was approx. 0.99 m deep (bottom at 19.92 m level) (fig. 7; 8).

When the filling of the pit was excavated, a total of 14 ceramic fragments were found (fig. 8). Among them, there are sherds of the grey wheel-made variety, and handmade wares in the manner of the Late Iron Age, as well as two fragments each of Early Roman amphorae and tableware (for the pottery finds cf. chapter 9.1). Consequently, the pit can likely be dated to the 1st century AD.

Inferring from the pit shape, it was probably not intended for food storage, but rather used for the extraction of building material. As with pit 5.1.2, it is not possible to decide with certainty whether the ceramic fragments ended up in pit 5.1.6. accidentally or deliberately as waste. The latter is less likely, because similarly to pit 5.1.2, no animal bones were found in pit 5.1.6.

8.3.2.3. Results and interpretation

In trench 5.1/2, three different features were examined. Feature 5.1.6 is most likely a pit for obtaining building material, while 5.1.2 is a possible scoop pit. The burial of a child was discovered on the bottom of pit 5.1.5 (cf. the contributions by L. Vagalinski et al., chapter 8.3.3).

The inventories suggest a dating around the middle, or the 2nd half of the 1st century, i.e. in the first decades of the Roman occupation. For comparison, there are no Roman finds in the Late Iron Age pit complexes of the 2nd and 1st century BC in Ruse (V. Varbanov, Ruse; *pers. comm.*). In this respect, the end of that pit field suggested by V. Varbanov (Върбанов 2013d, 39) in the last quarter of the 1st century, i.e., before Domitian's Dacian wars, seems likely to have been set too late.



Fig. 5. Feature 5.1.2. Profile (view from the north) (photo by S. Conrad)

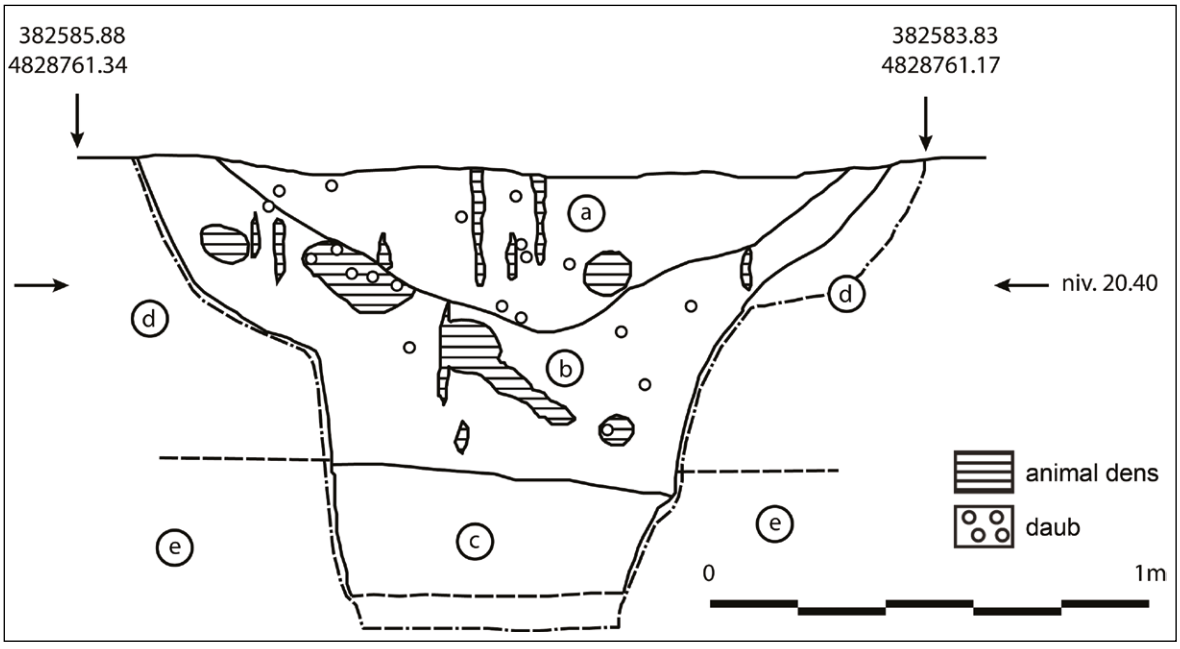


Fig. 6. Feature 5.1.2. Redrawing of the profile (redrawing by S. Conrad after original drawing by J. Becher); a – pale brown; loamy weakly humous; pieces of daub and charcoal. b – brown, with some yellowish spots; loamy, mixed with humous; pieces of daub. c – dark grey, spotty; loamy-sandy, humous. d – yellowish, with grey-brown spots; loamy (native; alluvial). e – brown; loamy-sandy (native; alluvial)



Fig. 7. Feature 5.1.6. Profile (view from the northwest) (photo by S. Conrad)

However, on the other hand, numerous Roman imported objects from the 1st and early 2nd century were found in the Piroboridava fortification in Eastern Dacia libera (Vulpe, Teodor 2003, 89-95 fig. 235–242).

Several vessels from the features 5.1.2, 5.1.5 and 5.1.6, especially the Roman finds, fit particularly well into the spectrum of finds from pits I and II, in sector X of Novae. These were dug during the wood

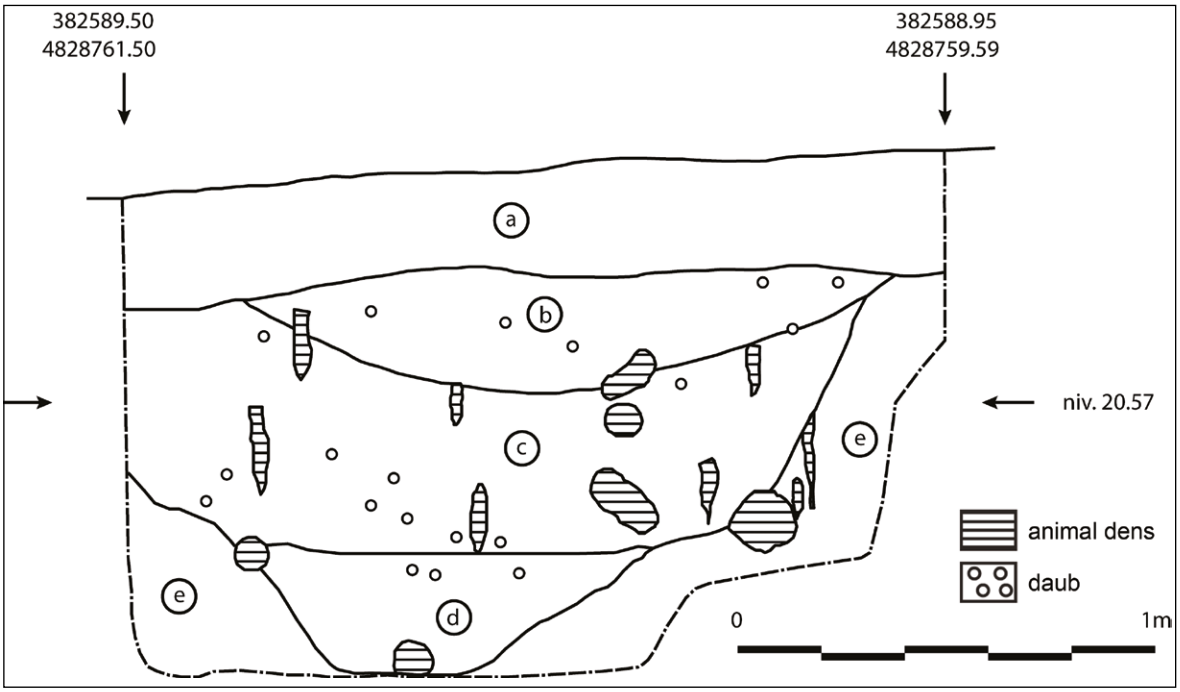


Fig. 8. Feature 5.1.6. Redrawing of the profile (redrawing by S. Conrad after original drawing by J. Becher); a – dark greyish brown; humous, loamy (arable layer). b – greyish brown, slightly pale and yellowish mixed; loamy; some daub pieces and small spots of limestone. c – greyish brown; loamy; some daub pieces and very few small spots of limestone. d – dark brown; loamy humous. e – yellowish, with grey-brown spots; loamy (native; alluvial)

and earth phase of the legionary camp in the middle or third quarter of the 1st century (Генчева 2002, 16–17; 82–92; 94–97; 100–102). It can therefore be assumed with some certainty that the three pits including the grave in pit 5.1.5 were established at this site when the Romans had already taken control of this section of the Danube[4].

The diverse character of the features 5.1.2, 5.1.5 and 5.1.6, and also the pattern of the geomagnetic mapping of the anomalies at site 5, give a possible indication that these are individual features on the edge of a settlement. The settlement could be indicated by a concentration of features and finds in a north-easterly direction (cf. the contributions by N. Kecheva et al., chapter 12, site 5).

РАННОРИМСКИ ЯМИ 5.1.2 И 5.1.6

Свен Конрад

(Резюме)

В сондаж 5.1, който е създаден в ареала на обект 5 в низината на р. Янтра, бяха идентифицирани и проучени три структури. Докато кръглата яма 5.1.2 може да бъде за черпене на вода, неправилната яма 5.1.6 много вероятно е създадена за изваждане на строителен материал. В насипа са открити относително малко находки. В допълнение към някои керамични фрагменти от късната желязна епоха са открити и ранноримски предмети. Двете ями, както и яма 5.1.5 с детското погребение датират към средата или втората половина на I в. сл. Хр.

Според геомагнитното картиране ямите са разположени много вероятно в периферията на малко селище, заобиколено от бивш криволичещ меандър на р. Янтра.

4 Cf. the dissenting opinion especially for the dating of the grave of L. Vagalinski et al., chapter 8.3.3, on which we will comment elsewhere.

8.3.3. The grave in pit 5.1.5

Lyudmil Vagalinski, Lyuba Traykova, Nadezhda Kecheva

Description: Trench 5.1 was located within the scatter of site 5 south of the area investigated by the geophysical survey (fig. 1). It was situated in the lowlands, encompassed by an old meander of the Yantra River. The location of trench 5.1 was consistent with the higher concentration of the artefacts recorded during the field surveys in the spring of 2018. The team (L. Vagalinski, S. Conrad, L. Traykova, N. Kecheva, S. Sabkova and German students) excavated trench 5.1 during August 24th – September 12th, 2018 (Вагалински et al. 2019, 84).

The total area of the trench was 18 m^2 with dimensions of 6 m along the northwest-southeast axis and 3 m along the northeast-southwest axis. The modern surface was flat. A GNSS receiver was used to measure the coordinates of the corners of the trench. Arbitrary levels were used and the excavation was carried out by hand by workers. Several pits were excavated in the trench (fig. 2). After the removal of the surface layer and reaching a level ▼20.68 m three pits were recorded in plan (fig. 3). Pit 5.1.5 was cut by the southern section of the trench. Initially, only the northwestern quarter of the pit was excavated so that half of the recorded pit could be investigated. At a level ▼19.75 m, a left side of a human skull and large handmade pottery fragments were excavated (fig. 4) together with the postcranial bones of a human skeleton. The excavated area was expanded to the west and north around the remains because it was too narrow and inconvenient to work (fig. 5). The excavation continued in the northeastern quarter of pit 5.1.5 where the area was also expanded to allow work to continue. A 0.4 m control section was left between the two quarters (fig. 6). The removed arbitrary levels to a level ▼19.69 m did not contain pottery fragments, animal or human bones or charcoals. Only a few small pieces of burnt clay were found. Work stopped in the northeastern quarter of the pit (fig. 7), after which sections were drawn, and the control section between the two quarters of pit 5.1.5 was removed (figs. 8, 9).

A southern extension of trench 5.1 was excavated in the place where it was assumed that the southern part of pit 5.1.5 was located. This was trench 5.2 which measured 2.50 m along the northwest-southeast axis and 1.50 m along the northeast-southwest axis (fig. 1). The layer between the ploughzone and the level of recording on pit 5.1.5 (fig. 9, 5a) was distinguished by density and colour, but it also contained the same Roman pottery fragments that were found in the upper layer (fig. 9, 5). Moreover, the upper part of a Roman amphora (fig. 10; cf. chapter 9.1, cat. No. P5/010) was found in both layers (fig. 9, 5, 5a). This indicated that the layer beneath the ploughzone (fig. 9, 5a) may have acquired a higher density and a lighter colour due to natural sedimentation processes. At a level of ▼20.70 m, the southern part of pit 5.1.5 was recorded as a darker soil than the surrounding lighter clay (fig. 11). Larger pottery fragments continued to emerge in the upper part of the fill of the pit (fig. 12). After the removal of the pit fill, it was found that the pit narrowed with depth (fig. 13). It was excavated into the natural ground. The pit width along the east-west axis at the recording level was 1.96 m. From there to the bottom of the pit the depth was 0.94 m. The pit width in the bottom level was around 1.20–1.30 m (fig. 9) and it was at the pit bottom that a skeleton was found.

According to the initial observations[5], the bones were in anatomical order, and the skull lay on its right side. A darker strip was visible on the forehead (fig. 14), which is thought to possibly be from an imprint of a textile or leather band that had been tied around the head. The possibility that the imprint was a result of precipitated water was rejected because it was not horizontal and was consistent with the transverse circumference of the skull. The position of the skeleton indicated that the body was laid to rest in a special position (figs. 15, 16, 17) (cf. the contributions by V. Russeva, chapter 10.4). The head of the skeleton was also pointing to the west. Beneath the skeleton and the pottery fragments on the eastern periphery of the pit, small charcoals were found scattered on the light brown, sterile clay at the bottom of the pit.

---

5 The initial observations on the field were conducted by Assoc. Prof. Dr. Victoria Russeva (Institute of Experimental Morphology, Pathology and Anthropology with Museum at the Bulgarian Academy of Sciences)

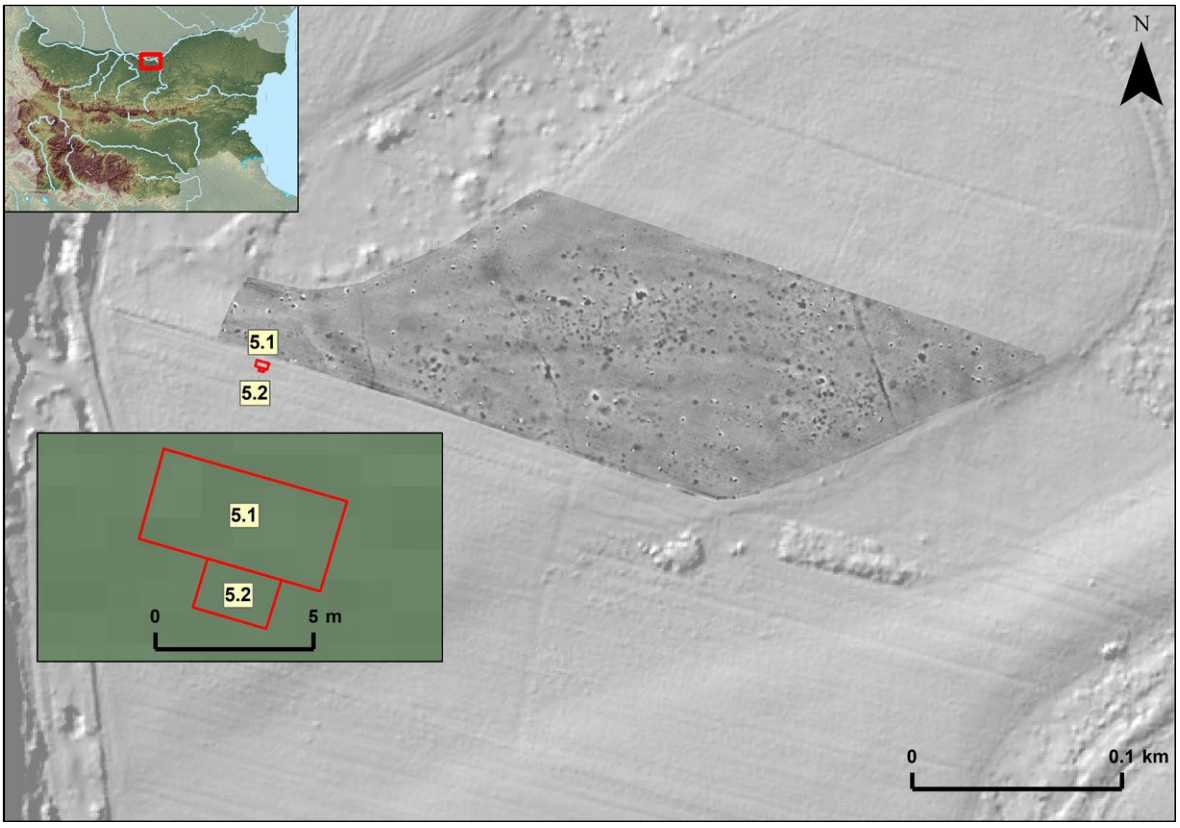


Fig. 1. Site 5, geophysical survey results in 2018 (cf. the contributions by B. Ullrich et al., chapter 6.1) and location of the trench 5.1 in 2018 (figure by N. Kecheva)

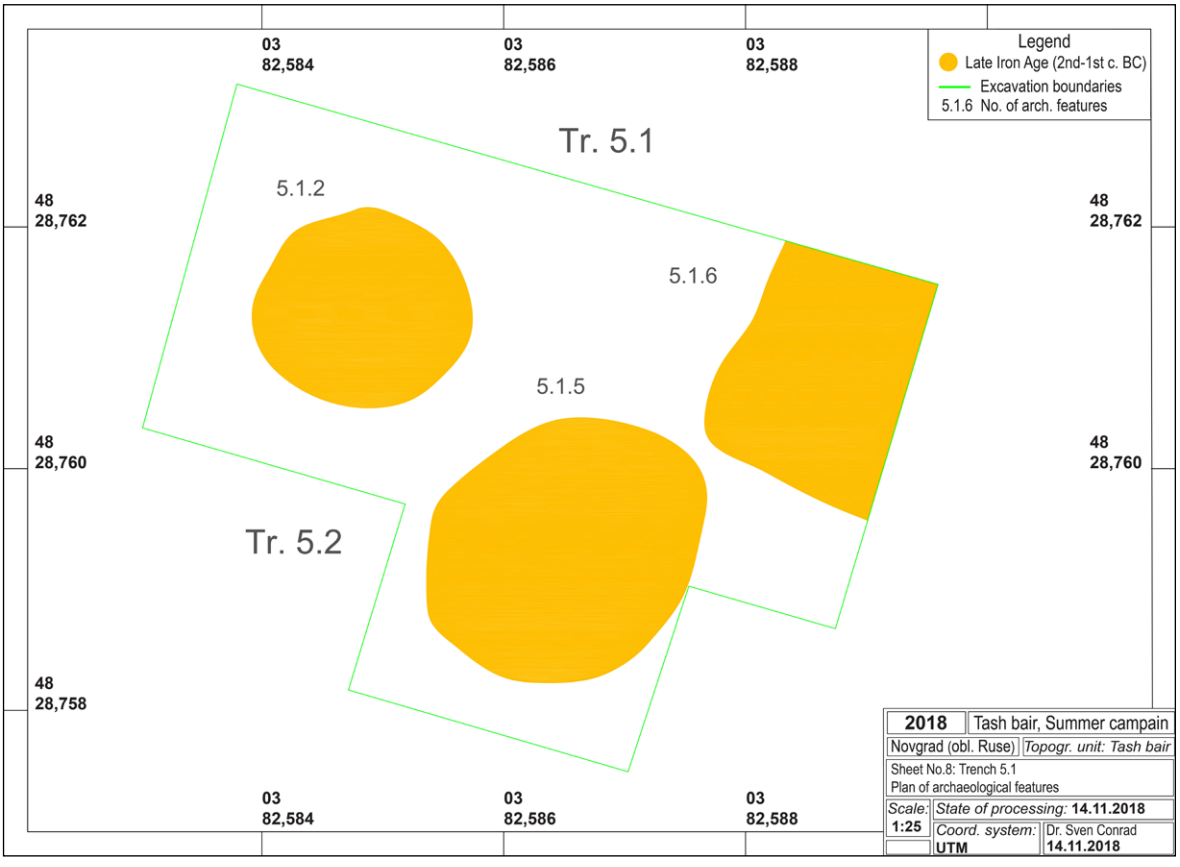


Fig. 2. Plan of the pits in trench 5.1 (drawing by S. Conrad, adapted by L. Traykova)



Fig. 3. Trench 5.1, level ▼20.68 m (photo by S. Conrad)



Fig. 4. The pit 5.1.5, level ▼19.75 m (photo by N. Kecheva)



Fig. 5. Extended area of the pit 5.1.5 (photo by N. Kecheva)

Analysis. The filling of pit 5.1.5 contained pottery fragments of the end of the Late Iron Age and the beginning of the Roman Imperial period. Fragments of a fruit bowl (cf. chapter 9.1, cat. No. P5/014) and a large vessel with two preserved tongue handles (cf. chapter 9.1, cat. No. P5/015) were discovered at the bottom of pit 5.1.5. They were made on a slow wheel and their closest parallels date back to the 1st c. BC – 1st c. AD (Vagalinski 2002, bowls type II, KY149-174; Върбанов 2013b, 196–199, 221, Табло II.



Fig. 6. Northeastern quarter, extended area of the pit 5.1.5, level ▼19.89 m (photo by N. Kecheva)

9, 230, Табло XI. 8; Zhivkov 2017, 224, pl. V. 23). Fragments from these two vessels were found in the upper layers of the pit fill, up to level ▼20.23 m. According to the stratigraphic distribution of the pottery fragments, this level was a boundary during the filling of the pit. Below this level, only fragments that are more typical of the Late Iron Age were recorded, and above were fragments from the Early Roman Imperial period (cf. chapter 9.1, table 12). In the humus soil of trench 5.2, two fragments from ceramic lamps were found (cat. Nos. SF 58, 59). Red slip decoration was visible on one of them which is dated to the middle, or the second half, of the 1st c. (cf. chapter 9.1, table 12).

The pottery fragments from the other two pits (5.1.2 and 5.1.6) in trench 5.1 (fig. 2) also included pieces dating to the end of the Late Iron Age and the beginning of the Roman Imperial period, but they were not stratigraphically arranged (cf. chapter 9.1, table 12). As such, this does not allow the comparison with the results from stratigraphic observations in pit 5.1.5. The three pits contained chronologically identical pottery fragments which were recorded at the same level. Most likely, the three pits were chronologically very close.

Interpretation and dating. The partial excavations in trenches 5.1 and 5.2 show a very small part of site 5. During the field surveys in 2018, a fragment of a millstone was found (cat. No. SF 56) as well as a fragment of a kiln grill for the production of pottery (cat. No. SF 57). Collected diagnostic pottery



Fig. 7. Northeastern quarter, extended area of the pit 5.1.5, level ▼19.69 m (photo by N. Kecheva)

fragments belong mostly to the Late Iron Age and the Roman period (cf. the contributions by N. Kecheva et. al., chapter 12, site 5).

The presence of a pit with a human skeleton at its bottom suggests that it was a grave. But it is questionable whether pit 5.1.5 was an ordinary burial. Only this pit out of the three excavated in tench 5.1 contained a human skeleton. According to their content, the other pits 5.1.2 and 5.1.6 may have been used for rubbish, from which clay was extracted for construction purposes, or they had a different purpose that was not as grave pits (cf. the contributions by S. Conrad, chapter 8.3.2). The stratigraphic distribution of the pottery fragments in the pit that was mentioned earlier raises the question of how and when the pit was filled. There are missing parts of the vessels (cf. chapter 9.1, cat. Nos. P5/014 and P5/015) that were found at the bottom of the pit and above the skeleton. Some of their fragments were found higher in the filling of the pit. This shows that the vessels were no longer intact when they arrived in the archaeological context. There are two possible explanations for this stratigraphic distribution of the pottery fragments: they were features of the burial rite, in which pottery vessels were broken and thrown into the burial pit while it was filled with earth; alternatively, the child was placed in a rubbish pit. The fact that pieces of vessels in it are missing above the level ▼20.23 m is important for dating the pit. The pottery fragments above this level were younger than those below it. The fragments from above date to the middle of the 1st c. AD (cf. chapter 9.1, table 12). They include a fragment of a Roman amphora (fig. 10) which was produced in Heraclea Pontica and was intended for wine transportation. It refers to type Hr II-1 according to Borislavova and dates back to the last quarter of the 1st c. (Borislavova 2018, 49, 50, fig. 3. 3–5). This pottery fragment gives a *terminus ante quem* for the dating of the pit with the skeleton of the child.

The stratigraphic results show that the pit was most probably filled in two phases. In the first stage, from the 1st c. BC to the middle of the 1st c. AD the pit was filled approximately to the level ▼20.23 m. This level was at almost half of the depth of the pit. At a later stage, around the middle and the second



Fig. 8. Northern half, extended area of the pit 5.1.5 (photo by N. Kecheva)

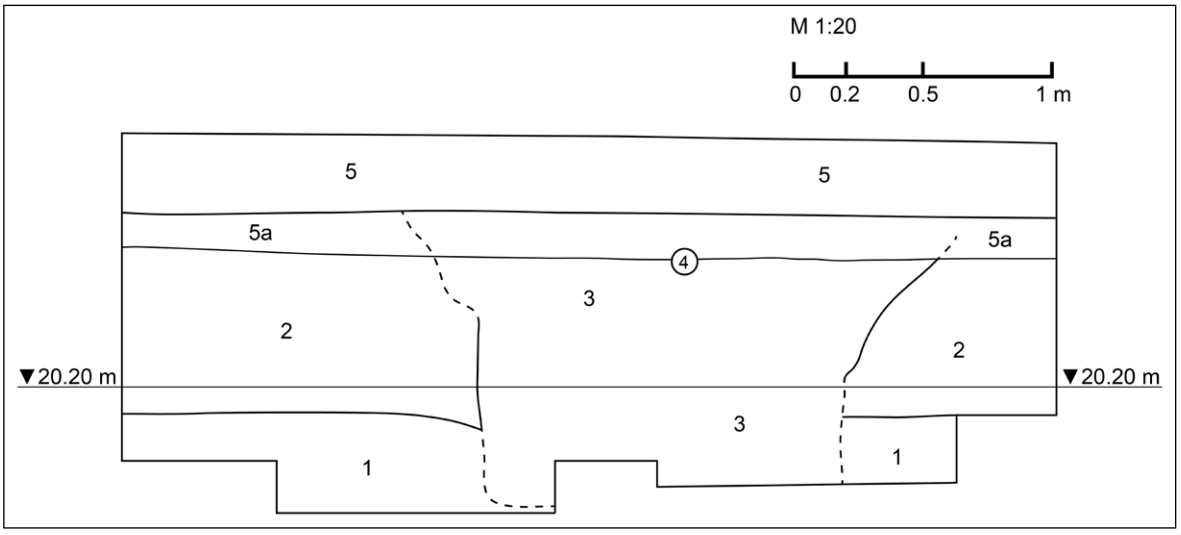


Fig. 9. Site 5. Trench 5.1, southern section: 1 – Light brown clay, sterile, with single white inclusions (soft stones with sizes under 1 × 1 cm) and black vertical strips from vegetation roots. A lot of bioturbations; 2 – Light brown clay, probable river deposit (it contains shells from mussels and small snails), with a large number of white inclusions some of which mark concentrations; black vertical strips from vegetation roots; separate pieces of burnt clay (with sizes under 0.5 × 0.5 cm). A lot of bioturbations; 3 – Pit 5.1.5, brown colour; it contained single handmade pottery fragments, small pieces of burnt clay (with sizes under 0.5 × 0.5 cm), bones. A lot of bioturbations; 4 – A recording level of pit 5.1.5; 5 – Dark brown layer, ploughzone, it contains: handmade and wheelmade pottery fragments; animal bones; 5a – Light brown dense layer that contains household Roman pottery fragments dated to the period of the second half of 1st–2nd c. The same fragments were found in layer (5) (drawing and interpretation by L. Traykova, N. Kecheva, L. Vagalinski)

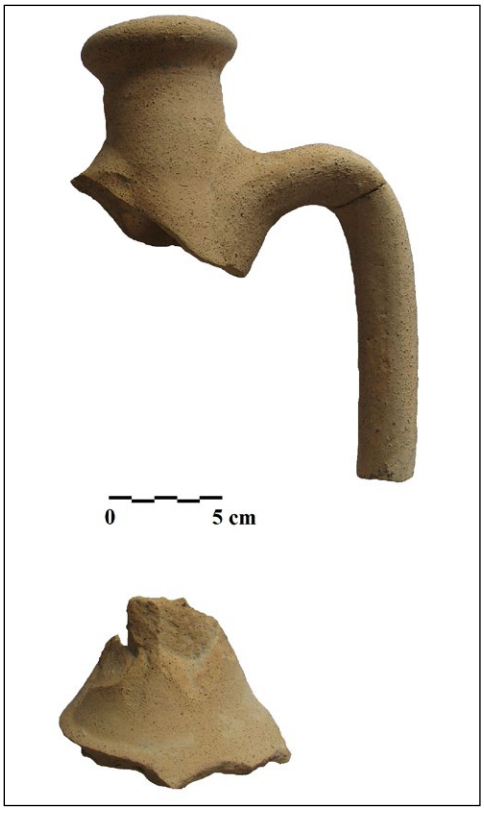


Fig. 10. Amphorae type Hr II-1 after Borislavova 2018 (photo by L. Vagalinski)



Fig. 11. Trench 5.2, southern half of the pit 5.1.5 (photo by L. Traykova)

half of the 1st c., the whole pit was filled in. The stratigraphic picture indicated that the child was buried in an existing rubbish pit. The strange position of the body also supports this conclusion. The absence of human remains in the adjacent pits (5.1.2 and 5.1.6) in trench 5.1 (fig. 2) also demonstrates that the three pits in the trench were not part of a burial site, but rather they had been used for rubbish or for digging a clean clay suitable for plastering the floor and walls of the dwellings.

Around the new era, the local population used obsolete structures as burial facilities. An abandoned pottery kiln was excavated 5 km to the north, in which a woman was subsequently casually buried (Vagalinski 2011a, 222, fig. 4) (fig. 18). The kiln was dated to the 1st c. BC – 1st c. AD. It immediately preceded the construction of the most significant and accurately dated among the Roman lime manufactories excavated so far. It was established by a division of the *legio I Italica* and operated briefly in the 70s of the 1st c. (Vagalinski 2011b, 54–55). It seems that the stratigraphic situation in the pit with the burial of the child represents the same historical transition of permanent imposition of Roman power on the southern bank of the Lower Danube.

Again in Northern Bulgaria to the southwest, in the land of Gorni Dabnik village, Dolni Dabnik municipality, a settlement dating to the 2nd–1st c. BC was excavated. The settlement included a pit that contained the skeleton of a 20-30-year-old woman and a skeleton of a rabbit at its bottom. The skeleton of the woman had bent upper and lower limbs to the right and the skull and torso were facing the ground (fig. 19). Charcoals and remains of charred millet and barley were found around and under the skull. A part of a Late La Tène iron fibula was found in the soil that had fallen into the skull. The pit is interpreted as an unusual burial within a settlement or a human sacrifice by analogy with examples from Thrace, dating from 5th–4th c. BC and Southern Romania from the 2nd–1st c. BC. It is characteristic of pits interpreted as human sacrifices that they were not in a burial context. Only a small amount of the excavated pits in large areas with multiple pits (cult or trash pits) contained human remains, and their bones in anatomical order show they were placed in unnatural postures during positioning of the body (Тонкова, Маджаров 2020, 516, обр. 2. 4, 517, обр. 3. 4; Tonkova 2010, 509–512) (fig. 19).



Fig. 12. Trench 5.2, southern half of the pit 5.1.5, level ▼20.56 m (photo by L. Traykova)



Fig. 13. The pit 5.1.5 in trenches 5.1 and 5.2 (photo by L. Traykova)



Fig. 14. Pit 5.1.5, the human skull (photo by N. Kecheva)



Fig. 15. Pit 5.1.5, the human skeleton under the pottery (photo by N. Kecheva)



Fig. 16. Pit 5.1.5, the human skeleton (photo by N. Kecheva)

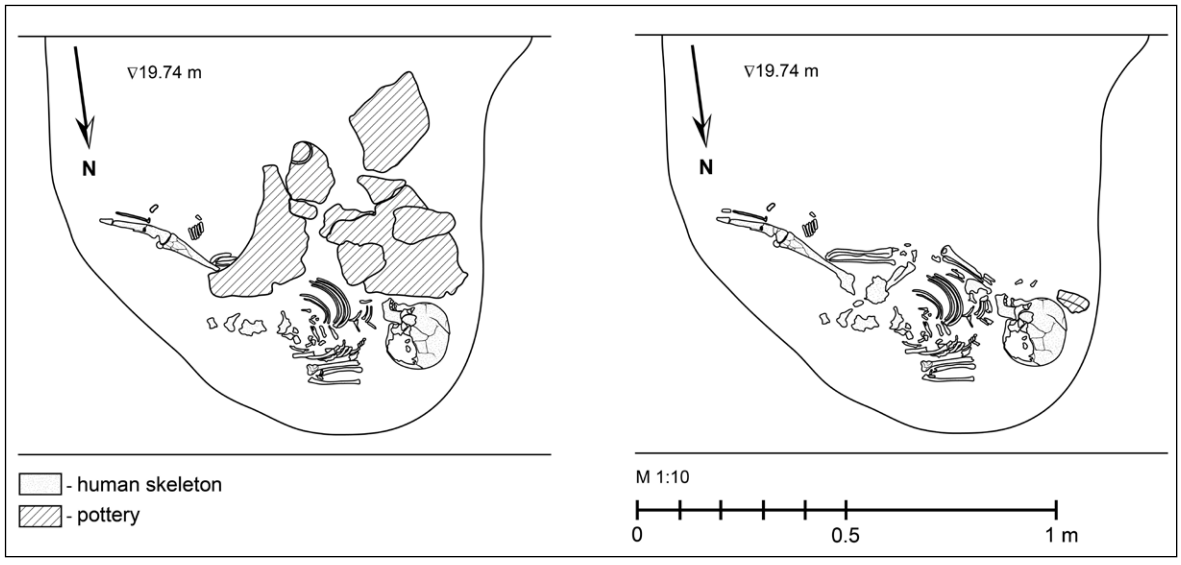


Fig. 17. Pit 5.1.5, the human skeleton before and after removing the pottery (drawing by L. Traykova)

The two pits with skeletons from the site near Gorni Dabnik village and pit 5.1.5 show similarities in terms of the position of the skull and torso – facing down, the upper limbs bent towards the body, as well as the presence of charcoals at the bottom. Both skeletons were oriented with the head to the west.

The context in which the three excavated pits in trenches 5.1 and 5.2 falls is not clear, but undoubtedly pit 5.1.5 with the child skeleton at the bottom cannot be defined as a regular burial. Whether it was a human sacrifice or a careless burial in a welded pit, this archaeological complex reveals a possible custom of the local tribes from the Late Iron Age.

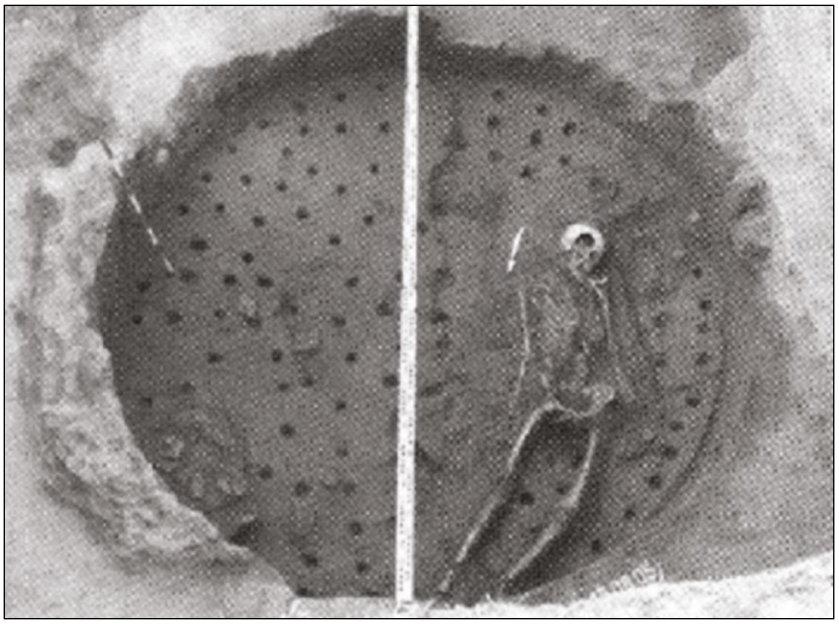


Fig. 18. Female burial on the pottery kiln's grate of pottery kiln near Krivina village, Tsenovo municipality (after Vagalinski 2011a, 222, fig. 4)



Fig. 19. Pit with a human skeleton (C6) near Gorni Dabnik village, Dolni Dabnik municipality (after Тонкова, Маджаров 2020, 516, обр. 2. 4)

ГРОБ В ЯМА 5.1.5

Людмил Вагалински, Люба Трайкова, Надежда Кечева

(Резюме)

Описание. Сондаж 5.1 в рамките на обект 5 (fig. 1) беше заложен южно от терена, на който беше направено геофизично изследване. Попада в един от меандрите на старото корито на р. Янтра. Не се очертаха ясни аномалии и изборът на място беше съобразен с по-голямата концентрация на материали, регистрирана при теренните издирвания от пролетта на 2018 г. (Вагалински et al. 2019, 84).

Общата площ на сондажа е 18 м^2. Теренът е равен. Работи се на механични пластове. Копае се само на ръка. В сондажа бяха регистрирани и проучени 3 ями (figs. 2, 3). Яма 5.1.5 е прерязана от южния профил на сондажа. Първоначално изчерпахме нейната северозападната четвърт. На ▼19,75 м беше разкрита лявата страна на човешки череп и големи фрагменти от керамични съдове, изработени на ръка (fig. 4). Установихме и наличие на скелет. Проучването продължи в североизточната четвърт на яма 5.1.5. Между двете четвъртини беше оставено контролно ребро

с широчина 0,40 м (fig. 6). Начертахме профилите и свалихме контролното ребро между двете четвъртини на яма 5.1.5 (figs. 8, 9).

Заложихме южно допълнение на сондаж 5.1, за да проучим южната част на яма 5.1.5 – сондаж 5.2 (fig. 1). След отнемането на пълнежа на ямата в сондаж 5.2 установихме, че ямата се стеснява в дълбочина (fig. 13). Вкопана е в стерилен пласт. Скелетът лежи на дъното на ямата.

Според първоначалните наблюдения[6] костите са в анатомичен порядък, черепът е на дясната си страна. На челото личи по-тъмна ивица (fig. 14). Вероятно е отпечатък от текстилна или кожена лента, която била вързана около главата. Позицията на скелета показва по-особена позиция на тялото при полагането (вж. приноса на В. Русева, глава 10.4). Под скелета и фрагментите керамика, както и по източната периферия на дъното на ямата открихме разпръснати дребни въглени.

Анализ. Пълнежът на яма 5.1.5 съдържа фрагменти керамика, характерни за края на късножелезния и началото на римския императорски период. На дъното на яма 5.1.5 бяха открити фрагменти от 2 керамични съда (вж. глава 9.1, кат. №№ P5/014 и P5/015), изработени на бавно колело. Най-близките им паралели се датират в периода I в. пр. Хр. – I в. сл. Хр. (Vagalinski 2002, bowls type II, KY149-174; Върбанов 2013b, 196 – 199, 221, Табло II. 9, 230, Табло XI. 8; Zhivkov 2017, 224, pl. V. 23). Фрагменти от тези съдове бяха открити и в по-горните пластове от пълнежа на ямата, до ниво ▼20,23 м. Според стратиграфското разпределение на керамиката това ниво играе ролята на граница в процеса на запълване на ямата. Под това ниво открихме само фрагменти, които са по-характерни за края на късния железен период, а над него и фрагменти от ранноимператорския римски период.

Керамичният материал от другите две ями в сондаж 5.1 – яма 5.1.2 и яма 5.1.6 (fig. 2), също включва фрагменти от края на късножелезния и ранния императорски период, но те не са разпределени стратиграфски (вж. глава 9.1, table 12). Това не позволява да се сравнят резултатите с тези от стратиграфските наблюдения в яма 5.1.5. Трите ями съдържат хронологично еднакъв керамичен материал и са разпознати на еднакво ниво. Това показва, че са изкопани по едно и също време.

Интерпретация и датировка. Проучената площ на сондажи 5.1 и 5.2 показва много малка част от обект 5. Фрагментите керамика, открити по време на теренните издирвания през 2018 г., са предимно от късния железен период и римския период (вж. приноса на Н. Кечева и др., глава 12, обект 5).

Наличието на яма със скелет на дъното предполага гробно съоръжение. Но дали яма 5.1.5 е обикновен гроб? От проучените три ями в сондаж 5.1 само тази съдържа човешки скелет. Според своето съдържание другите ями 5.1.2 и 5.1.6 може да са сметни или от тях е вадена глина за строителни нужди, или имат друго предназначение, но не са гробни (вж. приноса на С. Конрад, глава 8.3.2). Стратиграфското разпределяне на керамиката в ямата, споменато по-горе, повдига въпроса как и кога е била запълнена. Фрагментът от римска амфора (fig. 10) се датира в последната четвърт на I в. (Borislavova 2018, 49, 50, fig. 3. 3-5). Този керамичен фрагмент е сигурен *terminus ante quem* за ямата с детския скелет.

Стратиграфските ни резултати показват, че ямата е била запълнена най-вероятно на два пъти. При първия етап, в рамките на I в. пр. Хр. – средата на I в. сл. Хр., ямата била запълнена приблизително до ▼20,23 м, което е почти половината от нейната дълбочина. На по-късен етап, около средата и втората половина на I в., била запълнена цялата. Тази стратиграфска картина води към заключение, че детето е било погребано в налична яма за смет. Странната позиция на тялото също подкрепя този извод. Липсата на човешки останки в съседните ями (5.1.2 и 5.1.6) в сондаж 5.1 (fig. 2) също показва, че трите ями в сондажа не са част от некропол, а са по-скоро за смет или за изкопаване на чиста глина.

---

6 Огледът на място е извършен от доц. д-р Виктория Русева (ИЕМПАМ – БАН)

Около новата ера местното население използвало като гробни съоръжения излезли от употреба структури. На 5 км северно е проучена изоставена пещ за керамика, датирана в периода I в. пр. Хр. – I в. сл. Хр., в която впоследствие била небрежно погребана жена (Vagalinski 2011a, 222, fig. 4) (fig. 18).

В землището на с. Горни Дъбник, общ. Долни Дъбник (Северна България), е проучено селище с датировка II – I в. пр. Хр. Част от него е яма със скелет на 20 – 30-годишна жена и скелет на заек на дъното. Скелетът на жената е със свити горни и долни крайници, надясно, черепът и торсът са обърнати към земята (fig. 19). Ямата е интерпретирана като необичайно погребение в рамките на селище или човешко жертвоприношение. Характерно за интерпретираните като човешки жертвоприношения ями е, че те не са в погребален контекст. От проучените големи площи с множество ями (култови или сметни) само единици от тях съдържат човешки останки, а техните кости в анатомичен порядък показват неестествени пози при полагането (Тонкова, Маджаров 2020, 516, обр. 2. 4, 517, обр. 3. 4; Tonkova 2010, 509 – 512).

Ямата със скелет от с. Горни Дъбник и яма 5.1.5 показват сходство по отношение на позицията на черепа и торса – обърнати надолу, свити към тялото горни крайници, както и наличие на въглени по дъното. И двата скелета са ориентирани с глава на запад.

Контекстът, в който попадат трите проучени ями в сондажи 5.1 и 5.2, не е изяснен, но безспорно яма 5.1.5 с детски скелет на дъното не може да се определи като обичаен / редовен погребален обред. Независимо дали става въпрос за човешко жертвоприношение, или за небрежно трупополагане в заварена яма, този археологически комплекс разкрива обичай на местните племена от късния железен период.

8.3.4. Late Iron Age. Conclusion

Lyudmil Vagalinski, Lyuba Traykova, Nadezhda Kecheva

Features from the Late Iron Age were excavated in the areas of site 1 and site 5.

At site 1 (cf. the contributions by N. Kecheva et al., chapter 12, site 1), within trench 1.1, feature 1.1.6 was excavated in the northeast corner of trench 1.1-E and feature 1.1.15 in the northwest corner of 1.1-W. They belonged to a ditch with an E-W direction (cf. the contributions by L. Vagalinski et al. 8.3.1, figs. 9–12). The wheelmade and handmade pottery fragments found in its fill and mainly within the lower stratigraphic layers were used to date this ditch to the Late Iron Age (cf. chapter 9.1, tables 4, 5).

Due to the limited excavations, there is not enough data to determine the purpose of the ditch in trench 1.1 or to give an accurate size of the enclosed area. It can be assumed that the Late Iron ditch protected a settlement with an area of at least 1 ha. The results of the geophysical survey of site 1 (cf. the contributions by L. Vagalinski et al. 8.3.1, fig. 1), including the ditch, were not definite. A rough right angle was also recorded in the approximate centre of the Early Medieval earthwork fort suggesting that it is the southwestern end of a rectangular or trapezoidal enclosed area. No geophysical anomalies have been recorded to delineate an enclosed space to the east and north. A possible explanation is that the eastern Early Medieval ditch repeated the route of the older ditch in its northern part. Moreover, the northern side of the enclosed area may fall under the modern dirt road, or it could be located outside the terrain on which the geophysical survey was conducted.

Trench 5.1 was located within the site 5 scatter, south of the area investigated by the geophysical survey (cf. the contributions by N. Kecheva et al., chapter 12, site 5). Three pits with different shapes and probably different purposes were excavated. Pit 5.1.2 had an irregular funnel shape and was interpreted as a possible well (cf. the contributions by S. Conrad, chapter 8.3.2, fig. 5). Pit 5.1.6 was partially excavated; its shape in plan was rectangular or trapezoidal, with rounded angles, and it narrowed in depth. It was interpreted as a pit used for clay extraction for construction purposes (cf. the contributions by S. Conrad,

chapter 8.3.2, figs. 7, 8). A child skeleton was excavated in pit 5.1.5 (cf. the contributions by L. Vagalinski et al., chapter 8.3.3, fig. 15). Part of this pit was located in the southern section of 5.1. For the thorough investigation of the full extent of the pit, trench 5.1 was extended to the south – trench 5.2.

Wheelmade and handmade pottery fragments found in the fill of the pits included vessels from the Late Iron Age and Early Roman period, in the middle of the second half of the 1st c. (cf. chapter 9.1, table 12). Pits 5.1.2 and 5.1.6 were dated in the first decades of the Roman occupation (cf. the contributions by S. Conrad, chapter 8.3.2).

The stratigraphic pottery distribution in pit 5.1.5 showed a possible two-phase fill. Pottery fragments typical for the end of the Late Iron Age were recorded at the pit bottom and its lower section, while pottery fragments typical also for the Early Roman Imperial period were recorded at its upper section. Pit 5.1.5 with a child skeleton cannot be defined as a regular burial. Whether it was a human sacrifice or a careless burial in a welded pit, this archaeological complex reveals a possible custom of the local tribes from the Late Iron Age (cf. the contributions by L. Vagalinski et al., chapter 8.3.3)

The excavated pits in trenches 5.1 and 5.2 belonged to a possible periphery of a settlement. Furthermore, the excavated features from the Late Iron Age in site 1 and site 5 indicate habitation in the upper parts of the Tash Bair region as well as the lowlands located between the old meanders of the Yantra River (cf. the contributions by N. Kecheva et al., chapter 12, Maps and photos of the area covered in 2018 and 2019, fig. 3). This new data enriches the knowledge of the Lower Danube region habitation of south-eastern Europe during the Late Iron Age.

КЪСНА ЖЕЛЯЗНА ЕПОХА. ЗАКЛЮЧЕНИЕ

Людмил Вагалински, Люба Трайкова, Надежда Кечева

(Резюме)

Структури от късния железен период бяха проучени в площите на обект 1 и обект 5.

На обект 1 (вж. приноса на Н. Кечева и др., глава 12, обект 1) в рамките на в сондаж 1.1 бяха проучените структури 1.1.6 в североизточния ъгъл на 1.1-E и 1.1.15 в северозападния ъгъл на 1.1-W. Те принадлежат на ров с направление изток – запад (вж. приноса на Л. Вагалински и др., глава 8.3.1, figs. 9 – 12). Керамичните фрагменти, изработени на колело и ръка, открити в неговия пълнеж и главно тези от пластовете близо до дъното, позволяват този ров да се датира в късния железен период (вж. глава 9.1, tables 4, 5).

Поради ограничените като площ разкопки не разполагаме с достатъчно данни, за да определим предназначението на рова в сондаж 1.1, нито да заявим размера на ограденото пространство. Може да се предположи, че късножелезният ров е защитавал селище с площ поне 10 дка. Резултатите от геофизичното заснемане на обект 1 (вж. приноса на Л. Вагалински и др., глава 8.3.1, fig. 1) по отношение на този ров не са категорични. Регистрираният почти прав ъгъл в приблизителния център на ранносредновековното землено укрепление предполага, че е югозападен край на правоъгълна или трапецовидна ограден площ. Не са регистрирани геофизични аномалии, които да очертаят затворено пространство от изток и от север. Възможно обяснение е, че източният ранносредновековен ров е повторил трасето на по-стария ров в северната си част. Северната страна на ограденатa площ може да попада под съвременния черен път или да се намира извън терена, на който е направено геофизично изследване.

Сондаж 5.1 беше заложен южно от терена, на който беше направено геофизично изследване, в рамките на обект 5 (вж. приноса на Н. Кечева и др., глава 12, обект 5). В сондажа бяха проучени три ями с различна форма и вероятно различно предназначение. Яма 5.1.2 има неправилна фуниевидна форма, интерпретирана като вероятен кладенец (вж. приноса на С. Конрад, глава 8.3.2, fig. 5). Яма 5.1.6 е проучена частично. Нейната форма в план е правоъгъл-

на или трапецовидна, със заоблени ъгли, в дълбочина се стеснява, интерпретирана като изкоп за добив на глина за строителни нужди (вж. приноса на С. Конрад, глава 8.3.2, figs. 7, 8). В яма 5.1.5 разкрихме детски скелет (вж. приноса на Л. Вагалински и др., глава 8.3.3, fig. 15). Част от тази яма попадаше в южния профил на сондаж 5.1 и за пълното ѝ проучване направихме южно разширение на сондаж 5.1 – сондаж 5.2.

Керамичните фрагменти, изработени на колело и на ръка, открити в пълнежа на трите ями, показват форми от късния железен период, както и фрагменти от ранния римски период, отнесени към средата или втората половина на I в. (вж. глава 9.1, table 12). Датирането на ями 5.1.2 и 5.1.6 е отнесено към първите десетилетия от римската окупация (вж. приноса на С. Конрад, глава 8.3.2).

Според стратиграфското разпределение на керамиката в яма 5.1.5 вероятно нейното запълване е имало два етапа. На дъното и приблизително в долната половина на ямата открихме само фрагменти, които са по-характерни за края на късния железен период, а в горната половина и фрагменти от ранноимператорския римски период. Безспорно яма 5.1.5 с детски скелет на дъното не може да се определи като обичаен / редовен погребален обред. Независимо дали става въпрос за човешко жертвоприношение, или за небрежно трупополагане в заварена яма, този археологически комплекс разкрива обичай на местните племена от късния железен период (вж. приноса на Л. Вагалински и др., глава 8.3.3).

Контекстът, в който попадат трите проучени ями в сондажи 5.1 и 5.2, не е изяснен, но вероятно са част от периферията на селище.

Проучените структури от късния железен период от обект 1 и обект 5 показват обитаване както във височина, каквото е билото на близкия склон, така и в ниските места, обхванати от старите меандри на р. Янтра (вж. приноса на Н. Кечева и др., глава 12, Maps and photos of the area covered in 2018 and 2019, fig. 3). Те обогатяват нашето познание за обитаването на земите в Долнодунавския регион на Югоизточна Европа през късния железен период.

8.4. THE EARLY MEDIEVAL FORTIFICATIONS IN TRENCHES 1.1 AND 1.2

Lyudmil Vagalinski, Lyuba Traykova, Nadezhda Kecheva

Description: In the spring of 2018 during field surveys, a rectangular earthwork fort was recorded in site 1 (Вагалински et al. 2019, 84). The earthwork measured 200 × 200 m and was surrounded by a ditch and a rampart visible above the modern surface. The fort was first recorded during field surveys in 1999 (Вагалински et al. 2001a, 77). The results of the geophysical survey in 2018 also showed other negative linear anomalies inside the enclosed area (cf. the contributions by B. Ullrich et al., chapter 6.1). Attention was drawn to the intersection of two linear anomalies in the southwestern part of the fort (fig. 1). The stronger anomaly of the geophysical survey had an E-W direction and was almost parallel to the southern ditch of the fort. The team (L. Vagailnski, S. Conrad, L. Traykova, N. Kecheva, R. Krauß and German students) partially excavated these archaeological features between August 27th and September 24th 2019 (Вагалински et al. 2020a, 1177). The coordinates of the trench were created in GIS in WGS 1984 UTM Zone 35N coordinate system. GNSS receivers CHCNav i70 were used to trace the coordinate on the ground surface.

Trench 1.1 was located transversely according to the direction of the eastern ditch of the earthwork fort (north-south). It was situated in the middle of the ditch where the results of the geophysical survey showed that the ditch had been interrupted. The team assumed that this could be a possible place where an entrance to the earthwork fort was present. The trench area measured 49 m^2 and with the dimensions of 7 × 7 m. It was divided into two parts, eastern (1.1-E) and western (1.1-W), by a section with a 0.9 m width (fig. 1). The modern surface was found to be sloping from north to south and from west to east. The surface layer of trench 1.1 was the ploughzone (about 0.4 m) and was removed by machines. The

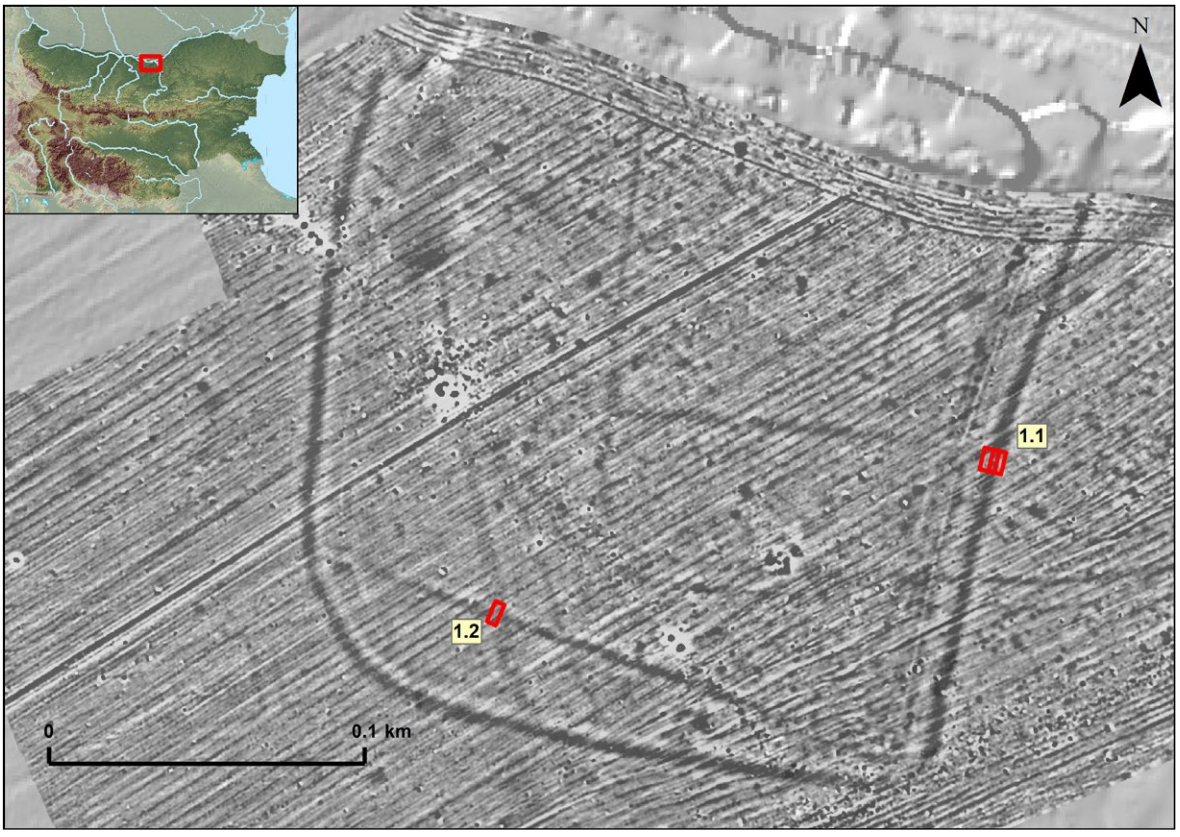


Fig. 1. Site 1, geophysical survey results in 2018 (cf. the contributions by B. Ullrich et al., chapter 6.1) and location of the trenches in 2019 (figure by N. Kecheva)

excavations continued with the removal of arbitrary levels. The first levels measured from ▼27.25 m in 1.1-E and to ▼27.82 m in 1.1-W.

Trench 1.1-E. With the excavation of an arbitrary level of ▼27.00–26.76 m in the eastern part of the trench, a lighter and dense yellow strip was visible. In the western part, the soil was darker, with a greyish-brown colour (fig. 2). At a level of ▼26.44 m in plan, next to the western section of the trench, the ditch and the entrance were recorded (fig. 3). From this level, at depth, the work continued only up to the ditch borders – in the northwest and southwest corners of the trench. The bottom of the ditch in the northwest corner was reached at ▼24.36 m (figs. 4, 5).

Trench 1.1-W. At a level ▼26.78 m in the western part of the trench the soil was light, while in the eastern part it was darker with greyish-brown colour (fig. 6). After the removal of an arbitrary level, ▼26.78–26.58 m, in the middle of the eastern section of the trench a concentration of relatively large handmade pottery fragments, animal bones, part of a human mandibula and a humerus were recorded (figs. 7, 8). After levelling at ▼26.58 m the ditch borders and the ditch passage were recorded in plan (fig. 9). It was found that the accumulation of larger pottery fragments, human and animal bones were part of a deposited layer on the passable part of the ditch. From this depth, the work continued only in the ditch borders – in the northeast and southeast corners of the trench. The ditch bottom in the northeast corner was reached at ▼24.35 m (fig. 10).

The contexts from trench 1 were numbered: 1.1.7 – trench 1.1-E, northwestern corner; 1.1.8 – trench 1.1-E, southwestern corner; 1.1.13 – trench 1.1-W, northeastern corner; 1.1.14 – trench 1.1-W, southeastern corner (fig. 11). The excavation of the ditch in contexts 1.1.8 and 1.1.14 was not finished due to the end of the excavation campaign.

The cross section of the excavated ditch had an irregular trapezoidal shape. The eastern/outer side of the ditch was more sloping and in its lower part was staircase-shaped, while the western/inner side had a greater slope. The bottom was almost flat, and its depth was over 2 m. Measured from the modern



Fig. 2. Trench 1.1-E, level ▼26.76 m (photo by Lea Valcov)



Fig. 3. Trench 1.1-E, level ▼26.44 m (photo by Lea Valcov)

surface to the bottom at the northern section, the depth was about 3.70 m, the maximum preserved width at the top was c. 5.40 m, and the narrowest part at the bottom was c. 1.7 m (fig. 12). The width at the top of the southern section was c. 5.80 m (fig. 13). The preserved width of the passage through the ditch in its upper part was c. 1.50 m (figs. 14, 15). Most likely, the walls of the passage collapsed and were added to the fill of the ditch. The ditch had been dug into sterile loess, and had cut into another, earlier ditch (figs. 11, 12) dating to the Late Iron Age (cf. the contributions by L. Vagalinski et al., chapter 8.3.1).

Trench 1.2 was situated on a cross point of two negative linear anomalies in the southwestern part of the earthwork fort (fig. 1). It had an area of 23.10 m^2 and dimensions 7 × 3.30 m. The modern surface there was almost flat. The surface layer was also removed by machines. Excavations at depth continued by hand with workers. The first arbitrary level was excavated to ▼29.91 m. At a level of ▼29.46 m in the middle of the trench a darker strip with an approximate width of 3 m and an east-west direction was recorded (fig. 16). This ditch was approximately parallel to the southern ditch of the earthwork fort. The soil south of the ditch was light yellow, but it was not sterile soil. In the northern part of the trench, the soil



Fig. 4. Trench 1.1-E, bottom of the ditch in NW corner level ▼24.36 m
(photo by L. Vagalinski)



Fig. 5. Trench 1.1-E, bottom of the ditch in NW corner level ▼24.36 m (photo by S. Conrad)



Fig. 6. Trench 1.1-W, level ▼26.78 m (photo by Lea Valcov)



Fig. 7. Trench 1.1-W, level ▼26.71 m (photo by S. Conrad)



Fig. 8. Trench 1.1-W, level ▼26.66 m (photo by S. Conrad)



Fig. 9. Trench 1.1-W, level ▼26.58 m (photo by Lea Valcov)



Fig. 10. Trench 1.1-W, bottom of the ditch in NE corner level ▼24.35 m (photo by L. Vagalinski)

was dark brown, but it was different to the soil in the middle of the trench. The trench was conditionally divided into three parts to distinguish the different contexts and to separate the artefacts from them. The ditch in the central part of the trench was numbered as context 1.2.5 (fig. 17). At a level of ▼29.30 m, the ditch with an east-west direction was visible (fig. 18). The excavation at depth continued only in its borders. Sections of the ditch were excavated until its bottom had been reached at ▼26.94 m (figs. 19,

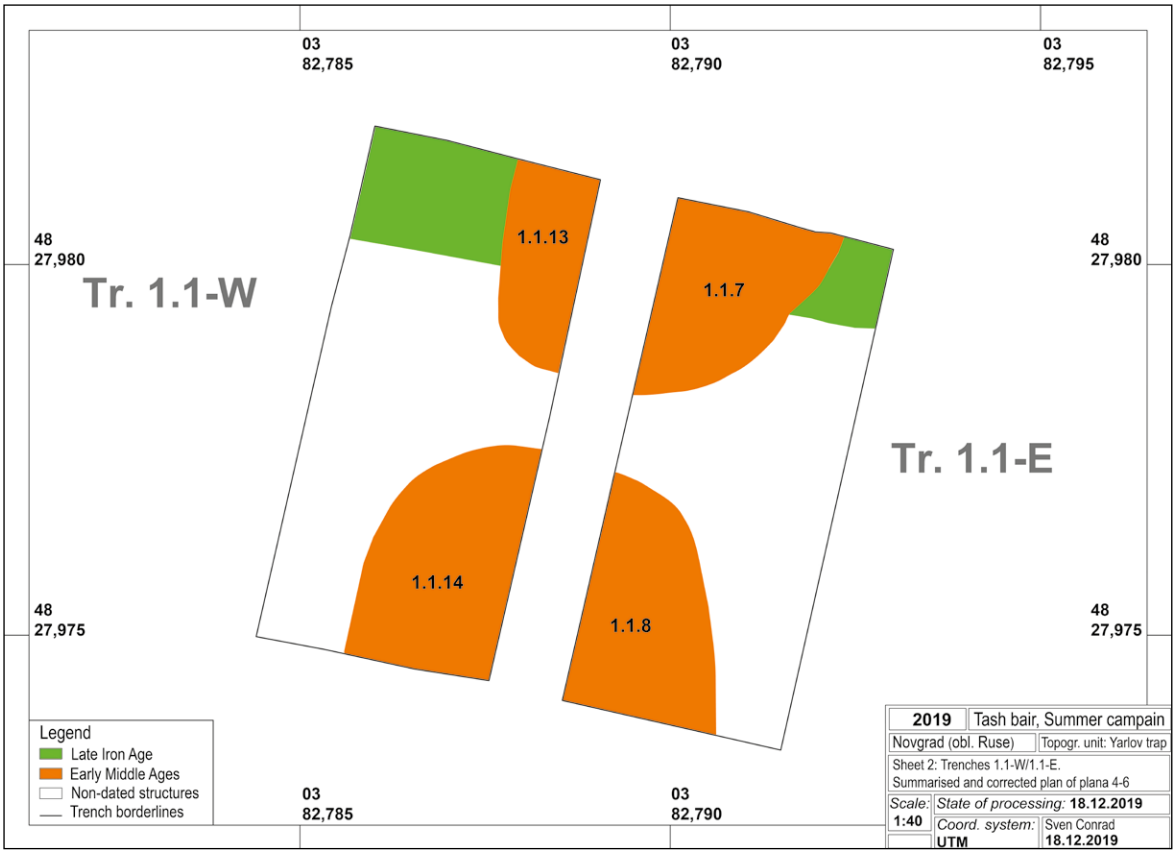


Fig. 11. Plan of the ditches in trench 1.1 (drawing by S. Conrad, adapted by L. Traykova)

20). The ditch crossed another earlier ditch (cf. the contributions by R. Krauß, S. Conrad, chapter 8.1), and it had been dug into the sterile loess (figs. 21, 22, 23).

The cross section of the excavated ditch was in the shape of an inverted trapezoid. The bottom was almost flat and its depth was at least 2.5 m. Measured from the modern surface to the bottom in the western section it was approximately 3.50 m. The maximum preserved width at the top measured about 2.50 m, and the narrowest part at the bottom was 1.50–1.60 m (figs. 22, 23).

Analysis and dating. Site 1 was inhabited throughout many periods – Late Neolithic, Iron Age, Roman period, Late Antiquity, and Middle Ages (Вагалински et al. 2019, 84; cf. the contributions by N. Kecheva et al., chapter 12, site 1). The ditch fill in trench 1.1 contained pottery fragments and various other finds (cf. the contributions by R. Krauß, chapter 9.2.1, cat. Nos. SF 35, 37, 41, 42, 44; L. Traykova, chapter 9.2.2, cat. Nos. SF 46–50) dated to all of these periods. Wheelmade pottery fragments found in the fill of the eastern ditch of the earthwork fort and especially in the layers close to the ditch bottom (cf. chapter 9.1, tables 6, 7) indicate that it could be dated to the Early Medieval period, during the period of the First Bulgarian Kingdom (681–1018). Two groups of Early Medieval pottery were distinguished including an early group dating to the end of 7th–8th c. and a late group dating from 9th to the beginning of the 11th c. The fragments from the earlier group were much fewer than those belonging to the late group. They belonged to the upper layers of the ditch fill in trench 1.1 only. The Early Medieval ditch in trench 1.2 did not contain pottery fragments from the early group (cf. chapter 9.1, part 9.1.2.6). This shows that due to erosion we observe an inverted stratigraphy which explains why pottery fragments from the late group were found in the bottom of the ditch, and pottery fragments from the earlier group were in the upper layers.

Rasho Rashev distinguished three main stages in the periodisation of the construction of medieval earthwork forts on the Lower Danube. The first stage began with the residence of Bulgarians who were under the rule of khan Asparuh in Northern Dobrudzha and Southern Bessarabia in the 660s and 670s.

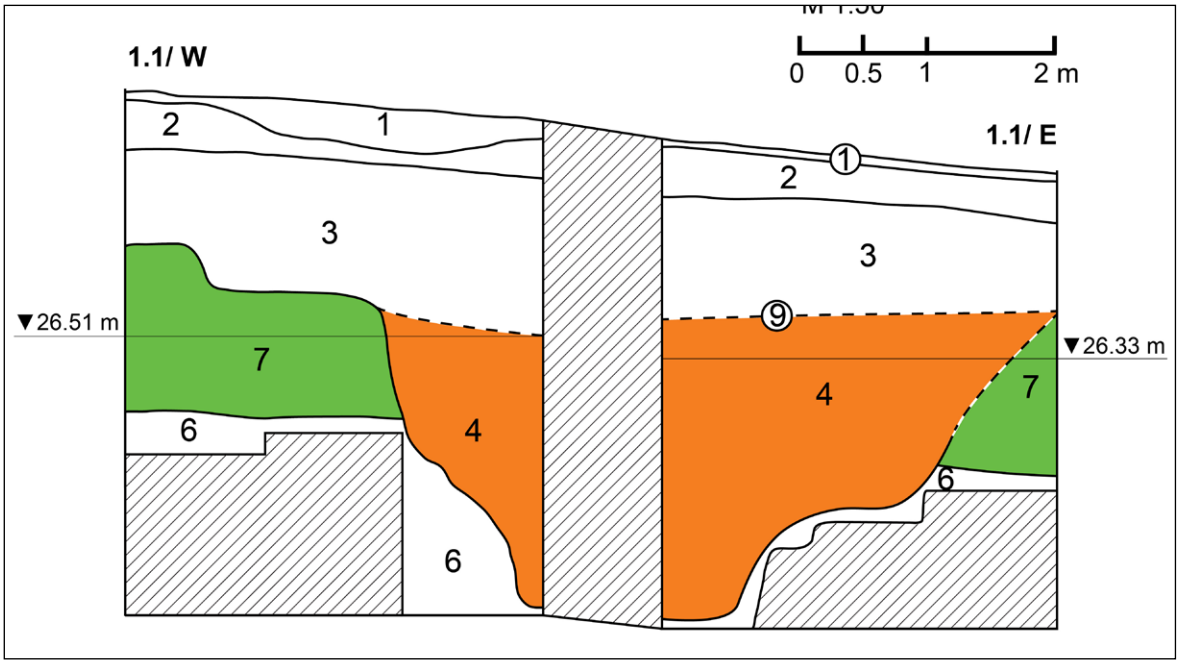


Fig. 12. Site 1. Trench 1.1, northern section: 1 – Loose and full of humus soil, greyish-brown layer – ploughzone. It contained pottery fragments. Pits of unrooted trees from an orchard were visible; 2 – Light brown loess, very dense layer, formed by erosion; it contained small pottery fragments, single charcoals, small pieces of burnt clay, single small stones; 3 – Dark grey full of humus layer, but not as much as layer No. 1. It contained small pottery fragments, single small stones, small and scattered pieces of burnt clay, lots of bioturbations; 4 – Fill of the Early Medieval ditch, brownish-black dense layer; it contained pottery fragments, medium- to small-size stones, single animal bones, single lumps of loess, scattered charcoals, single small pieces of burnt clay, single bioturbations. The artefacts cluster in the lower part of the ditch, close to the bottom, pottery fragments and stones were larger than those in the upper layers. In the northern section of trench No. 1.1/W there were strips of fallen loess lumps from the eastern side of the Early Medieval ditch; 6 – Sterile yellowish-brown loess; 7 – The fill of the earlier ditch with direction E–W, cut by the Early Medieval ditch. It contained ash strips, Late Neolithic pottery fragments, yellowish-brown loess lumps fallen from the ditch sides, single small stones, one flint; 9 – Early Medieval surface from which the ditch N-S was dug. It is almost the same as the surface of the other ditch probably because of the constant significant erosion (drawing and interpretation by L. Vagalinski, L. Traykova)

Border ramparts were built that had less protective functions. The second stage began with the expansion of the Bulgarian state in Moesia in 681 and ended at the beginning of the 9th c. The third stage was connected to the Bulgarian expansion in the southern direction according to a treaty with Byzantium in 815. The abandonment of the earthwork forts is dated to the end of the 9th – the beginning of the 10th c. (Рашев 1982, 121–125). The younger earthwork forts in Bulgaria were built in the middle of the 9th c. (Рашев 2008, 140–142). Given the above, we date the earthwork fort in the 8th–9th c. At this stage of the archaeological research, there are no solid arguments for more precise dating.

Interpretation. The ditch in trench 1.1 was part of a defensive feature of the Early Medieval earthwork fort.

According to the terminology defined by Rashev, the earthwork forts could be divided into ramparts and camps. The partially excavated earthwork fort could be defined as a camp – a feature with a geometrical shape (mostly rectangular) surrounded by a rampart or ditch. Usually, there is a berm between the rampart and the ditch so that the rampart does not slip into the ditch. The area of the earthwork camps in Early Medieval Bulgaria varies between 0.1 and several hundreds of hectares. The current camp area is around 4 ha. Sometimes a second ditch is recorded in the inner side that does not have a defensive purpose. It is formed by removing earth in order to achieve a greater height of the rampart since in the medieval earthwork fortifications the leading role is played by the rampart (Рашев 1982, 17).

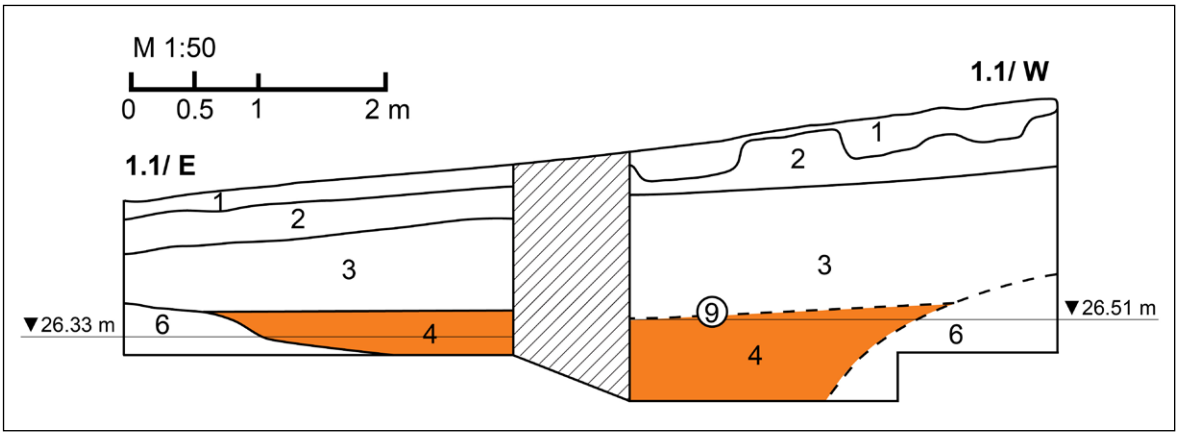


Fig. 13. Site 1. Trench 1.1, southern section: 1 – Loose and full of humus soil, greyish-brown layer – ploughzone. It contained pottery fragments. Pits of unrooted trees from an orchard were visible; 2 – Light brown loess, very dense layer, formed by erosion; it contained small pottery fragments, single charcoals, small pieces of burnt clay, single small stones; 3 – Dark grey full of humus layer, but not as much as layer No. 1. It contained small pottery fragments, single small stones, small and scattered pieces of burnt clay, lots of bioturbations; 4 – The fill of the Early Medieval ditch, brownish-black dense layer; it contained pottery fragments, medium- to small-size stones, single animal bones, single lumps of loess, scattered charcoals, single small pieces of burnt clay, single bioturbations. The artefacts clustered in the lower part of the ditch, close to the bottom, pottery fragments and stones were larger than those in the upper layers. In the northern section of trench No. 1.1/W there were strips of fallen loess lumps from the eastern side of the Early Medieval ditch; 6 – Sterile yellowish-brown loess; 9 – Early Medieval surface from which the ditch N-S was dug (drawing and interpretation by L. Vagalinski, L. Traykova)

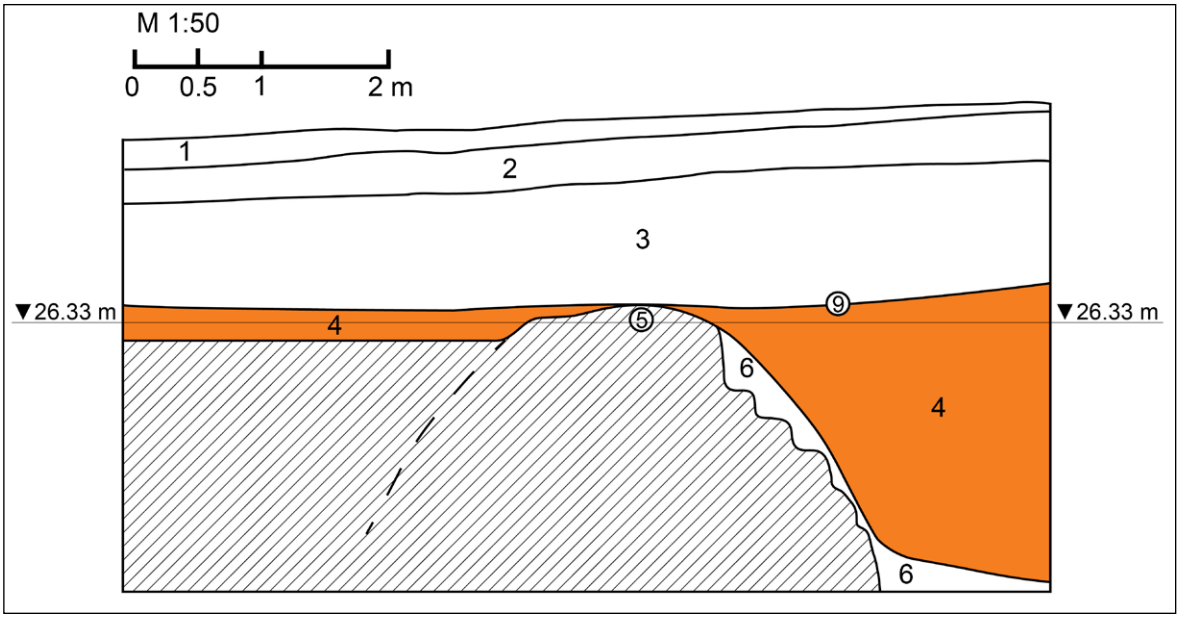


Fig. 14. Site 1. Trench 1.1-E, western section: 1 – Loose and full of humus soil, greyish-brown layer – ploughzone. It contained pottery fragments. Pits of unrooted trees from an orchard were visible; 2 – Light brown loess, very dense layer, formed by erosion; it contained small pottery fragments, single charcoals, small pieces of burnt clay, single small stones; 3 – Dark grey full of humus layer, but not as much as layer No. 1. It contained small pottery fragments, single small stones, small and scattered pieces of burnt clay, lots of bioturbations; 4 – The fill of the Early Medieval ditch, brownish-black dense layer; it contained pottery fragments, medium- to small-size stones, single animal bones, single lumps of loess, scattered charcoals, single small pieces of burnt clay, single bioturbations. The artefacts clustered in the lower part of the ditch, close to the bottom, pottery fragments and stones were larger than those in the upper layers. In the northern section of trench No. 1.1/W there were strips of fallen loess lumps from the eastern side of the Early Medieval ditch; 5 – A passage/path through the ditch – sterile yellowish-brown loess; 6 – Sterile yellowish-brown loess; 9 – Early Medieval surface from which the ditch N-S was dug (drawing and interpretation by L. Vagalinski, L. Traykova)

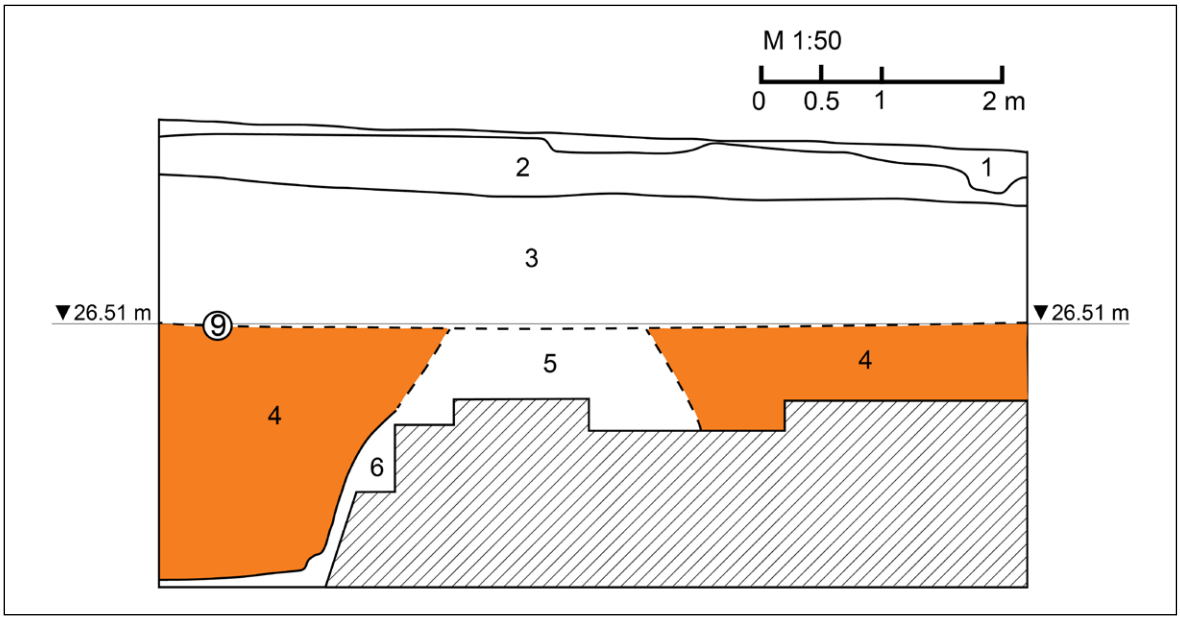


Fig. 15. Site 1. Trench 1.1-W, eastern section: 1 – Loose and full of humus soil, greyish-brown layer – ploughzone. It contained pottery fragments. Pits of unrooted trees from an orchard were visible; 2 – Light brown loess, very dense layer, formed by erosion; it contained small pottery fragments, single charcoals, small pieces of burnt clay, single small stones; 3 – Dark grey full of humus layer, but not as much as layer No. 1. It contained small pottery fragments, single small stones, small and scattered pieces of burnt clay, lots of bioturbations; 4 – The fill of the Early Medieval ditch, brownish-black dense layer; it contained pottery fragments, medium- to small-size stones, single animal bones, single lumps of loess, scattered charcoals, single small pieces of burnt clay, single bioturbations. The artefacts clustered in the lower part of the ditch, close to the bottom, pottery fragments and stones are larger than those in the upper layers. In the northern section of trench No. 1.1/W there were strips of fallen loess lumps from the eastern side of the Early Medieval ditch; 5 – A passage/path through the ditch – sterile yellowish-brown loess; 6 – Sterile yellowish-brown loess; 9 – Early Medieval surface from which the ditch N-S was dug (drawing and interpretation by L. Vagalinski, L. Traykova)

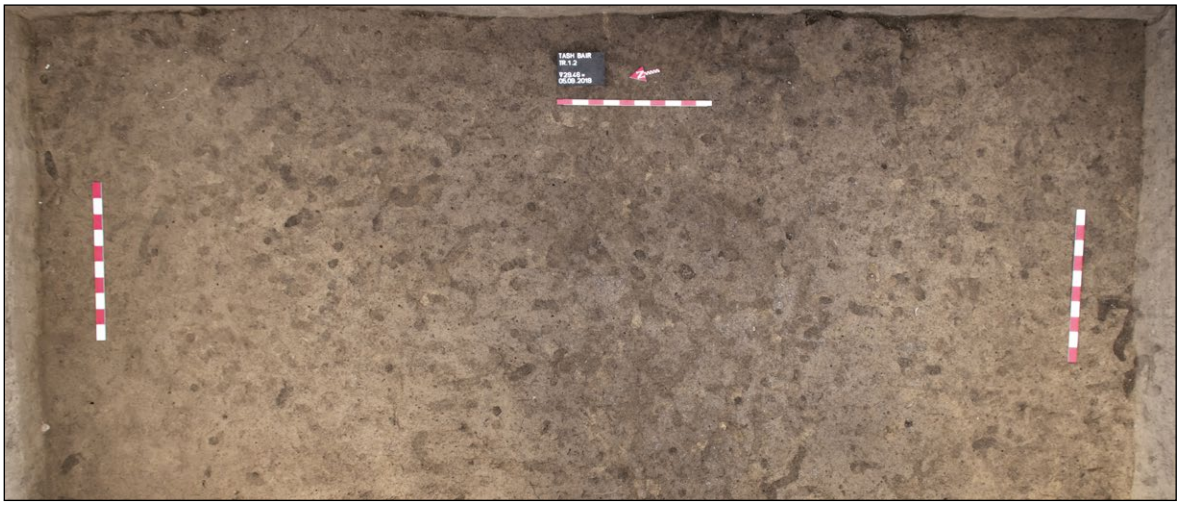


Fig. 16. Trench 1.2, level ▼29.46 m (photo by S. Conrad)

The ditch in trench 1.1 was not fully excavated during this campaign. Interpretation of the geophysical results shows that linear anomalies were inside the fort running parallel to the eastern and western sides. They could be part of limestone features (walls?) or palisade remains (cf. the contributions by B. Ullrich et al., chapter 6.1).

Rashev distinguished four groups of earthwork forts according to their location: in Pliska area; on the road Danube – Pliska – Rishki prohod passage – Southern Bulgaria; on the right bank of Danube

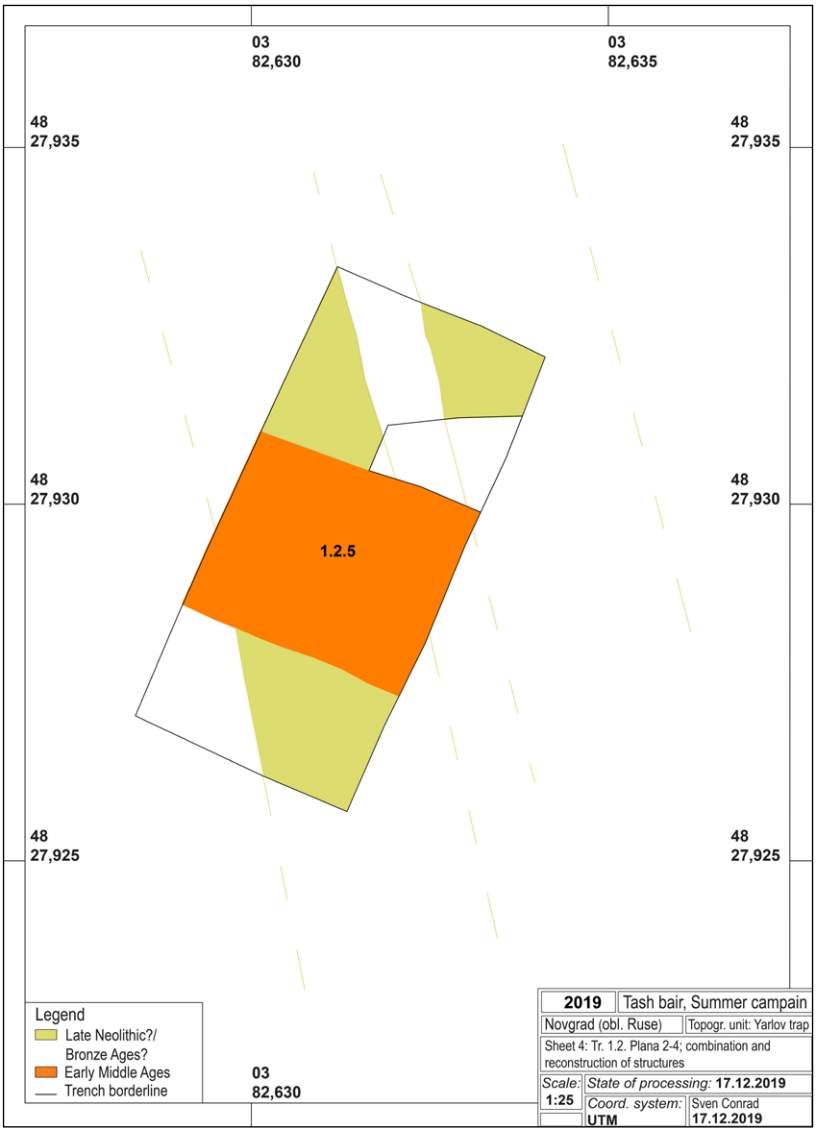


Fig. 17. Plan of the features in trench 1.2 (drawing by S. Conrad, adapted by L. Traykova)

between Ruse and Silistra; on the road between Pliska and the western border of the First Bulgarian Kingdom (Ostrovski, Hayredinski and Lomski ramparts) that are situated to the west of Pliska. The last group includes four fortifications from east to west: near Pobit kamak village, Razgrad municipality; near Starmen village, Byala municipality; near Borislav village, Pordim municipality; and near Stavertsi village, Dolna Mitropoliya municipality. Archaeological excavations have been conducted only on the site near Starmen village that is guarding a ford that crosses the Yantra River. The other three forts are only assumed to be dated to the Early Middle Ages due to the type of defensive features (Рашев 1982, 95, 109–117). These groups form an area of Bulgaria, bounded between the Danube, Stara Planina mountain, Black Sea and Yantra River. The most important earthwork barriers are located on the periphery of this area, and most of the localized camps are situated inside (Рашев 1982, 122). In a more recent study, the last group of sites located west of Pliska was not included in the main areas for the location of earthwork forts. Due to the structural features of the construction of the rampart, the fort near Starmen village is defined as a transitional variant between an earthwork fort and the later dated stone fortresses of the Tsar Asen group (Рашев 2008, 140). A possible reason for the exclusion of the group of forts between Pliska and the western border ramparts is the uncertain dating of three of the four forts mentioned in this group. The earthwork forts guarding the main road artery, Danube – Pliska – Rishki prohod passage, are located at approximately equal distances; the same as those south of Tutrakan rampart (Рашев 1982, 76, табл. XXIV, 117; Рашев 2008, 141). This peculiarity corresponds with Rashev's hypothesis that the location of the four forts on the road from Pliska to the western border ramparts since the distance



Fig. 18. Trench 1.2, level ▼29.30 m (photo by Lea Valcov)



Fig. 19. Trench 1.2, the bottom of the ditch 1.2.5, level ▼26.94 m (photo by S. Conrad)

between them is approximately the same. The complex structure of the fortification near the Starmen village (Рашев 2008, 140) suggests that it was probably built in several stages. Its strategic location at the ford of the Yantra River was probably connected by a road artery oriented east-west.

The available data on the inhabitation of the camps from their initial period as fortified settlements show that they were rarely used as such (Pliska, Kabiyuk Archaeological Reserve, near Han Krum village, Veliki Preslav municipality, and near Nova Cherna village, Tutrakan municipality). Permanently inhabited earthwork forts are recorded when the fortifications are no longer functioning and dwellings dug on the inside of the ramparts are discovered (near Popina village, Sitovo municipality, and near Kladentsi village, Tervel municipality). The functioning of these sites as unfortified settlements is referred to as the earliest in the period from the end of the 9th to the beginning of the 10th c. In other forts, no traces of



Fig. 20. Trench 1.2, western cross-section and the bottom of the ditch 1.2.5, level ▼26.94 m (photo by L. Vagalinski)



Fig. 21. Trench 1.2, eastern cross-section and the bottom of the ditch 1.2.5, level ▼26.94 m (photo by L. Vagalinski)

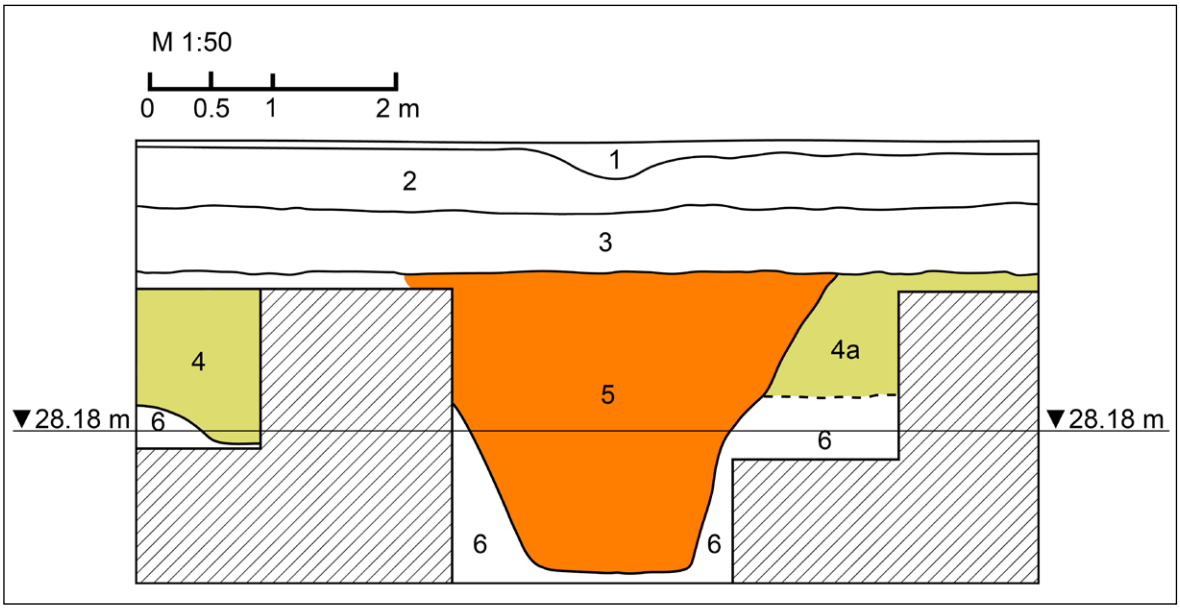


Fig. 22. Site 1. Trench 1.2, eastern section: 1 – Loose and full of humus soil, greyish-brown layer – ploughzone. It contained pottery fragments. Pits of unrooted trees from an orchard were visible; 2 – Light brown loess, very dense layer, formed by erosion; it contained small pottery fragments, single charcoals, small pieces of burnt clay, single small stones; 3 – Dark grey full of humus layer, but not as much as layer No. 1. It contained small pottery fragments, single small stones, small and scattered pieces of burnt clay, lots of bioturbations; 4 – The ditch was older than the Early Medieval ditch which it was cut by it, light brown dense layer. It contained Late Neolithic pottery fragments, animal bones, scattered charcoals, single pieces of yellowish-brown loess fallen from the sides of the ditch, single pieces of burnt clay, single traces of bioturbation; 4a – Layer/fill of the older ditch, light brown layer. It contained Late Neolithic pottery fragments, loess pieces fallen from the sides of the ditch, scattered charcoals, pieces of burnt clay. Probably (4) and (4a) are part of the same double ditch; 5 – Early Medieval ditch, greyish-brown dense filling. It contained pottery fragments, animal bones, single charcoals, single pieces of yellowish-brown loess fallen from the sides of the ditch; 6 – Sterile yellowish-brown loess (drawing and interpretation by L. Vagalinski, L. Traykova)

settlement are recorded (Rish village, Smyadovo municipality, Dunavets village, Tutrakan municipality, and near Kus village – part of Kaolinovo town). Synchronous settlements probably existed around the camps (Рашев 2008, 142). The partially excavated earthwork fort from site 1 falls in close proximity to the western periphery of the area separated by Rashev between the Danube, Stara Planina mountain, Black Sea and Yantra River. No archaeological excavations have been carried out inside the earthwork fort. This limits the possibilities for determining its purpose.

According to the results gathered during the field surveys in 2018 (Вагалински et al. 2019, 84), the Early Medieval pottery fragments that we recorded at site 1 are a relatively small amount for a permanently inhabited settlement (cf. the contributions by N. Kecheva et al., chapter 12, site 1). The quantity of these fragments from the Early Medieval ditches in trenches 1.1 and 1.2 is also small. The probable explanation for the small number of Early Medieval pottery fragments in the eastern ditch is the presence of a rampart on the western/inner side, which was a natural obstacle to the accumulation of artefacts from inside the fort. It should be pointed out that the deepest Early Medieval pottery fragments found in trench 1.1-W were discovered at a depth of more than 1 m above the bottom of the ditch (cf. chapter 9.1, table 7). During the field surveys in 2019 (Вагалински et al. 2020b, 18–20), Early Medieval sites located in the immediate vicinity of site 1 (cf. the contributions by N. Kecheva et al., chapter 12, sites 19–22) were recorded. It seems the Early Medieval earthwork fort was not permanently inhabited but defended the surrounding population in case of danger.

The ditch in trench 1.2 was not part of the large protective ditch of the earthwork fort because it was located inside the fort, almost parallel to its southern side. The geophysical survey shows that it was a separate linear negative anomaly (fig. 1). Its connection with other anomalies surrounding a certain area

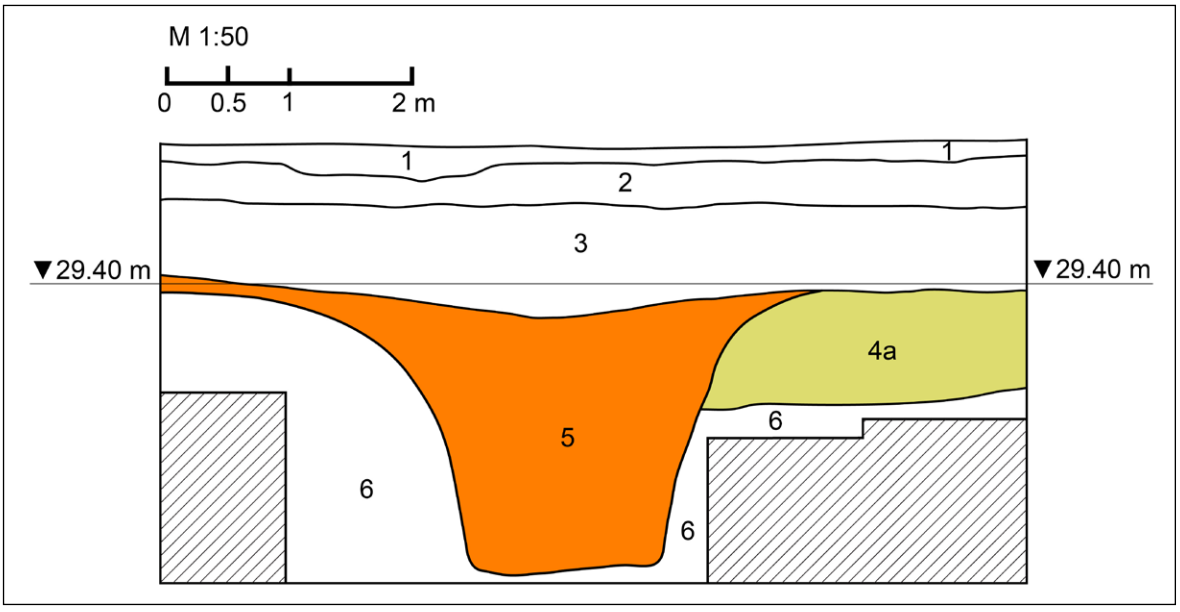


Fig. 23. Site 1. Trench 1.2, western section: 1 – Loose and full of humus soil, greyish-brown layer – ploughzone. It contained pottery fragments. Pits of unrooted trees from an orchard were visible; 2 – Light brown loess, very dense layer, formed by erosion; it contained small pottery fragments, single charcoals, small pieces of burnt clay, single small stones; 3 – Dark grey full of humus layer, but not as much as layer No. 1. It contained small pottery fragments, single small stones, small and scattered pieces of burnt clay, lots of bioturbations; 4a – Layer/fill of the older ditch, light brown layer. It contained Late Neolithic pottery fragments, loess pieces fallen from the sides of the ditch, scattered charcoals, pieces of burnt clay. 5 – Early Medieval ditch, greyish-brown dense filling. It contained pottery fragments, animal bones, single charcoals, single pieces of yellowish-brown loess fallen from the sides of the ditch; 6 – Sterile yellowish-brown loess (drawing and interpretation by L. Vagalinski, L. Traykova)

is not traced. The upper part of the ditch in trench 1.2 was twice narrower than the one in the ditch in trench 1.1 at approximately the same depth. The southern side of the fort was located at the lowest part of the terrain, and it could be assumed that in order not to be vulnerable, the rampart there had to be higher, which would explain the presence of the second narrower ditch in trench 1.2.

The distinction between two groups of Early Medieval pottery fragments shows a long period of use of the earthwork fort during the period of the First Bulgarian Kingdom (681–1018). The absence of fragments from the earlier group in the ditch fill in trench 1.2 allows us to assume that it may have been excavated at a slightly later stage. The removed soil was probably used to raise the level of the southern rampart or to repair other parts of the rampart. Statistics of the pottery fragments from the two ditches demonstrates that slightly more fragments were in the ditch fill in trench 1.2 but they were only from the late group (cf. chapter 9.1, part 9.1.2.6; chapter 9.1, table 7). The ditch in trench 1.2 probably did not have a rampart. The sloping terrain from north to south and the constant erosion are possible explanations for the higher number of pottery fragments in the ditch fill which had fallen into it from inside the fort. On one hand, terrain displacement and erosion are possible explanations for the lack of pottery fragments from the earlier group. On the other hand, they are also an indication that this inner ditch was probably not dug at the same time as the eastern ditch in trench 1.1. We assume that the two ditches mark two phases in the use of the fort. The excavation in the inner area and establishing the stratigraphy will complement the available data on its functions (refuge for surrounding population and/or a military camp?) and its stages of inhabitation during the Early Middle Ages.

РАННОСРЕДНОВЕКОВНИ ФОРТИФИКАЦИИ В СОНДАЖИ 1.1 И 1.2

Людмил Вагалински, Люба Трайкова, Надежда Кечева

(Резюме)

Описание. През пролетта на 2018 г. при теренно археологическо проучване беше документирано квадратно землено укрепление с размери около 200 на 200 м, оградено с ров и вал, видим над съвременния терен, разположено в границите на обект 1 (Вагалински et al. 2019, 84). Укреплението е регистрирано за пръв път при теренни проучвания през 1999 г. (Вагалински et al. 2001a, 77). Резултатите от геофизичното проучване показаха и други вкопани линейни аномалии вътре в рамките на укреплението (вж. приноса на Б. Улрих и др., глава 6.1). За проучването на част от тези аномалии заложихме два сондажа.

Сондаж 1.1 е заложен напречно върху източния ров (с направление север – юг) на земленото укрепление (fig. 1). Ситуиран е приблизително в средата, по направлението на рова, където според резултатите от геофизиката изглежда, че ровът прекъсва и там вероятно е оформен вход към укреплението. Сондажът е с площ 49 м^2 и размери 7 × 7 м, разделен на изток (1.1-E) и запад (1.1-W) от ребро с широчина 0,9 м (fig. 1). Теренът тук е с наклон от север на юг и от запад на изток. Повърхностният пласт в сондаж 1.1 от обработваема почва (около 0,40 м) беше отнет със земекопна техника. В дълбочина работата продължи на ръка, с отнемане на механични пластове.

Сондаж 1.1-E. На ▼26,44 м в план до западния профил на сондажа се очерта ровът и мястото, където е бил проходим (fig. 3). От тази дълбочина работата продължи само в очертанията на рова – в северозападния и югозападния ъгъл на сондажа. Неговото дъно в северозападния ъгъл на сондажа беше достигнато на ▼24,36 м (figs. 4, 5).

Сондаж 1.1-W. След изравняване на ▼26,58 м разграничихме в план очертанията на рова и прохода в него (fig. 9). Установихме, че струпването на по-големи фрагменти керамика, човешки и животински кости е в свлечен пласт, отложен върху проходимата част от рова. От тази дълбочина работата продължи само в очертанията на рова – в североизточния и югоизточния ъгъл на сондажа. Неговото дъно в североизточния ъгъл на сондажа беше достигнато на ▼24,35 м (fig. 10).

Структурите от проучения ров в сондаж 1 получиха следната номерация: 1.1.7 – сондаж 1.1-E, северозападен ъгъл; 1.1.8 – сондаж 1.1-E, югозападен ъгъл; 1.1.13 – сондаж 1.1-W, североизточен ъгъл; 1.1.14 – сондаж 1.1-W, югоизточен ъгъл (fig. 11). Поради ограничения срок на проекта не успяхме да довършим проучването на рова в структури 1.1.8 и 1.1.14.

Напречното сечение на проучения ров е с неправилна трапецовидна форма – източната / външна стена на рова е по-полегата и в долната си част е оформена стъпаловидно, докато западната / вътрешна стена е с по-голям наклон. Дъното е почти равно, а дълбочината му е била над 2 м. Измерена от съвременната повърхност до дъното при северния профил, дълбочината е около 3,70 м. Запазената широчина на прохода през рова в горната му част е около 1,50 м (figs. 14, 15). Най-вероятно стените на прохода са се обрушвали и са се добавили към пълнежа на рова. Ровът е вкопан в стерилен льос, но пресича друг, по-ранен ров (figs. 11, 12) от късния железен период (вж. приноса на Л. Вагалински и др., глава 8.3.1).

Сондаж 1.2 е заложен върху пресечната точка на двете вкопани линейни аномалии в югозападната част на земленото укрепление (fig. 1). Сондажът е с площ 23,10 м^2 и размери 7 × 3,30 м. Повърхностният пласт и тук също беше отнет със земекопна техника, а в дълбочина продължихме работата на ръка. Работи се на механични пластове. Сондажът беше разделен условно на три части с цел разграничаване на различни структури и разделяне на подемния материал. Ровът в централната част на сондажа е структура 1.2.5 (figs. 17, 18). Проучването в дълбочина продължи само в неговите очертания. Направихме разрези на рова до достигане

на неговото дъно на ▼26,94 м (figs. 19, 20). Ровът пресича друг по-ранен ров (вж. приноса на Р. Краус, С. Конрад, глава 8.1), а в дълбочина е вкопан в стерилен льос (figs. 21, 22, 23).

Напречното сечение на проучения ров е с форма на обърнат трапец. Дъното е почти равно, а дълбочината му е била поне 2,5 м. Измерена от съвременната повърхност до дъното при западния профил, тя е около 3,50 м.

Анализ и датировка. В пълнежа на рова в сондаж 1.1 открихме керамични фрагменти и различни находки (вж. приноса на Р. Краус, глава 9.2.1, кат. №№ SF 35, 37, 41, 42, 44; Л. Трайкова, глава 9.2.2, кат. №№ SF 46 – 50) от различни епохи. Керамичните фрагменти, изработени на колело, открити в пълнежа на източния ров на земленото укрепление и главно в пластовете близо до дъното (вж. глава 9.1, tables 6, 7), позволяват той да се отнесе към Ранното средновековие от периода на Първата българска държава (681 – 1018 г.). Разграничени са две групи ранносредновековна керамика: ранна от края на VII – VIII в. и късна от IX – началото на XI в. Фрагментите от ранната група са значително по-малко спрямо тези от късната група и принадлежат към горните пластове от запълването на рова само в сондаж 1.1. Според подемния материал ранносредновековният ров в сондаж 1.2 не съдържа фрагменти от ранната група. Това показва, че поради ерозията имаме обърната стратиграфия, което обяснява защо фрагменти от по-късната група са паднали на дъното на рова, а фрагментите от по-ранната група попадат в пластовете над тях.

Р. Рашев разграничава три основни етапа в периодизацията при изграждането на средновековни землени укрепления на Долен Дунав. Първият етап е отнесен към 60-те и 70-те години на VII в. Изграждат се пограничните валове, които имат не толкова защитни функции; вторият етап започва с утвърждаването на българската държава в Мизия през 681 г. и завършва в началото на IX в.; третият етап е свързан с разширяването на България на юг въз основа на договора с Византия от 815 година. За горна граница за изграждане на този тип укрепления в България е определена средата на IX век, а изоставянето им е отнесено в края на IX – началото на X в. (Рашев 1982, 121 – 125; Рашев 2008, 140 – 142). Предвид гореизложеното датираме земленото укрепление в VIII – IX век. На този етап от археологическото проучване липсват теренни аргументи за по-точна датировка.

Интерпретация. Ровът в сондаж 1.1 е част от отбранителното съоръжение на ранносредновековно землено укрепление.

Според терминологията, определена от Р. Рашев, проученото землено укрепление отговаря на определението за лагер – съоръжение с геометрична форма (най-често правоъгълна), очертана от насип / вал и ров. Понякога от вътрешната страна се проследява втори ров, който не е с отбранително предназначение. Той се образува от загребването на земна маса с цел постигане на по-голяма височина на вала, тъй като при средновековните землени укрепления водеща роля има валът (Рашев 1982, 17).

Валът на рова в сондаж 1.1 не беше проучен поради ограничените срокове на проекта. Интерпретацията на резултатите от геофизичното заснемане показва, че вътре в укреплението, успоредно на източната и западната страна, са регистрирани положителни линейни аномалии, вероятно произхождащи от варовикови структури (стени?) или останки от палисада (вж. приноса на Б. Улрих и др., глава 6.1).

Според разположението на земленните укрепления Р. Рашев разграничава четири групи, формиращи област от България, ограничена между Дунав, Стара планина, Черно море и р. Янтра. По периферията на тази област са разположени най-важните землени прегради, а вътре в нея са повечето локализирани лагери (Рашев 1982, 122). Наличните данни за обитаването на лагерите от началния им период показват, че те рядко са използвани като укрепени селища. Регистрирани са трайно обитавани землени укрепления, когато укрепителните съоръжения вече не са функционирали и са разкрити жилища, вкопани от вътрешната страна на валовете. Функционирането на тези обекти като неукрепени селища е отнесено най-рано в периода от

края на IX – началото на X в. При други укрепления не са открити следи от селищно обитаване. Вероятно са съществували синхронни селища около лагерите (Рашев 2008, 142).

Проученото землено укрепление от обект 1 попада в непосредствена близост до западната периферия на обособената от Р. Рашев област. Не са провеждани археологически разкопки вътре в рамките на земленото укрепление. Това ограничава възможностите за определяне на неговото предназначение. Фрагментите ранносредновековна керамика, открити на обект 1 при теренните издирвания през 2018 г. (Вагалински et al. 2019, 84) и от археологическите разкопки на ранносредновековните ровове в сондажи 1.1 и 1.2, са сравнително малко количество за трайно обитавано селище (вж. приноса на Н. Кечева и др., глава 12, обект 1). Вероятното обяснение за малкия брой ранносредновековни фрагменти в източния ров е наличието на вал от западната / вътрешна страна, който е бил естествено препятствие за натрупване на материали от вътрешността на укреплението. При теренните издирвания през 2019 г. (Вагалински et al. 2020b, 18 – 20) са регистрирани ранносредновековни обекти, разположени в близките околности на обект 1 (вж. приноса на Н. Кечева и др., глава 12). Поради малкото количество керамика от площта на земленото укрепление и наличието на ранносредновековни обекти в близост до него предполагаме, че то не е интензивно обитавано като селище.

Ровът в сондаж 1.2 не е част от големия защитен ров на земленото укрепление, а е разположен вътре в него, почти успоредно на южната му страна. Геофизичното заснемане показва, че той е самостоятелна линейна аномалия (fig. 1). Южната страна на укреплението е най-ниско разположената и може да се предположи, че за да не бъде уязвима, валът там е трябвало да бъде по-висок, което би обяснило наличието на втория по-тесен ров в сондаж 1.2. Статистиката за керамиката от двата рова показва малко повече керамични фрагменти в полза на рова в сондаж 1.2, но само от по-късната група. Самият ров в сондаж 1.2 вероятно не е имал вал. Спускането на терена от север на юг и постоянната ерозия са възможно обяснение за по-високия брой фрагменти, попаднали в него от вътрешността на укреплението. Споменатата денивелация на терена и ерозията от една страна са възможно обяснение за липсата на фрагменти от по-ранната група, а от друга са довод, че вероятно този вътрешен ров не е изкопан едновременно с източния ров в сондаж 1.1. Допускаме, че двата рова отбелязват две фази в използването на укреплението. Проучването чрез разкопки на неговата вътрешна площ и установяването на стратиграфията ще допълнят наличните данни за функциите (убежище за околното население и / или военен лагер?) и етапите му на обитаване през Ранното средновековие.

9. POTTERY AND SMALL FINDS

9.1. THE POTTERY FINDS (WITH CATALOGUE)

9.1.1. Prehistoric pottery

Raiko Krauß

9.1.1.1. The chronological framework for the prehistoric periods since the Mesolithic

The foundations for the relative chronology of the Bulgarian prehistory were established during the 1960s. They essentially go back to the parallelisation of the previously known finds with the chronological systems of Anatolia, the Aegean and southern Germany, as well as the stratigraphic observations on tell settlements in Thrace. Up until the end of the Second World War, these chronologies were predominantly based on the observations made on the strata sequences of Yunatsite, Kremikovtsi, Veselinovo, Sveti Kirilovo and Deve-Bargan (Birkner 1916; Миков 1933; Gaul 1948; Milojčić 1949). The excavations at tell Karanovo, whose basic stratigraphic sequence was presented in 1961 by Georgi Georgiev, were of great importance for the chronological division. On the basis of this, Henrieta Todorova constructed the chronological framework for the Neolithic and the Chalcolithic (Тодорова 1986; Тодорова, Вайсов 1993). The work of Krasimir Leshtakov, based on the excavations of the settlement mounds of Ezero, Nova Zagora, Dyadovo, Karanovo, Veselinovo, Sveti Kirilovo and Asara, was fundamental to understanding the Bronze Age structure (Лещаков 2000). A synthesis of the Early Iron Age structure was presented by Maria Chichikova (Čičikova 1971) who drew on the previous work, including the extensive geographical framework, of Bernhard Hänsel (1968; 1974a; 1976). For a long time, the absolute chronology of the finds was unclear since the dating from the nearest sites in the Middle East and Egypt (fixed in time via historical dates) only provided imprecise, and as we now know, also some incorrect results (cf. Milojčić 1949). It was only with the introduction of the ^{14}C method in archaeology that the first reliable dates were obtained, which were surprisingly much older than previously believed. By evaluating data series from the Berlin Radiocarbon Laboratory, Jochen Görsdorf and Yavor Boyadzhiev (1996) succeeded in presenting the first basic chronological framework for the Bulgarian prehistory. These were conventional measurements, for which mainly charcoal was used, or larger collections of bone were necessary to achieve the required amount of collagen. The calibration of the measured values was carried out using the curve published in 1993, initially with comparatively little dendrochronological data (Stuiver, Pearson 1993; Person, Stuiver 1993). It is noteworthy that the data from settlement sequences were already processed using the then highly innovative method of Archaeological Wiggle Matching (Weninger 1986).

The generally accepted chronological framework for the historical periods is essentially based on the periodisation, which follows the main epochs of the respective region, and which can be deduced from the written sources. Historical records for the Aegean and the Eastern Mediterranean region (which became more numerous in the first half of the first millennium BC) form the basis of the detailed historical framework for the younger periods (fig. 3). These individual periods are often significantly shorter than in prehistory, so that comparisons, for example of settlement intensities, are difficult. Archaeology, especially survey research based on unstratified finds, is faced with the difficulty that the chronology of the finds cannot always be brought into congruence with the historical periods (see below). This leads to certain shifts and blurring of the delimitations of the periods, especially since excavations on a larger scale at the Tash Bair are still missing for the time being. The current ongoing work within the project will help clarify the periodisation for the region[1].

1 Cf. Görsdorf/Bojadžiev 1996; Bojadžiev 1998; Bojadžiev 2007; Tsirtsoni 2016 and figure 1 in this study.

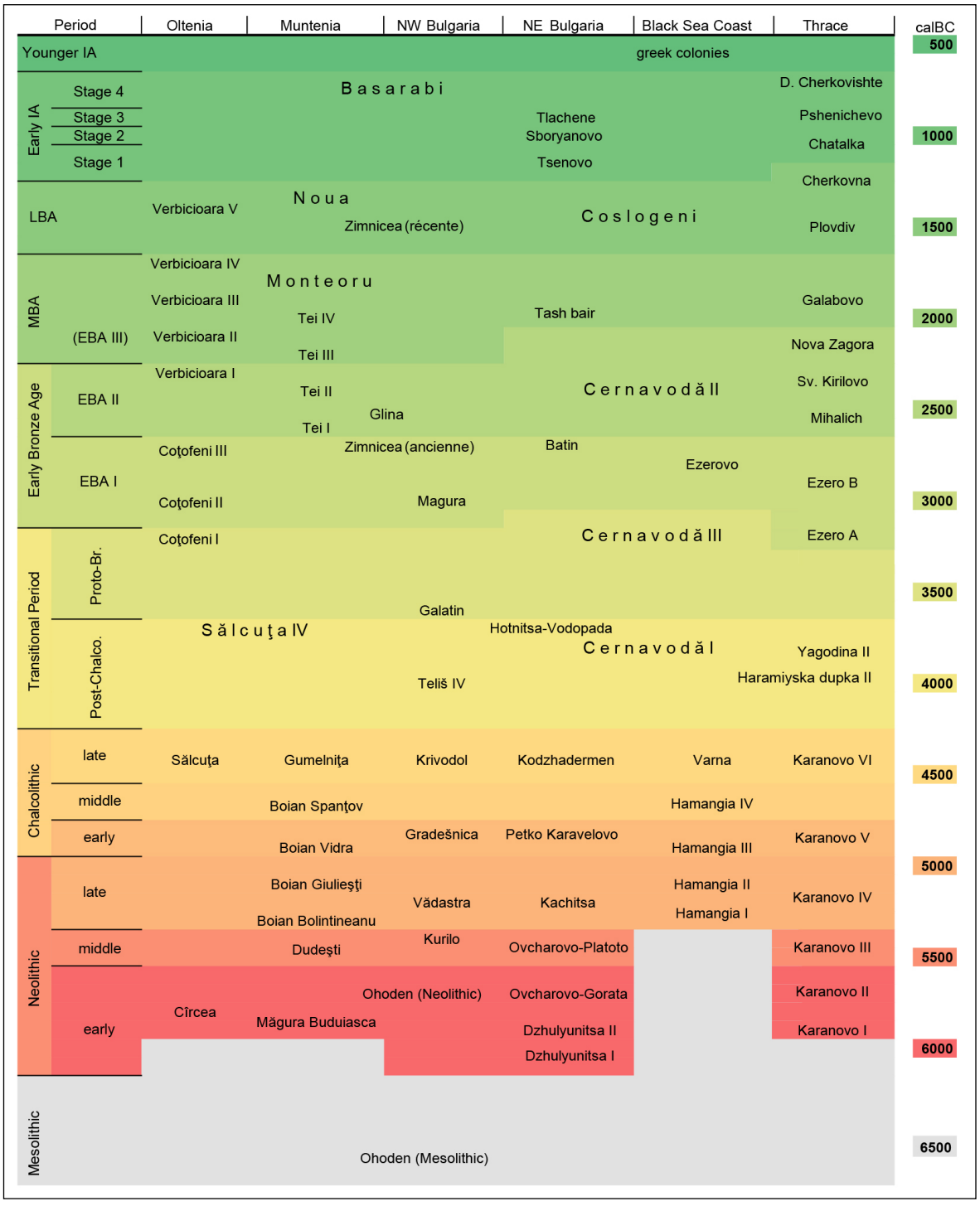


Fig. 1. Chronology of the prehistoric periods in the Eastern Balkan region (by R. Krauß)

The modifications and corrections to the chronological framework that have taken place in the 25 years since Görsdorf and Boyadzhiev's work, can largely be traced back to our work in northern Bulgaria (table 13). These are to be briefly summarised here.

Information on the *Mesolithic* settlement in northern Bulgaria was only very sparse until recently, although the well-studied zone of the Danube Gorges (Iron Gates) is not far away, and settlement of the lowlands on the Lower Danube is to be expected. In the well-known finds from the Pobiti Kamani near Varna, there are no indications of precise dating (Gatsov 1989); however, there are some indications of an even later dating for the chipped stone collections (Krauß 2007). It was only in the last few years that reliable features from the Mesolithic could be identified at the Ohoden site in northwestern Bulgaria

(Ганецовски et al. 2020), dating back to the first half of the 7th millennium BC. There are no materials from the surveys and excavations of the project published here that can be assigned to the Mesolithic.

The research in the catchment area of the Yantra, and in the neighbouring river valley to the east of the Rusenski Lom, was of great importance for determining the beginning of the *Neolithic* in northern Bulgaria and the entire Balkan region. The excavations in Dzhulyunitsa, which offered a complete stratigraphic sequence from the Early Neolithic, is worth mentioning here. The modelling of the Accelerator Mass Spectrometry (AMS) data (obtained therefrom on short-lived samples) made it possible to determine the beginning of the Neolithic settlement in this area to the 61st century BC (Krauß et al. 2014). This dating is further confirmed by the newly acquired AMS data from the Koprivets site in the Rusenski Lom catchment area (Marinova, Krauß 2014). This also made it clear that the older, high data from Dzhulyunitsa, but also that from Polyanitsa-Platoto in the catchment area of the Kamchia River, cannot be used to determine the advent of the Neolithic. The reasons for this are different. In Dzhulyunitsa, the high data could be identified as outliers due to the modelling of the entire data set (Krauß et al. 2014). This was partly because the samples were taken from pig bones which can have a reservoir effect similar to human bones. The small series of data from Polyanitsa-Platoto were measured on organic additions to the pottery by conventional measurements. These high values result from the mixed sample, which also contained fossil organic components from the clay (see the detailed discussion in Krauß 2014, 286–290).

The developed Early Neolithic in northern Bulgaria could be chronologically fixed by means of an extensive AMS data series on the material from the Ovcharovo-Gorata site in the catchment area of the Kamchia (Krauß 2014, 280–294). The time position is confirmed by the modelled data series obtained in the upper layers from Dzhulyunitsa (Krauß et al. 2014). The Neolithic material found during the surveys and excavations at Tash Bair can be assigned to later phases. However, an Early Neolithic date comes from the core T1C29_360 in the floodplain (RICH-28447). Small ceramic fragments and a flint artefact also come from the same drill section, indicating a site below the colluvium (cf. the contributions by A. López del Olmo et al., chapter 4).

The following sequence of the Middle and Late Neolithic in northern Bulgaria is comparatively poorly documented with radiocarbon data. To tackle this problem, a new series of ^{14}C dates was taken from the multi-layered site of Varbitsa, again in the catchment area of the Kamchia. This series is currently being evaluated and will be presented as part of a Tübingen dissertation. The raw data presented here from Varbitsa already help to better understand the older dates for the Middle and Late Neolithic.

The great mass of prehistoric finds from Tash Bair, namely from Site 1, can be assigned to the *Late Neolithic*. A differentiation within this epoch cannot be made due to the methodology used. But it is clear that different phenomena are represented in the material (Vădastra, Boian, Hamangia, Bulgarian Late Neolithic), which appear at different times within the Late Neolithic development. Different regional cultural groups, or people with differing traditions appear to be present at Tash Bair at the same time. This would be possible due to its geographical location at the intersection of the groups mentioned.

We have three radiocarbon dates from the corresponding contexts (Poz-120368; Poz-120370; Poz-120371) (cf. the contributions by R. Krauß, S. Conrad, chapter 8.1), dating to the 51st/50th century calBC, which correspond to the dates of the Late Neolithic layers of Kachitsa and Hotnitsa-Orlovka. The data series from Varbitsa is earlier and should therefore correspond to the Middle Neolithic. But here it is worth waiting for the modelling. New data from the Brankovtsi site in northwestern Bulgaria (Кечева et al. 2020) provides comparable values.

New data series from the well-known Chalcolithic tell settlements in northern Bulgaria and southern Romania, as well as the dating of the burials of the Varna I necropolis, have led to a fundamental reassessment of the chronology of the Chalcolithic. The initial conception of the chronological structure of the Chalcolithic can only be retained at its beginning, shortly after 5000 calBC (Görsdorf, Bojadžiev 1996). With the duration of the burials in Varna I being determined as spanning from the 46th to the 43rd century, the Bulgarian Late Chalcolithic was shifted to about 200 years earlier (Higham et al. 2007;

Krauß et al. 2017). These results are by no means surprising considering the introduction of AMS dating across Europe, which indicated that the Neolithic must be set earlier. There is broad agreement in the specialist community that the beginning of the Late Chalcolithic in the Lower Danube region should be around 4600 calBC (Hansen et al. 2008; Гайдарска 2011; Reingruber et al. 2011; Tsirtsoni 2016), and that the older approaches (cf. Görsdorf, Bojadžiev 1996; Bojadžiev 1998) must be discarded. The end of the Late Chalcolithic can be grasped even more clearly, as all tell settlements in this area break off at the latest by 4200 calBC (Hansen et al. 2008; Čohadžiev, Krauß 2019). Both, the low number of finds and a radiocarbon date (Poz-120369) indicate that the Tash Bair was settled or at least visited during the Late Chalcolithic (cf. the contributions by R. Krauß, S. Conrad, chapter 8.1).

In terms of research history, the following time is viewed as a Transitional period to the Early Bronze Age (Morintz, Roman 1968; Roman 1971; Georgieva 1993). Since this is a comparatively long period of time, it made sense to divide it into phases. The determination developed in southern Romania on the basis of the various sites of Cernavodă (Roman 1971; Morintz 2001) is suitable for this purpose, although it was only adopted selectively by Bulgarian research (cf. Nikolova 1999). Instead, Ivan Vajsov (2002) developed his own structure based on the sequence of burials in Durankulak, describing the 42nd to 37th century as the Post-Chalcolithic and the 36th to 32nd century as the Proto-Bronze Age.

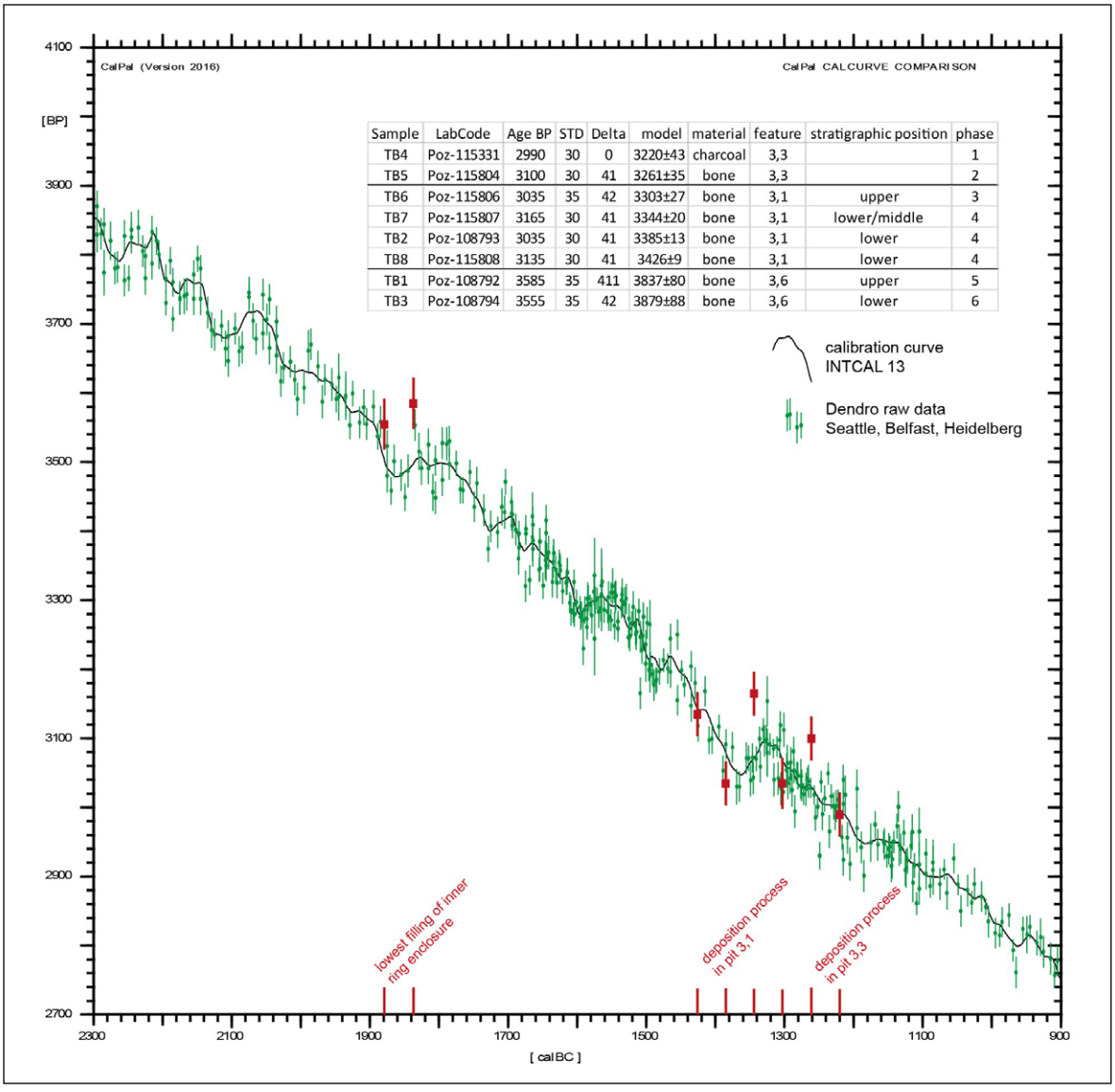
Interestingly, two data from the geomorphological drilling in the floodplain (T9C13_467; T9C17_280) lay within this timespan (RICH-28435; RICH-28446).

A separate problem is the determination of the beginning of the Early Bronze Age. Here the impression of a very early beginning of the Bronze Age tell settlements in Thrace arose too, based on the older conventionally charcoal dates from the Berlin Laboratory (cf. Görsdorf, Bojadžiev 1996). The re-evaluation of the data series from Ezero (Weninger 1995) in comparison to the settlement sequence of the Early Bronze Age Troy (Weninger, Easton 2014; Jung, Weninger 2015), and Kanlıgeçit in Turkish Thrace (Özdoğan, Parzinger 2012), led to a correction. The Early Bronze Age in Bulgaria does not begin until the 31st century BC, which is in line with the Bronze Age development in the Aegean (Weninger, Jung 2009; Weninger, Easton 2014).

The determination of the Middle Bronze Age on the lower course of the Danube is again closely related to our research in the catchment area of the Yantra and the neighbouring areas. Although, no tell settlements or larger stratigraphic sequences are known from northern Bulgaria during this period, the extensive finds can be linked to the sequences of the Tei and Verbicioara cultural groups in southern Romania (Krauß 2006a). The last ^{14}C data collected allow these facies to be narrowed down to the time between the 23rd and 17th century BC (Krauß (in press)-b). This chronological delimitation makes sense because it corresponds to the horizon of the Mycenaean Shaft Graves, which allows them to be connected over a large area with the Apa-Hajdúsámson hoarding horizon in the Carpathian Basin, which in turn corresponds to level Br-A2 of the South German Bronze Age (Hänsel 1968; David 2002; Metzner-Nebelsick 2013). The Bulgarian finds are located in a geographically middle position in-between the Aegean, and the Carpathian region.

As far as the beginning of the Late Bronze Age is concerned, the Zimnicea-Cherkovna-Plovdiv find horizon, which can be found over a large area in the Eastern Balkans, provides a good starting point (Alexandrescu 1973; Hänsel 1976; Panajotov 1989). The northern Bulgarian sites do not offer sufficient settlement stratigraphies for this period either, which is why it initially makes sense to look at the cultural development in the neighbouring areas. Significant highlights can certainly be seen here in the end of the Mycenaean palace culture and the fall of the Hittite Empire around 1200 BC (Jung, Weninger 2002).

The construction of the inner ditch at Tash Bair, Site 3, belongs to the Middle Bronze Age (cf. the contributions by L. Vagalinski et al., chapter 8.2.1). Corresponding ceramic finds come from the bottom layer of the ditch, and their time position is secured by ^{14}C data (fig. 2). This ditch was apparently still in use during the Late Bronze Age (and later during the Late Iron Age, and probably still during the Late Roman period). From the Late Bronze Age, we have radiocarbon dates from two different features within the enclosure, even if the finds from this period are not easily identifiable. We have a total of



Sample	LabCode	Age BP	STD	Delta	model	material	feature	stratigraphic position	phase
TB4	Poz-115331	2990	30	0	3220±43	charcoal	3,3		1
TB5	Poz-115804	3100	30	41	3261±35	bone	3,3		2
TB6	Poz-115806	3035	35	42	3303±27	bone	3,1	upper	3
TB7	Poz-115807	3165	30	41	3344±20	bone	3,1	lower/middle	4
TB2	Poz-108793	3035	30	41	3385±13	bone	3,1	lower	4
TB8	Poz-115808	3135	30	41	3426±9	bone	3,1	lower	4
TB1	Poz-108792	3585	35	411	3837±80	bone	3,6	upper	5
TB3	Poz-108794	3555	35	42	3879±88	bone	3,6	lower	6

Fig. 2. Gauss Monte Carlo Wiggle Matching of stratified radiocarbon samples from Bronze Age features at site 3 (by R. Krauß)

eight radiocarbon dates on short-lived samples (Poz-115331; Poz-115804; Poz-115806; Poz-115807; Poz-108793; Poz-115808; Poz-108792; Poz-108794), most of which can also be related to each other stratigraphically. Based on the stratigraphic position of the ^{14}C samples, we have developed an age model which contributes to a more precise dating of this structures (fig. 2). Accordingly, the construction of the inner ditch, and also likely the double circular ditch, fall within the 19th century calBC. Depositional processes can be observed during the 15th and 14th century, ending at the end of the 13th century calBC.

The primary determination of the Early Iron Age on the lower course of the Danube goes back to the division of Bernhard Hänsel (1976) and was further specified and labelled due to the later excavations, especially in Sboryanovo (Stoyanov 1997). Due to more recent work in Thrace, the groups of older stamp ceramics (Tsenovo), Sboryanovo and Tlachene identified by us (Krauß 2006a; Conrad, Krauß 2020) as well as finally the Basarabi culture (Vulpe 1965; 1986) can be paralleled with the groups in Thrace (Nekhrizov, Tzvetkova 2018) and delimited very precisely in absolute chronological terms (Conrad, Krauß 2020).

In the material from Tash Bair (specifically from Site 1) there is evidence of massive settlement during the Basarabi stage of the Early Iron Age. With some reservations, some finds can also be assigned to the earlier Tlachene stage. Further, detailed stratigraphic observations are also required to clarify the question of how the development within the Early Iron Age settlement is to be assessed.

9.1.1.2. Neolithic pottery[2]

The finds at site 1 (identical to Krauß 2006a, No. 48a) are dominated by Late Neolithic pottery. It is all relocated material, which is nevertheless partially very well preserved. A particularly extensive inventory comes from the survey carried out in spring 2001 and has already been presented in detail (Krauß 2006a, 185f. Plates 9–21). This is now being supplemented by the newer finds from survey and excavation soundings at the site. Since the excavations could not contribute to the clarification of the stratigraphy of the Late Neolithic settlement layers, this material can only be presented *en bloc*. Differentiations within the Late Neolithic pottery can only be made on the basis of typological criteria.

Large storage vessels with a narrow mouth rim appear with coarse pottery, the surface of which is usually roughened with finger-grooved barbotine. The rims are slightly offset and smoothed. One large vessel has a slightly fluted cylinder neck (cat. P1/187). There is a fragment of a sieve vessel (cat. P1/203) and the bottom plate of a coarse vessel with a multi-perforated base (cat. P1/230). So, it should be clear that many of these vessels were also used for production purposes. Further fragments of the coarse pottery can be added to form wide-bodied bowls, often with biconic walls. Many very thick sherds with impasto decoration show barely noticeable curvatures. These belong to cylindrical sockets, the so-called "Steckdosen" (cat. P1/010; P1/017; P1/176). These were often closed with dome-shaped or cylindrical lids (cat. P1/174; P1/186; P1/200; P1/201; P1/245). The fragment of a large vessel impasto decorated on the inner surface seems to have belonged to a wide-mouthed bowl (cat. P1/180).

The fine pottery shows various bowls, including simple conical and carinated shapes (cat. P1/028; P1/032-040). The pots are constructed in a similar way, with a biconical lower part and an often well offset conical narrowing neck, cylinder rim or a slightly protruding mouth (cat. P1/191; P1/196; P1/197). One bottom fragment belongs to an open bowl with a square contour (cat. P1/235). There are also spherical pots with a narrow mouth or a slightly S-shaped swinging rim (cat. P1/041; P1/193; P1/228) or with funnel rims (cat. P1/046; P1/213).

The vessels of the Vădastra culture are decorated using the chip carving technique and have elaborate and hybrid forms. Deviating from radially symmetrical basic shapes, the walls also repeatedly merge into angular cross-sections. In general, the range of types of Vădastra ceramics is very diverse, of which only an inaccurate impression can be gained from the shattered material of the Tash Bair. Among the finds, however, there are some larger fragments that belonged to such large vessels that change from a round to an angular cross-section (cat. P1/185).

A special form is a figuratively decorated lid, which is crowned by a human face (cat. P1/215). The narrow diameter of this piece suggests that it belongs to a bottle-shaped vessel. Another special shape is a foot with a round cross-section that is attached to a flat plate (cat. P1/199).

The fabric of the ceramic is remarkable due to the numerous organic additions that can be easily recognised in the fresh break. Despite the coarse sherds, many fabrics (ware groups) are very well smoothed on the surface and often also polished. The coarse ceramic is made from ware groups 1, 3, 5, 6, 8, 28, 36 and 44 (table 1; a detailed description of the pottery fabrics can be found in Krauß 2006a, 347–354). However, ware group 6 is predominant. The same recipes were also used for the production of fine ceramics, supplemented by ware groups 7, 9, 12, 20, 26, 35, 40 and 46. The coarse ceramics are often roughened with finger-grooved barbotine and sometimes also structured in patterns. As an additional decoration, two fragments have an applied ring over which the barbotine runs (cat. P1/220; P1/233). The inner surfaces of the vessels are also carefully smoothed and often also polished in the area of the vessel's mouth.

The decorations on Late Neolithic ceramics are very frequent and varied, there are hardly any undecorated vessels. Often several decorative techniques appear together on a single vessel. Specific types of decoration are combined with certain vessel shapes. The carinated bowls and pots of the North

2 The pottery is described chronologically, according to periods, and only secondarily according to sites. The references refer to the numbers in the ceramic catalogue (cat.). The types of prehistoric ceramic fabrics are given at the end.

Bulgarian Late Neolithic are often decorated with fluting or incisions in the shoulder area. The well-smoothed flutes run either vertically or diagonally, but sometimes they also form patterns. On a pot, a buckle on the belly of the vessel is framed by arched fluting (cat. P1/183). There is a large spiral in the form of fluting on a large bulbous vessel, which seems to fill the entire body (cat. P1/207). On some vessels, various decorative stripes alternate with fluting; this change in direction makes the ornamentation attractive. Sometimes fine punctures accompany the fluting (cat. P1/043; P1/243) or fill gussets between the fluting motifs (cat. P1/029; P1/044; P1/197). The incisions on the shoulder of bowls can consist of simple oblique lines or bands (cat. P1/061; P1/181; P1/212). But there are also more complex patterns of hook meanders (cat. P1/247). The line pattern on a pot fragment with an elongated, vertical buckle is remarkable. The bands formed by the incised lines have small incisions, like heads of music notes (cat. P1/190). A large biconical bowl is carved on the shoulder with arched lines and decorated with vertical lines on its conical base (cat. P1/181). These form bands, the inner surfaces of which are polished. The usual decorative forms of the Late Neolithic pottery also include mat impressions on the standing surfaces, which give an indication of how the vessels may have been made. The incised pattern on the bottom fragment of a vessel seems to be a decorative motif (cat. P1/249).

Among the finds from the Tash Bair, there are numerous Vădastra sherds with decorative patterns made using the chip carving technique, which are filled in with a white paste. There are diverse individual motifs, such as spiral meanders, zigzag lines, ladder bands, rows of lines or chessboard motifs. Often, however, the fragments are also filled with densely packed zigzag areas that are reminiscent of textile embroidery patterns or knotted patterns from oriental carpets. Some of these vessels are irregularly shaped (cat. P1/176; P1/185; P1/245). The areas between the incised patterns are sometimes painted with red paint (cat. P1/185; P1/199; P1/201; P1/206).

Typologically, the material can be assigned to different groups. The carinated bowls and pots with decorated shoulders are typical forms of the Bulgarian Late Neolithic (Тодорова, Вайсов 1993, 127–142), which can be paralleled with Karanovo IV in Thrace (Krauß 2008). In northern Bulgaria, the material from Kachitsa gave these facies their name. This group develops eastwards slightly into the Hamangia culture (Berciu 1966; Тодорова, Вайсов 1993, 142–147). Many of the finely fluted forms, especially the anthropomorphic vessel lid (cat. P1/215), are reminiscent of the Hamangia cultural group. Some of the incised and impasto-decorated pieces can be assigned to the Boian (Berciu 1974) or Vădastra culture (Gaul 1940). It is quite possible that these forms mark different phases of the Late Neolithic settlement on the Tash Bair.

The evaluation of the find materials reveals that various levels of the Boian culture are represented, especially on site 1. We have assigned this material to pottery style groups, which probably reflect different workshops. At least the Boian-Bolintineanu, Boian-Giuleşti and Boian-Vidra levels are represented in the material. It is possible that the development already begins with the Neolithic Dudeşti group. Thus, at the Tash Bair we record the entire Late Neolithic of the Lower Danube up to the Early Chalcolithic.

9.1.1.3. Chalcolithic pottery

The character of the Chalcolithic settlement at Tash Bair is still largely unclear. Already in the 2001 survey there were few surface finds from site 1 that could be assigned to the Boian-Giuleşti stage of the Chalcolithic in the lowlands of the Lower Danube (Krauß 2006a, 308). Of course, a part of the barbotine-decorated ceramics described in connection with the Late Neolithic material could also belong to the Chalcolithic. However, amongst the material from excavation trench 1.2, a vessel was found that can confidently be assigned to the Late Chalcolithic (cat. P1/242). It is a wide-mouthed bowl with a stepped, fluted edge. The last remains of a graphite painting can be seen on the outer edge of the vessel. The type of fabric of the vessel corresponds to our ware group 7. The vessel fits into the inventory of the settlement ceramics of the Kodzhadermen-Gumelnița-Karanovo VI complex (Тодорова 1986, 107–113).

9.1.1.4 . Bronze Age pottery

Bronze Age ceramics are difficult to differentiate among the prehistoric finds, especially if they are only individual fragments from surface collections. Very few vessel fragments from site 1 can be assigned to the final Early Bronze Age or the Middle Bronze Age. Among them, the fragment of a vessel with a possibly squared cross-section, appearing biconical in shape with a long, vertical tubular lug from the rim to the fold (cat. P1/226). This fabric corresponds to our group 6. Two fragments of widened tenon handles appear to belong to the Middle Bronze Age (cat. P1/222; P1/251), at least one of which can be identified as positioned on a vessel's rim. Both fragments are well smoothed on the surface; this ceramic fabric corresponds to groups 18 and 37.

Bronze Age finds come from site 3, most of which can be assigned to the Middle Bronze Age, and a small number to the Late Bronze Age. The Middle Bronze Age material from the filling sediment of the circular ditch (trench 3.6) and from a larger pit (feature 3.1), roughly in the centre of the roundel, is very well represented. There are bulbous bowls, some with pouring spouts and wishbone handles on the rims (cat. P1/086; P3/004; P3/030). There are pots with narrow mouths, partially with notched edges (cat. P3/003; P3/006; P3/007; P3/025; P3/036), and vertical ribbon handles with oval cross-sections (cat. P3/010; P3/013). Bulbous cups with ribbon handles that are slightly over the rim and that lead from the rim to the belly, are also characteristic (cat. P3/012; P3/022; P3/027). Some vessels have smaller humps or grip pegs on the body (cat. P3/026; P3/039). Otherwise, the ceramics from the Middle Bronze Age are undecorated. The surfaces are well smoothed and rarely polished on the outside. Typical fabrics of the pottery are 13, 18, 36, 37 and 39.

Spherical shapes with a sharp break to the rim, which can be reconstructed as spherical kantharoi, can be clearly assigned to the earlier Bronze Age development at site 3 (cat. P3/034; P3/035). These vessels also have handles that are semi-circular in cross-section and have a flat top (cat. P3/038). Fragments of wide-bodied pots with notched strips below the rim can only be generally assigned to the Bronze Age (cat. P3/024; P3/037). Large handles on the lower part of large storage vessels seem to belong more to the Late Bronze Age (cat. P1/026). The fabrics of the Late Bronze Age ceramics hardly differ from those of the Early Bronze Age. Specifically, the ware groups 13, 16, 18, and 37 are to be mentioned.

Because of the characteristic cups and spouted vessels, the Middle Bronze Age finds from Tash Bair can be paralleled with Phase III of the Tei culture in Muntenia (Leahu 1966). The spherical kantharoi represent the later phases Tei IV and V (Христова 2002; Krauß 2006b), or the approximately simultaneously existing Zimnicea-Cherkovna-Plovdiv group (Alexandrescu 1973; Hänsel 1976).

9.1.1.5. Pottery of the Early Iron Age

The finds from the Early Iron Age are predominantly from the 2001 survey on site 1 and are only supplemented selectively by the more recent excavation and survey finds. Large storage vessels with protruding lip rims and some bulbous pots were documented under the coarse ceramics (cat. P1/081; P1/082; P1/085; P1/113; P1/114). It is known that the majority of these are tall pots with slightly bulbous walls, which have edges that bend at differing degrees. These are usually without handles and only rarely have short knobs (cat. P1/125).

The coarse ceramic is rarely smoothed and has rather rough surfaces. The ware groups 28, 31, 34, and 37 are represented. The only decorations on the coarse pottery are notched strips (cat. P1/101; P1/103; P1/106; P1/110), which run parallel to the rim and are sometimes doubled. Vertical speckled lines, as well as notched edges (although the thickened edge is sometimes designed like a dotted strip) are also typical.

The forms of fine ceramics are much more diverse. In particular, bowl shapes with edges that curve in or swing out in an S-shape are known. The characteristic jugs with a so-called Hallstatt profile should appear on closed forms (cf. Krauß 2006a, Taf. 65, 5; Taf. 70, 6). These are vessels with a bulbous lower part that tapers conically at the bottom, a conical neck and a funnel rim. Due to the degree of

fragmentation, only a few pieces of the more recent finds can be assigned to such forms (possibly cat. P1/077, P1/083 or P1/111). These jugs are the leading forms of the Hallstatt Period and also appear in the Balkans. A special form of the Basarabi style are very large bowls with a comparatively small dome-shaped bowl in the centre and an oversized, cantilevered rim zone that is curved in the other direction and very lavishly decorated with stamped ornaments (cat. P1/102; P1/180; P1/227). There are also single-handled cups with curved or bent vertical handles (P1/119–124). The handles are oval or ribbon-shaped in cross section. The latter sometimes concave.

The surfaces of fine ceramics are often well smoothed which is sometimes achieved by polishing. Characteristic types of wares are 14, 23, 28, 35, 39, and in particularly 40. A characteristic feature of Basarabi fine ceramics is the extravagant tendency to decorate the vessels. Often complex fluting patterns are combined with fine stamp motifs. With the help of small cogwheels or unrollable clay stamps, entire areas between the decorative motifs were roughened in the manner of a notch cutting technique, which were then filled in with a white paste. The stamp technique distinguishes this Iron Age type of notch cut from the Late Neolithic. Spiral motifs and chains of rhombuses are popular. Sometimes the engraved motifs also form hatched bands that run vertically over the surface of the vessel. S-hook chains are also known from the 2001 survey material. There are also individual small buckles on the edge of bowls with a curving wall or humps on the widest part of the bowls. The tendency towards ornamentation is also seen in the cup handles, which are often fluted or decorated with fine stamp motifs.

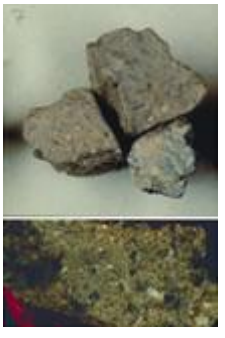
The general development of the Early Iron Age in the Lower Danube has been previously explained (Hänsel 1976; Conrad, Krauß 2020), and at least stages III (Tlachene) and IV (Basarabi) at Tash Bair have been proven (Krauß 2006a, 96–100). A more precise chronological delimitation of the beginning of the Early Iron Age settlement is not currently possible with the excavations carried out thus far. In any case, the Basarabi settlement was very massive. So far, there is no other site in Bulgaria with such an enormous number of finds.

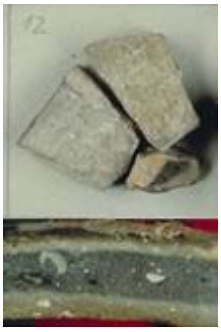
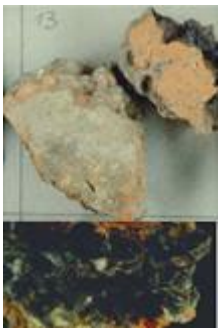
9.1.1.6. Fabrics (ware groups) of the prehistoric pottery

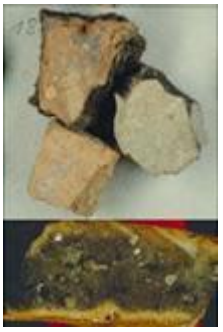
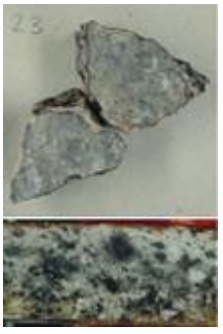
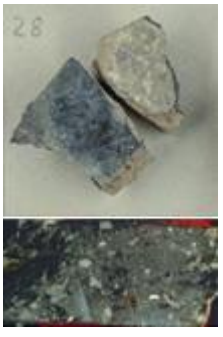
The types of ware groups that are relevant to the Tash Bair prehistoric ceramic finds are listed here (table 1). The descriptions of the ceramic wares are excerpts of those described already in Krauß 2006a, 347–354, hence the non-consecutive numbering. The colour is indicated according to the Munsell Colour code for soils.

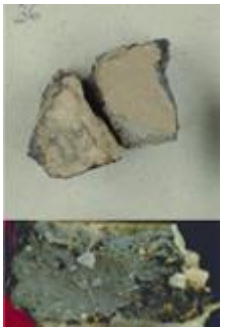
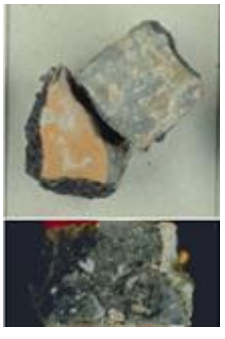
Table 1. Fabrics (ware groups) of the prehistoric pottery

Fabric 1 Hard to very hard fired fabric, very dense. Breakage fine-grained and stratified. Small, very fine mineral components, sand and mica, with small organic additions, probably grain chaff. Uniform structure with directed texture. Often of varying colours on the interior and exterior. The interior is often black, and the external surface colour changes from black and brown tones to yellow or orange with a grey brake core. The surface is often covered with engobe and polished internally and externally. Outer surface: 10YR5/3; inner surface: 2.5Y2.5/1; break 10YR5/4; break core 2.5Y4/1.	

Fabric 3 Hard, dense fabric with granular breakage. Lots of mineral components, mica, limestone and rock grit, medium-sand. Uniform structure. The break is dark grey to black. The surface is lighter and often covered with barbotine. Inner surface: 2.5Y6/3; barbotine: 10YR6/4; break: 2.5Y3/1.	
Fabric 5 Fine-pored, soft fabric with slate like fractures. Lots of organic additions – grain chaff or manure. Straightened texture. Even brick-red ware. Porous surface. Inner and outer surface: 2.5YR6/8; break: 2.5YR6/8.	
Fabric 6 Fine-pored, soft fabric with a schist-like break. Lots of organic additions – grain chaff or manure. Few mineral components, sand and medium-fine lime. Uneven structure with directional texture. Surface colours yellow and brown tones. Most pieces have a deep black break. For a few, the colour of the break does not differ from the surface colour. In some cases, the exterior is coated with clay slip and polished. Inner and outer surface: 10YR6/4; clay slip: 5YR4/4; break: 10YR2/1; 10YR6/4; 10YR5/3; break core: 10YR2/1.	
Fabric 7 Soft, porous and sandy fabric with granular breakage. Many mineral constituents – sand, limestone and gravel. Few, very fine organic additions. Uniform structure. The break is brown-black and only slightly darker than the porous surface. The surface can be smoothed. Inner and outer surface: 10YR4/2; break: 10YR4/1; 10YR2/1.	
Fabric 8 Hard, coarse-pored fabric with grainy, lightly layered breakage. Lots of very coarse limestone additions and grain chaff. Uneven structure. Brick-red body with a slightly lighter surface. Some pieces are decorated with barbotine on the outside. Inner and outer surface: 10R5/6; barbotine: 10R7/4; break: 10R5/8.	

Fabric 9 Hard and dense fabric with a smooth break. Few, very fine mineral components – sand. Even texture. The exterior is brownish in colour, the interior is grey to black. In the break the colours merge. The exterior and interior are very tight and polished. Outer surface: 10YR5/4; inner surface: 10YR2/1; 10YR5/1; break: 7.5YR2.5/1; 7.5YR3/2.	
Fabric 12 Fine-pored, hard fabric with a smooth break. Few, very fine mineral components. Occasional fine pieces of lime. Uniform structure. Grey exterior and interior, with the break being slightly darker. The surface is polished externally and internally. Inner and outer surface: 10YR6/1; break: 10YR4/1	
Fabric 13 Hard, porous fabric with a shell-like fracture. Lots of very coarse mineral components – chamotte and coarse gravel. Probably also organic ingredients. Uneven structure. The surface of the sherds is orange-red, the break is black. The exterior and interior are coated with a clay slip and smoothed. Inner and outer surface (slip): 5YR6/8; break: 10YR4/1.	
Fabric 14 Hard, coarse-pored fabric with grainy cracks. Lots of very coarse additions of limestone and gravel. Uneven structure. Evenly grey-brown coloured sherds. Smoothed surface. Outer surface: 2.5Y5/4; inner surface: 2.5Y6/3; break: 2.5Y6/4.	
Fabric 16 Hard, porous fabric with granular break. Lots of medium-fine mineral and organic components – sand, chamotte, mussel shells and very fine grain chaff. Uniform structure. Exterior is reddish-brown, and interior is brown-grey. The break is black-grey. The surface of the vessel can be polished. Outer surface: 5YR6/8; 10YR6/4; 10YR7/3; inner surface: 2.5Y4/1; 10YR6/4; break: 5YR7/1 with lots of black spots.	

Fabric 18 Hard, fine-pored fabric with granular breakage. Medium-fine mineral components – mica and gravel. Uneven structure. Orange-brown exterior and interior with a black breakage. Some pieces show a thin black core when broken. Inner and outer surface: 5YR6/4; 5YR7/6; 10YR6/4; break: 5YR5/6; 5YR4/1, 5YR2.5/1; break core: 7.5YR5/1.	
Fabric 20 Hard, fine-pored fabric with a smooth break. Few, very fine organic lean components, probably grain chaff. Even fewer mineral particles. Uniform structure. The sherds are uniformly grey to brownish in colour. Inner and outer surface: 5YR5/6; 5YR6/1; break: 5YR5/6; 5YR6/1.	
Fabric 23 Hard to very hard, fine-pored fabric with granular breakage. Lots of very fine organic ingredients. These are only recognisable as small black points in the bevel. Homogeneous structure. Uniformly grey-black colour of the break. External surfaces are also grey-black. Very fine reddish-brown layer below the surface. The outer surface is polished. Outer surface: 10YR5/1; inner surface: 10YR2/1; break: 2.5YR6/1.	
Fabric 26 Very hard, dense fabric with a smooth break. Many very fine mineral components – lime and sand. Homogeneous structure. Evenly grey body. The surface is very dense and smooth. Inner and outer surface: 10YR5/1: break: 10YR6/1.	
Fabric 28 Hard sounding, dense fabric with fine-grained breakage. Few, very fine mineral components – sand. Homogeneous structure. Even black body with slightly lighter outer surfaces. The exterior and interior are polished. Fabric of the fluted and stamped ceramic. Outer surface: 2.5Y2.5/1; inner surface: 2.5Y5/1; break: Gley4/N.	

Fabric 31 Hard, fine-pored fabric with granular breakage. Many coarse mineral components – chamotte, lime and rock grit (grain sizes up to 3 mm). Also, mussel or snail gravel. Uneven structure. Reddish-brown body with a narrow grey core. Inner and outer surface: 10YR7/3; break (at the edges): 10YR7/3; break core: 10YR4/1.	
Fabric 34 Soft, coarse-pored fabric with a cracked fracture. Many very coarse mineral components – chamotte, lime, rock grit (grain sizes up to 3 mm). Very irregular structure. The exterior is reddish-brown, the interior is grey-black. In the break, the colour zones merge into one another. The surface of the vessel is slightly smoothed but still grainy. Outer surface: 5YR6/6; inner surface: 5YR4/2; break: 10YR7/4; 10YR4/2.	
Fabric 35 Hard, porous fabric with granular breakage. Lots of medium-fine mineral particles – mostly chamotte, less limestone and rock gravel. Irregular structure. Grey to brownish body with colour zones merging into one another. The surface of the vessel is smoothed. Inner and outer surface: 5YR6/4; break: 5YR4/1.	
Fabric 36 Very hard, fine-pored fabric with granular breakage. Few, medium-fine mineral components – limestone and rock gravel. Uneven structure. Even black-grey coloured body with slightly lighter outer surfaces. The surface is smoothed. Outer surface: 10YR6/4; inner surface: 2.5Y4/1; break: Gley4/N.	
Fabric 37 Very hard to hard sounding, fine-pored fabric with granular breakage. Few, coarse mineral components – quartz and rock gravel. Uneven structure. Uniform black-grey body with slightly lighter outer surfaces. The surface of the vessel can be coated with a clay slip. Inner and outer surface: 5YR6/1; slip: 5YR6/8; break: Gley4/N.	

Fabric 39 Hard, dense fabric with fine-grained breakage. Lots of mineral constituents – fine quartz sand, mica, medium-sized pieces of lime and a few, very fine chamotte. Uniform structure. Brown body with a thin grey core. The exterior is smoothed and, in some cases, polished. Inner and outer surface: 5YR6/4; break: 5YR6/6; break core: 5YR5/2.	
Fabric 40 Hard to very hard, fine-pored fabric with splintery breakage. Lots of mineral components – gravel and few, very fine organic additions. Uniform structure. The sherds are deep black in the break. The internal and external surface is covered with a brown clay slip. The exterior is also polished. Inner and outer surface (slip): 10YR5/3; break: 10YR2/1.	
Fabric 44 Hard, dense fabric with granular breakage. Many mineral components – medium-fine rock grit and calcite. Uneven structure. Brown break and darker smoothed surface. Outer and inner surface: 7.5YR2.5/1; break: 5YR6/4.	
Fabric 46 Hard, dense fabric with a smooth break. Very fine, silty mineral components. Homogeneous structure. Even black sherds. The exterior is polished, the interior is smoothed, and in some cases also polished. Inner and outer surface: 2.5Y2.5/1; break: 2.5Y2.5/1.	

КЕРАМИКА ОТ ПРАИСТОРИЯТА

Райко Краус

(Резюме)

Хронологически рамки

Археологията, особено проучванията, основаващи се на нестратифицирани находки, се сблъсква с трудността, че хронологията на находките невинаги може да бъде приведена в

съответствие с историческите периоди. Това води до известни разместванията и размиване на границите на периодите, особено след като засега все още липсват по-мащабни разкопки на Таш баир. Текущата работа в рамките на проекта ще помогне за изясняване на периодизацията за региона. Промените и корекциите в хронологическата система, настъпили през последните десетилетия, до голяма степен могат да бъдат проследени в Северна България.

Информацията за мезолитното заселване в Северна България доскоро беше твърде оскъдна, въпреки че добре проучената зона на Железни врати се намира наблизо и може да се очаква заселване на низините по долното течение на Дунав. От добре известните находки от Побити камъни край Варна няма дати за точна датировка. Едва през последните няколко години в местността Оходен в Северозападна България могат да бъдат установени надеждни следи от мезолита, датирани в първата половина на VII хил. пр. Хр. В публикуваните тук материали, добити по проекта, липсват такива от мезолита.

Проучванията във водосборния басейн на р. Янтра и в съседната речна долина на изток от р. Русенски Лом са от голямо значение за определяне началото на неолита в Северна България и целия Балкански регион. Тук заслужава да се споменат разкопките при Джулюница, които предложиха пълна стратиграфска последователност през ранния неолит. Моделирането на радиовъглеродните дати позволи да се определи началото на неолитното заселване в този район към LXI в. пр. Хр.

Развитият ранен неолит в Северна България може да бъде хронологически определен чрез обширна серия от AMS дати от обекта Овчарово-Гората във водосборния басейн на р. Камчия. Времевата позиция се потвърждава от моделираната серия дати, получена от горните слоеве на Джулюница. Неолитният материал, открит по време на проучванията и разкопките по Таш баир, може да бъде отнесен към по-късните фази на тази епоха.

Средният и късният неолит в Северна България са сравнително слабо документирани с радиовъглеродни дати. За да се справим с този проблем, беше взета нова серия от ^{14}C дати от многослойния обект Върбица, разположен отново във водосборния басейн на р. Камчия.

Голямата маса праисторически находки от Таш баир, а именно от обект 1, могат да бъдат отнесени към късния неолит. Разграничение в рамките на тази епоха не може да бъде направено на този етап от проучването на обекта. Но е ясно, че в материала са представени различни културни явления (Въдастра, Боян, Хаманджия, български късен неолит), които се появяват в различни периоди от развитието на късния неолит. Изглежда, че на Таш баир по едно и също време присъстват различни регионални културни групи или групи от хора с различни културни традиции.

Новите серии данни от известните халколитни селищни могили в Северна България и Южна Румъния, както и датирането на погребенията от Варненския халколитен некропол доведоха до основна преоценка на хронологията на каменно-медната епоха на Балканите. Първоначалната представа за хронологията на халколита може да се запази само за неговото начало, малко след 5000 calBC. С определянето на продължителността на погребенията във Варна I, която обхваща периода от XLVI до XLIII в. пр. Хр., българският късен халколит е изместен с около 200 години по-рано. Тези резултати в никакъв случай не са изненадващи, като се има предвид въвеждането на AMS датирането в цяла Европа, което показа, че периодите на неолита трябва да се определят по-рано. В специализираната общност съществува широко съгласие, че началото на късния халколит в региона на Долен Дунав трябва да бъде около 4600 calBC и че предходните датировки трябва да бъдат отхвърлени. Краят на късния халколит може да бъде определен още по-ясно, тъй като животът на всички селищни могили в този район прекъсва най-късно около 4200 calBC.

От гледна точка на история на проучванията следващият период се разглежда като преходен към ранната бронзова епоха. Тъй като това е сравнително дълъг период от време, беше логично да се раздели на фази. Така ранният етап беше определен като пост-енеолит, а по-късният – като прото-бронз.

Отделен проблем е определянето на началото на ранната бронзова епоха. И тук възникна съмнение в твърде ранното начало на селищните могили от бронзовата епоха в Тракия, основано на стари датировки от берлинската лаборатория, добити от овъглена дървесина. Преоценката на поредицата от дати от селищната могила Езеро в сравнение с Троя и Канлъгечит в Турска Тракия доведе до корекция. Ранната бронзова епоха в България започва едва през XXXI в. пр. Хр., което е в съответствие с развитието на бронзовата епоха в регионите покрай Егейско море.

Определянето на средната бронзова епоха по долното течение на Дунав отново е тясно свързано с изследванията във водосборния басейн на р. Янтра и съседните райони. Въпреки че от Северна България не са известни значителни селища или по-големи стратиграфски отлагания от този период, многобройни находки могат да се свържат с културните групи Тей и Вербичоара в Южна Румъния. Последните датировки позволяват тези културни явления да бъдат отнесени времево между XXIII и XVII в. пр. Хр.

Що се отнася до началото на късната бронзова епоха, хоризонтът Зимнича-Черковна-Пловдив, който е разпространен на голяма територия в Източните Балкани, представлява добра отправна точка. Севернобългарските обекти също не предлагат достатъчно селищни стратиграфии за този период, поради което първоначално има смисъл да се разгледа културното развитие в съседните области. Съществени акценти тук със сигурност могат да се видят в края на микенската дворцова култура и падането на Хетската империя около 1200 г. пр. Хр.

Изграждането на вътрешния ров по Таш баир, обект 3, се отнася към средната бронзова епоха. Съответните керамични находки произхождат от най-долния слой на рова, а тяхната времева позиция е обезпечена с радиовъглеродни данни. Очевидно този ров е бил използван и през късната бронзова епоха, а и по-късно – през късната желязна епоха, а вероятно – и през късния римски период. От късната бронзова епоха имаме радиовъглеродни дати от два различни сондажа в рамките на заграждението, въпреки че находките от този период не са лесно разпознаваеми. Разполагаме с общо осем радиовъглеродни дати от краткотрайни материали. Въз основа на стратиграфската позиция на ^{14}C пробите разработихме хронологически модел, който допринася за по-точното датиране на тези структури. Така изграждането на вътрешния ров, а също така вероятно и на двойния кръгъл ров попадат в рамките на XIX в. calBC. Процесите на отлагане се наблюдават през XV и XIV в., като приключват в края на XIII в. calBC.

Първичното определяне на ранната желязна епоха по долното течение на Дунав е започнато през 70-те г. на XX в. и е доуточнено благодарение на по-късни разкопки, особено в Сборяново. Благодарение на по-скорошни изследвания културните групи с ранната щампована керамика (Ценово), Сборяново, Тлачене и накрая културата Басараб могат да бъдат съпоставени с групите в Тракия и да бъдат разграничени много точно като абсолютната хронология.

В материалите от Таш баир (по-конкретно от обект 1) има данни за значително заселване през етап Басараб на ранната желязна епоха. С известна несигурност някои находки могат да бъдат отнесени и към по-ранния етап Тлачене. Необходими са подробни стратиграфски наблюдения, за да се изясни въпросът как се развива обитаването през ранната желязна епоха.

Неолитна керамика

При находките от обект 1 преобладава къснонеолитната керамика. Става въпрос за изцяло преотложен материал, който обаче е частично добре запазен. Особено богат набор произхожда от проучването, проведено през пролетта на 2001 г., което е вече представено подробно. Сега той се допълва с по-нови находки от разкопките на обекта. Тъй като сондажите не можаха да допринесат за изясняване на стратиграфията на къснонеолитните селищни пластове, този материал може да бъде представен само анблок. Разграниченията в рамките на къснонеолитната керамика могат да бъдат направени само въз основа на типологични критерии.

От типологична гледна точка материалът може да бъде отнесен към различни групи. Биконичните купи и гърнетата с украсени рамена са типични форми за българския късен неолит,

които могат да бъдат съпоставени с Караново IV в Тракия. В Северна България материалът от Качица дава името на тази местна група от късния неолит. Тази група се развива леко на изток в културата Хаманджия. Много от фино набраздените форми, особено антропоморфният капак на съдовете, напомнят за културната група Хаманджия. Някои от врязаните и украсени с бяла паста парчета могат да бъдат отнесени към културата Боян или Вадастра. Напълно възможно е тези форми да маркират различни фази на късноеолитното селище на Таш баир.

Халколитна керамика

Характерът на халколитното селище на Таш баир все още е до голяма степен неясен. Още при проучването през 2001 г. бяха открити малко повърхностни находки от обект 1, които могат да бъдат отнесени към етапа Боян-Джулещ на халколита в низините на Долен Дунав. Разбира се, част от украсената в барботино техника керамика, описана във връзка с късноеолитния материал, също би могла да принадлежи към халколита. Въпреки това сред материала от сондаж 1.2 беше открит съд, който със сигурност може да бъде отнесен към късния халколит. Това е купа с широко гърло и стъпаловидно профилиран ръб. Върху външния ръб на съда се виждат следи от графитна рисунка. Видът на глината на съда отговаря на нашата група изделия 7. Съдът се вписва в селищната керамика на комплекса Коджадермен-Гумелница-Караново VI.

Керамика от бронзовата епоха

Керамиката от бронзовата епоха е трудна за разпознаване сред праисторическите находки, особено ако става дума само за отделни фрагменти, събрани от повърхността. Много малко чирепи от обект 1 могат да бъдат отнесени към края на ранната бронзова епоха или към средната бронзова епоха. Сред тях е и фрагментът от съд с вероятно квадратно сечение, изглеждащ биконичен по форма, с дълъг вертикален тръбен улей от ръба до сгъвката. Глиненото тесто съответства на нашата група 6. Два фрагмента от разширени дръжки с пъпки изглежда принадлежат на средната бронзова епоха, като поне единият от тях може да бъде идентифициран като разположен върху ръба на съда. И двата фрагмента имат добре загладена повърхност; тази технологична обработка съответства на групи 18 и 37.

Находките от бронзовата епоха произхождат от обект 3, като повечето от тях могат да бъдат отнесени към средната бронзова епоха, а малък брой – към късната бронзова епоха. Много добре е представен материалът от средната бронзова епоха от пълнежния седимент на кръглия ров (сондаж 3.6) и от една по-голяма яма (сондаж 3.1), разположена приблизително в центъра на кръга.

Заради характерните чаши и съдове с чучур находките от средната бронзова епоха от Таш баир могат да бъдат съпоставени с фаза III на културата Тей в Мунтения. Сферичните кантароси представляват по-късните фази Тей IV и V или приблизително едновременно съществуващата група Зимнича-Черковна-Пловдив.

Керамика от ранната желязна епоха

Находките от ранната желязна епоха произхождат предимно от проучването на обект 1 през 2001 г. и са допълнени само избирателно с артефакти от по-новите проучвания. Големи съдове за съхранение с изпъкнали ръбове и някои гърнета с луковици са документирани в групата на грубата керамика. Известно е, че по-голямата част от тях са високи гърнета с леко луковични стени, чиито устийни ръбове са извити под различен ъгъл. Тези съдове са обикновено без дръжки и само в редки случаи имат къси издатъци.

Общото развитие на ранната желязна епоха по долното течение на Дунав е обяснено от нас по-рано. В Таш баир са доказани поне етапи III (Тлачене) и IV (Басараб). По-прецизно хронологическо определяне на началото на селището от ранната желязна епоха засега не е възможно. Във всеки случай селището Басараб е било много мащабно. Досега в България не е известно такова, съдържащо огромен брой находки.

9.1.2. Late Iron Age to Medieval pottery

Sven Conrad

9.1.2.1. The regional chronology of the historical periods before the background of the chronological framework of the Eastern Balkans and the Aegean

In the generally accepted chronology of the Eastern Balkans, the end of the Early Iron Age is equated with the end of the Archaic period and the beginning of the Classical period, i.e. around the year 500 BC or with the end of the Persian Wars around 490 BC. In Central European chronology, this also corresponds to the turn from the Hallstatt Period D to the Early Latène A (fig. 3). However, this demarcation does not prove to be applicable for the chronological differentiation of Early and Late Iron Age settlements on the basis of survey finds and in the absence of larger excavations.

Instead, the emergence of the fine and slightly sandy, grey (monochrome) wheelmade pottery is of decisive importance for the chronological differentiation of the survey finds from Early and Late Iron Age settlements. Almost 50 years ago, B. Hänsel (1974b, 210–212) had already linked the adoption of the potter's wheel in the Thracian regions with the founding of the Greek colonies on the Black Sea coast. Meanwhile, well-dated archaic contexts in Histria (Alexandrescu 1977; Lungu 2009) and Apollonia Pontica (Ников 2012, 146–152) confirm Hansel's assumption that the appearance of grey wheelmade wares can be limited to the turn of the 7th to the 6th century BC. During the 6th century BC, this pottery became common in the Thracian territories north and south of the Balkans, imitating mainly the forms of Greek vessels (cf. also Bouzek, Domaradzka 2009, 199–204; Bozkova 2015, 233–234). In the absence of other reliable indicators for differentiating between Early and Late Iron Age settlements, we use the appearance of this pottery as a fixed point for the dating of Early and Late Iron Age settlements in the surveys (fig. 3; cf. also Conrad 2006, 312).

Another problem concerns the internal chronology of the Late Iron Age period on the Lower Danube. For the Thracian regions south of the Balkan Mountains, it is customary to keep following the Aegean chronology and speaking of a Hellenistic period. Its beginning is usually equated with the death of Alexander the Great in 323 BC (Delev 2015a; 2015b; cf. Ross et al. 2018, chronology table p. XIV). Shortly before that, there had been a decisive turning point with the conquest of Thrace by Philip II of Macedon in 341/340 BC and the associated destructions. The areas north of the Balkans were probably largely spared from these events except for a brief foray by Philip II into NE Thrace (Delev 2015a, 49–52). The circumstances and the current state of research do not allow the delimitation and definition of a Hellenistic period along the Lower Danube.

Based on observations made during excavations and other research in recent years, a rather continuous development seems to be emerging on the Lower Danube for the Late Iron Age. The fortified hill settlements of Svishtov and Byala (Krauß 2006a, No. 1; 90; Conrad 2006, 312–315) apparently existed until the beginning of the Roman occupation. However, Daniel Spânu (2014, 110–120, pl. 27/2) points out a discontinuity in the fortification of Zimnicea during the 3rd century BC. It could be related to the Celtic migration and the founding of their kingdom which existed until 218 BC (Strobel 1996, 153–174; Delev 2015b, 60; Emilov 2015). However, the increase in fortifications and settlements on both sides of the Danube during the 2nd and 1st century BC is striking. They can possibly be associated with the rise of the Dacian Kingdom to the north of the Danube. In our working area for example, this concerns the fortification of Scaidava near Batin (Вербанов 2015) and the ritual pit complex of Ruse (Вербанов 2013a).

The grey, monochrome wheelmade wares remain the determining lead ceramic assemblage for the dating of contexts throughout the entire Early and Late Iron Age period. A chronological differentiation is difficult to make on the basis of small fragments of wheelmade wares alone, and seldom possible from handmade pottery. Wherever possible, however, we have tried to differentiate between the early and late phases on the basis of the fabric and the shapes.

The grey wheelmade pottery (together with handmade wares) still made up a very large proportion of the ceramic finds in the first decades of the Roman occupation. This is proved by the

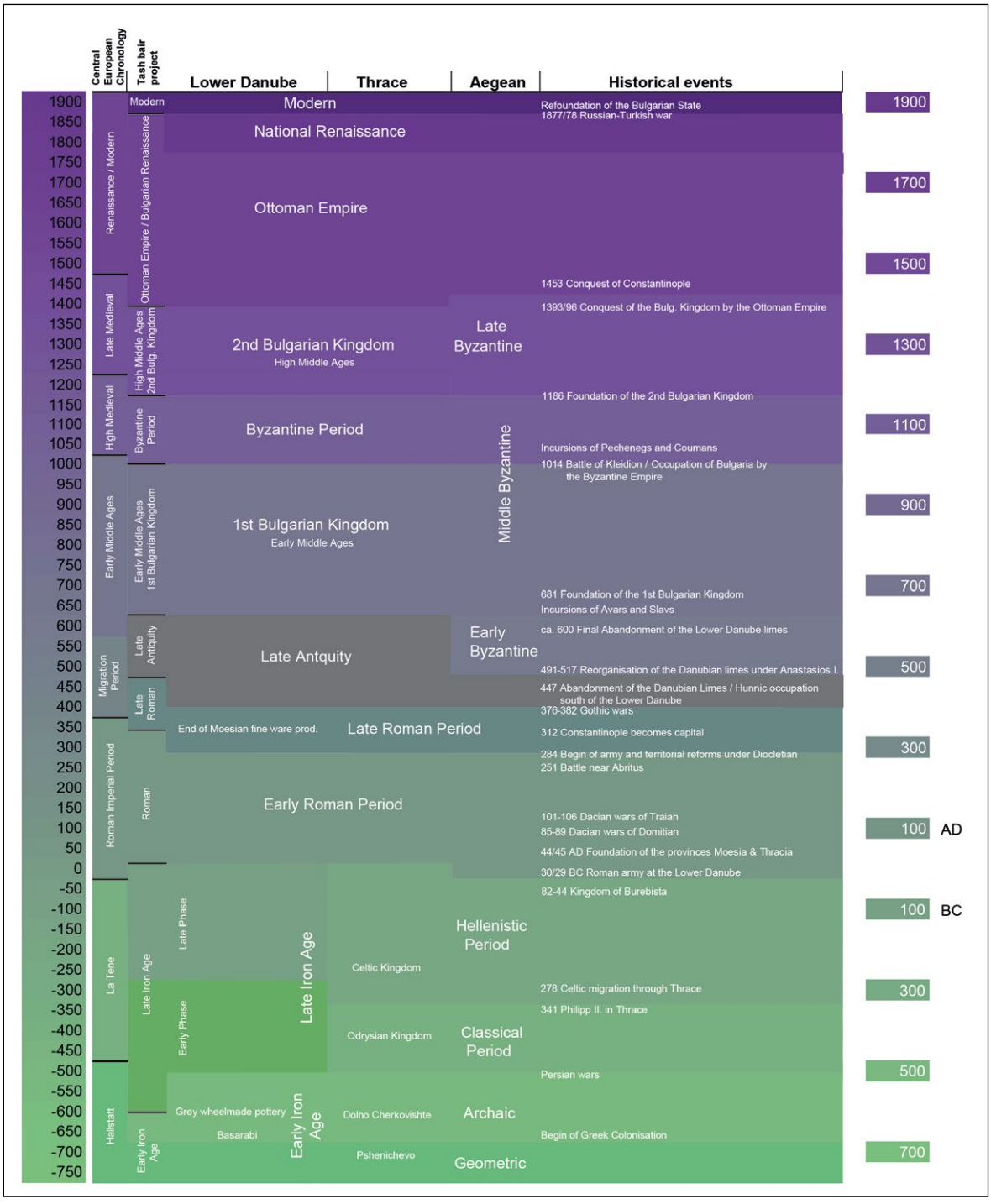


Fig. 3. Chronological framework of the historical periods of the Eastern Balkans and the adjacent regions (by S. Conrad)

pottery finds during the excavations in site 5 (cf. the contributions by L. Vagalinski et al., chapter 8.3.3), and also by the finds in the features from the 1st century AD in the Novae legionary camp (Генчева 2002). A sharp demarcation between the Late Iron Age and the Roman period, which would coincide with the creation of the independent province of Moesia with an own governor and its expansion to the lower reaches of the Yantra in 44 AD, is therefore not possible on the basis of the surface finds (Suceveanu 1971; Suceveanu, Barnea 1991, 26; cf. Tomas 2016, 20–21). As a result, the pottery finds indicate another blurred transition period which spans at least half a century from the middle to the end of the 1st century.

Based on the survey finds of the working area, the Roman settlement becomes clearly tangible only with the increased emergence of Moesian red slip wares in the first decades of the 2nd century. A large part of this pottery came from the workshops of Butovo and Pavlikeni (Sultov 1985), located in the territory of Nicopolis ad Istrum. On the basis of stratigraphically dated finds, and which could also be proven with further scientific analyses, the workshops of Pavlikeni were likely in production throughout the 2nd and 3rd century. This is contrary to Stiliyan Ivanov's (2019) assumption that these workshops were only in production during the 2nd century. As can also be seen from the high proportion of these wares among the tableware of Period A in the Late Roman fort Iatrus, the finds from the Butovo workshops are dominant during the first half of the 4th century (Daszkiewicz, Schneider 2007; Conrad 2007a; 2007b). Due to the current absence of alternative indicators, the Moesian red slip ware is considered the main chronological indicator. This shifts the dividing line between the Roman and Late Roman times for the survey finds and consequently the corresponding sites to the middle of the 4th century. As a result, it should be accepted that neither the Gothic invasions of the 3rd century nor the Tetrarchic and Constantinian periods can be depicted on the basis of the survey finds.

The Late Roman period is resultingly shortened in our chronological scheme to the period from the middle of the 4th to about the middle of the 5th century. This is contrary to the accepted chronological schemes which start with Constantine the Great, or even in the middle of the 3rd century. Above all, the finds from the castrum Iatrus can be used as parallels, particularly the amphorae like Late Roman 1 and Late Roman 2, as well as various characteristic pot shapes (Böttger 1982; Conrad 2007a). The destruction of Iatrus, presumably in the course of the Huns' invasion and its abandonment for around three decades, marks an important historical fixed point in the working area (von Bülow 1994, 15–16; 1995a, 43–46)

The Late Antiquity is well documented by the periods D1 and D2 at the fortified settlement in the castrum Iatrus under Anastasios and Justinian between 480 and 600 (von Bülow 1994, 16–20; 1995b; 1995c). However, in the current state of research, there were no finds available from Tash Bair dating to the Late Antiquity.

With the abandonment of the Danube Limes around 600 and the relocation of the Byzantine border to the ridge of the Balkan Mountains, the Byzantine Empire lost control of the areas north of the Balkan Mountains for several centuries.

Various groups of immigrants, mainly Slavs, subsequently settled in these areas. After the immigration of the Bulgarians, these areas were gradually incorporated into their newly founded kingdom in the year 681, situated in what is now NE Bulgaria (Божилов, Гюзелев 1999a, 27–103). On the basis of the archaeological finds alone, it is difficult to subdivide the almost three and a half centuries long Early Medieval period, which is representative of the First Bulgarian Kingdom (681–1018). More recent studies open the possibility to make at least a rough subdivision into an early phase (end of the 7th until the beginning of the 9th century) and a late phase (from the 9th until the beginning of the 11th century; cf. below).

With the victory in the battle of Kleidion in 1014, the Byzantines ended the Bulgarian statehood for almost two centuries in 1018 (so-called Byzantine period) (Божилов, Гюзелев 1999a, 341–343). While the Byzantine rule south of the Balkan mountains proved to be relatively stable, the Danube border could not be held permanently. This led to a second wave of the Great Migration, during which amongst others, the tribes of Pechenegs and Coumans settled south of the Danube. These processes are only sporadically documented archaeologically and through individual finds, for example at the fort Iatrus (Въжарова 1981; Wendel 1986, 200). At Tash Bair and in its vicinity there are only some stray finds from this Byzantine era which do not indicate permanent settlement.

In the years 1185/86, the two nobles Asen and Teodor (as Tsar Petar IV) used a phase of weakness in the Byzantine Empire (involved in defensive battles against the Ottomans and further weakening by internal unrest) as an opportunity to uprise and restore the Bulgarian state. The Second Bulgarian Kingdom in the period of the High Middle Ages was initially limited to the areas north of the Balkan Mountains and also expanded to the south (Божилов, Гюзелев 1999a, 421–526).

In 1396, the Second Bulgarian Kingdom was conquered by the Ottomans who established a long-lasting rule (Божилов, Гюзелев 1999b, 7–35). Their rule was increasingly called into question from the middle of the 18th century when the monk Paisius from Hilendar gave impetus for the development of a Bulgarian national consciousness in his 'Istoriya slavyanobalgarska' published in 1762. The general signs of decline of the Ottoman Empire favoured the emergence of the liberation movements in the 19th century. This historical phase of the national rebirth, which is important in terms of the history of ideas and the historical course, cannot, however, be archaeologically grasped.

The liberation of the Bulgarian lands took place in the course of the Russo-Turkish War of 1876/77, whereby the independent Bulgarian statehood was restored, and Bulgaria entered the Modern Age.

9.1.2.2. The pottery from the Late Iron Age until the Middle Ages. Preliminary remarks

The pottery finds come from both the excavations and field surveys. The finds from the latter are naturally broken into very small pieces and often have washed and rolled surfaces. Most of the finds were first examined in the field. The determination, including the assignment to a fabric group and the statistical recording, took place in the base after the pieces had been washed. Well-preserved and typologically clearly identifiable fragments (mostly rim fragments) were documented by drawings. They form the basis of the catalogue, in which the items are arranged by sites and subsequently distinguished in survey and excavation finds. The order of the items on the plates follows the order in the catalogue.

The ceramic fabrics list gives a detailed description of the Tash Bair finds (table 2). This was drawn up for the finds of the Late Iron Age to the Ottoman period from the extensive field surveys at the Lower Yantra (Iatrus-Krivina, vol. VII [in prep.]). The numbering continues the corresponding list by R. Krauß (2006a, 347–354) for the prehistoric periods[3]. For some individual finds and imports (amphorae), a detailed description of the sherds is given instead of separate categories of fabrics.

Although there are different sites at Tash Bair, it is a very limited geographical region. This justifies the comprehensive, summarising evaluation of the ceramic finds in the following part. The statistical analyses of finds from the excavations are given in chapter 9.1.3. The tables with the statistical recording of survey finds can be found in table 1 in chapter 12.

It is clear that with the pieces presented here, only a small, partially representative excerpt from the find material can be given. Furthermore, since only a representative selection was taken from the survey polygons for determination and dating, no reliable ratio between the individual ware groups of each period can be determined.

9.1.2.3. Late Iron Age pottery

The pottery finds of the Late Iron Age come from the field surveys as well as from the targeted excavations on the inner ditch of site 3 (3.6) and the ditch 1.1.6 / 15 in site 1 (cf. the contributions by L. Vagalinski et al., chapters 8.2.1 and 8.3.1). The finds consist of fragments from imported amphorae, fine pottery and coarse fabrics. The latter were used for handmade vessels and those made on the slow wheel.

Whenever possible, attempts were made to differentiate between the pottery from the early (6th–3rd century BC) and late phase (2nd–1st century BC). This is somewhat problematic due to the fragmentary condition of the finds and the difficulties in the distinction of the material from the two phases. Furthermore, there is a lack of comprehensive studies on Late Iron Age ceramics in the whole region. After all, the pottery from the Ruse pit complex was the first to be a comprehensive complex of finds from the later phase of the Late Iron Age in the region (Върбанов 2013b; 2013c). The older reviews by the Romanian authors Ion H. Crişan (1969) and Emil Moscalu (1983) refer mainly to finds north of the Danube, from the Carpathian region and Transylvania. These reviews also present a more limited range of ceramic types and forms, and mainly focus (especially in the case of Moscalu) on the finds of

3 Cf. also the description of fabrics for the pottery finds from the Neolithic to the Early Iron Age by R. Krauß in this contribution (cf. chapter 9.1.1, table 1).

the older phase (6th–3rd c. BC). From imported and local transport amphorae, only few body fragments were found, which cannot be determined with regard to typology and origin.

The fabrics. Six different fabrics (Nos. 49–54) were identified among the finds of the fine grey wheelmade pottery. Four of them belong to the grey monochrome fabrics (Nos. 49–52). Fabric 49, which is characterised by a homogeneous, grey to grey-olive-coloured body with a clay-ground, matt-glossy coating, apparently occurs almost exclusively in the first phase from the 6th to the 4th century. Fabric 50 with a dark, often grey-black coating, on the other hand, seems to have been widespread throughout the Late Iron Age. The light grey, often provided with a glossy polish, fabric 51 and the darker, slightly sandy fabric 52, on the other hand, most likely come from the later phase of the Late Iron Age.

The dating of the wall fragments is based mainly on the fabrics and therefore may be fraught with considerable uncertainties. At the same time, the fragmentary state of preservation often does not allow any conclusions to be drawn about the exact shape of the vessel. Nevertheless, the finds reveal a broad typological range, which become a little bit more limited and more specific in the later (Hellenistic) phase (Bozkova 2015, 233).

The fine and slightly sandy wares also include fabrics 53 and 54 of the younger phase, which are technologically connected to the grey fabrics, but differ in colour due to oxidizing burns or special admixtures. Among the finds from the excavations and surveys, there are body fragments only and no typologically identifiable finds of these wares (cf. also Bozkova 2015, 237).

The handmade wares (including vessels made on the slow wheel) were divided into three wares (Nos. 55–57), which are characterised by a more or less severe sand tempering and a brittle, somewhat fissured structure in the break. Very typical is fabric 57 that appears with a light brown (in some cases somewhat stained), mostly slip-coated surface, and often has a dark core. Due to the more careful surface treatment, the use of the slow wheel, and some individual shapes (such as the garland-shaped plastic strips), it is often possible to assign vessels to the younger phase (2nd–1st c. BC).

Pottery types of the early phase of the Late Iron Age (approx. 6th–3rd c. BC). Relatively frequently among the finds are fragments of amphorae with flat bottoms or hydriai with base ring (cat. P5/002; P17/004; P18/001; P19/004-005), including several bottom and handle fragments that were not included in the catalogue. Large and small craters (cat. P1/126–129; P17/003) are typical (cf. Bozkova 2015, 234), especially for the early phase. Throughout the Late Iron Age, depending on their overall shape, jugs or cups can be dated relatively easily (the latter often with over-the-rim handles) (cat. P1/209; P19/006).

Most of the plates and bowls belong to the widespread type with inwardly curved rims (cat. P1/223; P18/003–004; P19/007–008; P24/007) (Bozkova 2015, 233), which have a certain range of variations in the detail forms. The bowl with the short, slanted rim P1/134 seems to be a variant of these bowls with inwardly curved rims. P1/133 is a small bowl with an open vessel form which is not very common so far.

The so-called fruit bowls – large bowls or plates on a high (hollow) foot – form an important and common type of vessel, which also occurs in large numbers as a handmade variant (cf. Върбанов 2013b, 198–199 pl. 9,34–37; 10,1–42). A small vessel foot (cat. P1/205) could come from such a small fruit bowl or a jug.

The fragment of a bowl in the form of a lekane with a horizontal handle (cat. P34/001), which undoubtedly belongs to the early phase (5th–4th century BC), is interesting and shows the formal connection to Greek models (cf. Bozkova 2015, 233–234).

Other fragments belong to (storage?) vessels and dolia (for example cat. P1/228), although their typological assignment is not always certain due to the small size of the fragments.

Plates with an inwardly curved rim and various detailed shapes form an important part of the handmade vessels too (cat. P3/018; P18/003–004; P19/009). They are the counterpart to the corresponding vessels in fine grey wares (see above). The fragment of a plate with a strongly curved rim from site 19 (cat. P19/009), is strongly related to the tradition of the Early Iron Age vessels with a turban rim. This remarkable fragment can undoubtedly be dated back to the 6th century. The foot cat. P1/138 can be assigned to a large fruit bowl.

Other typologically identifiable rim fragments belong to pots with an open profile (cat. P19/011; 18/005), while some partly decorated fragments come from pots in general (cat. P1/139; P18/006–007).

Pottery types of the late phase of the Late Iron Age (approx. 2nd–1st c. BC). Individual specimens with thickened, flattened rims (cat. P25/001) and kinked walls (cat. P1/136) are made in the monochrome grey fabrics. These pottery types, like the broad rim of a fruit bowl (cat. P5/003), a fragment of a jar (cat. P5/004), a small dolium (cat. P5/005), and a storage vessel (cat. P18/005) can likely be assigned to the younger phase (2nd–1st century BC).

A pot with a funnel edge (cat. P24/008) and some sherds of decorated vessels might be attributed to handmade vessels of the late phase of the Late Iron Age too.

9.1.2.4. Pottery of the Roman period

Early Roman pottery (1st c. AD). The pits investigated in trench 5.1 (site 5) are so far the only structures from the Roman period that have been found during the excavations at the Tash Bair sites. An interesting range of Early Roman pottery was found in these structures (cf. also table 12). To a large extent, it consisted of fragments of vessels that had been made in the Late Iron Age manner. Most of these are handmade vessels or vessels made on the slow wheel (cat. P5/014–025), which more or less can be assigned to the handmade fabrics of the Late Iron Age No. 55 and 56. However, there were also some fragments of monochrome fine grey wares (cat. P5/013; P5/026). In addition, some fragments of vessels of Roman origin were found, including the omphalos base of a jug (cat. P5/012), small fragments of other fine wares, and lamp fragments (cf. the contributions by L. Traykova, chapter 9.2.2, cat. Nos. SF 58, 59). There are also some characteristic imported amphorae (cat. P5/010–011). These pieces provide a relatively reliable dating of the find complex of the middle or second half of the 1st century AD.

These finds make it clear that the Late Iron Age pottery tradition was continued in the Early Roman period. A strict chronological delimitation of the sites at this transition based on the surface finds is difficult, if not impossible. Handmade vessels of the Late Iron Age tradition can still be found in the 3rd and 4th century, although they only make up a small proportion of the vessel finds in this time period (Conrad 2007a, 243–244 fig. 40; 262–263 fig. 62; Александрова 2013, 62–74).

Roman pottery of the 2nd to mid-4th c. In contrast, the Roman fragments found during field surveys can only generally be assigned to the period between the 2nd and the 1st half of the 4th century. This is largely due to the fragmentation and the state of preservation. In addition, as indicated by the finds from the investigated pits at site 5, the number of clearly identifiable pieces from the Early Roman period is relatively low overall. Furthermore, the detailed chronology of the vessels covered with glossy slip and the assignment to individual workshops has not yet been sufficiently clarified.

Even if the percentage shares of pottery finds cannot be precisely quantified, the fine wares undoubtedly make up the largest part of the survey finds from the Imperial period. Mostly, these are hard-fired ceramics, which are usually covered with a red to reddish brown gloss slip; sometimes referred to as the Moesian sigillata. According to the different properties and qualities, we have distinguished four wares (Nos. 58–60; 62). The production of this pottery was most likely established by immigrants from Asia Minor at the beginning of the 2nd century. As research in recent years shows, in addition to the important and long-known workshops of Butovo and Pavlikeni (Sultov 1985), other production centres may have existed, for example in Nicopolis ad Istrum and in the major military sites on the Danube (cf. Conrad 2007a, 222–223; Baranowski et al. 2021).

The vessel fragments show a wide range of shapes and details, which is reflected for example in the repertoire of Pavlikeni's workshop. In the first half of the 4th century, the workshops in Butovo were apparently the main suppliers of Moesian red slip wares, before they probably came to an end shortly after the middle of the 4th century (Daszkiewicz, Schneider 2007, with the Conrad 2007b, catalogue). We have also noticed a great variety of shapes among the red slip wares from the Iatrus fort (Conrad 2007a, 222–223). The detailed chronology and typological development of the vessel shapes have not yet been defined, and it is not clear if this variability and certain differences in the fabrics at one site are

indicative of chronological depth. Often the vessels are decorated with stamp, barbotine or scroll wheel patterns (cf. Ivanov 2019, 22–25).

The majority of the typologically clearly identifiable finds are bowls and plates; bowls with a slightly curved rim being the most common. The body wall can be rounded or kinked and the rim shapes can be very diverse (cat. P1/146–147; P2/009–010; P2/012–013; P12/004–005; P18/012). In addition, there are also smaller specimens that tend to show open forms with or without a broad rim (cat. P1/145; P2/008; P2/011; P2/014; P18/013). A small conical bowl (cat. P2/015) is a rather unusual and rare form.

The individual forms of the plates differ from each other quite clearly. They come in the variants with thickened (cat. P2/005–006), broadly outcurved (cat. P18/010), narrow-horizontal (cat. P1/143; P2/007) and vertical rims (cat. 18/011), whereby individual forms are also found here clearly different from each other.

Typical and common are the flat-bottomed table amphorae (cat. P1/142; P12/001–002; P2/004), pots (cat. P2/016) and cauldrons (cat. P1/150; P2/017–018; P18/014), which certainly served as storage or mixing vessels. Thin-walled vessels such as cups (cat. P12/003; P18/009), beakers, jugs and kantharoi are typologically proven among the survey finds to a small extent or not at all. However, they made up a large proportion of the production and excavation finds (Sultov 1985, pl. 32–38; Falkner 1999, pl. 9.34–35; 9.38; 9.40–42; Conrad 2007a, cat. 758–778; 862–864; 881–883; 885–887; 934–939).

Five wares (Nos. 63–67) were distinguished among the coarse wares of the Roman period. Only a few fragments from vessels made of these fabrics could be assigned typologically, a. o. the typical pots with beaded rims of the 2nd–3rd c. (cat. P1/152–153; P12/007), with lid groove (cat. P1/154; P1/156; P 12/008; P18/015–016) and with slanted rims (cat. P12/009; P18/017; P1/155). The rim of a bowl made of grey coarse ware (P12/006) has striking parallels to the red slip ware pieces (P2/014; P18/013).

The pots cat. P1/155–156; P12/009; P18/015–017, together with the bowl fragment P1/151, were of the characteristic whitish-yellowish kaolin fabric (No. 63) which was in use in the Lower Danube during the 3rd, and the first half of the 4th c. (cf. Conrad 2007a, 242–243,261–262 fig. 59; 843–844 fig. 61,853; Dyczek 2009; 2016).

There is also a simply profiled pot with an outcurved rim (cat. P18/018) and the cauldron fragment (cat. 02/091), which has an unusual rim that has not yet been observed elsewhere.

In addition to the two Early Imperial amphorae from Heraclea Pontica from pit 5.1.5 (cat. P5/010–011), the amphorae collected during field surveys form a small but typical range of amphorae which were delivered to the territories at the limes and beyond during the Roman period (cf. Dyczek 2001). The double handle cat. P5/007 as well as the foot cat. P2/002 belong to the amphorae of the Dressel 2–4 group probably produced in the East Aegean region. They can only generally be dated to the 1st to 2nd century. The other pieces, on the other hand, belong mainly to the time frame from the end of the 2nd to the first half of the 4th century. The fragments cat. P1/140; P1/141 and probably also the foot cat. P5/009 belong to the type Zeest 85 originating from the northern Pontus area. The funnel-shaped mouths cat. P2/003; 5/008; 18/008 are to be assigned to the periphery of the amphora Dressel 24 sim., which very likely comes from the Aegean region.

9.1.2.5. Late Roman pottery

Among the survey finds of the Late Roman pottery, only imported amphorae and coarsely tempered pottery (mainly kitchen ware) can be distinguished. Three rim fragments of amphorae Iatrus I1 = LR Amphora 2 (cat. P1/158; P2/020; P12/010), each from the second half of the 4th century, were recorded on the Tash Bair sites. There is also a foot of an amphora from North African production (cat. P2/021) and a foot of an early example of an amphora Iatrus I6 = Kuzmanov 10 (cat. P1/159).

Among the Late Roman coarse wares, four fabrics were set (Nos. 71–74), but the number of finds is relatively small. Of the survey finds, only a bowl (cat. P1/160), two pot fragments (cat. P1/161;

P12/011) and a lid (cat. P1/162) could be included in the catalogue as clearly typologically identified items. According to the relatively small number and the dating of the corresponding sherds among the collected material, the Late Roman sites at Tash Bair seem to end before the end of the 4th century.

The finds from the upper backfill layers of trench 3.6, including amphora fragments Iatrus I1 = LRA 2 and pot sherds (cat. P3/021–023), belong without any doubt to the first half of the 5th century. They likely prove that after the villa complexes and village settlements had been abandoned, some of the former residents or new settlers had very likely withdrawn to the prehistoric enclosure.

9.1.2.6. Early Medieval Pottery

The finds of the Early Medieval pottery sherds (included in the catalogue after the statistically recording) come from vessels which are strongly sand-tempered, wheelmade, and are of fine orange and fine grey fabrics.

The wheelmade coarse wares are divided into four different fabrics (Nos. 75–78) according to their texture, colour and shape. Despite the clear identification of the sherds, this group of fabrics has evaded more precise dating for a long time because of its unspecific shape (especially the rims) and its variable decoration (mostly done with a comb-like tool and often uncharacteristic texture). For this pottery group, Galina Grozdanova (2018) recently suggested at least a rough distinction between the finds from the advanced 7th / 8th century and the 9th / 10th century based on the findings in the excavations at Garvan and Popina, where she also used the preliminary work of Rasho Rashev (Рашев 2014, 181–184). Rashev had previously proposed a similar distinction between vessels that had been produced on the slow (type AII) and fast (type AIII) wheel. Further subgroups resulted from the type of decoration. However, Rashev did not draw any conclusions for the chronology of the two groups from this distinction.

On this basis, the dating of the finds from our investigations is possible with certain reservations which are due to the fragmentary preservation. For a reliable assessment, among other things, knowledge of the entire ornamentation is also necessary.

According to the criteria established by Grozdanova, the thick-walled, somewhat roughly shaped fragments cat. P1/163; P19/012; P21/002 can be assigned to the early group, which typically have short and an outward leaning rim. More or less at the same time as this early group, vessels made on the slow potter's wheel of grey fine ware, appear. This kind of pottery can be traced back to a nomadic pottery tradition, and can therefore connected with the Proto-Bulgarians (cf. Рашев 2014, 184–186, Grozdanova 2018, 27–28). The items in fabric 83 in the catalogue include three items with a burnished or smoothed surface (cat. P1/170; P1/172; P34/002), as well as another three items in ware 85 with a slightly rough surface (cat. P1/169; P1/171; P34/003). The latter are often decorated with incised wave bands. This group very likely appeared at the same time as the handmade vessels, of which only a few uncharacteristic wall fragments were found (ware No. 87).

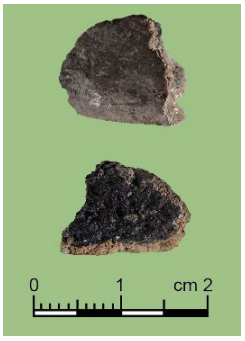
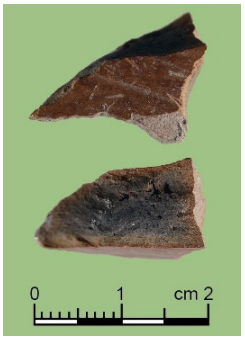
The remaining pieces of the sandy coarse ware come from relatively thin-walled vessels most likely made on the fast potter's wheel. There are more or less pronouncedly outward leaning rims with rounded (cat. P1/221; P1/224; P12/006), pointed (cat. P21/003–004; P37/001) and flattened, angularly offset lips (cat. P1/164–167; P1/210; P19/013–014; P20/001; P21/005). In addition, there is a kinked, slightly thickened edge of a larger storage vessel (cat. P1/225). On the basis of the rim shapes and decorations (as far as they are recognisable) these pieces can be assigned to the younger group, i.e. to the period from the 9th to the beginning of the 11th century.

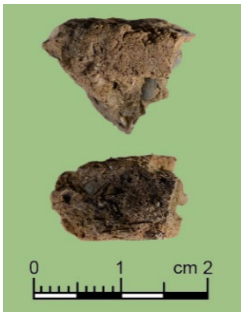
Several items made of orange-coloured fine clay (ware No. 80) were recorded, but only the rim fragments cat. P1/168; P1/225 could be clearly identified as pot rims and were included in the catalogue. Furthermore, fragments of the characteristic double-handled jars were observed. Vessels made of this ware occur in both the early and later phases of the Early Middle Ages.

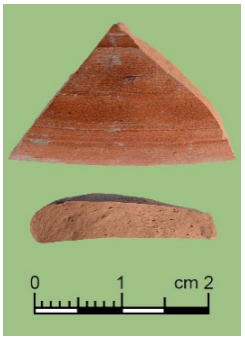
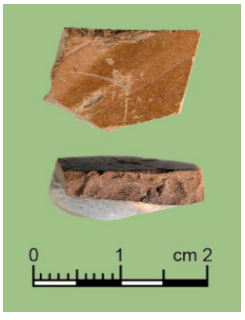
The find spectrum is completed by some statistically recorded fragments of glazed vessels (ware 31).

Table 2. Fabrics (ware groups) of the pottery from the Late Iron Age to the Ottoman period

Fabric No.	Fabric	Cat. No.	Dating	Photo
Late Iron Age (- Early Roman period)				
Fine fabrics (wheelmade)				
49	*Fracture:* Fine grey fabric; hard fired. Mostly smooth fracture; porous and splintery in places. Modest tempering with silty sand; individual fine (lime?) pieces. Some vessels with a core of different colour. Samples: 5/N to 5/1 5GY (Gley 1) (fracture); 6/N (Gley 1) (core) *Surface and finish:* Clay-ground, very smooth surface (sometimes olive-grey), often polished. Samples: 5/N to 6/N (Gley 1)	P1/126–P1/128; P1/209; P1/223; P5/002; P5/013; P5/026; P17/004; P19/008; P24/007	LIA (very likely 6th–3rd c.)	
50	*Fracture:* Dark grey to dark greyish brown, sometimes greyish black, fine fabric; very hard fired; mostly smooth fracture with individual porous areas. Very little silty sand, very few medium-sized pieces of limestone. A part of the vessels has a light grey to grey, partly two-coloured layered core. Samples: 4/N (Gley 1) to 10YR 4/1 (fracture); 4/N to 6/N (Gley 1), partly with a thin outer layer; 10YR 4/1 (core) *Surface and finish:* Carefully smoothed surface with partly streaked, polished black or dark grey coating. Samples: 2.5/5PB (Gley 2) to 2.5Y 2.5/1	P1/131; P1/133; P1/135; P1/137; P1/205; P1/208; P18/001; P19/005–P19/007; P25/001; P34/001	LIA	
51	*Fracture:* Grey to light grey, hard and fine; mostly smooth, sometimes slightly grainy. Samples: 7/N (Gley 1) *Surface and finish:* Carefully smoothed, often polished. Vessels of the latest phase of the Late Iron Age (2nd–1st c. BC) and the Early Roman Imperial period (1st c.), often show a shiny polished surface. Samples: 7/N to 8/N (Gley 1)	P1/129; P1/134; P1/136; P5/003–P5/005	LIA (especially 2nd – 1st c. BC [–1st c. AD])	

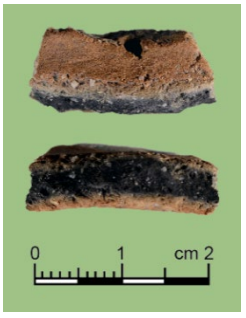
Fabric No.	Fabric	Cat. No.	Dating	Photo
52	*Fracture:* Grey to dark grey, middle hard and middle fine fabric; grainy and porous fracture (some vessels may have been produced on slow wheel); slightly fragile structure. A part of the vessel has a thick dark grey or blackish core. Modest tempering with fine and middle fine sand; some bigger pieces (dm. 2–3 mm). Samples: 5/N to 4/N (Gley 1) (fracture); 2,5/N (Gley 1) (core) *Surface and finish:* Moderate smoothed dark grey to greyish black surface; slightly grainy. Samples: 4/N (Gley 1)	P1/130; P1/138; P19/004	LIA (2nd – 1st c. BC)	
53	*Fracture:* Red brown to dark red-brown, hard and fine; mostly smooth with individual medium-fine pores. Very little silty sand. A part of the vessel has a light grey to light grey brown core. Samples: 5YR 4/6 to 7.5YR 5/6 - 4/6 (fracture); 5/10G (Gley 2); 5YR 5/1 (core) *Surface and finish:* Brown to red-brown surface with a polished coating. Samples: 5YR 4/4; 7YR 6/4	P1/132; P17/003	LIA, 2nd – 1st c. BC (–1st c. AD?)	
54	*Fracture:* Some vessels show a certain variety in colour of No. 53; their fracture is light yellowish to white-yellowish. Samples: 2.5Y 9/1 to 2.5Y 9/2 (White Page) *Surface and finish:* The mostly polished surface has the same colour as the fabric; there can be orange spots Samples: 2.5Y 9/2 to 7.5YR 8,5/2 (White Page)		LIA, 2nd – 1st c. BC (–1st c. AD?)	

Fabric No.	Fabric	Cat. No.	Dating	Photo
Coarse fabrics (hand- and slow wheelmade)				
55	*Fracture:* Light brown to yellowish light brown; sometimes greyish brown (secondarily fired); grainy and with fissures. Coarse (middle sandy), slightly fragile. Most of the vessels have a thick black or greyish black core. Samples: 7.5YR 7/6 to 7.5YR 6/4 (similar) (fracture); 2.5/N (Gley 1) (core) *Surface and finish:* Light brown to yellowish light brown fabric; the surface is not very carefully smoothed. Often with attached mouldings with fingerprints. Samples: 7.5YR 7/6 to 7.5YR 6/4 (similar)	P1/139; P5/017; P5/022; P5/023	LIA	
56	*Fracture:* Greyish black to black; surface layers light brown to light reddish brown. Slightly grainy and with fine fissures. Light coarse (fine sandy), slightly fragile. Samples: 2.5/N (Gley 1) (fracture/core); 10YR 8/4 to 7/4 (similar); 5YR 6/4 (similar) (surface layers) *Surface and finish:* Light brown to light reddish brown; carefully smoothed surface (often slow wheelmade). Most vessels with attached mouldings with fingerprints. Samples: 10YR 7/4 (similar) to 5YR 6/4 (similar)	P3/018; P4/001; P5/014; P5/018–P5/021; P5/024; P5/025; P18/003–P18/007; P19/009; P19/010; P24/008	LIA	
57	*Fracture:* Reddish brown; thin surface layers grey to brownish grey. Slightly grainy. Light coarse (fine sandy); strong mica temper. Samples: 2YR 6/4 (similar) (fracture/core); 2YR 3/1 to 7.5YR 3/1 (similar) (surface layers) *Surface and finish:* Grey to brownish grey; carefully smoothed surface (slow wheelmade). Samples: 2YR 3/1 to 7.5YR 3/1 (similar)	P5/015; P19/011	LIA, 2nd–1st c. BC (–1st c. AD)	

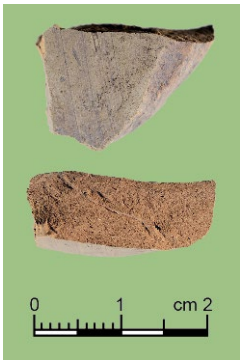
Fabric No.	Fabric	Cat. No.	Dating	Photo
Roman period (1st – mid 4th c.)				
Fine fabrics				
58	*Fracture:* Red brown to light red-brown, fine and very hard fired fabric; smooth, fine cracks, sometimes slightly leafy structure. Very hard with a uniform structure. In some cases, very fine single pieces of sand or lime. Samples: 2.5YR 5/4...6 *Surface and finish:* Dense, light red to light red-brown glossy coating. Some of the vessels decorated with barbotine or rouletting. Samples: 2.5YR 5/8	P1/143; P1/145; P1/146–P1/148; P2/005; P2/006; P2/008–P2/010; P2/014–P2/017; P12/003; P18/010; P18/011; P18/013	RP (2nd–1st half of 4th c.)	
59	*Fracture:* Light brown (sometimes light reddish brown) to beige coloured, fine and very hard, with uniform structure; smooth fracture; individual pores. Individual fine grains of sand. Samples: 7.5YR 7/4 ... 6; 2.5YR 5/4...6 *Surface and finish:* Uneven, red-brown to dark red-brown, partially spotty, matt glossy slip. Some of the vessels decorated with barbotine or scroll wheel. Samples: 2.5Y 2.5/3; 2.5YR 4/8; 5YR 2.5/2	P1/142; P1/144; P1/150; P2/007; P2/013; P2/018; P12/001; P12/002; P12/004; P12/005; P18/009; P18/012; P18/014	RP (2nd–1st half of 4th c.)	
60	*Fracture:* Beige to light brown, sometimes dark brown fine and very hard fabric with a uniform structure; smooth break. Single pieces of very fine sand. Samples: 10YR 7/6; 10YR 6/6 *Surface and finish:* Brown, matt glossy slip. Samples: 7.5YR 4/6; 7.5YR 5/6	P2/011; P2/012	RP (2nd–1st half of 4th c.)	
62	*Fracture:* Red brown to dark red brown; smooth, slightly grainy fracture. Light fine sandy tempering. Samples: 7.5YR 5/8 (similar) *Surface and finish:* Red brown, matt slip. Samples: 7.5YR 5/6 (similar)		RP (2nd–1st half of 4th c.)	

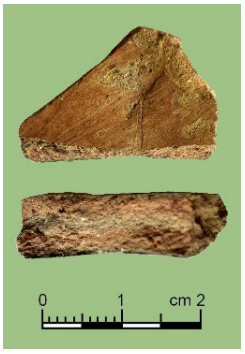
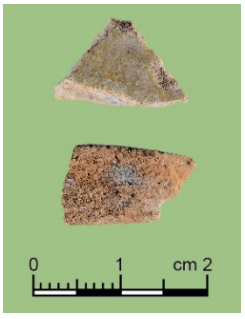
Fabric No.	Fabric	Cat. No.	Dating	Photo
Coarse fabrics				
63	*Fracture:* Light yellow to whitish-yellow fine and relatively hard fired, with a uniform structure; granular and fine-pored. Medium-strong, fine sand and brick-dust tempering with single coarse grains. Samples: 2.5Y 8/2...3 *Surface and finish:* Rough surface of similar colour like the fracture; the outside and especially the rim is often sooted. Samples: 2.5Y 8/2...3	P1/151; P1/155; P1/156; P12/009; P18/015–P18/017	RP (3rd–1st half of 4th c.)	
64	*Fracture:* Grey, granular, middle fine, relatively hard. Strong tempering with fine sand. Samples: 5...4/N (Gley 1) *Surface and finish:* Rough, granular, fabric-like coloured surface. Samples: 5...4/N (Gley 1)	P1/152; P12/006; P12/008	RP	
65	*Fracture:* Grey to dark grey-brown, granular middle-fine, relatively hard fabric; partially smooth fracture. Some pieces have dark grey or blackish grey core. Medium-strong tempering with fine sand; in rare cases with single coarse grains. Samples: 7.5YR 5/1; 5/N (Gley 1) (fracture); 7.5YR 2.5/1; 2.5/N (Gley 1) (core) *Surface and finish:* Rough, fabric-like coloured surface, sometimes darker (dark to blackish grey). Samples: 7.5YR 5/1; 2.5/N	P1/153; P1/154; P12/007	RP	
66	*Fracture:* Light grey brown to light greyish red brown fabric. Some characteristics are similar to No. 65. Samples: 7.5YR 6/2; 10YR 6/2 *Surface and finish:* Slightly rough, fabric like coloured surface. Samples: 7.5YR 6/2; 10YR 6/2	P1/157	RP; LRP	

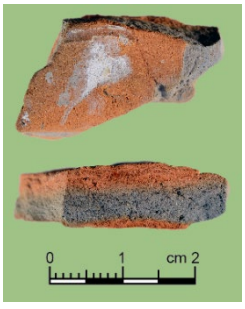
Fabric No.	Fabric	Cat. No.	Dating	Photo
67	*Fracture:* Red brown fabric; fine and hard fired. Middle strong, fine sand temper; sometimes with small lime pieces. Smooth fracture, with some fissures. Samples: 10R 5/8 *Surface and finish:* Light red brown, relatively carefully smoothed. Samples: 10R 6/8	P2/019	RP	
Late Roman period				
Fine fabrics				
70	*Fracture:* Dark grey to dark olive grey, very fine, with a uniform structure; smooth, very slightly porous fracture surface; sometimes slight tempering with fine sand. Samples: 4/N; 3/N (Gley 1) *Surface and finish:* Dark grey to black grey surface; in some cases, flat or ornamentally burnished. Inside mostly slightly rough. Samples: 2.5/N (Gley 1); 2.5/5PB (Gley 2)		LRP	
Coarse fabrics				
71	*Fracture:* Similar to No. 65; with a modest to strong tempering of middle coarse to coarse sand. Samples: 4/N; 3/N (Gley 1) *Surface and finish:* Slightly darker and more granular surface. Samples: 2.5/N (Gley 1); 2.5 / 5PB (Gley 2)	P1/160; P1/162; P3/021	LRP (4th–5th c.)	
72	*Fracture:* Light grey to grey, hard; with a modest tempering of fine sand. Relatively smooth fracture. Samples: 6…8/N (Gley 1) *Surface and finish:* Accurately formed, fabric-like coloured or dark grey surface, sometimes slightly rough. Samples: 6…8/N (Gley 1)	P1/161	LRP (4th–5th c.)	

Fabric No.	Fabric	Cat. No.	Dating	Photo
73	*Fracture:* Reddish brown to dark reddish brown, hard fabric; grainy fracture. Samples: 2.5YR 4/8; 2.5YR 3/6 *Surface and finish:* Slightly rough, fabric-like coloured surface; sometimes slightly carelessly shaped. Samples: 2.5YR 4/6; 10R 4/6; 10R 5/3	P3/019; P3/020	LRP (2nd half 4th–5th c.)	
74	a. Outer thin layer light reddish brown, middle fine, grey core. Hard fired; less sand tempering. Samples: 10R 7/6 *Surface and finish:* a. Carefully shaped surface; outside with dark green to yellowish dark green glaze; inside fabric-like coloured. Samples: 5/10Y; 4/5GY (outside) 10Y-5GY); 7...8/N (Gley 1) (inside). b. Like 74a, but with yellowish-ochre glaze. Samples: 2.5Y/7...8/4		a. LRP (2nd half 4th–5th c.) b. RIP/LRP (2nd half 3rd–4th c.)	
Early Middle Ages				
Coarse fabrics				
75	*Fracture:* Dark grey to grey black core with surface layers of light brown to red-brown colour. Middle fine fabric with rather uniform structure. Middle strong, fine sand tempering; individual larger grains. Samples: 5YR 4/3...6; 5YR 5/3...6; 7.5YR 5/3... 4 (surface layers); 7.5YR 2.5 / 1; 10YR 3/2...3 (core) *Surface and finish:* Rather carefully formed surface; slightly granular, sometimes with secondary soot. On the outer surface in the shoulder and body zone, ornamentation of very variable shape, often incised with a comb instrument. Samples: 5YR 4/3...6; 5YR 5/3...6 (outside); 7.5YR 5/3...4 (inside)	P1/164; P1/165; P1/210; P19/012; P19/013; P20/001; P21/003–P21/005; P34/002; P34/003; P37/001	EMA (10th c.)	

Fabric No.	Fabric	Cat. No.	Dating	Photo
76	*Fracture:* Similar to No. 75, but uniformly fired throughout with red-brown to dark red-brown colour. Very strong sand tempering of medium grain size. Samples: 5YR 5/6; 10R 5/6...8 *Surface and finish:* Fabric like surface, rather carefully shaped; partly dark grey to black-grey soot on the outside. Samples: 5YR 5/6; 10R 5/6...8	P1/167	EMA	
77	*Fracture:* Outside black-grey, inside dark red-brown to dark grey-brown; dark grey to grey-black fracture, slightly granular. Medium hard fired; medium-fine with a rather uniform structure. Medium-strong sand temper with fine grain. Samples: 2.5Y 2.5 / 1; 5YR 3/2...3 *Surface and finish:* Rough to slightly rough surface, black-grey to dark greyish brown outside, dark grey inside. Incised decorations on the outside (shoulder and body) with a comb-like instrument. Samples: 2.5Y 2.5 1; 10R 4/3...6 (outside); 10YR 3/1...2 (inside)	P1/163; P1/166; P1/211; P1/224; P19/014; P21/002	EMA	
78	*Fracture:* Very similar to No. 75. Stronger sand temper; more fragile texture. Samples: 2.5YR 6...7/6 (fracture); 2.5YR 2.5/1 (core) *Surface and finish:* Very similar to No. 75. More granular and less carefully shaped surface. Samples: 2.5YR 7/6		EMA (end 10th c./11th c./pecheneg vessels)	

Fabric No.	Fabric	Cat. No.	Dating	Photo
Light orange fine fabric				
80	*Fracture:* Ochre- or light orange coloured, very fine; sometimes with a slightly darker core. Smooth break with uniform structure; some individual pores only. Samples: 7.5YR 8/4...6; 5YR 7/8 (fracture); 2.5YR 7/8; 2.5YR 6/8 (core) *Surface and finish:* Clay-ground surface; outside sometimes with grey-yellow to light grey-yellow engobe. On some vessels in the rim or shoulder area incised decoration with a comb-like instrument, mostly in the form of a wave band. Samples: 2.5Y 8/3...4; 10YR 8/3; 7.5YR 8/6 (outside); 7.5YR 8/4...6 (inside)	P1/168; P1/225	EMA	
Grey fine fabric (slow wheelmade)				
83	*Fracture:* Dark grey to grey-brown, very fine fabric with dark grey or dark core; hard fired. Mostly smooth, in places slightly grainy and slightly splintered fracture. Few, very fine mica; occasionally individual coarse pieces of lime. Samples: 2.5Y 4/1...2; 10YR 4/2...4 (fracture); 6/N; 5/N (Gley 1) (core) *Surface and finish:* Olive-grey to dark-grey, sometimes black-grey smooth surface; flat or ornamental burnishing. Samples: 10YR 3/1; 10YR 2/1 (outside); 10YR 5/2...4 (inside)	P1/170; P1/172	EMA	

Fabric No.	Fabric	Cat. No.	Dating	Photo
85	*Fracture:* Grey to dark grey, sometimes pale yellowish brown with pale grey core. Fine fabric; very hard fired. Slightly granular fracture; modest sandy tempering of medium grain size; few, very fine mica. Samples: 5...4/N (Gley1); 5YR 7/6 *Surface and finish:* Grey to dark grey, sometimes yellowish brown. Soapy-soft or very slightly rough finish; in a few cases, irregularly polished on the outside. Some vessels with incised wave band decoration. Samples: 10YR 5/1; 10YR 4/1; 5YR 6/6-8	P1/169; P1/171; P34/002; P34/003	EMA	
Glazed fabric				
86	*Fracture:* Light grey to grey, middle fine, hard fabric; often with a dark grey layer under the glaze coating. Modest to strong fine sand tempering. Samples: 8...7/N; 2.5/N *Surface and finish:* Outside with dark green, spotty glaze; fabric-like coloured on the inside. Samples: 5GY/2 (10Y-5GY) (outside)		EMA	
Handmade				
87	*Fracture:* Dark red brown to dark greyish red brown, coarse; slightly fragile; with dark grey to greyish black core or inside. Strong sandy tempering, with medium sized grains. Samples: 2.5YR 4/3...4 (fracture); 2.5YR 3/1 – 5YR 2.5/1 (inside/ core) *Surface and finish:* Fabric-like coloured, relatively rough surfaces. Samples: 2.5YR 5/4; 2.5YR 3/1		EMA	

Fabric No.	Fabric	Cat. No.	Dating	Photo
High Middle Ages				
Coarse Fabric				
88	*Fracture:* Red-brown, fine and hard; some vessels with a grey to light grey, separated core. Slightly grainy and slightly splintery fracture. Medium sand temper of medium grain size. Individual coarse pieces of lime; sometimes a little very fine mica. Samples: 2.5YR 5/8 - 2.5YR 4/8 (fracture); 10YR 6/1; 10YR 5/1 (core) *Surface and finish:* Clay-ground, slightly rough surface. Often horizontal, narrow grooves in the shoulder area. Pots are often stained black-grey on the outside, secondary burned and sooty. Samples: 2.5YR 4...8 (outside); 2.5YR 5/8...2.5YR 4/8 (inside)		HMA (Second Bulgarian Kingdom)	
Glazed Fabric				
89	*Fracture:* Like No. 88, but only some have slightly separated grey-brown core. Low sand tempering of fine grain size. Mostly used for bowls with a stand ring. Samples: 2.5YR 5/8 - 2.5YR 4/8 (fracture); 10YR 5...6/1 (core) *Surface and finish:* Inner surface with coloured glaze painting (sgrafitto), predominantly in white, brown and green tones on white engobe. The outlines of the ornaments are often incised before the paint is applied. Samples: 2.5YR 5/8 - 2.5YR 4/8 (outside)		HMA (Second Bulgarian Kingdom)	

КЕРАМИКА ОТ КЪСНАТА ЖЕЛЯЗНА ЕПОХА ДО СРЕДНОВЕКОВИЕТО

Свен Конрад

(Резюме)

*Х*ронологичното разделение на селищната история от късната желязна епоха до Средновековието на Таш баир и в околностите му следва основно общоприетата периодизация, използвана в българската археология. Тъй като датирането на структури и открити при разкопките слоеве често се основава изключително на керамични находки, невинаги е възможно да се определят ясни граници на периодите по тази схема.

Периодизация на керамичните находки

Началото на късната желязна епоха не съвпада – както обикновено е прието – с прехода от Халщатско време към Латенския период, но е белязано от появата на сиви съдове, направени на колело на границата между VI и V в. пр. Хр. Находките от късната желязна епоха се състоят от фрагменти от вносни амфори, фина сива керамика и парчета от грубо изработени глинени съдове. Последните били оформени на ръка или на бавно (ръчно) грънчарско колело. Бяха разграничени шест технологични групи в рамките на сивата керамика, изработена на колело, и три за керамика, изработена на ръка.

При възможност са правени опити да се разграничи керамиката от ранната (VI – III в. пр. Хр.) и късната фаза (II – I в. пр. Хр.). Ръчно изработената керамика не е или само в много ограничена степен е подходяща за по-точно определение на датировката. Вносните транспортни амфори изглежда са използвани в по-голям брой едва през по-късната фаза на късната желязна епоха.

Преходът към римско време също не може да се определи въз основа на създаването на римския лимес в началото на I в. сл. Хр. или спрямо организацията на провинция Мизия под *legatus Augusti* през 44 г. сл. Хр., защото сивата керамика, направена на колело, все още се произвежда през първите десетилетия на римската власт. Интересна колекция на римска керамика от I в. сл. Хр. произлиза от ями на обект 5.

Водещ керамичен и хронологичен индикатор за римския период е фината керамика с червено покритие, която е разделена в четири групи. Тя показва голямо разнообразие на типове и варианти. Голяма част от тази керамика е произведена в работилниците на Бутово и Павликени в територията на Никополис ад Иструм. Тяхното унищожаване в средата на IV в. дава крайна хронологична рамка за тази епоха, определена от керамичните находки. Други малобройни находки като кухненска керамика (пет технологични групи, вкл. т. нар. каолинови изделия) и някои транспортни амфори също са използвани за датиране.

Следващият късноримски период е представен само от находки от втората половина на IV в. Тук са характерни амфори, които показват доставка от Средиземноморието. Слабо обитаване през първата половина на V в. разкриват само находки от вътрешния ров на обект 3.

Евентуално заселване през VI в. на Таш баир и околностите му не може да бъде доказано по намерените артефакти.

През Ранното средновековие възниква обширно селище, особено на обект 1 и околностите му. То включва и археологически обекти по речните меандри в низините. Нему принадлежи и землено укрепление с валове. Обичайно преобладават съдовете, източени на грънчарски кръг, украсени с гребен и бурин. Те са разделени в четири технологични групи. Някои от тези съдове могат да бъдат отнесени към ранна (VII – VIII в.) и късна фаза (IX – X в.). Открити са още фрагменти от сива керамика с изгладена или полирана повърхност, които могат да се свържат с номадската традиция (т.нар. „пастирски тип“ керамика), парчета от оранжеви фини съдове и няколко чирепа от глазирани и ръчно изработени съдове.

9.1.3. Pottery statistics from the excavations of different features

Sven Conrad, Raiko Krauß

9.1.3.1. The pottery statistics from the excavations on site 1

Trench 1.2, features 1.2.4/6 and 1.2.7/8. Various cultural-historical groups can be recognised within the Late Neolithic materials from the double ditch in trench 1.2. Some of the material belongs to the the Vădastra culture, which occurs mainly in Oltenia. Other finds can be assigned to the Boian culture, which is mainly widespread in Muntenia. In addition, material from the Bulgarian Late Neolithic occurs, and individual forms can also be attributed to the Hamangia culture. All of the mentioned cultural groups represent regional manifestations of the Late Neolithic in the Balkans, the exact temporal relationship of which cannot be precisely determined. All of the groups mentioned show a development over time which may overlap. The common find position in the ditch alone is not sufficient to determine whether there is a geographical overlay of all four cultural groups or whether the find material at Tash Bair occurs in chronological succession.

The recording of the finds was done according to the different types of surface treatments and decorations. In some cases, these are specific to one of the mentioned culture groups. Most of the finds can only be characterised as Neolithic in general and were recorded according to the surface treatment or the shape of the vessel. There are other finds, such as stone axes, hammer stones and grinders, which belong to the typical inventory of Neolithic settlements. However, these cannot be assigned to any specific cultural group. Numerous finds of mudbricks offer an indication of the houses of the Neolithic settlement but can also come from houses of more recent times. Since they are associated with the Late Neolithic finds, their weight was determined (table 3).

The Late Neolithic material is numerous and offers a clear indication of the earliest history of backfilling this ditch. In addition, surface finds from the Late Neolithic are concentrated in the area enclosed by the ditch. Remarkably, the Late Neolithic finds in this area are also very numerous even in the more recent features; in many cases they represent the dominant find category.

A few finds from the Late Chalcolithic in the ditch fill are remarkable. At least one wide bowl can be safely assigned to the Kodzhadermen-Gumelnița-Karanovo VI stage of the Chalcolithic. These finds are the only evidence of settlement activity on Tash Bair in the middle of the 5th millennium BC. A larger settlement chamber from this time can only be found near Borovo and Volovo, approx. 30 km southeast of Tash Bair (Krauß 2006a, 219–222). Compared to the Late Neolithic, however, the Chalcolithic settlement cannot have been very large if one considers the small number of finds.

Trench 1.1-E/W, feature 1.1.6/15. Prehistoric fragments (Neolithic, Bronze Age, Early Iron Age) make up the largest proportion of the ceramics from the two parts of this ditch at site 1 (fig. 4; 5; 6; 7; features 1.1.6 / 15) (cf. the contributions by L. Vagalinski et al., chapter 8.3.1), with a total number of 850 pieces (91.2%) (tables 4, 5). In particular, there is an impressive range of Late Neolithic finds among them. Their large number is due to the long and intensive settlement at the site especially during the Late Neolithic. It seems to indicate that the core of the settlement is in the immediate vicinity.

While the few Roman (3) and Early Medieval (4) individual pieces from the upper excavation layers in ditch 1.1.6 are most likely secondary entries via the many animal dens, the Late Iron Age fragments are spread over almost its entire backfill. With a total of 68 pieces (8%), including 22 pieces of grey wheelmade wares, 45 pieces of handmade wares and a fragment of an imported amphora, their share is sufficiently significant for dating[4].

Only the small foot of a fruit bowl (cat. P1/205), which can only generally be assigned to the Late Iron Age, was included in the catalogue. All other fragments are wall fragments of different vessels (fig. 8). On the basis of the ceramic wares represented, only very few pieces, especially from the upper

4 Excavations carried out in another section of this ditch in 2022 showed that it has to be dated in the Late Neolithic. These results will be published in the next volume.

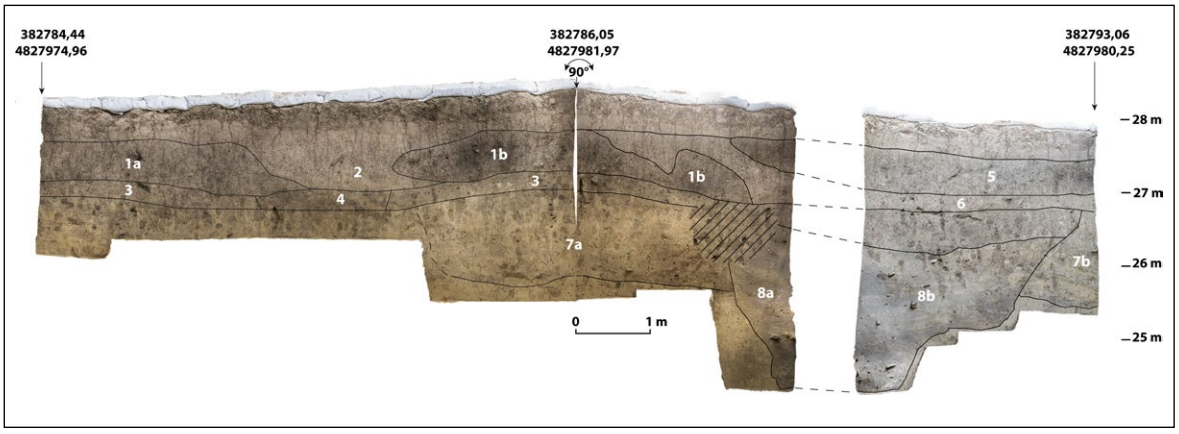


Fig. 4. Trench 1.1-W/E, north profile (combined), and trench 1.1-W, west profile. Legend: 1a – Shifted rampart (feature 1.1.5); 1b – Shifted rampart (features 1.1.1; 1.1.5); 2 – Gateway of the Early Medieval fortress; 3 – Ancient surface; 4 – Gateway surface; 5 – Modern colluvium; 6 – Post-Medieval surface with colluvium; 7a – Late Iron Age ditch (feature 1.1.15); 7b – Late Iron Age ditch (feature 1.1.6); 8a – Early Medieval ditch (feature 1.1.13); 8b – Early Medieval ditch (feature 1.1.7) (by the authors using an orthophoto obtained from a SfM model by M. Offermann)

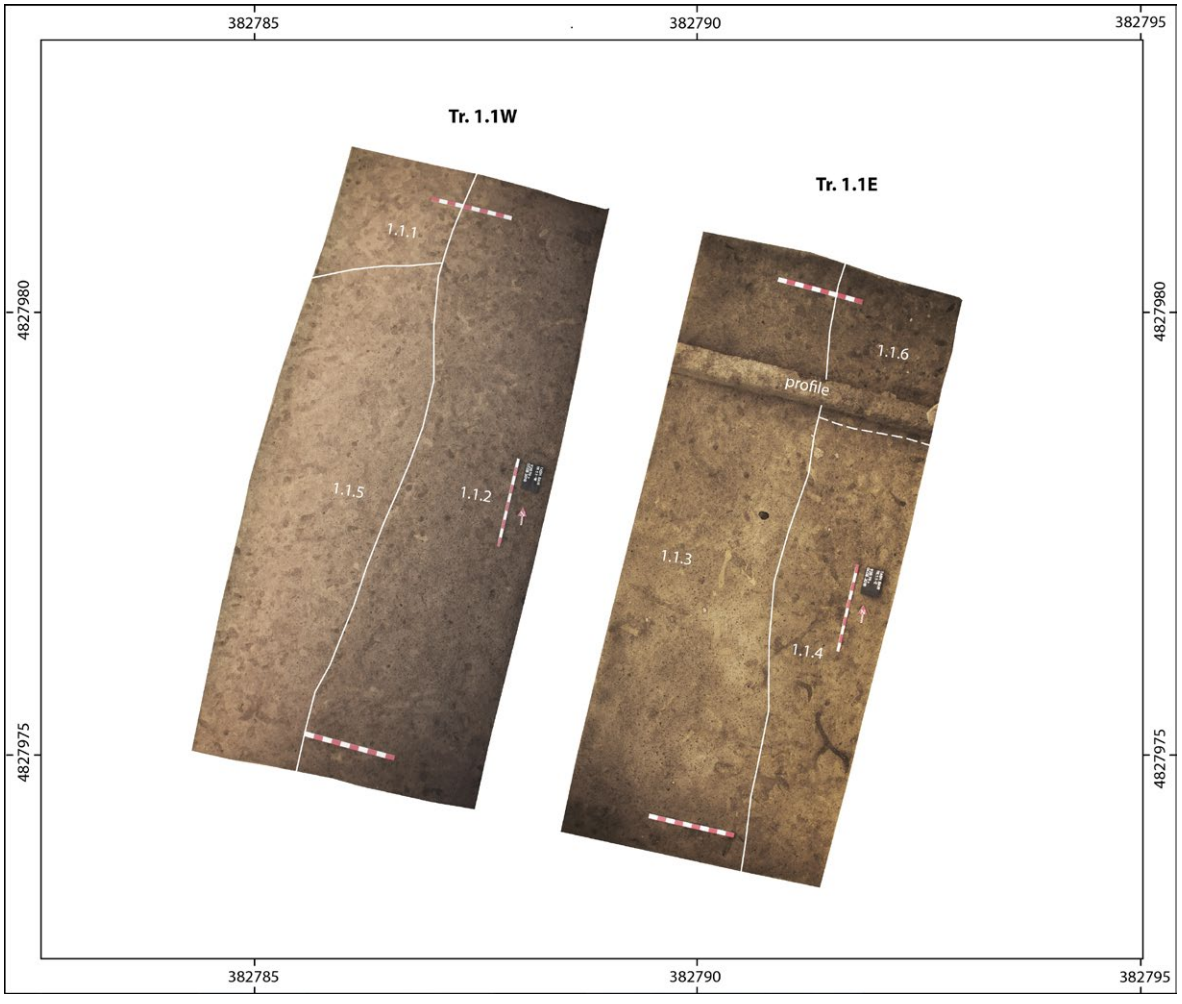


Fig. 5. Trench 1.1-W/E, planum 3 (niv. 26.78–26.76 m). Interpretation of features: 1.1.1, 1.1.5 – eroded material of the secondarily shifted Early Medieval rampart; 1.1.2, 1.1.5 – top layer of the filling of the Early Medieval ditch; 1.1.4 – colluvium; 1.1.6 – earlier ditch (Late Iron Age) (by S. Conrad using an orthophoto obtained from a SfM model by M. Offermann)

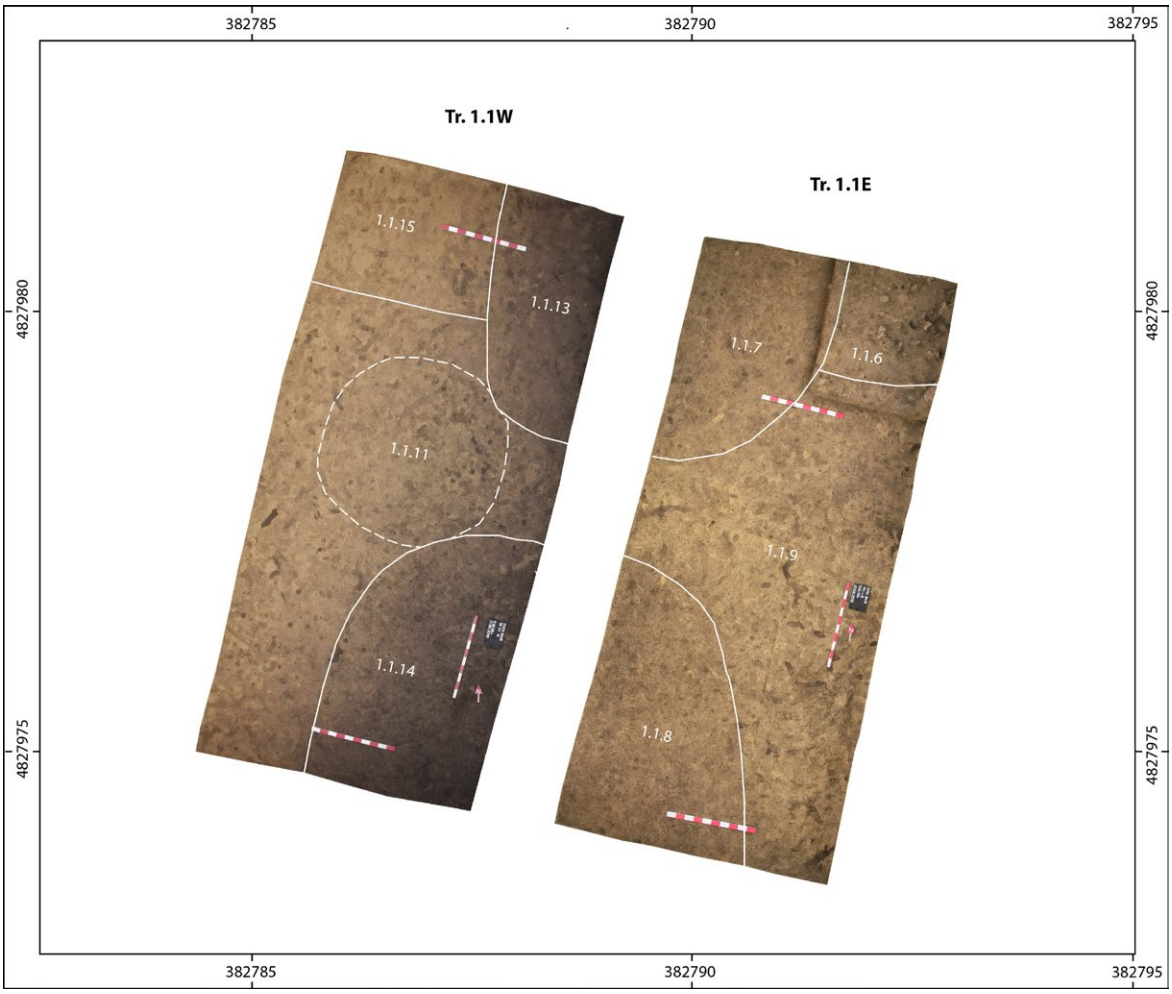


Fig. 6. Trench 1.1-W/E, planum 4 (niv. 26.58–26.53 m). Interpretation of features: 1.1.7/13 and 1.1.8/14 – ditch heads at the doorway of the medieval fortification; 1.1.6/15 – earlier ditch (Late Iron Age); 1.1.9 – colluvium (transition to the sterile loess); 1.1.11 – concentration of finds in the doorway of the Early Medieval fortification (partially sunken in the sterile loess) (by S. Conrad using an orthophoto obtained from a SfM model by M. Offermann)

backfill layers, can be assigned to the 2nd to 1st century BC. By far the largest part belongs to the older phase of the Late Iron Age between the 5th and 3rd century BC.

The Early Medieval ditches in trench 1.1-W/E (feature 1.1.7/13) and trench 1.2 (feature 1.2.5). The statistics of the ceramic finds from the northern ditch end, at the gate (features 1.1.7/13) and the SW inner ditch of the earthwork fortification (feature 1.2.5) at site 1 (fig. 4; 6; 7; 11), prove that Early Medieval ceramics represent in both cases the youngest and therefore chronologically relevant group of finds (tables 6–8). But again, in these cases, most of the finds are from prehistoric periods that got into the ramparts and into the ditches in the course of backfilling. In addition, finds from the Late Iron Age, the Roman Imperial and Late Roman period were found, but in significantly fewer numbers, like the Early Medieval finds. A single Modern sherd probably got into the backfill via an animal den (table 8).

The Early Medieval pottery fragments from these ditches and from the downwards shifted ramparts are all relatively small in size (fig. 9; 10; 12; 13). There were no matching pieces, which suggests that they only got into the backfill after a relocation. Two pieces included in the catalogue (cat. P1/224–225) originate from the downwards shifted rampart of the fortification.

Apart from two sherds of handmade vessels and two fragments of grey fine wares with burnished decoration from the upper layers of the infills (tables 6, 7), the majority of the Early Medieval fragments (determined by decoration and rim shape) can be assigned to the more recent period of the Early Middle

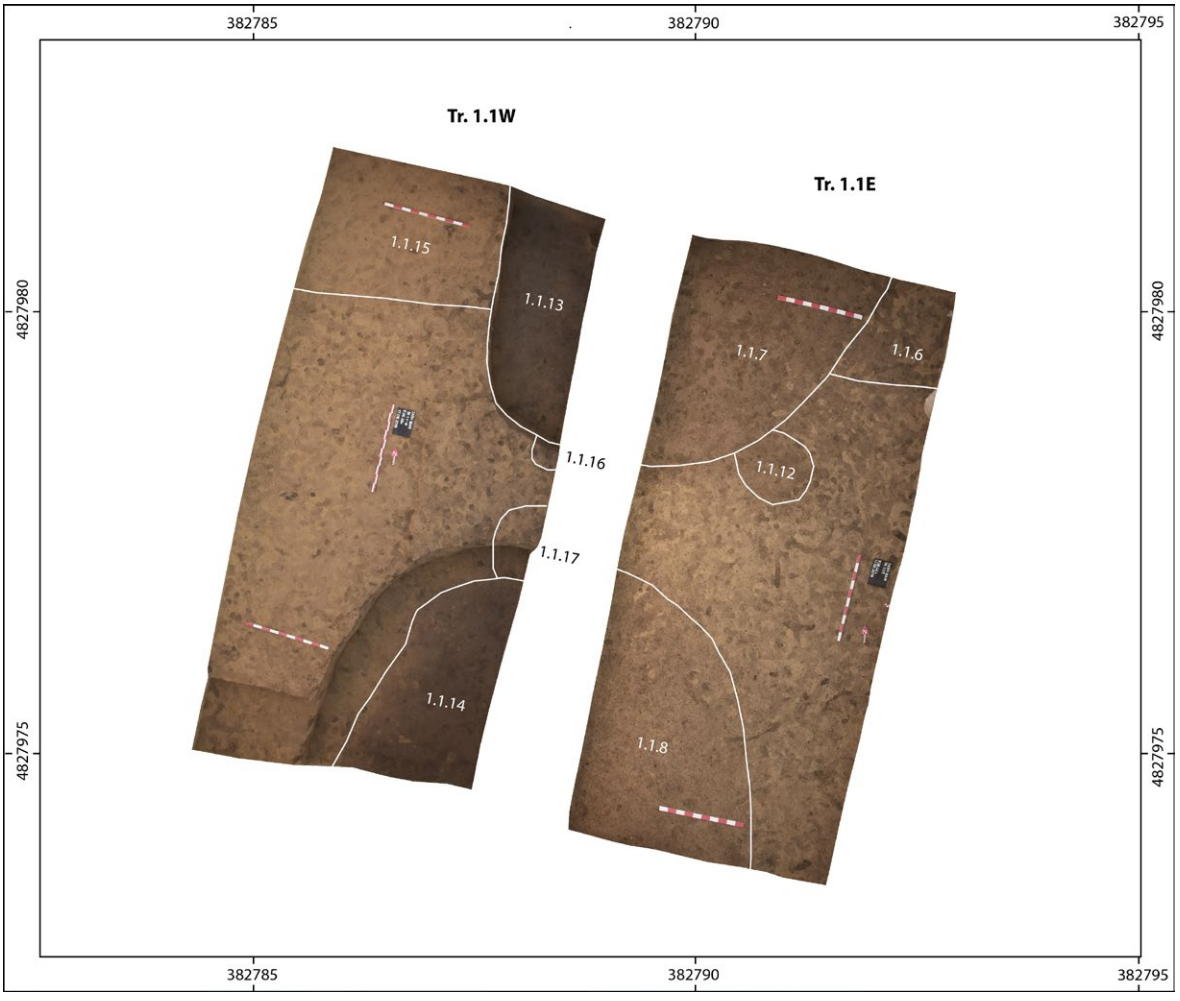


Fig. 7. Trench 1.1-W/E, planum 5 (26.38–26.44 m). Interpretation of features: 1.1.7/13 and 1.1.8/14 – ditch heads at the doorway of the Early Medieval fortification; 1.1.6/15 – earlier ditch (Late Iron Age); 1.1.12 – pit (not dated); 1.1.16 – post hole (?; Early Medieval); 1.1.17 – pit (not dated) (by S. Conrad using an orthophoto obtained from a SfM model by M. Offermann)



Fig. 8. Feature 1.1.15. Pottery of the Late Iron Age (selection) (by S. Conrad)

Table 3. Features 1.2.4/6 and 1.2.7/8; detailed pottery finds statistics (part 1)

Feature	LNL untreated	LNL barbotine	LNL smoothed	LNL polished	LNL channeled	LNL fine black polished (Boian)	LNL incised & channeled (Vădastra)	LNL storage vessel decored (Vădastra)	LNL Vădastra lid	NL storage vessel	Bulbous/biconical coars with barbotine	bowl with straight wall, coars	bowl with straight wall, fine	carinated bowl fine undecorated	carinated bowl fine channeled shoulder	carinated bowl fine scretched decoration	fine complex profiled with fine channeling (Boian)	large bowl with cone handle	coarse closed pot
1.2.6 W (outer) ditch																			
layer above ditch 29.46–29.30 m	6	4					3	2											
29.30-28.95 m	1	1																	1
28.95–28.70 m	40	6	4	1		7	3												3
28.70–28.50 m	106	13	6	3	1	3	6	1			2						2		1
28.50–28.23 m																			
28.23–28.01 m	1	1																	
1.2.4 W (outer) ditch																			
layer above ditch 29.46–29.30 m	31	7	1			5	3			2		2					1	1	1
29.30–29.08 m	20	2	1	3		4	2										1		2
29.08–28.84 m	25	6	2			8	1	1											1
28.84–28.58 m	29	13	1	2	1	2	1	3	2	2							3		
28.58–28.11 m	7	3				4	6										2		
1.2.7/8 E (inner) ditch																			
29.30–28.94 m	49	12				6	2					2		1		1			1
28.94–28.78 m	8	7					4						2				1		1
28.78–28.60 m	18	5	2		1	10	6				1	1				1	4		3
28.60–28.40 m	9	2	1		2		2												
28.40–28.10 m	34	7	1	2	1	4	4		2										1

Table 3. Features 1.2.4/6 and 1.2.7/8; detailed pottery finds statistics (part 2)

Feature	fine closed pot	footed vessel	box like	Chalcolithic dish	mudbrick in gram	oven plate fragments	grinding stone fragments	hammer stone fragments	stone axe fragments	Remarks	Younger material	Catalogue
1.2.6 W (outer) ditch												
layer above ditch 29.46–29.30 m					115					mixed	5 pieces Late Iron Age; 2 later prehistory	
29.30-28.95 m	1				8	2						
28.95–28.70 m					209					mixed	2 Late Iron Age (?) fragments, 1 fragment of Roman tile; 2 Medieval ceramic fragments	P1/239
28.70–28.50 m	1				155	2	1			1 big stone plate and another smaller stone	1 very small Medieval sherd (1 cm) and one Early Iron Age (1 cm), possibly from animal activity	P1/236–P1/238
28.50–28.23 m					40	3						P1/232
28.23–28.01 m												
1.2.4 W (outer) ditch												
layer above ditch 29.46–29.30 m			1							mixed	1 Roman, 1 Medieval, 5 Late Iron Age; 3 Early Iron Age	P1/233–P1/235
29.30–29.08 m				1	6					mixed		P1/242
29.08–28.84 m					41					mixed	1 fragment of Roman tile	
28.84–28.58 m		1			295	1				mixed	2 pieces Roman ceramic	
28.58–28.11 m					214							P1/240; P1/241
1.2.7/8 E (inner) ditch												
29.30–28.94 m	1				24			2				P1/246–P1/248
28.94–28.78 m						2						P1/243
28.78–28.60 m	1					2	1					
28.60–28.40 m												
28.40–28.10 m	1				35	1	1					P1/244; P1/245

Table 4. Trench 1.1-E. Feature 1.1.6, pottery statistics

Level (m)	Prehistory	LIA sum	LIA	LIA	LIA	Roman	EMA	Catalogue
			wheelmade	handmade	amphora		wheelmade	
26.76–26.67	**128**	**3**	1	2		**3**	**2**	P1/173–P1/181; P1/188; P1/198; P1/201; P1/205
26.67–26.24 no measured coordinates	**184**	**33**	10	23			**1**	
measured coordinates	**112**	**14**	4	10			**1**	P1/182–P1/184; P1/199
26.24–26.16	**14**	**1**		1				P1/186; P1/187; P1/204
26.16–26.08	7	**2**	1	1				
26.00–25.83	**39**	**1**		1				P1/189
25.83–25.39	**93**	**8**	4	3	1			P1/194; P1/195; P1/202
bottom	**17**							
Sum	**594**	**62**	20	41	1	**3**	**4**	

Table 5. Trench 1.1-W. Feature 1.1.15, pottery statistics

Level (m)	Prehistory	LIA sum	LIA	LIA	LIA	Roman	EMA	Catalogue
			wheelmade	handmade	amphora		wheelmade	
1.1.15W_26.38–26.20	**33**							
1.1.15W_26.20–25.99	**84**	**2**		2				
1.1.15W_25.99–25.77	**38**	**1**		1				P1/192; P1/193
1.1.15W_25.77–25.57	**8**							
1.1.15E_26.38–26.23	**14**	**1**		1				P1/190; P1/191; P1/196; P1/197
1.1.15E_26.23–26.05	**19**							
1.1.15E_26.05–25.88	**9**							
1.1.15E_25.88–25.77	**51**	**2**	2					
Sum	**256**	**6**	2	4				

Table 6. Trench 1.1-E. Feature 1.1.7 (NW ditch), pottery statistics

Level (m)	Prehistory	LIA				Roman					Late Roman			EMA						Catalogue
		Sum	wheelmade	handmade	amphora	Sum	amphora	fine	coarse	bricks/tiles	Sum	amphora	coarse	Sum	coarse (wheel)	fine	burnished	glazed	handmade	
26.44–26.24	**64**	**5**	4	1		**4**	2	2		3	**1**		1	**11**	10	1				
26.24–26.00	**33**	**3**		3		**1**	1				**3**	1	2	**3**	1		2			
26.00–25.83	**49**	**2**	1	1		**5**	3	2		1				**7**	2	3		2		P1/210
25.83–25.61	**43**	**1**	1			**2**	1	1		4				**1**	1					
25.61–25.39	**16**	**2**	1	1		**3**	1	1	1	2				**2**	1			1		
25.39–25.17	**23**	**3**		3		**2**	2			1				**1**	1					
25.17–24.97	**13**	**2**		2										**6**	5	1				
24.97–24.78	**13**	**2**	1	1																
24.78–24.56	**29**	**5**	1	4		**1**		1		1				**5**	4	1				
24.56–24.36	**11**	**5**	2	3																P1/208
Sum	**294**	**30**	11	19		**18**	10	7	1	**12**	**4**	1	3	**36**	25	6	2	3		

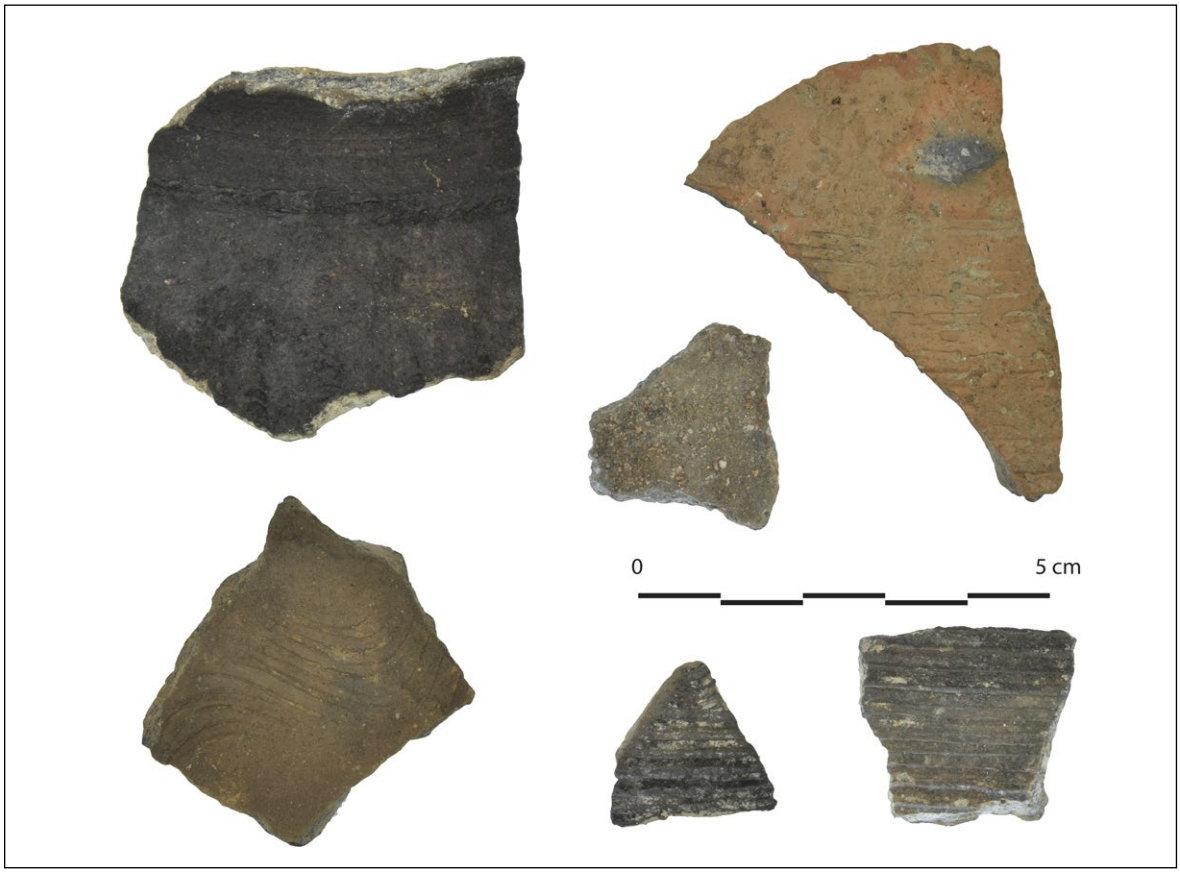


Fig. 9. Feature 1.1.7/13. Early Medieval pottery (niv. 25.17–24.56 m) (by S. Conrad)

Table 7. Trench 1.1-W. Feature 1.1.13 (NE ditch), pottery statistics

Level (m)	Prehistory	LIA				Roman					Late Roman			EMA						Catalogue
		Sum	wheelmade	handmade	amphora	Sum	amphora	fine	coarse	bricks/tiles	Sum	amphora	coarse	Sum	coarse (wheel)	fine	burnished	glazed	handmade	
26.58–26.38	**15**	**2**	2			**1**			1					**5**	4				1	
26.38–26.21	**14**					**1**			1					**2**	1	1				
26.21–26.04	**22**													**2**	2					
26.04–25.86	**25**	**5**	4	1										**3**	1	1			1	P1/206; P1/207; P1/209
25.86–25.65	**51**	**3**	1	2																
25.65–25.48	**5**													**2**	1	1				P1/211
25.48–25.28	**6**	**1**	1							1										
25.28–25.09	**3**																			
25.09–24.89	**2**																			
24.89–24.70	**1**																			
24.70–24.35	**2**																			
Sum	**146**	**11**	8	3		**2**			2	1	**0**			**14**	9	3			2	

Ages, i.e. from the 9th to the beginning of the 11th century (cf. cat. P1/210–211). It is not possible to derive a reliable date for the construction of the fortification from these finds.

9.1.3.2. The pottery statistics from the excavations on site 3

The inner ditch in trench 3.6. In the backfilling of the ditch (cf. the contributions by L. Vagalinski et al., chapter 8.2.1), between the bottom at approx. 57.49 m and niv. 58.58 m (fig. 14), in addition to the usual, difficult-to-determine prehistoric sherds, three Middle Bronze Age and four common Bronze Age sherds were found. Between niv. 58.58 m and 60.37 m, apart from two Bronze Age, three Early Iron Age and several common prehistoric pieces, only Late Iron Age finds were recorded (table 9). In the excavation layer between 58.80 m and 58.58 m (approx. 1.20 m above the bottom), a fragment of a handmade bowl with an inwardly curved rim (cat. P3/018) was found. This fragment dates back to the 6th / 5th century BC. As the latest finds, these Late Iron Age sherds determine the dating of the backfill in the middle part of the ditch.

In the upper part between the surface and level 60.37 m, in addition to prehistoric finds, numerous Late Roman sherds were found. These include wall fragments from amphorae Iatrus I1 (LR Amphora 2), which date to the first half of the 5th century. This dating is confirmed by the rims (cat. P3/019–021) and wall sherds of several pots (table 9; fig. 15). Besides that, some Late Roman roof tile fragments (fig. 16) and a bronze bell (cat. No. SF 54) (cf. the contributions by L. Traykova, chapter 9.2.2) came to light. These Late Roman finds continue until approx. 60 cm above the bottom of the trough-shaped, rounded layer boundary (maximum depth at approx. niv. 59.50 m) which divides the relatively homogeneous,

Table 8. Trench 1.2. Feature 1.2.5 (EMA ditch), pottery statistics

Level (m)	Prehistory	LIA				Roman					Late Roman			EMA						mod.	Catalogue
		Sum	wheelmade	handmade	amphora	Sum	amphora	fine	coarse	bricks/tiles	Sum	amphora	coarse	Sum	coarse(wheel)	fine	burnished	glazed	handmade		
29.46–29.30	**71**	**13**	7	6		**10**	2	5	3	4	**3**		3								
S_29.30–29.07	**90**	**8**	3	5		**15**	5	9	1		**3**		3	**8**	7	1					
S_29.07–28.89	**63**	**9**	5	4		**6**	2	4		1	**2**	1	1	7	7						
S_28.89–28.71	**106**	**21**	14	7		**12**	2	5	5	2				**26**	25			1			
S_28.71–28.49	**104**	**9**	7	2		**9**	2	3	4	1				**3**	3						
S_28.49–28.29	**97**	**9**	6	3		**3**		1	2		**1**		1	**2**	2						
S_28.29–28.10	**89**	**5**	3	2		**2**		2			**1**		1							1	P1/250; P1/251
S_28.10–27.92	**6**	**2**	1	1		**1**	1														
S_27.92–27.75	7	**3**		3																	
S_27.75–27.54	**51**	**16**	5	11										**1**	1						
S_27.54–27.35	**2**	**1**	1			**1**			1												
S_27.35–27.12	**19**	**6**	2	4		**3**	1		2	1				**2**	2						
S_27.12–26.94	**1**													**1**	1						
N_29.30–28.84	**12**	**4**	1	3		**2**	1	1		2				**1**	1						
N_28.84–28.58	**3**					**1**	1														
N_28.58–27.98	**37**	**3**	1	2																	P1/249
N_27.98–27.54	**27**	**2**	1	1						2				**1**	1						
N_27.54–26.94	**3**	**1**	1							1											
Sum	**788**	**112**	58	54		**65**	17	30	18	14	**10**	1	9	**52**	50	1		1		**1**	

grey-humous backfill in the upper part from the yellowish-brown backfill in the lower part. It can be suggested that this boundary can be related to the occupation of the site during the Late Roman period.

These observations prove that the ditch was more or less open since the Middle Bronze Age or regularly cleaned in its phases of use. In this context the observation of rapid natural backfilling of the excavated Bronze Age in the small enclosure near Drama is interesting. The fully excavated ditch, which is situated on a moderate slope, was filled with a 1.80 m thick layer of colluvium over the course of eight years (Lichardus et al. 2000, 30–32). This makes it clear that such ditches had to be cleaned regularly in order to maintain their shape and functionality. In the case of the enclosure at the Tash Bair, it is possible that the slope favoured the washing out of the sediment during heavy rainfall, which could be intensified by the demolished terrace. Furthermore, it must be considered that erosion processes on the hillside most likely caused considerable surface erosion, and therefore the trench was significantly deeper at that time.

Trenches 3.2–5, feature 3.2.1: Finds and dating. Besides the bronze knife (cat. No. SF 53; cf. the contributions by R. Krauß, E. Pernicka, chapter 10.1) and large pieces of daub, very few datable pottery

Table 9. Ditch in trench 3.6. Pottery statistics according to the excavated layers

Level (m)	Prehistory, undetermined	MBA	LBA	BA	EIA	Prehistory, sum	LIA	LIA	LIA	LIA	RIP	LR	LR	LR	LR roof-tiles	Daub	Catalogue
								amphorae	wheelmade	handmade			amphorae	coarse			
61.33 (Surface)–61.07	29	1	1			31	5		4	1		11	4	7			P1/008; P1/014; P1019
61.07–60.89	24	2				26	2		2			4		4			P1/004
60.89–60.72	8	1	1	2		12	5		3	2	2	22	1	21	4	2	P1/006; P1/007; P1/017
60.72–60.37	27	1		1		29	8		3	5		4		4	2		P1/005; P1/012; P1/015; P1/020; P1/021
60.37–60.12	4		1			5											P1/013
60.12–59.87	4					4											
59.87–59.62	0					0	2	1	1								
59.62–59.35	4				1	4	2			2							
59.35–59.07	5					5	4			4							
59.07–58.80	11		1		1	13				4							P1/016
58.80–58.58	5				1	6	5		1	4						5	P1/018
58.58–58.32	6					6											
58.32–58.03	13	2		2		17											P1/011
58.03–57.49	4			2		6											P1/002; P1/003; P1/009; P1/010

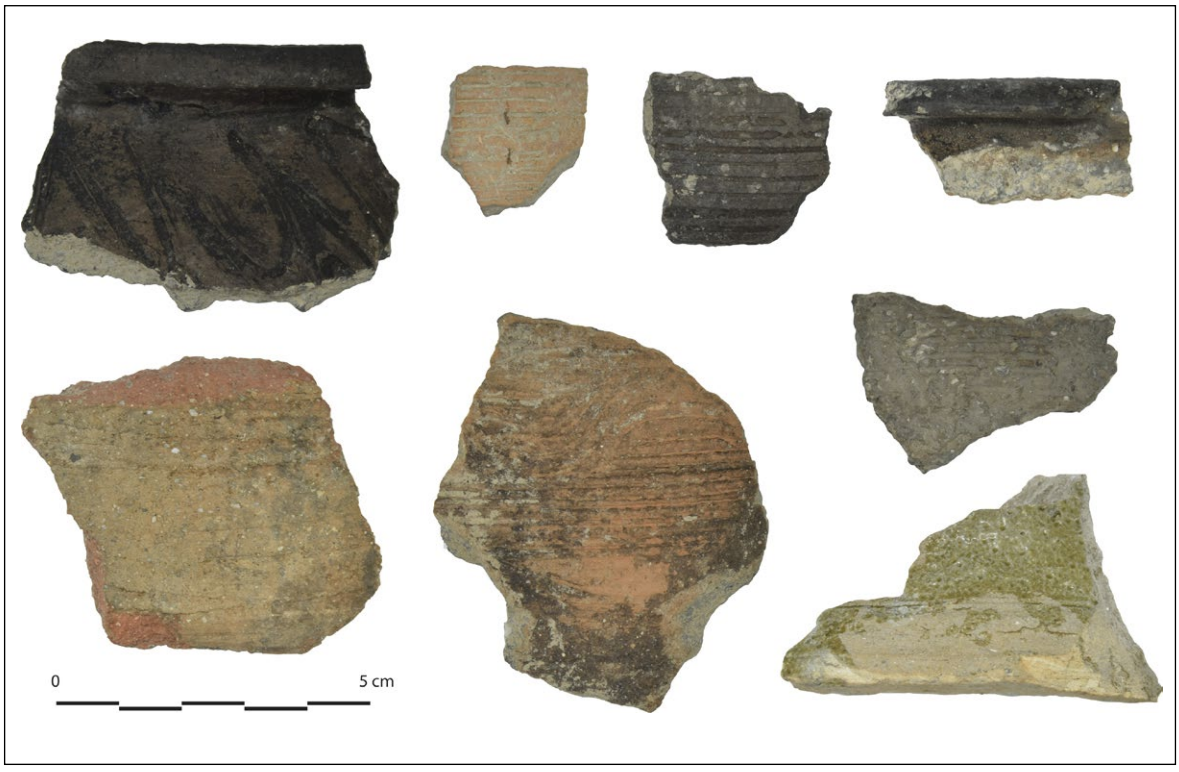


Fig. 10. Feature 1.1.7/13. Early Medieval pottery (niv. 27.35–25.17 m) (by S. Conrad)

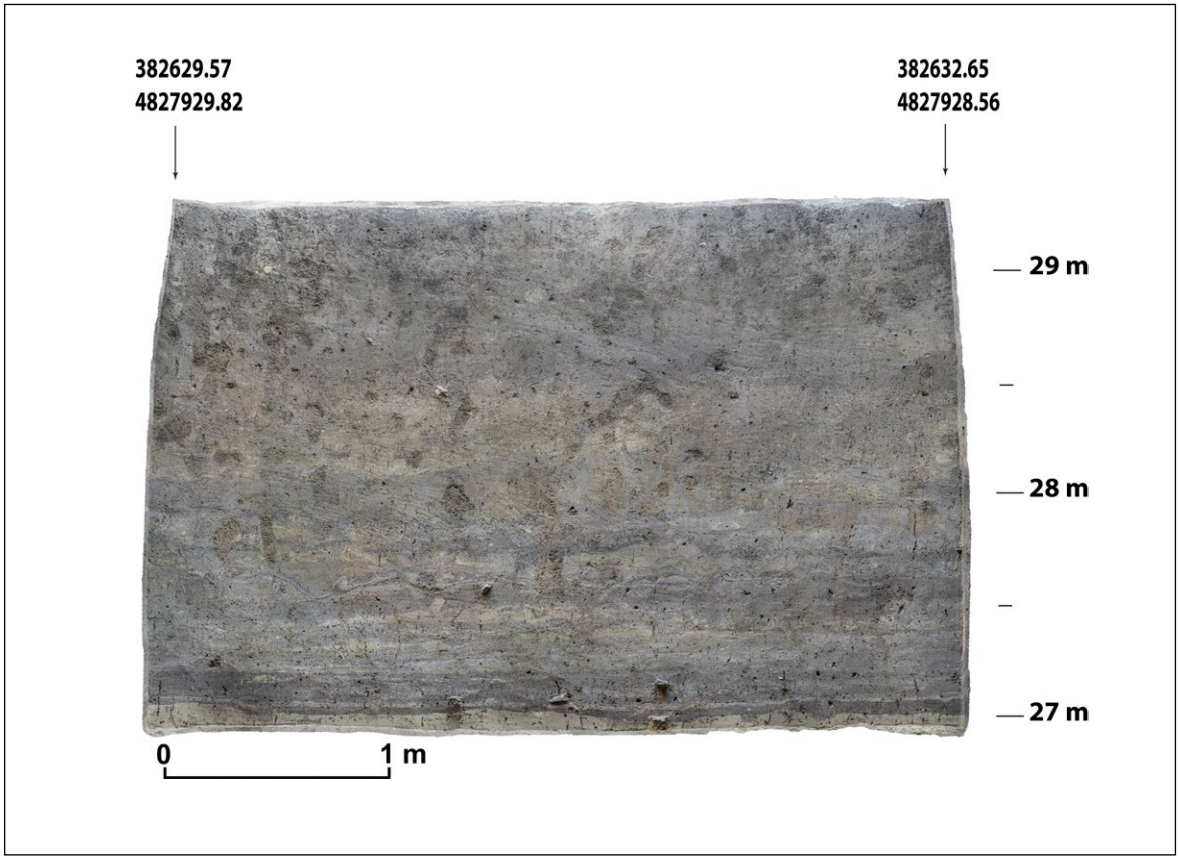


Fig. 11. Feature 1.2.5, north profile of the longitudinal section. Orthophoto obtained from a SfM model (by M. Offermann)



Fig. 12. Feature 1.2.5. Early Medieval pottery (niv. 27.35–26.94 m) (by S. Conrad)

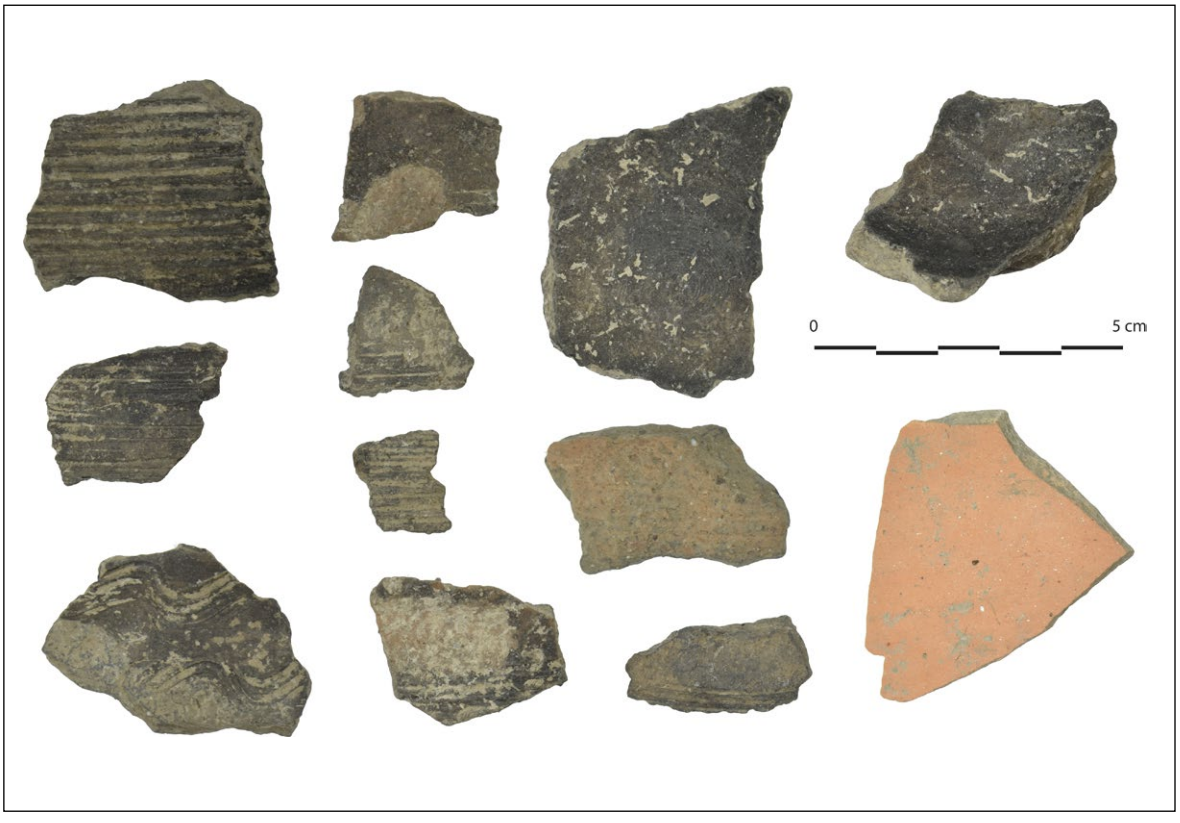


Fig. 13. Feature 1.2.5. Early Medieval pottery (niv. 28.89–27.49 m) (by S. Conrad)



Fig. 14. Trench 3.6, north profile. Stratigraphical distribution of the pottery finds (by the authors using an orthophoto obtained from a SfM model by M. Offermann). Legend: 1 – (Prehistory) / Bronze Age; 2 – (Prehistory) / Middle Bronze Age / Bronze Age; 3 – (Prehistory); 4 – (Prehistory) / Bronze Age / Late Iron Age; 5 – (Prehistory) / Bronze Age / Early Iron Age / Late Iron Age; 6 – (Prehistory) / Late Iron Age; 7 – (Prehistory) / Early Iron Age / Late Iron Age; 8 – Late Iron Age; 9 – (Prehistory); 10 – (Prehistory) / Late Bronze Age; 11 – (Prehistory) / Middle Bronze Age / Bronze Age / Late Iron Age / Late Roman period; 12 – (Prehistory) / Middle Bronze Age / Late Bronze Age / Late Iron Age /Roman period / Late Roman period; 13 – (Prehistory) / Middle Bronze Age / Late Iron Age / Late Roman period; 14 – (Prehistory) / Middle Bronze Age / Late Bronze Age / Late Iron Age / Late Roman period; 15 – Pit 3.1.1: (Prehistory) / Middle Bronze Age / Bronze Age



Fig. 15. Trench 3.6. Late Roman pottery sherds found in the upper filling of the ditch (selection) (by S. Conrad)



Fig. 16. Trench 3.6. Late Roman roof tile fragments from the upper filling of ditch (by S. Conrad)



Fig. 17. Feature 3.2.1, northeast profile. Orthophoto obtained from a SfM model (by M. Offermann)

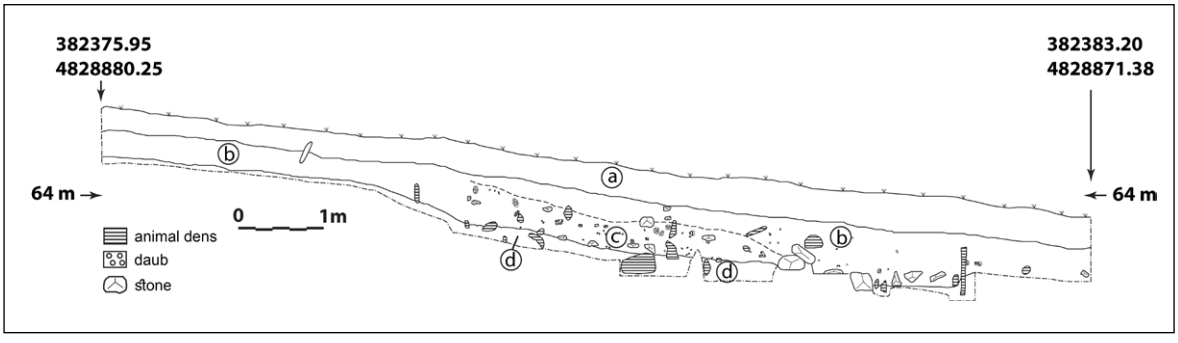


Fig. 18. Feature 3.2.1, northeast profile. Drawing (by S. Conrad and S. Roller). a – plough layer; greyish brown, humous. b – light grey, yellowish mixed, slightly humous, homogeneous; some charcoal and burnt clay pieces; single small stones. c – like b, but bigger pieces of burnt clay (house masonry) and wood; small, middle and large stones. d – natural ground (yellowish loess)

Table 10. Feature 3.2.1, pottery statistics according to the excavated layers

Position	Prehistory	LBA	BA	Catalogue
Trench 3.2				
Surface – planum 1 (ca. 64.00–63.48 m)	7			P3/024
planum 1-2 (63.48–63.36 m)	1			
planum 2-3 (63.36–63.26 m)	15	1	2	
planum 3 – end (63.26–ca. 62.90 m)	7			
Trench 3.3 + 3.3 south				
humous – planum 1 (64.36–64.08 m)	4			
planum 1-2 (64.08–63.77 m)	4			
planum 2-3 (63.77–63.38 m)	14	1		P3/025; P3/026
Trench 3.4				
Surface (ca. 64.30 m) – 64.14 m	1			
63.94–63.77 m	5			
Trench 3.5				
Surface – planum 1 (ca. 64.30 m)	1			
levelling (64.26–63.85 m)	8			

sherds were found in the layer of burnt house debris in the filling of the feature 3.2.1 (cf. the contributions by L. Vagalinski, L. Traykova, chapter 8.2.2) (fig. 17; 18). Among the sum of 71 sherds, two sherds from the Late Bronze Age and two sherds with a common date to the Bronze Age were registered (table 10). The other finds are uncharacteristic sherds of handmade pottery. The dating of the feature was primarily based on the ^{14}C data obtained from one of the few animal bones and a charcoal.

Trench 3.1., pit 3.1.1/2. During the excavations of the pit, a total of 204 ceramic fragments were recovered, the position of which was partly documented by individual measurements (table 11). Of these finds, four pieces could be assigned to the Middle Bronze Age, five to the Late Bronze Age and 10 in common to the Bronze Age. The dating of the remaining 185 prehistoric sherds could not be narrowed down due to the lack of special characteristics.

The dating of the feature to the Late Bronze Age was backed up by the ^{14}C data obtained from four animal bones (cf. the contributions by R. Krauß, chapter 9.1.1).

9.1.3.3. The pottery statistics from the excavations on site 5

Trench 5.1., feature 5.1.2. In the backfilling of the pit, in addition to pieces of charcoal and a few daub pieces, only ten relatively small pottery fragments were found (table 12; fig. 19). There are three fragments of Early Roman amphorae as well as a fragment of grey wheelmade fabric and six fragments of handmade ware in the Late Iron Age manner. Due to their small size, none of these fragments could be typologically determined.

Trench 5.1/2., feature 5.1.5. Fragments of a fruit bowl (cat. P5/014) and a large, high pot (cat. P5/015) were added as grave goods to the burial of the child on the floor of pit 5.1.5. The dating of both vessels cannot be narrowed down, but they can easily be connected to common types of the Late Iron Age handmade pottery or to the repertoire of Early Roman ceramics made in a Late Iron Age tradition.

Table 11. Feature 3.1.1/2. Pottery statistics according to excavated layers including the single finds measured. Layer a: niv. 61.68 m (planum 1) – ca. 61.40 m; layer b: ca. 61.40 m – ca. 61.25 m; layer c: ca. 61.25–60.98 m

FindID	Find No.	GPS measure (m)	Position – planum or level (m)	Layer	Prehistory	MBA	LBA	BA	Catalogue
TB18.3.1-c12			Surface – pl. 1 (61.92–61.68 m)		12				
Qu. A									
TB18.3.1-c3;c5			61.68–61.58	a	9	1		4	P3/030; P3/033; P3/044–P3/046
TB18.3.1-c1			61.58–61.48	a	22				
TB 18.3.1-m1	Find2	61.49		a				1	P3/047
TB18.3.1-c2;c4			61.48–61.38	a(-b)	4			2	P3/032; P3/042
TB18.3.1-m2	Find3	61.41		a(-b)		1			P3/029
TB18.3.1-m5	Find16	61.47		a			1		P3/027
TB18.3.1-c11			61.43–61.33	(a-)b	11				
TB18.3.1-c6			61.38–61.28	b	23			2	
TB18.3.1-m3	Find6	61.36		b	1				
TB18.3.1-m10	Find21	61.26	planum 2	b			1		P3/037
TB18.3.1-m6	Find17	61.25	planum 2	b		1			P3/028
TB18.3.1-m13	Find24	61.27	planum 2	b	1		1		P3/039
TB18.3.1-m14	Find25	61.25		b	1				
TB18.3.1-m11	Find22	61.25		b	2				
TB18.3.1-m7	Find18	61.26		b	1				
TB18.3.1-m8, m5	Find16,19	61.26		b		1			
TB18.3.1-m12	Find23	61.30		b	1				
TB18.3.1-c7			61.28–61.18	(b-)c	11				
TB18.3.1-m15	Find29	61.01		b				1	P3/040
TB18.3.1-m9	Find20	61.24		(b-)c	1				
TB18.3.1-m17	Find32	60.94		c	1				
TB18.3.1-c8			61.18–61.08	c	38			1	P3/041
TB18.3.1-m4	Find9	61.21		c	1				
TB18.3.1-m16	Find30	60.98		c	1				
TB18.3.1-c9			61.13–61.03	c	4				
TB18.3.1-c13			61.08–60.98	c	3				
Qu. B									
TB18.3.1-c15				a	12		1	2	P3/031; P3/034; P3/035; P3/038
TB18.3.1-c10; c14; c18				b	15		1		P3/036
TB18.3.1-c16; c19				c	7				

Table 12. Statistics of pottery finds from features 5.1.2, 5.1.5 and 5.1.6

Feature	Level (m)	RIP	RIP	RIP	RIP	LIA manner	LIA manner	LIA manner	LIA manner	Catalogue
		sum	fine ware	coarse	amphorae	sum	wheelmade	handmade	amphorae	
5.1.2	20.68–20.28				3		1	6		
5.1.5 (Tr. 5.2.)	21.18–20.77 (humous)		9		47**		4	29		P5/010; P5/011; P5/019; P5/024
	20.77–20.70						4	2	1	P5/013; P5/016; P5/025
	20.70–20.56		1	1	5		3	27		P5/012; P5/020–P5/023
	20.56–20.49		1		1		3	11		P5/018
	20.49–20.38							1	1	
	20.38–20.23		2					3		P5/017
	20.23–20.06							1		
5.1.5 (Tr. 5.1)	20.68–20.23		2	1			5	7		
	20.65–19.80						1	8	1	
	19.76						1			
5.1.5 grave	19.80–19.75							2*		P5/014; P5/015
5.1.6			1	1	2		5	5		P5/026
*reconstructed parts of two vessels **6 amphorae of type Šelov can be recognised										



Fig. 19. Feature 5.1.2. Pottery (niv. 20.68–20.28 m) (by S. Conrad)

The careful design and uniform surface suggest the use of the slow wheel. The relatively fine clay used in the manufacture of the pot cat. P5/015, its strong mica tempering as well as the inclined handles are unusual among the material from the sites at the Tash Bair and suggest a special manufacture or an import.

In the backfilling of pit 5.1.5 above the grave, a relatively large number of pottery fragments were found in comparison to the other two pits 5.1.2 and 5.1.6 (fig. 20; 21). The larger part comes from vessels that were made in a Late Iron Age tradition. Handmade vessels, however, take up the majority of the finds (cat. P5/016–025). Their shape and their decoration also clearly reflect the Late Iron Age tradition. The relatively carefully crafted shapes and surfaces, which require regular use of the slow potter's wheel, are often striking.

No direct parallel is known for the rim fragment of a cauldron cat. P5/025 with a faceted upper side of the rim, but it can be related to the kinked edge and body shapes of other vessel types (cat. P5/016; P5/026; cf. Върбанов 2013c, cat. 218; 222; 223; 230 pl. 5,2.6.7.14). Indeed, for some of the ceramics from the later phase of the Late Iron Age (2nd–1st century BC) and the vessels made in the local tradition from the Early Roman Imperial period (see below), a tendency towards a more pronounced structure of the vessel bodies and more sharply defined individual forms can be observed.

A wheelmade bowl fragment of grey ware cat. P4/013 has a typical rim profile for vessels of this type from Late Iron Age (2nd–1st c. BC) and the Early Roman Empire (see parallels in the catalogue).

Furthermore, a significant number of fragments of Early Imperial Roman ceramics were found (table 12; fig. 20, 21). Among them, some characteristic pieces were recovered, including the omphalos bottom of a red-clay jug with traces of red engobe (cat. P5/012) and fragments of amphorae from Heraclea Pontica (Šelov type A = Borislavova type Hr I / II) (cat. P5/010). In addition, several other wall fragments of Roman fine and coarse wares were registered.



Fig. 20. Feature 5.1.5 (trench 5.2). Pottery from the filling of the pit (selection) (niv. 20.56–20.49 m) (by S. Conrad)



Fig. 21. Feature 5.1.5 (trench 5.1). Pottery from the filling of the pit (selection) (niv. 20.70–20.56 m) (by S. Conrad)



Fig. 22. Feature 5.1.6. Pottery (selection) (by S. Conrad)

Fragments of the amphorae from the Šelov A = Borislavova type Hr I / II (cat. P5/010–011), Roman fine ware and two lamp fragments (cf. the contributions by L. Traykova, chapter 9.2.2, cat. Nos. SF 58, 59) were found in the plough horizon above, which apparently disturbed the backfill of the pit.

Trench 5.1., feature 5.1.6. During the excavation of the filling of the pit, a total of 14 ceramic fragments were found (table 12; fig. 22). Five fragments each belong to vessels of grey wheelmade and handmade fabrics in the Late Iron Age design, among them, according to shape and fabric, a bowl fragment in grey wheelmade ware cat. P5/026. However, parallel examples from Valchedram, Yakimovo and Ruse prove that the kinked vessel profile, together with the shining surface of the fabric, is common during the latest phase of the Late Iron Age and the early phase of the Roman occupation of the Lower Danube. Furthermore, two fragments each of Early Roman amphorae and fine ware were found, among them the bottom fragment of a jug with reddish brown engobe. They can be dated in the 1st c. AD.

Acknowledgements

The members of the research team accompanied the material processing with advice and technical support. With Piotr Dyczek (Warsaw) and Varbin Varbanov (Ruse) we were able to discuss in detail the ceramic finds from the Late Iron Age and Early Roman Imperial period. Judith Berning (Stuttgart) took on restoration work, including the reconstruction of vessels from the pit 5.1.5.

The large part of the handmade pottery was drawn by Achim Frey (Tübingen). Additionally, Further drawings were carried out by Doncho Karakolev (Ruse), Julia Becher, Lea Valcov and Jonas Sprißler (Tübingen). The pencil drawings were converted into Indian ink by Doncho Karakolev (Ruse). The digital processing and implementation were in the hands of Jonas Sprißler. Publications that were difficult to access were provided by Evgeniya Gencheva (Sofia) and Florian Matei-Popescu (Bucharest).

We would like to take this opportunity to thank everyone for their support.

СТАТИСТИКА НА КЕРАМИЧНИ НАХОДКИ ОТ РАЗКОПКИТЕ НА РАЗЛИЧНИ СТРУКТУРИ

Свен Конрад, Райко Краус

(Резюме)

Обект 1. Сондаж 1.2, структури 1.2.4/6 и 1.2.7/8. В къснонеолитните материали могат да се разпознаят различни културно-исторически групи. Има материал от културата Въдастра, Боянската култура, материал от българския късен неолит и отделни форми също могат да бъдат отнесени към културата Хаманджия. Всички посочени културни групи представляват регионални прояви на късния неолит на Балканите, чието точно времево отношение не може да бъде прецизно определено. Поради общото местонамиране само в рововете в момента не може да се реши дали това е географско наслагване на четирите групи на този обект, или материалите на Таш баир са отложени хронологично един след друг. Забележителни са няколко находки от късния халколит в запълването на рова. Поне една широка купа може да бъде причислена със сигурност към етапа Коджадермен-Гумелница-Караново VI от периода на халколита. Тези находки са единственото доказателство за селищна дейност на Таш баир в средата на V хил. пр. Хр.

Обект 1. Сондаж 1.1-W/E, структура 1.1.6/15. Праисторически фрагменти (неолит, бронзова епоха, ранна желязна епоха) съставляват най-голям дял от керамиката, открита в двете части на този ров на обект 1 (вж. приноса на Л. Вагалински и др., глава 8.3.1), в общия им брой от 850 броя (91,2%). По-специално сред тях има впечатляващ набор от къснонеолитни находки. Големият им брой се дължи на дългото и интензивно обитаване на мястото, особено през късния неолит. Изглежда, ядрото на селището е в непосредствена близост. Докато няколкото римски (3) и ранносредновековни (4) отделни чирепи от горните слоеве в структурата 1.1.6 са много вероятно попаднали вторично чрез животни, фрагментите от късната желязна епоха са разпръснати в почти целия пълнеж на структурата. С общо 68 броя (8%), включително 22 броя сиви, изработени на бързо колело, 45 броя фрагменти на ръчно изработени съдове и един фрагмент от вносна амфора, техният дял е достатъчно значим за датиране.

Обект 1. Сондаж 1.1-W/E (структура 1.1.7/13) и сондаж 1.2 (структура 1.2.5). Статистиката на керамичните находки от северния край на ранносредновековния ров при портата (структура 1.1.7/13) и югозападния вътрешен ров на земното укрепление (обозначение 1.2.5) на обект 1 доказват, че ранносредновековната керамика и в двата случая представлява най-младата и следователно хронологично релевантна група находки. Но отново в тези случаи повечето от находките са от праисторически периоди, попаднали в землените валове и в рововете при тяхното засипване.

Обект 3. Вътрешен ров в сондаж 3.1.6. Разпределението на находките в запълването на рова показва, че след построяването и функционирането му през средната бронзова епоха той е използван в някои следващи периоди. В по-долните слоеве има парчета от бронзовата епоха, някои от които могат да бъдат отнесени към средната и късната бронзова епоха. Горните пластове и съответните находки показват, че е използван през ранната и късната желязна епоха. Слоят на хумусово запълване над ниво на използване показва, че последното функциониране е през късноримския период.

Обект 3. Сондажи 3.2 – 5, структура 3.2.1. Освен бронзовия нож (кат. № SF 53; вж. приноса на Р. Краус, Е. Перницка, глава 10.1) и големи парчета мазилки, в слоя от изгорели жилища са открити много малко керамични парчета в попълването на структура 3.2.1 (вж. приноса на Л. Вагалински, Л. Трайкова, глава 8.2.2), които могат да се датират. Сред сбора от 71 фрагменти са регистрирани два фрагмента от късната бронзова епоха и два фрагмента с обща датировка към бронзовата епоха.

Обект 3. Сондаж 3.1, структура 3.1.1/2. При разкопките на яма 3.1.1/2 са открити общо 204 керамични фрагмента, чието положение е частично документирано чрез индивидуални измервания (table 11). От тези находки четири чирепа могат да бъдат отнесени към средната бронзова епоха, пет – към късната бронзова епоха и 10 – най-общо към бронзовата епоха. Датировката на останалите 185 праисторически фрагменти не може да бъде стеснена поради липсата на специфични белези. Датирането на ямата към късната бронзова епоха е подкрепено от данните от ^{14}C, получени от една от малкото животински кости и въглен.

Обект 5. Сондаж 5.1, структури 5.1.2 и 5.1.6. В засипването на ямите освен парчета въглен и няколко парчета мазилки са открити само 10, съответно 14 сравнително малки керамични фрагменти (table 12; fig. 19). Има три фрагмента от ранноримски амфори и други съдове, както и фрагменти, характерни за късната желязна епоха керамични групи – сива керамика, изработена на колело и съдове, оформени на ръка.

Обект 5. Сондаж 5.1/2, структура 5.1.5. Фрагменти от фруктиера (кат. № P5/014) и голямо високо гърне (кат. № P5/015) са сложени като гробен дар в погребението на дете на дъното на яма 5.1.5. Датировката на двата съда не може да бъде стеснена, но те могат лесно да се свържат с често срещаните типове ръчно изработена керамика от късната желязна епоха или с репертоара от локална ранноримска керамика, изработена в традиция от късната желязна епоха. Заради внимателното изработване и равномерната повърхност може да се предполага използване на бавно колело. Сравнително фината глина, използвана при производството на съда, кат. № P5/015, силният примес на слюда, както и наклонените дръжки са необичайни за керамичния комплекс от обектите на Таш баир и предполагат специална изработка или внос. В запълването на яма 5.1.5 над гроба са открити фрагменти от късната желязна епоха и много ранноримски чирепи. Съответно трите ями 5.1.2, 5.1.5 и 5.1.6 могат да бъдат датирани заедно в средата или втората половина на I в. Погребението в яма 5.1.5 също може да бъде включено в тази времева рамка.

Table 13. Radiocarbon data from northern Bulgaria (radiocarbon data from Tash Bair is between Nos. 158–182)

No.	Site	Lab code	^{14}C-age [BP]	Material	calBC 2σ	δ^{13}C [‰PDB]	Phase/ context	Depth	Comment	Source
1	Banyata	Bln-202	4242 ± 100	---	3120–2520	n.d.				Görsdorf, Bojadžiev 1996
2	Banyata	Bln-405	4075 ± 100	---	2960–2360	n.d.				Görsdorf, Bojadžiev 1996
3	Borovo	Bln-1763	2620 ± 40	charcoal	860–740	n.d.	tumulus III			Görsdorf, Bojadžiev 1996
4	Brankovtsi	Poz-120640	6410 ± 40	charcoal (Cornus sp.)	5500–5300		36.4.pit.coal2			Kecheva et al. 2023; site info – Кечева et al. 2020; sample provided by N. Kecheva
5	Brankovtsi	Poz-120639	6390 ± 40	charcoal (Cornus sp.)	5510–5270		36.4.5MP.flotation			Kecheva et al. 2023; site info – Кечева et al. 2020; sample provided by N. Kecheva
6	Brankovtsi	Poz-120752	6260 ± 40	charcoal (Cornus sp.)	5340–5140		TR.22.3MP_up2			Kecheva et al. 2023; site info – Кечева et al. 2020; sample provided by N. Kecheva
7	Brankovtsi	Poz-120751	6240 ± 40	charcoal (Salix sp.)	5360–5040		TR.22.3MP_down			Kecheva et al. 2023; site info – Кечева et al. 2020; sample provided by N. Kecheva
8	Brankovtsi	Poz-120641	6210 ± 40	charcoal (Cornus sp.)	5320–5000		TR.22.3MP_up1			Kecheva et al. 2023; site info – Кечева et al. 2020; sample provided by N. Kecheva
9	Durankulak	Bln-2122	5700 ± 50	---	4690–4410	n.d.				Görsdorf, Bojadžiev 1996
10	Durankulak	Bln-2111	5495 ± 60	charcoal	4490–4210	n.d.				Görsdorf, Bojadžiev 1996
11	Durankulak	Bln-2121	5475 ± 50	charcoal	4420–4220	n.d.				Görsdorf, Bojadžiev 1996
12	Durankulak	Bln-3532	3910 ± 70	charcoal & charred sediment	2580–2180	n.d.	house 15			Görsdorf, Bojadžiev 1996
13	Durankulak	Bln-3529	3490 ± 60	charcoal & charred sediment	1950–1670	n.d.	house 15			Görsdorf, Bojadžiev 1996
14	Durankulak	Bln-3528	3400 ± 60	charcoal & charred sediment	1860–1540	n.d.	house 15			Görsdorf, Bojadžiev 1996
15	Durankulak	Bln-3530	3160 ± 60	charcoal & charred sediment	1550–1310	n.d.	house 15			Görsdorf, Bojadžiev 1996
16	Durankulak	Bln-2570	2960 ± 60	charcoal, detritus & sand	1380–980	n.d.	house IVa			Görsdorf, Bojadžiev 1996
17	Durankulak	Bln-2571	2930 ± 50	charcoal, detritus & sand	1300–980	n.d.	house 1			Görsdorf, Bojadžiev 1996

No.	Site	Lab code	^{14}C-age [BP]	Material	calBC 2σ	δ^{13}C [‰PDB]	Phase/ context	Depth	Comment	Source
18	Durankulak	Bln-2569	2850 ± 50	charcoal, detritus & sand	1160–880	n.d.	house Vb			Görsdorf, Bojadžiev 1996
19	Dzhulyunitsa	OxA-24937	7588 ± 37	bone (Sus)	6500–6380	-20.24	Profile Sond. 18/21, Dzh I (spit 7)	116.11	radiometric outlier	Krauß et al. 2014
20	Dzhulyunitsa	KN-5776	7400 ± 40	charcoal	6410–6170	n.d.				Provided by Bernhard Weninger (Cologne), Krauß (in press)-a; sample provided by N. Elenski
21	Dzhulyunitsa	KN-5777	7225 ± 45	charcoal	6250–5970	n.d.				Provided by Bernhard Weninger (Cologne), Krauß (in press)-a; sample provided by N. Elenski
22	Dzhulyunitsa	OxA-24934	7195 ± 37	bone (Bos)	6110–5990	-19.73	Planum in front of Profile Sond. 18/21, Dzh I	115.70		Krauß et al. 2014
23	Dzhulyunitsa	OxA-24981	7185 ± 40	bone (Bos)	6110–5990	-20.76	Profile Sond. 18/21, Dzh II (spit 1)	116.41		Krauß et al. 2014
24	Dzhulyunitsa	OxA-24939	7171 ± 36	bone (Ovis)	6090–5970	-19.59	Profile Sond. 18/21, Dzh II (spit 2)	116.26		Krauß et al. 2014
25	Dzhulyunitsa	OxA-24979	7145 ± 38	bone (Bos)	6080–5960	-20.26	Planum in front of Profile Sond. 18/21, Dzh I	115.96		Krauß et al. 2014
26	Dzhulyunitsa	OxA-25047	7140 ± 40	charcoal	6080–5960	-24.38	Profile Sond. 18/21, Dzh III	117.01		Krauß et al. 2014
27	Dzhulyunitsa	OxA-24977	7136 ± 40	bone (Bos)	6070–5950	-20.11	Profile Sond. 18/21, Dzh II (spit 1)	116.41		Krauß et al. 2014
28	Dzhulyunitsa	OxA-24938	7134 ± 35	bone (Bos)	6070–5950	-19.20	Profile Sond. 18/21, Dzh I (spit 4)	116.06		Krauß et al. 2014
29	Dzhulyunitsa	OxA-25044	7095 ± 40	charcoal	6070–5870	-25.87	Planum in front of Profile Sond. 18/21, Dzh I	116.05		Krauß et al. 2014
30	Dzhulyunitsa	OxA-25042	7095 ± 40	charcoal	6070–5870	-24.29	Planum in front of Profile Sond. 18/21, Dzh I	115.76		Krauß et al. 2014
31	Dzhulyunitsa	KN-5747	7094 ± 47	charcoal	6070–5870	n.d.				Provided by Bernhard Weninger (Cologne), Krauß (in press)-a; sample provided by N. Elenski

No.	Site	Lab code	^{14}C-age [BP]	Material	calBC 2σ	δ^{13}C [‰PDB]	Phase/ context	Depth	Comment	Source
32	Dzhulyunitsa	KN-5775	7085 ± 40	charcoal	6040–5880	n.d.				Provided by Bernhard Weninger (Cologne), Krauß (in press)-a; sample provided by N. Elenski
33	Dzhulyunitsa	OxA-25033	7084 ± 36	bone	6040–5880	-20.28	Planum in front of Profile Sond. 18/21, Dzh I	115.92		Krauß et al. 2014
34	Dzhulyunitsa	OxA-24933	7084 ± 36	bone	6040–5880	-20.28	DZH 21-116			Provided by Bernhard Weninger (Cologne), Krauß (in press)-a; sample provided by N. Elenski
35	Dzhulyunitsa	OxA-24936	7083 ± 36	bone	6040–5880	-19.09	Profile Sond. 18/21, Dzh I (spit 13)	115.40		Krauß et al. 2014
36	Dzhulyunitsa	OxA-32777	7075 ± 37	bone (human)	6030–5870	n.d.	DZHU 10–I0706			Provided by Bernhard Weninger (Cologne), Krauß (in press)-a; sample provided by N. Elenski
37	Dzhulyunitsa	OxA-24931	7066 ± 38	bone (Ovis)	6030–5870	-20.00	Profile Sond. 18/21, Dzh I (spit 3)	116.16		Krauß et al. 2014
38	Dzhulyunitsa	OxA-25043	7055 ± 40	charcoal	6020–5860	-25.76	Profile Sond. 18/21, Dzh II (spit 1)	116.41		Krauß et al. 2014
39	Dzhulyunitsa	OxA-24978	7054 ± 39	bone (Ovis)	6020–5860	-20.44	Profile Sond. 18/21, Dzh II (spit 2)	116.26		Krauß et al. 2014
40	Dzhulyunitsa	OxA-24932	7053 ± 35	bone (Ovis)	6020–5860	-19.93	Profile Sond. 18/21, Dzh I (spit 3)	116.16		Krauß et al. 2014
41	Dzhulyunitsa	KN-5774	7050 ± 50	charcoal	6030–5830	n.d.				Provided by Bernhard Weninger (Cologne), Krauß (in press)-a; sample provided by N. Elenski
42	Dzhulyunitsa	OxA-25040	7049 ± 39	charcoal	6020–5860	-24.83	Profile Sond. 18/21, Dzh I (spit 3)	116.16		Krauß et al. 2014
43	Dzhulyunitsa	OxA-24935	7026 ± 35	bone (Bos)	6020–5820	-20.46	Profile Sond. 18/21, Dzh II	116.56		Krauß et al. 2014
44	Dzhulyunitsa	OxA-24980	7011 ± 38	bone (Bos)	6030–5790	-19.97	Profile Sond. 18/21, Dzh I (spit 8)	116.05		Krauß et al. 2014
45	Dzhulyunitsa	OxA-25046	6950 ± 40	charcoal	5930–5730	-25.59	Profile Sond. 18/21, Dzh II	116.20		Krauß et al. 2014
46	Dzhulyunitsa	OxA-25045	6686 ± 39	charcoal	5680–5520	-25.35	Profile Sond. 18/21, Dzh IV	117.31		Krauß et al. 2014

No.	Site	Lab code	^{14}C-age [BP]	Material	calBC 2σ	δ^{13}C [‰PDB]	Phase/ context	Depth	Comment	Source
47	Dzhulyunitsa	PSUAMS-1836	6615 ± 30	bone (human)	5640–5480	n.d.	No7 (Early Neolithic)–I2521			Provided by Bernhard Weninger (Cologne), Krauß (in press)-a; sample provided by N. Elenski
48	Galatin	hv-12756	5090 ± 280	---	4510–3270	n.d.				Provided by Bernhard Weninger (Cologne), Krauß (in press)-a
49	Galatin	Bln-3316	4480 ± 50	---	3410–2970	n.d.				Görsdorf, Bojadžiev 1996
50	Galatin	Bln-3317	4360 ± 50	---	3130–2850	n.d.				Görsdorf, Bojadžiev 1996
51	Golyamata Peshtera	Bln-2112	5900 ± 70	---	4940–4620	n.d.				Görsdorf, Bojadžiev 1996
52	Golyamo Delchevo	Bln-923	5970 ± 100	charcoal	5110–4630	n.d.	Hor. 5, Qu. 326	3.29		Görsdorf, Bojadžiev 1996
53	Golyamo Delchevo	Bln-925	5940 ± 100	charcoal	5070–4590	n.d.	Hor. 3, Qu. 563	4.08		Görsdorf, Bojadžiev 1996
54	Golyamo Delchevo	Bln-922	5930 ± 120	charcoal	5120–4520	n.d.	Hor. 7, Qu. 954	3.92		Görsdorf, Bojadžiev 1996
55	Golyamo Delchevo	Bln-924	5840 ± 100	charcoal	4940–4460	n.d.	Hor. 4, Qu. 431	3.87	same like Bln-966	Görsdorf, Bojadžiev 1996
56	Golyamo Delchevo	Bln-966	5780 ± 100	charcoal	4850–4410	n.d.	Hor. 4, Qu. 431	3.87	same like Bln-924	Görsdorf, Bojadžiev 1996
57	Golyamo Delchevo	Bln-920A	5640 ± 100	charcoal	4720–4280	n.d.	Hor. 12, Qu. 462	1.19	same like Bln-920	Görsdorf, Bojadžiev 1996
58	Golyamo Delchevo	Bln-920	5590 ± 100	charcoal	4650–4250	n.d.	Hor. 12, Qu. 462	1.19	same like Bln-920A	Görsdorf, Bojadžiev 1996
59	Golyamo Delchevo	Bln-921	5515 ± 100	charcoal	4560–4160	n.d.	Hor. 9, Qu. 431	2.90		Görsdorf, Bojadžiev 1996
60	Hotnitsa-Orlovka	KN-5769	6370 ± 40	charcoal	5490–5250	-25.72	Sond. 3, Grube 1, unterstes Niveau	k.A.		Provided by Bernhard Weninger (Cologne), Krauß (in press)-a; sample provided by V. Ilcheva
61	Hotnitsa-Orlovka	KN-5768	6305 ± 35	charcoal	5360–5200	-25.67	Sond. 1, Qu. 23, Grube 3 neben Südprofil	1.92		Provided by Bernhard Weninger (Cologne), Krauß (in press)-a; sample provided by V. Ilcheva
62	Hotnitsa-Orlovka	KN-5766	6195 ± 40	charcoal	5280–5000	-25.53	Sond. 1, Qu. 23, Grube 3 neben Südprofil	1.60		Provided by Bernhard Weninger (Cologne), Krauß (in press)-a; sample provided by V. Ilcheva
63	Hotnitsa-Orlovka	KN-5767	6055 ± 40	charcoal	5070–4830	-26.35	Sond. 1, Qu. 23, Grube 3 neben Südprofil	1.60		Provided by Bernhard Weninger (Cologne), Krauß (in press)-a; sample provided by V. Ilcheva
64	Hotnitsa-Vodapada	Bln-3682	5110 ± 50	---	4030–3750	n.d.				Görsdorf, Bojadžiev 1996
65	Hotnitsa-Vodapada	Bln-3683	4950 ± 60	charcoal	3910–3590	n.d.				Görsdorf, Bojadžiev 1996

No.	Site	Lab code	^{14}C-age [BP]	Material	calBC 2σ	δ^{13}C [‰PDB]	Phase/ context	Depth	Comment	Source
66	Hotnitsa-Vodapada	Bln-3684	4950 ± 60	charcoal	3910–3590	n.d.				Görsdorf, Bojadžiev 1996
67	Hotnitsa-Vodapada	Bln-3685	4890 ± 60	charcoal	3810–3570	n.d.				Görsdorf, Bojadžiev 1996
68	Hotnitsa-Vodapada	Bln-3680	4830 ± 60	charcoal	3740–3460	n.d.				Görsdorf, Bojadžiev 1996
69	Hotnitsa-Vodapada	Bln-3681	4830 ± 60	charcoal	3740–3460	n.d.				Görsdorf, Bojadžiev 1996
70	Kachitsa	Bln-1686	6190 ± 50	charcoal	5280–5000	n.d.	Grube, Hor. 3, Sekt. 8	0.80	Plateau in cal curve	Görsdorf, Bojadžiev 1996
71	Kachitsa	Bln-1687	6170 ± 55	charcoal	5280–4960	n.d.	Grube, Hor. 3, Sekt. 8	0.80	Plateau in cal curve	Görsdorf, Bojadžiev 1996
72	Kachitsa	Bln-1685	6160 ± 55	charcoal	5270–4950	n.d.	Grube, Hor. 3, Sekt. 8	1,20-1,30	Plateau in cal curve	Görsdorf, Bojadžiev 1996
73	Koprivets	Poz-63237	7090 ± 80	bone (radius dist., Bos)	6110–5790	n.d.	trench Я1	-1.35	1% Coll	Marinova, Krauß 2014
74	Koprivets	Poz-63236	7020 ± 50	bone (humerus, dist. Bos taurus)	6030–5790	n.d.	trench Я1	-1.30	0,4% Coll	Marinova, Krauß 2014
75	Koprivets	Poz-63238	6930 ± 50	bone (radius prox., Bos)	5930–5690	n.d.	trench Я1	-1.30	0,7 Coll	Marinova, Krauß 2014
76	Krivodol	Bln-2114	5445 ± 45	---	4380–4220	n.d.				Görsdorf, Bojadžiev 1996
77	Krivodol	Bln-2113	5295 ± 40	charcoal	4270–3990	n.d.				Görsdorf, Bojadžiev 1996
78	Krivodol	Bln-2115	5295 ± 45	seeds	4290–3970	n.d.				Görsdorf, Bojadžiev 1996
79	Ohoden	Poz-88724	8010 ± 40	Bone (Cervus elaphus)	7110–6750		Mesolithic pit, scull 3			Unpublished; site info – Ганецовски et al. 2020; sample provided by G. Ganetsovski
80	Ohoden	Poz-88723	7840 ± 40	Bone (Cervus elaphus)	6780–6580		Mesolithic pit, scull 2			Unpublished; site info – Ганецовски et al. 2020; sample provided by G. Ganetsovski
81	Ohoden	Poz-82519	7650 ± 50	Bone (Cervus elaphus)	6610–6410		Mesolithic pit, scull 1			Unpublished; site info – Ганецовски et al. 2020; sample provided by G. Ganetsovski
82	Ohoden	KN-5655	6830 ± 45	charcoal	5790–5630	n.d.	Struktur 1	k.A.		Ганецовски 2009
83	Ohoden	KN-5704	6770 ± 50	charcoal	5750–5590	-25.33	Westprofil M13	k.A.		Provided by Bernhard Weninger (Cologne), Krauß (in press)-a; sample provided by G. Ganetsovski
84	Ohoden	KN-5703	6675 ± 35	charcoal	5650–5530	-24.50	Eingrabung M13,4	1.00		Provided by Bernhard Weninger (Cologne), Krauß (in press)-a; sample provided by G. Ganetsovski

No.	Site	Lab code	^{14}C-age [BP]	Material	calBC 2σ	δ^{13}C [‰PDB]	Phase/ context	Depth	Comment	Source
85	Omurtag	hv-12378	5575 ± 115	0.00	4650–4210	n.d.				Provided by Bernhard Weninger (Cologne), Krauß (in press)-a
86	Omurtag	hv-12379	5530 ± 185	0.00	4800–3920	n.d.				Provided by Bernhard Weninger (Cologne), Krauß (in press)-a
87	Ovcharovo-Gorata	Poz-18480	6900 ± 40	bone (Bos)	5880–5680	-21.3	Hor. IV, big pit in the east		0,8% Coll	Krauß 2014
88	Ovcharovo-Gorata	Poz-16984	6890 ± 40	bone (Bos)	5880–5680	-13.1	Hor. I, Qu. Ж7	-0.1	4,1% Coll	Krauß 2014
89	Ovcharovo-Gorata	Poz-16985	6890 ± 40	bone (Ovis/ Capra)	5880–5680	-13.1	Hor. I, Qu. M6	-0.2	2,5% Coll	Krauß 2014
90	Ovcharovo-Gorata	Poz-18491	6810 ± 40	bone	5750–5630	-19	Hor. II, Qu. Г (N 4,63/O 1,21)	-0.15	11,2% Coll	Krauß 2014
91	Ovcharovo-Gorata	Poz-18486	6800 ± 40	bone	5750–5630	-19.9	Hor. I, Qu. 63 (N 4,10/O 2,40)		0,5% Coll	Krauß 2014
92	Ovcharovo-Gorata	Poz-18490	6780 ± 40	bone	5740–5620	-18.2	Hor. III, Qu. 115 (N 0,80/O 2,40)	-1.3	9,5% Coll	Krauß 2014
93	Ovcharovo-Gorata	Poz-18483	6750 ± 40	bone	5740–5580	-22.2	Hor. II, Qu. M1 (N 1,20/O 3,80)	-0.1	0,4% Coll	Krauß 2014
94	Ovcharovo-Gorata	Poz-18489	6750 ± 40	bone (Bos)	5740–5580	-16.9	Qu. 62/2 (N 0,70/O 1,90)		6,2% Coll	Krauß 2014
95	Ovcharovo-Gorata	Poz-18494	6690 ± 40	bone (Bos/ Cervus)	5680–5520	-13.8	Hor. IV, Qu. 30, house pit	-0.2	6,6% Coll	Krauß 2014
96	Ovcharovo-Gorata	Bln-1544	6688 ± 60	charcoal	5700–5500	n.d.	Hor. I		same like Bln-1620	Görsdorf, Bojadžiev 1996
97	Ovcharovo-Gorata	Poz-18493	6670 ± 40	bone (Bos)	5670–5510	-19.9	Hor. I, Qu. 61/3 (N 4,30/O 1,25) pit	-0.3	5,3% Coll	Krauß 2014
98	Ovcharovo-Gorata	Poz-18487	6660 ± 40	bone (Ovis/ Capra)	5660–5500	-18.9	Hor. IV, Qu. 24, Sondage	-0.2	0,6% Coll	Krauß 2014
99	Ovcharovo-Gorata	Poz-18484	6640 ± 40	bone (Bos)	5650–5490	-20.6	Hor. III, Qu. 104 (N 0,30/O 2,80)	-0.1	0,5% Coll	Krauß 2014
100	Ovcharovo-Gorata	Bln-2032	6555 ± 70	charcoal and ashes	5640–5400	n.d.	Hor. III, Qu. 33	-0.26	high ash content	Görsdorf, Bojadžiev 1996
101	Ovcharovo-Gorata	Poz-16986	6500 ± 40	bone (Ovis/ Capra)	5550–5350	-14.1	Hor. III, Qu. 115/125	-1.3	2,2% Coll	Krauß 2014
102	Ovcharovo-Gorata	Bln-1620	6463 ± 50	charcoal	5520–5320	n.d.	Hor. I		same like Bln-1544	Görsdorf, Bojadžiev 1996

No.	Site	Lab code	^{14}C-age [BP]	Material	calBC 2σ	δ^{13}C [‰PDB]	Phase/ context	Depth	Comment	Source
103	Ovcharovo-Gorata	Bln-2030	6125 ± 45	charcoal and ashes	5270–4910	n.d.	Hor. III, Qu. 61, pit	-0.6	to young, high ash content	Görsdorf, Bojadžiev 1996
104	Ovcharovo-Gorata	Bln-2031	5440 ± 50	charcoal and ashes	4370–4210	n.d.	Hor. III, Qu. 61, pit	-0.3	to young, high ash content	Görsdorf, Bojadžiev 1996
105	Ovcharovo-Platoto	Bln-1356	6480 ± 60	---	5550–5310	n.d.	Pit, layer I	k.A.		Görsdorf, Bojadžiev 1996
106	Ovcharovo-Platoto 2	Bln-1547	5140 ± 60	charcoal	4100–3740	n.d.				Görsdorf, Bojadžiev 1996
107	Ovcharovo-Platoto 2	Bln-1510	5024 ± 60	charcoal	4010–3650	n.d.				Görsdorf, Bojadžiev 1996
108	Ovcharovo-Platoto 2	Bln-1511	4885 ± 80	charcoal	3870–3470	n.d.				Görsdorf, Bojadžiev 1996
109	Petko Karavelovo	KN-5770	5980 ± 30	charcoal	4970–4770	-25.21	Sekt. N, Pfostenloch von Haus 1	k.A.		Provided by Bernhard Weninger (Cologne), Krauß (in press)-a; sample provided by A. Chohadzhiev
110	Petko Karavelovo	KN-5772	5900 ± 45	charcoal	4870–4670	n.d.	Sekt. N, Pfostenloch von Haus 1	k.A.		Provided by Bernhard Weninger (Cologne), Krauß (in press)-a; sample provided by A. Chohadzhiev
111	Polyanitsa	Bln-1496	6396 ± 60	charcoal and soil	5500–5260	n.d.	oven 71/2, Hor. 7	2.35	old wood effect	Görsdorf, Bojadžiev 1996
112	Polyanitsa	Bln-1495	6290 ± 60	charcoal and sand	5400–5120	n.d.	Obj. 14/13, Hor. 7	2.94	old wood effect	Görsdorf, Bojadžiev 1996
113	Polyanitsa	Bln-1492	3240 ± 80	charcoal and soil	1710–1350	n.d.	fireplace, Hor. 7	k.A.	radiometric outlier	Görsdorf, Bojadžiev 1996
114	Polyanitsa-Platoto	Bln-1571	7535 ± 80	ceramic, organic temper	6530–6210	n.d.	Hor. 1, Qu. 49	-0.40	fossil organic	Görsdorf, Bojadžiev 1996
115	Polyanitsa-Platoto	Bln-1613	7380 ± 60	ceramic, organic temper	6430–6070	n.d.	Hor. 1, Qu. 153	-0.40	fossil organic	Görsdorf, Bojadžiev 1996
116	Polyanitsa-Platoto	Bln-1613A	7275 ± 60	ceramic, organic temper	6260–6020	n.d.	Hor. 1, Qu. 153	-0.40	fossil organic	Görsdorf, Bojadžiev 1996
117	Polyanitsa-Platoto	Bln-1512	7140 ± 80	ceramic, organic temper	6170–5850	n.d.	Hor. 1, Qu. 153	-0.40		Görsdorf, Bojadžiev 1996
118	Povelyanovo	Bln-1141	5595 ± 100	wood	4650–4250	n.d.				Görsdorf, Bojadžiev 1996
119	Povelyanovo	Bln-1140	5520 ± 100	wood	4560–4160	n.d.				Görsdorf, Bojadžiev 1996
120	Provadia	Prov 01	6796 ± 43	---	5750–5630					Provided by Bernhard Weninger (Cologne), Krauß (in press)-a; sample provided by V. Nikolov
121	Provadia	Prov 11	6503 ± 44	---	5550–5350					Provided by Bernhard Weninger (Cologne), Krauß (in press)-a; sample provided by V. Nikolov

No.	Site	Lab code	^{14}C-age [BP]	Material	calBC 2σ	δ^{13}C [‰PDB]	Phase/ context	Depth	Comment	Source
122	Provadia	Prov 13	6432 ± 39	---	5510–5310					Provided by Bernhard Weninger (Cologne), Krauß (in press)-a; sample provided by V. Nikolov
123	Provadia	Prov 12	6365 ± 40	---	5490–5250					Provided by Bernhard Weninger (Cologne), Krauß (in press)-a; sample provided by V. Nikolov
124	Provadia	Prov 03	6248 ± 42	---	5370–5050					Provided by Bernhard Weninger (Cologne), Krauß (in press)-a; sample provided by V. Nikolov
125	Provadia	Prov 10	5849 ± 39	---	4810–4610					Provided by Bernhard Weninger (Cologne), Krauß (in press)-a; sample provided by V. Nikolov
126	Provadia	Prov 17	5841 ± 44	---	4820–4580					Provided by Bernhard Weninger (Cologne), Krauß (in press)-a; sample provided by V. Nikolov
127	Provadia	Prov 09	5838 ± 41	---	4820–4580					Provided by Bernhard Weninger (Cologne), Krauß (in press)-a; sample provided by V. Nikolov
128	Provadia	Prov 06	5830 ± 39	---	4800–4560					Provided by Bernhard Weninger (Cologne), Krauß (in press)-a; sample provided by V. Nikolov
129	Provadia	Prov 08	5795 ± 42	---	4760–4520					Provided by Bernhard Weninger (Cologne), Krauß (in press)-a; sample provided by V. Nikolov
130	Provadia	Prov 15	5785 ± 43	---	4750–4510					Provided by Bernhard Weninger (Cologne), Krauß (in press)-a; sample provided by V. Nikolov
131	Provadia	Prov 07	5781 ± 41	---	4750–4510					Provided by Bernhard Weninger (Cologne), Krauß (in press)-a; sample provided by V. Nikolov
132	Provadia	Prov 05	5779 ± 42	---	4750–4510					Provided by Bernhard Weninger (Cologne), Krauß (in press)-a; sample provided by V. Nikolov
133	Provadia	Prov 02	5765 ± 42	---	4740–4500					Provided by Bernhard Weninger (Cologne), Krauß (in press)-a; sample provided by V. Nikolov

No.	Site	Lab code	^{14}C-age [BP]	Material	calBC 2σ	δ^{13}C [‰PDB]	Phase/ context	Depth	Comment	Source
134	Provadia	Prov 16	5702 ± 42	---	4670–4430					Provided by Bernhard Weninger (Cologne), Krauß (in press)-a; sample provided by V. Nikolov
135	Provadia	Prov 18	5691 ± 44	---	4650–4410					Provided by Bernhard Weninger (Cologne), Krauß (in press)-a; sample provided by V. Nikolov
136	Provadia	Prov 04	5617 ± 43	---	4540–4340					Provided by Bernhard Weninger (Cologne), Krauß (in press)-a; sample provided by V. Nikolov
137	Provadia	Prov 14	5595 ± 42	---	4520–4320					Provided by Bernhard Weninger (Cologne), Krauß (in press)-a; sample provided by V. Nikolov
138	Samovodene	KIA-42166	6960 ± 30	bone (Bos)	5940–5740	-19.83	Horizont B1	k.A.	radiometric outlier	Scheu 2012
139	Samovodene	KIA-42165	6635 ± 30	bone (Bos)	5630–5510	-20.84	Horizont A	k.A.		Scheu 2012
140	Samovodene	KIA-42168	6545 ± 30	bone (Bos)	5560–5440	-20.88	Horizont B	k.A.		Scheu 2012
141	Samovodene	KIA-42167	6475 ± 25	bone (Bos)	5510–5350	-19.94	Horizont B1/B2	k.A.		Scheu 2012
142	Smyadovo	Bln-1667	5840 ± 50	---	4830–4550	n.d.				Görsdorf, Bojadžiev 1996
143	Smyadovo	Bln-2120a	5700 ± 80	---	4750–4350	n.d.				Görsdorf, Bojadžiev 1996
144	Smyadovo	Bln-2116	5680 ± 50	---	4640–4400	n.d.				Görsdorf, Bojadžiev 1996
145	Smyadovo	Bln-1668	5665 ± 50	---	4620–4380	n.d.				Görsdorf, Bojadžiev 1996
146	Smyadovo	Bln-1669	5650 ± 50	---	4600–4360	n.d.				Görsdorf, Bojadžiev 1996
147	Smyadovo	Bln-2119	5630 ± 60	---	4600–4320	n.d.				Görsdorf, Bojadžiev 1996
148	Smyadovo	Bln-2118	5590 ± 60	---	4550–4310	n.d.				Görsdorf, Bojadžiev 1996
149	Smyadovo	Bln-2120	5480 ± 70	---	4470–4190	n.d.				Görsdorf, Bojadžiev 1996
150	Smyadovo	Bln-2185	5420 ± 50	---	4370–4170	n.d.				Görsdorf, Bojadžiev 1996
151	Smyadovo	Bln-2117	5400 ± 40	---	4360–4160	n.d.				Görsdorf, Bojadžiev 1996
152	Sushina	Poz-67096	5790 ± 40	charcoal	4740–4540					Čohadžiev, Krauß 2019
153	Sushina	Poz-67097	5740 ± 40	charcoal	4720–4480					Čohadžiev, Krauß 2019
154	Sushina	Poz-91621	5730 ± 40	charcoal	4700–4460					Čohadžiev, Krauß 2019
155	Sushina	Poz-67099	5710 ± 40	charcoal	4680–4440					Čohadžiev, Krauß 2019
156	Sushina	Poz-91619	5680 ± 40	hordeum vulgare (nudum)	4610–4410					Čohadžiev, Krauß 2019

No.	Site	Lab code	^{14}C-age [BP]	Material	calBC 2σ	δ^{13}C [‰PDB]	Phase/ context	Depth	Comment	Source
157	Sushina	Poz-67098	5625 ± 35	charcoal	4540–4340					Čohadžiev, Krauß 2019
158	Tash Bair	RICH-28078	11094 ± 47	Bulk	11160–10920		T4C6_420			Unpublished, thesis A. López del Olmo
159	Tash Bair	RICH-28447	7151 ± 33	Bulk	6080–5960		T1C29_360			Unpublished, thesis A. López del Olmo
160	Tash Bair	Poz-120370	6170 ± 40	bone (Cervus elaphus)	5240–5000		TB 2019. Tr.1.2/1.2.4 NW			Unpublished, this project
161	Tash Bair	Poz-120368	6155 ± 35	bone (Bos)	5260–4980		TB 2019. Tr.1.2 NE/1-2-7/8			Unpublished, this project
162	Tash Bair	Poz-120371	6120 ± 35	bone (Bos)	5250–4930		TB 2019. Tr1.2NE/1.2 7/8			Unpublished, this project
163	Tash Bair	Poz-120369	5545 ± 35	bone (large ungulate)	4470–4310		TB 2019. Tr1.2/1.2.4 NW			Unpublished, this project
164	Tash Bair	RICH-28446	5294 ± 28	Bulk	4280–4000		T9C17_280			Unpublished, thesis A. López del Olmo
165	Tash Bair	RICH-28435	5075 ± 27	Wood	3990–3750		T9C13_467			Unpublished, thesis A. López del Olmo
166	Tash Bair	Poz-108792	3585 ± 35	bone, bone (Bos taurus)	2040–1840		trench 3.6, ditch filling			Unpublished, this project
167	Tash Bair	Poz-108794	3555 ± 35	bone	2010–1770		trench 3.6, ditch filling			Unpublished, this project
168	Tash Bair	Poz-115807	3165 ± 30	bone, bone (Bos taurus)	1510–1390		trench 3.1			Unpublished, this project
169	Tash Bair	Poz-115808	3135 ± 30	bone	1470–1350		trench 3.1			Unpublished, this project
170	Tash Bair	Poz-115804	3100 ± 30	bone	1450–1290		trench 3.3			Unpublished, this project
171	Tash Bair	Poz-115806	3035 ± 35	bone, bone (Bos taurus)	1430–1190		trench 3.1			Unpublished, this project
172	Tash Bair	Poz-108793	3035 ± 30	bone, Bos?	1410–1210		trench 3.1			Unpublished, this project
173	Tash Bair	Poz-115331	2990 ± 30	charcoal	1350–1110		trench 3.3			Unpublished, this project
174	Tash Bair	RICH-28068	2600 ± 26	Bulk	830–750		T10C4_215			Unpublished, thesis A. López del Olmo
175	Tash Bair	RICH-28437	2473 ± 59	Seeds (Silene and Carex)	840–360		T8C13_683			Unpublished, thesis A. López del Olmo
176	Tash Bair	RICH-28052	2411 ± 25	Piece of bark	570–370		T1C9_430			Unpublished, thesis A. López del Olmo

No.	Site	Lab code	^{14}C-age [BP]	Material	calBC 2σ	δ^{13}C [‰PDB]	Phase/ context	Depth	Comment	Source
177	Tash Bair	RICH-28436	2243 ± 24	Piece of bark	420–180		T4C4_332			Unpublished, thesis A. López del Olmo
178	Tash Bair	RICH-28439	1997 ± 48	Seeds	120 BC–120 AD		T9C9_747			Unpublished, thesis A. López del Olmo
179	Tash Bair	RICH-28048	1912 ± 25	Piece of wood	20–140 AD		T7C23_654			Unpublished, thesis A. López del Olmo
180	Tash Bair	RICH-26700	1814 ± 33	Seeds	90–290 AD		T8C3_430			Unpublished, thesis A. López del Olmo
181	Tash Bair	RICH-28448	1506 ± 24	Bulk	500–620 AD		T7C24_325			Unpublished, thesis A. López del Olmo
182	Tash Bair	RICH-28438	1012 ± 25	Seeds	970–1050 AD		T4C7_226			Unpublished, thesis A. López del Olmo
183	Telish	Bln-2240	5400 ± 50	seeds	4400–4080	n.d.				Görsdorf, Bojadžiev 1996
184	Telish	Bln-2388	5330 ± 50	charcoal	4320–4000	n.d.				Görsdorf, Bojadžiev 1996
185	Telish	Bln-2243	5295 ± 70	charcoal	4310–3950	n.d.				Görsdorf, Bojadžiev 1996
186	Telish	Bln-2241	5240 ± 50	seeds	4260–3900	n.d.				Görsdorf, Bojadžiev 1996
187	Telish	Bln-2242	5230 ± 50	charcoal	4230–3910	n.d.				Görsdorf, Bojadžiev 1996
188	Telish	Bln-2244	5170 ± 50	charcoal	4090–3850	n.d.				Görsdorf, Bojadžiev 1996
189	Telish-Laga	Ua-20609	2725 ± 40	charcoal	950–790		Iron Age pit			Merkyte 2005
190	Tell Hotnitsa	KN-5765	5765 ± 30	charcoal	4720–4520	n.d.	Qu. 76, house 8	0.42		Provided by Bernhard Weninger (Cologne), Krauß (in press)-a; S. Chohadzhiev
191	Tell Hotnitsa	KN-5763	5720 ± 30	charcoal	4660–4460	-24.45	Qu. CC, house level	3.20		Provided by Bernhard Weninger (Cologne), Krauß (in press)-a; S. Chohadzhiev
192	Tell Hotnitsa	KN-5762	5680 ± 35	charred cereal grains	4590–4430	-24.03	Hor. III, Obj. 34, house 6	1.33		Provided by Bernhard Weninger (Cologne), Krauß (in press)-a; S. Chohadzhiev
193	Tell Hotnitsa	KN-5764	5660 ± 35	charcoal	4570–4410	-19.25	Qu. CC, Obj. 34, Profile	3.10		Provided by Bernhard Weninger (Cologne), Krauß (in press)-a; S. Chohadzhiev
194	Tell Hotnitsa	KN-5761	5595 ± 35	charcoal	4500–4340	-24.94	Qu. CC	3.00		Provided by Bernhard Weninger (Cologne), Krauß (in press)-a; S. Chohadzhiev
195	Tell Hotnitsa	Bln-125	5560 ± 100	---	4590–4230	n.d.	Hor. 1	0.90		Görsdorf, Bojadžiev 1996

No.	Site	Lab code	^{14}C-age [BP]	Material	calBC 2σ	δ^{13}C [‰PDB]	Phase/ context	Depth	Comment	Source
196	Tell Ovcharovo	Bln-1546	5989 ± 80	woden remains and sand	5090–4690	n.d.	Hor. 3, Qu. 244	4.47		Görsdorf, Bojadžiev 1996
197	Tell Ovcharovo	Bln-1493	5940 ± 80	ashy sand	5030–4630	n.d.	Hor. 5	k.A.		Görsdorf, Bojadžiev 1996
198	Tell Ovcharovo	Bln-1545	5845 ± 40	seeds and charcoal	4830–4590	n.d.				Görsdorf, Bojadžiev 1996
199	Tell Ovcharovo	Bln-1362	5805 ± 60	cereals	4810–4490	n.d.				Görsdorf, Bojadžiev 1996
200	Tell Ovcharovo	Bln-1368	5800 ± 60	charcoal, floor cover	4790–4510	n.d.	Hor. 3, Qu. 602	4.07		Görsdorf, Bojadžiev 1996
201	Tell Ovcharovo	Bln-1366	5747 ± 60	charcoal, floor cover	4740–4460	n.d.	Hor. 7, Qu. 511	2.70		Görsdorf, Bojadžiev 1996
202	Tell Ovcharovo	Bln-1361	5705 ± 60	cereals	4720–4400	n.d.				Görsdorf, Bojadžiev 1996
203	Tell Ovcharovo	Bln-1360	5685 ± 60	charcoal	4670–4390	n.d.				Görsdorf, Bojadžiev 1996
204	Tell Ovcharovo	Bln-1367	5676 ± 60	charcoal/Detritus, floor cover	4660–4380	n.d.	Hor. 6, Qu. 452	4.50		Görsdorf, Bojadžiev 1996
205	Tell Ovcharovo	Bln-1365	5664 ± 60	grains and charcoal	4640–4360	n.d.	Hor. 8, Qu. 633	3.14		Görsdorf, Bojadžiev 1996
206	Tell Ovcharovo	Bln-1359	5640 ± 60	charcoal	4610–4330	n.d.				Görsdorf, Bojadžiev 1996
207	Tell Ovcharovo	Bln-1363	5620 ± 60	charcoal	4590–4310	n.d.				Görsdorf, Bojadžiev 1996
208	Tell Ovcharovo	Bln-1364	5610 ± 60	charcoal	4560–4320	n.d.	Hor. 8, Qu. 341	2.05		Görsdorf, Bojadžiev 1996
209	Tell Ovcharovo	Bln-1358	5525 ± 60	charcoal	4500–4260	n.d.				Görsdorf, Bojadžiev 1996
210	Tell Ovcharovo	Bln-1357	5420 ± 60	charcoal	4410–4090	n.d.				Görsdorf, Bojadžiev 1996
211	Tell Ruse	Bln-4098	5800 ± 80	charcoal	4850–4450	n.d.	Hor. 12	2,90-3,00		Görsdorf, Bojadžiev 1996
212	Tell Ruse	Bln-4097	5720 ± 60	charcoal	4730–4410	n.d.	Hor. 12	2,90-3,10		Görsdorf, Bojadžiev 1996
213	Tell Ruse	Bln-4099	5650 ± 70	charcoal	4650–4330	n.d.	Hor. 7	2.30		Görsdorf, Bojadžiev 1996
214	Varbitsa	Poz-108842	6895 ± 35	bone (Ovis/ Capra)	5860–5700		XII, spit 22			Unpublished; site info – Венелинова, Григоров 2016; 2017; 2019; sample provided by S. Venelinova
215	Varbitsa	Poz-108838	6890 ± 40	bone (Ovis)	5880–5680		XV, spit 31			Unpublished; site info – Венелинова, Григоров 2016; 2017; 2019; sample provided by S. Venelinova
216	Varbitsa	Poz-82522	6880 ± 40	Bone (Bos taurus)	5870–5670		Sondage 1, spit 26			Unpublished; site info – Венелинова, Григоров 2016; 2017; 2019; sample provided by S. Venelinova

No.	Site	Lab code	^{14}C-age [BP]	Material	calBC 2σ	δ^{13}C [‰PDB]	Phase/ context	Depth	Comment	Source
217	Varbitsa	Poz-108892	6880 ± 40	bone (Ovis/ Capra)	5870–5670		VII A, spit 17			Unpublished; site info – Венелинова, Григоров 2016; 2017; 2019; sample provided by S. Venelinova
218	Varbitsa	Poz-108839	6870 ± 40	bone (Bos taurus)	5860–5660		XIV, spit 30			Unpublished; site info – Венелинова, Григоров 2016; 2017; 2019; sample provided by S. Venelinova
219	Varbitsa	Poz-108844	6870 ± 40	bone (Bos taurus)	5860–5660		X, spit 19			Unpublished; site info – Венелинова, Григоров 2016; 2017; 2019; sample provided by S. Venelinova
220	Varbitsa	Poz-108895	6850 ± 40	bone (Bos taurus)	5810–5650		V, spit 18			Unpublished; site info – Венелинова, Григоров 2016; 2017; 2019; sample provided by S. Venelinova
221	Varbitsa	Poz-108840	6840 ± 40	bone (Bos taurus)	5800–5640		XIII, spit 29			Unpublished; site info – Венелинова, Григоров 2016; 2017; 2019; sample provided by S. Venelinova
222	Varbitsa	Poz-82523	6830 ± 40	bone (Bos taurus)	5790–5630		Sondage 1, spit 24			Unpublished; site info – Венелинова, Григоров 2016; 2017; 2019; sample provided by S. Venelinova
223	Varbitsa	Poz-108891	6820 ± 40	bone (Bos taurus)	5780–5620		VIII, spit 16			Unpublished; site info – Венелинова, Григоров 2016; 2017; 2019; sample provided by S. Venelinova
224	Varbitsa	Poz-88725	6815 ± 35	bone (Bos taurus)	5760–5640		Sondage 1, spit 18			Unpublished; site info – Венелинова, Григоров 2016; 2017; 2019; sample provided by S. Venelinova
225	Varbitsa	Poz-108843	6800 ± 35	bone (Ovis/ Capra)	5750–5630		XI, spit 25			Unpublished; site info – Венелинова, Григоров 2016; 2017; 2019; sample provided by S. Venelinova
226	Varbitsa	Poz-108896	6790 ± 40	bone (Bos taurus)	5740–5620		IV, spit 11			Unpublished; site info – Венелинова, Григоров 2016; 2017; 2019; sample provided by S. Venelinova
227	Varbitsa	Poz-108846	6760 ± 40	bone (Bos taurus)	5730–5610		IX, spit 17			Unpublished; site info – Венелинова, Григоров 2016; 2017; 2019; sample provided by S. Venelinova
228	Varbitsa	Poz-108893	6730 ± 40	bone (Ovis)	5730–5570		VI, spit 19			Unpublished; site info – Венелинова, Григоров 2016; 2017; 2019; sample provided by S. Venelinova

No.	Site	Lab code	^{14}C-age [BP]	Material	calBC 2σ	δ^{13}C [‰PDB]	Phase/ context	Depth	Comment	Source
229	Varbitsa	Poz-108882	6730 ± 40	bone (Bos taurus)	5730–5570		II B, spit 13			Unpublished; site info – Венелинова, Григоров 2016; 2017; 2019; sample provided by S. Venelinova
230	Varbitsa	Poz-108897	6690 ± 40	bone (Bos taurus)	5680–5520		III A, spit 9			Unpublished; site info – Венелинова, Григоров 2016; 2017; 2019; sample provided by S. Venelinova
231	Varbitsa	Poz-82520	6300 ± 40	Bone (Bos taurus)	5350–5190		sondage 1, spit 12			Unpublished; site info – Венелинова, Григоров 2016; 2017; 2019; sample provided by S. Venelinova
232	Varna	MAMS-15093	6158 ± 24	shell Dentalium	5240–5000	-10	symbolic 27		marine reservoir effect	Krauß et al. 2016
233	Varna	MAMS-15094	6118 ± 24	shell Dentalium	5240–4920	-13	symbolic 41		marine reservoir effect	Krauß et al. 2016
234	Varna	OxA-X-225647	5860 ± 60	antler (Cervus)	4880–4560	-212	burial 294			Higham et al. 2018
235	Varna	OxA-13865	5855 ± 34	bone (human)	4810–4650	-184	burial 111			Higham et al. 2007
236	Varna	OxA-19875	5849 ± 39	bone (human)	4810–4610	-181	burial 51			Higham et al. 2018
237	Varna	OxA-19929	5831 ± 39	bone (human)	4810–4570	-190	burial 78			Higham et al. 2018
238	Varna	OxA-13688	5787 ± 30	bone (human)	4740–4540	-193	burial 158			Higham et al. 2007
239	Varna	OxA-23619	5771 ± 31	bone (human)	4720–4520	-184	burial 121 ?			Higham et al. 2018
240	Varna	OxA-13848	5766 ± 36	bone (human)	4720–4520	-190	burial 117			Higham et al. 2007
241	Varna	OxA-13846	5757 ± 34	bone (animal)	4710–4510	-194	burial 111			Higham et al. 2007
242	Varna	OxA-19928	5752 ± 37	bone (human)	4730–4490	-191	burial 78			Higham et al. 2018
243	Varna	OxA-23617	5739 ± 32	bone (human)	4690–4490	-188	burial 72			Higham et al. 2018
244	Varna	OxA-24041	5735 ± 31	bone (human)	4690–4490	-189	burial 127			Higham et al. 2018
245	Varna	OxA-13254	5732 ± 33	bone (human)	4710–4470	-185	burial 255			Higham et al. 2007
246	Varna	OxA-19878	5730 ± 33	bone (human)	4680–4480	-188	burial 85			Higham et al. 2018
247	Varna	OxA-19880	5728 ± 34	bone (human)	4700–4460	-194	burial 129			Higham et al. 2018
248	Varna	OxA-X-225643	5725 ± 45	antler (Cervus)	4720–4440	-226	burial 143			Higham et al. 2018
249	Varna	OxA-X-225646	5725 ± 40	bone (animal)	4700–4460	-184	burial 293			Higham et al. 2018
250	Varna	OxA-13685	5720 ± 29	bone (human)	4660–4460	-184	burial 43			Higham et al. 2007
251	Varna	OxA-23616	5719 ± 32	bone (human)	4660–4460	-193	burial 67 ?		same sample like OxA-23615 ?	Higham et al. 2018

No.	Site	Lab code	^{14}C-age [BP]	Material	calBC 2σ	δ^{13}C [‰PDB]	Phase/ context	Depth	Comment	Source
252	Varna	OxA-23615	5717 ± 32	bone (human)	4660–4460	-188	burial 67		same sample like OxA-23616 ?	Higham et al. 2018
253	Varna	OxA-19931	5715 ± 55	bone (human)	4710–4430	-191	burial 151			Higham et al. 2018
254	Varna	OxA-18576	5710 ± 33	antler (Cervus)	4650–4450	-194	burial 111			Higham et al. 2018
255	Varna	OxA-X-225831	5703 ± 36	antler (Cervus)	4640–4440	-185	burial 143			Higham et al. 2018
256	Varna	OxA-13251	5702 ± 32	bone (human)	4620–4460	-186	burial 112			Higham et al. 2007
257	Varna	OxA-19927	5702 ± 39	bone (human)	4640–4440	-193	burial 256			Higham et al. 2018
258	Varna	OxA-13690	5700 ± 30	bone (animal)	4610–4450	-197	burial 143			Higham et al. 2007
259	Varna	OxA-19924	5696 ± 37	bone (human)	4630–4430	-193	burial 179			Higham et al. 2018
260	Varna	OxA-24042	5690 ± 31	bone (human)	4600–4440	-194	burial 87			Higham et al. 2018
261	Varna	OxA-13689	5690 ± 32	bone (human)	4600–4440	-197	burial 143			Higham et al. 2007
262	Varna	OxA-19925	5689 ± 38	bone (human)	4620–4420	-191	burial 197			Higham et al. 2018
263	Varna	OxA-23623	5688 ± 32	bone (human)	4600–4440	-189	burial 286		same sample like OxA-23264	Higham et al. 2018
264	Varna	OxA-19877	5687 ± 34	bone (human)	4600–4440	-196	burial 84			Higham et al. 2018
265	Varna	OxA-13253	5685 ± 33	bone (human)	4600–4440	-186	burial 125			Higham et al. 2007
266	Varna	OxA-19879	5678 ± 34	bone (human)	4590–4430	-195	burial 126			Higham et al. 2018
267	Varna	OxA-13252	5672 ± 34	bone (human)	4580–4420	-189	burial 121			Higham et al. 2007
268	Varna	OxA-23620	5668 ± 33	bone (human)	4580–4420	-194	burial 139			Higham et al. 2018
269	Varna	OxA-13691	5668 ± 32	bone (human)	4560–4440	-196	burial 215			Higham et al. 2007
270	Varna	OxA-19923	5666 ± 37	bone (human)	4580–4420	-191	burial 171			Higham et al. 2018
271	Varna	OxA-19930	5665 ± 39	bone (human)	4580–4420	-190	burial 154			Higham et al. 2018
272	Varna	MAMS-15095	5662 ± 27	bone (human)	4550–4430	-267	burial 43			Krauß et al. 2016
273	Varna	OxA-13693	5660 ± 29	bone (human)	4550–4430	-200	burial 225			Higham et al. 2007
274	Varna	OxA-23622	5659 ± 31	bone (human)	4550–4430	-185	burial 182			Higham et al. 2018
275	Varna	OxA-23614	5658 ± 32	bone (human)	4550–4430	-191	burial 47			Higham et al. 2018
276	Varna	OxA-23621	5658 ± 32	bone (human)	4550–4430	-190	burial 174			Higham et al. 2018
277	Varna	OxA-13692	5657 ± 30	bone (human)	4550–4430	-196	burial 44			Higham et al. 2007
278	Varna	OxA-23618	5655 ± 32	bone (human)	4550–4430	-192	burial 89			Higham et al. 2018
279	Varna	OxA-13694	5654 ± 36	bone (human)	4570–4410	-198	burial 137			Higham et al. 2007
280	Varna	OxA-23624	5654 ± 31	bone (human)	4550–4430	-190	burial 286		same sample like OxA-23263	Higham et al. 2018

No.	Site	Lab code	^{14}C-age [BP]	Material	calBC 2σ	δ^{13}C [‰PDB]	Phase/ context	Depth	Comment	Source
281	Varna	OxA-23625	5646 ± 31	bone (animal? human?)	4560–4400	-190	burial 286			Higham et al. 2018
282	Varna	OxA-13686	5639 ± 32	bone (human)	4550–4390	-195	burial 11			Higham et al. 2007
283	Varna	OxA-19871	5638 ± 35	bone (human)	4560–4360	-187	burial 34			Higham et al. 2018
284	Varna	OxA-19870	5631 ± 35	bone (human)	4550–4350	-184	burial 32			Higham et al. 2018
285	Varna	OxA-19867	5629 ± 34	bone (human)	4550–4350	-178	burial 25			Higham et al. 2018
286	Varna	OxA-13250	5626 ± 31	bone (human)	4540–4340	-186	burial 94			Higham et al. 2007
287	Varna	OxA-19926	5618 ± 39	bone (human)	4540–4340	-190	burial 249			Higham et al. 2018
288	Varna	OxA-225644	5610 ± 45	antler (Cervus)	4530–4330	-193	burial 182			Higham et al. 2018
289	Varna	OxA-19876	5608 ± 35	bone (human)	4530–4330	-186	burial 69			Higham et al. 2018
290	Varna	OxA-23626	5608 ± 32	bone (human)	4510–4350	-190	burial 294			Higham et al. 2018
291	Varna	OxA-19869	5599 ± 34	bone (human)	4500–4340	-186	burial 30			Higham et al. 2018
292	Varna	OxA-23612	5590 ± 31	bone (Cervus)	4490–4330	-186	burial 28			Higham et al. 2018
293	Varna	OxA-23613	5585 ± 32	bone (human)	4490–4330	-191	burial 46			Higham et al. 2018
294	Varna	OxA-19873	5583 ± 35	bone (human)	4490–4330	-186	burial 45			Higham et al. 2018
295	Varna	OxA-23611	5574 ± 31	bone (human)	4480–4320	-185	burial 28			Higham et al. 2018
296	Varna	OxA-19874	5574 ± 33	bone (human)	4490–4330	-186	burial 50			Higham et al. 2018
297	Varna	OxA-13687	5569 ± 32	bone (human)	4480–4320	-191	burial 10			Higham et al. 2007
298	Varna	OxA-19868	5567 ± 34	bone (human)	4480–4320	-187	burial 30			Higham et al. 2018
299	Varna	OxA-18577	5564 ± 30	bone (animal)	4480–4320	-193	burial 286			Higham et al. 2018
300	Varna	OxA-X-225645	5555 ± 45	antler (Cervus)	4480–4320	-189	burial 286			Higham et al. 2018
301	Varna	OxA-18575	5550 ± 31	bone (animal)	4480–4320	-189	burial 28			Higham et al. 2018
302	Varna	OxA-24043	5539 ± 32	bone (human)	4470–4310	-189	burial 261			Higham et al. 2018
303	Varna	OxA-24044	5531 ± 31	bone figurine (animal)	4470–4310	-216	burial 40			Higham et al. 2018
304	Varna	OxA-13811	5530 ± 36	bone (animal)	4470–4310	-202	burial 117			Higham et al. 2007
305	Varna	MAMS-15097	5508 ± 27	bone (human)	4420–4300	-287	burial 167			Krauß et al. 2016
306	Varna	MAMS-15098	5472 ± 28	bone (human)	4390–4230	-352	burial 288			Krauß et al. 2016
307	Varna	Poz-71452	5420 ± 35	bone (human)	4370–4210	n.d.	burial 209			Krauß et al. 2016
308	Varna	OxA-19872	3728 ± 31	bone (human)	2240–2000	-190	burial 38		Bronze Age	Higham et al. 2018
309	Varna	Poz-71453	3585 ± 35	bone (human)	2040–1840	n.d.	burial 33		Bronze Age	Krauß et al. 2017

Catalogue and plates of the pottery finds

Introductory Remarks

The pottery finds are sorted according to the site where they were found. Within the sites, a separation was made according to finds from the surveys and from the excavations, each in a chronological order. The relevant section of the catalogue is assigned to the tables on the opposite page.

The – if available – dating of the cited reference pieces from other sites forms the essential basis for the dating of the pottery finds. In the case of the excavation finds, the context and the stratigraphic position also had to be considered.

Achim Frey, Doncho Karakolev, Raiko Krauß and Sven Conrad provided the basic drawings for the plates. The photos are from Raiko Krauß and Sven Conrad. Jonas Sprißler was responsible for processing the pottery profiles and designing the plates.

Abbreviations

b – bottom diameter
d – diameter
dmax – maximal diameter of the vessel's body
ft. – feature
h – height
hf – fragment height
m – mouth diameter
niv. – niveau
pl. – planum
pol. – polygon
qu. – quadrant
th – thickness
tr. – trench
w – width
wf – fragment width

BA – Bronze Age
CL – Chalcolithic
EIA – Early Iron Age
EMA – Early Middle Age
ERP – Early Roman period
LIA – Late Iron Age
LNL – Late Neolithic
LRP – Late Roman period
MBA – Middle Bronze Age
RP – Roman period

SITE 1. Survey

Site 1, survey: Late Neolithic pottery

P 1/001. Site 1; pol. 7LT4. – Middle fragment with double buckle. – Dimensions (cm): dmax 33.6; wf 6.6; hf 6.5. – Fabric 3, slipped. – Dating: LNL.

P 1/002. Site 1; pol. 7LT3. – Rim fragment of a bulbous pot with conical to cylindrical neck. – Dimensions (cm): m 11.4; wf 3.8; hf 3.9. – Fabric 1, smoothed and polished surface. – Dating: LNL.

P 1/003. Site 1; pol. 7NK1. – Rim fragment of a large storage vessel with a narrow mouth. – Dimensions (cm): m 38.7; wf 3.1; hf 6.1. – Fabric 3, finger grooved barbotine. – Dating: LNL.

P 1/004. Site 1; pol. 7LV2. – Rim fragment of a cylindrical neck. – Dimensions (cm): m 14.6; wf 3.3; hf 3.1. – Fabric 6, smoothed surface. – Dating: LNL.

P 1/005. Site 1; pol. 188. – Rim fragment of a funnel neck. – Dimensions (cm): m ca. 13; wf 4.6; hf 2.2. – Fabric 1, slipped. – Dating: LNL.

P 1/006. Site 1; pol. 1-6. – Rim fragment of a bulbous coarse vessel with a slightly outward curving lip. – Dimensions (cm): m 7.2; wf 4.0; hf 2.7. – Fabric 6, smoothed surface. – Dating: LNL.

P 1/007. Site 1; pol. 188. – Rim fragment of a wide-bodied bowl. – Dimensions (cm): wf 3.3; hf 2.2. – Fabric 1, smoothed and polished surface, vertical channeling. – Dating: LNL.

P 1/008. Site 1; pol. 187NK1. – Rim fragment of a large decorated vessel. – Dimensions (cm): dmax 34; m 13.8; wf 6.2; hf 4.4. – Fabric 6, impasto horizontal lines parallel to the rim. – Dating: LNL (Vădastra).

P 1/009. Site 1; pol. 7LT3. – Middle fragment with impasto. – Dimensions (cm): wf 6.1; hf 4.7. – Fabric 3, impasto zig-zag lines with hatched fields in between. – Dating: LNL (Vădastra).

P 1/010. Site 1; pol. 7LT3. – Shoulder piece of a large cylindrical lid. – Dimensions (cm): wf 4.0; hf 3.9. – Fabric 5, complex impasto motif with rhomboid filling of the bands. – Dating: LNL (Vădastra).

P 1/011. Site 1; pol. 7LT3. – Rim fragment of a cylindrical vessel part. – Dimensions (cm): m 9.7; wf 4.4; hf 4.3. – Fabric 5, impasto, spiraloid motif with gussets filled with striations. – Dating: LNL (Vădastra).

P 1/012. Site 1; pol. 7NK1. – Middle fragment of a large impasto decorated vessel. – Dimensions (cm): wf 6.5; hf 4.2. – Fabric 3, wide meander motif with well-preserved white impasto. – Dating: LNL (Vădastra).

P 1/013. Site 1; pol. 7SS4. – Middle fragment of a large vessel. – Dimensions (cm): wf 5.1; hf 5.2. – Fabric 8, wide band motif with gusset filled with striations. – Dating: LNL (Vădastra).

P 1/014. Site 1; pol. 7LV2. – Middle fragment of a large bulbous impasto decorated vessel. – Dimensions (cm): wf 5.0; hf 4.2. – Fabric 3, empty field framed by an impasto band with rhombuses. – Dating: LNL (Vădastra).

P 1/015. Site 1; pol. 7LT1. – Rim fragment of a vessel with conical mouth. – Dimensions (cm): m 25.8; wf 6.4; hf 5.4. – Fabric 3, horizontal linear bands impasto filled parallel to the rim. – Dating: LNL (Vădastra).

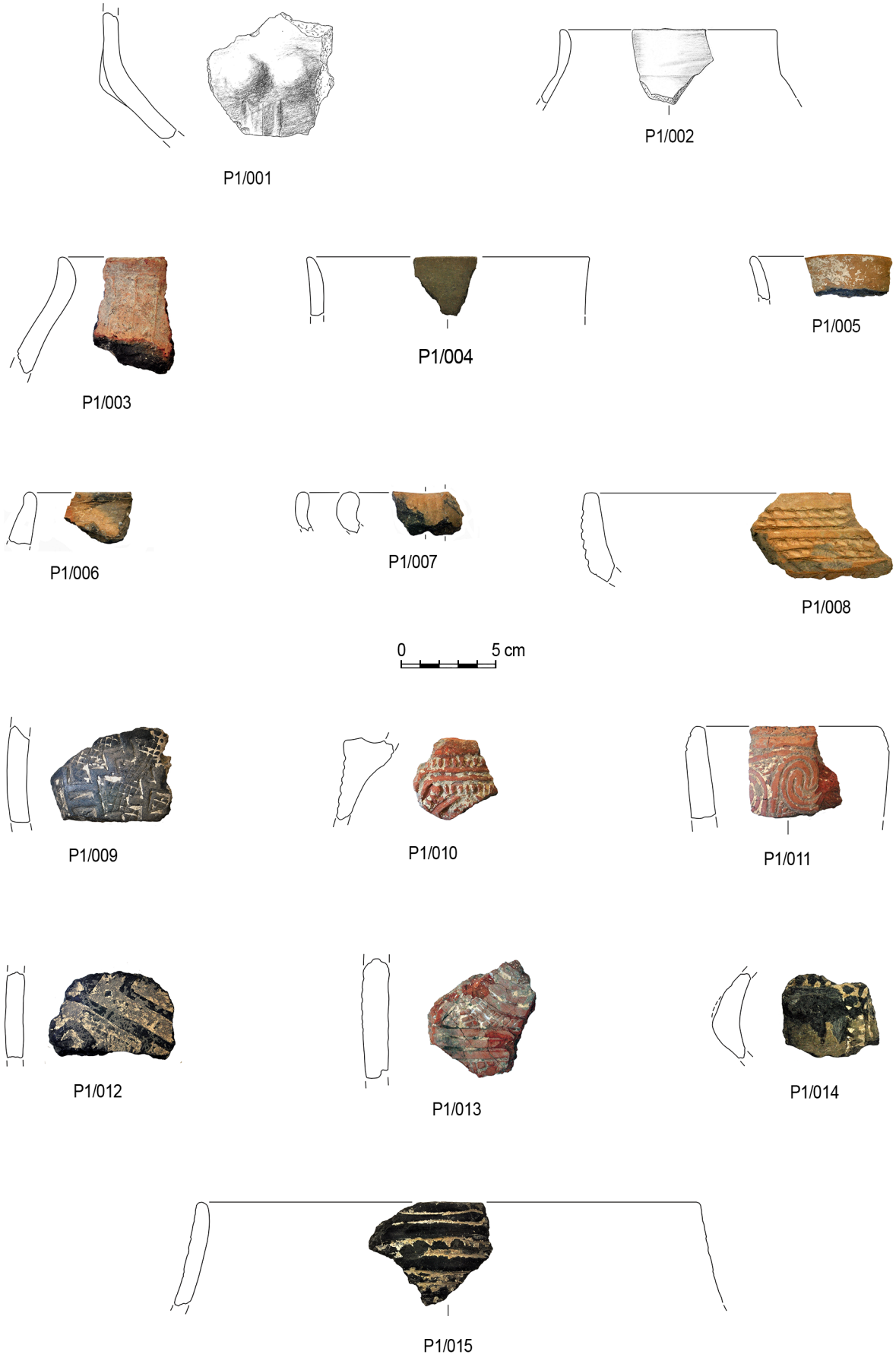


Plate 1. Site 1, survey: Late Neolithic pottery (P1/001–P1/015)

SITE 1. Survey

Site 1, survey: Late Neolithic pottery

P 1/016. Site 1; pol. 7LT1. – Rim fragment of a large vessel with conical mouth. – Dimensions (cm): m 28.2; wf 3.5; hf 3.3. – Fabric 3, horizontal bands impasto filled with rhombuses. – Dating: LNL (Vădastra).

P 1/017. Site 1; pol. 188LV3. – Middle fragment of a huge cylindrical vessel. – Dimensions (cm): wf 6.2; hf 5.5. – Fabric 5, horizontal linear bands, framing a field filled with spared worked zig-zag and impasto. – Dating: LNL (Vădastra).

P 1/018. Site 1; pol. 188LV3. – Middle fragment of a huge cylindrical vessel. – Dimensions (cm): wf 5.4; hf 5.3. – Fabric 3, intertwined meander motifs with hatched gussets, impasto. – Dating: LNL (Vădastra).

P 1/019. Site 1; pol. 187NK1. – Middle fragment of a huge bulbous vessel. – Dimensions (cm): wf 6.6; hf 8.9. – Fabric 3, angular meander motifs with hatched spaces and a smoothed zone. – Dating: LNL (Vădastra).

P 1/020. – Site 1; pol. 7SS4. – Middle fragment. – Dimensions (cm): wf 4.2; hf 3. – Fabric 3, impasto decorated. – Dating: LNL (Vădastra).

P 1/021. Site 1; pol. 189SC1. – Rim fragment of a large vessel with conical mouth. – Dimensions (cm): m 5.7; wf 3.5; hf 3.5. – Fabric 8, zig-zag impasto filled fields below the lip. – Dating: LNL (Vădastra).

P 1/022. Site 1; pol. 188SC3. – Middle fragment of a huge bulbous vessel. – Dimensions (cm): wf 3.0; hf 4.1. – Fabric 8, zig-zag impasto filled fields with smoothed fields in between. – Dating: LNL (Vădastra).

P 1/023. Site 1; pol. 187. – Middle fragment of a huge vessel. – Dimensions (cm): wf 5.0; hf 5.3. – Fabric 6, zig-zag impasto filled field framed by lines. – Dating: LNL (Vădastra).

P 1/024. Site 1; pol. 6. – Middle fragment of a huge vessel. – Dimensions (cm): wf 5.2; hf 6.1. – Fabric 5, zig-zag impasto filled field. – Dating: LNL (Vădastra).

P 1/025. Site 1; pol. 6. – Middle fragment of a huge cylindrical vessel. – Dimensions (cm): wf 6.0; hf 5.8. – Fabric 6, angular meander motifs with hatched spaces, impasto. – Dating: LNL (Vădastra).

P 1/026. Site 1; pol. 7. – Rim fragment of a stepped neck with a curved profile. – Dimensions (cm): m 10.8; wf 8.1; hf 7.2. – Fabric 3, band and spiral motifs with hatched gussets, impasto, below the zone of the lip. – Dating: LNL (Vădastra).

P 1/027. Site 1; pol. 7LT3. – Middle fragment of a huge vessel. – Dimensions (cm): wf 2.8; hf 4.1. – Fabric 6, meander motif impasto. – Dating: LNL (Vădastra).

P **1/028.** Site 1; pol. 7LT4. – Rim fragment of a small carinated bowl with a slightly outward curving lip. – Dimensions (cm): m 11.9; wf 3.7; hf 3.8. – Fabric 12, vertical channeling on the vessels shoulder. – Dating: LNL (North Bulgarian LNL).

P 1/029. Site 1; pol. 7LT4. – Middle fragment of a small bulbous pot. – Dimensions (cm): m 14.6; wf 5.5; hf 4.3. – Fabric 12, channeled bands with gussets filled with fine incisions. – Dating: LNL (Hamangia like).

P 1/030. Site 1; pol. 187NK1. – Rim fragment of a huge funnel neck. – Dimensions (cm): m 5.9; wf 3.2; hf 2.8. – Fabric 6, oblique flutings below the rim zone. – Dating: LNL (North Bulgarian LNL).

P 1/031. Site 1; pol. 7LT3. – Rim fragment of a small bulbous pot with a slightly outward curving lip. – Dimensions (cm): m 15.5; wf 3; hf 3.2. – Fabric 12, vertical channeling below the rim zone. – Dating: LNL (North Bulgarian LNL).



Plate 2. Site 1, survey: Late Neolithic pottery (P1/016–P1/031)

SITE 1. Survey

Site 1, survey: Late Neolithic pottery

P 1/032. Site 1; pol. 7LV4. – Rim fragment of a carinated bowl. – Dimensions (cm): dmax 34; m 17.5; wf 5.3; hf 4.4. – Fabric 12, vertical channeling on the shoulder. – Dating: LNL (North Bulgarian LNL).

P 1/033. Site 1; pol. 188SS2. – Rim fragment of a carinated bowl with offset lip rim. – Dimensions (cm): wf 1.4; hf 2.0. – Fabric 3, vertical channeling on the shoulder. – Dating: LNL (North Bulgarian LNL).

P 1/034. Site 1; pol. 7NK2. – Shoulder fragment of a carinated bowl with offset lip rim. – Dimensions (cm): wf 3.8; hf 4.5. – Fabric 12, vertical channeling on the shoulder. – Dating: LNL (North Bulgarian LNL).

P 1/035. Site 1; pol. 7NK5. – Rim fragment of a carinated bowl with a slightly S-curved lip. – Dimensions (cm): m 16.0; wf 3.0; hf 2.5. – Fabric 12, vertical channeling on the shoulder. – Dating: LNL (North Bulgarian LNL).

P 1/036. Site 1; pol. 7LT2. – Rim fragment of a wide carinated bowl with outward arching lip. – Dimensions (cm): m 16.4; wf 2.9; hf 2.3. – Fabric 6, undecorated but with a thin horizontal score line marking the lip zone. – Dating: LNL (North Bulgarian LNL).

P 1/037. Site 1; pol. 7NK5. – Rim fragment of a carinated bowl with a slightly S-curved lip. – Dimensions (cm): dmax 23.0; m 22.7; wf 2.9; hf 2.7. – Fabric 3, traces of vertical channeling on the shoulder. – Dating: LNL (North Bulgarian LNL).

P 1/038. Site 1; pol. 7LT2. – Rim fragment of a carinated bowl with offset lip rim. – Dimensions (cm): d 19.4; m 20.2; wf 3.3; hf 3.4. – Fabric 12, undecorated. – Dating: LNL (North Bulgarian LNL).

P 1/039. Site 1; pol. 7LV7. – Rim fragment of a carinated bowl with offset lip rim. – Dimensions (cm): m 19.6; wf 4.5; hf 4.4. – Fabric 12, vertical channeling on the shoulder. – Dating: LNL (North Bulgarian LNL).

P 1/040. Site 1; pol. 7LV1. – Rim fragment of a small bulbous pot. – Dimensions (cm): m 20.9; wf 4.0; hf 3.4. – Fabric 12, oblique flutings on the shoulder. – Dating: LNL (North Bulgarian LNL).

P 1/041. Site 1; pol. 7LT1. – Rim fragment of a fine carinated bowl with high shoulder and slightly offset lip. – Dimensions (cm): dmax 34.0; wf 5.0; hf 5.1. – Fabric 3, vertical channeling on the shoulder. – Dating: LNL (North Bulgarian LNL).

P 1/042. Site 1; pol. 7SS1. – Rim fragment of a large vessel with conical shoulder and offset lip. – Dimensions (cm): m 5.7; wf 4.3; hf 3.7. – Fabric 6, vertical channeling on the shoulder. – Dating: LNL (North Bulgarian LNL).

P 1/043. Site 1; pol. 7LT1. – Middle fragment of a small bulbous pot. – Dimensions (cm): wf 3.4; hf 2.8. – Fabric 3, channeled lines in combination with fine incisions. – Dating: LNL (Hamangia like).

P 1/044. Site 1; pol. 187NK1. – Middle fragment of a small carinated pot. – Dimensions (cm): m 19.3; wf 3.9; hf 4.0. – Fabric 12, on the shoulder oblique channeling in two directions with fine triangular incisions in the gusset. – Dating: LNL (North Bulgarian LNL).

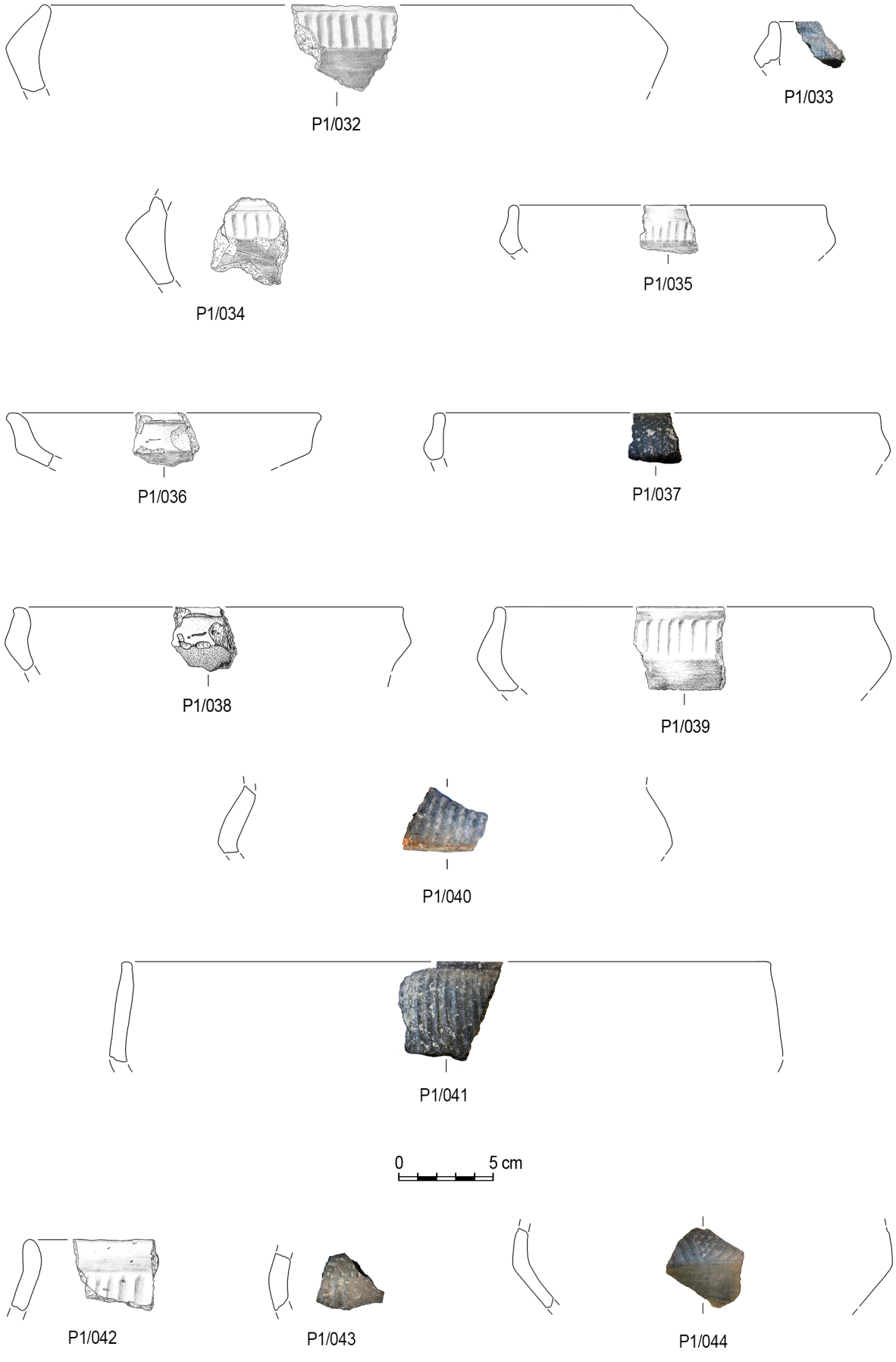


Plate 3. Site 1, survey: Late Neolithic pottery (P1/032–P1/044)

SITE 1. Survey

Site 1, survey: Late Neolithic pottery

P 1/045. Site 1; pol. 187NK1. – Rim fragment of a round bowl with straight wall. – Dimensions (cm): m 17.9; wf 5.7; hf 4.6. – Fabric 6, flat fishbone channeling. – Dating: LNL (North Bulgarian LNL).

P 1/046. Site 1; pol. 187NK1. – Funnel rim fragment. – Dimensions (cm): m 6.7; wf 3.4; hf 3.3. – Fabric 12, rough horizontal channeling. – Dating: LNL.

P 1/047. Site 1; pol. 8NK1. – Middle fragment of a bulbous vessel. – Dimensions (cm): m 11.7; wf 2.9; hf 2.1. – Fabric 6, oblique flutings combined with horizontal channels. Dating: LNL (Hamangia like).

P 1/048. Site 1; pol. 187NK1. – Fragment of the lower part of a conical vessel. – Dimensions (cm): wf 4.1; hf 4.7. – Fabric 3, unorganised oblique channeling. – Dating: LNL.

P 1/049. Site 1; pol. 188Y2. – Middle fragment of a large vessel. – Dimensions (cm): wf 5.9; hf 4.4. – Fabric 1, crossing channels limited by a groove. – Dating: LNL.

P 1/050. Site 1; pol. 15. – Rim fragment of a fine carinated bowl with high shoulder and slightly offset lip. – Dimensions (cm): m 27.0; wf 4.2; hf 4.5. – Fabric 12, fine oblique channeling on the shoulder. – Dating: LNL (North Bulgarian LNL).

P 1/051. Site 1; pol. 1-6. – Middle fragment of a coarse biconical vessel. – Dimensions (cm): wf 5.7; hf 4.0. – Fabric 6, smoothed surface. – Dating: LNL.

P 1/052. Site 1; pol. 15. – Middle fragment of a coarse pot. – Dimensions (cm): wf 3.1; hf 3.0. – Fabric 6, buckle with deep channels. – Dating: LNL.

P 1/053. Site 1; pol. 188. – Middle fragment of a bulbous vessel. – Dimensions (cm): wf 2.0; hf 2.9. – Fabric 8, fishbone channeling. – Dating: LNL.

P 1/054. Site 1; pol. 187NK1. – Fragment of a little lid with with a cone-shaped top. – Dimensions (cm): wf 3.2; hf 2.1. – Fabric 3, undecorated. – Dating: LNL.

P 1/055. Site 1; pol. 187NK1. – Rim fragment of a flat bowl with a straight wall. – Dimensions (cm): m 18.1; wf 4.1; hf 2.1. – Fabric 6, horizontal scratches on the exterior. – Dating: LNL.

P 1/056. Site 1; pol. 7LT6. – Rim fragment of a conical rim with offset lip. – Dimensions (cm): m 18.5; wf 2.8; hf 3.0. – Fabric 6, fine score marking the lip. – Dating: LNL.

P 1/057. Site 1; pol. 7LT1. – Rim fragment of a flat bowl with a straight wall. – Dimensions (cm): d 37; wf 7.8; hf 5.5. – Fabric 6, unorganized scratches on the exterior. – Dating: LNL.

P 1/058. Site 1; pol. 188LV3. – Rim fragment of a slightly outward-curving cylindrical neck. – Dimensions (cm): m 13.5; wf 4.3; hf 4.4. – Fabric 20, smoothed surface. – Dating: LNL.

P 1/059. Site 1; pol. 8LV1. – Middle fragment of a large vessel. – Dimensions (cm): wf 2.4; hf 2.3. – Fabric 8, smoothed surface with incised lines forming simple spiral bands. – Dating: LNL.

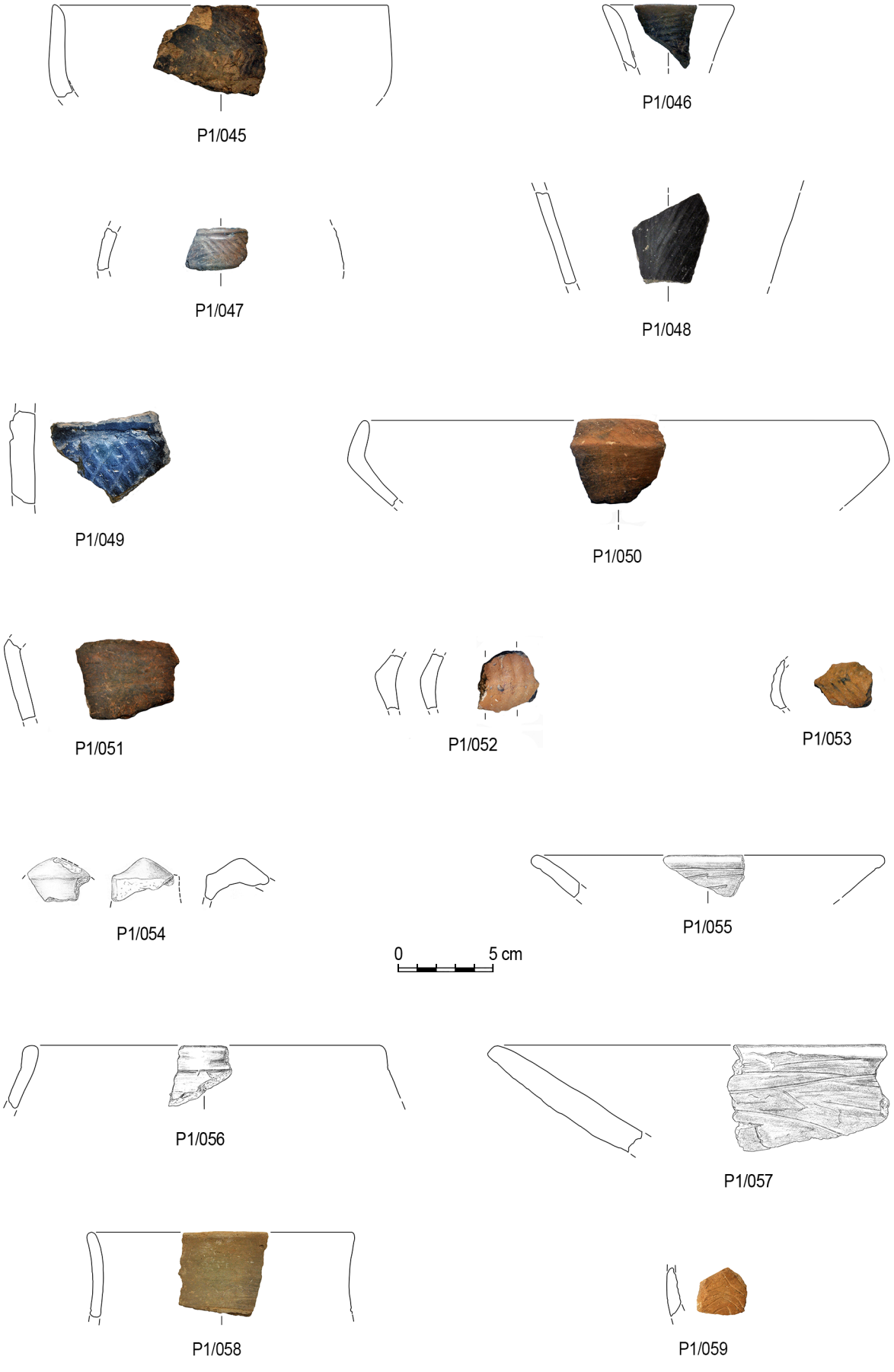


Plate 4. Site 1, survey: Late Neolithic pottery (P1/045–P1/059)

SITE 1. Survey

Site 1, survey: Late Neolithic pottery

P 1/060. Site 1; pol. 187NK1. – Bottom fragment of a large vessel. – Dimensions (cm): b 7.4; wf 2.9; hf 1.2. – Fabric 3, incision lines for impasto filling. – Dating: LNL (Vădastra).

P 1/061. Site 1; pol. 8LT5. – Shoulder part of a small carinated bowl with offset lip. – Dimensions (cm): wf 5.0; hf 3.5. – Fabric 12, curved scratches forming an ornamental frieze on the shoulder and two linear parallel scratches on the lower part. – Dating: LNL (North Bulgarian LNL).

P 1/062. Site 1; pol. 7LT5. – Middle fragment of a large vessel. – Dimensions (cm): wf 3.4; hf 3.2. – Fabric 3, fine angular meander motif with white impasto filling. – Dating: LNL (Vădastra).

P 1/063. Site 1; pol. 188LV4. – Middle fragment of a large vessel. – Dimensions (cm): wf 4.3; hf 3.1. – Fabric 5, scratched angular intertwining meander motifs. – Dating: LNL (Vădastra).

P 1/064. Site 1; pol. 188NK1. – Middle fragment of a large bulbous vessel. – Dimensions (cm): wf 3.8; hf 3.5. – Fabric 3, linear scratches with traces of white impasto. – Dating: LNL (Vădastra).

P 1/065. Site 1; pol. 14. – Middle fragment of a large vessel. – Dimensions (cm): wf 5.0; hf 4.1. – Fabric 6, curved score lines. – Dating: LNL (Vădastra).

P 1/066. Site 1; pol. 5. – Middle fragment of a large vessel. – Dimensions (cm): wf. 4.9; hf 3.6. – Fabric 3, scratches on smoothed surface. – Dating: LNL (Vădastra).

P 1/067. Site 1; pol. 7LT7. – Middle fragment of a large vessel with straight walls. – Dimensions (cm): wf 2.0, hf 1.6. – Fabric 6, angular meander motifs. – Dating: LNL (Vădastra).

P 1/068. Site 1; pol. 7LT1. – Fragment of a cylindrical neck. – Dimensions (cm): m 7.7; wf 7.9; hf 6.9. – Fabric 3, crossing scratches on the shoulder. – Dating: LNL (Vădastra).

P 1/069. Site 1; pol. 7LT1. – Rim fragment of a bulbous pot with an outward-curving lip. – Dimensions (cm): m 20.1; wf 4.3; hf 5.1. – Fabric 6, small incisions below the lip and one oblique scratch on the body. – Dating: LNL.

P 1/070. Site 1; pol. 7LT7. – Conical vessel's foot with concave base. – Dimensions (cm): b 2.6; hf 1.7. – Fabric 6, undecorated. – Whitish adhesion to the bottom of the vessel (food residue?). – Dating: LNL.

P 1/071. Site 1; pol. 7NK7. – Fragment of a funnel neck. – Dimensions (cm): m 15.4; wf 3.0; hf 3.1. – Fabric 12, wide deep horizontal flutings. – Dating: LNL.

P 1/072. Site 1; pol. 188NK5. – Rim fragment of a bowl with inverted lip. – Dimensions (cm): wf 3.7; hf 2.8. – Fabric 6, wide deep horizontal flutings. – Dating: LNL.

P 1/073. Site 1; pol. 187NK1. – Rim fragment of a fine small vessel with straight walls. – Dimensions (cm): m 15.9; wf 1.8; hf 1.3. – Fabric 3, fine incisions at the lip. – Dating: LNL.

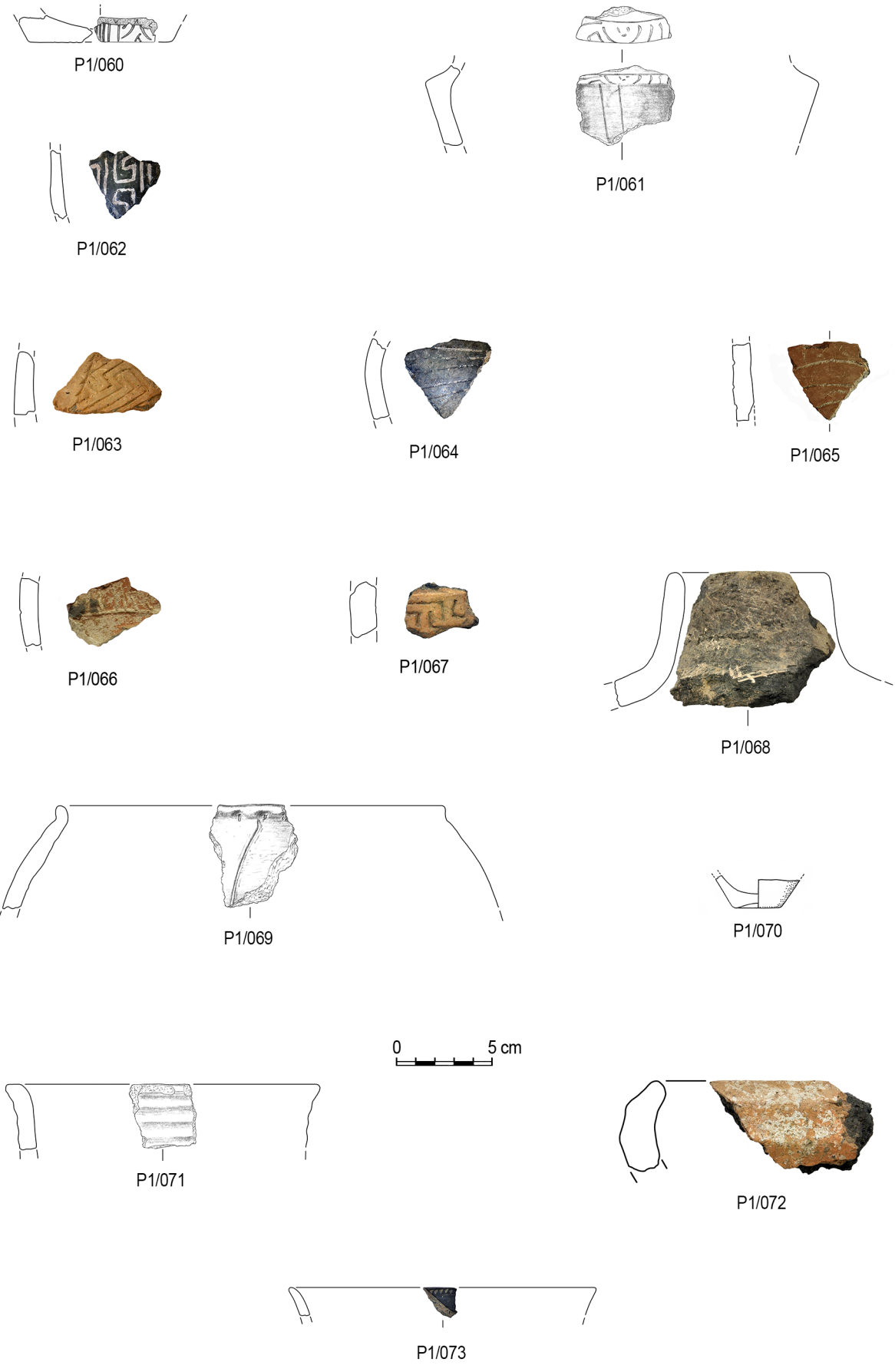


Plate 5. Site 1, survey: Late Neolithic pottery (P1/060–P1/073)

SITE 1. Survey

Site 1, survey: Bronze Age pottery

P 1/074. Site 1; pol. 20. – Rim fragment of a bowl with an outward-curving rim. – Dimensions (cm): wf 2.5; hf 1.8. – Fabric 39, notched lip. – Dating: BA.

P 1/075. Site 1; pol. 7NK4. – Rim fragment of a bulbous pot with a narrow mouth. – Dimensions (cm): m 21.8; wf 5.2; hf 4.0. – Fabric 13, fingertip strip below the rim. – Dating: BA.

P 1/076. Site 1; pol. 7LT2. – Rim fragment of a large bowl with straight walls. – Dimensions (cm): wf 5.5; hf 5.6. – Fabric 18, notched lip, small buckle and oblique plastic stripe on the wall. – Dating: BA.

P 1/077. Site 1; pol. 7LV7. – Middle fragment from the transition point between the shoulder and neck of the vessel. – Dimensions (cm): wf 3.7; hf 3.0. – Fabric 36, polished with incised triangle motif filled with lines. – Dating: BA.

P 1/078. Site 1; pol. 7NK2. – Rim fragment of a pot. – Dimensions (cm): m 25.5; wf 2.2; hf 2.5. – Fabric 29, small pits below the lip. – Dating: BA.

P 1/079. Site 1; pol. 7NK2. – Rim fragment of a closed vessel. – Dimensions (cm): wf 2.8; hf 2.4. – Fabric 37, notched lip, rough surface. – Dating: BA.

P 1/080. Site 1; pol. 188SC5. – Handle fragment with triangular cross-section. – Dimensions (cm): wf 1.5; hf 2.3. – Fabric 36. – Dating: BA.

P 1/081. Site 1; pol. 187LV3. – Rim fragment of a conical upper part of a pot with a slightly outward-curving rim. – Dimensions (cm): m 15.5; wf 2.3; hf 2.5. – Fabric 39, untreated. – Dating: BA.

P 1/082. Site 1; pol. 189SC1. – Rim fragment of a closed pot with a slightly outward curving rim. – Dimensions (cm): wf 3.4; hf 4.1. – Fabric 36, smoothed surface. – Dating: BA.

P 1/083. Site 1; pol. 187LV2. – Middle fragment of a bulbous vessel. – Dimensions (cm): wf 3.2; hf 2.4. – Fabric 13, horizontal line of incisions and scratched lines. – Dating: BA.

P 1/084. Site 1; pol. 7LV4. – Funnel rim fragment. – Dimensions (cm): m 10.9; wf 2.3; hf 1.1. – Fabric 18, notched lip. – Dating: BA.

P 1/085. Site 1; pol. 7LV4. – Rim fragment of a large pot with a slightly outward-curving lip. – Dimensions (cm): d 22.0; wf 5.6; hf 4.5. – Fabric 37, slip. – Dating: BA.

P 1/086. Site 1; pol. 7LT3. – Fragment of a whishbone handle. – Dimensions (cm): wf 2.2; th 1.2. – Fabric 36. – Dating: MBA.

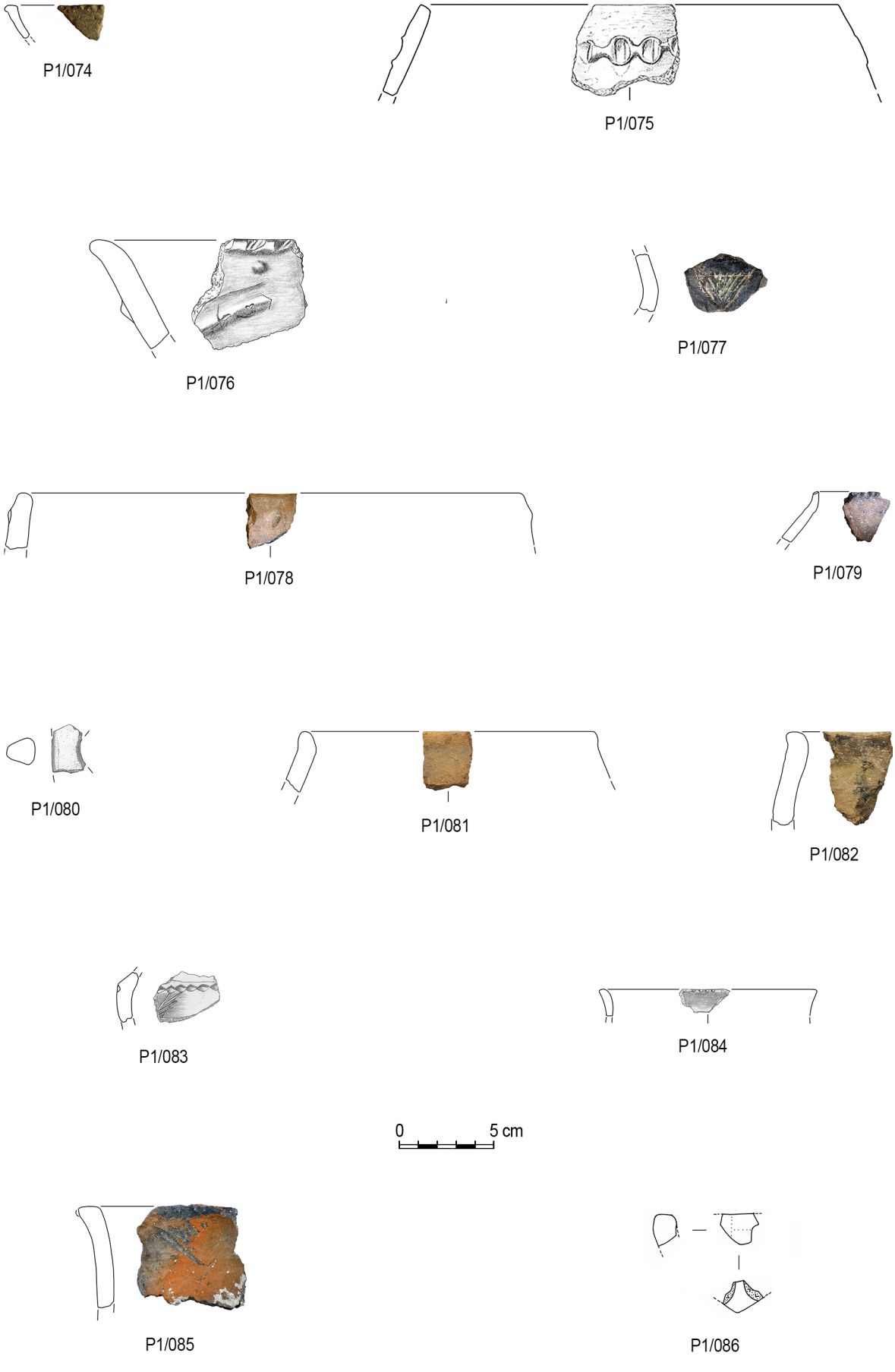


Plate 6. Site 1, survey: Bronze Age pottery (P1/074–P1/086)

SITE 1. Survey

Site 1, survey: Early Iron Age pottery

P 1/087. Site 1; pol. 188NK5. – Rim fragment of a roll rim bowl. – Dimensions (cm): m 21.2; wf 3.2; hf 1.8. – Fabric 35, untreated. – Dating: EIA (Basarabi/8th–7th c. BC).

P 1/088. Site 1; pol. 7SS5. – Rim fragment of a roll rim bowl. – Dimensions (cm): wf 1.7; hf 1.2. – Fabric 40, wide, oblique circumferential fluting and a vertically running band with scroll wheel decoration. Dating: EIA (Basarabi/8th–7th c. BC).

P 1/089. Site 1; pol. 187NK4. – Rim fragment of a roll rim bowl. – Dimensions (cm): wf 2.0; hf 1.8. – Fabric 34, oblique circumferential fluting. – Dating: EIA (Basarabi/8th–7th c. BC).

P 1/090. Site 1; pol. 187NK4. – Small rim fragment of open vessel. – Dimensions (cm): wf 1.5; hf 1.9. – Fabric 40, small band with scroll wheel incision. – Dating: EIA (Basarabi/8th–7th c. BC).

P 1/091. Site 1; pol. 7SS4. – Rim fragment of a roll rim bowl. – Dimensions (cm): m 17.1; wf 2.6; hf 1.3. – Fabric 40, wide, oblique circumferential fluting. – Dating: EIA (Basarabi/8th–7th c. BC).

P 1/092. Site 1; pol. 8LT2. – Rim fragment of a roll rim bowl. – Dimensions (cm): m 17.0; wf 3.2; hf 3.0. – Fabric 40, complex channeling in combination with incised bands made by scrolling wheel or stamping. A small hump on the belly of the vessel, which is covered entirely by the ornament. – Dating: EIA (Basarabi/8th–7th c. BC).

P 1/093. Site 1; pol. 8NK2. – Rim fragment of a roll rim bowl. – Dimensions (cm): m 14.8; wf 13.8; hf 1.6. – Fabric 40, oblique circumferential fluting and a small hump below the widest part of the vessel. – Dating: EIA (Basarabi/8th–7th c. BC).

P 1/094. Site 1; pol. 8NK2. – Rim fragment of a roll rim bowl. – Dimensions (cm): m 15.9; wf 3.8; hf 1.6. – Fabric 40, complex channeling in combination with incised bands made by scrolling wheel or stamping. – Dating: EIA (Basarabi/8th–7th c. BC).

P 1/095. Site 1; pol. 7LV4. – Rim fragment of a roll rim bowl. – Dimensions (cm): wf 4.5; hf 2.7. – Fabric 40, horizontal wide fluting framed by horizontal stamp bands. – Dating: EIA (Basarabi/8th–7th c. BC).

P 1/096. Site 1; pol. 7LT3. – Rim fragment of a roll rim bowl. – Dimensions (cm): m 22.3; wf 2.8; hf 2.1. – Fabric 40, complex channeling in combination with incised bands made by scrolling wheel or stamping. – Dating: EIA (Basarabi/8th–7th c. BC).

P 1/097. Site 1; pol. 182. – Rim fragment of a roll rim bowl. – Dimensions (cm): wf 4.8; hf 3.7. – Fabric 40, horizontal fluting. – Dating: EIA (Basarabi/8th–7th c. BC).

P 1/098. Site 1; pol. 183. – Rim fragment of a roll rim bowl. – Dimensions (cm): wf 3.5; hf 2.2. – Fabric 35, oblique fluting. – Dating: EIA (Basarabi/8th–7th c. BC).

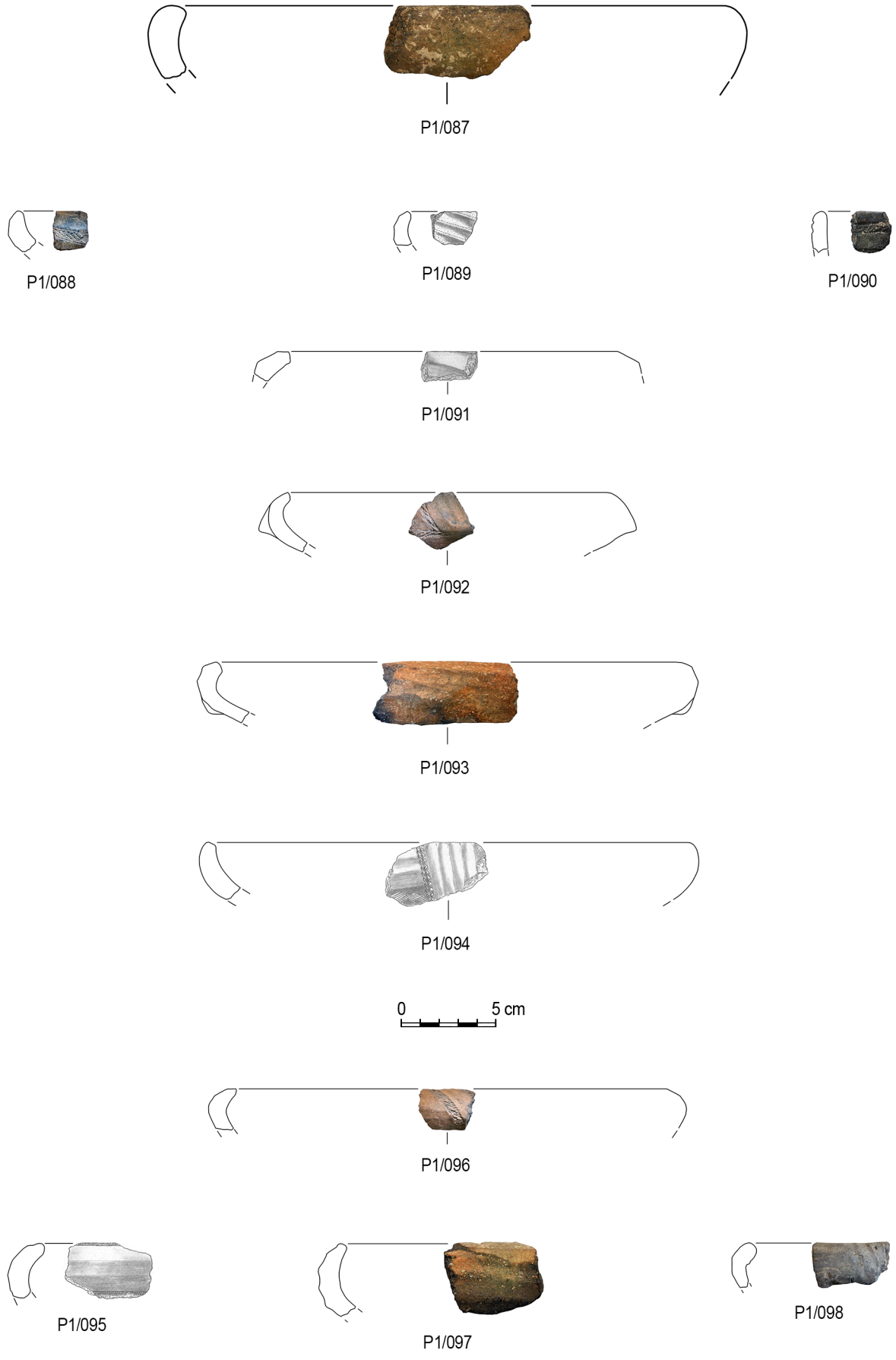


Plate 7. Site 1, survey: Early Iron Age pottery (P1/087–P1/098)

SITE 1. Survey

Site 1, survey: Early Iron Age pottery

P 1/099. Site 1; pol. 188SS4. – Rim fragment of an open vessel. – Dimensions (cm): wf 3.5; hf 3.6. – Fabric 35, embellished with roller wheel imprints. Individual triangles and lines. – Dating: EIA (Basarabi/8th–7th c. BC).

P 1/100. Site 1; pol. 7LT7. – Middle fragment of a bulbous vessel. – Dimensions (cm): wf 4.0; hf 1.8. – Fabric 40, remnants of scroll wheel decorations. – Dating: EIA (Basarabi/8th–7th c. BC).

P 1/101. Site 1; pol. 7LT2. – Rim fragment of a wide storage vessel. – Dimensions (cm): wf 4.6; hf 3.0. – Fabric 39, notched rim and wide bar with notches below the edge. – Dating: EIA (Basarabi/8th–7th c. BC).

P 1/102. Site 1; pol. 7LT1. – Middle fragment of a wide bowl with convex outward curving rim zone. – Dimensions (cm): wf 3.7; hf 4.5. – Fabric 29, stamped triangle in a line. – Dating: EIA.

P 1/103. Site 1; pol. 183. – Middle fragment of a storage vessel. – Dimensions (cm): wf 5.6; hf 3.7. – Fabric 34, horizontal dotted band. – Dating: EIA.

P 1/104. Site 1; pol. 15. – Small middle fragment of a fine bulbous vessel. – Dimensions (cm): wf 3.0; hf 2.2. – Fabric 28, remnants of scroll wheel or stamped bands. – Dating: EIA (Basarabi/8th–7th c. BC).

P 1/105. Site 1; pol. 181. – Middle fragment of a roll rim bowl. – Dimensions (cm): wf 3.5; hf 3.0. – Fabric 40, horizontal fluting combined with a band of scroll wheel decoration. – Dating: EIA (Basarabi/8th–7th c. BC).

P 1/106. Site 1; pol. 183. – Rim fragment of a wide storage vessel. – Dimensions (cm): wf 4.5; hf 5.1. – Fabric 39, notched protruding rim and wide bar with notches below the edge. – Dating: EIA.

P 1/107. Site 1; pol. 189SC1. – Rim fragment of a roll rim bowl. – Dimensions (cm): wf 2.5; hf 2.2. – Fabric 40, horizontally fluting. – Dating: EIA (Basarabi/8th–7th c. BC).

P 1/108. Site 1; pol. 188Y4. – Rim fragment of a closed bowl. – Dimensions (cm): wf 1.8; hf 2.2. – Fabric 40, undecorated. – Dating: EIA.

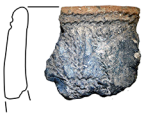
P 1/109. Site 1; pol. 187Y5. – Rim fragment of a roll rim bowl. – Dimensions (cm): wf 2.5; hf 2.8. – Fabric 28, small hump below the widest part of the body. – Dating: EIA (Basarabi/8th–7th c. BC).

P 1/110. Site 1; pol. 7SS4. – Rim fragment of a wide storage vessel. – Dimensions (cm): d 40.0; wf 3.6; hf 2.9. – Fabric 39, notched protruding rim and wide bar with notches below the edge. – Dating: EIA.

P 1/111. Site 1; pol. 8NK2. – Middle fragment of a fine vessel. – Dimensions (cm): wf 3.6; hf 3.5. – Fabric 28, remnants of a buckle, decorated with complex stamped motifs, a vertically zone is left out. – Dating: EIA (Basarabi/8th–7th c. BC).

P 1/112. Site 1; pol. 7SS6. – Middle fragment of a large bulbous vessel. – Dimensions (cm): wf 6.3; hf 5.9. – Fabric 39, two parallel incised lines. – Dating: EIA.

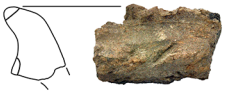
P 1/113. Site 1; pol. 187NK4. – Rim fragment of a large vessel with a narrow mouth. – Dimensions (cm): wf 3.6; hf 2.3. – Fabric 34, hatched rim. – Dating: EIA.



P1/099



P1/100



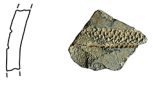
P1/101



P1/102



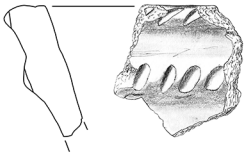
P1/103



P1/104



P1/105



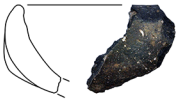
P1/106



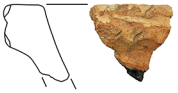
P1/107



P1/108



P1/109



P1/110

0 5 cm



P1/111



P1/112



P1/113

Plate 8. Site 1, survey: Early Iron Age pottery (P1/099–P1/113)

SITE 1. Survey

Site 1, survey: Early Iron Age pottery

P 1/114. Site 1; pol. 8NK1. – Rim fragment of a vessel with a narrow mouth. Dimensions: wf 3.8; hf 2.3. – Fabric 31, hatched rim. – Dating: EIA.

P 1/115. Site 1; pol. 8NK1. – Middle fragment of a fine vessel. Dimensions: wf 3.0; hf 2.6. – Fabric 28, complex stamped motif filled with parallel scroll wheel lines. – Dating: EIA (Basarabi/8th–7th c. BC).

P 1/116. Site 1; pol. 7LT6. – Middle fragment. Dimensions: wf 3.0; hf 2.0. – Fabric 40, remnants of scroll wheel decorations, crossing lines. – Dating: EIA (Basarabi/8th–7th c. BC).

P 1/117. Site 1; pol. 182. – Middle fragment. Dimensions: wf 4.2; hf 3.6. – Fabric 40, scroll wheel lines in combination with channeling. – Dating: EIA (Basarabi/8th–7th c. BC).

P 1/118. Site 1; pol. 183. – Fragment of a handle pin. Dimensions: wf 3.7; hf 3.4. – Fabric 28, stepped on the lower (upper?) side. – Dating: EIA (Gava-style).

P 1/119. Site 1; pol. 8LT3. – Ribbon handle. Dimensions: wf 2.5; hf 4.1. – Fabric 40, parallel flutings. – Dating: EIA (Basarabi/8th–7th c. BC)

P 1/120. Site 1; pol. 8LT3. – Ribbon handle. Dimensions: wf 1.6; hf 4.4. – Fabric 40, parallel flutings. – Dating: EIA (Basarabi/8th–7th c. BC).

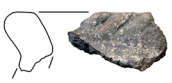
P 1/121. Site 1; pol. 8LT2. – Ribbon handle. Dimensions: wf 1.6; hf 2.3. – Fabric 40, parallel flutings. – Dating: EIA (Basarabi/8th–7th c. BC).

P 1/122. Site 1; pol. 7LV7. – Ribbon handle. Dimensions: wf 2.2; hf 2.7. – Fabric 39, D-shaped cross-section, undecorated. – Dating: EIA.

P 1/123. Site 1; pol. 182. – Ribbon handle. – Dimensions: wf 4.1; hf 5.2. – Fabric 40, remnants of stamped decoration. – Dating: EIA (Basarabi/8th–7th c. BC).

P 1/124. Site 1; pol. 182. – Ribbon handle. – Dimensions: wf 4.9; hf 9.5. – Fabric 40, parallel flutings. – Dating: EIA (Basarabi/8th–7th c. BC).

P 1/125. Site 1; pol. 7NK7. – Round handle pin. – Dimensions: wf 4.0; hf 5.0. – Fabric 40, undecorated. – Dating: EIA.



P1/114



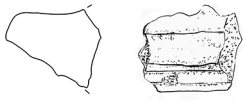
P1/115



P1/116



P1/117



P1/118



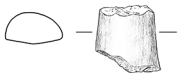
P1/119



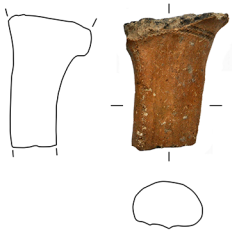
P1/120



P1/121



P1/122



P1/123

0 5 cm



P1/124



P1/125

Plate 9. Site 1, survey: Early Iron Age pottery (P1/114–P1/125)

SITE 1. Survey

Site 1, survey: Late Iron Age pottery

P 1/126. Site 1; pol. 182. – Large crater, rim fragment. Massive rim, slanted on the exterior. – Dimensions (cm): m 35; hf 4.1; wf 14.2. – Fabric 49; exterior grey, polished; interior greyish black; dark greyish core. – Parallels: similar to Moscalu 1983, type 23a pl. 86,4 (Alexandria; 6th–5th c. BC). – Dating: LIA.

P 1/127. Site 1; pol. 6. – Crater; rim fragment. Outward curving, short rim with thickened lip; spherical body. – Dimensions (cm): m 28; hf 2.3; wf 4.5. – Fabric 49. Grey fabric, obviously burnished (rolled). Dark grey core. – Parallels: probably rim of a low crater like Moscalu 1983, type 23a pl. 96. – Dating: LIA (5th–4th c. BC?).

P 1/128. Site 1; pol. 187SC3. – Crater, rim fragment. Slightly slanted, thickened rim with flat upper part. – Dimensions (cm): m 32; h 2.4; wf 4.1. – Fabric 49. Olive-grey surface; grey core. – Parallels: Moscalu 1983, type 23/g pl. 98,4 (Ravna; 6th c. BC); 102,4 (Alexandria – Pod; 2nd half of 7th–6th c. BC). – Dating: LIA (ca. 6th–5th c. BC).

P 1/129. Site 1; pol. 23. – Small crater, rim fragment. Slightly slanted, thickened rim; steeply sloped wall. – Dimensions (cm): m 18; hf 2.1; wf 2.7. – Fabric 51. – Parallels: Moscalu 1983, type 23a pl. 96.4 (Ravna; 6th–5th c. BC). 5 (Braničevo; 4th c. BC). – Dating: LIA (6th–4th c. BC).

P 1/130. Site 1; pol. 188Y1. – Bowl, rim fragment. Outward curving, relatively narrow gripper rim. – Dimensions (cm): m 27; hf 2.2; wf 3.7. – Fabric 52. Fine sand; rolled surface. – Parallels: Върбанов 2013b, no. 105 pl. 3,50 (2nd–1st c. BC). – Dating: LIA (2nd–1st c. BC).

P 1/131. Site 1; pol. 187Y4. – Bowl, wall fragment; S-shaped curve with part of a thickened rim. – Dimensions (cm): hf 3.8; wf 6.2. – Fabric 50. Dark olive-grey; matt burnished. – Parallels: Вагалински 2002, bowls type 3 var. 1 КУ 176 (Valchedram; 1st c. BC/1st c. AD); Върбанов 2013b, no. 206 pl. 4,34 (2nd–1st c. BC). Moscalu 1983, type 16/d pl. 84,10 (Murighiol; 4th c. BC) is probably a precursor of this type. – Dating: LIA (2nd–1st c. BC).

P 1/132. Site 1; pol. 16. – Bowl, S-shaped wall fragment. Similar to p1/131 but more upright. – Dimensions (cm): hf 4.3; wf 4.7. – Fabric 53. Red brown; fine with whitish inclusions. Thin whitish painting on the surface; dark brown spots from secondary firing. – In regarding the basic form of the vessel and parallels in grey fabric, cf. cat. P 1/131. – Dating: LIA (2nd–1st c. BC/1st c. AD).

P 1/133. Site 1; pol. 187Y4. – Bowl, unprofiled rim fragment; slightly incurving. Flattened, slightly inclined upper side. – Dimensions (cm): m 13; hf 2.4; wf 3.2. – Fabric 50; blackish grey. – Parallels: Moscalu 1983, type 10d pl. 80,6 (Rasova; 6th–5th c. BC). 8 (Branicevo; 5th c. BC). – Dating: LIA (6th–5th c. BC).

P 1/134. Site 1, pol. 187NK3. – Bowl, rim fragment. S-shaped profile with thickened, slanted rim. – Dimensions (cm): m 32; hf 3.8; wf 4.7. – Fabric 51. Light grey surface; rolled. – Parallels: similar to Moscalu 1983, type 16a pl. 85,2 (Bugeac; 4th c. BC). 8 (Nalbant; 5th–4th c. BC). – Dating: LIA (5th–4th c. BC).

P 1/135. Site 1; pol. 7LT3. – Bowl, rim fragment. Slightly inwardly turned upper part, with a narrow strip on the exterior. The rim is beveled towards the interior. – Dimensions (cm): m 18; hf 3.9; wf 8.1. – Fabric 50. Dark olive-grey to black-grey surface; burnished. Dark olive-grey core. – Parallels: no exact parallel. For the similar type of the vessel cf. Crişan 1969, pl. 35, 1.9 (Ciumeşti; 3rd–1st c. BC). – Dating: LIA (3rd–1st c. BC).

P 1/136. Site 1 (offsite); pol. 394. – Bowl, rim fragment. Short slanted rim, steep wall with sharp angle towards the bottom. – Dimensions (cm): m ca. 22; hf 3.1; wf 4.4. – Fabric 51. Rolled surface. – Parallels: cf. Върбанов 2013b, no. 74; 78; 83 pl. 3,19.23.28 with similar profiles of the vessel (2nd–1st c. BC). The type exists as handmade variant as well, cf. Върбанов 2013a, no. 265 pl. 9,31 (2nd–1st c. BC). – Dating: LIA (2nd–1st c. BC).

P 1/137. Site 1; pol. 189NK5. – Pot or storage vessel; rim fragment. Slanted rim, thickened in the exterior; rounded lip. Conically widened upper part of the vessel. – Dimensions (cm): m 18; hf 3.3; wf 4.9. – Fabric 50. Greyish brown fracture; dark grey surface. – Parallels: no exact parallel. probably similar type like Върбанов 2013b, no. 373 pl. 9,1. – Dating: LIA.

P 1/138. Site 1; pol.187. – Fruit bowl; fragment of the thick-walled foot. – Dimensions (cm): hf 4.1; b 17; wf 5.8. – Fabric 52 (slow wheel?); exterior olive brown to dark grey, a little bit polished; interior dark grey to olive-greyish brown, slightly smoothed; black core. – Parallels: cf. Върбанов 2013a, no. 369; 373 pl. 12,33.37. – Dating: LIA.

P 1/139. Site 1; pol. 26. – Pot, wall fragment with fingerprinted strip. – Dimensions (cm): hf 4.3; wf 4.9. – Fabric 55 greyish-brown, slightly rough surface; blackish-grey core; brittle and slightly fissured fracture. – Exact determination of type and dating not possible. – Dating: LIA.

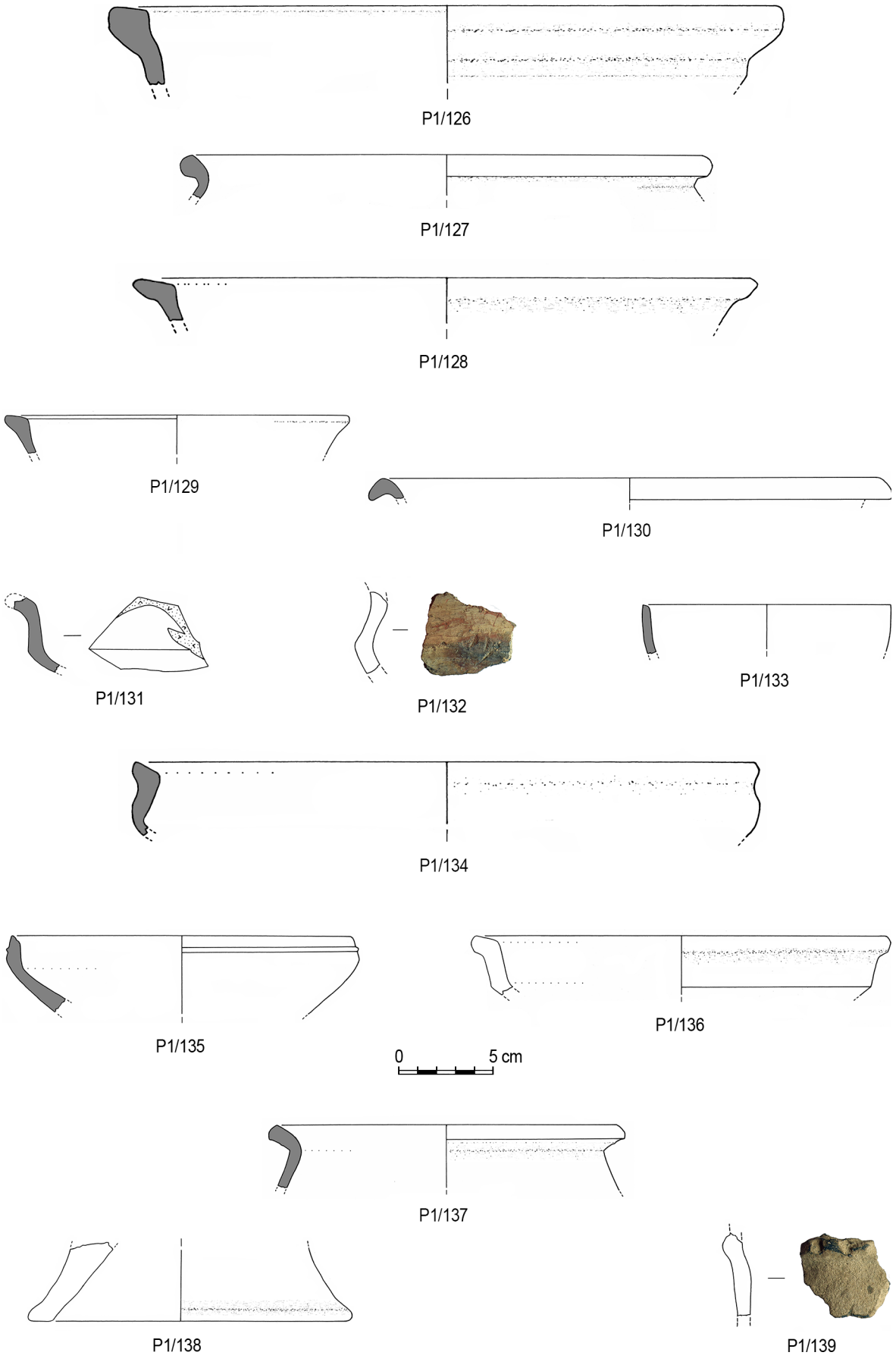


Plate 10. Site 1, survey: Late Iron Age pottery (P1/126–P1/139)

SITE 1. Survey

Site 1, survey: Roman pottery

P 1/140. Site 1; pol. 13. – Amphora, rim fragment. Slightly flared and thickened rim, undercut on the exterior. Dimensions (cm): m 17; hf 5.6; wf 6.6. – Reddish brown, sandy fabric (with some dark inclusions); fabric-coloured engobe. – Parallels: Зеест 1960, type 85; Hayes 1983, type 35; 36; Conrad 2007a, cat. 753. – Dating: RP (2nd–3rd c.).

P 1/141. – Site 1; pol. 188. – Amphora with beaded rim; undercut exterior. Nearby, a handle fragment was found which most likely belongs to this vessel. – Dimensions (cm): m ca. 14; hf 9.4; wf 7.8. – Reddish brown to dark reddish brown, sandy fabric; greyish to olive-brown core; fabric-coloured engobe. – Cf. cat. P 1/140. – Dating: RP.

P 1/142. Site 1 (offsite), pol. 392. – Amphora, rim fragment. Funnel-shaped mouth with beaded lip. – Dimensions (cm): m 14; hf 2.3; wf 5.6. – Fabric 59. Rolled surface. – Parallels: Falkner 1999, cat. 898 (mid-2nd c.); Conrad 2007a, cat. 757 (2nd half of 3rd c.). – Dating: RP (2nd–1st half of 4th c.).

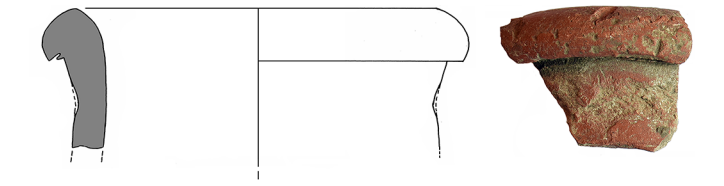
P 1/143. Site 1; pol. 18. – Plate, rim fragment. Horizontal rim with an attached narrow strip on the top in interior; sloping wall. – Dimensions (cm): m 26; hf 3; wf 7.5. – Fabric 58. – Parallels: Falkner 1999, cat. 393; 394; Conrad 2007a, cat. 788 (2nd half of 3rd c.). – Dating: RP (2nd–1st half of 4th c.).

P 1/144. Site 1; pol. 188SC2. – Bowl, rim fragment. Thickened rim with rounded profile. Open body form with rounded wall. – Dimensions (cm): m 21; hf 2.6; wf 3.5. – Fabric 59. Rolled surface. – Parallels: Falkner 1999, cat. 630. – Dating: RP.

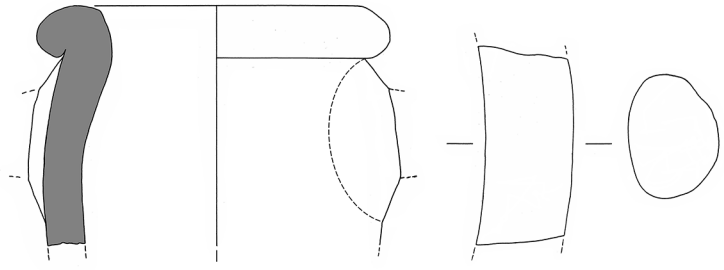
P 1/145. Site 1; pol. 8. – Small bowl or plate, fragment. Vertical upper part with unprofiled, rounded lip; two horizontal grooves on the exterior. Curved wall in the lower part. – Dimensions (cm): m 15; hf 3.7; wf 5.8. – Fabric 58. – Parallels: similar to Falkner 1999, cat. 534; 537; 547; Conrad 2007a, cat. 888 (1st half of 4th c.). – Dating: RP (2nd–1st half of 4th c.).

P 1/146. Site 1; pol. 13. – Bowl, rim fragment. Short, slanted rim with flat groove on the interior. Vertical, slightly curved and relatively thin side wall. Stylised floral barbotine decoration and incised groove on the exterior; probably sharp bend to the lower part of vessel. – Dimensions (cm): m ca. 28; hf 3.7; wf 5.8. – Fabric 58. – Parallels: Sultov 1985, bowls type 1 pl. 28,7; Falkner 1999, cat. 467 (2nd c.); Conrad 2007a, 834 (3rd c.); 921 (1st half of 4th c.). – Dating: RP (2nd–1st half of 4th c.).

P 1/147. Site 1; pol. 187NK5. – Bowl, rim fragment. Slightly incurved upper part of the vessel; rounded lip with a flat groove on the exterior bottom part of vessel. Two rows of narrow notches, applied by rouletting are preserved. – Dimensions (cm): m 22; hf 2.1; wf 3.5. – Fabric 58. – Parallels: no exact parallel. For similar rim form, cf. Conrad 2007a, cat. 822. – Dating: RP.



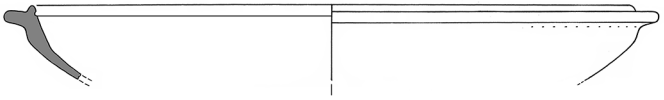
P1/140



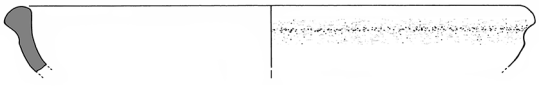
P1/141



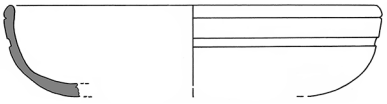
P1/142



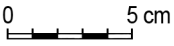
P1/143



P1/144

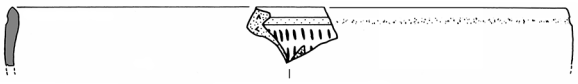


P1/145





P1/146



P1/147

Plate 11. Site 1, survey: Pottery of the Roman period (P1/140–P1/147)

SITE 1. Survey

Site 1, survey: Roman pottery

P 1/148. Site 1; pol. 12. – Bowl, fragment of the stand ring. – Dimensions (cm): hf 1.9; b (stand ring) 8; wf 3.6. – Fabric 58. – Dating: RP (2nd–1st half of 4th c.)

P 1/149. Site 1; pol. 187LV2. – Plate or bowl; fragment of the stand ring. – Dimensions (cm): hf 1.7; b (stand ring) 7; wf 3.2. – Terra Sigillata (gallic?). Dark brick-red fracture; tight dark red coat. – Dating: RP (1st–3rd c.)

P 1/150. Site 1; pol. 189LV1. – Crater (or cauldron?); rim fragment. – Dimensions (cm): m 20; hf 2.2; wf 5.3. – Fabric 59; badly adhering slip. – Parallels: Falkner 1999, cat. 687. Dating: RP.

P 1/151. Site 1; pol. 9. – Bowl, rim fragment. Thickened rim with flat upper side, slightly slanted towards interior. – Dimensions (cm): m 20; hf 1.7; wf 4.8. – Fabric 63. – Parallels: Falkner 1999, cat. 266; 272 (very likely residual). – Dating: RP (2nd–1st half of 4th c.)

P 1/152. Site 1; pol. 18. – Pot, rim fragment. Slanted rim, beaded to the exterior; shallow groove to the interior. – Dimensions (cm): m 26; hf 2.7; wf 4.8. – Fabric 64. Grey, very sandy fabric; light grey core. – Parallels: Falkner 1999, cat. 81–83 (very likely residual). – Dating: RP (2nd half of 2nd/3rd c.).

P 1/153. Site 1; pol. 189SS3. – Pot, rim fragment. Slightly out-curved rim with strongly beaded profile; short neck kinked to the shoulder. – Dimensions (cm): m 20; h 3.8; wf 6.5. – Fabric 65. – Parallels: Sultov 1985, pot type 1 pl. 43,1. – Dating: RP (2nd–3rd c.).

P 1/154. Site 1; pol. 23. – Pot, rim fragment. Relatively short, slanted and beaded rim with a shallow groove on the interior. – Dimensions (cm): m ca. 14; hf 3.3; wf 3.5. – Fabric 65. exterior grey, greyish-brown, interior reddish brown, grey core; coarse sandy temper. – Parallels: Falkner 1999, cat. 97; 103. – Dating: RP (2nd–1st half of 4th c.).

P 1/155. Site 1; pol. 188LV3. – Pot, rim fragment. Slanted, flat rim; conical upper part of the body. – Dimensions (cm): m 21; hf 2.4; wf 3.5. – Fabric 63. Light pink fracture; sooted rim. – No parallel. – Dating: RP (2nd–1st half of 4th c.).

P 1/156. Site 1; pol. 189SC3. – Pot, rim fragment. Slightly slanted, thickened rim; short, kinked neck. – Dimensions (cm): m 18; hf 2.0; wf 3.1. – Fabric 63; sooted rim. – No parallel. – Dating: RP (2nd–1st half of 4th c.).

P 1/157. Site 1; pol. 187SC5. – Beaker-like pot; rim fragment. – Dimensions (cm): m 17; hf 2.0; wf 7.7. – Fabric 66. – Parallels: probably an early variant of the beaker-like pots, cf. Conrad 2007a, 220–221 fig. 12; 13. – Dating: RP.

Site 1, survey: Late Roman pottery

P 1/158. Site 1; pol. 188NK5. – Amphora, rim fragment. Funnel-shaped mouth; thickened, rounded mouth. – Dimensions (cm): m 17; hf 4.8; wf 4.8. – Reddish brown, fine. Light brown engobe. – Parallels: Riley 1979, LRA2; Böttger 1982, amphora I1. – Dating: LRP (end of 4th–1st half of 5th c.).

P 1/159. Site 1; pol. 26. – Amphora, foot. Slightly elongated, rounded and thickened. – Dimensions (cm): hf 4.0; b (foot) 3. – Light reddish brown, greyish core. Very coarse temper. – Parallels: very likely foot of Böttger 1982, amphora I6; Кузманов 1985, type 10; Dobreva 2017, 267–268. – Dating: LRP.

P 1/160. Site 1; pol. 22. – Bowl, rim fragment. Thickened and beaded rim, slightly inclined towards the interior. – Dimensions (cm): m 18; hf 1.9; wf 5. – Fabric 71. – Parallels: Falkner 1999, cat. 272 (buff coloured ware). – Dating: LRP.

P 1/161. Site 1; pol. 8LV3. – Pot, rim fragment. Slanted rim with flat upper side and a grooved underside. – Dimensions (cm): m 18; hf 1.7; wf 5.5. – Fabric 72; dark grey surface. – Parallels: cf. Böttger 1982, pot type 3. – Dating: LRP.

P 1/162. Site 1; pol. 15. – Lid, rim fragment. Inclined rim, banded interior. – Dimensions (cm): m 19; hf 2.9; Wf 6.5. – Fabric 71; blackish grey. – Parallels: cf. for example Böttger 1982, cat. 510 (per. C; 1st half of 5th c.). – Dating: LRP.

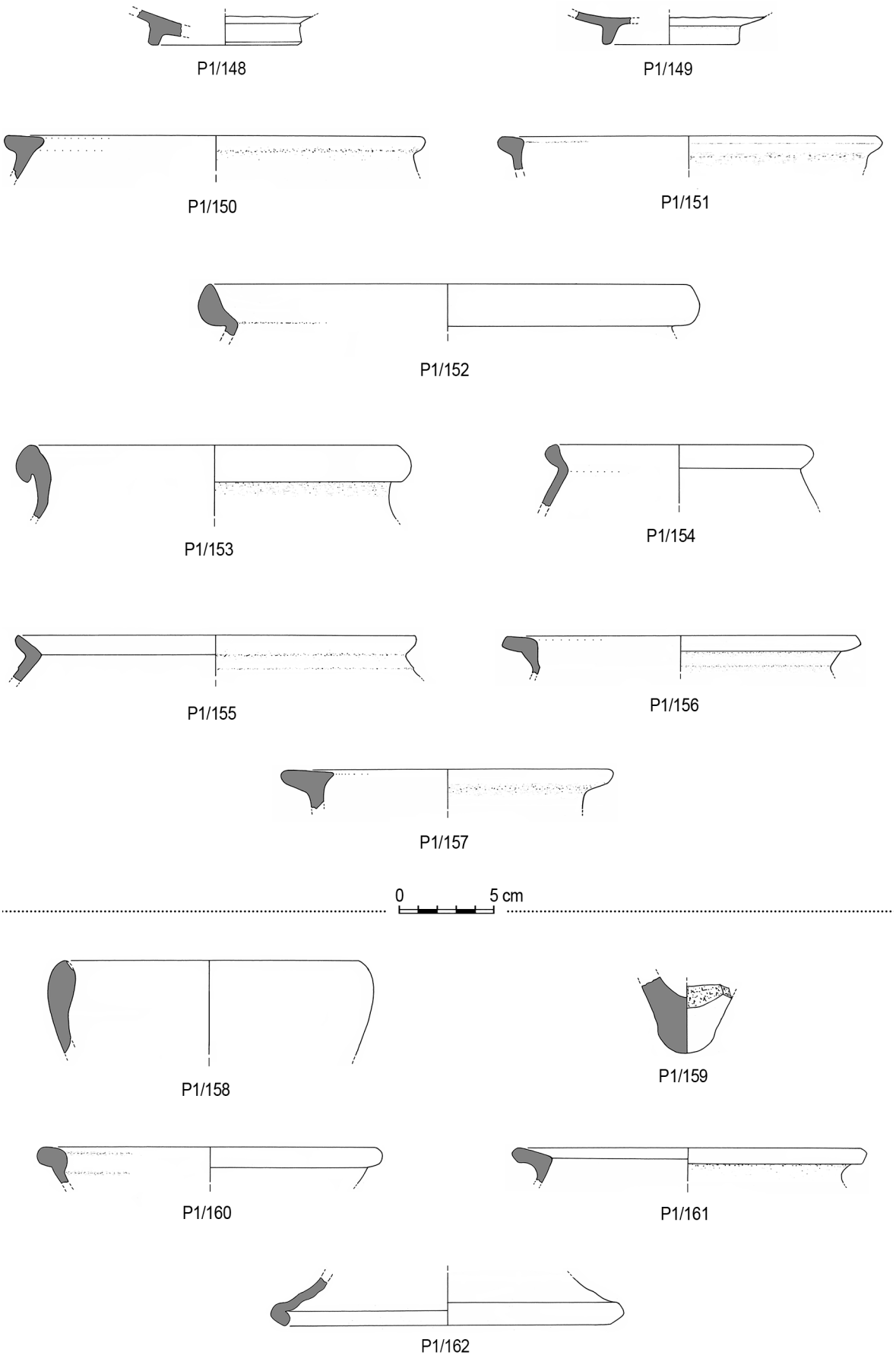


Plate 12. Site 1, survey: Pottery of the Roman period (P1/148–P1/157); Late Roman pottery (P1/158–P1/162)

SITE 1. Survey

Site 1, survey: Early Medieval pottery

P 1/163. Site 1; pol. 188Y3. – Pot, rim fragment. Short, sharply outcurving rim. Horizontally incised lines on the shoulder of the vessel. – Dimensions (cm): m 14; hf 3.1; wf 5.2. – Fabric 77; sandy surface. – Parallels: Wendel 1986, type Krivina pl. 34,6.11; group 5 pl. 27,6.8. – Dating: EMA.

P 1/164. Site 1; pol. 188LV3. – Pot, rim fragment. Simply profiled rim, outcurving in exterior. – Dimensions (cm): m 17; hf 3.6; wf 6.0. – Fabric 75. – Parallels: Wendel 1986, type 3 pl. 29,4.7. – Dating: EMA.

P 1/165. Site 1; pol. 188SC1. – Pot, rim fragment. Wide rim with thickened and angularly profiled lip. Incised horizontal line on the neck; narrow wave band on the upper part of the shoulder. – Dimensions (cm): m 28; hf 3.6; wf 5.5. – Fabric 75. – Parallels: Wendel 1986, type 3 pl. 29,1.6. – Dating: EMA.

P 1/166. Site 1; pol. 8SS2. – Pot, rim fragment of a small, thin-walled pot. Out-curving rim, undercut exterior. Traces of an incised waved band on the shoulder. – Dimensions (cm): m 12; hf 2.8; wf 6. – Fabric 77; sooted rim. – Parallels: Wendel 1986, type 2 pl. 29,10. – Dating: EMA.

P 1/167. Site 1; pol. 18. – Large pot, rim fragment. Spherical body; short, relatively sharp outcurving and steeply slanted rim with thickened, rounded lip. – Dimensions (cm): m 27; hf 3.5; wf 7. – Fabric 76. – No parallel. – Dating: EMA.

P 1/168. Site 1; pol. 188SC4. – Pot, rim fragment. Beaded rim, slightly outcurving. – Dimensions (cm): m 12; hf 3; wf 5.8. – Fabric 80. – Parallels: Wendel 1986, 143 pl. 36.13.14. – Dating: EMA.

P 1/169. Site 1; pol. 187LV5. – Pot, rim fragment. Beaded rim with small undercut, with a slight outward lean. – Dimensions (cm): m 21; hf 3.6; wf 2.5. – Fabric 85. – Parallels: Wendel 1986, grey pottery 144 pl. 36,31.32; Рашев 2014, 186–188 group C; Дончева–Петкова 2016, 74–84. – Dating: EMA.

P 1/170. Site 1 (offsite), pol. 392. – Pot, rim fragment. Spherical body; very slight outward lean, beaded rim. – Dimensions (cm): m 15; hf 3.6; wf 5.2. – Fabric 83. Light greyish brown fabric with light reddish brown core. Slightly burnished surface. – Cf. cat. P 1/169. – Dating: EMA.

P 1/171. Site 1; pol. 188Y3. – Pot, rim fragment. Outward lean, beaded rim. – Dimensions (cm): hf 4.8; wf 4.1. – Fabric 85. Reddish grey brown fracture with light ochre grey core; some white inclusions. ochre brown, polished surface. – Cf. cat. P 1/169. – Dating: EMA.

P 1/172. Site 1; pol. 188Y3. – Pot, rim fragment. Outward lean beaded rim. – Dimensions (cm): hf 3.6; wf 3.7. – Fabric 83 (cf. cat. P 1/171). – Cf. cat. P 1/169. – Dating: EMA.

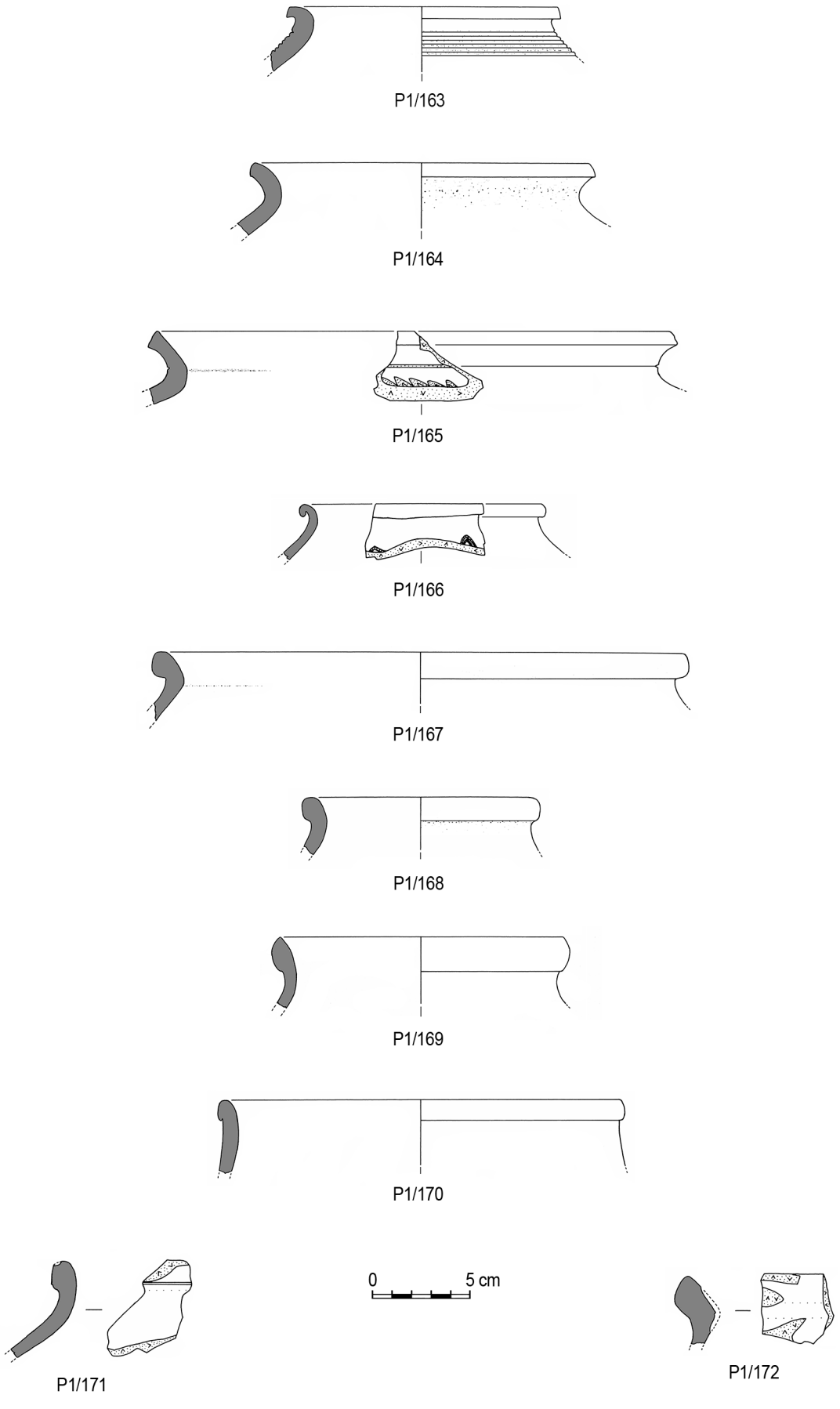


Plate 13. Site 1, survey: Early Medieval pottery (P1/163–P1/172)

SITE 1. Excavations

Trench 1.1-W/E, features 1.1.6/15 (Late Iron Age ditch)

Features 1.1.6/15: Neolithic pottery

P 1/173. Site 1; tr. 1.1-E; ft. 1.1.6; niv. 26.70. – Middle fragment of a large bulbous vessel. – Dimensions (cm): wf 5.4; hf 5.3. – Fabric 3, incised decoration, lines framed by small triangles. – Dating: LNL (Vădastra).

P 1/174. Site 1; tr. 1.1-E; ft. 1.1.6; niv. 26.75. – Middle fragment of the upper conical part of a vessel. – Dimensions (cm): wf 5.6; hf 9.5. – Fabric 3, incised decoration, lines framed by small triangles. – Dating: LNL (Vădastra).

P 1/175. Site 1; tr. 1.1-E; ft. 1.1.6; niv. 26.71. – Middle fragment of the upper conical part of a vessel. – Dimensions (cm): wf 5.6; hf 6.1. – Fabric 3, incised decoration, lines framed by small triangles. – Dating: LNL (Vădastra).

P 1/176. Site 1; tr. 1.1-E; ft. 1.1.6; niv. 26.62. – Middle fragment. – Dimensions (cm): wf 5.7; hf 7.3. – Fabric 3, incised lines. – Dating: LNL (Vădastra).

P 1/177. Site 1; tr. 1.1-E; ft. 1.1.6; niv. 26.64. – Middle fragment of a large vessel with straight walls. – Dimensions (cm): wf 14.0; hf 8.6. – Fabric 3, complex zig-zag-motif in impasto technique. – Dating: LNL (Vădastra).

P 1/178. Site 1; tr. 1.1-E; ft. 1.1.6; niv. 26.65. – Middle fragment of a fine vessel. – Dimensions (cm): wf 4.6; hf 5.4. – Fabric 3, incised curvilinear motif with white impasto. – Dating: LNL (Vădastra).

P 1/179. Site 1; tr. 1.1-E; ft. 1.1.6; niv. 26.70. – Middle fragment of a fine vessel. – Dimensions (cm): wf 4.9; 6.8. – Fabric 3, complex spiral motifs in impasto technique. – Dating: LNL (Vădastra).

P 1/180. Site 1; tr. 1.1-E; ft. 1.1.6; niv. 26.68. – Rim fragment of a large open vessel. – Dimensions (cm): wf 4.8; hf 6.3. – Fabric 3, straight crossing scratches, which extend over the edge of the vessel. – Dating: LNL (Vădastra).

P 1/181. Site 1; tr. 1.1-E; ft. 1.1.6; niv. 26.63. – Almost entire profile of a large carinated bowl, only the bottom is missing. – Dimensions (cm): m 26.5; wf 12.3; hf 12.4. – Fabric 44, linear scratches. On the shoulder arched motifs; on the lower part parallel lines, the in between spaces are filled differently with remnants of (red?) colour, resulting in bands. – Dating: LNL (North Bulgarian LNL).

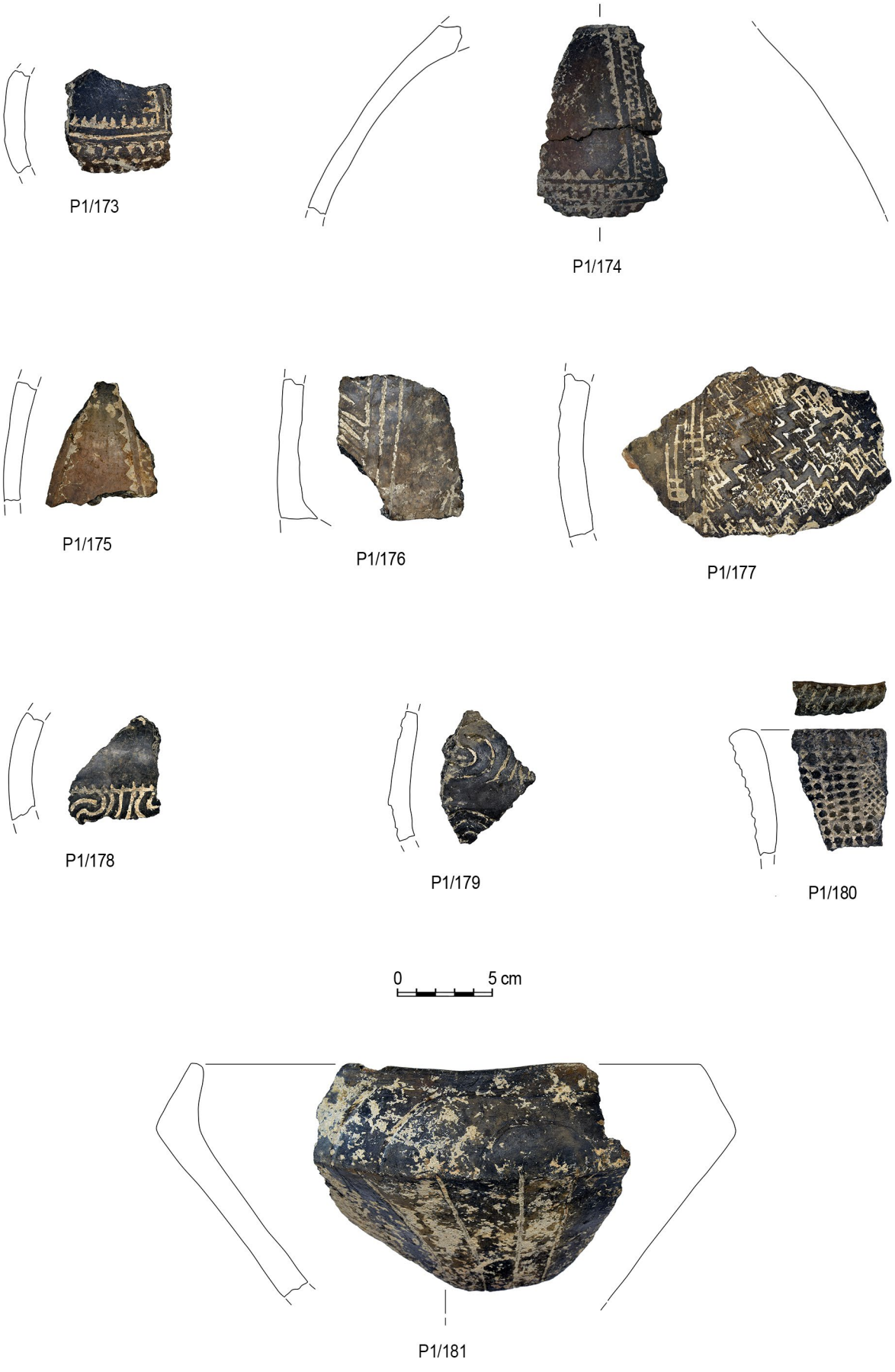


Plate 14. Site 1, excavations: Late Neolithic pottery (P1/173–P1/181)

SITE 1. Excavations

Trench 1.1-W/E, features 1.1.6/15 (Late Iron Age ditch)

Features 1.1.6/15: Neolithic pottery

P 1/182. Site 1; tr. 1.1-E; ft. 1.1.6; niv. 26.58. – Rim fragment of a spherical pot. – Dimensions (cm): m 16.0; wf 7.8; hf 5.3. – Fabric 6, barbotine with small structuring vertical lines. – Dating: LNL.

P 1/183. Site 1; tr. 1.1-E; ft. 1.1.6; niv. 26.67. – Middle piece of a jug-like large vessel, bottom and rim missing. – Dimensions (cm): wf 8.3; hf 7.8. – Fabric 46, polished, on the shoulder fine flutings framing a buckle in concentric arches. – Dating: LNL (North Bulgarian LNL).

P 1/184. Site 1; tr. 1.1-E; ft. 1.1.6; niv. 26.66. – Middle piece of a large pot with conical lower and cylindrical upper part, bottom and rim missing. – Dimensions (cm): wf 13.8; hf 10.9. – Fabric 9, remnants of fine fluting on the shoulder. – Dating: LNL (North Bulgarian LNL).

P 1/185. Site 1; tr. 1.1-E; ft. 1.1.6; niv. 27.00–26.76. – Lower part of a large vessel stand. The cross section is slightly squared. – Dimensions (cm): wf 8.5; hf 9.0. – Fabric 6, complex impasto decorations with white paste and remnants of red colour. – Dating: LNL (Vădastra).

P 1/186. Site 1; tr. 1.1-E; ft. 1.1.6; pl. 6; niv. 26.24. – Fragment of a spherical lid. – Dimensions (cm): wf 5.4; hf 4.2. – Fabric 6, fine impasto decorations and polished surface. Along the rim there is a row of small squares with metope motifs above them. – Dating: LNL (Vădastra).

P 1/187. Site 1; tr. 1.1-E; ft. 1.1.6; pl. 6; niv. 26.24. – Cylindrical and slightly concavely curved rim of a huge storage vessel. – Dimensions (cm): m 20.1; wf 21.2; hf 7.6. – Fabric 5, barbotine with vertical finger grooves. – Dating: LNL.

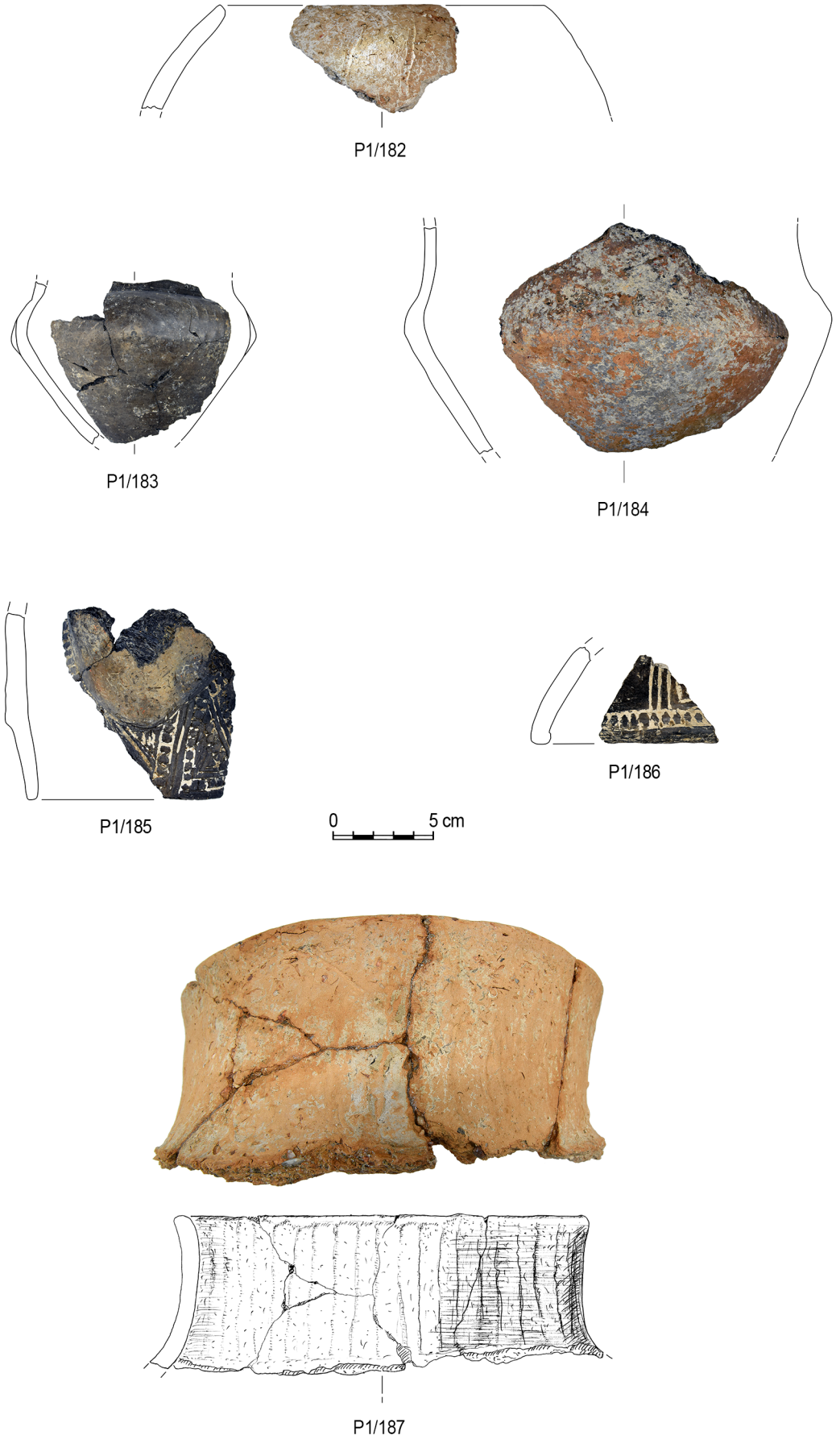


Plate 15. Site 1, excavations (trench 1.1-W/E, features 1.1.6/15): Late Neolithic pottery (P1/172–P1/187)

SITE 1. Excavations

Trench 1.1-W/E, features 1.1.6/15 (Late Iron Age ditch)

Features 1.1.6/15: Neolithic pottery

P 1/188. Site 1; tr. 1.1-E; ft. 1.1.6; niv. 26.76–26.67. – Cylindrical neck of a large vessel. – Dimensions (cm): m 12.9; wf 7.1; hf 4.7. – Fabric 6, complex scratched motifs all over the surface of the fragment. – Dating: LNL.

P 1/189. Site 1; tr. 1.1-E; ft. 1.1.6; niv. 26.00–25.83. – Rim fragment of a large vessel with straight walls. – Dimensions (cm): wf 5.5; hf 8.2. – Fabric 6, zig-zag pattern in chip carving technique with impasto. – Dating: LNL (Vădastra).

P 1/190. Site 1; tr. 1.1-W; ft. 1.1.15; niv. 26.38–26.23. – Middle fragment of a small bulbous jug with a vertically prolonged hump. – Dimensions (cm): wf 4.1; hf 4.3. – Fabric 9, thin incised lines forming curvilinear motifs with small incisions like musical notes. – Dating: LNL.

P 1/191. Site 1; tr. 1.1-W; ft. 1.1.15; niv. 26.38–26.20. – Biconical pot with a conical neck, lip and bottom missing. – Dimensions (cm): wf 8.6; hf 7.9. – Fabric 46, polished, on the shoulder fine oblique flutings in changing directions. – Dating: LNL (North Bulgarian LNL).

P 1/192. Site 1; tr. 1.1-W; ft. 1.1.15; niv. 25.88–25.77. – Biconical pot with a conical neck, lip and lower part missing. – Dimensions (cm): wf 6.8; hf 7.3. – Fabric 46, polished, different flutings bands, horizontal, fishbone-like and oblique over the whole fragment. – Dating: LNL (North Bulgarian LNL).

P 1/193. Site 1; tr. 1.1-W; ft. 1.1.15; niv. 25.99–25.77. – Small bulbous pot with slightly conical neck, bottom missing. – Dimensions (cm): m 11.7; wf 5.7; hf 7.7. – Fabric 6, smoothed, undecorated. – Dating: LNL.

P 1/194. Site 1; tr. 1.1-E; ft. 1.1.6; niv. 25.39 (bottom). – Middle fragment of a bulbous vessel. – Dimensions (cm): wf 9.1; hf 5.8. – Fabric 6, changing curvilinear, spiraloid and meander motifs in impasto technique. – Dating: LNL (Vădastra).

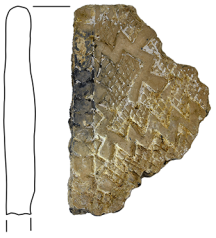
P 1/195. Site 1; tr. 1.1-E; ft. 1.1.6; niv. 25.39 (bottom). – Rim fragment of an open vessel. – Dimensions (cm): b 6.3; wf 3.4; hf 4.0. – Fabric 3, linear incisions with white paste forming a hook motif and parallel lines. – Dating: LNL.

P 1/196. Site 1; tr. 1.1-W; ft. 1.1.15; niv. 26.38–26.20. – Biconical pot with a conical neck, lip and lower part missing. – Dimensions (cm): wf 6.8; hf 8.2. – Fabric 28, excellently polished, horizontal flutings on the neck, oblique in changing directions on the middle zone. – Dating: LNL (North Bulgarian LNL).

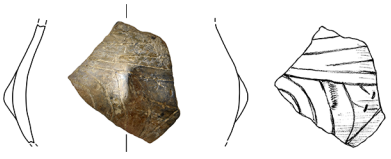
P 1/197. Site 1; tr. 1.1-W; ft. 1.1.15; niv. 26.38–26.20. – Middle fragment of a small bulbous jug. – Dimensions (cm): wf 3.8; hf 4.0. – Fabric 46, perfectly polished, oblique flutings in changing directions with fine incised dots in the gusset. – Dating: LNL (Hamangia-like).



P1/188



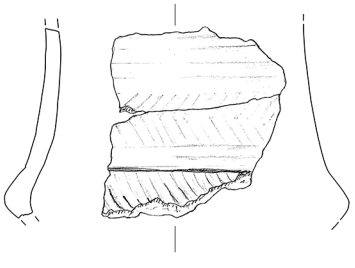
P1/189



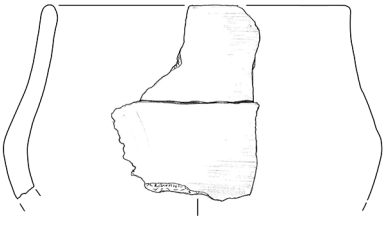
P1/190



P1/191



P1/192



P1/193



P1/194

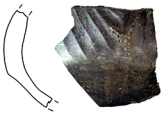


P1/195

0 5 cm



P1/196



P1/197

Plate 16. Site 1, excavation (trench 1.1-W/E, features 1.1.6/15): Late Neolithic pottery (P1/188–P1/197)

SITE 1. Excavations

Trench 1.1-W/E, features 1.1.6/15 (Late Iron Age ditch)

Features 1.1.6/15: Neolithic pottery

P 1/198. Site 1; tr. 1.1-E; ft. 1.1.6; niv. 26.76–26.67. – Cylindrical base that widens towards the bottom. – Dimensions (cm): b 13.0; wf 5.3; hf 3.4. – Fabric 6, impasto incisions, concentric circles. – Dating: LNL (Vădastra).

P 1/199. Site 1; tr. 1.1-E; ft. 1.1.6; niv. 26.51. – Small foot with round cross-section on the rest of a plate. – Dimensions (cm): wf 3.8; hf 3.2; Foto: wf 4.1; hf 3.1. – Fabric 3, remnants of red colour. – Dating: LNL.

P 1/200. Site 1; tr. 1.1-E; ft. 1.1.6; niv. 27.00–26.76. – Spherical lid. – Dimensions (cm): b 14.1; wf 7.9; hf 4.5. – Fabric 6, fine ladder tapes and rhombic chains in impasto technique as concentrical bands. – Dating: LNL (Vădastra).

P 1/201. Site 1; tr. 1.1-E; ft. 1.1.6; niv. 26.72. – Cylindrical lid with a vaulted top. – Dimensions (cm): wf 8.2; hf 3.5. – Fabric 6, impasto remnants on the side and traces of red colour on top. – Dating: LNL (Vădastra).

P 1/202. Site 1; tr. 1.1-E; ft. 1.1.6; niv. 25.83–25.39. – Flat lid. – Dimensions (cm): b 3.5; wf 4.9; hf 3.5. – Unclear fabric, even bone-like, undecorated. – Dating: LNL.

P 1/203. Site 1; tr. 1.1-E; ft. 1.1.6; niv. 27.00–26.76. – Middle fragment of a sieve. – Dimensions (cm): wf 6.8; hf 4.0. – Fabric 6, multiple perforated sherd. – Dating: LNL.

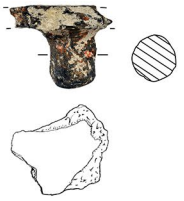
P 1/204. Site 1; tr. 1.1-E; ft. 1.1.6; niv. 26.24–26.14. – Middle fragment from the shoulder of a bulbous vessel. – Dimensions (cm): dmax 24.0; wf 10.0; hf 4.0. – Fabric 3, traces of incised lines. – Dating: LNL.

Features 1.1.6/15: Late Iron Age pottery

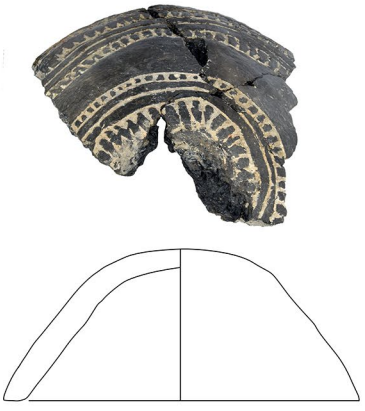
P 1/205. Site 1; tr. 1.1-E; ft. 1.1.6 (ditch); niv. 26.70. – Fruit bowl (or jug?), low foot. – Dimensions (cm): hf 2.7; b (foot) 4.8. – Fabric 50. – Parallels: Moscalu 1983, type 4a/b; 24a pl. 66,5.14. 20 (4th–3rd c. BC). – Dating: LIA.



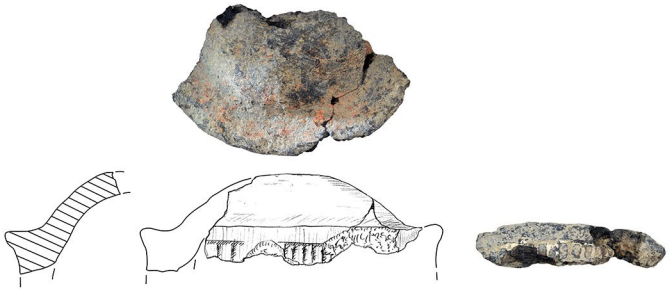
P1/198



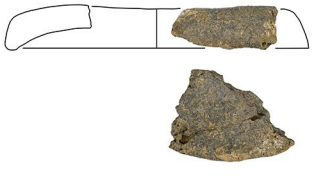
P1/199



P1/200



P1/201



P1/202

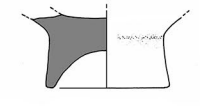


P1/203

0 5 cm



P1/204



P1/205

Plate 17. Site 1, excavation (trench 1.1-W/E, features 1.1.6/15): Late Neolithic pottery (P1/198–P1/204); Late Iron Age pottery (P1/205)

SITE 1. Excavations

Trench 1.1-W/E, features 1.1.7/13 (Early Medieval ditch)

Features 1.1.7/13: Neolithic pottery

P 1/206. Site 1; tr. 1.1-W; ft. 1.1.13; niv. 26.04–25.86. – Rim fragment of a large open vessel. – Dimensions (cm): wf 5.3; hf 7.2. – Fabric 6, incised lines forming a spiral motif and parallel lines, remnants of red colour. – Dating: LNL (Vădastra).

P 1/207. Site 1; tr. 1.1-W; ft. 1.1.13; niv. 26.04–25.86. – Wall fragment of a large bulbous vessel. – Dimensions (cm): wf 16.6; hf 19.3. – Fabric 3, slipped and smoothed, one large spiral shaped by fingertips over the whole fragment. – Dating: LNL.

Features 1.1.7/13: Late Iron Age pottery

P 1/208. Site 1; tr. 1.1-E; ft. 1.1.7 (EMA ditch) (niv. 24.56–24.36). – Amphora-shaped dolium, rim fragment. Funnel-shaped mouth with out-curved, triangular rim. – Dimensions (cm): m 24; hf 3.7; wf 10.5. – Fabric 50. Dark grey surface, burnished. – Parallels: rim profile and upper part of the vessel similar to Moscalu 1983, type 1 pl. 67 (Zimnicea, 3rd c. BC); 68. – Dating: LIA.

P 1/209. Site 1; tr. 1.1-W; ft. 1.1.13 (EMA ditch) (niv. 26.04–25.86). – Jug, fragment of the lower part with attachment traces of the stand ring. – Dimensions (cm): hf 3.0; b (stand ring) 4.7; wf 9.5. – Fabric 49. Dark grey, polished surface; relatively rough inner surface. – Parallels: cf. Moscalu 1983, pl. 74. – Dating: LIA.

Features 1.1.7/13: Early Medieval pottery

P 1/210. Site 1; tr. 1.1-E; ft. 1.1.7 (ditch); niv. 26.00–25.83. – Pot, rim fragment. Spherical body; flat, relatively sharp outward leaning rim with thickened, angulated lip. Incised wave bands on the shoulder and on the rim. – Dimensions (cm): m 13; hf 3.5; wf 5.9. – Fabric 75. Sooty exterior. – Parallels: Wendel 1986, group 3 pl. 25,1; type 5 pl. 31,4.5. – Dating: EMA.

P 1/211. Site 1; tr. 1.1-W; ft. 1.1.13 (ditch); niv. 25.65–25.48. – Pot, rim fragment. Spherical body; outward leaning rim with rounded lip. – Dimensions (cm): m 13; hf 1.8; wf 3.7. – Fabric 77. Sooty exterior. – Parallels: Wendel 1986, type Krivina pl. 34,7; 35,4. – Dating: EMA.

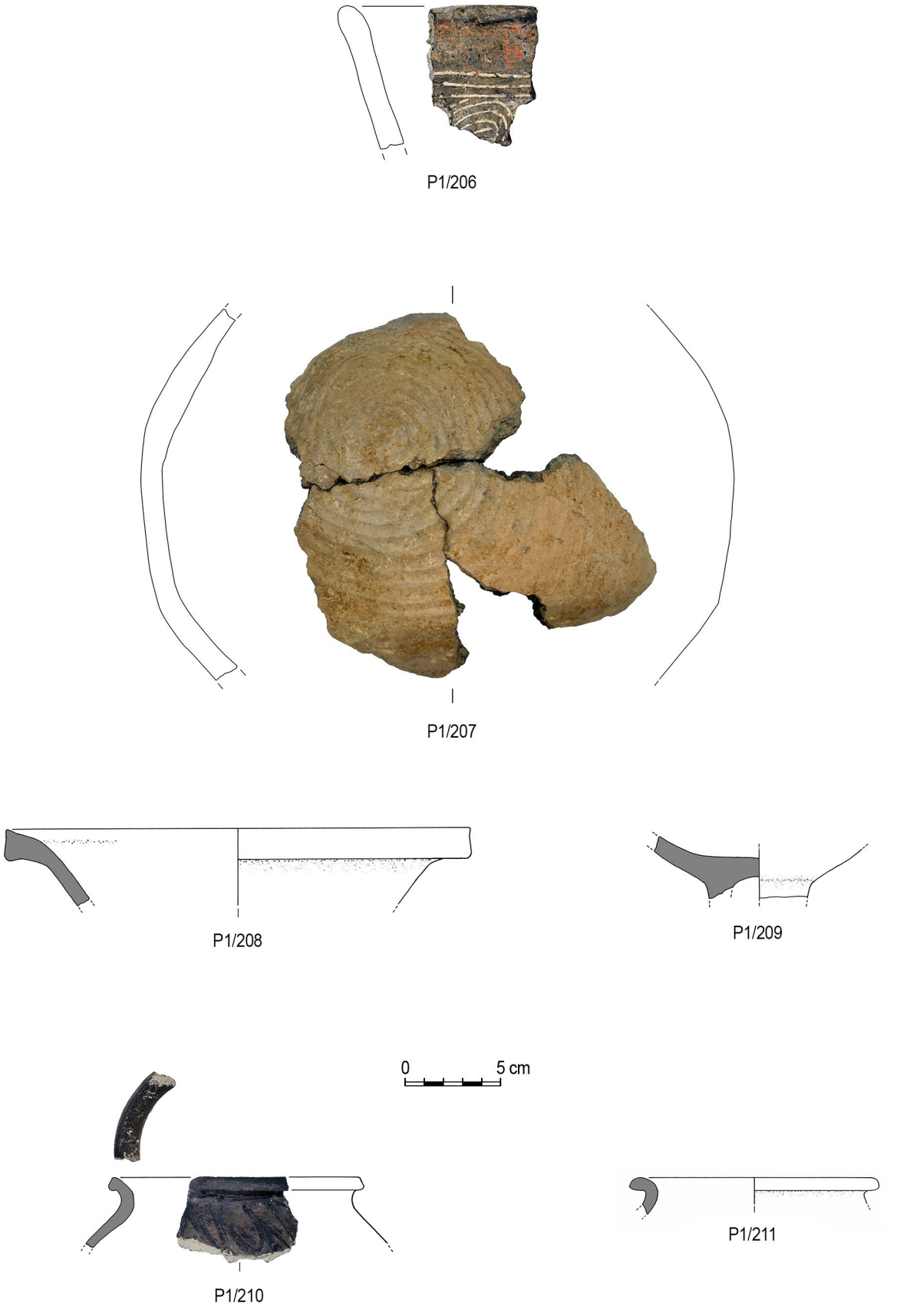


Plate 18. Site 1, excavation (trench 1.1-W/E, features 1.1.7/13): Late Neolithic pottery (P1/206–P1/207); Late Iron Age pottery (P1/208–P1/209); Early Medieval pottery (P1/210–P1/211)

SITE 1. Excavations

Trench 1.1-W/E, Early Medieval and Post-Medieval features

Features 1.1.2-4 (Early Medieval shifted rampart): Neolithic pottery

P 1/212. Site 1; tr. 1.1-W; ft. 1.1.1; niv. 27.22–27.00. – Rim fragment of a carinated bowl. – Dimensions (cm): m 16.5; wf 4.1; hf 3.1. – Fabric 36, oblique incision lines below the rim. – Dating: LNL (North Bulgarian LNL).

P 1/213. Site 1; tr. 1.1-W; ft. 1.1.1; niv. 27.22–27.00. – Rim fragment of a pot with slightly funnel mouth. – Dimensions (cm): m 16.0; wf 6.5; hf 6.1. – Fabric 40, remnants of fine vertical parallel lines on the shoulder. – Dating: LNL.

P 1/214. Site 1; tr. 1.1-W; ft. 1.1.1; from N-profile (niv. 27.21). – Top of a mushroom-shaped lid. – Dimensions (cm): d 11.3; wf 9.7; hf 3.2. – Fabric 6, zig-zag lines in impasto technique forming chains of small squares. – Dating: LNL (Vădastra).

P 1/215. Site 1; tr. 1.1-W; ft. 1.1.2; niv. 27.00–26.78. – Cylindrical lid with a a highly stylised human face on top. – Dimensions (cm): wf 2.8; hf 3.1. – Fabric 6, fine incision lines around the body with scratches forming ladder bands. The top is plastically formed in the shape of a humanoid face with a raised nose, the eyes are indicated by small balls that are placed below the nose. – Dating: LNL (Hamangia-like).

P 1/216. Site 1; tr. 1.1-W; ft. 1.1.2; niv. 27.00–26.78. – Wall fragment of a large vessel. – Dimensions (cm): wf 9.2; hf 10.9. – Fabric 3, zig-zag pattern in chip carving technique with impasto over the entire fragment. – Dating: LNL (Vădastra).

P 1/217. Site 1; tr. 1.1-W; ft. 1.1.2; niv. 26.78–26.58. – Rim fragment of a bulbous pot with narrow mouth. – Dimensions (cm): m 17.3; wf 5.2; hf 4.3. – Fabric 7, with fingers structured barbotine below the rim. – Dating: LNL.

P 1/218. Site 1; tr. 1.1-W; ft. 1.1.2; niv. 26.78–26.58. – Rim fragment of a bulbous pot with narrow mouth. – Dimensions (cm): m 16.3; wf 8.3; hf 4.6. – Fabric 5, undecorated. – Dating: LNL.

P 1/219. Site 1; tr. 1.1-W; ft. 1.1.2; niv. 26.78–26.58. – Rim fragment of a bulbous pot with narrow mouth. – Dimensions (cm): m 16.5; wf 6.5; hf 6.8. – Fabric 7, with fingers structured barbotine below the rim. – Dating: LNL.

P 1/220. Site 1; tr. 1.1-W; ft. 1.1.2; niv. 26.78–26.58. – Middle fragment of a large storage vessel. – Dimensions (cm): wf 7.2; hf 7.3. – Fabric 3, barbotine, ring-shaped applicated motif covered by the plastically formed barbotine. – Dating: LNL.

P 1/221. Site 1; tr. 1.1-W; ft. 1.1.4; niv. 26.76–26.53. – Rim fragment of a carinated bowl. – Dimensions (cm): m 17.3; wf 6.2; hf 4.7. – Fabric 6, fine vertical channeling on the shoulder. – Dating: LNL (North Bulgarian LNL).

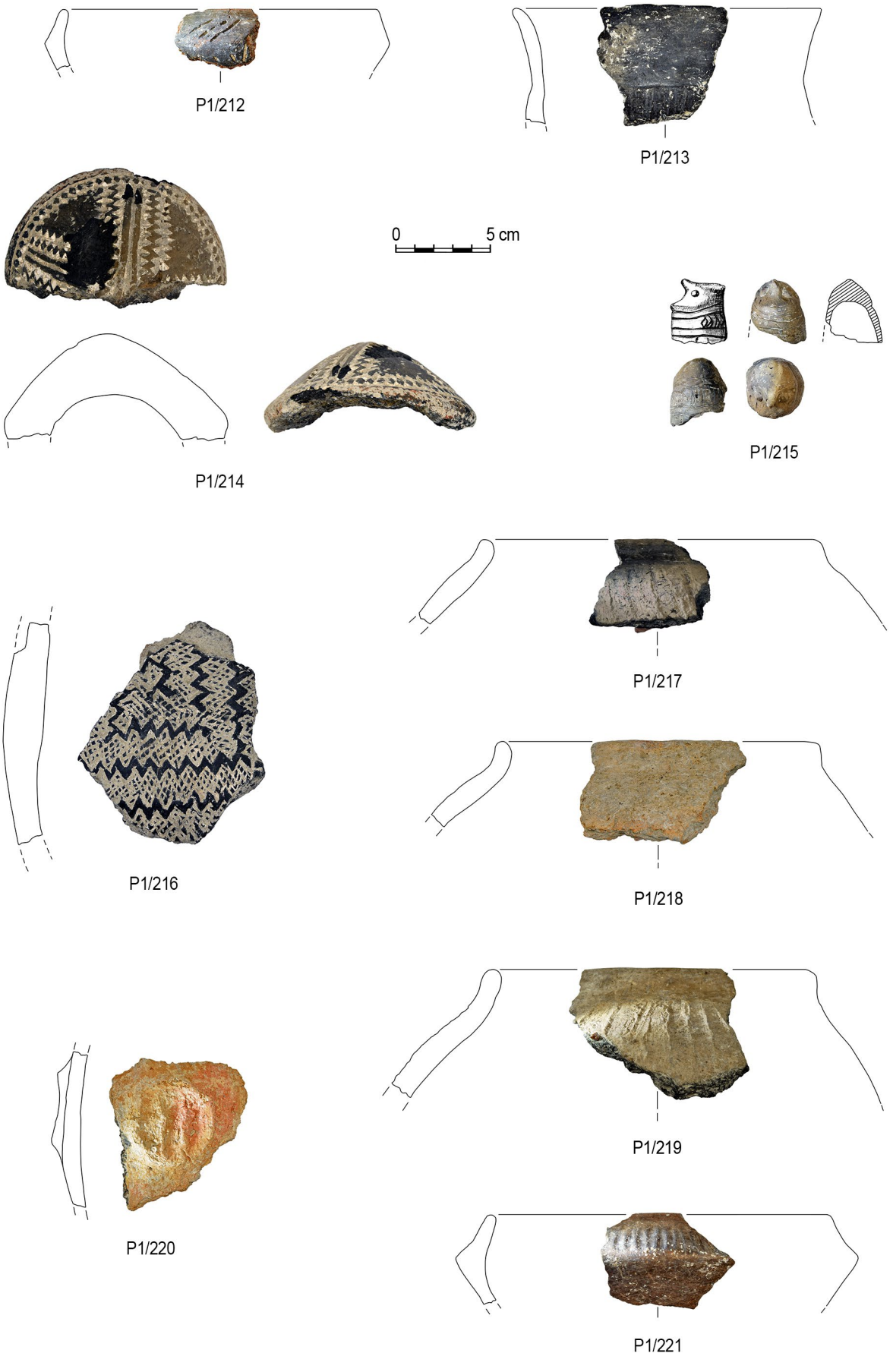


Plate 19. Site 1, excavation (trench 1.1-W/E, features 1.1.2–4): Late Neolithic pottery (P1/212–P1/221)

SITE 1. Excavations

Trench 1.1-W/E, Early Medieval and Post-Medieval features

Features 1.1.2-4 (Early Medieval shifted rampart): Bronze Age pottery

P 1/222. Site 1; tr. 1.1-W; ft. 1.1.4; niv. 28.84–28.58. – Fragment of a grip handle with a widened end. – Dimensions (cm): wf 2.6; hf 3.3. – Fabric 13, smoothed. – Dating: BA.

Features 1.1.2-4 (Early Medieval shifted rampart): Late Iron Age pottery

P 1/223. Site 1; tr. 1.1-E; Ft. 1.1.4 (niv. 26.76–26.53). – Bowl, rim fragment. Slightly inwardly curved rim; two narrow, flat grooves on the exterior of the upper part. – Dimensions (cm): m 23; hf 2.7; wf 4.9. – Fabric 49. Dark grey, ochre-grey core. – Parallels: Moscalu 1983, type 10a pl. 75,1-4 (5th–4th c.); for the grooves under the rim cf. ibid. pl. 78,2.3 (Alexandria, 550–450 BC). – Dating: LIA (5th–4th c. BC).

Features 1.1.2-4 (Early Medieval shifted rampart): Early Medieval pottery

P 1/224. Site 1; tr. 1.1-W; ft. 1.1.2 (shifted rampart); niv. 26.78–26.58. – Pot, rim fragment. Spherical body; outwards turned rim with rounded lip. A row of stamped small squares and a waveband on the shoulder. – Dimensions (cm): m 12; hf 3.1; wf 2.0. – Fabric 77. – Parallels: Wendel 1986, type 4 pl. 30,1.3. – Dating: EMA.

P 1/225. Site 1; tr. 1.1-W; ft. 1.1.2 (shifted rampart); niv. 26.78–26.59. – Pot, rim fragment. Spherical body; outwards turned rim beaded outwards. – Dimensions (cm): m 11; hf 2.3; wf 3.7. – Fabric 80.
Parallels: Wendel 1986, pl. 36,14. – Dating: EMA.

Trench 1.1-E, feature 1.1.9 (niveau level): Bronze Age pottery

P 1/226. Site 1; tr. 1.1-E; ft. 1.1.9; niv. 26.74. – Rim fragment of a biconical vessel, slightly squared in cross-section with vertical tubular lugs at the one preserved edge. – Dimensions (cm): m 10.8; wf 9.0; h 6.0. – Fabric 18, smoothed, traces of the tool used are visible on the surface. – Dating: BA.

Trench 1.1-E, feature 1.1.9 (niveau level): Early Iron Age pottery

P 1/227. Site 1; tr. 1.1-E; ft. 1.1.9; niv. 26.44–26.24. – Middle fragment of a bowl with a convex outcurving wide rim. – Dimensions (cm): wf 5.4; hf 5.9. – Fabric 40, the inner surface is incised with fine scrolling wheel or stamping, forming complex spiraloid motifs. – Dating: EIA (Basarabi/8th–7th c. BC)

Trench 1.1-W, feature 1.1.11 (Early Medieval gateway): Late Neolithic pottery

P 1/228. Site 1; tr. 1.1-W; ft. 1.1.11. – Rim fragment of a jug with slightly conical neck. – Dimensions (cm): m 8.0; wf 5.7; hf 5.0. – Fabric 46, small hump on the shoulder framed by fine channeling. – Dating: LNL (North Bulgarian LNL).

P 1/229. Site 1; tr. 1.1-W; ft. 1.1.11; niv. 27.00. – Rim fragment of a bulbous pot with narrow mouth. – Dimensions (cm): m 12.8; wf 7.3; hf 7.1. – Fabric 7, with fingers structured barbotine below the rim. – Dating: LNL.

P 1/230. Site 1; tr. 1.1-W; ft. 1.1.11. – Bottom fragment with secondary perforated base. – Dimensions (cm): b 13.6; wf 10.3; hf 7.6. – Fabric 3, vertical finger grooved barbotine on the surface. – Dating: LNL.

Trench 1.1-W, feature 1.1.16 (Early Medieval gateway): Early Iron Age pottery

P 1/231. Site 1; tr. 1.1-W; ft. 1.1.16; niv. 26.58–26.19. – Rim fragment of a wide bowl. – Dimensions (cm): m 29.4; wf 5.1; hf 3.0. – Fabric 40, fine channeled decoration in combination with stamped motifs on the inner surface. – Dating: EIA (Basarabi/8th–7th c. BC).

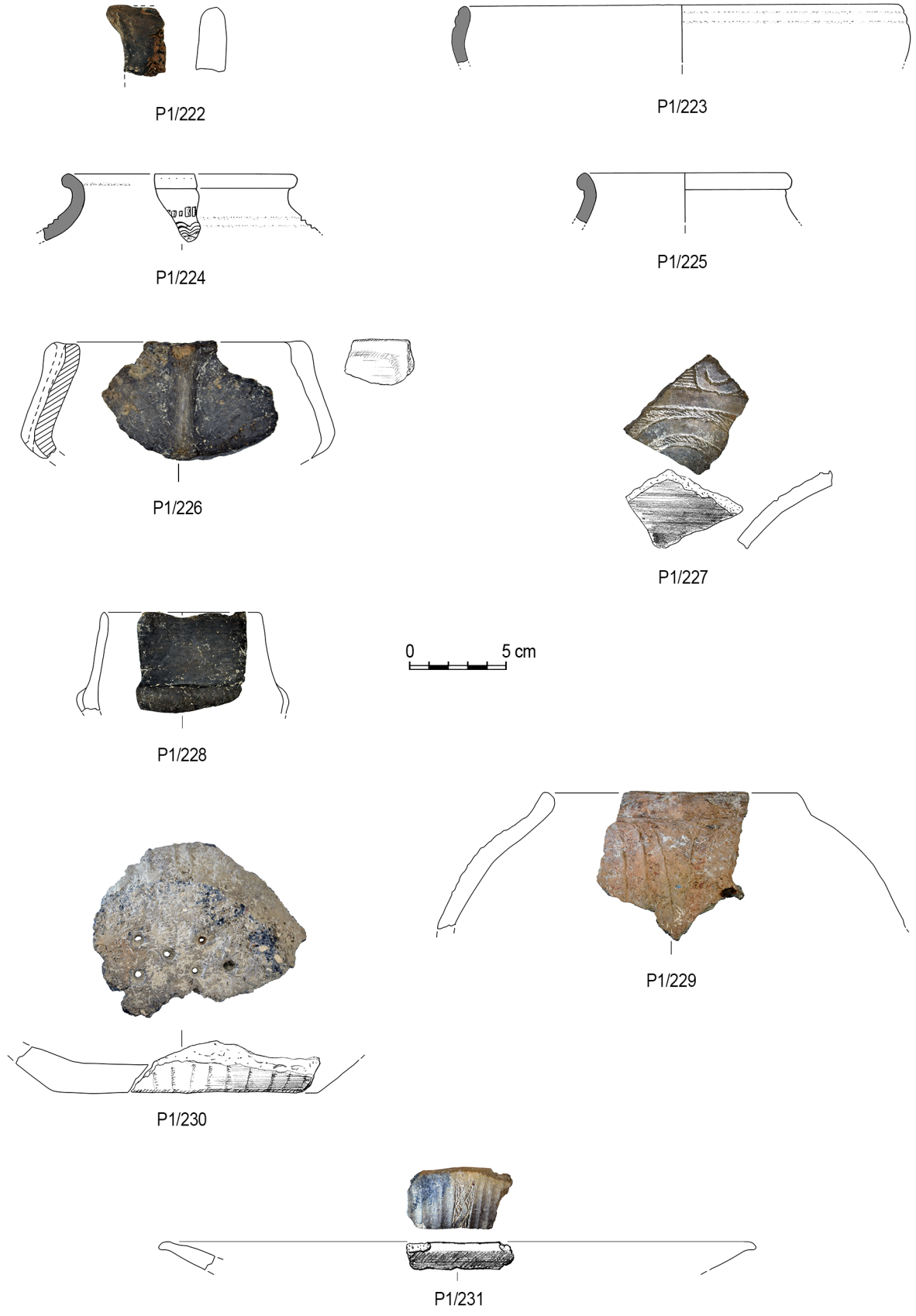


Plate 20. Site 1, excavations (trench 1.1-W/E, features 1.1.2–4): Bronze Age pottery (P1/222); Late Iron Age pottery (P1/223); Early Medieval pottery (P1/224–P1/225). – Site 1, excavations (trench 1.1-E, feature 1.1.9): Bronze Age pottery (P1/226); Early Iron Age pottery (P1/227). – Site 1, excavations (trench 1.1-W, feature 1.1.11): Late Neolithic pottery (P1/228–P1/230). – Site 1, excavations (trench 1.1-W, feature 1.1.16): Early Iron Age pottery (P1/231)

SITE 1. Excavations

Trench 1.2, feature 1.2.4/6 (Western / outer Neolithic ditch)

Feature 1.2.4/6: Neolithic pottery

P 1/232. Site 1; tr. 1.2; ft. 1.2.6; niv. 28.50–28.23. – Rim fragment of an open bowl with a straight wall. – Dimensions (cm): m 16.9; wf 3.7; hf 3.3. – Fabric 3, undecorated. – Dating: LNL.

P 1/233. Site 1; tr. 1.2; ft. 1.2.4; niv. 29.46–29.30. – Middle fragment of a bulbous vessel. – Dimensions (cm): wf 4.2; hf 7.4. – Fabric 5, rough surface. Plastic application in form of a ring. – Dating: LNL.

P 1/234. Site 1; tr. 1.2; ft. 1.2.4; niv. 29.46–29.30. – Rim fragment of a bulbous pot. – Dimensions (cm): m 11.8; wf 4.3; hf 6.5. – Fabric 5, fine incised lines, forming bands. – Dating: LNL.

P 1/235. Site 1; tr. 1.2; ft. 1.2.4; niv. 29.46–29.30. – Flat bowl, rectangular in shape. – Dimensions (cm): m 17.5; wf 5.1; hf 3.5. – Fabric 6, remnants of impasto decoration on the outer surface. – Dating: LNL (Vădastra).

P 1/236. Site 1; tr. 1.2; ft. 1.2.6; niv. 28.70–28.56. – Middle fragment of a small jug. – Dimensions (cm): dmax 11.0; wf 2.3; hf 3.1. – Fabric 28, oblique flutings on the shoulder. – Dating: LNL (North Bulgarian LNL).

P 1/237. Site 1; tr. 1.2; ft. 1.2.6; niv. 28.70–28.56. – Middle fragment. – Dimensions (cm): wf 7.0; hf 8.2. – Fabric 6, zig-zag pattern in chip carving technique with impasto over the entire fragment. – Dating: LNL (Vădastra).

P 1/238. Site 1; tr. 1.2; ft. 1.2.6; niv. 28.70–28.56. – Middle fragment. – Dimensions (cm): wf 10.9; hf 6.3. – Fabric 5, wide, hatched areas for an impasto filling. – Dating: LNL (Vădastra).

P 1/239. Site 1; tr. 1.2; ft. 1.2.6; niv. 28.95–28.70. – Middle fragment. – Dimensions (cm): wf 6.1; hf 6.2. – Fabric 6, complex impasto motif with hatched areas in between the raised linear motif. – Dating: LNL (Vădastra).

P 1/240. Site 1; tr. 1.2; ft. 1.2.4; niv. 28.58–28.11. – Large fragment of a spherical lid. – Dimensions (cm): m 21.5. – Fabric 6, complex meander motifs made out of zig-zag lines in impasto technique. – Dating: LNL (Vădastra).

P 1/241. Site 1; tr. 1.2; ft. 1.2.4; niv. 28.58–28.11. – Shoulder fragment of a large biconical vessel. – Dimensions (cm): wf 11.4; hf 12.0. – Fabric 6, large metopes filled with zig-zag lines in impasto technique. – Dating: LNL (Vădastra).

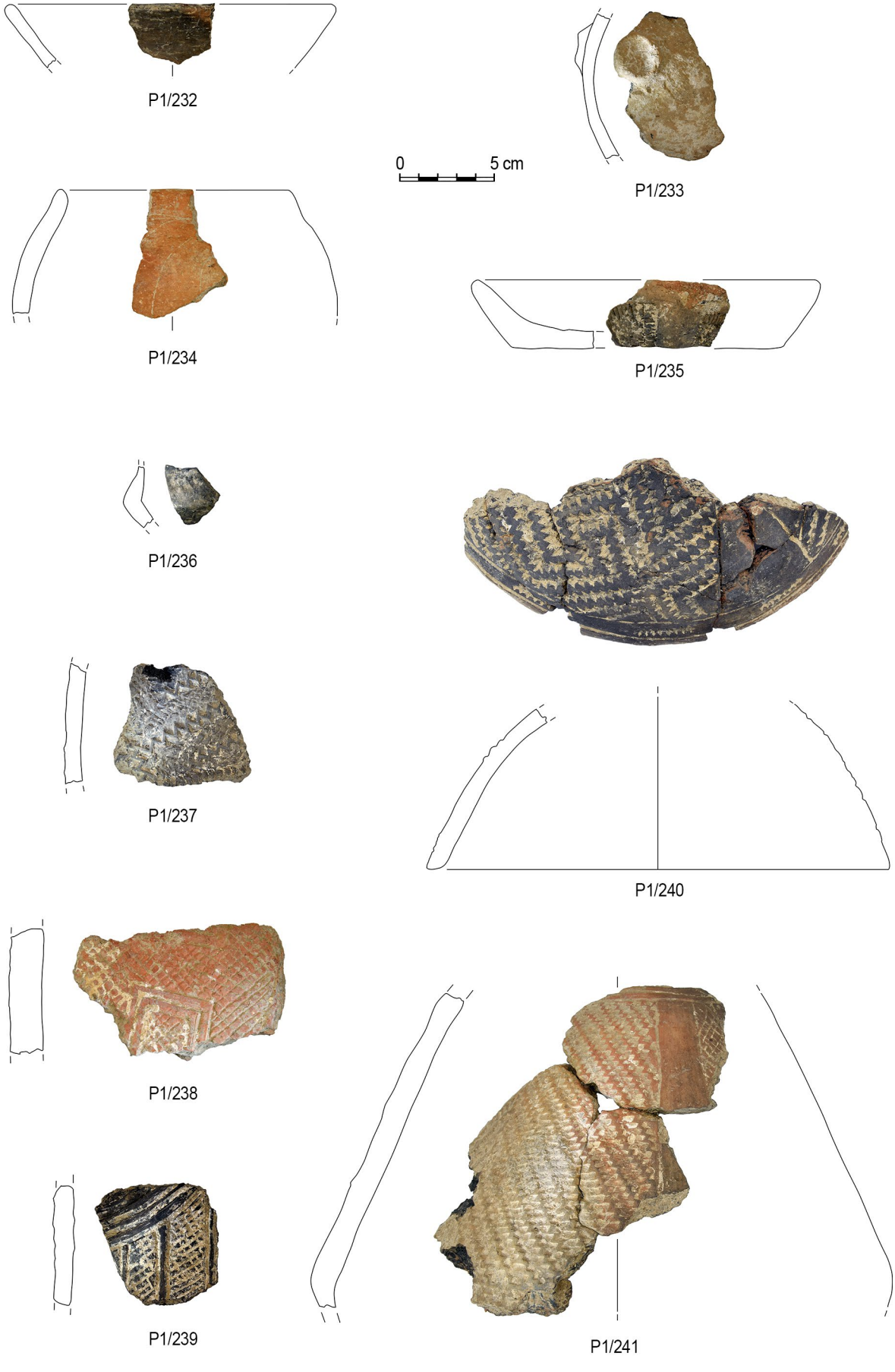


Plate 21. Site 1, excavations (trench 1.2, feature 1.2.4/6): Late Neolithic pottery (P1/232–P1/241)

SITE 1. Excavations

Trench 1.2, feature 1.2.4/6 (Western / outer Neolithic ditch)

Feature 1.2.4/6: Chalcolithic pottery

P 1/242. Site 1; tr. 1.2; ft. 1.2.4; niv. 29.30–29.08. – Larger fragment of a carinated bowl with out-curving lip-rim, bottom missing. – Dimensions (cm): m 31.0. – Fabric 7, polished, remnants of graphite paint. – Dating: CL (Kodzhadermen-Gumelnița-Karanovo VI).

Trench 1.2, feature 1.2.7/8 (Eastern / inner Neolithic ditch)

Feature 1.2.7/8: Neolithic pottery

P 1/243. Site 1; tr. 1.2; ft. 1.2.7/8; niv. 28.94–28.78. – Biconical pot with offset cylindrical rim. – Dimensions (cm): m 14.3; wf 13.5; hf 6.0. – Fabric 46, fine fishbone channeling on the shoulder framed by tiny little incisions. – Dating: LNL (Hamangia-like).

P 1/244. Site 1; tr. 1.2; ft. 1.2.7/8; niv. 28.40–28.10. – Rim fragment of a bowl with rolled rim. – Dimensions (cm): wf 5.1; hf 4.1. – Fabric 6, a chain of squares in impasto technique below the rim. – Dating: LNL (Vădastra).

P 1/245. Site 1; tr. 1.2; ft. 1.2.7/8; niv. 28.40–28.10. – Shoulder fragment of a profiled vessel with a slightly angular cross-section. – Dimensions (cm): wf 9.9; hf 4.9. – Fabric 6, deep incised complex decoration in impasto technique contouring the tectonic of the vessel, framed metopes. – Dating: LNL (Vădastra).

P 1/246. Site 1; tr. 1.2; ft. 1.2.7/8; niv. 29.30–28.94. – Rim fragment of a carinated bowl. – Dimensions (cm): m 23.4; wf 3.5; hf 4.8. – Fabric 6, slipped, undecorated. – Dating: LNL.

P 1/247. Site 1; tr. 1.2; ft. 1.2.7/8; niv. 29.30–28.94. – Rim Fragment of a small bowl with narrow mouth. – Dimensions (cm): m 16.5; wf 3.8; hf 3.1. – Fabric 7, fine incised meander motif below the lip. – Dating: LNL.

P 1/248. – Site 1; tr. 1.2; ft. 1.2.7/8; niv. 29.30–28.94. – Rim fragment of a bulbous bowl with secondary perforated wall. – Dimensions (cm): m 22.2; wf 9.1; hf 4.0. – Fabric 8, undecorated. – Dating: LNL.

Trench 1.2, feature 1.2.5 (Early Medieval ditch)

Feature 1.2.5: Neolithic pottery

P 1/249. Site 1; tr. 1.2; ft. 1.2.5; niv. 28.58–27.58. – Bottom fragment of the conical lower part of a vessel. – Dimensions (cm): b 4.9; wf 3.0; hf 1.8. – Fabric 46, fine incised parallel lines on the bottom of the fragment. – Dating: LNL.

P 1/250. Site 1; tr. 1.2; ft. 1.2.5; niv. 28.29–28.10. – Rim fragment of a wide bowl with straight walls, bottom missing. – Dimensions (cm): m 14.4; wf 2.9; hf 5.0. – Fabric 3, undecorated. – Dating: LNL.

Feature 1.2.5: Bronze Age pottery

P 1/251. Site 1; tr. 1.2; ft. 1.2.5; niv. 28.29–28.10. – Fragment of a rim standing handle with a widened end. – Dimensions (cm): wf 3.3; hf 3.6. – Fabric 18. – Dating: BA.

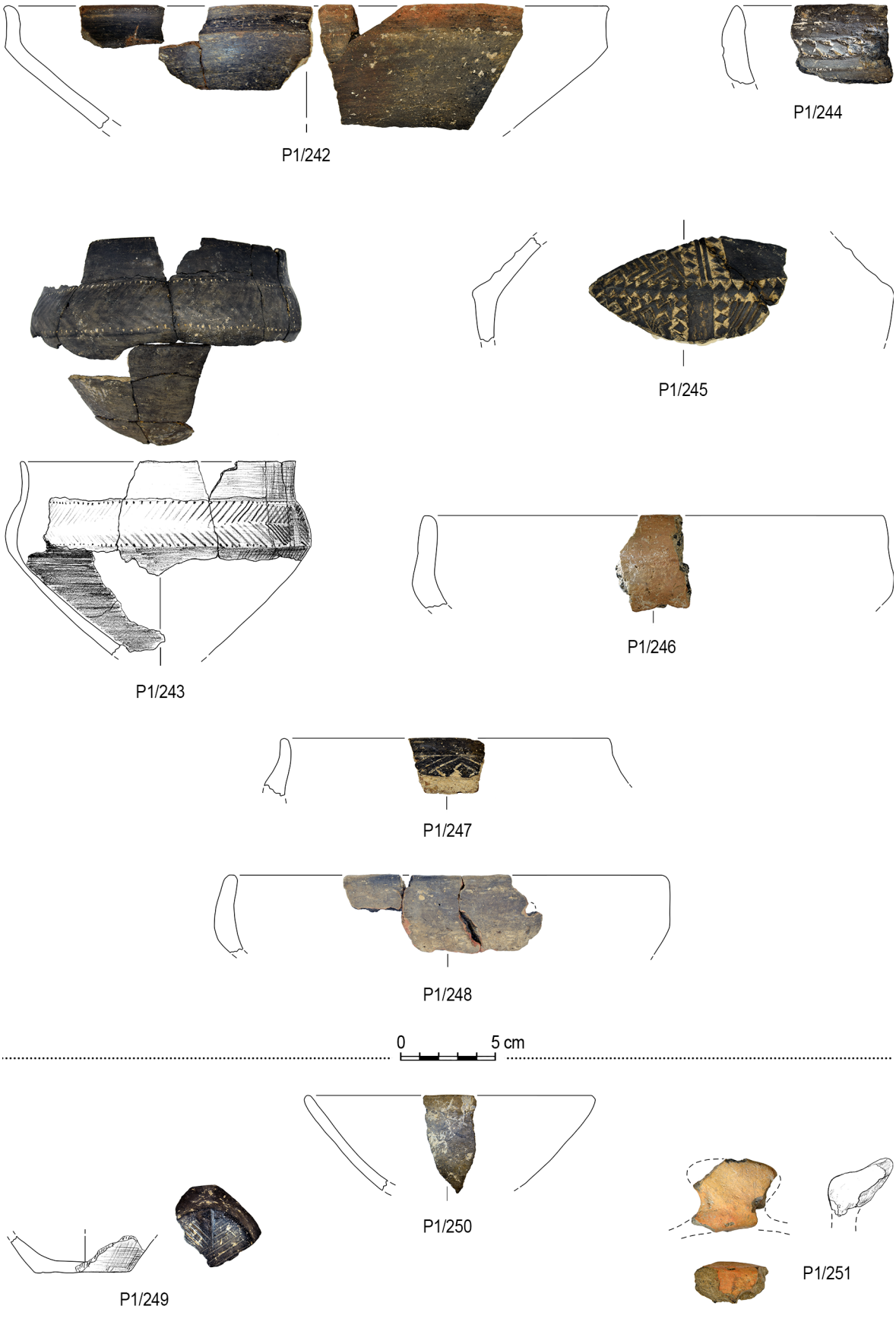


Plate 22. Site 1, excavations (trench 1.2, feature 1.2.4/6): Chalcolithic pottery (P1/242). – Site 1, excavations (trench 1.2, feature 1.2.7/8): Late Neolithic pottery (P1/243–P1/248). – Site 1, excavations (feature 1.2.5): Late Neolithic pottery (P1/249–P1/250); Bronze Age pottery (P1/251)

SITE 2. Survey

Site 2, survey: Late Neolithic pottery

P 2/1. Site 2; pol. 31. – Middle fragment. – Dimensions (cm): wf 6.2; hf 4.1. – Fabric 5, zig-zag impasto with white paste over the whole fragment. – Dating: LNL (Vădastra).

Site 2, survey: Roman pottery

P 2/002. Site 2; pol. 193. – Amphora, massive cylindrical foot, slightly retracted in the middle. – Dimensions (cm): hf 11.2; b (foot, max.) 6.4. – Light reddish brown fabric; coarse sandy temper (with some dark inclusions); traces of a light ochre engobe. – Parallels: very likely a foot of an amphora Dressel 1879, type 2–4, cf. cat. 5/007. – Dating: RP (1st–2nd c.).

P 2/003. Site 2; pol. 31. – Amphora, rim fragment. Funnel-shaped mouth with slightly thickened and slanted to the interior rim; flat groove on the upper side. – Dimensions (cm): m 18; hf 7.2; wf 7.6. – Light reddish brown fabric with some fine inclusions; yellowish ochre engobe. – Parallels: Dressel 1879, type 24 sim., cf. Hayes 1983, type 18; Opaiț 2007, 628–629 fig. 2,7–9; Dobreva 2017, 233–237 fig. 143; 147, 2. – Dating: RP (2nd–3rd c.).

P 2/004. Site 2; pol. 108/109. – Amphora, rim fragment. funnel-shaped mouth with beaded lip. – Dimensions (cm): m 14; hf 4.2; wf 6.3. – Light grey, fine fabric, with grey core. ochre-coloured slip. – Parallels: similar to Falkner 1999, cat. 888; 894 (2nd–1st half of 4th c.). – Dating: RP (2nd–1st half of 4th c.).

P 2/005. Site 2; pol. 192. – Plate, (or lid bowl) rim fragment. Horizontal rim; sloping and slightly turned wall. – Dimensions (cm): m 20; hf 1.9; wf 4.3. – Fabric 58; rolled and damaged. – Parallels: similar to Falkner 1999, cat. 346; 359; 397 (2nd–1st half of 4th c.). – Dating: RP (2nd–1st half of 4th c.)

P 2/006. Site 2; pol. 192. – Plate, rim fragment. Thickened lip with wide, horizontal upper side which is profiled with three flat grooves. – Dimensions (cm): m 22; hf 1.5; wf 6.5. – Fabric 58. – Parallels: Conrad 2007a, cat. 804 (2nd half of 3rd c.). – Dating: RP (3rd–1st half of 4th c.)

P 2/007. Site 2; pol. 110. – Plate, rim fragment. Similar profile to cat. 2/006; slightly slanting rim. Flat groove on the interior; relatively sharp bend of the wall to the lower part. – Dimensions (cm): m 36; hf 3.4; wf 8.3. – Fabric 59; light ochre fabric; brownish red, poorly adhering slip. – Parallels: Falkner 1999, cat. 389; Conrad 2007a, cat. 897 (1st half of 4th c.). – Dating: RP (2nd–1st half of 4th c.).

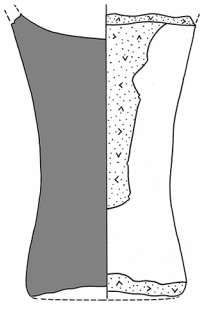
P 2/008. Site 2; surface (no exact location). – Small bowl, fragment. Profile of the vessel similar to cat. P 1/145; the grooves on the exteriors are missing. Rouletted circles on the interior. Shallow groove around the flat bottom. – Dimensions (cm): m 16; h 4.0; b 4.4; wf 8.2. – Fabric 58. – Cf. cat. P 1/145. – Dating: RP (2nd–1st half of 4th c.).

P 2/009. Site 2; pol. 204. – Bowl, rim fragment. Slightly inwardly inclined (carinated) upper part with a slanted, beaded rim. Sharp bend to the lower part. – Dimensions (cm): m 25; hf 5.3; wf 7.3. – Fabric 58; rolled surface. – Parallels: Falkner 1999, cat. 446; Conrad 2007a, cat. 924 (1st half of 4th c.). – Dating: RP (2nd–1st half of 4th c.).

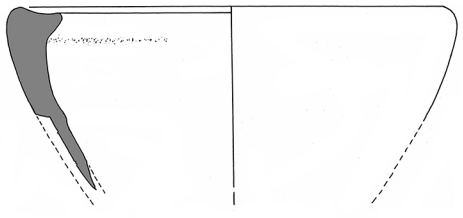
P 2/010. Site 2; pol. 38. – Bowl, rim fragment. Straight, slightly inclined upper part with rounded lip. Sharp bend to the lower part, which is marked with a narrow handlebar. Further decorations with grooves and barbotine on the exterior. – Dimensions (cm): m 22; hf 5.2; wf 7.3. – Fabric 58; badly rolled and damaged. – Parallels: similar profile to Sultov 1985, dish type 1a pl. 26,1; but no exact parallel for the details. – Dating: RP (2nd–3rd c.?).



P2/001

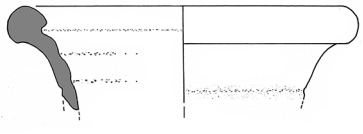


P2/002

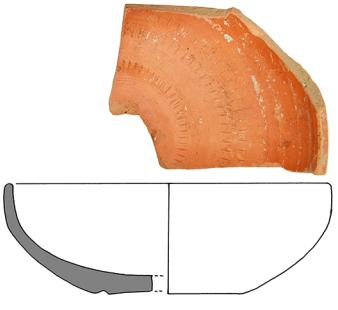


P2/003

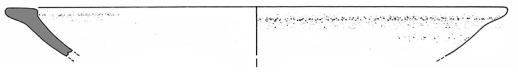
0 5 cm



P2/004



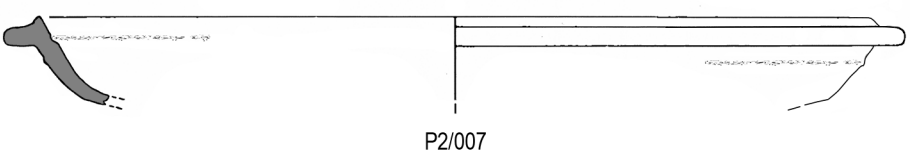
P2/008



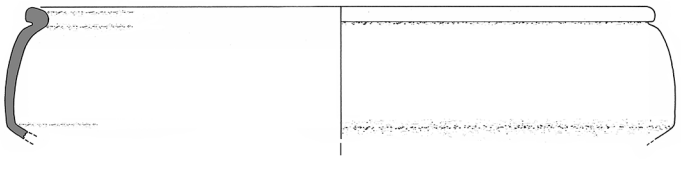
P2/005



P2/006



P2/007



P2/009



P2/010

Plate 23. Site 2, survey: Late Neolithic pottery (P2/001); Roman pottery (P2/002–010)

SITE 2. Survey

Site 2, survey: Roman pottery

P 2/011. Site 2; pol. 39. – Bowl, rim fragment. Narrow horizontal rim; Sloping, slightly curved wall. – Dimensions (cm): m ca. 16; hf 2.3; wf 3.9. – Fabric 60. Grey fabric with brown slip; traces of processing with a chip-like instrument on the exterior. – Parallels: similar to Falkner 1999, cat. 613 (2nd–1st half of 4th c.); Conrad 2007a, cat. 816 (1st half of 4th c.). – Dating: RP (2nd–1st half of 4th c.).

P 2/012. Site 2; pol. 32. – Bowl, rim fragment. Curved wall, slanted rim with small groove. – Dimensions (cm): m 23; hf 6.5; wf 5.5. – Fabric 60. – Parallels: Sultov 1985, dish type 3 pl. 29,5. Similar to Conrad 2007a, cat. 919; 926 (1st half of 4th c.). – Dating: RP (2nd–1st half of 4th c.).

P 2/013. Site 2; pol. 205. – Bowl, rim fragment. Slightly curved wall; slanted, narrow rim. Incised groove on the exterior, likely sharp kink towards the lower part. – Dimensions (cm): m ca. 15; hf 4.9; wf 6.2. – Fabric 5. – Parallels: Conrad 2007a, cat. 925 (1st half of 4th c.). – Dating: RP (2nd–1st half of 4th c.).

P 2/014. Site 2; pol 193. – Bowl, rim fragment. Wide curved rim, slanted to the exterior; slightly curved wall. – Dimensions (cm): m 12; hf 3.2; wf 5.5. – Fabric 58; slightly faceted rim (traces of processing with a chip-like instrument). – Parallels: Sultov 1985, bowl type 6a pl. 31; Falkner 1999, cat. 422; 423 (2nd–1st half of 4th c.); Conrad 2007a, cat. 908 (1st half of 4th c.). – Dating: RP (2nd–1st half of 4th c.).

P 2/015. Site 2; pol. 31. – Small bowl, rim fragment. Sloping, slightly inwardly curved wall; the lip is emphasised by a narrow groove. – Dimensions (cm): m 11; hf 2.8; wf 4. – Fabric 58. On the exterior under the rim traces of processing with a chip-like instrument. – Parallels: Falkner 1999, cat. 597 (2nd–1st half of 4th c.). – Dating: RP (2nd–1st half of 4th c.).

P 2/016. Site 2; pol. 196. – Pot / storage vessel (or krateriskos?), rim fragment. Flared rim with a groove on the exterior; narrow groove in the neck zone. – Dimensions (cm): m 15; hf 2.8; wf 4.3. – Fabric 58. – Parallels: similar to Falkner 1999, cat. 853; 855; Conrad 2007a, cat. 936; 937 (1st half of 4th c.). – Dating: RP (2nd–1st half of 4th c.).

P 2/017. Site 2; pol. 190. – Storage vessel / cauldron, rim fragment. Strongly inwardly inclined upper part of the vessel; wide, slightly inwardly slanted rim. – Dimensions (cm): m 19; hf 2.3; wf 14.5. – Fabric 58; shiny dark reddish brown slip. Badly damaged. – Parallels: Böttger 1982, cauldron type 1; Sultov 1985, jar type 1 pl. 39; Falkner 1999, cat 877. – Dating: RP (2nd–1st half of 4th c.).

P 2/018. Site 2; pol. 39. – Storage vessel / cauldron, rim fragment. Moderately inclined upper part of the wall; thickened rim to the in- and exterior, with curved upper side. – Dimensions (cm): m 30; hf 2.3; wf 6.8. – Fabric 59; rolled surface. – Parallels: similar to Falkner 1999, cat. 875. – Dating: RP (2nd c.?).

P 2/019. Site 2; pol. 31. – Storage vessel / cauldron, rim fragment. Beaded, horizontal rim, slightly sloping to the exterior; short neck. Spherical body. – Dimensions (cm): m 28; hf 3.6; wf 6.9. – Fabric 67. Light reddish brown, sandy fabric; outer surface ochre brow. – No parallel. – Dating: RP (3rd–1st half of 4th c.).

Site 2, survey: Late Roman pottery

P 2/020. Site 2; pol. 110. – Amphora, rim fragment. Funnel-shaped mouth with a thickened, rounded rim. – Dimensions (cm): m 20; hf 4.2; wf 7.5. – Light reddish brown, fine fabric with some fine inclusions; yellowish engobe. – Parallels: Riley 1979, LRA 2; Böttger 1982, amphora I1 (2nd half of 4th c.). – Dating: LRP (2nd half of 4th c.).

P 2/021. Site 2; surface (no exact location). – Amphora, foot. Massive, cylindrical shape, slightly expanded upwards. – Dimensions (cm): hf 11.2; b (foot) 4.6. – Greyish-reddish brown, slightly sandy fabric; brown engobe. Black spotted (secondarily fired). – Parallels: Böttger 1982, amphora I2 (2nd half of 4th c.); Keay 1984, type 25. – Dating: LRP (2nd half of 4th c.).

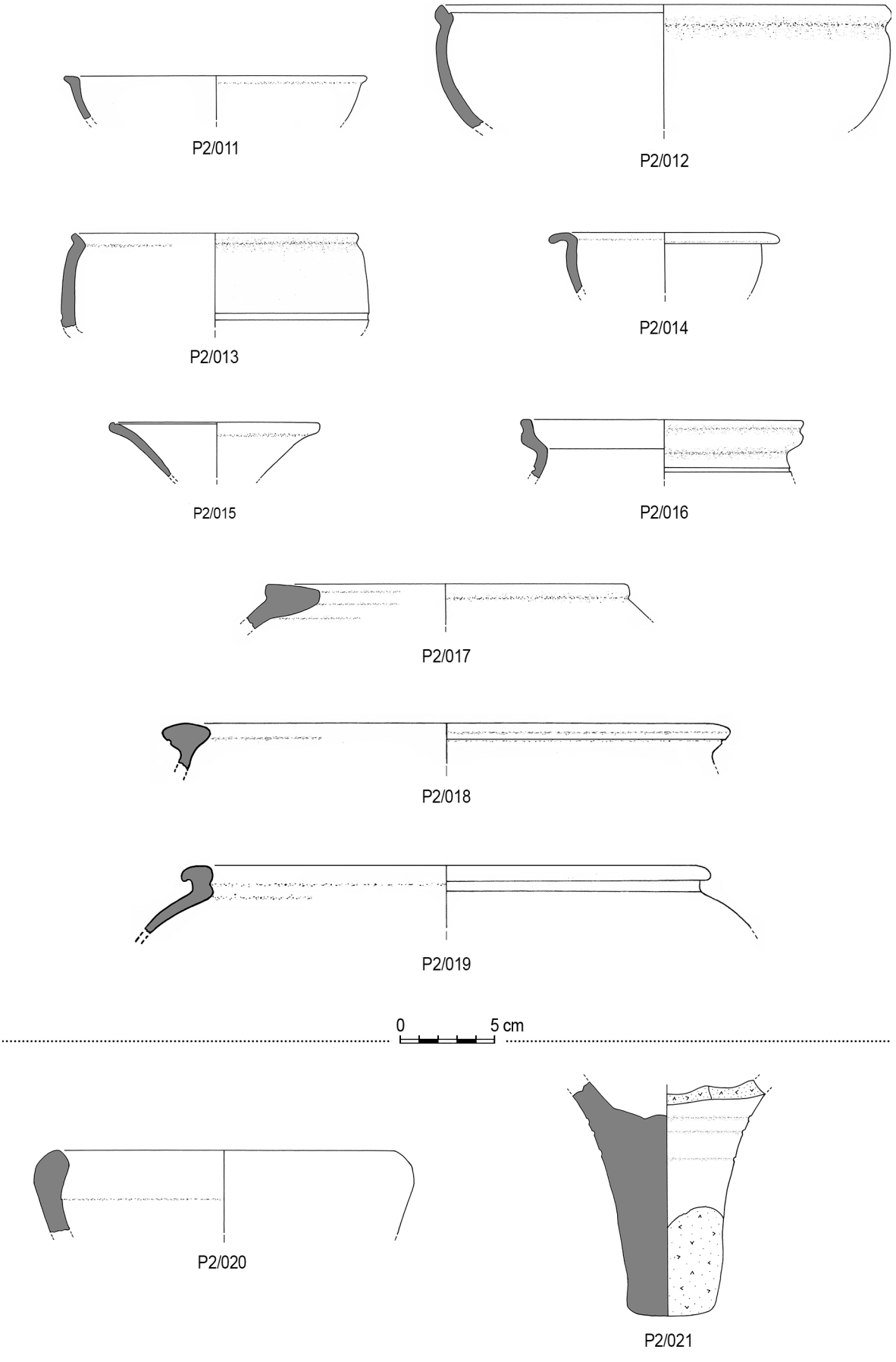


Plate 24. Site 2, survey: Roman pottery (P2/011–P2/019); Late Roman pottery (P2/020–P2/021)

SITE 3. Survey

Site 3, survey: Early Iron Age pottery

P 3/001. Site 3; pol. 120 (offsite). – Rim fragment of a wide open mouth of a storage vessel. – Dimensions (cm): m 33.0; wf 4.9; hf 6.0. – Fabric 14, notched rim and notched bar running parallel below the edge. – Dating: EIA.

SITE 3. Excavations

Trench 3.6 (inner ditch)

Trench 3.6 (ditch): Bronze Age pottery

P 3/002. Site 3; tr. 3.6; pl. 6; niv. 58.03. – Rim fragment of a bulbous pot with narrow mouth. – Dimensions (cm): m 20.6; wf 7.3; hf 8.9. – Fabric 39, undecorated. – Dating: BA.

P 3/003. Site 3; tr. 3.6; pl. 6; niv. 58.03. – Upper part of a small bulbous pot with offset cylinder edge. – Dimensions (cm): m 8.1; wf 6.5; hf 5.9. – Fabric 13, wavy rim and a small hump on the shoulder of the vessel. – Dating: MBA.

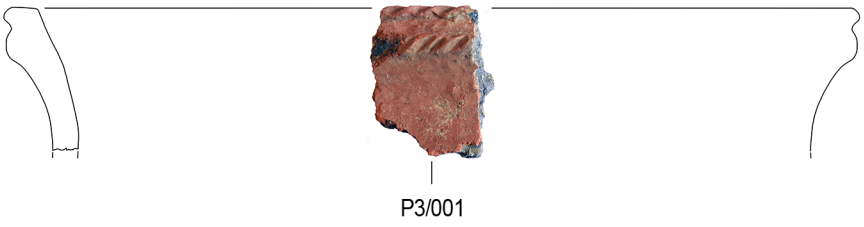
P 3/004. Site 3; tr. 3.6; niv. 61.07–60.89. – Fragment of a wishbone handle. – Dimensions (section/in cm): hf 3.8; wf 1.5 wf. – Fabric 13, undecorated. – Dating: MBA.

P 3/005. Site 3; tr. 3.6; niv. 60.72–60.37. – Spout fragment. – Dimensions (cm): d 2.5; dmax 3.6; wf 3.6; hf 3.5. – Fabric 39, undecorated. – Dating: MBA.

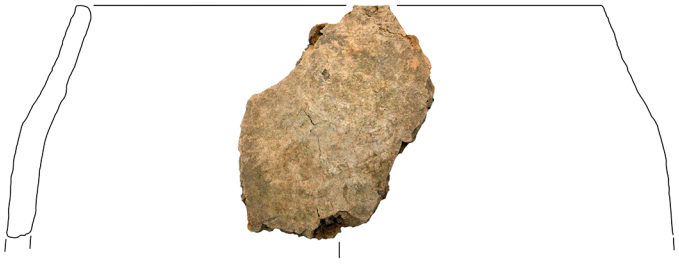
P 3/006. Site 3; tr. 3.6; niv. 61.07–60.89. – Middle fragment of a small bulbous pot with narrow mouth. – Dimensions (cm): m 4.5; wf 4.9; hf 5.5. – Fabric 18, undecorated. – Dating: BA.

P 3/007. Site 3; tr. 3.6; niv. 60.89–60.72. – Rim fragment of a bulbous pot with funnel rim. – Dimensions (cm): m 17.8; wf 4.9; hf 4.8. – Fabric 18, undecorated. – Dating: MBA.

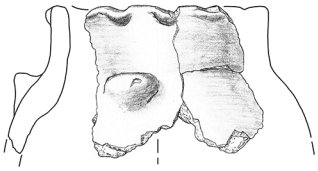
P 3/008. Site 3; tr. 3.6; niv. 61.33–61.07. – Rim fragment of a spherical bowl with a spout. – Dimensions (cm): m 20.7; wf 6.5; hf 5.5. – Fabric 39, undecorated. – Dating: MBA.



P3/001



P3/002



P3/003

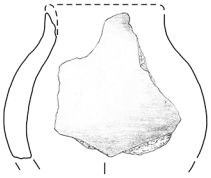


P3/004

0 5 cm



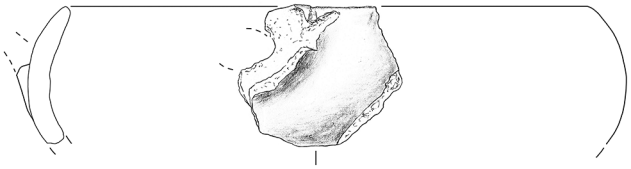
P3/005



P3/006



P3/007



P3/008

Plate 25. Site 3, survey: Early Iron Age pottery (P3/001) – Site 3, excavations (feature 3.6): Bronze Age pottery (P3/002–008)

SITE 3. Excavations

Trench 3.6 (inner ditch)

Trench 3.6 (ditch): Late Bronze Age pottery

P 3/009. Site 3; tr. 3.6; niv. 58.03–57.49. – Middle fragment of a large storage vessel. – Dimensions (cm): wf 8.0; hf 8.1. – Fabric 18, handle in the form of a double hump on the belly. – Dating: BA.

P 3/010. Site 3; tr. 3.6; niv. 58.03. – Fragment of a ribbon handle with oval cross section. – Dimensions (cm) wf 4.5; hf 2.8. – Fabric 18, undecorated. – Dating: BA.

P 3/011. Site 3; tr. 3.6; niv. 58.32–58.03. – Rim fragment of a vessel with straight wall. – Dimensions (cm) wf 3.3; hf 3.5. – Fabric 39, parallel scratches on the rim. – Dating: BA.

P 3/012. Site 3; tr. 3.6; niv. 60.72–60.37. – Middle fragment of small mug with a handle. – Dimensions (cm) wf 6.2; hf 5.3. – Fabric 18, undecorated. – Dating: BA.

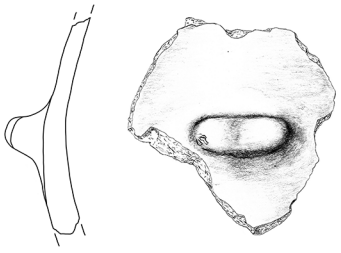
P 3/013. Site 3; tr. 3.6; niv. 60.37–60.12. – Fragment of a ribbon handle with oval cross-section. – Dimensions (cm): wf 1.9; hf 5.0. – Fabric 18, undecorated. – Dating: BA.

P 3/014. Site 3; tr. 3.6; niv. 61.33–61.07. – Rim fragment of a vessel with straight wall. – Dimensions (cm) wf 4.1; hf 4.5. – Fabric 18, undecorated. – Dating: BA.

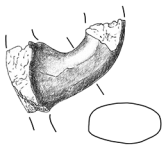
P 3/015. Site 3; tr. 3.6; niv. 60.72–60.37. – Rim fragment of a small vessel with slightly out-curving rim. – Dimensions (cm) m 6.9; wf 1.9; hf 1.9. – Fabric 18, undecorated. – Dating: BA.

P 3/016. Site 3; tr. 3.6; niv. 59.07–58.80. – Lower fragment of a vessel with a slightly concave base. – Dimensions (cm): b 3.7; wf 3.9; hf 2.0. – Fabric 18, undecorated. – Dating: BA.

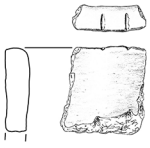
P 3/017. Site 3; tr. 3.6; niv. 60.89–60.72. – Rim fragment of a spherical bowl. – Dimensions (cm) m 21.4; wf 6.4; hf 4.7. – Fabric 18, undecorated. – Dating: BA.



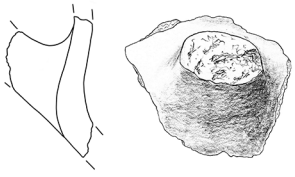
P3/009



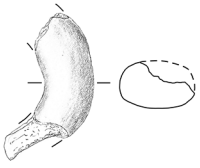
P3/010



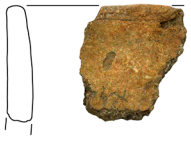
P3/011



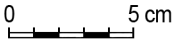
P3/012



P3/013

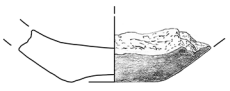


P3/014

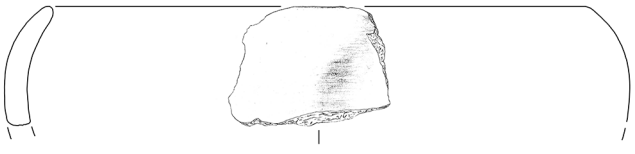




P3/015



P3/016



P3/017

Plate 26. Site 3, excavations (feature 3.6): Bronze Age pottery (P3/009–P3/017)

SITE 3. Excavations

Trench 3.6 (inner ditch)

Trench 3.6 (ditch): Late Iron Age pottery

P 3/018. Site 3; tr. 3.6; ft. 3.6 (ditch); niv. 58.80–58.58. – Bowl, rim fragment. Incurved rim; rounded lip. – Dimensions (cm): m 24; hf 3.2; wf 3.7. – Fabric 56. Made with slow wheel. – Parallels: Moscalu 1983, type 11b pl. 53,2.4.5.6 (Alexandria-Vii; mid-6th–mid-5th c. BC). – Dating: LIA (6th–5th c. BC).

Trench 3.6 (ditch): Late Roman pottery

P 3/019. Site 3; tr. 3.6 (humus); niv. 61.33–61.07. – Pot, rim fragment. Slanted rim with flat upper side. – Dimensions (cm): m 16; hf 2.4; wf 5.1. – Fabric 73; large pebble (d 4 mm) in the temper. Sooty rim. – Parallels: Böttger 1982, pot type 2. – Dating: LRP (1st half of 5th c.).

P 3/020. Site 3; tr. 3.6 (ditch); niv. 60.72–60.38. – Pot, rim fragment. Slanted rim, slight groove. – Dimensions (cm): m 14; hf 2.8; wf 5.2. – Fabric 73. Sooty rim. – Parallels: Böttger 1982, pot type 2. – Dating: LRP (1st half of 5th c.).

P 3/021. Site 3; tr. 3.6 (ditch); niv. 60.72–60.38. – Pot, rim fragment. Slightly grooved rim, slanted outwards. – Dimensions (cm): m 16; hf 1.2; wf 5.1. – Fabric 71. Sooty rim. – Parallels: Böttger 1982, pot type 5. – Dating: LRP (1st half of 5th c.).

Trench 3.6, Feature 3.6.1 (pit): Bronze Age pottery

P 3/022. Site 3; tr. 3.6; ft. 3.6.1; niv. 60.72–59.81. – Middle fragment of small mug with a handle. – Dimensions (cm): wf 5.9; hf 5.5. – Fabric 37, undecorated. – Dating: BA (MBA?)

P 3/023. Site 3; tr. 3.6; ft. 3.6.1; niv. 60.72–59.81. – Rim fragment of a vessel with out-curving lip. – Dimensions (cm): m 4.0; wf 3.6; hf 3.7. – Fabric 37, undecorated. – Dating: BA.

Trenches 3.6.2-5, feature 3.2.1 (depression / pit)

Feature 3.2.1: Late Bronze Age pottery

P 3/024. Site 3; tr. 3.2; ft. 3.2.1; niv. 63.77–63.57. – Rim fragment of a large storage vessel with straight upper part. Dimensions (cm): m 22.6; wf 5.6; hf 6.5. – Fabric 18, fingertip strip below the edge. – Dating: BA.

P 3/025. Site 3; tr. 3.3; ft. 3.2.1; niv. 63.56. – Shoulder fragment of a bulbous pot with narrow rim. – Dimensions (cm): wf 6.6; hf 7.1. – Fabric 18, undecorated. – Dating: LBA.

P 3/026. Site 3; tr. 3.3 south; ft. 3.2.1; niv. 63.60. – Middle fragment of a large storage vessel. – Dimensions (cm): wf 7.0; hf 4.7. – Fabric 18, solid, downwardly inclined tenon handle. – Dating: BA.

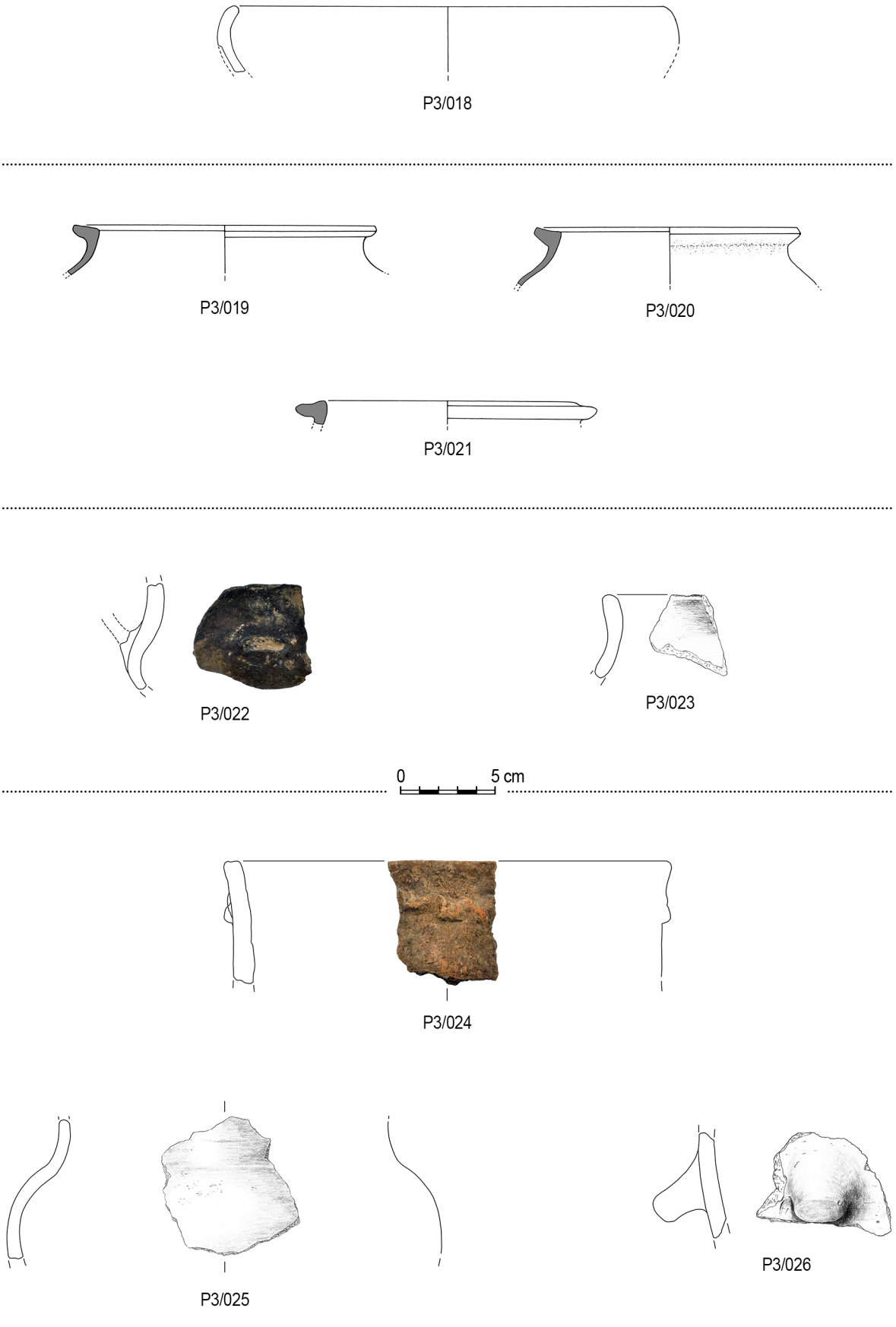


Plate 27. Site 3, excavations (feature 3.6): Late Iron Age pottery (P3/018); Late Roman pottery (P3/019–P3/021). – Site 3, excavations (feature 3.6.1): Bronze Age pottery (P3/022–P3/023). – Site 3, excavations (feature 3.2.1): Bronze Age pottery (P3/024–026)

SITE 3. Excavations

Trench 3.1, feature 3.1.1/2 (pit)

Feature 3.1.1/2: Bronze Age pottery

P 3/027. Site 3; tr. 3.1; ft. 3.1.1/2; layer c; niv. 61.47–61.26. – Small, spherical cup with an over-the-rim handle with an oval cross-section. – Dimensions (cm): dmax 10.5; m 8.3; wf 6.9; hf 8.3. – Fabric 37, undecorated. – Dating: MBA.

P 3/028. Site 3; tr. 3.1; ft. 3.1.1/2; qu. A; layer a–b; niv. 61.25. – Middle fragment of a large spouted vessel. – Dimensions (cm): wf 10.1; hf 10.5. – Fabric 37, undecorated. – Dating: MBA.

P 3/029. Site 3; tr. 3.1; ft. 3.1.1/2; qu. A; layer b; niv. 61.41. – Rim fragment of a large bowl with ribbon handle from the rim to the body. – Dimensions (cm): wf 12.3; hf 6.2. – Fabric 18, undecorated. – Dating: MBA.

P 3/030. Site 3; tr. 3.1; ft. 3.1.1/2; qu. A; layer a; niv. 61.68–61.58. – Fragment of a wishbone handle. – Dimensions (cm): wf 2.3; hf 1.6. – Fabric 37, undecorated. – Dating: MBA.

P 3/031. Site 3; tr. 3.1; ft. 3.1.1/2; qu. B; layer a. – Rim fragment of a pot with narrow mouth. – Dimensions (cm): m 19.4; wf 3.9; hf 3.9. – Fabric 18, undecorated. – Dating: BA.

P 3/032. Site 3; tr. 3.1; ft. 3.1.1/2; qu. A; layer a; niv. 61.48–61.38. – Rim fragment of a pot with straight lip. – Dimensions (cm): wf 2.9; 2.7. – Fabric 18, undecorated. – Dating: BA.

P 3/033. Site 3; tr. 3.1; ft. 3.1.1/2; qu. A; layer a; niv. 61.68–61.58. – Rim fragment of a pot with funnel mouth. – Dimensions (cm): m 13.0; wf 5.1; hf 3.6. – Fabric 18, undecorated. – Dating: BA.

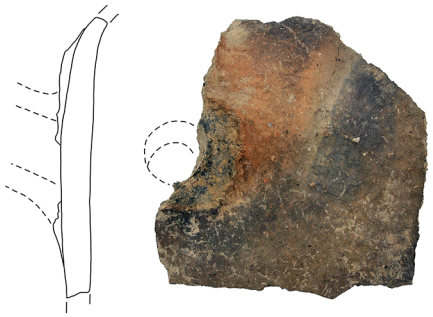
P 3/034. Site 3; tr. 3.1; ft. 3.1.1/2; qu. B; layer a. – Shoulder fragment of a small mug. – Dimensions (cm): wf 2.7; hf 2.3. – Fabric 18, undecorated. – Dating: BA.

P 3/035. Site 3; tr. 3.1; ft. 3.1.1/2; qu. B; layer a; niv. 61.48–61.38. – Shoulder fragment of spherical pot with offset neck. – Dimensions (cm): wf 7.0; hf 5.2. – Fabric 18, undecorated. – Dating: LBA.

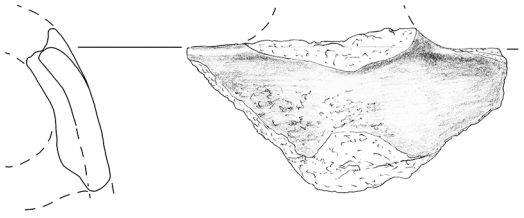
P 3/036. Site 3; tr. 3.1; ft. 3.1.1; qu. B; layer b. – Upper part of a bulbous pot with S-profiled rim. – Dimensions (cm): m 18.1; wf 10.3; hf 9.9. – Fabric 18, smoothed and slipped, undecorated. – Dating: LBA.



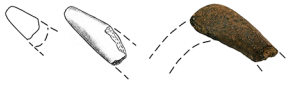
P3/027



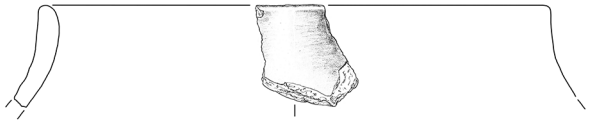
P3/028



P3/029



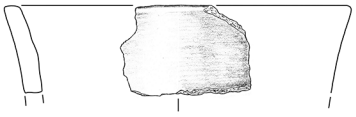
P3/030



P3/031



P3/032

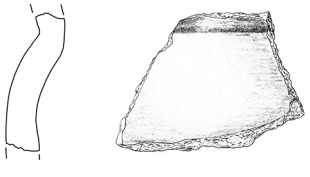


P3/033



P3/034

0 5 cm



P3/035



P3/036

Plate 28. Site 3, excavations (feature 3.1.1/2): Bronze Age pottery (P3/027–P3/036)

SITE 3. Excavations

Trench 3.1, feature 3.1.1/2 (pit)

Feature 3.1.1/2: Bronze Age pottery

P 3/037. Site 3; tr. 3.1; ft. 3.1.1/2; qu. A; layer b; niv. 61.26. – Rim fragment of a storage pot with outcurving lip. – Dimensions (cm): m 24.5; wf 8.0; hf 8.3. – Fabric 37, fingertip strip below the edge. – Dating: LBA.

P 3/038. Site 3; tr. 3.1; ft. 3.1.1/2; qu. B; layer a. – Fragment of a ribbon handle with D-shaped cross-section. – Dimensions (cm): wf 2.7; hf 2.4. – Fabric 18, undecorated. – Dating: BA.

P 3/039. Site 3; tr. 3.1; ft. 3.1.1/2; qu. A; layer b; niv. 61.27. – Middle fragment of a storage vessel. – Dimensions (cm): wf 8.8; hf 4.7. – Fabric 18, tenon handle in the form of a double hump. – Dating: LBA.

P 3/040. Site 3; tr. 3.1; ft. 3.1.1/2; qu. A; layer b; niv. 61.01. – Rim fragment of a small elongated pot with a massive vertical handle bar on the side towards the lower part, narrowing from top to bottom. – Dimensions (cm): wf 3.1; hf 4.3. – Fabric 18, undecorated. – Dating: BA.

P 3/041. Site 3; tr. 3.1; ft. 3.1.1/2; qu. A; layer c; niv. 61.18–61.08. – Fragment of a ribbon handle with D-shaped cross-section. – Dimensions (cm): wf 2.2; hf 2.3. – Fabric 18, undecorated. – Dating: BA.

P 3/042. Site 3; tr. 3.1; ft. 3.1.1/2; qu. A; layer b; niv. 61.47. – Upper part of a bulbous pot with S-profiled rim. – Dimensions (cm): m 19.2; wf 17.1; hf 8.1. – Fabric 18, undecorated. – Dating: BA.

P 3/043. Site 3; tr. 3.1; ft. 3.1.1/2; qu. A; layer a; niv. 61.68–61.58. – Rim fragment of the conical upper part of a vessel. – Dimensions (cm): wf 4.0; hf 2.6. – Fabric 18, notched rim. – Dating: BA.

P 3/044. Site 3; tr. 3.1; ft. 3.1.1/2; qu. A; layer a; niv. 61.68–61.58. – Fragment of a small buckle. – Dimensions (cm): wf 3.1; hf 1.8. – Fabric 18, undecorated. – Dating: BA.

P 3/045. Site 3; tr. 3.1; ft. 3.1.1/2; qu. A; layer b; niv. 61.68–61.58. – Rim fragment of the conical upper part of a vessel. – Dimensions (cm): wf 3.0; hf 3.8. – Fabric 18, undecorated. – Dating: BA.

P 3/046. Site 3; tr. 3.1; ft. 3.1.1/2; qu. A; layer b; niv. 61.68–61.58. – Rim fragment of the conical upper part of a vessel. – Dimensions (cm): wf 3.2; hf 2.8. – Fabric 18, undecorated. – Dating: BA.

P 3/047. Site 3; tr. 3.1; ft. 3.1.1/2; qu. A; layer a; niv. 61.49. – Rim fragment of a funnel mouth. – Dimensions (cm): m 11.6; wf 5.3; hf 4.4. – Fabric 18, undecorated. – Dating: BA.

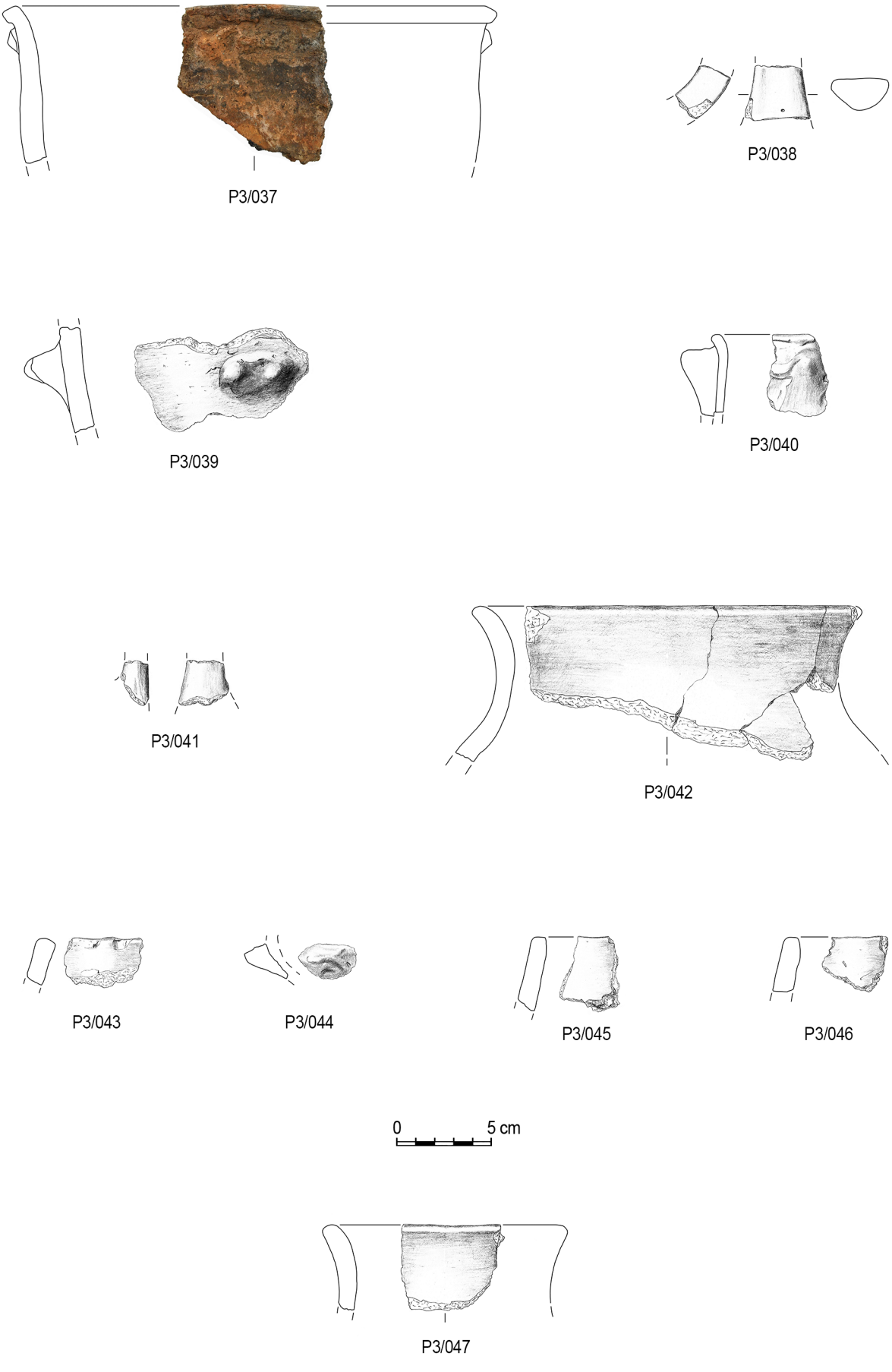


Plate 29. Site 3, excavations (feature 3.1.1/2): Bronze Age pottery (P3/037–P3/047)

SITE 4. Survey

Site 4, survey: Late Iron Age pottery

P 4/001. Site 4; pol. 225. – Cup, rim fragment. Slanted rim; spherical body. – Dimensions (cm): m 12; hf 2.2; wf 3.2. – Fabric 56. Rolled and washed surface; likely wheel made. – Parallels: Върбанов 2013b, no. 341 pl. 2,57 (grey fabric; 2nd–1st c.). – Dating: LIA (2nd–1st c. BC).

SITE 5. Survey

Site 5, survey: Early Iron Age pottery

P 5/001. Site 5; pol. 166. – Fragment of a wide tenon handle. – Dimensions (cm): wf 6.3; hf 3.0. – Fabric 28. – Dating: EIA.

Site 5, survey: Late Iron Age (- Early Roman) pottery

P 5/002. Site 5; pol. 162. – Hydria or large jug; stand ring. – Dimensions (cm): hf 4.4; b (stand ring) 11. – Fabric 49. – Cf. cat. P 17/004. – Dating: LIA.

P 5/003. Site 5; pol. 162. – Large plate or (fruit -?) bowl, rim fragment. Wide, horizontal rim with curved cross-section. Sharp bend to the wall. – Dimensions (cm): m 45.5; hf 1.7; wf 10.2. – Fabric 51; rolled and washed surface. – Parallels: cf. Върбанов 2013b, no. 188 pl. 4,16 (2nd–1st c. BC). – Dating: LIA (2nd–1st c. BC/1st c. AD).

P 5/004. Site 5; pol. 162. – Jar(?), rim fragment. Simply profiled, out-curved rim. – Dimensions (cm): m 18; hf 2.1; wf 6.2. – Fabric 51. – Parallels: cf. Moscalu 1983, type 23c1 (with horizontal handles) pl. 100,2 (Bugeac, 4th c. BC); Върбанов 2013b, cat. 389; 390 pl. 9,17.18 (2nd–1st c. BC). – Dating: LIA.

P 5/005. Site 5; pol. 170. – Small dolium, fragment of the bottom with thickened foot. Incised grooves on the exterior. – Dimensions (cm): m 14.2; hf 5.1; b 6; wf 7.5. – Fabric 51; exterior grey; interior dark grey, stained. – No parallel. – Dating: LIA (-ERP?).

P 5/006. Site 5; pol. 163. – Pot, wall fragment with small round attachment with imprint. – Dimensions (cm): hf 3.7; wf 4.1. – Fabric 55. – Parallels: similar attachments mainly in the later phase of the LIA, cf. for example Върбанов 2013a, pl. 2,15–19; 3,1.2.7.8 (2nd–1st c. BC). – Dating: LIA (2nd–1st c. BC/1st c. AD).

Site 5, survey: Roman pottery

P 5/007. Site 5; pol. 165. – Amphora, fragment of a double handle. – Dimensions (cm): wf 8.3. – Ochre engobe; sandy, reddish brown fabric with light reddish brown outer layer. – Parallels: Dressel 1879, type 2–4; Dyczek 2001, type 1; Генчева 2002, cat. 106 pl. 34,2 (mid-2nd half of 1st c.); Dobreva 2017, 294–295 fig. 216; 217. – Dating: RP (1st–2nd c.).

P 5/008. Site 5; pol. 142. – Amphora, rim fragment. Funnel-shaped mouth with rounded, slightly thickened rim. – Dimensions (cm): m 15; hf 2.7; wf 4.8. – Ochre fabric and engobe; light reddish brown core; fine. Rolled surface. – Parallels: Dressel 1879, type 24 sim. D, cf. Opaiț 2007, 632. – Dating: RP (2nd half of 3rd c.–1st half of 4th c.).

P 5/009. Site 5; pol. 176. – Amphora, foot with rounded and slightly thickened end; flat bottom with small hole. – Dimensions (cm): hf 7.4; b (foot) 3.5. – Dark reddish brown, sandy, micaceous fabric; middle coarse temper. – Not classified; foot belongs probably to an amphora like cat. P 1/140; P 2/002 or similar. – Dating: RP (2nd–3rd c.?).

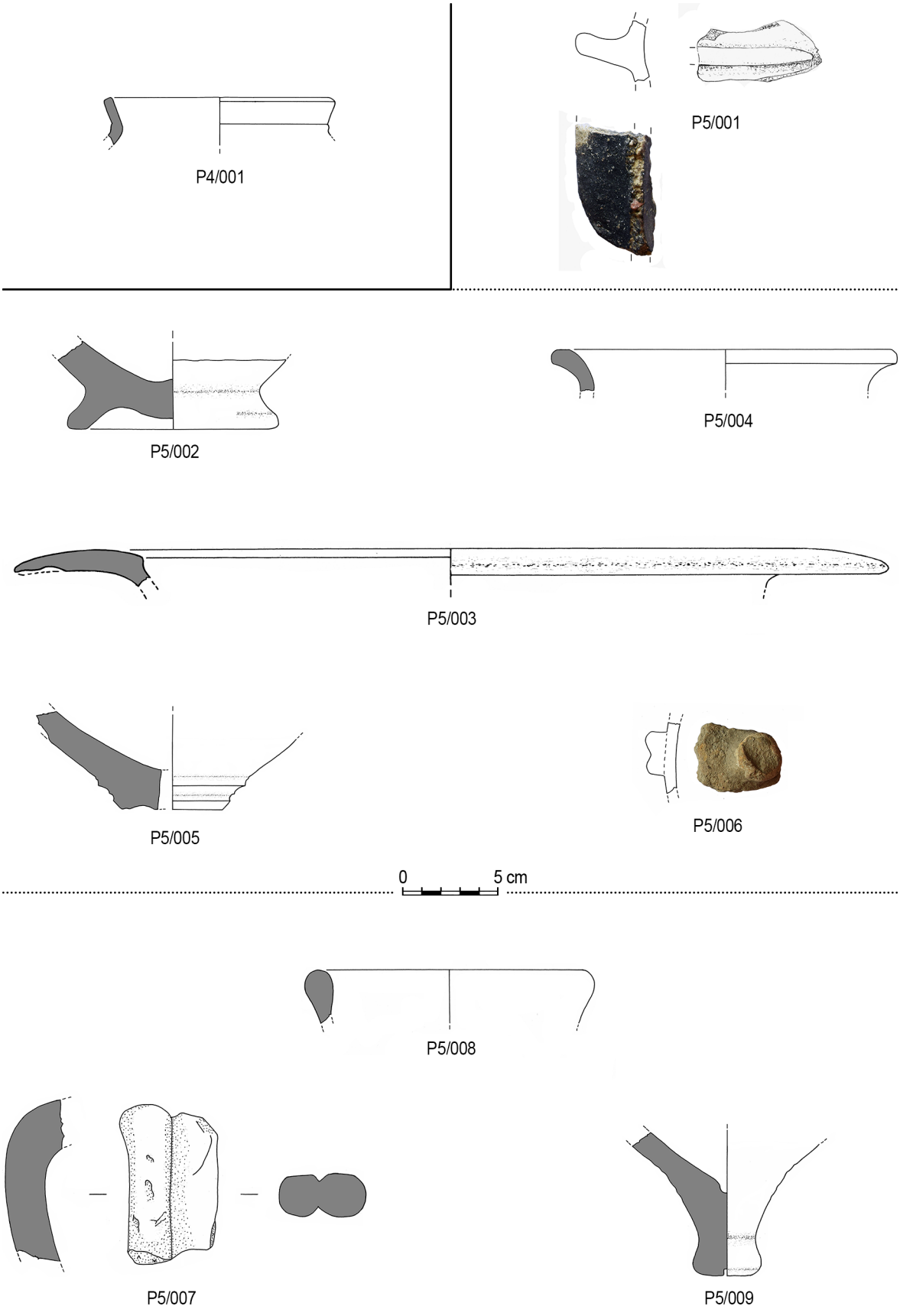


Plate 30. Site 4, survey: Late Iron Age pottery (P4/001). – Site 5, survey: Early Iron Age pottery (P5/001); Late Iron Age (– Early Roman) pottery (P5/002–P5/006); Roman pottery (P5/007–P5/009)

SITE 5. Excavations

Site 5, excavations: Roman pottery

P 5/010. Site 5; tr. 5.2; ft. 5.1.5 (pit); niv. 21.18–20.77 (humus); several fragments also in the lower filling of the pit. – Amphora, with different preserved parts: mouth with thickened rim and with partly preserved handles, part of the neck, and several fragments of the body. – Dimensions (cm): m 6.9; hf 24) (reconstr.). – Light yellowish, sandy fabric with some fine, dark inclusions. – Parallels: Зеест 1960, type 64b; Šelov 1986, type A; Böttger, Šelov 1998, 32 type 26A; Генчева 2002, cat. 104 pl. 33,3; Внуков 2003, type C IV A1/A2; Внуков 2016; Dobreva 2017, 249–250 fig. 164; Borislavova 2018, type Hr I (mid-1st–beg. 2nd c.). – Dating: ERP (mid to 2nd half of the 1st c. AD).

P 5/011. Site 5; tr. 5.1. Humus layer. – Amphora, rim fragment. Slightly flared and thickened rim. – Dimensions (cm): m 8; hf 5.9; wf 4.6. – Light yellowish, sandy fabric; roughly sandy surface. – Parallels: Генчева 2002, cat. 234 pl. 33,2; Borislavova 2018, type Hr II (mid-1st–beg. 2nd c.). Cf. also cat. P 5/010. – Dating: ERP (mid to 2nd half of the 1st c. AD).

P 5/012. Site 5; tr. 5.2; ft. 5.1.5 pit; niv. 20.70–20.56. – Jug, fragment of the bottom; shaped as an omphalos. – Dimensions (cm): hf 1.0; b 6.8. – Light reddish brown, slightly sandy fabric. Traces of reddish brown engobe. – Parallels: Генчева 2002, cat. 88; 90; 210 pl. 25,3; 26,1; 31,2. – Dating: ERP (mid to 2nd half of the 1st c. AD).

P 5/013. Site 5; tr. 5.2; ft. 5.1.5 (pit); niv. 20.77–20.70. – Bowl; large fragment with rim. Wide, slightly outcurved wall with an almost vertical upper part narrow grip rim with surface sloping outwards. – Dimensions (cm): m 28.5; hf 9.5; wf 15.7. – Fabric 49. Olive brown fabric with blackish grey spotted surface; grey core. – Parallels: bowls with similar profiles from early features in Novae, cf. Генчева 2002, cat. 195; 156; 244; pl. 22,1–3 (mid to 2nd half of 1st c. AD), but already in the pit sanctuary in Ruse, cf. Върбанов 2013a, no. 67; 105; 106 pl. 3,12 (with sharp turn in the wall).50.51 (2nd–1st c. BC); Вагалински 2002, bowl type I var. 1; КУ 134 (Vulchedrum; 1st c. BC to 1st/2nd c. AD), КУ140; КУ143 (Kula-Castra Martis; 1st c. AD) with similar profiles (partly burnished). – Dating: ERP (mid to 2nd half of the 1st c. AD).

P 5/014. Site 5; tr. 5.1; ft. 5.1.5 (grave); niv. 19.75. – Fruit bowl (slow wheel made), approx. a quarter of the broken vessel is preserved (restored); the foot is missing. Wide rim, gently slanting to the interior; sharp kink to the upper vertical wall, which sharply bends to the sloping lower part. – Dimensions (cm): m 34; hf 11.6). – Fabric 56. Carefully smoothed surface. – Parallels: Crişan 1969, Taf. 52,16 (2nd–1st c. BC); Върбанов 2013a, no. 321; 323 pl. 11,8.10 (2nd–1st c. BC). – Dating: ERP (mid to 2nd half of the 1st c.).

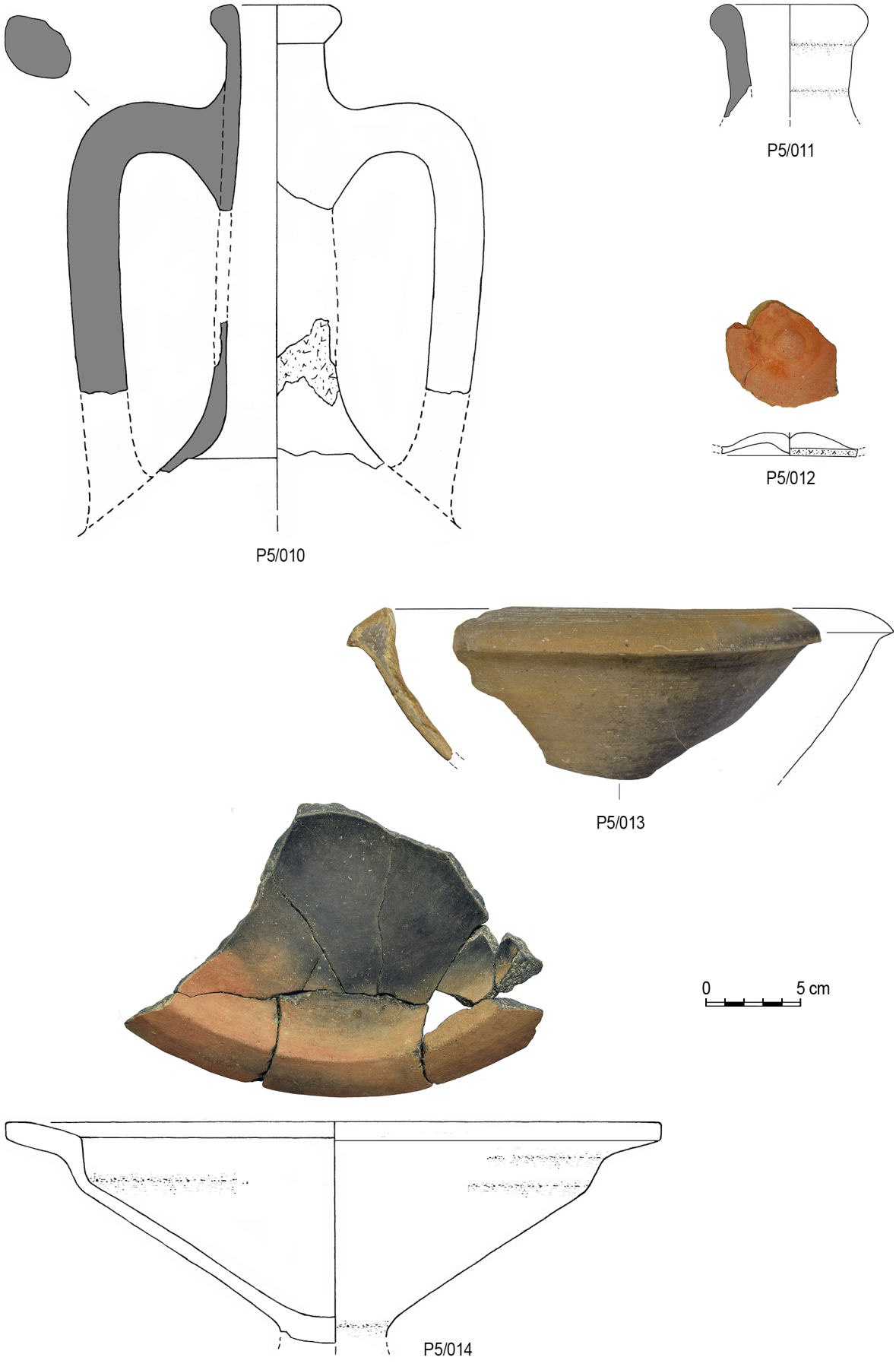


Plate 31. Site 5, excavations: Roman pottery (P5/010–P5/014)

SITE 5. Excavations

Site 5, excavations: Roman pottery

P 5/015. Site 5; tr. 5.1; ft. 5.1.5 (grave); niv. 19.75. – Large, beaker-shaped vessel (slow wheel made); large fragments without bottom, had apparently been deposited as grave goods. Heavily fragmented; partly restored. The handles (two are preserved) are attached at an angle to the axis of the vessel. – Dimensions (cm): hf 19.6; b ca. 11.8. – Fabric 57, with a large quantity of mica. Carefully smoothed surface. – Parallels: profile of the vessel (without ornaments) similar to Crişan 1969, Taf. 28,13 (Ghenci; 3rd–2nd c. BC); Moscalu 1983, type 3c pl. 16,1 (Cerna; 5th–4th c. BC).5 (Cernica-Bukarest; 425–400 BC); Чичикова 1984, type 1 fig. 1 pl. 1; Върбанов 2013a, no. 36–41 pl. 2,1–6. – Dating: ERP (mid to 2nd half of the 1st c. AD).

P 5/016. Site 5; tr. 5.1; ft. 5.1.5 (pit); niv. 20.77–20.32. – Jar (slow wheel made), several wall fragments without rim and bottom. The moderately sloping shoulder with the relatively sharp bend towards the concave lower part is preserved. – Dimensions (cm): d 25.5 (shoulder); hf 10.7; wf 10.1. – Dark greyish brown to greyish black fracture; very coarse. Black outer surface, carelessly formed and slightly smoothed, with minor damage. – Parallels: no exact parallel. Jars and jugs with a sharp bend in the middle of the body were found in the pit sanctuary in Ruse, cf. Върбанов 2013a, no. 381–385 pl. 12,8–12 (2nd–1st c. BC). – Dating: ERP (mid to 2nd half of the 1st c. AD).

P 5/017. Site 5; tr. 5.1; ft. 5.1.5 (filling of the pit); niv. 20.38–20.23. – Pot (handmade); several fragments are preserved, from which the profile was reconstructed. Beaker-like form of the vessel with slightly spherical wall (bottom not preserved); Slightly out curved and beaded rim. Flat incised, ovoid ornaments on the exterior. – Dimensions (cm): m 14; hf 9.7) (reconstr.). – Fabric 55. – Parallels: Генчева 2002, cat. 121 pl. 40,3 (mid to 2nd half of 1st c. AD); profile also very likely similar to the fragments Върбанов 2013a, no. 88–90 pl. 4,1–3 (2nd–1st c. BC). No exact parallel for the incised ornament found. – Dating: ERP (mid to 2nd half of the 1st c. AD).

P 5/018. Site 5; tr. 5.2; ft. 5.1.5 (pit); niv. 20.56–20.49. – Pot (handmade); two fragments from the upper part with rim. Bulbous, obviously rather thick-walled body with narrow neck; funnel-shaped upper part with unprofiled rim; angulated lip. Two rows of irregular notches in the neck zone; smaller, oblique notches in greater distances on the exterior of the rim. – Dimensions (cm): m ca. 16.5; hf 10.5; wf 9.2. – Fabric 56. Very coarse; rough surface. – Parallels: type of the thick-walled vessel like Crişan 1969, 161–163 Abb. 75; 76 pl. 77,4 (Moigrad).12 (Poiana; Moigrad; Sf. Gheorghe; 1st c. BC – 1st c. AD); Moscalu 1983, type 2d pl. 24,1 (Brăiliţa; 4th–3rd c. BC); Генчева 2002, cat. 117; pl. 39,1 (mid to 2nd half of 1st c. AD). Cf. also Върбанов 2013a, no. 94 pl. 4,7 (2nd–1st c. BC). No exact parallel for the ornamentation. – Dating: ERP (mid to 2nd half of the 1st c. AD).

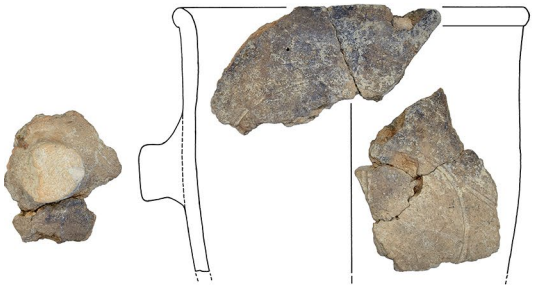


P5/015



P5/016

0 5 cm



P5/017



P5/018

Plate 32. Site 5, excavations: Roman pottery (P5/015–P5/018)

SITE 5. Excavations

Site 5, excavations: Roman pottery

P 5/019. Site 5; tr. 5.2; humus layer above ft. 5.1.5; niv. 21.18–20.77. – Large bowl or pot (handmade); rim fragment. Straight, sloping wall with unprofiled, flattened rim. – Dimensions (cm): m ca. 40; hf 5.7; wf 6.9. – Fabric 56; smoothed and carefully formed surface. – Parallels: the fragment probably belongs to a bowl like Върбанов 2013a, no. 250; 251 pl. 9,16.17 (2nd–1st c. BC). – Dating: LIA (2nd/1st c. BC) or ERP (mid to 2nd half of the 1st c. AD).

P 5/020. Site 5; tr. 5.2; 5.1.5 (pit); niv. 20.70–20.56. – Pot (handmade); two fragments of the rim. Funnel-shaped rim, slightly curved. – Dimensions (cm): m 20; hf 5.5; wf 11.1. – Fabric 56; smoothed and carefully formed surface. – Parallels: high, funnel-shaped rims at vessels like Moscalu 1983, type 1e pl. 7,3 (Enisala; 4th c. BC).4 (Calnia; 4th c. BC); Генчева 2002, cat. 171 pl. 39,3 (mid to 2nd half of 1st c. AD). Similar rims were found in the pit sanctuary of Ruse, cf. Върбанов 2013a, no. 23; 26 pl. 1;13.19 (2nd–1st c. BC). – Dating: ERP (mid to 2nd half of the 1st c. AD).

P 5/021. Site 5; tr. 5.2; ft. 5.1.5 (pit); niv. 20.70–20.56. – Pot (handmade); large fragment of the lower part with bottom. Roughly formed; very thick-walled; stepped bottom. On the interior of the bottom footstep of an animal (dog?). – Dimensions (cm): hf 6.5; b 13.2. – Fabric 55. Very coarse; rough surface (similar to cat. P 05/018). – Parallels: thick-walled bottom of a pot like Върбанов 2013a, no. 125; 128 pl. 5,31.34 (2nd–1st c. BC). – Dating: ERP (mid to 2nd half of the 1st c. AD).

.

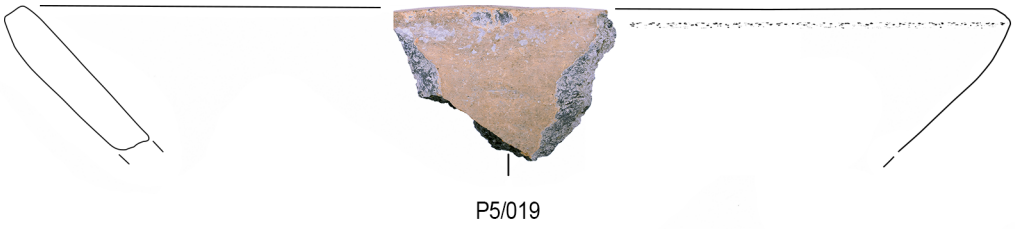
P 5/022. Site 5; fr. 5.2; ft. 5.1.5 (pit); niv. 20.70–20.56. – Pot (slow wheel made?); wall fragment. Incised lines and a semicircle on the surface; partly preserved. – Dimensions (cm): hf 5.3; wf 8.5. – Fabric 55. – Parallels: cf. the fragments with deeper incised lines: Върбанов 2013a, no. 88–90 pl. 4,1–3 (2nd–1st c. BC). – Dating: ERP (mid to 2nd half of the 1st c. AD).

P 5/023. Site 5; fr. 5.2; ft. 5.1.5 (pit); niv. 20.70–20.56. – Pot (slow wheel made?); one wall fragment. Part of an attached waved moulding with fingertip prints preserved. – Dimensions (cm): hf 7.1; wf 8.4. – Fabric 55. – Parallels: garland-like curved mouldings with fingertip prints especially on vessels from the pit sanctuary in Ruse, cf. for example Върбанов 2013a, no. 36–38; 41;43; 44 pl. 2,1–3.6.8.9. – Dating: ERP (mid to 2nd half of the 1st c. AD).

P 5/024. Site 5; tr. 5.2.; humus layer above pit 5.1.5; niv. 21.18–20.77. – Pot (slow wheel made?); one wall fragment. Relatively flat relief attachment with an incised oblique cross. – Dimensions (cm): hf 5.6; wf 5.3. – Fabric 56. – Parallels: Crişan 1969, Taf. 74,6 (Sighişoara; 1st c. BC – 1st c. AD); Върбанов 2013a, no. 4; 152 pl. 1;4; 6,11 (2nd–1st c. BC). – Dating: (LIA–) ERP (mid to 2nd half of the 1st c. AD or [residual?] 2nd/1st c. BC).

P 5/025. Site 5; tr. 5.2; ft. 5.1.5 (pit); niv. 20.77–20.70. – Storage vessel / cauldron; rim fragment. Strongly out-curved rim with faceted upper side, which is slightly inclined. Bulbous body. – Dimensions (cm): m ca. 29; hf 3.6; wf 7.8. – Fabric 56. – Parallels: no exact parallel. Faceted rims on fruit bowls from the pit complex in Ruse, cf. Върбанов 2013b, cat. 218; 222; 223; 230 pl. 5,2.6.7.14 (wheel made). – Dating: ERP (mid to 2nd half of the 1st c. AD)

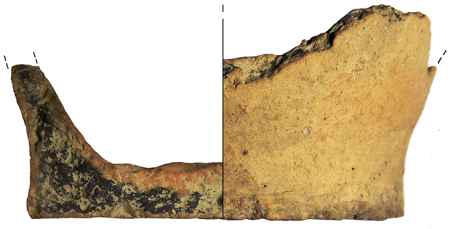
P 5/026. Site 5, tr. 5.1; ft. 5.1.6 (pit). – Fruit bowl (or plate?), rim fragment. Relatively wide, curved rim, slightly slanting to the interior. Sharp kink to the upper vertical wall which bends to the moderately inclined lower part. – Dimensions (cm): m 28; hf 3.5; wf 4.8. – Fabric 49. Dark grey fabric; grey, with shiny polished surface. Traces of processing with chip-like instrument. – Parallels: similar profiles: Вагалински 2002, bowls type II var. 3; КУ165 (Yakimovo; 1st c. BC – 2nd c. AD); bowls type II var. 4; КУ169 (Vulchedrum; 1st c. BC – 1st/2nd c. AD); КУ170 (Yakimovo; 1st c. BC – 2nd c. AD); Върбанов 2013b, no. 209 pl. 4,37 (2nd–1st c. BC), with burnished surface. Dating: ERP (mid to 2nd half of the 1st c. AD).



P5/019



P5/020





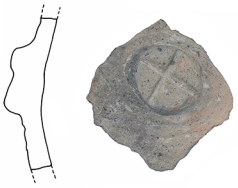
P5/021



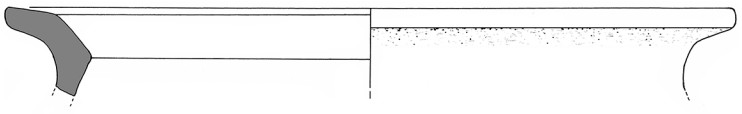
P5/022



P5/023

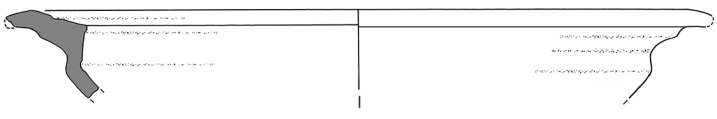


P5/024



P5/025

0 5 cm



P5/026

Plate 33. Site 5, excavations: Roman pottery (P5/019–P5/026)

SITE 12. Survey

Site 12, survey: Roman pottery

P 12/001. Site 12; pol. 243. – Amphora, rim fragment. Funnel-shaped mouth, on the exterior a combination of two beadings separated by a groove. – Dimensions (cm): m 17; hf 3.4; wf 6.8. – Fabric 59. Rolled surface. – Parallels: Falkner 1999, cat. 908 (2nd c.). – Dating: RP (2nd c.).

P 12/002. Site 12; pol. 243. – Amphora, rim fragment. Slightly funnel-shaped mouth, on the exterior a projected beading with a circumferential groove. – Dimensions (cm): m 15; hf 3.5; wf 6.5. – Fabric 59. – Parallels: similar to Falkner 1999, cat. 914 (end 2nd–1st half of 3rd c.). – Dating: RP (end 2nd–1st half of 3rd c.).

P 12/003. Site 12; pol. 244. – Cup, rim fragment; slightly turned and funnel-shaped extended. – Dimensions (cm): m 9; hf 2.0; wf 3.0. – Fabric 58. – Parallels: Böttger 1982, cup type I; Sultov 1985, cup type 2 pl. 32,6; Falkner 1999, cat. 757; 758; Conrad 2007a, cat. 771 (2nd half of 3rd c.); 883 (1st half of 4th c.). – Dating: RP (2nd–1st half of 4th c.).

P 12/004. Site 12; pol. 243. – Bowl, rim fragment. Vertical, slightly curved upper part; slightly beaded rim which is emphasised by a groove on the exterior. Sharp bend to the lower part. – Dimensions (cm): m 28; hf 5.8; wf 6.5. – Fabric 59. – Parallels: Sultov 1985, bowls type 1c pl. 29,1; Falkner 1999, cat. 432; 441 (2nd–1st half of 4th c.); Conrad 2007a, cat. 924; 925 (1st half of 4th c.). – Dating: RP (2nd–1st half of 4th c.).

P 12/005. Site 12; pol. 243. – Bowl, rim fragment. Spherical body; outwards turned rim with rounded lip. – Dimensions (cm): m 24; hf 4.4; wf 3.1. – Fabric 59. – Cf. cat. P 2/009; P 2/013; P 12/004. – Dating: RP (2nd–1st half of 4th c.).

P 12/006. Site 12; pol. 234. – Bowl, rim fragment. Similar form of the vessel to cat. P 2/014; slimmer shape and more slanted rim. – Dimensions (cm): m 14; hf 2.6; wf 4.5. – Fabric 64. Rough surface. – In regarding the fabric, the piece is a variant of this type made in red slipware, cf. cat. P 2/014; P 18/013. – Dating: RP (2nd–1st half of 4th c.).

P 12/007. Site 12; pol. 234. – Pot, rim fragment. Strongly outwards turned rim, beaded on the downside; flat upper side. – Dimensions (cm): m ca. 18; hf 2.2; wf 2.3. – Fabric 65. – Parallels: Falkner 1999, cat. 98; 108 (residual). – Dating: RP (2nd half of 2nd/3rd c.).

P 12/008. Site 12; pol. 243. – Pot, rim fragment. Slanted, beaded rim with a shallow groove on the interior. – Dimensions (cm): m ca. 18; hf 2.6; wf 3.1. – Fabric 64. Rough surface. – Cf. cat. P 18/016. – Dating: RP (3rd c.–1st half of 4th c.).

P 12/009. Site 12; pol. 234. – Pot, rim fragment. Flat, slanted rim. – Dimensions (cm): m 16; hf 2.4; wf 4.0. – Fabric 63. – Parallels: Falkner 1999, cat. 277; 278 (probably residual); Conrad 2007a, cat. 868 (2nd half of 3rd c.). – Dating: RP (3rd c. – 1st half of 4th c.).

Site 12, survey: Late Roman pottery

P 12/010. Site 12; pol. 244. – Amphora, rim fragment. Similar to cat. P 2/020, but with narrower mouth. – Dimensions (cm): m ca. 14; hf 6.0; wf 5.2. – Dark reddish brown, slightly fine sandy fabric; light yellowish engobe. – Parallels: Riley 1979, LRA 2; Böttger 1982, amphora I1 (2nd half of 4th c.). – Dating: LRP (2nd half of 4th c.).

P 12/011. Site 12; pol. 244. – Pot, rim fragment. Flat, slanted rim. – Dimensions (cm): m 18; hf 2.0; wf 4.2. – Fabric 71. – Parallels: Böttger 1982, pot type 3. – Dating: LRP.

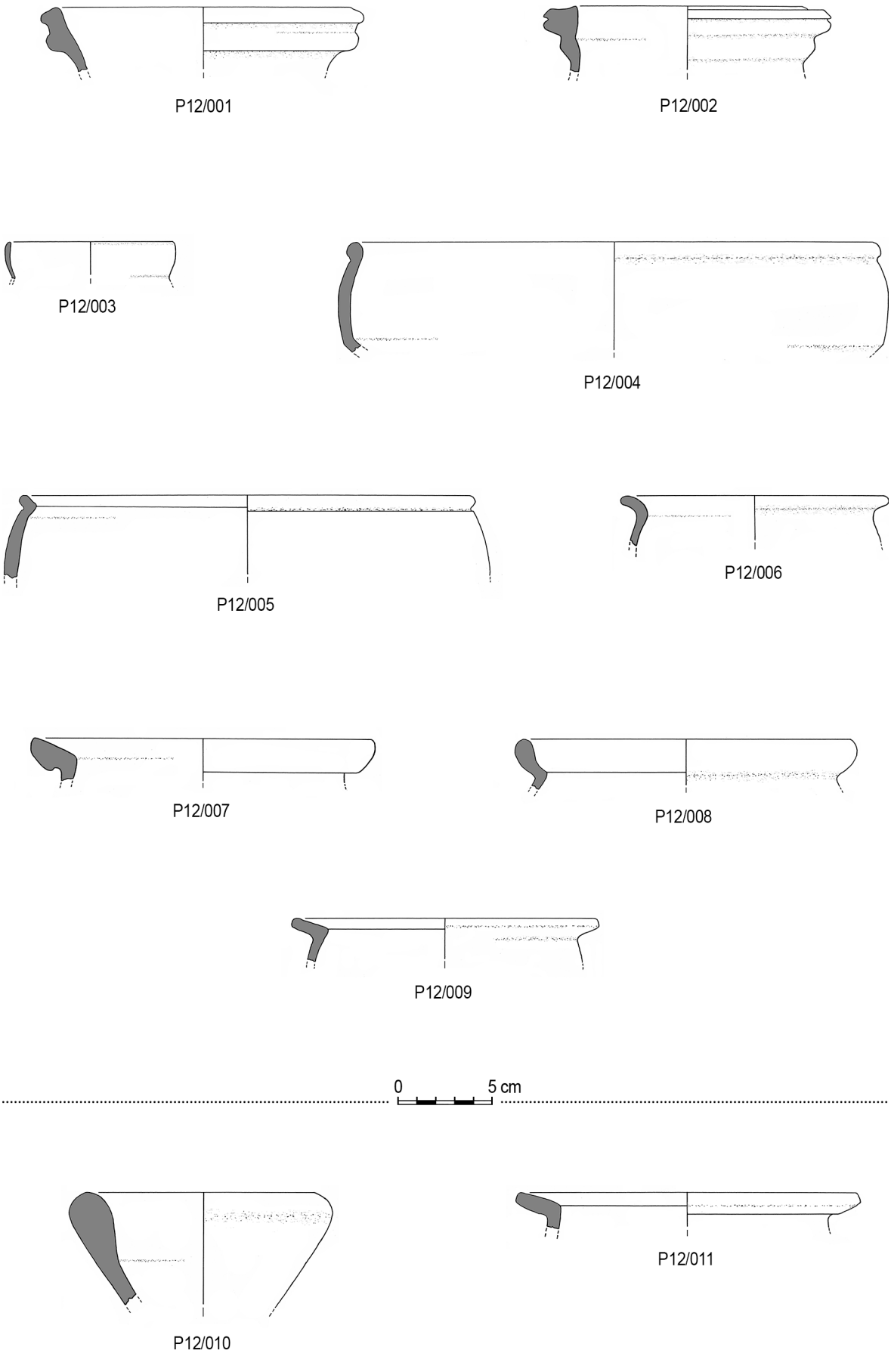


Plate 34. Site 12, survey: Roman pottery (P12/001–P12/009); Late Roman pottery (P12/010–P12/011)

SITE 17. Survey

Site 17, survey: Early Iron Age pottery

P 17/001. Site 17; pol. 411. – Middle fragment of a straight walled vessel. – Dimensions (cm): wf 5.8; hf 3.4. – Fabric 40, linear incised motif. – Dating: EIA.

P 17/002. Site 17; pol. 458. – Fragment of a wide tenon handle. – Dimensions (cm): wf 10.3; hf 7.2. – Fabric 28, slipped, undecorated. – Dating: EIA.

Site 17, survey: Late Iron Age pottery

P 17/003. Site 17; pol. 412. – Crater, rim fragment. Thickened, hammer-like profile, slightly inclined. – Dimensions (cm): m 126; hf 2.2; wf 4.6. – Fabric 53. – Parallels: Moscalu 1983, type 23 pl. 102,3 (Alexandria; 550–450 BC). – Dating: LIA.

P 17/004. Site 17 (offsite); pol. 415. – Hydria, fragment of the stand ring. – Dimensions (cm): hf 3.2; b (stand ring) 10.8; wf 10.5. – Fabric 49. – Parallels: cf. Moscalu 1983, type 22 a/c pl. 94,1 (Piscul Sadovei, 5th–3rd c. BC). – Dating: LIA.

SITE 18. Survey

Site 18, survey: Late Iron Age pottery

P 18/001. Site 18; pol. 451. – Amphora or hydria, rim fragment. Flared rim, thickened, angularly profiled. Conical neck. – Dimensions (cm): m 16; hf 2.8; wf 6.0. – Fabric 50. – Parallels: no exact parallel for the rim form. The rim could belong to an amphora like Moscalu 1983, type 22c pl. 95,4 (Dolno Sahrane). 6 (Adamclisi). Cf. also Bouzek, Domaradzka 2009, fig. 13,3; Ников 2012, fig. 18 (Apollonia, 6th c. BC) or a small amphora-shaped dolium like Moscalu 1983, type 1 pl. 67 (Zimnicea, 3rd c. BC); pl. 68. – Dating: LIA (5th–4th c. BC).

P 18/002. Site 18; pol. 447. – Storage vessel / cauldron, rim fragment. Slanted rim with slightly thickened, rounded lip. – Dimensions (cm): m 32; hf 2.1; wf 6.9. – Light grey to light orange, fine fabric; some dark, middle fine sand. Rolled surface. – Parallels: Върбанов 2013b, no. 382 fig. 9,10 (2nd–1st c. BC). – Dating: LIA (2nd–1st c. BC).

P 18/003. Site 18; pol. 458. – Plate, rim fragment. Inwardly curved, thickened rim with rounded lip. – Dimensions (cm): m ca. 26; hf 3.0; wf 4.9. – Fabric 56. Light greyish brown, sandy fabric with black core; polished inner surface. – Parallels: Moscalu 1983, type 11b pl. 53,2.4.5.6 (Alexandria-Vii; mid-6th–mid-5th c. BC). – Dating: LIA (6th–5th c. BC).

P 18/004. Site 18; pol. 458. – Plate, rim fragment. Inwardly curved rim with thickened, slightly angulated lip. – Dimensions (cm): m 32; hf 4.4; wf 7.1. – Fabric 56; hand or slow wheel made. Dark greyish brown, sandy fabric with black core; black spotted surface. – Parallels: Moscalu 1983, type 11b pl. 52,10 (Bugeac; 4th c. BC). – Dating: LIA (ca. 4th c. BC).

P 18/005. Site 18; pol. 450. – Pot, rim fragment; very slightly slanted wall, a little bit spherical. Unprofiled rim with flat upper side; horizontal fingerprinted strip. – Dimensions (cm): m 15; h 5.2; wf 5.4. – Fabric 56. Slightly blackish brown spotted. – Parallels: Върбанов 2013a, no. 36 pl. 2,1 (2nd–1st c. BC). Similar rim profile for the vessel Moscalu 1983, type 3a pl. 14,1 (Gruia; 6th c. BC). – Dating: LIA (2nd–1st c. BC).

P 18/006. Site 18; pol. 459. – Pot, wall fragment with small handle. – Dimensions (cm): hf 6.1; wf 3.4. – Fabric 56. – Parallels: these handles often appear with other attachments at handmade pots, cf. Moscalu 1983, type 9d1.d2.f pl. 41; 42 (ca. 5th–3rd c. BC). – Dating: LIA (5th–3rd c. BC).

P 18/007. Site 18; pol. 459. – Pot, wall fragment with fingerprinted strip. – Dimensions (cm): hf 6.3; wf 7.1. – Fabric 56. – Exact determination of type and dating not possible. – Dating: LIA.

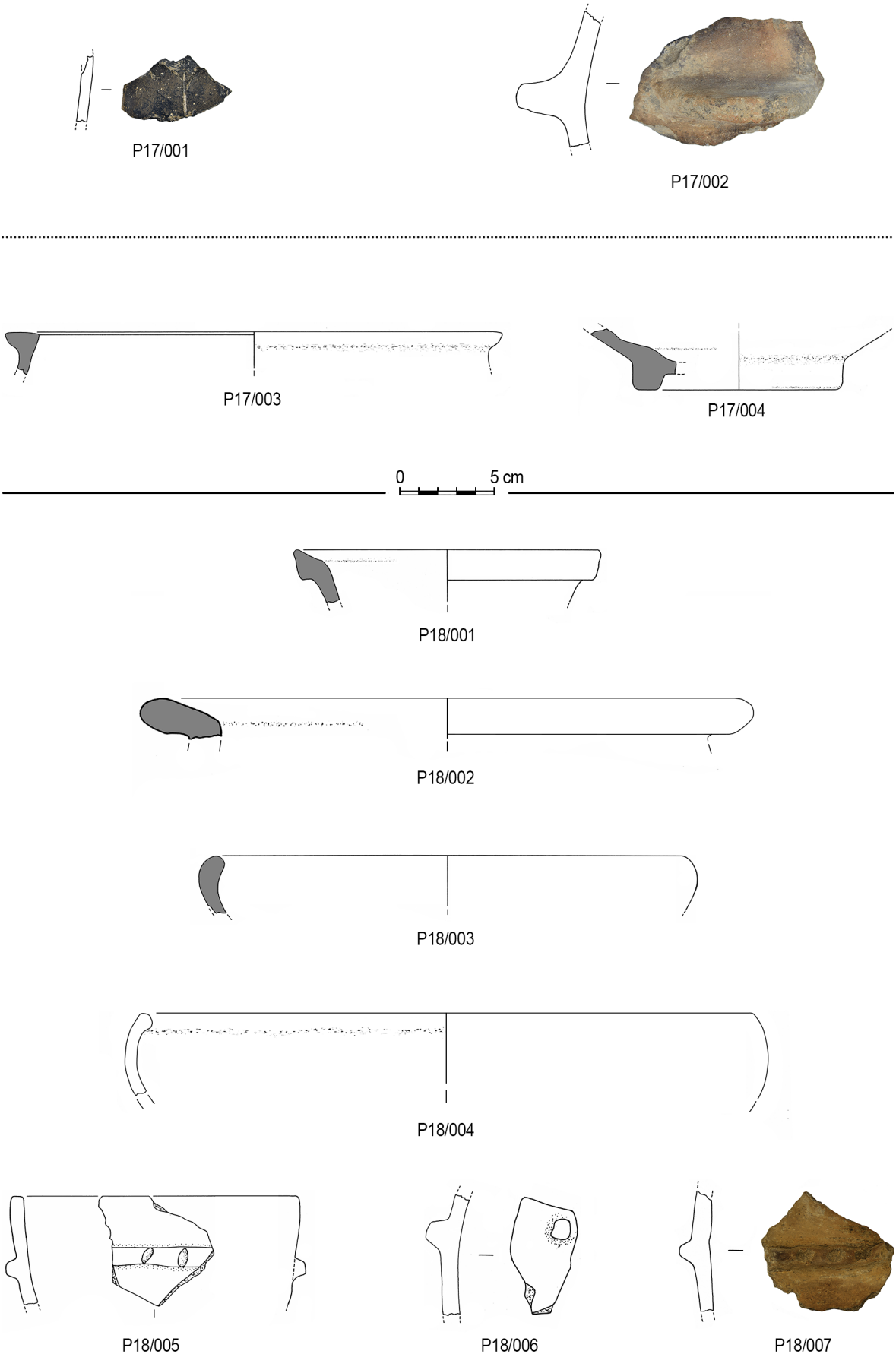


Plate 35. Site 17, survey: Early Iron Age pottery (P17/001–P17/002); Late Iron Age pottery (P17/003–P17/004). – Site 18, survey: Late Iron Age pottery (P18/001–P18/007)

SITE 18. Survey

Site 18, survey: Roman pottery

P 18/008. Site 18; pol. 459. – Amphora, rim fragment. Funnel-shaped mouth, slightly inclined. Rounded lip with a relatively sharp edge to the interior. – Dimensions (cm): m 16; hf 5.3; wf 10.2. – Reddish brown, fine fabric; light ochre engobe. – Dressel 1879, type 24 sim., cf. Opaiț 2007, 628–629 fig. 2,4–6; Dobreva 2017, 233–237 fig. 145. – Dating: RP (2nd–3rd c.).

P 18/009. Site 18; pol. 459. – Cup; only the conical, thick-walled lower part is preserved. Incised horizontal groove, small stand ring. – Dimensions (cm): hf 4.5; b (stand ring) 3.5. – Fabric 59 (without slip; probably rolled). Traces of soot. – No parallel. – Dating: RP.

P 18/010. Site 18; pol. 459. – Plate, rim fragment. Wide curved rim that merges into the swinging, moderately sloping wall without a step. – Dimensions (cm): m 27; hf 3.3; wf 7.5. – Fabric 58. – Sultov 1985, dishes type 3 pl. 26, 5; Conrad 2007a, cat. 800; 801 (3rd c.); 904 (1st half of 4th c.). – Dating: RP (2nd–1st half of 4th c.).

P 18/011. Site 18; pol. 459. – Plate, rim fragment. Vertical side wall with unprofiled rim; relatively sharp bend to the lower part. – m 24; hf 2.7; wf 4.1. – Fabric 58. – Sultov 1985, dish type 7 pl. 28,4; Falkner 1999, cat. 507–510; Conrad 2007a, cat. 896 (with narrow groove on the exterior under the rim) (1st half of 4th c.). – Dating: RP (2nd–1st half of 4th c.).

P 18/012. Site 18; pol. 459. – Small bowl, rim fragment. Slanted rim with rounded lip and shallow groove; curved wall with grooves on the exterior. – Dimensions (cm): m 14; hf 3.0; wf 6.3. – Fabric 59. Rolled surface.
Similar to Sultov 1985, bowl type 6a pl. 30; Falkner 1999, cat. 795–797; Conrad 2007a, cat. 832; 833; 837 (2nd half of 3rd c.). – Dating: RP (2nd–1st half of 4th c.).

P 18/013. Site 18; pol. 459. – Bowl, rim fragment. Curved rim; spherical body with slightly inwardly inclined wall of the upper part. – Dimensions (cm): m 16; hf 3.2) wf 3.6. – Fabric 58. – Conrad 2007a, cat. 843 (2nd half of 3rd c.). Cf. cat. P 02/014; P 12/006. – Dating: RP (2nd–1st half of 4th c.).

P 18/014. Site 18; pol. 459. – Storage vessel / cauldron, rim fragment. Similar profile to cat. P 2/017. – Dimensions (cm): m 35; hf 2.7; wf 7.7. – Fabric 59. Rolled surface. – Cf. cat. P 2/017. – Dating: RP (2nd–1st half of 4th c.).

P 18/015. Site 18 (offsite); pol. 436. – Pot, rim fragment. Slanted, beaded rim with a shallow groove on the interior. Attachment of handle under the rim. – Dimensions (cm): m 18; hf 3.0; wf 5.6. – Fabric 63.
Cf. cat. P 12/008. – Dating: RP (3rd–1st half of 4th c.).

P 18/016. Site 18; pol. 447. – Pot, rim fragment. Slanted, slightly beaded rim with a shallow groove on the interior. – Dimensions (cm): m 16; hf 2.1; h 2.7. – Fabric 63. Sooty rim. – Böttger 1982, pot type 1 (1st half of 4th c.); Sultov 1985, pot type 3 pl. 43; Falkner 1999, cat. 278 (very likely residual); Conrad 2007a, cat. 851; 852 (2nd half of 4th c.). – Dating: RP (3rd c. – 1st half of 4th c.).

P 18/017. Site 18; pol. 459. – Pot, rim fragment. Flat, steeply slanted rim. – Dimensions (cm): m 16; hf 4.3; wf 8.5. – Fabric 63. Sooty rim. – Cf. cat. P 12/009. – Dating: RP (3rd c. – 1st half of 4th c.).

P 18/018. Site 18; pol. 459. – Pot, rim fragment. Very slightly thickened rim with round lip, turned outwards. – Dimensions (cm): m ca. 17; hf 1.9; wf 3.7. – Fabric 65. – Conrad 2007a, cat. 855 (2nd half of 3rd c.). – Dating: RP (3rd c. – 1st half of 4th c.).

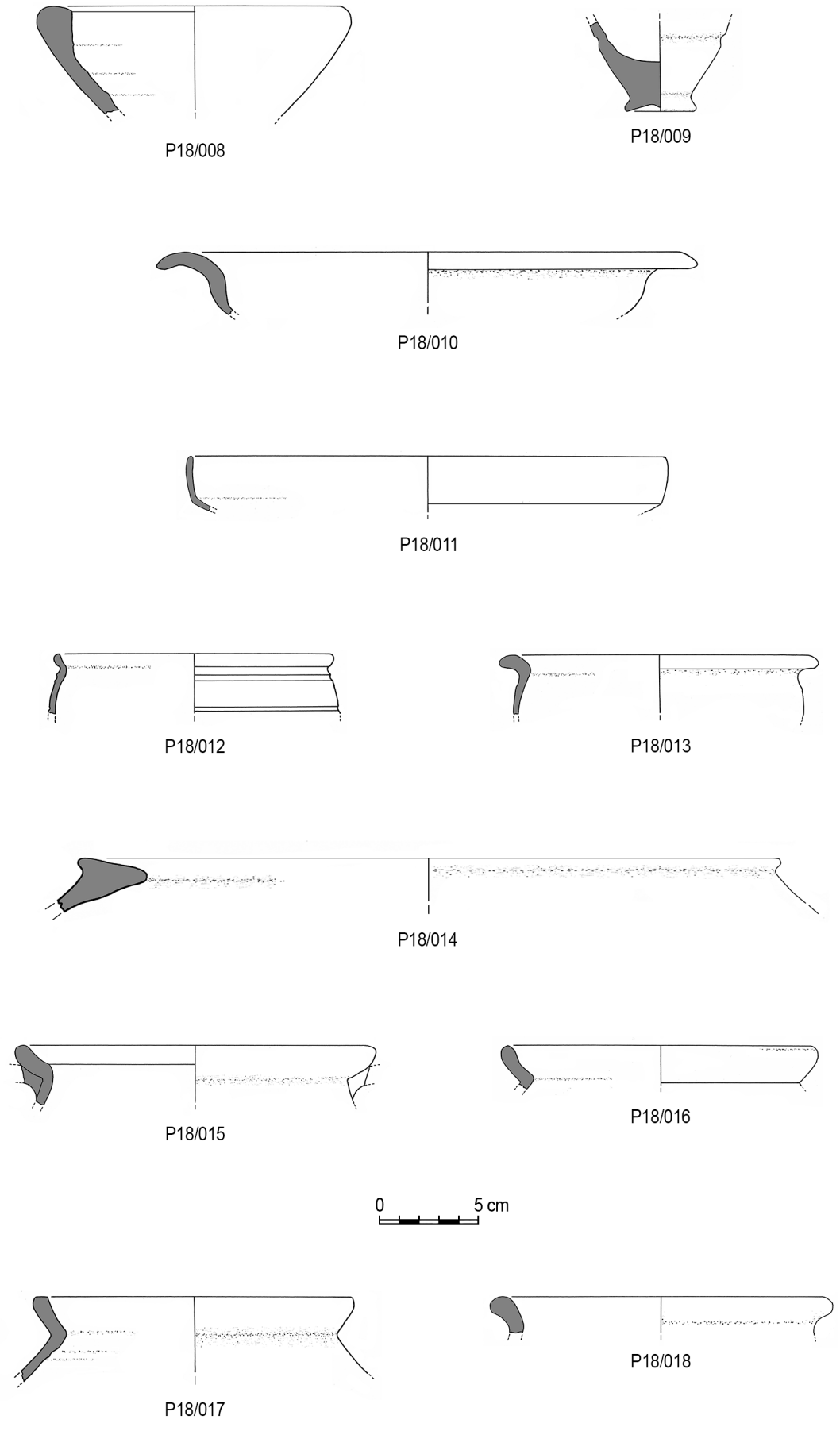


Plate 36. Site 18, survey: Roman pottery (P18/008–P18/018)

SITE 19. Survey

Site 19, survey: Early Iron Age pottery

P 19/001. Site 19; pol. 499. – Fragment of a ribbon handle with flat cross-section. – Dimensions (cm): wf 5.0; hf 4.1. – Fabric 14. – Dating: EIA.

P 19/002. Site 19; pol. 499. – Rim fragment of a rolled rim bowl. – Dimensions (cm): wf 2.1; hf 2.8. – Fabric 40. – Dating: EIA (Basarabi/8th–7th c. BC).

P 19/003. Site 19; pol. 499. – Middle fragment. – Dimensions (cm): wf 2.0; hf 1.4. – Fabric 40. – Dating: EIA.

Site 19, survey: Late Iron Age pottery

P 19/004. Site 19; pol. 503. – Amphora, hydria or large jug, rim fragment. Flared, funnel-like rim, barely profiled. – Dimensions (cm): m 16; hf 1.9; wf 5.1. – Fabric 52. Dark grey, fine fabric; olive-grey surface. – Parallels: nonspecific profile of the mouth, probably like Moscalu 1983, type 22a pl. 94, 2 (Canlia, 4th c. BC). 3 (Brezovo, 440/30 BC).4 Plevna (4th–3rd c. BC); Върбанов 2013b, no. 261 pl. 7,3 (2nd–1st c. BC; jug with burnished ornaments). – Dating: LIA (5th–3rd c. BC?).

P 19/005. Site 19; pol. 491. – Amphora, hydria or similar, rim fragment. Horizontal, angularly profiled rim; funnel-shaped upper part of the neck. – Dimensions (cm): m ca. 16; hf 1.5; wf 3.1. – Fabric 50. – Parallels: cf. Moscalu 1983, type 22a pl. 94,1 (piscul Sadovei, 5th–3rd c. BC); Bouzek, Domaradzka 2009, fig. 13,5; Върбанов 2013b, no. 288 pl. 7,30; 294 pl. 7;36 from the Thracian pit complex in Ruse / Sexaginta Prista (2nd–1st c. BC), but with burnished surface. – Dating: LIA (very likely 5th–3rd c. BC).

P 19/006. Site 19; pol. 491. – Cup (or small jug / beaker), bottom fragment with stand ring. – Dimensions (cm): hf 2.9; b (stand ring) 6.2; wf 5.3. – Fabric 50. – Parallels: Чичикова 1984, no. I.121 fig. 13 (4th–3rd c. BC); Moscalu 1983, type 6a pl. 72,8–15; 73,1.2 (6th–4th c. BC); Върбанов 2013b, pl. 6,52–60 (2nd–1st c. BC). – Dating: LIA.

P 19/007. Site 19; pol. 503. – Plate (or bowl), rim fragment. Rim profile similar to cat. 24/007, but the rim is slightly beaded and the vessel form is more open. – Dimensions (cm): m ca. 26; hf 2.0; wf 3.5. – Fabric 50. Grey, fine fabric; dark grey, polished surface. – Parallels: Moscalu 1983, type 10b pl. 77,10 (Alexandria, 550–450 BC); Върбанов 2013b, no. 22; 23 pl. 1,2.3 (Early Hellenistic). – Dating: LIA (5th–3rd c. BC?).

P 19/008. Site 19; pol. 501. – Plate (or bowl), rim fragment. Slanted wall; only the rounded and slightly thickened lip is inwardly curved. – Dimensions (cm): m 28; hf 3.3; wf 3.6. – Fabric 49. Rolled surface. – Cf. cat. P 19/007. – Dating: LIA (5th–3rd c. BC?).

P 19/009. Site 19; pol. 505. – Plate or bowl, rim fragment. Strongly inwardly curved rim; horizontal groove on the exterior. – Dimensions (cm): m ca. 30; hf 3.7; wf 4.1. – Fabric 56; hand or slow wheel made. – Parallels: Crişan 1969, 50–53 type 1 fig. 9,5; 10 pl. 10 (7th–6th c. BC). – Dating: LIA (7th–6th c. BC).

P 19/010. Site 19; pol. 503. – Bowl, rim fragment. Turned profile; flat lip with slightly rounded edges. – Dimensions (cm): m ca. 20; hf 5.3; wf 5.4. – Fabric 56. Probably made on slow wheel. – Parallels: Moscalu 1983, type 11b pl. 53,1.3 (Alexandria-Vii; mid-6th–mid-5th c. BC). – Dating: LIA.

P 19/011. Site 19; pol. 491. – Pot, rim fragment. Straight wall, slightly inclined; barely profiled rim with flat upper side. – Dimensions (cm): m 24; hf 4.0; wf 5.0. – Fabric 57. – No parallel. – Dating: LIA.

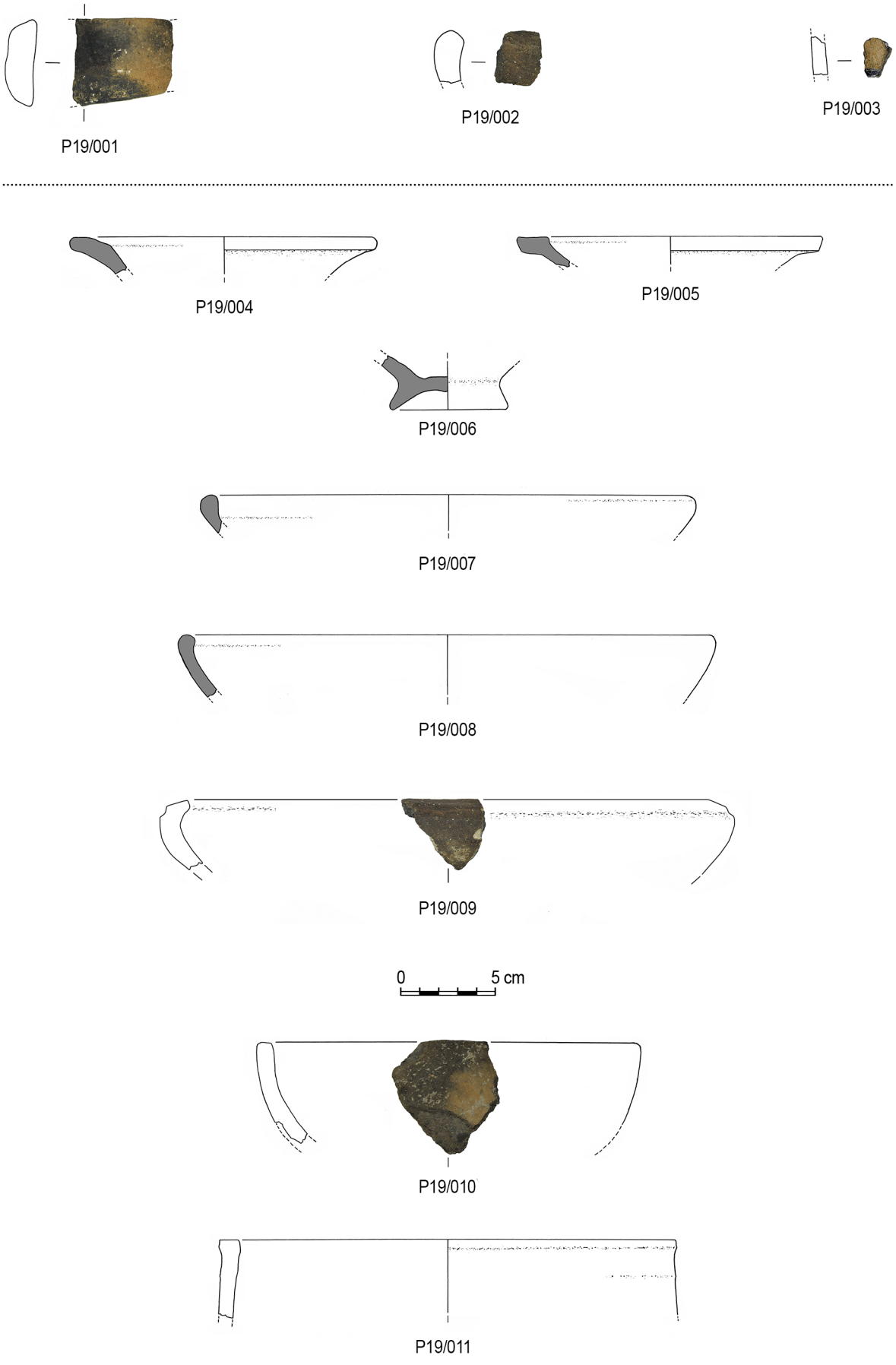


Plate 37. Site 19, survey: Early Iron Age pottery (P19/001–P19/003); Late Iron Age pottery (P19/004–P19/011)

SITE 19. Survey

Site 19, survey: Early Medieval pottery

P 19/012. Site 19; pol 466. – Pot, rim fragment. Spherical body; very short outwards turned rim which tapers towards the lip. Wave band on the shoulder. – Dimensions (cm): m 12; hf 2.9; wf 4.5. – Fabric 75. – Parallels: Wendel 1986, type Krivina pl. 34,6.9. – Dating: EMA.

P 19/013. Site 19; pol 479. – Pot, rim fragment. Spherical body; outwards turned rim with angulated lip. – Dimensions (cm): m 16; hf 2.8; wf 4.3. – Fabric 75. – Parallels: Wendel 1986, type 5 pl. 31,2.4. – Dating: EMA.

P 19/014. Site 19; pol 499. – Pot, rim fragment. Spherical body; flat, relatively sharply outwards turned rim with thickened, angulated lip. – Dimensions (cm): m ca. 14; hf 2.4; wf 3.6. – Fabric 77. – Parallels: Wendel 1986, type Krivina pl. 35,1. – Dating: EMA.

SITE 20. Survey

Site 20, survey: Early Medieval pottery

P 20/001. Site 20 (offsite); pol. 545. – Pot, rim fragment. Spherical body; outwards turned rim with slightly angulated lip. Incised horizontal lines with crossing bundles of lines. – Dimensions (cm): m ca. 14; hf 5.0; wf 7.5. – Fabric 75. – Parallels: Wendel 1986, group 4 pl. 26,2; type 5 pl. 31,2. – Dating: EMA.

SITE 21. Survey

Site 21, survey: Early Iron Age pottery

P 21/001. Site 21; pol. 588. – Middle fragment of a storage vessel with a wide horizontal buckle. – Dimensions (cm): hf 4.5; wf 5.8. – Fabric 40. – Dating: EIA.

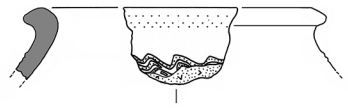
Site 21, survey: Early Medieval pottery

P 21/002. Site 21; pol. 521. – Pot, rim fragment. Spherical body; very short outwards turned rim with rounded lip, which has a sharp edge on its underside. Incised horizontal lines on the shoulder. – Dimensions (cm): m 13; hf 2.8; wf 4.0. – Fabric 77. – Parallels: Wendel 1986, type Krivina pl. 34,6.8. – Dating: EMA.

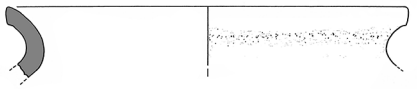
P 21/003. Site 21; pol. 585. – Pot, rim fragment. Spherical body; sharply outwards turned rim with angulated lip. Incised horizontal lines with notches on the shoulder. – Dimensions (cm): m 15; hf 2.5; wf 5.1. – Fabric 75. – Parallels: Wendel 1986, type Krivina pl. 34,10; 35,11. – Dating: EMA.

P 21/004. Site 21; pol. 585. – Pot, rim fragment. Spherical body; moderately outwards turned rim. Incised wave band with horizontal lines underneath on the shoulder. – Dimensions (cm): m 16; hf 6.2; wf 6.3. – Fabric 75. Sooty rim. – Parallels: Wendel 1986, type 7 pl. 33,1.2.4.5. – Dating: EMA.

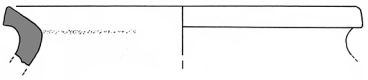
P 21/005. Site 21; pol. 585. – Pot, rim fragment. Spherical body; flat, relatively sharply outwards turned, irregularly shaped rim with angulated lip. Two incised wavebands on the shoulder. – Dimensions (cm): m 13; hf 3.4; wf 6.1. – Fabric 75. – Parallels: Wendel 1986, type 5 pl. 31,2. – Dating: EMA.



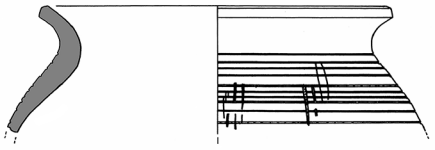
P19/012



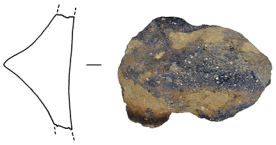
P19/013



P19/014

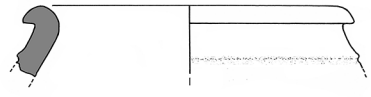


P20/001



P21/001

0 5 cm



P21/002



P21/003



P21/004



P21/005

Plate 38. Site 19, survey: Early Medieval pottery (P19/012–P19/014). – Site 20, survey: Early Medieval pottery (P19/001). – Site 21, survey: Early Iron Age pottery (P21/001); Early Medieval pottery (P21/002–P21/005)

SITE 24. Survey

Site 24, survey: Early Iron Age pottery

P 24/001. Site 24; pol. 817. – Rim fragment of a roll rim bow. – Dimensions (cm): hf 2.6; wf 3.5. – Fabric 40, oblique flutings. – Dating: EIA (Basarabi/8th–7th c. BC).

P 24/002. Site 24; pol. 819. – Rim fragment of a coarse pot. – Dimensions (cm): m 21; hf 6.0; wf 5.1. – Fabric 14, fingertip strip on the edge. – Dating: EIA.

P 24/003. Site 24; pol. 819. – Rim fragment of a funnel rim. – Dimensions (cm): m 28; hf 4.7; wf 7.8. – Fabric 40. – Dating: EIA.

P 24/004. Site 24; pol. 818. – Raised bottom fragment. – Dimensions (cm): b 10; hf 3.5; wf 5.1. – Fabric 40. – Dating: EIA.

P 24/005. Site 24; pol. 819. – Middle fragment. – Dimensions (cm): hf 7.3; wf 6.0. – Fabric 41. – Dating: EIA.

P 24/006. Site 24; pol. 818. – Middle fragment. – Dimensions (cm): hf 5.7; wf 7.0. – Fabric 42, fingertip strip. – Dating: EIA.

Site 24, survey: Late Iron Age pottery

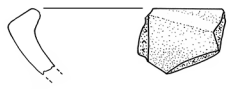
P 24/007. Site 24; pol. 817. – Plate or bowl, rim fragment. Inwardly curved rime with rounded lip. – Dimensions (cm): m 26; hf 2.2; wf 4.2. – Fabric 49. – Parallels: Чичикова 1984, type 26 no. I.67 fig. 10 (4th–3rd c. BC); Moscalu 1983, type 10b pl. 76 (6th–4th c. BC). – Dating: LIA (5th–3th c. BC).

P 24/008. Site 24; pol. 818. – Plate or bowl, rim fragment. Inwardly curved rim with rounded lip. – Dimensions (cm): m 25; hf 3.9; wf 5.1. – Fabric 56. – Parallels: cf. for example Moscalu 1983, type 2d pl. 24,3 (Enisala; 4th c. BC); type 6b pl. 24,9 (Brăiliţa; 4th–3rd c. BC); Върбанов 2013a, no. 94 pl. 4,7 (2nd–1st c. BC). – Dating: LIA (2nd–1st c. BC).

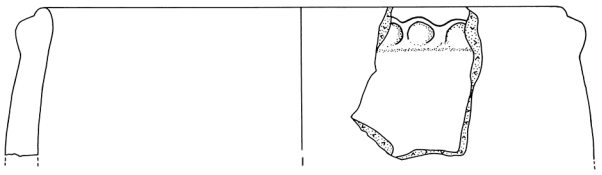
SITE 25. Survey

Site 25, survey: Late Iron Age pottery

P 25/001. Site 25; pol. 833 (north of the burial mound). – Plate, rim fragment. Open form with relatively shallow body; thickened rim with slightly slanted upper side. – Dimensions (cm): m 22; hf 1.9; wf 3.8. – Fabric 50. – Parallels: Върбанов 2013b, no. 108; 109 pl. 3,53.54 (2nd–1st c. BC). – Dating: LIA (2nd–1st c. BC?).



P24/001



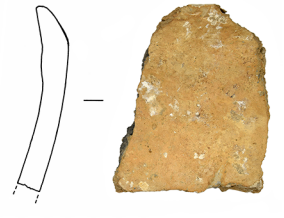
P24/002



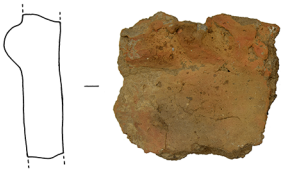
P24/003



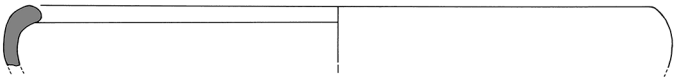
P24/004



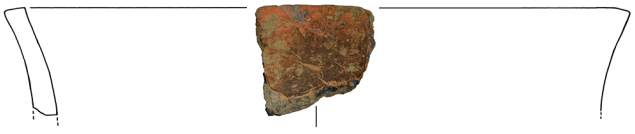
P24/005



P24/006

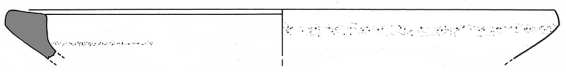


P24/007



P24/008

0 5 cm



P25/001

Plate 39. Site 24, survey: Early Iron Age pottery (P24/001–P24/006); Late Iron Age pottery (P24/007–P24/008). – Site 25, survey: Late Iron Age pottery (P25/001)

SITE 34. Survey

Site 34, survey: Late Iron Age pottery

P 34/001. Site 34; pol. 877. – Bowl (Lekane), wall fragment with part of the horizontal handle. – Dimensions (cm): d (body) ca. 30; hf 4.8; wf 7.3. – Fabric 50. – Parallels: cf. Moscalu 1983, type 20a/b pl. 88 (5th–3rd c. BC); Върбанов 2013b, cat. pl. 1,8 (5th–4th c. BC). – Dating: LIA (5th–3rd c. BC).

Site 34, survey: Early Medieval pottery

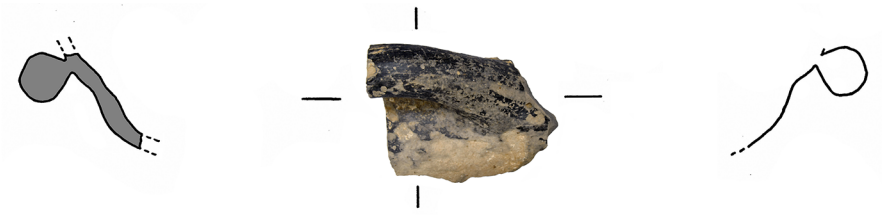
P 34/002. Site 34; pol. 875. – Pot, rim fragment. Spherical body; outwards turned rim with rounded lip. – Dimensions (cm): m 15; hf 5.4; wf 6.5. – Fabric 83. Less temper of sand and pieces of limestone. Irregularly burnished outer surface. – Parallels: Wendel 1986, grey pottery 144 pl. 36,30. – Dating: EMA.

P 34/003. Site 34; pol. 875. – Pot, wall fragment. Horizontal groove with a zone of burnished cross hatch below. – Dimensions (cm): hf 6.4; wf 5.5. – Fabric 85. Slightly rough surface. – Cf. cat. P 34/002. – Dating: EMA.

SITE 37. Survey

Site 37, survey: Early Medieval pottery

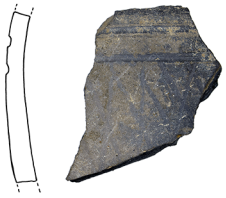
P 37/001. Site 37; pol. 837. – Pot, rim fragment. Spherical body; outwards turned rim with rounded lip, which has a sharp edge on its underside. – Dimensions (cm): m 14; hf 2.8; wf 3.2. – Fabric 75. Sooty rim. – Parallels: Wendel 1986, type Krivina pl. 34,6.9; 35,4. – Dating: EMA.



P34/001

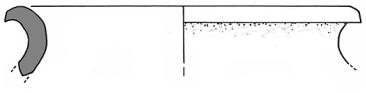


P34/002



P34/003

0 5 cm



P37/001

Plate 40. Site 34, survey: Late Iron Age pottery (P34/001); Early Medieval pottery (P34/002–P34/003). – Site 37, survey: Early Medieval pottery (P37/001)

9.2. SMALL FINDS (WITH CATALOGUE)

9.2.1. Small finds from prehistory

Raiko Krauß

The collection of small finds contains a large number of polished stone tools. Some of these can be addressed as axes and adzes or are fragments of such. The basic distinguishing feature is the way of hafting these implements, which can be read from the shape of the artefacts (Hahn 1991, 286–291; Willms 2012). Axes are hafted parallel to the cutting edge (fig. 1a), in the simplest case through a hole in the handle or an inserted intermediate chuck. These chucks usually are made fom antler (Probst-Böhm 2016). Stone axes can also be held by a split stile, which is tightened by a lacing. So that the axes do not slip through, they are often provided with a circumferential notch, but such pieces are not represented in our material. According to the parallel hafting, stone axes are symmetrical in the longitudinal section and the blade wears out on one side during use (SF 02; 06; 37). Used axe blades are therefore often at an angle, which is reinforced by resharpening (Klimscha 2016, 65–79).

Adzes, on the other hand, are hafted across the handle. This requires an angled stile to which the stone tool is tied (Hahn 1991, 286–291; Stöckli et al. 1995, 159–168; Willms 2012). For this reason, they must have a flat bottom (fig. 1b). They are therefore asymmetrical in the cross-section (SF 01; 05; 08; 21; 37; 41). Adzes are used like hoes, which is why the cutting edge is usually worn evenly. However, there are also adzes that are hafted in intermediate chucks (fig. 2). In this case, the blade cross-section can also be shaped differently. Hatchets and adzes can therefore be distinguished by their transversal cut and the wear and tear on the blade. The angle at which the sides are to the neck is less meaningful for a differentiation. Both axes and adzes occur with almost parallel sides. However, trapezoidal outlines are more common for axes, which can be explained by their hafting, as the wedge shape is more likely to work into the shaft during use and thus stabilise itself.

To be differentiated from axes and adzes are shaft hole axes, which are attached directly to the handle. The body of stone shaft hole axes is approximately square in cross-section. In the material from Tash Bair and the surveys in the surrounding area, however, there were no stone implements that could clearly be referred to shaft hole axes. They did not appear in Bulgaria until the Chalcolithic, whereas stone axes and adzes appeared in the Early Neolithic and remained in use until the Bronze Age (Klimscha 2016).

The raw materials used for the stone axes and adzes found in 2018 were determined macroscopically by Patrick Schmidt (Tübingen University). For most of the pieces, it is volcanic rocks, such as granites. In one case an olivine basalt could be identified. Few pieces consist of sedimentary rock, such as limestone or slate. The stone axes and adzes are all very badly worn, and in few cases we have just splinters from such tools. The signs of wear effected not only the blades but also the neck, which shows that they were also used as chisels – possibly secondarily. Some pieces were also used as pestles for mortars (SF 05). In general, the recycling of stone axes for all sorts of purposes seems to be the rule rather than the exception (Klimscha 2016, 79–104).



Fig. 1. Examples for hafting of stone axes (a) and stone adzes (b); a (left): collection of the Institute for Prehistory, Early History and Medieval Archaeology in Tübingen, b (right): Keefer 1993, 98

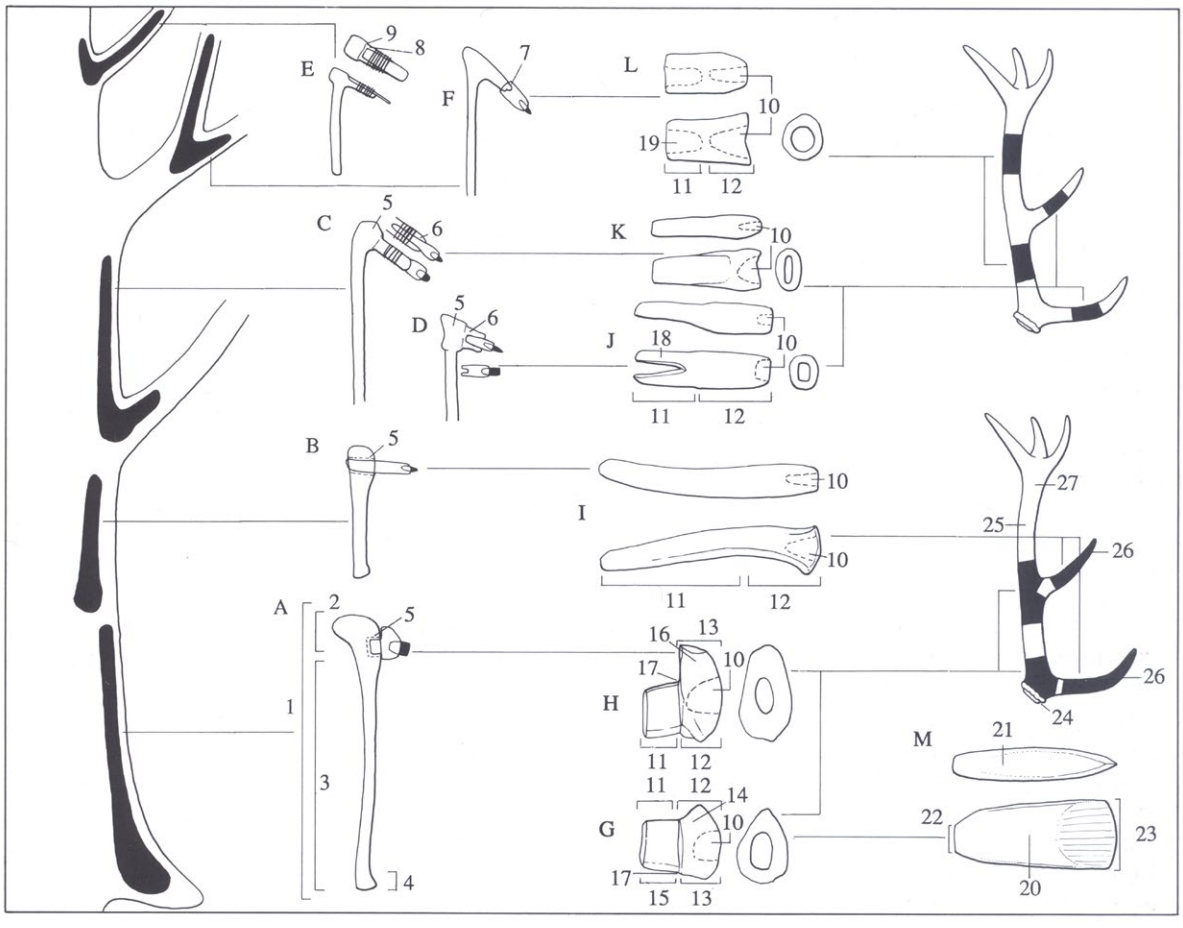


Fig. 2. Use of wood and antlers to make axe or adze shafts with or without intermediate chucks (Stöckli et al. 1995, 161, Abb. 96)

At least three pieces are documented in the material that originally served as a mortar pestle (SF 12; 16; 22). Both are made of limestone. As a rule, pestles have a round cross-section (Klimscha 2014, 175, Taf. 68.9) and can also be clearly differentiated from axes and adzes as fragments. All kinds of solid surfaces could have served as bases for the mortar. Real stone mortars were not found. Although some broken stone pieces found could have derived from stone mortars, they were difficult to identify as such. Stone mortars are part of the standard inventory of prehistoric settlements and appear at the beginning of the Neolithic in the Balkans (Тодорова, Вайсов 1993, 170). They remain in use until historical times and can hardly be assigned to a specific epoch due to their shape. However, it is noticeable that in historical times only the mortars themselves were made of stone, whereas the pestles were often made of wood. In this respect, the stone pestles seem to belong to the prehistoric period, with a clear focus on the Neolithic.

Some fragments of grinding stones are represented in the material (SF 17; 18; 43; 60; 62). The grinding stones of the Neolithic and Chalcolithic in Bulgaria do not have a specific basic shape and can only be identified on the basis of the concave work surfaces created by the rubbing process itself. Different types of rock material of both volcanic and sedimentary origin were used as grinding stones. They were essential for grinding grain, which is why they are an integral part of the Neolithic package (Gehlen 2012, 840–844). Grindstones were also used for grinding coloured minerals such as hematite, malachite or azurite. They are also the most important piece of equipment for the production of polished stone tools and jewellery items. Accordingly, it is to be expected that they would have come in different sizes and with different grain fineness. In principle, stone grinders can be used indefinitely, which is why they were often used until the work surface was broken. Commonly, they were also used on both sides, resulting

in two convex surfaces. Grinding stones were also used in later prehistoric periods but have a clear focus in the Neolithic and Chalcolithic (Тодорова, Вайсов 1993, 169–171). With the advent of rotary mills from the Bronze Age onwards, there should be less grindstones represented in the archaeological record.

Furthermore, some round picking or hammer stones are documented in the finds (SF 09; 11; 15; 19; 44; 61; 70). The use of these implements as such is revealed by the surrounding picking tracks. In northern Bulgaria, the Neolithic-Chalcolithic hammer stones often consist of flint bulbs, which are often naturally round and handy (Klimscha 2014, 175, Taf. 68.1–6,7,8). However, many pieces appear almost perfectly round, which may have been a result of use alone (Hahn 1991, 296f.) (fig. 3). Simple river pebbles or rounded limestone were also used as hammer stones. These pieces could be used for smoothing stone surfaces or for mortars. However, as devices for flint knapping, they are only suitable in the very first stages, such as peeling off the cortex and roughly dressing the striking platform (Weiner 2012). Nevertheless, for all of these pieces, their use as sling shots should also be considered. They can be thrown straight out of the hand or thrown with the help of a loop (Korfmann 1972). It is also possible to use several of these balls tied together as bolas. Due to the evident lack of projectile points in the archaeological record of Neolithic sites, it is very likely that slingshots were used for hunting and fighting. It was not until the Chalcolithic that projectile points made of flint and animal bones appeared at the sites of the lower course of the Danube (Čohadžiev, Krauß 2019, 77–80). However, even then, projectile points were not numerous enough to indicate that the use of slingshots would have become completely uncommon. The handiness also makes a device originally intended as a hammer stone a practical weapon (SF 63). The fragments represented in the material suggest weaponry as a possible secondary use. Such re-use can also have taken place in historical times, for example with the Romans (fig. 4).

Some pieces with an irregular shape could be used as smoothing stones (SF 10; 13), for example to smoothen the surfaces of vessels during pottery making. Other types of use are also conceivable, which is why these items cannot be assigned to a specific prehistoric or historical epoch. The piece SF 10 is reminiscent of teardrop-shaped stone pendants from the Pfyn culture (Matuschik, Schlichtherle 2016, 73, Abb. 73), which only shows how diverse the interpretations can be.

Two differently shaped stone objects are represented in the material found, whose common feature is a linear channel (SF 35; 36). Both are ideal as straighteners, for example for arrow shafts or for debarking small twigs (Gehlen 2012, 850–852). Objects of this kind belong to the inventory of prehistoric sites, but usually cannot be assigned to a specific epoch.

The piece SF 14 has no recognisable shape and the narrow groove can be identified as the trace of a saw. Apparently, this piece was discarded before the target product could be made or it was casually used to sharpen stone blades (cf. Klimscha 2016, 57–60, Abb. 48).

SF 20 is the wall fragment of a Late Neolithic ceramic vessel that was ground into a small disc. Small boring pits can be seen on both sides, but these are slightly offset, and they don't go through the piece. It is also possible that it was not intended to perforate the sherd, but rather it is a kind of marking. Many of these ceramic disks come from the Neolithic settlements of northern Bulgaria, either with or without a perforation or with an attached bore, like in our piece (fig. 5). These objects could be used in

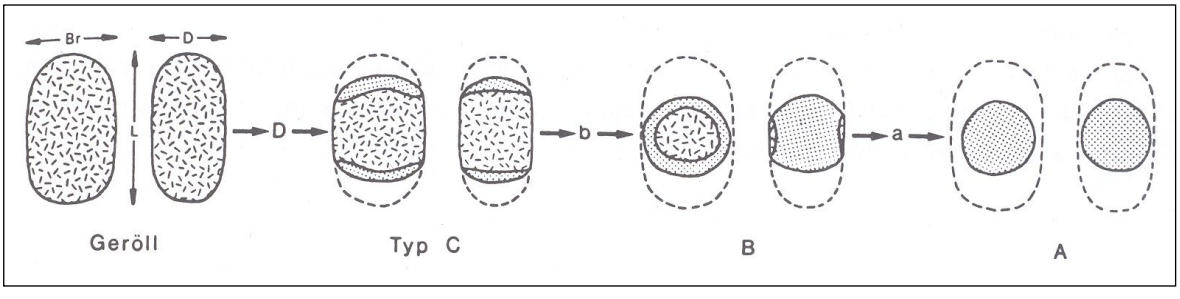


Fig. 3. Manufacturing of hammer stones (Hahn 1991, Abb. 91)



Fig. 4. Roman slinger in the Dacian War. Detail of a relief from Trajan's Column

many ways, as tokens, game buttons, counting aids or amulets. However, as decorative elements alone they are a bit unspectacular.

Another ceramic object (SF 45) can be identified as a tool for incising plastic decorations on ceramic surfaces. The piece is wedge-shaped with a slightly thickened neck and a flat, slightly arched and comb-like notched stamp surface. In the centre of the piece has a through-hole that was made before the stamp was burned. This would have allowed the piece to be threaded and if necessary also worn as a pendant. Such combs were used to make the characteristic rolling wheel impressions on the Early Iron Age ceramics (especially Basarabi, but also Tlachene), which were filled in with a white paste after firing (Ailincăi et al. 2004). Carola Metzner-Nebelsick (1997) pointed out that these objects can also

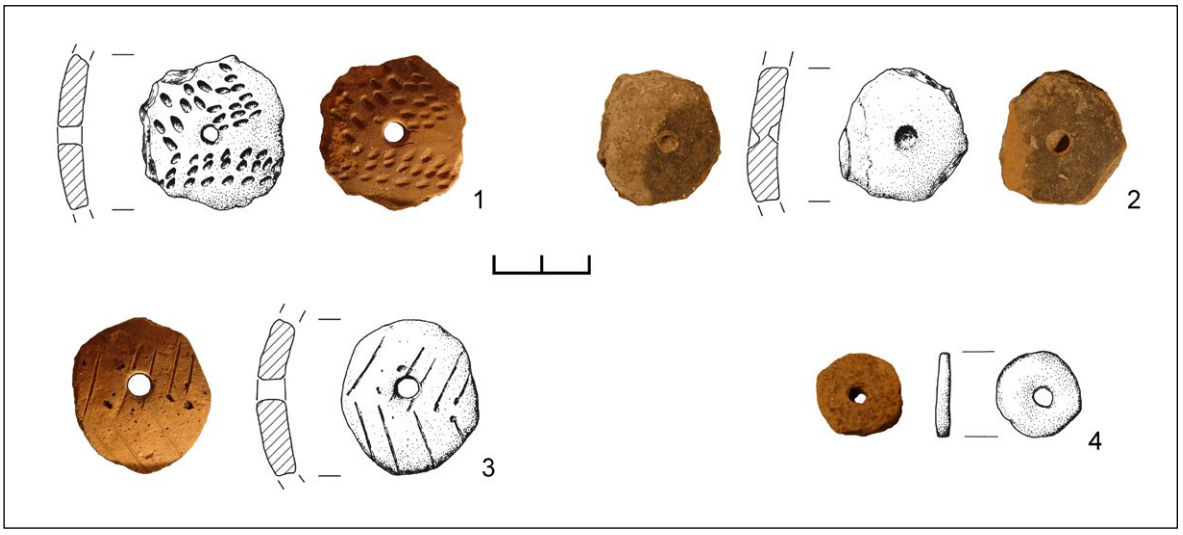


Fig. 5. Neolithic tokens made from pottery fragments. Ovcharovo-Gorata (after Krauß 2014, Abb. 106)

have symbolic meaning. In fact, similarly shaped miniature objects appeared in a wide variety of shapes in the Early Iron Age of the Carpathian area. In addition, there is the perforation of our piece, which enhances the amulet character. However, for ceramic production, these objects have a very practical use. The piece fits into a large group of related stamps with a crest from the areas north of the Danube (fig. 6). In addition to the fragment of a clay stamp with a preserved working edge (Krauß 2006a, Tab. 99.6), this is already the second copy from site 1 at Tash Bair.

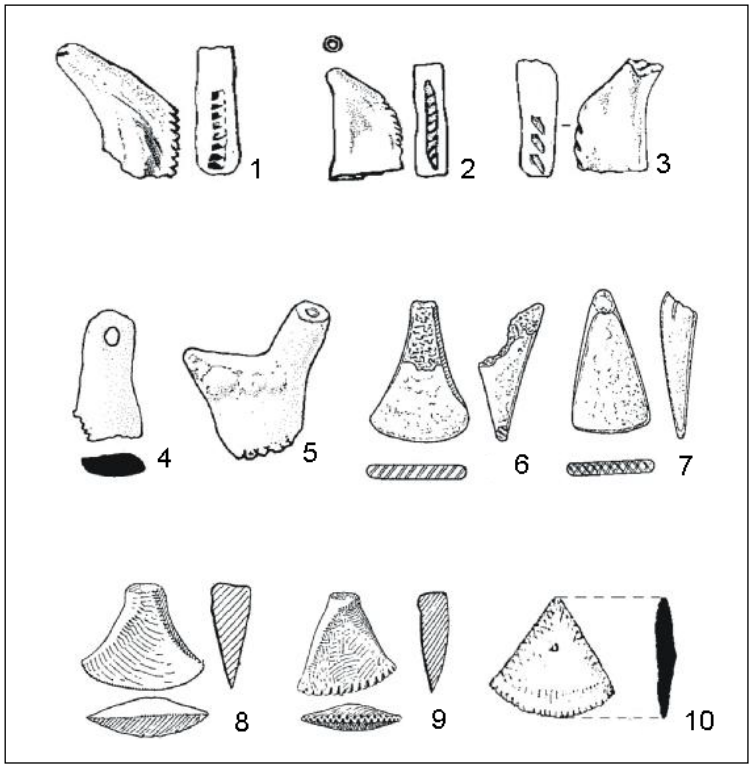


Fig. 6. Early Iron Age clay ceramic stamps of the Basarabi group (different scale) (Ailincăi et al. 2004, Fig. 8)

МАЛКИ НАХОДКИ ОТ ПРАИСТОРИЯТА

Райко Краус

(Резюме)

Колекцията от малки находки идва от различни обекти на Таш баир и неговата околност, главно от обект 1. Тя съдържа по-голям брой загладени каменни оръдия. Сред тях са някои брадви, тесли и секири, както и пестици за хавани, гладилки, хромелни камъни и чукалки. За последните се обсъжда използването им и като камъни за прашка. Сред керамичните находки има няколко керамични фрагменти, вторично заоблени на дискове, някои с дупка в средата. Малък керамичен предмет с назъбен ръб може да се определи като щампа за украса на керамика от ранната желязна епоха.

Catalogue and plates of the small finds from prehistory

Abbreviations
d – diameter
h – height
l – length
niv. – niveau
Pol. – polygon
th – thickness
Tr. – trench
w – width

Cat. No.	Coordinates	Type	Description	Dimensions	Chronology	Site ID
SF 01	Pol. 6	fragment of a stone axe or adze	Flake from the surface of a stone axe or adze made from a volcanic rock, probably olivine-basalt (P. Schmidt).	w 5.1 × th 3.1 × 7.5 cm	Prehistory	site 1
SF 02	Pol. 186	stone axe fragment	Preserved neck of a stone axe with rectangular cross-section made from a volcanic rock (P. Schmidt). Trapezoidal shape.	w 4.0 × th 5.5 × l 4.5 cm	Prehistory	site 1
SF 03	Pol. 188SS1	stone axe fragment	Preserved side of a stone axe with rectangular, probably almost quadrangular, cross-section. Volcanic rock (P. Schmidt).	3.86 × 2.56 × 2.0 cm	Prehistory	site 1
SF 04	Pol. 7LV7	stone axe fragment	Upper part of a stone axe with possibly oval cross-section. Volcanic rock (P. Schmidt).	5.09 × 4.75 × 1.52 cm	Prehistory	site 1
SF 05	Pol. 7LT4	stone adze	Stone adze with D-shaped cross-section. Neck and cutting edge are reduced by secondary use as a pestil for mortaring. Sedimentary siliceous rock (P. Schmidt).	w 6.9 × th 4.5 × l 10.08 cm	Prehistory	site 1
SF 06	Pol. 7LT7	stone adze	Stone adze with rectangular cross-section and flattened lower side. The cutting edge is asymmetrically worn. Probably limestone (P. Schmit).	w 3.6 × th 1.47 × l 5.62 cm	Prehistory	site 1
SF 07	Pol. 8LV1	stone axe fragment	Preserved neck of a stone axe with rectangular to round cross-section made from limestone (P. Schmidt).	3.6 × 3.6 × l 2.4 cm	Prehistory	site 1
SF 08	Pol. 7LT1	stone axe	Stone axe with rectangular cross-section. Trapezoidal shape with slightly curved flanks and straight neck and cutting edge. Slightly shipped at the sides. Limestone (P. Schmidt).	w 4.35 × th 1.4 × l 6.24 cm	Prehistory	site 1



Plate 1. SF 01–08 – small finds from site 1, field survey (figure by R. Krauß)

Cat. No.	Coordinates	Type	Description	Dimensions	Chronology	Site ID
SF 09	Pol. 186	hammer stone	Naturally rounded handy chissel, broken on one side. Vulcanic rock (compared to other pieces with petrological determination).	w 8.3 × th 5.5 × d 9.4 cm	Neolithic-Chalcolithic	site 1
SF 10	Pol. 190	smooth stone	Naturally chisel, artificially flattened on one side. Volcanic rock (compared to other pieces with petrological determination).	w 7.3 × th 2.3 × l 10.3 cm	Undefined	site 1
SF 11	Pol. 7LT1	hammer stone	Naturally rounded handy chisel with picking marks on the side. Volcanic rock (compared to other pieces with petrological determination).	d 5.22 × 4.62 × th 5.65 cm	Neolithic-Chalcolithic	site 1
SF 12	Pol. 7LT3	fragment of a pestle	Middle segment of a cylindrical pestil from a mortar. Limestone (compared to other pieces with petrological determination).	5.09 × 4.75 cm and 1.52 l of the fragment	Neolithic	site 1
SF 13	Pol. 7LV5	smooth stone	Naturally formed chisel in the form of a square with rounded edges. Volcanic rock (compared to other pieces with petrological determination).	5.15 × 5.34 × th 1.75 cm	Undefined	site 1
SF 14	Pol. 187SC2	fragment of a work-piece	Stone with a sawn groove. Unclear mineralogy (P. Schmidt).	3.2 × 2.5 × 1.23 cm	Undefined	site 1
SF 15	Pol. 7NK1	hammer stone	Naturally rounded handy chisel with picking marks on the side. Volcanic rock (compared to other pieces with petrological determination).	8.4 × 6.87 × 5.6 cm	Neolithic-Chalcolithic	site 1



Plate 2. SF 09–15 – small finds from site 1, field survey (figure by R. Krauß)

Cat. No.	Coordinates	Type	Description	Dimensions	Chronology	Site ID
SF 16	Pol. 7LT2	fragment of a pestle	Preserved half of a neck from a cylindrical pestle from a mortar. Limestone (compared to other pieces with petrological determination).	w 4.7 × th 2.77 × l 5.3 cm	Neolithic	site 1
SF 17	Pol. 189SS1	grinder fragment	Edge of the lower part of a grinder with one concave work surface. Limestone (compared to other pieces with petrological determination).	18.0 × 11.0 × th 3.7 cm	Neolithic-Chalcolithic	site 1
SF 18	Pol. 7NK2	grinder fragment	Edge of the lower part of a grinder with one concave work surface. Limestone (compared to other pieces with petrological determination).	19.0 × 12.0 × th 4.7 cm	Neolithic-Chalcolithic	site 1
SF 19	Pol. 7NK2	hammer stone	Naturally rounded handy chisel with picking marks on one end. Volcanic rock (compared to other pieces with petrological determination).	4.3 × 3.9 × 8.25 cm	Neolithic-Chalcolithic	site 1
SF 20	Pol. 7LT1	ceramic token	Fragment of Neolithic pottery, secondary rounded with small dimples in the middle of the outer surfaces.	d 3.85 × 3.5 × th 1.18 cm	Late Neolithic	site 1
SF 21	from the surface of site 1	stone axe	Small stone axe rectangular cross-section from a dark volcanic rock (compared to other pieces with petrological determination). Conical sides and conical, slightly curved sides. The cutting edge is also slightly curved. Entirely preserved.	w 3.05 × th 1.1 × l 3.6 cm	Prehistory	site 1
SF 22	from the surface of site 1	pestle	Lime stone pestle from a mortar. The working surface is broken and scratching marks on all sides from agricultural machines.	w 6.0 × th 4.9 × l 12.3 cm	Neolithic	site 1



Plate 3. SF 16–22 – small finds from site 1, field survey (figure by R. Krauß)

Cat. No.	Coordinates	Type	Description	Dimensions	Chronology	Site ID
SF 35	Tr. 1.1-E, at niv. 26.75 m, 1.60 m from its SE corner and 2.76 m from the SW corner	shaft straightener	Spherical stone, probably limestone, with a linear groove. The piece was originally probably perfectly round and is broken on one side.	5.0 × 5.2 × 4.0 cm	Prehistory	site 1
SF 36	Tr. 1.1-W, feature 1.1.11, E 382787.310; N 4827978.317; niv. 26.69 m	shaft straightener	Fragment of an elongated, very coarse sandstone with a curved underside and smoothed top, on which there is a 0.9 cm wide, elongated channel. The piece was probably originally longer because it broke off at both ends.	w 3.5 × th 3.1 × l 5.3 cm	Prehistory	site 1
SF 37	Tr. 1.1-E, NW corner, at niv. 24.78 m	stone adze	Weathered granite stone axe with a D-shaped cross-section. The cutting edge and the neck as well as the curved side are chipped. Heavily sintered when found.	w 4.65 × th 2.35 × l 7.15 cm	Prehistory	site 1
SF 38	Tr. 1.1, surface find from the ploughing horizon	stone axe	Stone axe with a rectangular cross-section. Made of sedimentary rock, either a fine sandstone or limestone (P. Schmit). After a negative test with acid, however, it is more likely to be assessed as lime-free and therefore sandstone. Cutting edge and the neck are bumped. Sintered surface.	w 5.4 × th 2.5 × l 8.8 cm	Prehistory	site 1
SF 39	Tr. 1.2, surface find from the ploughing horizon	flake from stone axe or adze	Flake from a grinded tool, probably stone axe with one preserved smoothed surface. Volcanic rock (P. Schmidt).	2.4 × 3.15 × 1.2 cm	Prehistory	site 1
SF 40	Tr. 1.1-E, NE corner, above feature 1.1.6, at niv. 27.00–26.76 m	stone axe fragment	Preserved neck of a flat stone axe made from a volcanic rock (P. Schmidt). On the curved (ventral) side the surface is well preserved.	w 5.55 × th 2.5 × l 4.7 cm	Prehistory	site 1
SF 41	Tr. 1.1-W, at niv. 26.40 m. At the east profile of the trench, 2.30 m from its SE corner	stone axe fragment	Preserved neck of a stone axe with rectangular cross-section made from a volcanic rock (compared to other pieces with petrological determination).	w 4.7 × th 3.0 × l 4.0 cm	Prehistory	site 1
SF 42	Tr. 1.1-W, at niv. 27.22–27.00 m	stone axe fragment	Preserved neck of a stone axe with rectangular cross-section made from a limestone (compared to other pieces with petrological determination). The neck is bumped.	w 4.8 × th 4.4 × l 5.9 cm	Prehistory	site 1
SF 43	Tr. 1.1-E, NE corner, above feature 1.1.6, at niv. 27.00–26.76 m	grinder fragment	Edge of the lower part of a grinder. The piece was used on both sides until it was completely worn out and is then likely to have broken. One edge is still preserved. Volcanic rock.	10.5 × 7.6 × th 3.35 cm	Neolithic-Chalcolithic	site 1



Plate 4. SF 35–43 – small finds from site 1, excavations (figure by R. Krauß)

Cat. No.	Coordinates	Type	Description	Dimensions	Chronology	Site ID
SF 44	Tr. 1.1-E, at niv. 26.44–26.24 m, east and central part of the trench	hammer stone fragment	A handy chisel from limestone. Possibly used in prehistory as a hammer stone. Broken and sintered.	4.0 × 5.8 × 3.9 cm	Neolithic-Chalcolithic	site 1
SF 45	Tr. 1.2, at niv. 29.75–29.67 m, in the SE corner of the trench	ceramic clay stamp comb	Early Iron Age ceramic stamp. A small, conically shaped wedge with a rounded neck and a wide, comb-shaped notched stamp surface. These pieces were used to incise the characteristic comb stitch decorations on the Early Iron Age (Basarabi) ceramics. The item was pierced before firing and could be threaded. The piece is in excellently preserved and only broken on one corner of the stamp blade.	w 2.1 × th 1.1 × l 3.1 cm	Early Iron Age	site 1
SF 53	Tr. 3.2, at niv. 63.55 m	bronze knife	Knife with a straight back and a short tang made of tin bronze.	w 0.9 × th 0.3 × l 5.9 cm	Late Bronze Age	site 3
SF 60	Pol. 450	grinder fragment	Lower part of a prehistoric grinding stone. Bumped from all sides. Volcanic rock.	w 9.4 × th 5.7 cm × l 13.4	Neolithic-Chalcolithic	site 18
SF 61	Pol. 450	hammer stone	Rounded silex core with radial picking marks.	w 7.05 × l 5.65 × h 5.9 cm	Neolithic-Chalcolithic	site 18
SF 62	Pol. 505	grinder fragment	Lower part of a prehistoric grinding stone. Bumped from all sides. Volcanic rock.	w 5.25 × l 10.1 × h 2.8 cm	Neolithic-Chalcolithic	site 19
SF 63	Pol. 505	sling shot fragment	Fragment of a spherical lime stone.	w 4.8 × l 5.3 × h 2.1 cm	Prehistory	site 19
SF 70	Pol. 816	hammer stone	Spherically shaped lime stone with radial picking traces.	w 5.7 × th 4.4 cm	Neolithic-Chalcolithic	site 24



Plate 5. SF 44–45 – small finds from site 1, excavations; SF 53 – small find from site 3, excavations; SF 60–61 – small finds from site 18, field survey; SF 62–63 – small finds from site 19, field survey; SF 70 – small find from site 24, field survey (figure by R. Krauß)

9.2.2. Small finds from Antiquity and Early Middle Ages

Lyuba Traykova

SITE 1

Glass

Glass bracelet, cat. No. SF 23, plate 6.

According to the main characteristics, such as colour and plastic design, this fragment belongs to the La Tène type of glass bracelets. Thea Elisabeth Haevernick is developing one of the main typologies of Celtic glass bracelets from the Late Iron Age for the territory of Continental Europe. The basis of this typology includes the profiling of the upper surface and the presence of additional decoration (Haevernick 1960). Colour is added to these criteria as an addition, but they are also applied later by other scientists in the development of new typologies for certain regions. For instance, the numbers of the groups or types are repeated with small differences in the details. Such typologies have been developed for the territory of Poland (Karwowski 1997), Romania (Németi 2000, Vaida 2006), Eastern Hungary (Tankó 2006), Austria (Karwowski 2004) and separately for North Tyrol (Zerobin 2017), the Lower Rhine region (Roymans, Verniers 2010), Brittany / Western France (Dinard et al. 2011), and Slovakia (Čambal, Štrbík 2014). The dating of this type of bracelets made of blue glass for the listed regions dates to the second half of the 3rd – the last quarter of the 2nd c. BC (fig. 1a, b).

For the territory of Bulgaria, Mieczysław Domaradzki outlines the development of the Celtic glass bracelets, but no typology was created. Despite this, he has identified several known types. Blue glass bracelets with plastic ribs, often decorated with white paste inlay are the most popular ones. They were found only north of Stara Planina mountain. More than ten fragments of glass bracelets have been found in the two residential levels from the 3rd to the 2nd c. BC on the Tsarevets Hill (Домарадски 1984, 140; обр. 6). Separate single finds have also been published (Lazarov 2006, fig. 21; Anastassov 2011, 231, fig. 8).

Cat. No. SF 23 best corresponds to the definition of M. Karwowski's type 7a, variant 1 (fig. 1a). Bracelets with five longitudinal ribs; the middle rib is usually the highest and widest without additional decoration. The cuts between all the ribs are quite shallow. They are made mainly of translucent blue glass and much less often of purple, brown and green glass. The type is widespread in the period LT C1 / LT C2, which corresponds to the second half of 3rd – the first quarter of the 2nd c. BC (Karwowski 2004, 23, 77–78; table 17; 228, 229, table 18).

Statistics show that most of the finds were from settlements and a smaller number were from graves (Karwowski 2006, 142; Roymans, Verniers 2010, 201; Dinard et al. 2011, 150, fig. 1; 107; Čambal, Štrbík 2014, 108–109, Tabela 1; Zerobin 2017, 2, Abb. 02). For the studied sites from the territory of Slovenia, it is noted that this type does not appear in the graves from the end of the Middle La Tène period (Čambal, Štrbík 2014, 107).

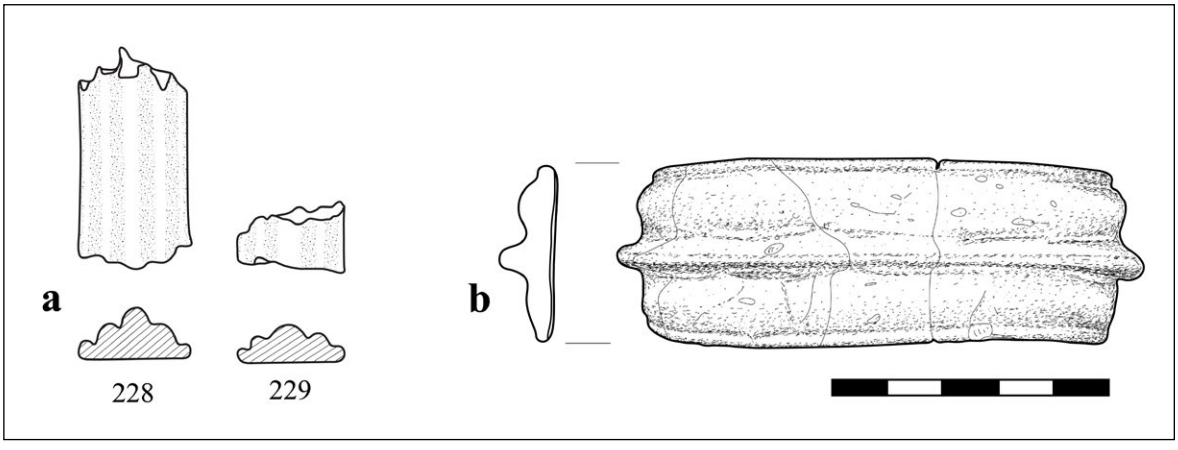


Fig. 1. Glass bracelets: a – after Karwowski 2004, 23, Tafel 17. 228, 229; b – Zerobin 2017, Taf. 6.11

The number of well-dated grave finds with glass bracelets is relatively small. This makes it difficult to determine the chronological boundaries of individual finds or entire typological groups of glass bracelets. The chronological system developed for the areas where grave finds were recorded could not be applied automatically everywhere. Moreover, archaeological artefacts from one region do not always correspond to the chronology in other regions (Karwowski 2006, 138).

Cat. No. SF 23 was found during a field survey, i.e. from the surface and it has no exact archaeological context. Site 1 is multi-layered. The recorded pottery fragments show habitation from the Late Neolithic to the Early Middle Ages. The Late Iron Age is represented by fragments from the 5th–3rd c. BC and 2nd/1st c. BC – 1st c. AD. (cf. the contributions by N. Kecheva et al., chapter 12, site 1). It could be assumed that there were settlements there during Late Iron Age. Without finds with archaeological context, the dating of the cat. No. 23 could be approximately related to the period 3rd–2nd c. BC.

Ceramic – cat. Nos. SF 24–26, SF 46, SF 47.

Ceramic stamp, cat. No. SF 24, plate 6.

Ceramic stamps were used to stamp a decoration or the name of the manufacturer. Vessels with such decorations are more often found than the stamps themselves. They can be unilateral or bilateral. The motifs include floral, geometric or combined ornaments. The stamps were used to create relief decoration in the manufacture of moulds for vessels or directly on the vessels themselves.

Ten stamps for pottery were excavated in the production centre near Pavlikeni town, Veliko Tarnovo district. Several of them are covered with a slip, including the working part. The production was carried out in the period from the end of the 1st to the 3rd c. All vessels found in the production centre were wheelmade (Владкова 2010, 258–259, 263, обр. 1.в–е). Ceramic lamps are wheelmade and made in a mould, and the stamps of the moulds show the name of the manufacturer (Владкова 2013, 161–162).

A double-sided stamp, with a body shaped like that of cat. No. SF 24 was found in a destroyed kiln in Mezdra town, Vratsa district (fig. 2a). Its two working sides have floral ornaments. Evidence for the production of cups dating to the 3rd c. was also found in the kiln (Лука 2006, 164, 168, обр. 7).

Several ceramic stamps (fig. 2b) for dish moulds with relief plant and geometric decoration have been found in Montana town (Димитрова-Милчева 2008, 143, обр. 29).

A stamp with a similar body shape (fig. 2c) and preserved working part was found in a ceramic production centre in Budapest town (Nagy 2017, 220, fig. 25). This centre is one of the earliest for the

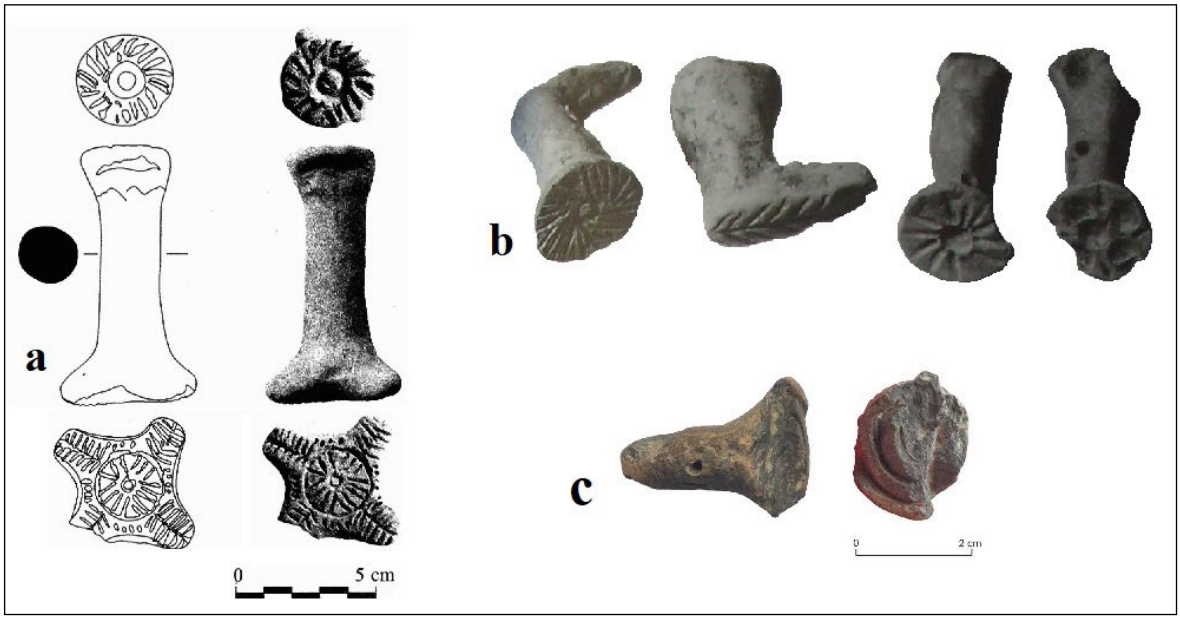


Fig. 2. Ceramic stamps: a – after Лука 2006, 168, обр. 7; b – after Димитрова-Милчева 2008, 143, обр. 29; c – Nagy, 220, fig. 25

region. Its production reflects the transition from the 1st c. when the surviving Celtic traditions were mixed with the new Roman influence. The production of the centre dates from the middle of the 1st c. to the middle of the 2nd c. In the 3rd c. it certainly no longer functions (Nagy 2017, 16, 21–22).

Cat. No. SF 24 is a stray find and is fragmented. The fracture does not allow to determine whether this stamp was double-sided or single-sided. The saved working part is also damaged, and it is not possible to establish what the image in the central field was. The good workmanship of finely refined clay, hard firing and slip covering dated this seal to the period 1st–3rd c. Its presence is associated with local, specialised, ceramic production of vessels with stamped or applied decoration.

Ceramic spindle whorls, cat. No. SF 25, plate 6, cat. No. SF 46, plate 11.

Ceramic spindle whorls with these forms – biconical (cat. No. SF 25) and disc-shaped (cat. No. SF 46) were found from the Neolithic to the Middle Ages (Александрова 2017, 358, обр. 10.1. 1, 2, 9–12, обр. 10.4. 2; Cholakov 2015, 135, fig. 6. 8; Рашев 2008, Табло XCIV. 1–31). Both spindle whorls have no archaeological context – cat. No. SF 25 was found during the field survey and cat. No. SF 46 from the excavations; the latter had fallen into a lower deposited layer due to erosion of the terrain. Cat. No. SF 25 was made from well-purified and evenly baked clay. Based on its manufacture, it can be assumed that it dates to Antiquity. Cat. No. SF 46 is a very small fragment, and the admixture of coarse sand in the dough is not a reliable indicator for the dating of this find.

Ceramic loom weight, cat. No. SF 26, plate 6.

The find is fragmented, but it can most likely be attributed to the type of pear-shaped weights. They are characteristic and widespread in Thrace during the Late Iron Age. Such were found in near Koprivlen village, Blagoevgrad district (Димитрова 2002, фиг. 166. 1, 2, 4–6), Emporion Pistiros near Vetren village, Pazardzhik district, and Seuthopolis near Kazanlak town, Stara Zagora district (Dimova 2016, 644, tabl. 2, 667, tabl. 5, 672, fig. 7.b). Loom weights from this type are dated in 4th–3rd c. BC and have been found near Karshevitsa, Southeastern Serbia (Popović, Vranić 2006, 311, fig. 2). A collective find from the ancient city of Heraclea Sintica, near Rupite village, Blagoevgrad district, shows that the form was used during the Roman period (Cholakov 2015, 136, 135, fig. 6. 1) (fig. 3).

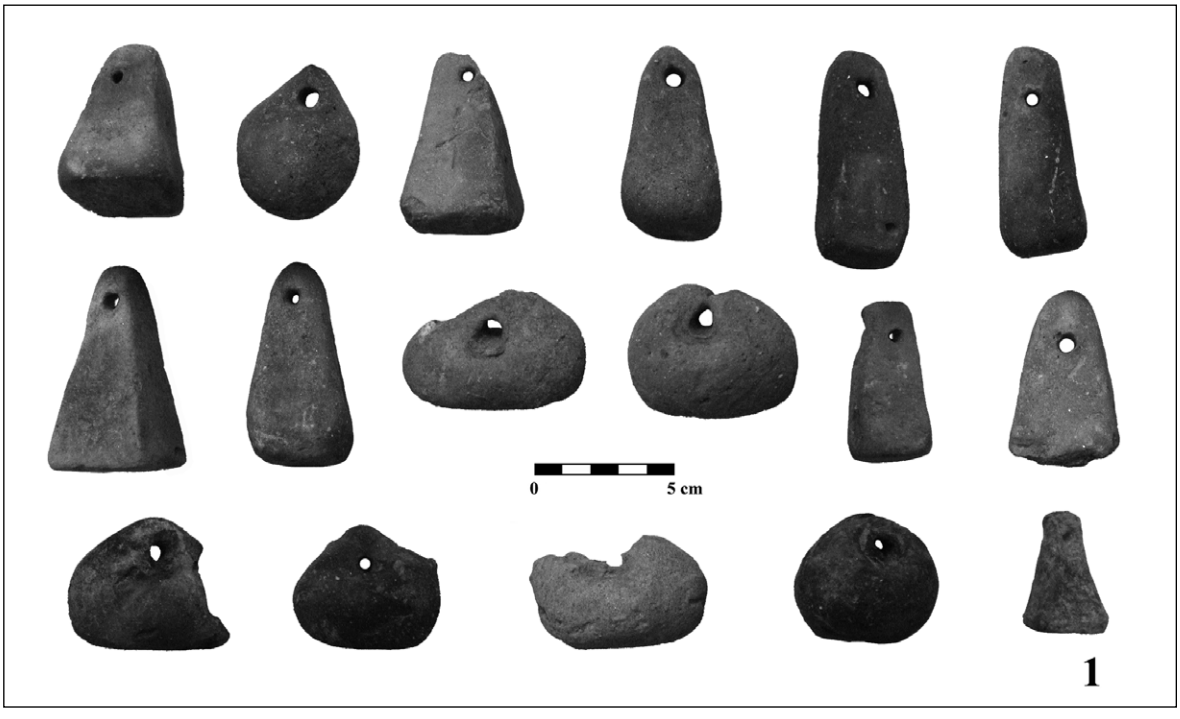


Fig. 3. Ceramic loom weights (after Cholakov 2015, 135, fig. 6. 1)

Ceramic lamp fragment, cat. No. SF 47, plate 11.

The fragment of the lamp is part of the tank with a break to the shoulders.The section of the lamp shows that it most likely belongs to the types of lenticular lamps with a biconvex tank. These types date from the last quarter of the 4th c. BC to the third quarter of the 2nd c. BC (Кузманов 1992, 15; Кузманов, Минчев 2018, 37, 41, 43). The preserved part of this lamp does not show diagnostic parts, which makes it difficult to refer to a specific type. The section corresponds to types X, XII and XIII of the typology of the collection of ceramic lamps from Regional Museum of History – Varna (Кузманов, Минчев 2018, Табло XCVI. 67, 106, 109, 110, Табло XCVII. 66, 76–78, 81, 92, 98, 107, Табло XCIX. 72, 90, 91, 96, 99, 102–105, 111, Табло CI. 63, 69, 75, 87, 89, 100, 101, Табло CII. 68, 71, 79, 94, 97, 108).

We excavated a trench from Late Iron Age in trench 1.1 (cf. the contributions by L. Vagalinski et al., chapter 8.3.1). Its filling contains several pottery fragments from the upper part of the filling of the ditch, which dates to the 2nd–1st c. BC. The more significant number of fragments dates back to the 5th–3rd c. BC (cf. chapter 9.1, part 9.1.2.3.). The fragment from lamp with cat. No. SF 47 had fallen into a layer where the upper boundary of the ditch is unclear. It is not possible to determine with certainty whether the fragment is part of the filling of the trench or the eroded layers of earth. The find does not provide sufficiently definite marks to be dated more accurately than the last quarter of the 4th c. BC to the third quarter of the 2nd c. BC.

Marble

Marble weight, cat. No. SF 34, plate 10.

Similar weights made of coarse-grained white marble have been found in the ancient Transmarisca fortress in Tutrakan town (Вагалински 1995, 72, фиг. 1). The weights do not have a clear archaeological context. The analysis of the material, the form and the inscriptions, as well as the mentioned analogies, do not give reliable data for more precise dating. They are dated to the end of the 1st c. – the end of the 6th c. (Вагалински 1995, 68–70, 73).

Six marble, biconical weights found in Durostorum fortress in Silistra town provide more information. Four of them were found during archaeological excavations, in a building that was part of the *canabae* of the *Legio XI Claudia*. The building was burned in 238 during the attack of the Carps, Goths and Sarmatians, or in 251–255 during the invasion of the Goths. The marble weights weigh between 10 and just over 36 Roman libra (Йотов 2017, 73, 74, обр. 1–6).

Stone, especially limestone, was a commonly used material for the manufacture of commercial weights. From 525 stone weights from the period 1st c. BC – 1st c. AD, found in Jerusalem, only 4 were made of stone other than limestone (Reich 2009, 176). The weights were usually marked with the appropriate weight relative to the Roman libra; weight marking is applied to stone (Mutz 1983, 57, Abb. 38. 10, 11) and bronze weights (Božič 2005, 330, Abb. 37).

Cat. No. SF 34 has an incised mark on the upper surface. This sign marks the number 35, written in Roman numerals in a ligature[5]. The inscription of the number 30 with Roman numerals in a ligature can be seen on a tombstone from Abritus near Razgrad town (fig. 4), dating to the end of the 2nd c. – the first half of the 3rd c. (Conrad 2004, 223; Tafel 120.3). The weight is 9.93 kg, intended to weigh 35 Roman libra; it should be approximately 11.46 kg. The weights do not reach 1.53 kg which is needed to match the weight of the marked 35 Roman libra. An explanation for the lost weight can be attributed to the small broken pieces on the underside and the missing handle. It was certainly used to calibrate the weight, particularly if we assume that an iron rod with a diameter of 2.5 cm and a length of 30 cm was used for the handle, the ends of which were thinned to fit into the rings and its weight would have been about 1 kg (the density of the iron is 7.874 g/cm^3).

Cat. No. SF 34 is a stray find. Its dating could be placed in the wide range of the period 1st–6th c. Despite the lack of archaeological context, this find brings additional information about the site. The

5 The team is thankful to Nicolay Sharankov for the epigraphic consultation made for the inscription.

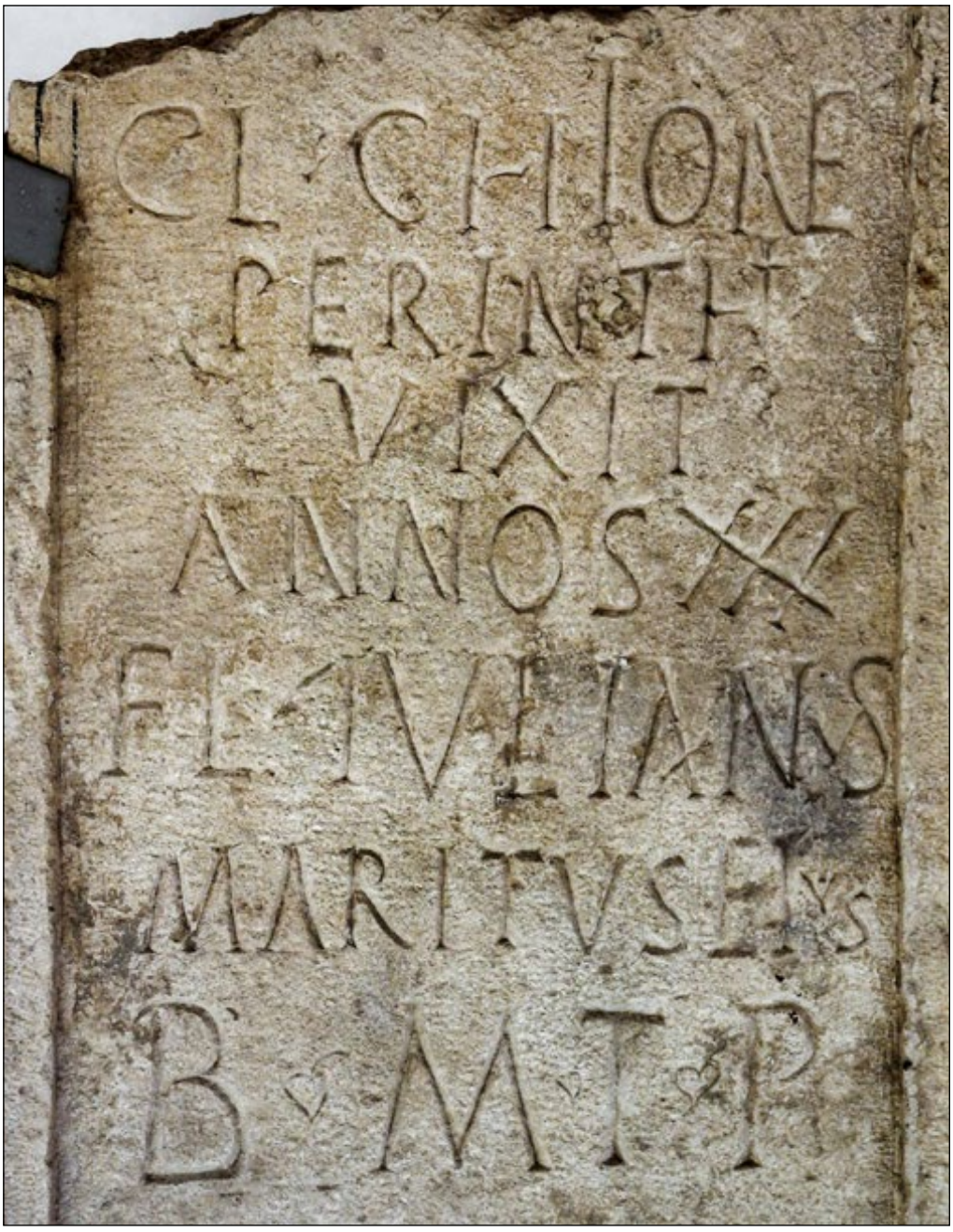


Fig. 4. Gravestone stele with the Roman numeral 30 in ligature (after Conrad 2004, 223; Tafel 120.3)

discovery of a relatively large weight near site 1 is evidence of the development of commercial activity in the area. Most likely, the trade was related to the production of agricultural products. It would be difficult to determine without archaeological excavations whether the produce, the subject of local trade, came from a Roman villa or a settlement.

Stone – cat. Nos. SF 27–33.

Stone loom weight, cat. No. SF 31, plate 8.

The antique stone loom weights for the vertical loom repeat the shapes of those made of clay. The most commonly used shapes in ceramic weights are pyramidal with pronounced or rounded edges or conical. The rounded contours of the stone weights are probably due to the peculiarities of the processing of the stone raw material. The stones are usually conical with a round or elliptical base. In the ancient town of Heraclea Sintica near Rupite village, Blagoevgrad district, pyramidal loom weights with rounded

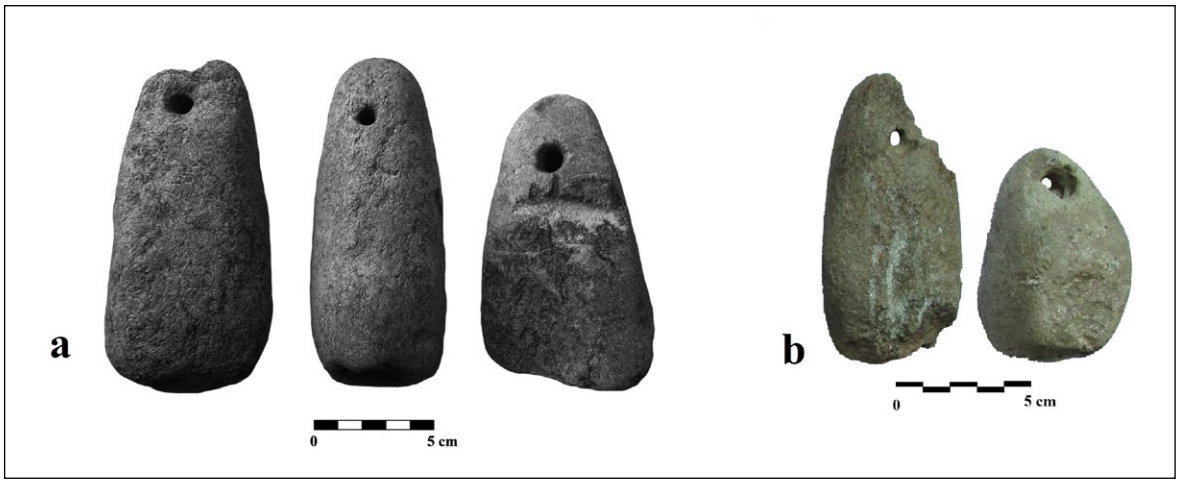


Fig. 5. Stone loom weights: a – after Cholakov 2015, 133, fig. 5. 11–13; b – after Трайкова, Тагарева 2021

edges in cultural layers of the 3rd–4th c. are also found (Cholakov 2015, 136; 133, fig. 5. 11–13) (fig. 5a). Two stone loom weights together with coins minted in the last quarter of the 4th c. and the first quarter of the 5th c. were found in a settlement from the urban territory of Heraclea Sintica (Трайкова, Тагарева 2021, 841) (fig. 5b).

Four whetstones, cat. Nos. SF 27–29, plate 7, cat. No. SF 30, plate 8.

The whetstone was a stone tool used for sharpening various cutting tools. The most common type of stone used to make whetstones are sandstones, due to their granular structure and abrasive properties. Since the four fragments were found on the surface during field surveys they have no archaeological context. They are quite fragmented and without context, thus it is difficult to determine the chronological periods in which they were used.

Two fragments of millstones, cat. Nos. SF 32–33, plate 9.

Both fragments were found during field surveys, and they have no archaeological context. They are fragments of the upper parts of round millstones used by hand. The preserved dimensions of the fragments do not suggest propulsion by animal power or water. They were used to grind cereals for household needs and their discovery suggests the existence of a settlement.

Iron /Fe/ – cat. Nos. SF 48–50.

Iron bridle, cat. No. SF 48, plate 11.

The fragment was discovered during excavations, but it was recorded in a deposited layer due to terrain erosion (cf. the contributions by L. Vagalinski et al., chapter 8.4, fig. 12, layer 2). The preserved part is small and fragmented, but it appears to have an S-shaped curved body. One end was completed with a ring shape. The curved part at the broken end suggests that it was also shaped like a ring and this shape indicates that both ends were connected by additional elements. Depending on the size and shape, the object is most likely part of a bridle of a horse – a bit. A bit is located in the mouth of the horse and is composed of two identical elements, i.e. the bit is twofold. At both ends of the bit, metal rings or elements of another shape are used to connect the side straps around the head of the horse (fig. 6). The lack of archaeological context and the additional elements to the bridle do not allow a reliable dating for this find. Different variants of bridles with a two-component bit are found in settlements and fortresses from the Early Middle Ages – 8th–11th c. (fig. 7), but the appearance of the two-component bridles dates as far back as the Late Iron Age (Йотов 2004, 135, 136, табло LXVII. 724–730, табло LXVIII. 732–735).

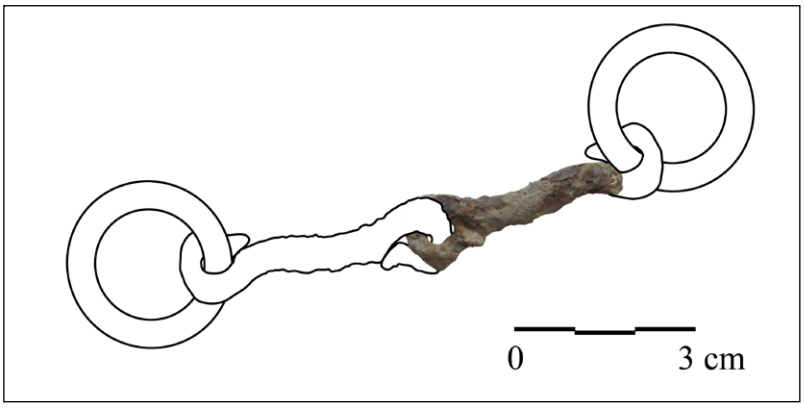


Fig. 6. Graphic reconstruction of part of a horse bridle (drawing by L. Traykova)

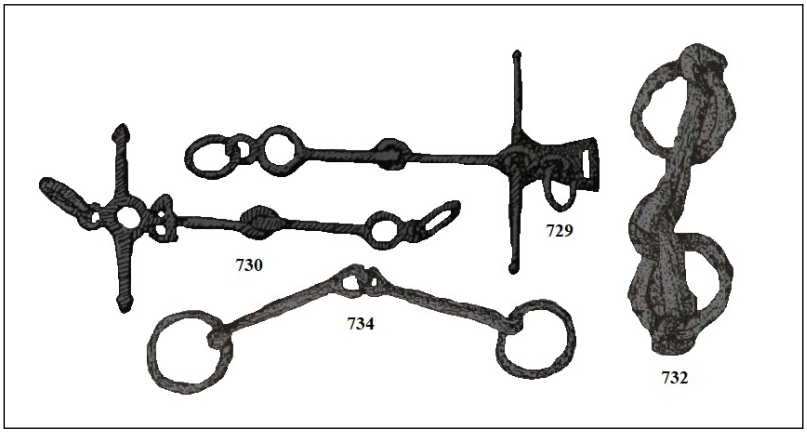


Fig. 7. Iron bridles (after Йотов 2004, табло LXVII. 729, 730, табло LXVIII. 732, 734)

Two arrowheads, cat. Nos. SF 49, 50, plate 11.

Cat. No. SF 49 was discovered during excavations of the fill of an Early Medieval ditch (cf. the contributions by L. Vagalinski et al., chapter 8.4, fig. 12, layer 4). Arrowheads of this type have been published by various authors dating from the 7th to the 9th c. to the 14th c. (Витлянов 1993, 125–126, таблица II. V/A 1; Момчилов 2003, 296, 309, обр. 6. ж–п; Николов 2005, 78, 87, табло V. 23–25; Момчилов 2010, 138, 139, 146, обр. 1. 11–12). In the summarizing publication about the Medieval armament of Valeri Yotov, this arrowhead corresponds to group II, type 2, variant A, and is dated between 7th–11th c., but it is more widespread across the period 10th–11th c. (Йотов 2004, 29, табло XXIII. 337–347).

Cat. No. SF 50 was discovered during excavations in a dark humus layer over the filling of an Early Medieval ditch (cf. the contributions by L. Vagalinski et al., chapter 8.4, fig. 12, layer 3). The appearance of the form dates back to Antiquity (Момчилов 1994, 54; Николов 2005, 78). In the Middle Ages the type dates back to a wide chronological range from the 8th to the 14th c. (Витлянов 1993, 121, таблица I. I/A 1; Момчилов 1994, 54, табло IV.24; Николов 2005, 78, 86, табло IV.18). In the classification of Valeri Yotov, it corresponds to group I, type 1, variant A, and is dated to the 7th–11th c. (Йотов 2004, 25, табло V. 32–59, табло VI. 60–65).

SITE 2

Two fragments of millstones, cat. Nos. SF 51, 52, plate 12.

These two fragments were similar to cat. Nos. SF 32–33. They were found during field surveys and have no archaeological context. These were parts of round millstones used by hand. The find cat. No. SF 51 was part of the top part, and the other one was part of the lower part of a millstone. The predominant part of the pottery of site 2 is from the Roman period (cf. the contributions by N. Kecheva et al., chapter 12, site 2). The two millstone fragments could also be dated to this period.



Fig. 8. Bronze bell (after Andreeva, Atanasov 2020, 482, cat. No. 389)

SITE 3

Bronze bell, cat. No. SF 54, plate 13.

The bell was found during excavations and was recorded in a deposited layer due to erosion of the terrain. Antique bells are made of bronze or iron and more often they have a pyramidal shape.

Bronze and iron bells were found in three collective finds from Slovenia. The publication reviews the development of forms. The typology is based on the shape of the bell, the shape of the suspension attachment, the shape of the base, the metal and the dimensions. Examples from the Lower Danube – Sucivada (Romania), Sadovets and Iatrus (Bulgaria), which have a pyramidal shape, are also included. There is a tendency for the dating of the types, mainly for those with a pyramidal shape. There is no strict distinction in time for the two main forms – pyramidal and cylindrical, which are used throughout Antiquity (Božič 2005, 315–319).

Pyramidal bells made of iron and conical bell made of bronze were found in Castra Martis in Kula town, Vidin district (Bulgaria). They are dated to the period 4th–5th c. In the description of the iron bells, it is noted that they have a thin copper coating (Атанасова 2005, 214, табл. II. 35, 37, 39, 40, 42).

A pyramidal bell made of copper is published as found in Belokopitovo village, Shumen district (Bulgaria). It is part of a collective find with metal artefacts. The form occurs from the 1st to the 6th c., but it is most often distributed in the 4th c. (Cholakov, Atanasov 2007, 258, 260, fig. 9).

A bell that is an exact analogue to cat. No. SF 54 was found in a site near Kozlovets village, Veliko Tarnovo district (Bulgaria) (fig. 8). It was discovered during excavation of a context with artefacts dating to the 2nd–3rd c. (Andreeva, Atanasov 2020, 482, cat. No 389).

Ceramic fishing net weight, cat. No. SF 55, plate 13.

The weight was found during excavations and was recorded in a deposited layer due to erosion of the terrain. Most of the pottery fragments in this layer are dated to the Late Antiquity (cf. chapter 9.1, part 9.1.2.5.). The weight was cut from a hard-fired tile, and it could be dated to the same period as the pottery.

SITE 5

Millstone, cat. No. SF 56, plate 14.

The fragment is a part of round millstones used by hand. It was found during a field survey and it does not have an archaeological context. The artefacts discovered in site 5 include pottery fragments dated to the Late Iron Age, Roman period and Late Antiquity (cf. the contributions by N. Kecheva et al., chapter 12, site 5).

Fragment of the grate of a pottery kiln, cat. No. SF 57, plate 14.

The fragment was also found during field surveys, and it has no archaeological context. This fragment was part of the periphery of the grate of a pottery kiln. The rounded end of the fragment suggests that the kiln was round or semicircular in shape, while the preserved part of the hole in the fragment shows that the diameter of this hole was about 3 cm.

The presence of a grate illustrates that the kiln was two-chambered, with vertical traction, and the grate itself was constant (Харизанов 2019, 38–40). According to the description of Alexander Harizanov, the diameter of the holes varied between 3–4 and 10–12 cm. It has been suggested that smaller holes were preferred when firing large quantities of products for a longer time due to the better-controlled access of hot gases moving into the upper chamber (Харизанов 2019, 39). The earliest two-chambered pottery kilns in Bulgaria date from the beginning of the Late Iron Age (Харизанов 2019, 42–47).

The available data and the lack of an archaeological context do not allow a reliable dating of the fragment of the grate, respectively the kiln. It could be placed in the wide boundaries between Late Iron Age and Late Antiquity. Determining the purpose of the kiln either for household pottery or tiles and bricks is currently only speculative. During the field surveys, a significant amount of tiles and bricks were found (cf. the contributions by N. Kecheva et al., chapter 12, site 5). It is more likely that the kiln was round or semi-circular, which suggests that it was more for the production of household pottery.

The finds with cat. Nos. SF 56 and SF 57 demonstrates that there was a settlement within site 5. The millstone (cat. No. SF 56) was used for household purposes. Its purpose for grinding grain indicates agricultural production, which required a sedentary society. The pottery kiln (cat. No. SF 57) also supports the existence of a settlement in the area.

Two ceramic lamp fragments, cat. Nos. SF 58, 59, plate 14.

Both fragments were found during excavations of the surface layers above the excavated pit (cf. the contributions by L. Vagalinski et al., chapter 8.3.3, fig. 10, layers 5, 5a). The ceramic fragments found in the arbitrary level date from the end of the Late Iron Age to the Early Roman Imperial period (cf. chapter 9.1, table 10). The finds cat. Nos. 58 and 59 are very small fragments, and it is probable that cat. No. SF 58 was part of a multi-wick lamp. The stratigraphic position of the two fragments of lamps suggests that they are likely to date to the Early Roman Imperial period.

SITE 19

The finds at site 19 were discovered during field surveys, and have no archaeological context. The recorded artefacts at site 19 include pottery fragments from the Early Iron Age, Late Iron Age, Roman period, Late Antiquity and Early Middle Ages (cf. the contributions by N. Kecheva et al., chapter 12, site 19).

Coin, cat. No. SF 65, plate 15.

The coin of Emperor Claudius (41–54) was rather erased, which shows that it was in circulation for a long time. The discovery of an Early Roman Imperial coin is evidence of the Early Roman presence in this area. With the annexation of the Thracian kingdom of Rhoemetalces III in 45 and the establishment of the legionary camp at Novae in 45–46, the mouth and upper course of the Yantra River were now part of the Roman province of Moesia (Тачева 2004, 54; Генчева 2002, 7).

Ceramic stopper/ Fishing net weight, cat. No. SF 66, plate 15.

It could not be determined with certainty whether the find is a stopper or was prepared for use as a weight for a fishing net, although it has not been drilled. Usually, stoppers are cut from the walls of vessels. Fragments of tiles were most often reused for cutting weights for fishing nets.

SITE 22

The finds at site 22 were discovered during field surveys, and they have no archaeological context. The recorded artefacts include pottery fragments dated to Late Iron Age, Roman period, Late Antiquity and Early Middle Ages (cf. the contributions by N. Kecheva et al., chapter 12, site 22).

Two fragments of millstones, cat. Nos. SF 67–68, fig. plate 16.

The fragments were fragments of the upper parts of round millstones used by hand.

Ceramic spindle whorl, cat. No. SF 69, plate 16.

Disc-shaped ceramic spindle whorls were found in contexts dating to between the Neolithic and the Middle Ages (Александрова 2017, 358, обр. 10.1–3, 359, обр. 10.2. 1–5, 361, обр. 10.4. 2; Рашев 2008, Табло XCIV. 13–16). An admixture of a lot of sand in the dough and the poor firing are not reliable indicators for the dating of this find.

SITE 27

Iron knife, cat. No. SF 71, plate 16.

It was found in a burial mound during a field survey and is probably a find from a grave that has been destroyed by looters (cf. the contributions by N. Kecheva et al., chapter 12, site 27). The knife is fragmented and strongly corroded. There are no other artefacts that could date the burial mound and the grave.

МАЛКИ НАХОДКИ ОТ АНТИЧНОСТТА И РАННОТО СРЕДНОВЕКОВИЕ

Люба Трайкова

(Резюме)

Малките находки от проведените проучвания са представени според местонамирането им по обекти. От общо регистрирани 38 обекта находки са открити в площите на 7 от тях – обекти: 1, 2, 3, 5, 19, 22 и 27. Повечето от тях нямат точен археологически контекст, тъй като са открити при теренни издирвания или в компрометирани пластове плитко под съвременната повърхност. Това наложи тяхното датиране да бъде направено предимно по паралели с аналогични находки.

Най-много като количество, разнообразни като материал за изработка и хронологично разпространение са находките от обект 1: стъклена гривна (кат. № SF 23, plate 6); керамичен печат за украса на керамика (кат. № SF 24, plate 6); керамични прешлени за вретено (кат. № SF 25, plate 6, кат. № SF 46, plate 11); фрагмент от керамична лампа (кат. № SF 47, plate 11); керамична тежест за стан (кат. № SF 26, plate 6); мраморна търговска тежест (кат. № SF 34, plate 10); каменна тежест за стан (кат. № SF 31, plate 7); четири каменни бруса (кат. №№ SF 27-29, plate 7, кат. № SF 30, plate 8); два фрагмента от хромели (кат. №№ SF 32-33, plate 9); фрагмент от желязна юзда (кат. № SF 48, plate 11); две железни стрели (кат. №№ SF 49, 50, plate 11). Наличието на сравнително голям брой находки от обект 1 спрямо останалите обекти може да се обясни с по-голямата площ, с по-интензивните археологически проучвания, проведени там, както и с широките хронологични граници, в които е обитаван.

Находките от останалите обекти са предимно фрагменти от хромели и керамични предмети. Бъдещи разширени проучвания на тези обекти ще допринесат за прецизирането на хронологията на относително датираните предмети.

Catalogue and plates of the small finds from Antiquity and Early Middle Ages

Abbreviations
d – diameter
h – height
l – length
niv. – niveau
r – radius
Pol. – polygon
th – thickness
Tr. – trench
w – width

Cat. No.	Coordinates	Type	Description	Dimensions	Chronology	Site ID
SF 23	Pol. 11	glass bracelet	A fragment of glass bracelet with five longitudinal ribs without additional decoration, made of semi-transparent blue glass, the incisions between all the ribs are of rather shallow depth; the midrib is tallest and widest.	d 8.0 cm, l 3.5 cm, w 1.1 cm	3rd–2nd c. BC	site 1
SF 24	Pol. 20	ceramic stamp	Ceramic stamp, fragmented, the working part is round, with circles in relief, conical handle, red-slip coating, very well purified light red clay, hard-fired.	d of working section 2.2 cm, l 2.35 cm	1st–3rd c.	site 1
SF 25	Pol. 7SS7	ceramic spindle whorl	Ceramic spindle whorl, fragmented, biconical shape, well purified light red clay, hard-fired.	h 2.0 cm, w 2.2 cm	Antiquity	site 1
SF 26	Pol. 188	ceramic loom weight	Pear-shape or fiddle-shape, fragmented, pinched at the top in order to make a hole for hanging, upper part is missing, well purified light red clay.	w 6.0 cm, h 3.5 cm, th 3.85 cm	Roman period	site 1

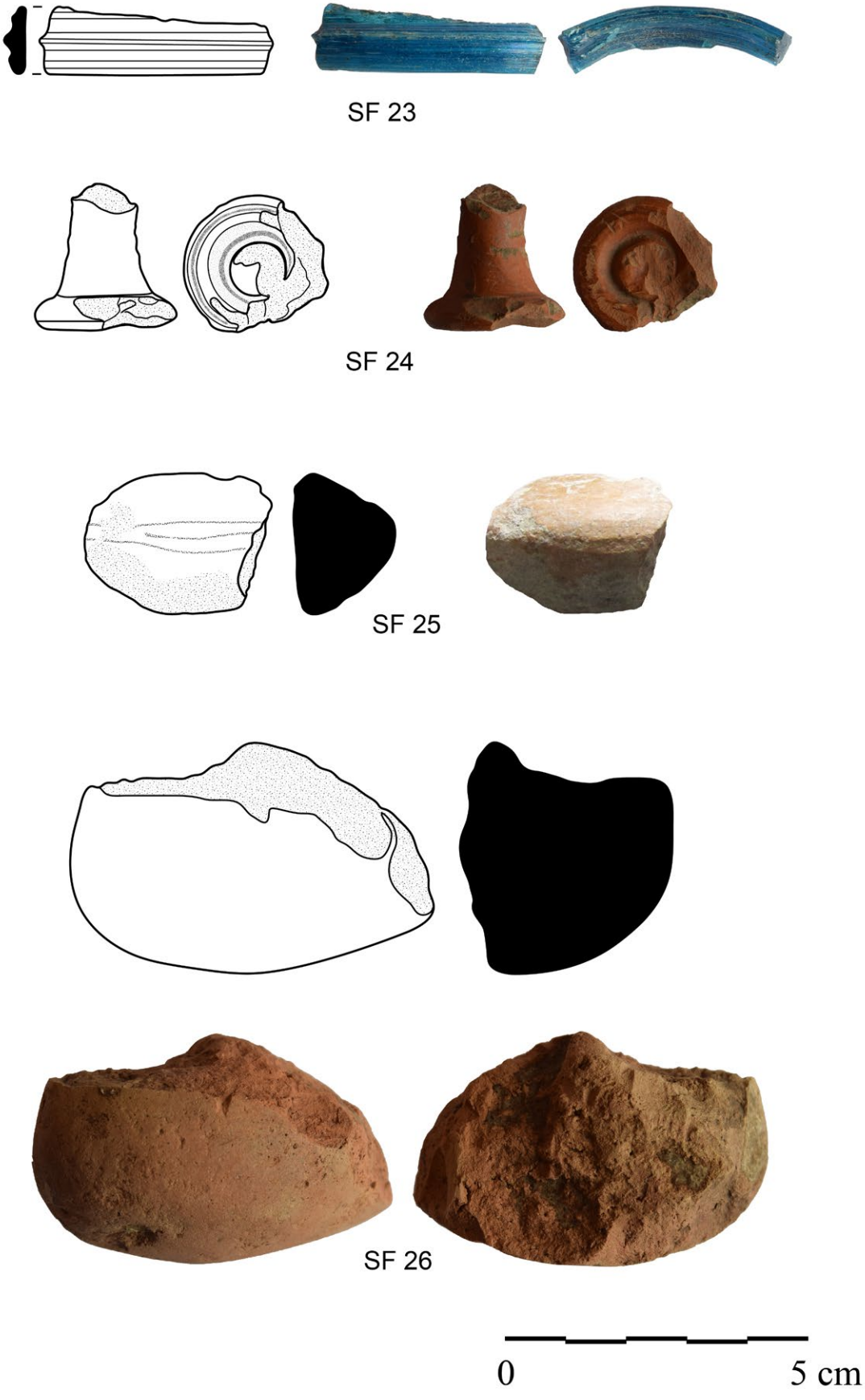


Plate 6. SF 23–26 – small finds from site 1, field survey (figure by L. Traykova)

Cat. No.	Coordinates	Type	Description	Dimensions	Chronology	Site ID
SF 27	Pol. 182	whetstone	Whetstone, fragmented, made from fine-grained sandstone.	l 3.5 cm, w 1.95 cm, th 0.65 cm	Undefined	site 1
SF 28	Pol. 188	whetstone	Whetstone, fragmented, made from fine-grained sandstone.	l 2.86, w 2.07, th 0.65 cm	Undefined	site 1
SF 29	Pol. 187NK1	whetstone	Whetstone, fragmented, made from coarse-grained sandstone.	l 4.32, w 4.0, th 1.4 cm	Undefined	site 1

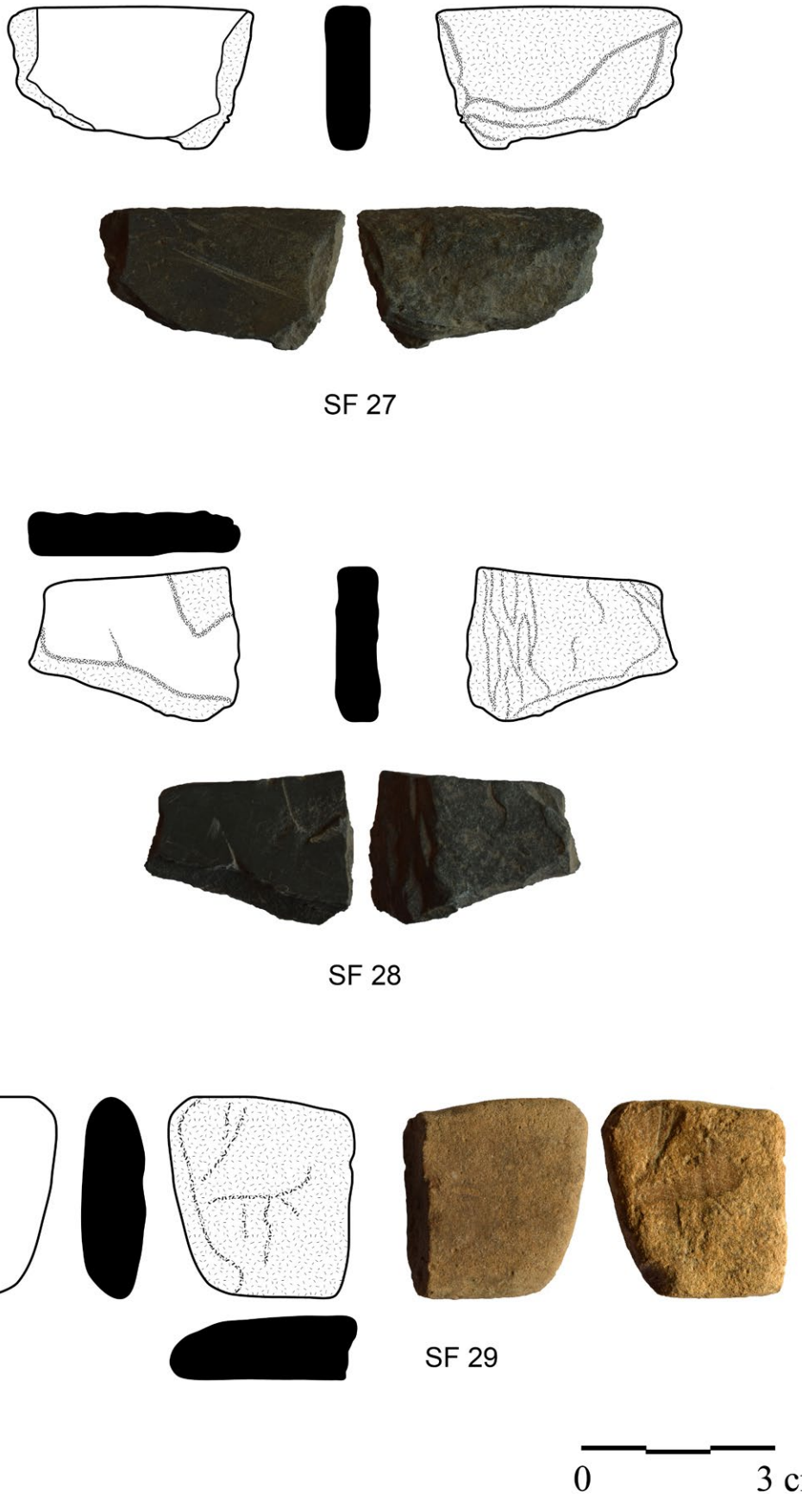
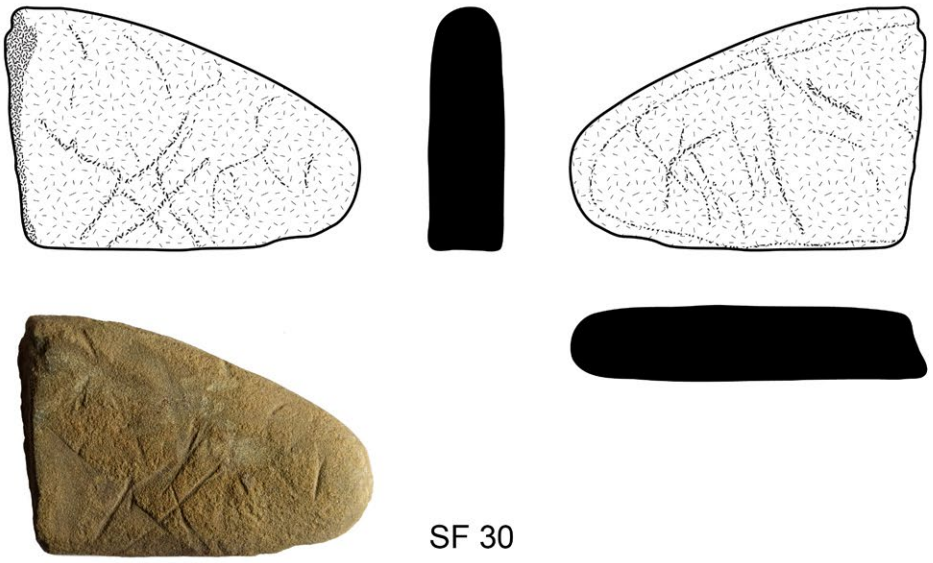


Plate 7. SF 27–29 – small finds from site 1, field survey (figure by L. Traykova)

Cat. No.	Coordinates	Type	Description	Dimensions	Chronology	Site ID
SF 30	Pol. 7LT5	whet-stone	Whetstone, fragmented, made from coarse-grained sandstone.	l 6.72 cm; w 4.46 cm, th 1.4 cm	Undefined	site 1
SF 31	Between sites 1 and 2	stone loom weight	Stone loom weight, the lower part is missing, elliptical cross section, covered with limescale.	h 7.4 cm, d 7.0 x 5.5 cm	Roman period	site 1



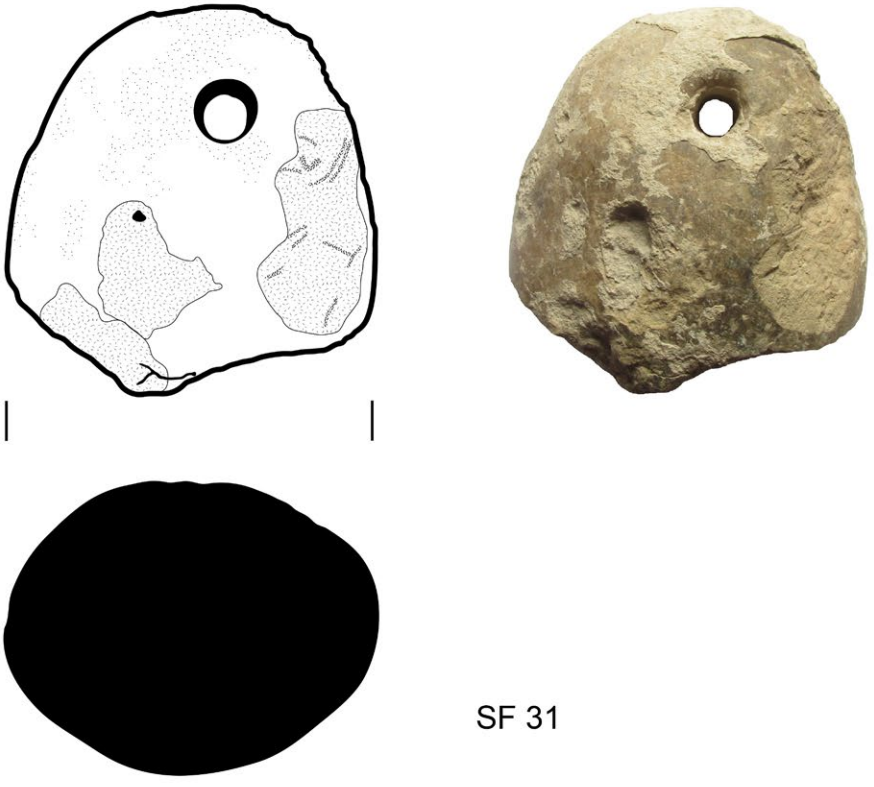


Plate 8. SF 30–31 – small finds from site 1, field survey (figure by L. Traykova)

Cat. No.	Coordinates	Type	Description	Dimensions	Chronology	Site ID
SF 32	Pol. 188SC3	mill-stone	Millstone, fragmented, upper part of round hand grinder, made of solid stone.	5.2 x 8.2 cm; th 5.25 cm	Undefined	site 1
SF 33	Pol. 393	mill-stone	Millstone, fragmented, upper part of round hand grinder, made of very porous limestone.	r 17.8 cm, max. th 6.25 cm	Undefined	site 1

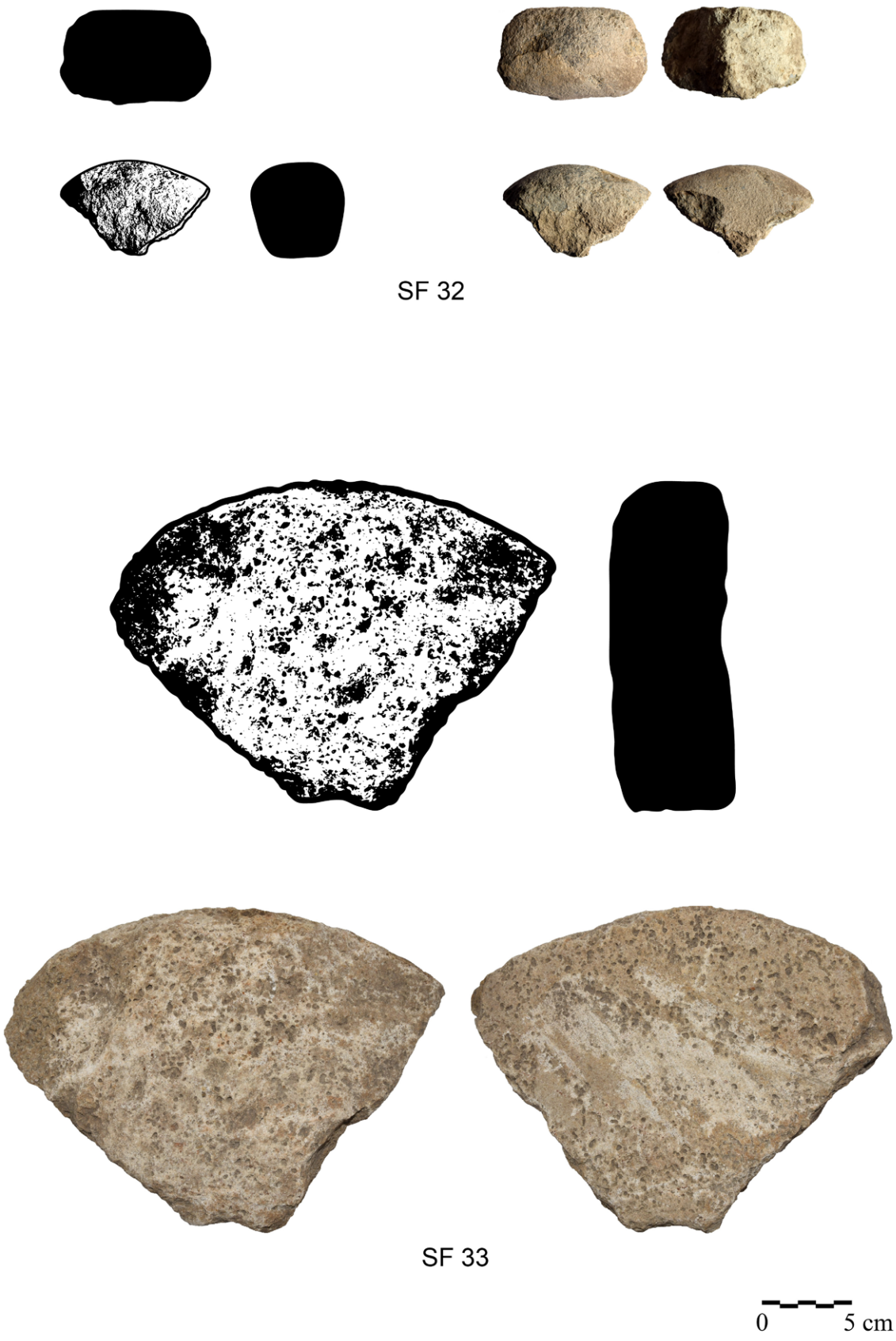


Plate 9. SF 32–33 – small finds from site 1, field survey (figure by L. Traykova)

Cat. No.	Coordinates	Type	Description	Dimensions	Chronology	Site ID
SF 34	West of Site 1	marble weight	Marble weight, made from coarse-grained white marble, with two iron rings for a handle, one of which is fragmented, 4 incised oblique lines intersected by 1 horizontal line.	d 23.0 x 22.0 cm; th 11.0 cm, weight 9.93 kg	1st–6th c.	site 1

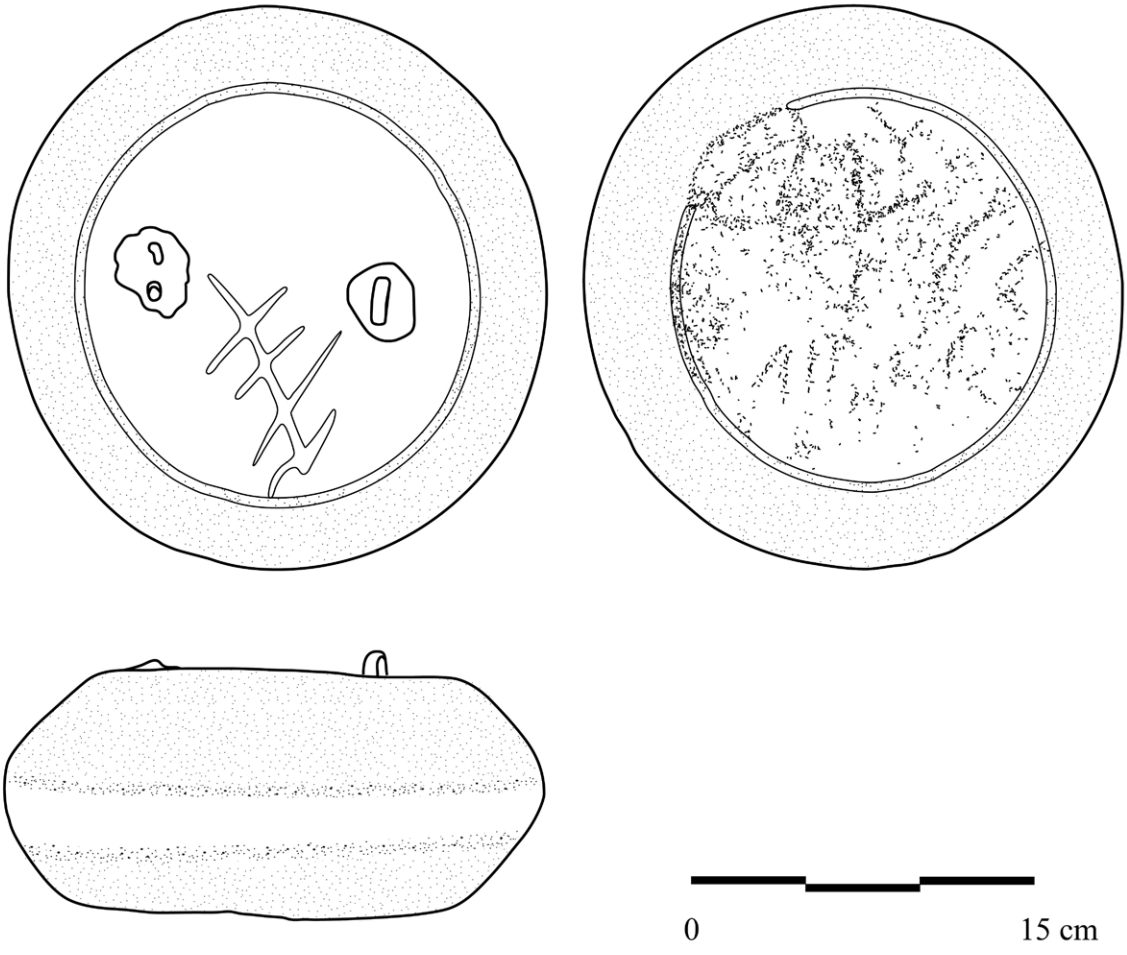




Plate 10. SF 34 – small find from site 1, stray find (figure by L. Traykova)

Cat. No.	Coordinates	Type	Description	Dimensions	Chronology	Site ID
SF 46	Tr. 1.1-W, at niv. 27.82–27.59 m	ceramic spindle whorl	Ceramic spindle whorl, fragmented, discoid shape, with a lot of sand and pebbles in the clay.	outer d 3.6 cm, inner d about 1.1 cm	Undefined	site 1
SF 47	Tr. 1.1-E, at niv. 27.00 m	ceramic lamp	Ceramic lamp, fragmented, wheelmade, very well purified light grey clay, surfaces are light brown-grey in colour, lentil-shaped lamp with biconvex reservoir.	outer d 8 cm, bottom diam. about 2.6 cm, preserved h 1.8 cm, max. w 4.9 cm	the last quarter of the 4th c. BC to the third quarter of the 2nd c. BC	site 1
SF 48	Tr. 1.1-W, NE corner at niv. 27.59–27.48 m	iron bridle	Iron bridle, fragment, rectangular cross section.	l 3.7 cm, outer d of the ring 1.1 cm, inner d of the ring 0.4 cm, th 0.6 x 0.5 cm	Undefined	site 1
SF 49	Tr. 1.1-W, at niv. 26.40 m. At the east profile of the trench, 2.30 m from its SE corner	iron arrow-head	Iron arrowhead, elongated pyramidal shape, with a spike, square cross-section of the spike.	l 8.6 cm, th of the spike 0.5 cm	10th–11th c.	site 1
SF 50	Tr. 1.1-E, at niv. 27.11 m, 3.80 m from SE corner 2.80 m from SW corner of the trench	iron arrow-head	Iron arrowhead, flat, leaf-shaped, with a spike, between the blade and the spike there is a ring in relief.	blade: l 6.9 cm, max. w 2.6 cm, th 0.3 cm; spike: l 4.1 cm, max. w 0.5 cm	7th–11th c.	site 1

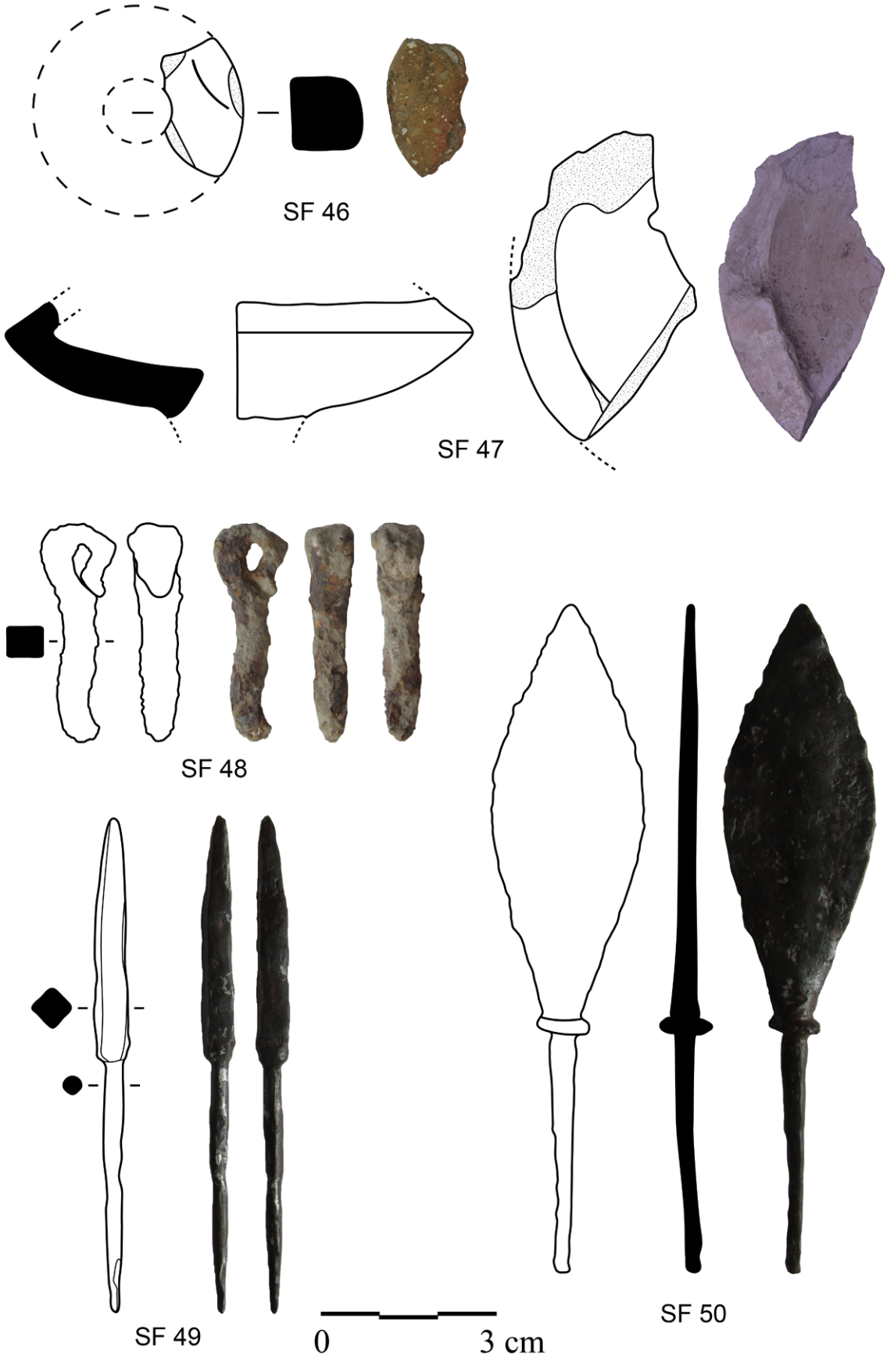


Plate 11. SF 46–50 – small finds from site 1, excavations (figure by L. Traykova)

Cat. No.	Coordinates	Type	Description	Dimensions	Chronology	Site ID
SF 51	Pol. 238	millstone	Millstone, fragmented, upper part of round hand grinder, made of very porous limestone.	r 11.5 cm, max. th 7.5 cm	Undefined, Roman	site 2
SF 52	Found on the road	millstone	Millstone, fragmented, lower part of round hand grinder, made of very porous limestone.	r 16 cm, th 9.2 cm	Undefined, Roman	site 2



Plate 12. SF 51–52 – small finds from site 2, field survey (figure by L. Traykova)

Cat. No.	Coordinates	Type	Description	Dimensions	Chronology	Site ID
SF 54	Tr. 3.6, at niv. 61.07–60.89 m	bronze bell	Bronze bell for a domestic animal, the tongue is missing, rectangular suspension attachment is soldered to the bell, it has an elliptical hole.	l 6.5 cm, d 3.75 × 3.4 cm	2nd–3rd c.	site 3
SF 55	Tr. 3.6, at niv. 60.72–60.37 m	fishing net weight	Fishing net weight, cut from tile, round hole in the middle.	d 6.1 cm, th 2.2 cm	Late Antiquity	site 3



Plate 13. SF 54–55 – small finds from site 3, excavations (figure by L. Traykova)

Cat. No.	Coordinates	Type	Description	Dimensions	Chronology	Site ID
SF 56	Pol. 176	mill-stone	Millstone, fragmented, lower part of round hand grinder, made of very porous limestone.	10.6 x 9.2 cm, th 5.3 cm	Undefined	site 5
SF 57	Pol. 162	grate of pottery kiln	Fragment of grate of pottery kiln.	6.0 x 5.0 x 4.15 cm	between Late Iron Age and Late Antiquity	site 5
SF 58	Tr. 5.2, pit 5.1.5, at niv. 21.18–20.77 m	ceramic lamp	Fragment of ceramic lamp.	l 4.1 cm, w 2 cm	Early Roman Imperial period	site 5
SF 59	Tr. 5.2, pit 5.1.5, at niv. 21.18–20.77 m	ceramic lamp	Fragment of ceramic lamp.	2 × 1.3 cm, th 0.2 cm	Early Roman Imperial period	site 5

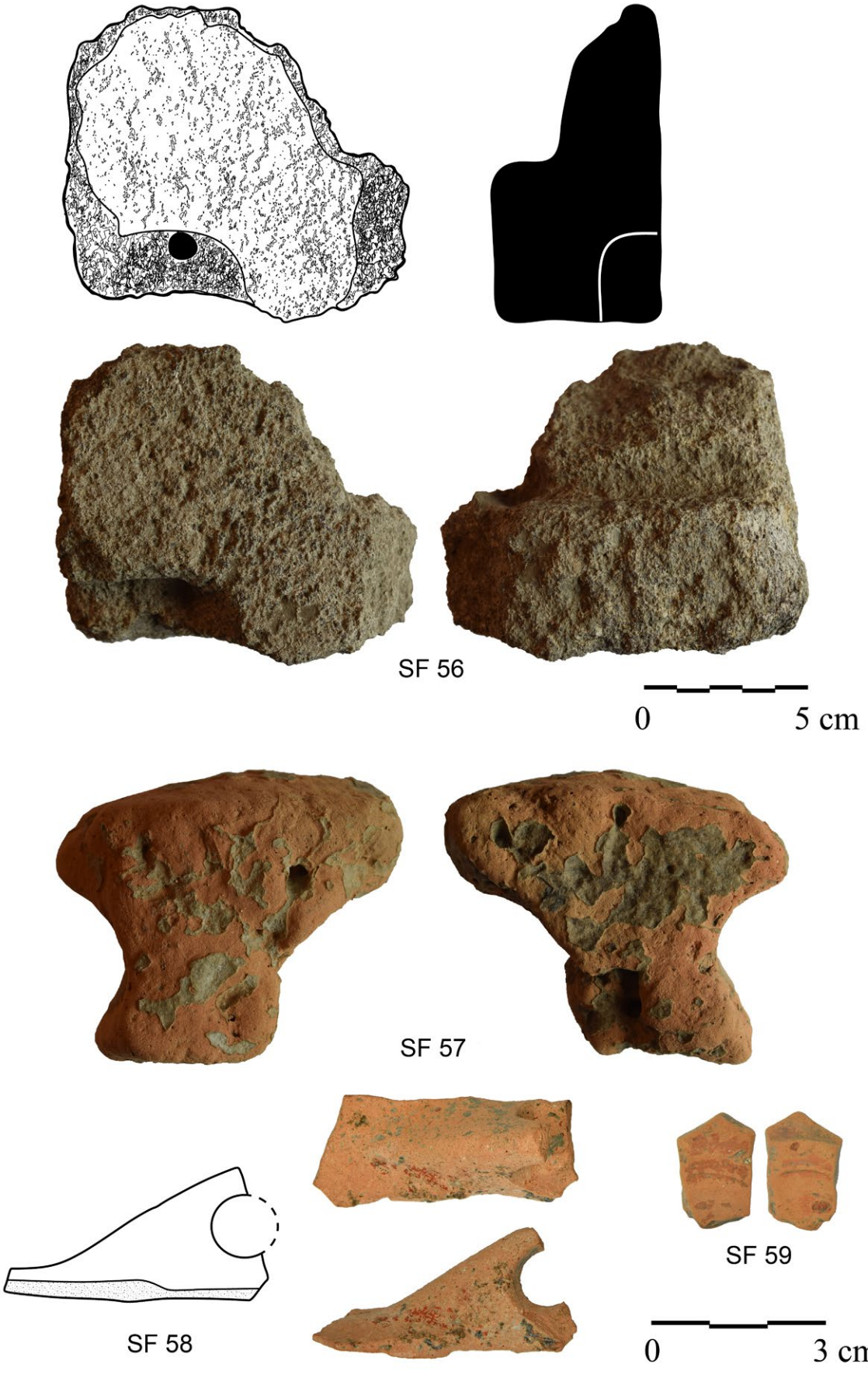


Plate 14. SF 56–57 – small finds from site 5, field survey; SF 58–59 – small finds from site 5, excavations (figure by L. Traykova)

Cat. No.	Coordinates	Type	Description	Dimensions	Chronology	Site ID
SF 64	Pol. 475	whet-stone	Whetstone, fragmented, made from fine-grained stone.	l 5.4 cm, max. w 3.2 cm, max. th 3.7 cm	Undefined	site 19
SF 65	Pol. 498	coin	Bronze coin of Emperor Claudius I (41–45), obverse: bare head left, reverse: the image is not preserved.	d 28/27 mm, weight 8.55 g, th 0.3 cm	Early Roman Imperial period	site 19
SF 66	Pol. 529	ceramic stopper / fishing net weight	Ceramic stopper or fishing net weight, cut from tile.	d 6.8 x 5.85 cm, th 2,05 cm	Undefined	site 19

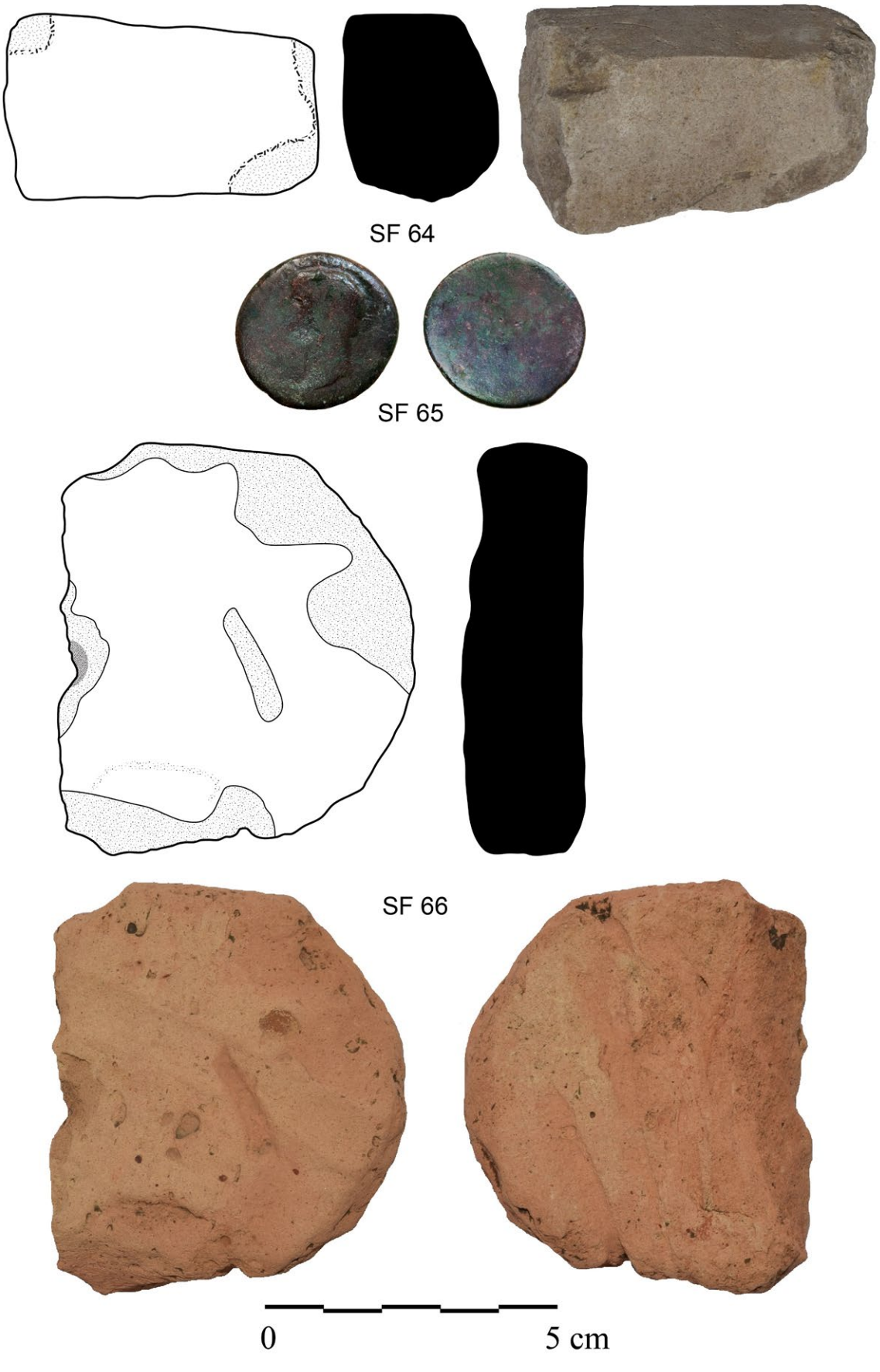


Plate 15. SF 64–66 – small finds from site 19, field survey (figure by L. Traykova)

Cat. No.	Coordinates	Type	Description	Dimensions	Chronology	Site ID
SF 67	Pol. 671	millstone	Millstone, fragmented, upper part of round hand grinder, made of limestone.	l 16.6 cm, r 12.5 cm, th 5.6 cm	Undefined	site 22
SF 68	Pol. 672	millstone fragment	Millstone, fragmented, upper part of round hand grinder, made of limestone.	l 17.5 cm, r 9.2 cm, th 7.5 cm	Undefined	site 22
SF 69	Pol. 695	ceramic spindle whorl	Ceramic spindle whorl, fragmented, with a lot of sand in the clay.	outer d 2.7 cm, inner d 1 cm, th 1.7 cm	Undefined	north of site 22
SF 71	Mound	iron knife	Fragment of an iron knife, very corroded.	l 5.4 cm, w 1.9 cm	Undefined	site 27

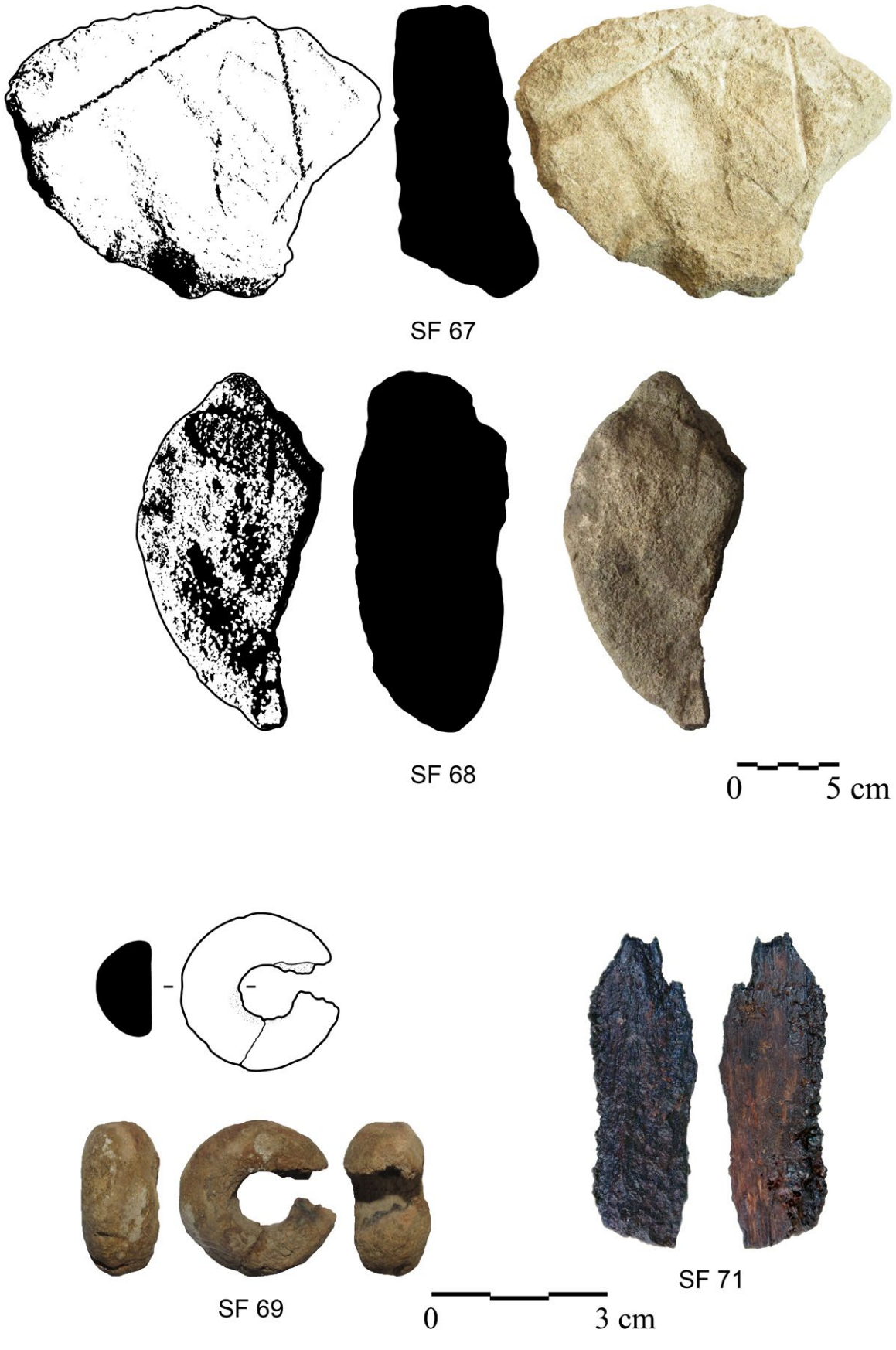


Plate 16. SF 67–68 – small finds from site 22, field survey; SF 69 – small find north of site 22, field survey; SF 71 – small find from site 27, field survey (figure by L. Traykova)


www.naim.bg